

**A ROBUST TOPOLOGICAL PRELIMINARY DESIGN
EXPLORATION METHOD WITH MATERIALS DESIGN
APPLICATIONS**

A Dissertation
Presented to
The Academic Faculty

by

Carolyn Conner Seepersad

In Partial Fulfillment
of the Requirements for the Degree
Doctor of Philosophy in Mechanical Engineering

Georgia Institute of Technology
September 2004

Copyright © Carolyn Conner Seepersad 2004

**A ROBUST TOPOLOGICAL PRELIMINARY DESIGN EXPLORATION
METHOD WITH MATERIALS DESIGN APPLICATIONS**

Approved by:

Farrokh Mistree, Chair
Professor, Mechanical Engineering

Janet K. Allen, Co-Chair
Senior Research Scientist,
Mechanical Engineering

David L. McDowell, Co-Chair
Regents' Professor, Mechanical
Engineering

Joe Cochran
Professor, Materials Science & Engineering

Christiann J. J. Paredis
Assistant Professor, Mechanical Engineering

David W. Rosen
Professor, Mechanical Engineering

Kwok Tsui
Professor, Industrial & Systems Engineering

Date Approved:
September 14, 2004

ACKNOWLEDGMENTS

You cannot teach a person anything--you can only help him to find for himself.
Galileo Galilei

Throughout my life, family, friends, and mentors have joined their voices in a continuous chorus, reverberating with the lyrics, “You can.” Synchronously, they have provided the supporting rhythm and accompaniment without which the song of my accomplishments would have been arduous, if not impossible, to compose. In short, they have given me a tremendous gift—a song of life—with all of the resources, knowledge, love, support, and inspiration that have helped me grow as a person and as a professional. They have helped me “find for myself.” There are many members of this ‘chorus’ that I wish to acknowledge.

My family are the most consistent and often the most audible members of this chorus. I have been blessed with wonderful parents; they have never failed to encourage me, to challenge me, and to support me as only parents can do. Mom continues to inspire me in spirit as she did in life. My husband, Clyde, is a blessing. His support, encouragement, love, and steady, uplifting nature make me a better person. I can only begin to express my appreciation, admiration, and affection for the rest of my family and friends and for the many teachers and mentors who have joined in the “You can” chorus through the years. “Anything is possible if you have faith (Mark 9:23).”

For the past few years, some of the most influential members of the chorus have been my advisors. I cannot begin to thank Farrokh Mistree and Janet Allen for their encouragement and for “helping me to find for myself.” I know that I am not alone among Farrokh and Janet’s current and former students when I remark that their dreams

for me are even bigger than my dreams for myself. Farrokh and Janet's enthusiasm, vision, insight, and gifts for encouraging students to set and meet high aspirations are truly unique. I also extend my warmest thanks to David McDowell, one of the most motivational and visionary educators I have ever known. Many of the innovative ideas in this dissertation have grown directly from discussions with him. I cannot thank him enough for truly believing that *design* is an essential part of materials design and for leading the way for young researchers like myself to build foundations for a new field. Dr. McDowell has a wonderful ability to motivate students to work very hard and challenge themselves abundantly—not because they are afraid of failure or rebuke but because they *want* to succeed. After my periodic meetings with Dr. McDowell, I am so excited about my own work that it's difficult to set it aside for long.

Singing harmony in the chorus are the members of the Systems Realization Laboratory with their diverse, challenging, sustaining, and motivational voices. I extend thanks to Hae-jin Choi and Marco Fernandez for their assistance with the thermal analysis models and to Marco for being such a patient 'sounding board' and wonderful friend. Olu Ogunsanya and Thang Nguyen have been helpful with many aspects of the case studies. Thang has been tremendously helpful with the FLUENT and ANSYS analyses for the combustor liner example. Most of all, I would like to thank all of the faculty and students in the SRL for their friendship and challenging discussions and for collectively making the lab a wonderful place to work, to learn, to grow, and to have fun. Thanks to Chris, Matt, Marco, Jitesh, Hae-jin, Andrew, Yao, Rakesh, Nate, and all of the past inhabitants of SRL 264 for being such wonderful friends and colleagues and for all of their support and pleasant distractions over the years.

I offer a special thanks to the members of my committee—Farrokh Mistree, Janet Allen, David McDowell, Joe Cochran, Chris Paredis, David Rosen, and Kwok Tsui—for their valuable advice and feedback on this dissertation. Benjamin Dempsey graciously provided the finite difference thermal analysis code for the structural heat exchanger example. Joe Cochran and his colleagues in the Lightweight Structures Group have graciously shared their knowledge and experience with linear cellular materials. Dr. McDowell’s students and postdoctoral researchers, including Rajesh Kumar and Aijun Wang, have been very helpful throughout the course of this research.

Finally, I thank the Fannie and John Hertz Foundation, the National Science Foundation Graduate Fellowship program, the Georgia Tech President’s Fellowship program, and Achievement Rewards for College Scientists for the financial support that made my graduate study feasible. The structural heat exchanger and combustor liner examples are based in part on the objectives of ONR Contract N00014-02-1-0926, “Linear Alloys for Thermal Management and Structures” with Project Monitor Dr. Steven Fishman. Financial support is gratefully acknowledged from the Air Force Office of Scientific Research, Multi-University Research Initiative (1606U81). Krister Svanburg is gratefully acknowledged for supplying the MMA algorithm used in this dissertation.

As an aspiring young professor, it is the author’s hope and pledge that she will become a strong voice in the “You can” choruses of many young people in the decades to come.

TABLE OF CONTENTS

ACKNOWLEDGMENTS	iii
TABLE OF CONTENTS	vi
LIST OF TABLES	xiv
LIST OF FIGURES	xviii
LIST OF SYMBOLS	xxv
SUMMARY	xxxvi
CHAPTER 1 FOUNDATIONS FOR ESTABLISHING A ROBUST TOPOLOGICAL PRELIMINARY DESIGN EXPLORATION METHOD	1
1.1 MATERIALS DESIGN—A NEW FRONTIER FOR ENGINEERING SYSTEMS DESIGN	3
1.1.1 Materials Design Challenges	7
1.1.2 The Materials Design Focus of this Dissertation: Mesoscopic Material Structure, Topology, and Prismatic Cellular Materials	12
1.2 FRAME OF REFERENCE	21
1.2.1 Topology Design	22
1.2.2 Robust Design and Multidisciplinary Concept Exploration	30
1.2.3 Multiobjective Decision-Making and the Compromise Decision Support Problem	38
1.3 RESEARCH FOCUS, CONTRIBUTIONS, AND STRATEGY	40
1.3.1 Fundamental Research Questions and Hypotheses	41
1.3.2 Research Contributions	47
1.4 AN OVERVIEW AND VALIDATION STRATEGY FOR THIS DISSERTATION	53

CHAPTER 2	ROBUST, MULTIFUNCTIONAL TOPOLOGY DESIGN FOR MATERIALS DESIGN APPLICATIONS: REVIEW OF LITERATURE AND IDENTIFICATION OF RESEARCH OPPORTUNITIES	63
2.1	DESIGN METHOD REQUIREMENTS FOR THE RTPDEM	63
2.2	MULTIOBJECTIVE DECISION SUPPORT AND THE COMPROMISE DSP	69
2.3	TOPOLOGY DESIGN	81
2.3.1	Robust Topology Design	100
2.3.2	Multifunctional Topology Design	107
2.4	ROBUST DESIGN AND ROBUST CONCEPT EXPLORATION	114
2.4.1	The Taguchi Approach for Robust Design	115
2.4.2	Improvements and Extensions of Taguchi's Robust Design Methodology for Engineering Design Applications	119
2.4.3	Robustness in the Early Stages of Multidisciplinary Design	126
2.4.4	Robust Design for Multidisciplinary Applications	133
2.5	RESEARCH OPPORTUNITIES	139
2.5.1	Research Question 1: Robust Topology Design	139
2.5.2	Research Question 2: Multifunctional Topology Design	141
2.5.3	Research Question 3: Compromise DSP for Multifunctional, Robust Topology Design	143
2.6	CHAPTER SYNOPSIS	145
CHAPTER 3	AN OVERVIEW OF THE ROBUST TOPOLOGICAL PRELIMINARY DESIGN EXPLORATION METHOD	146
3.1	AN INTRODUCTION TO THE ROBUST TOPOLOGICAL PRELIMINARY DESIGN EXPLORATION METHOD	147
3.1.1	Phase I: Formulate a Robust Topology Design Space	147
3.1.2	Phase II: Formulate a Robust Topology Design Problem	149
3.1.3	Phase III: Establish Simulation Framework	149

3.1.4	Phase IV: Solve the Robust Topology Design Problem	150
3.2	THE RESEARCH HYPOTHESES AND THEIR RELATIONSHIP WITH THE ROBUST TOPOLOGICAL PRELIMINARY DESIGN EXPLORATION METHOD	150
3.3	ADDRESSING HYPOTHESIS 1—ESTABLISHING ROBUST DESIGN METHODS FOR TOPOLOGY DESIGN	153
3.3.1	Phase 1: Formulate a Robust Topology Design Space	154
3.3.2	Phase 2: Formulate a Robust Topology Design Problem	169
3.3.3	Phase 3: Establish Simulation Framework	174
3.3.4	Phase 4: Solving the Robust Topology Design Problem	188
3.4	ADDRESSING HYPOTHESIS II—MULTIDISCIPLINARY ROBUST TOPOLOGY DESIGN	192
3.4.1	Basic Assumptions and Motivation for Multidisciplinary Robust Topology Design	194
3.4.2	A Multi-Stage Robust Design Approach for Multifunctional Topology Design	200
3.5	EXTENDING TOPOLOGY DESIGN TECHNIQUES BEYOND THE STRUCTURAL DOMAIN—A THERMAL TOPOLOGY DESIGN APPROACH	209
3.5.1	Critical Design Issues and Conventional Design Approaches for Thermal Topology and Parametric Design	212
3.5.2	Thermal Topology Design Approach	218
3.6	THEORETICAL STRUCTURAL VALIDATION FOR THE RTPDEM	239
3.7	CHAPTER SYNOPSIS	250
CHAPTER 4	DESIGN OF PRISMATIC CELLULAR MATERIALS	252
4.1	DESIGN, ANALYSIS, AND FABRICATION OF PRISMATIC CELLULAR MATERIALS	253
4.2	EXAMPLES OF PRISMATIC CELLULAR MATERIALS DESIGN	260
4.2.1	Overview and Materials Design Relevance of Three Prismatic Cellular Materials Design Examples	261

4.2.2	The Role of the Examples in Validating the Research Hypotheses	265
4.3	CHAPTER SYNOPSIS	272
CHAPTER 5	MULTIFUNCTIONAL DESIGN OF PRISMATIC CELLULAR MATERIALS FOR STRUCTURAL HEAT EXCHANGERS	273
5.1	AN OVERVIEW OF MULTIFUNCTIONAL DESIGN OF CELLULAR STRUCTURAL HEAT EXCHANGERS	274
5.2	VALIDATION AND VERIFICATION WITH THE EXAMPLE	276
5.2.1	Empirical Structural Validation	277
5.2.2	Empirical Performance Validation	279
5.3	INSTANTIATING THE DESIGN APPROACH FOR THIS EXAMPLE	281
5.3.1	Implementing Phase 1 of the RTPDEM: Formulating a Design Space	282
5.3.2	Implementing Phase 2 of the RTPDEM: Formulating a Compromise DSP for Prismatic Cellular Materials Design for a Structural Heat Exchanger	284
5.3.3	Implementing Phase 3 of the RTPDEM: Analysis Models and Simulation Infrastructure for Prismatic Cellular Material Design for a Structural Heat Exchanger	286
5.4	PRESENTATION AND DISCUSSION OF STRUCTURAL HEAT EXCHANGER DESIGNS	290
5.4.1	Designing Baseline Prismatic Materials for the Structural Heat Exchanger Application	292
5.4.2	Designing Multifunctional Prismatic Cellular Materials for the Structural Heat Exchanger Example	297
5.4.3	Verification and Validation of Resulting Designs	300
5.5	CRITICAL DISCUSSION OF THE EXAMPLE RESULTS	302
5.6	CHAPTER SYNOPSIS	307

CHAPTER 6	ROBUST TOPOLOGY DESIGN OF PRISMATIC CELLULAR MATERIALS FOR STRUCTURAL APPLICATIONS	310
6.1	AN OVERVIEW OF ROBUST TOPOLOGY DESIGN OF STRUCTURAL UNIT CELLS	311
6.2	VALIDATION AND VERIFICATION WITH THE EXAMPLE	316
6.2.1	Empirical Structural Validation	316
6.2.2	Empirical Performance Validation	319
6.3	INSTANTIATING THE ROBUST TOPOLOGICAL PRELIMINARY DESIGN EXPLORATION METHOD AS THE DESIGN APPROACH FOR THIS EXAMPLE	322
6.3.1	Implementing Phase 1 of the RTPDEM: Formulating the Robust Topology Design Space for Cellular Materials Design	322
6.3.2	Implementing Phase 2 of the RTPDEM: Formulating the Robust Topology Design Problem for Cellular Materials Design	328
6.3.3	Implementing Phase 3 of the RTPDEM: Analysis Models and Simulation Infrastructure for Cellular Materials Design	333
6.4	PRESENTATION AND DISCUSSION OF ROBUST CELLULAR MATERIAL DESIGNS	341
6.4.1	Results for Robust Topology Design for Dimensional Variation—Experimental Stage 1A for Design Cases 1 and 2	341
6.4.2	Results for Robust Topology Design for Dimensional and Topological Variation—Experimental Stage 1B for Design Cases 1 and 2	347
6.4.3	Verification of Results—Experimental Stage 3	353
6.5	CRITICAL DISCUSSION OF THE RESULTS	363
6.6	CHAPTER SYNOPSIS	370

CHAPTER 7	MULTIFUNCTIONAL, ROBUST TOPOLOGY DESIGN OF COMBUSTOR LINERS	372
7.1	AN OVERVIEW OF MULTIFUNCTIONAL, ROBUST TOPOLOGY DESIGN OF COMBUSTOR LINERS	373
7.2	VALIDATION AND VERIFICATION WITH THE EXAMPLE	380
	7.2.1 Empirical Structural Validation	381
	7.2.2 Empirical Performance Validation	385
7.3	INSTANTIATING THE ROBUST TOPOLOGICAL PRELIMINARY DESIGN EXPLORATION METHOD AS THE DESIGN APPROACH FOR THIS EXAMPLE	388
	7.3.1 Implementing Phase 1 of the RTPDEM: Formulating a Robust Multifunctional Topology Design Space for A Cellular Combustor Liner	388
	7.3.2 Implementing Phase 2 of the RTPDEM: Formulating the Robust Multifunctional Topology Design Problem for a Cellular Combustor Liner	392
	7.3.3 Implementing Phase 3 of the RTPDEM: Analysis Models and Simulation Infrastructure for a Cellular Combustor Liner	399
	7.3.4 Verification and Validation of the Structural and Thermal Simulations for the Combustor Liner Example Problem	408
	7.3.5 Multifunctional Design with the RTPDEM	420
7.4	PRESENTATION AND DISCUSSION OF COMBUSTOR LINER DESIGNS	423
	7.4.1 Structural Design Results for Range-Based and Model-Based, Multi-stage, Multifunctional Topology Design for Stages 1A and 1B of the Experimental Plan of Table 7.3	425
	7.4.2 Thermal Design Results for Range-Based, Multi-stage, Multifunctional Topology Design for Stage 1A of the Experimental Plan in Table 7.3	433
	7.4.3 Thermal Design Results for Model-Based, Multi-stage, Multifunctional Topology Design for Stage 1B of the Experimental Plan in Table 7.3	438

	7.4.4 Results for Stage 2: Comparing the Performance of the Designed Structures with the Performance of a Heuristically Designed Structure	446
7.5	CRITICAL DISCUSSION OF THE EXAMPLE RESULTS	448
7.6	CHAPTER SYNOPSIS	456
CHAPTER 8	CLOSURE	458
8.1	A SUMMARY OF THIS DISSERTATION	458
8.2	ANSWERING THE RESEARCH QUESTIONS AND VALIDATING THE RESEARCH HYPOTHESES	462
8.2.1	Hypothesis 1: Robust Topology Design	463
8.2.2	Hypothesis 2: Multifunctional, Robust Topology Design	470
8.2.3	Hypothesis 3: Compromise DSP for Multifunctional, Robust Topology Design	476
8.2.4	Theoretical Performance Validation of Hypotheses 1, 2, and 3	480
8.3	ACHIEVEMENTS AND CONTRIBUTIONS	483
8.3.1	Contributions to the Field of Design Methodology	483
8.3.2	Achievements in Thermal Topology Design and Analysis	487
8.3.3	Achievements and Contributions in the Field of Materials Design	488
8.4	LIMITATIONS AND OPPORTUNITIES FOR FUTURE WORK	490
8.4.1	Materials Design Opportunities	490
8.4.2	Additional Opportunities	495

APPENDIX A	ADDITIONAL VALIDATION OF THE APPROXIMATE FINITE ELEMENT/FINITE DIFFERENCE SIMULATION MODELS FOR COMBUSTOR LINER DESIGN	499
	A.1 PARAMETRIC DESIGN VALIDATION	499
	A.2 VALIDATION OF TOPOLOGY DESIGN	505
REFERENCES		510
VITA		526

LIST OF TABLES

Table 1.1	Requirements for Robust, Multifunctional Topological Designs and Associated Design Methods	20
Table 1.2	Mapping Requirements to Research Questions and Hypotheses	43
Table 3.1	Theoretical Capabilities and Limitations of the RTPDEM	241
Table 4.1	Materials Design Capabilities Demonstrated in Each Example	262
Table 5.1	Experimental Plan and Outline	280
Table 5.2	Summary of Design Parameters for the Structural Heat Exchanger Example	282
Table 5.3	Two-Stage Design Approach	291
Table 5.4	Example Prismatic Cellular Material Designs for the Structural Heat Exchanger Application	295
Table 5.5	Convergence Plots for 12x4 Designs in Table 5.4	302
Table 6.1	Requirements for Prismatic Cellular Materials for a Structural Application	311
Table 6.2	Experimental Plan and Outline	320
Table 6.3	Summary of Design Parameters for Structural Unit Cell Example	327
Table 6.4	Goal Target Values, Constraint Limits, Design Variable Bounds, and Weights	333
Table 6.5	Robust vs. Non-Robust Periodic Unit Cell Designs for Effective Stiffness in Both Principal Directions, Considering Dimensional Variation Only	343

Table 6.6	Robust vs. Non-Robust Periodic Unit Cell Designs for Effective Stiffness in Both Principal Direction and in Shear, Considering Dimensional Variation Only	344
Table 6.7	Robust vs. Non-Robust Periodic Unit Cell Designs for Effective Stiffness in Both Principal Directions, Considering Topological and Dimensional Variation	347
Table 6.8	Robust vs. Non-Robust Periodic Unit Cell Designs for Effective Stiffness in Principal Directions, Considering Topological and Dimensional Variation	348
Table 6.9	Robust vs. Non-Robust Periodic Unit Cell Designs for Effective Stiffness in Principal Directions, Considering Topological and Dimensional Variation	352
Table 6.10	Comparison of Finite Elements and Theoretical Approximations for Effective In-Plane Elastic Stiffness Properties	354
Table 6.11	Robust vs. Non-Robust Periodic Unit Cell Designs for Effective Stiffness in Both Principal Directions (9x9 nodal mesh)	356
Table 6.12	Additional Local Minima for Unit Cell Designs for Design Case 2 (Effective Stiffness in Both Principal Directions and in Shear) (5x5 nodal mesh)	359
Table 6.13	Convergence Plots for Designs in Table 6.5, 6.6, 6.7, 6.8, and 6.9	362
Table 7.1	Requirements for Prismatic Cellular Materials for a Combustor Liner Application	378
Table 7.2	Conditions for a Combustor Liner Application	379
Table 7.3	Experimental Plan and Outline	386
Table 7.4	Summary of Design Parameters for Combustor Liner Example	392
Table 7.5	Goal Targets, Design Variable Bounds, Constraint Limits, and Weights for Combustor Liner Design	398

Table 7.6	Comparisons of ANSYS and Approximate FE Model Stress Predictions for the Structure in Figure 7.9 with Thermal Expansion and the Boundary Conditions Indicated in the Table and in Figure 7.7	412
Table 7.7	Boundary and Operating Conditions for FE/FD Algorithm Validation with FLUENT	413
Table 7.8	Comparison of FLUENT and FE/FD Results for Heat Transfer and Fluid Temperatures	416
Table 7.9	Comparison of FLUENT and FE/FD Results for Cell Wall Temperature Distribution	417
Table 7.10	Robust Structural Design Results	426
Table 7.11	Non-Robust Structural Design Results	427
Table 7.12	Results of Range-Based Stage 1A Thermal Design, Based on the Robust Structural Design of Table 7.10, Modified for Thermal Performance within the Ranges Specified by the Structural Designer	437
Table 7.13	Results of Range-Based Stage 1A Thermal Design, Based on the Non-Robust Structural Design of Table 7.11, Modified for Thermal Performance within Ranges Consistent with Those for Robust Designs in Table 7.12	438
Table 7.14	Results of Stage 1B Thermal Design, Based on the Robust Structural Design of Table 7.10, Modified Exclusively for Thermal Performance within Broad Ranges	441
Table 7.15	Results of Model-Based Stage 1B Thermal Design, Based on the Robust Structural Design of Table 7.11, Modified for Thermal <i>and Structural</i> Performance within Broad Ranges. A Family of Designs is Illustrated with a Range of Tradeoffs Between Structural and Thermal Performance.	442
Table 7.16	Data for a Heuristically Designed Structure	446
Table A.1	Boundary and Operating Conditions for Parametric Design Trials	501
Table A.2	A Comparison of Approximate Analytical Gradients in the FE/FD Algorithm with Numerical Approximations	502

Table A.3	Initial and Final Values for Design Variables and Responses for Parametric Design Trials of Thermal Topology Design Algorithm	502
Table A.4	A Comparison of Approximate Analytical Gradients in the FE/FD Algorithm with Numerical Approximations	506
Table A.5	Initial and Final Values for Design Variables and Responses for Topology Design Trials of Thermal Topology Design Algorithm	507

LIST OF FIGURES

Figure 1.1	An Aircraft as a Complex, Hierarchical, Multi-scale System	5
Figure 1.2	Products and Materials as Complex, Multi-scale, Hierarchical Systems	7
Figure 1.3	Olson’s Hierarchical Concept of ‘Materials by Design’	8
Figure 1.4	A Hierarchy of Material Length and Time Scales	10
Figure 1.5	Topological and Continuous Transformations of a Simple Object	13
Figure 1.6	Ordered, Prismatic Cellular Materials	15
Figure 1.7	Sample Multifunctional Applications for Prismatic Cellular Materials	18
Figure 1.8	Size, Shape and Topology Design of a Cantilever Beam	23
Figure 1.9	A Binary Approach for Topology Design	24
Figure 1.10	A Ground Structure for Topology Design	26
Figure 1.11	Changes in Cantilever Beam Structure as Load Direction Changes	27
Figure 1.12	Optimal vs. Robust Solutions	31
Figure 1.13	Computing Infrastructure for the Robust Concept Exploration Method	33
Figure 1.14	Integration of Robust and Topology Design Tools with the Compromise DSP to Establish the RTPDEM	42
Figure 1.15	A Summary of Design Requirements, Foundations, Contributions, and Applications of the RTPDEM	48
Figure 1.16	The Validation Square	55
Figure 1.17	Validation Strategy for this Dissertation	57
Figure 1.18	A Dissertation Overview and Roadmap	58

Figure 2.1	A Family of Structural Heat Exchangers, Exhibiting a Range of Multiobjective Tradeoffs	64
Figure 2.2	Potential Sources of Performance Variation in a Prismatic Cellular Material	67
Figure 2.3	Flexibility in Preliminary Design Specifications	68
Figure 2.4	Mathematical Formulation of the Compromise DSP	77
Figure 2.5	Pareto Solutions and Goal Targets in the Compromise DSP	78
Figure 2.6	A Design Domain for Topology Optimization	83
Figure 2.7	A Highly Connected Ground Structure	85
Figure 2.8	Local Buckling Analysis in Discrete Topology Optimization	90
Figure 2.9	Perforated and Layered Microstructure Material Models	91
Figure 2.10	A Cantilever Beam Designed with the Artificial Material or SIMP Topology Optimization Approach	93
Figure 2.11	Changes in Cantilever Beam Structure as Load Direction Changes	100
Figure 2.12	Sample Heat Sink	110
Figure 2.13	Effect of Wall Removal on the Geometry of a Fluid Passageway	111
Figure 2.14	Taguchi's Quality Loss Function	116
Figure 2.15	Robust Design for Variations in Noise Factors and Control Factors	117
Figure 2.16	Computing Infrastructure for the Robust Concept Exploration Method	128
Figure 2.17	Comparing Two Designs with Respect with Respect to a Range of Requirements	130
Figure 2.18	Decomposable vs. Integral Systems	138
Figure 2.19	Dissertation Roadmap	144

Figure 3.1	Steps of the Robust Topological Preliminary Design Exploration Method	148
Figure 3.2	Relationship Between the Research Hypotheses and the RTPDEM	151
Figure 3.3	Phase I of the RTPDEM	155
Figure 3.4	A Ground Structure for Topology Design	156
Figure 3.5	Potential Sources of Variation in Topology Design	158
Figure 3.6	Relating Nominal Control Factor Values and Control Factor Tolerance Ranges	161
Figure 3.7	Examples of Topological Variation	168
Figure 3.8	Phase 2 of the RTPDEM: Formulating a Robust Topology Design Problem	169
Figure 3.9	Decision Support Problem Formulation for Robust Topology Design	171
Figure 3.10	Phase 3 of the RTPDEM: Solving a Robust Topology Design Problem	174
Figure 3.11	Phase 4 of the RTPDEM: Solving the Robust Topology Design Problem	188
Figure 3.12	Computing Infrastructure for the RTPDEM	189
Figure 3.13	A Closer Look at the Solution Process for the RTPDEM	190
Figure 3.14	A Multifunctional, Multi-stage Implementation of the RTPDEM	193
Figure 3.15	A General Multifunctional Topology Design Problem Formulation	194
Figure 3.16	Multistage, Multifunctional Topology Design via Communication of Ranges of Design Specifications	201
Figure 3.17	Communicating Robust Ranges of Design Specification	203

Figure 3.18	Communicating Robust Ranges of Design Specifications and Robust Sets of Possible Topologies	203
Figure 3.19	Multi-stage, Multifunctional Robust Topology Design via Communication of Ranged Sets of Design Specification and Physics-Based Approximate Models	206
Figure 3.20	Heat Sink Example	213
Figure 3.21	Examples of Linear Cellular Alloys	215
Figure 3.22	Discretizations for Continuous (Left) and Discrete (Right) Topology Optimization Approaches	219
Figure 3.23	Effect of Wall Removal on the Geometry of a Fluid Passageway	221
Figure 3.24	A Sample Thermal Ground Structure	222
Figure 3.25	Finite Element Analysis of a Thermal Ground Structure	224
Figure 3.26	A Plane, Linear, Rectangular Finite Element	225
Figure 3.27	Dissertation Roadmap	249
Figure 4.1	Standard Cell Topologies for Prismatic Cellular Materials	254
Figure 4.2	The Prismatic Cellular Materials Fabrication Process at Georgia Tech	255
Figure 4.3	Examples of Processing-Related Variations in Prismatic Cellular Materials	256
Figure 4.4	Design Method Requirements as Motivated by Prismatic Cellular Materials Design	259
Figure 4.5	Dissertation Roadmap	271
Figure 5.1	Compact, Forced Convection Heat Exchanger with Graded, Rectangular, Prismatic, Cellular Materials	275
Figure 5.2	Characteristic Fan Curve	283
Figure 5.3	Compromise DSP Formulated for Structural Heat Exchanger Design	284

Figure 5.4	Multifunctional Design Approach	287
Figure 5.5	FD Nodal Placement on a Typical Cross-Section of Cellular Material	288
Figure 5.6	Solution Process	290
Figure 5.7	Total Heat Transfer Rate for Periodic Rectangular Cell LCAs with Various Numbers of Rows and Columns	294
Figure 5.8	Tradeoffs Between Total Heat Transfer and Effective Stiffness for 12x2, 12x3, and 12x4 LCA Structures	298
Figure 5.9	Illustration of Multifunctional Tradeoffs for Prismatic Cellular Materials Designs with 12x4 Cells	299
Figure 5.10	Dissertation Roadmap	308
Figure 6.1	Stress Tensor at a Point in an LCA Structure	312
Figure 6.2	Effective Elastic Properties of Standard Cellular Topologies	313
Figure 6.3	Outline of Examples in this Chapter	321
Figure 6.4	Initial Ground Structures for Cellular Material Topology Design	323
Figure 6.5	Decision Support Problem for Robust Topology Design of Unit Cells with Dimensional Variation Only	330
Figure 6.6	Decision Support Problem for Robust Topology Design of Units Cells with Topological and Dimensional Variation	331
Figure 6.7	Decision Support Problem for Deterministic Topology Design of Unit Cells	332
Figure 6.8	Examples of Standard Periodically Repeating Unit Cells	354
Figure 6.9	Dissertation Roadmap	369
Figure 7.1	A Schematic of a Gas Turbine Engine	374
Figure 7.2	Initial Ground Structure for Structural Topology Design. The Illustrated Domain is a 1/32 Fraction Slice of the Entire Cylindrical Combustor Liner.	390

Figure 7.3	Sample Standard Ground Structure for Thermal Topology Design	391
Figure 7.4	Compromise DSP for Robust Topology Design by the Structural Designer in the Combustor Liner Example	395
Figure 7.5	Compromise DSP for Thermal Topology Design for Range-Based, Multi-Stage, Multifunctional Topology Design for Stage 1A of the Combustor Liner Example	396
Figure 7.6	Compromise DSP for Thermal Topology Design for Model-Based, Multi-stage, Multifunctional Topology Design for Stage 1B of the Combustor Liner Example	397
Figure 7.7	Boundary Conditions for Structural Topology Design	400
Figure 7.8	Boundary Conditions for Thermal Topology Analysis and Design	403
Figure 7.9	Details of Cellular Heat Exchanger Structure for FE/FD Algorithm Validation with FLUENT	410
Figure 7.10	Schematic of the Approximate Structural Finite Element Model	411
Figure 7.11	Mesh Convergence Study for FLUENT Analysis	414
Figure 7.12	Finite Element Discretization for Thermal Analysis of the Cellular Mesostructure Illustrated in Figure 7.9	414
Figure 7.13	Mesh Convergence Plot for the FE/FD Algorithm	416
Figure 7.14	Comparison of FLUENT and FE/FD Predictions of Heat Transfer for a Range of Source Temperatures	419
Figure 7.15	Sequence of Events for Range-Based, Multi-Stage, Multifunctional Topology Design for Stage 1A of Table 7.3	421
Figure 7.16	Sequence of Events for Model-Based, Multi-stage, Multifunctional Topology Design for Stage 1B in Table 7.3	423
Figure 7.17	Convergence Plots for Non-Robust (Left) and Robust (Right) Structural Topology Design	431
Figure 7.18	Structural Topology Design Based on a 5x4 Node Mesh	432

Figure 7.19	Convergence Plot for Thermal Redesign of the Robust Structural Design	444
Figure 7.20	Convergence Plot for Thermal/Structural Design with Broad Ranges. The Resulting Design is on the Right-Hand Side of Tables 7.14 and 7.15.	445
Figure 7.21	Dissertation Roadmap	455
Figure 8.1	The Hierarchical Nature of Materials Design	492
Figure A.1	Basic Structure for Parametric Design Validation	500
Figure A.2	Convergence Plots for Parametric Design Trials of Thermal Topology Design Algorithm	503
Figure A.3	A Convergence Plot for the Topology Design Trial of the Thermal Topology Design Algorithm	508

LIST OF SYMBOLS

CHAPTER 2

A_i	Cross-sectional area of the i^{th} member
$A_i(x)$	Achievement function
$C_i(X)$	Capability of the system
d_i^+, d_i^-	Deviation variables
d_i	Axial deformation of i^{th} element
$D_i(X)$	Demand to the system
e_i	Strain of i^{th} element
E_i	Elastic modulus of the i^{th} element
E^o	Elasticity tensor
E_x / E_s	Effective elastic stiffness in x-direction
E_y / E_s	Effective elastic stiffness in y-direction
f	Number of loading conditions
f^*	Set of ideal or utopian objective values
f_i	i^{th} objective
G_i	Goal value
$g_i(X)$	System constraint function
I_i	Moment of inertia of the i^{th} element
L	Quality loss

L_i	Length of the i^{th} member
l_i	Node-to-node length of the i^{th} element
m	Number of objectives
n	Number of design variables
N_i	Normal force of element i
p	Number of equality constraints
Q	Heat Transfer
q	Inequality constraints
T	Target value
V	Total volume of structure
w_i	Weight of i^{th} objective
X_i	System Variables
x_i	i^{th} design variable
$x_{i,L}$	Lower bounds for the i^{th} design variables
$x_{i,U}$	Upper bounds for the i^{th} design variables
x_L	Vector of lower bounds
x_U	Vector of upper bounds
Z	Objective function
y	System performance in a quality loss function
ρ	Density
μ_y	Expected value of the response

σ_y^2	Variance of the response
σ_i^k	Stress in the i^{th} element for loading condition k
Ω	Spatial domain

CHAPTER 3

$A_i(X, P)$	Goal Achievement function
C^G	Number of nodes in initial ground structure
C^D	Number of nodes in derived structure
C^R	Number of nodes in realized structure
c_{p_i}	Specific heat of the fluid
D	Depth
D_{H_i}	Hydraulic diameter for the i^{th} fluid cell
d_i^+, d_i^-	Deviation variables in a compromise DSP
d_m	In-plane depth of a cell wall
E	Modulus of elasticity
$f_i(x)$	Objective function
f_i	The Darcy friction factor for the i^{th} fluid cell
$g_i(x)$	Constraint function
H	Height
K	Stiffness matrix
k_x	Thermal conductivity of the material in x direction

k_y	Thermal conductivity of the material in y direction
L	Load
L_i	Total passage length of the i^{th} fluid cell
l_m	In-plane length of a cell wall
\dot{M}	Mass flow rate
m	Number of objectives
N	The total number of elements in the full ground structure
Nu	Nusselt number
N_ϕ	Number of nodes in the set Φ
n	Number of design variables
P	Noise factor designation
p	Number of constraints
Pr	Prandtl number
\dot{Q}_i	Rate of steady state heat transfer for the i^{th} fluid cell
\hat{q}_n	Heat flux specified along the boundary
R^D	Set of nodes in the derived structure
R^G	Set of nodes in the initial ground structure
R^R	Set of nodes in the realized structure
S_1	Lateral Surface
S_2	Lateral Surface
T_{in}	Inlet temperature

T_{out}	Outlet temperature
T_s	Heat Source Temperature
$T_{\infty 1}, T_{\infty 2}$	Ambient temperatures of the surrounding fluid medium on lateral surface
$T_{\infty \Gamma}$	Ambient temperature of fluid medium along the boundary
t_m	In-plane thickness of a cell wall
V_i	Mean fluid velocity for the i^{th} fluid cell
v_f	Volume fraction
W	Width
w	Weight function
X	Vector of control factors
X^D	Control factors for the derivative structure
X^G	Control factors for the initial ground structure
$x_{i,L}$	Lower bounds for the i^{th} design variable
$x_{i,U}$	Upper bounds for the i^{th} design variable
X_L	Lower bound
X^M	Missing control factors or elements
X_{MinMfg}	Minimum manufacturable area
X^R	Control factors for the realized structure
Z	Objective function
β_1, β_2	Convective heat transfer coefficients
β_{Γ}	Convective heat transfer coefficient of the fluid medium along the boundary

χ^R	Space of acceptable topologies or possible sets of realized elements
δA	Goal variation function
δg	Constraint variation function
δP	Noise factor variation function
δX	Control factor variation function
Γ	Boundary
γ_i	Probability of i^{th} experiment
μ	Mean Value
Φ	The set of nodes that define the surface surrounding incremental fluid cell I
θ	Direction of applied load
ρ_{inlet}	Mean fluid density at the heat sink inlet for the i^{th} fluid cell
ρ_m	Density of a thermal topology element m
σ	Standard Deviation
Ω	Spatial domain
ψ_j^e	Finite element approximation function

CHAPTER 5

c_p	Specific heat of substance
D	Depth
d_i^+, d_i^-	Deviation variables in a compromise DSP
\tilde{E}_x / E_s	Overall structural elastic stiffness in x-direction
\tilde{E}_y / E_s	Overall structural elastic stiffness in y-direction

H	Height
h_i	Height of the i^{th} row of cells
k_s	Thermal conductivity
\dot{M}	Mass flow rate
N_H	Number of columns of cells
N_V	Number of rows of cells
\dot{Q}	Overall rate of steady state heat transfer
t_H	Thickness of horizontal cell walls
T_{in}	Inlet Temperature
T_s	Heat Source Temperature
t_V	Thickness of vertical cell walls
W	Width
w_i	Width of the i^{th} column of cells

CHAPTER 6

A_e	In-plane area of element e
A_u	Area of unit cell
A_U	Area of entire unit cell domain
C	Tensor of elastic constants
C^G	Nodes in the initial ground structure
$[C^H]$	Homogenized tensor of elastic constants
$\{d_e\}$	Vector of displacements for element e

d_i^+, d_i^-	Deviation Variables in a compromise DSP
E_0	Young's modulus of a fully dense material
E_s	Young's modulus of a solid, sintered material
$\{F^{\epsilon^0}\}$	Vector of nodal loads that induce the initial strain field, $\{\epsilon^0\}$
$[K]$	Global stiffness matrix
$[k_e]$	Stiffness matrix for element e
N^D	Number of nodes in derived structure
N^G	Number of nodes in initial ground structure
N^R	Number of nodes in realized structure
P	Porosity
R^D	Set of nodes in the derived or designed structure
R^G	Set of nodes in the initial ground structure
R^M	Set of nodes in the realized structure
RVE	Representative Volume Element
S^j	Sample space of possible combinations of elements, taken j at a time
\bar{U}	Average strain energy
v_f	Volume Fraction
W_i	Weight of i^{th} objective
X_i	Element area
Z	Objective function
$\Delta C_{ij}(X)$	Range of elastic constant values (for dimensional variation)

$\Delta_{\mu} C_{ij}(X)$	Mean range of elastic constant values (for topological and dimensional variation)
ΔX	Tolerance range function
ϵ_i	Strain
$\{\epsilon^0\}$	Test strain field
γ_v	Probability of experiment v
μ_{Cij}	Mean value of an elastic constant
σ_{Cii}	Standard deviation of an elastic constant
σ_{xx}	Normal stress
$\sigma_{xy}(x \neq y)$	Shear Stress

CHAPTER 7

$[B_i]$	Strain-displacement matrix
C_i	Compliance of overall structure
CTE	Coefficient of thermal expansion
D	Diameter
$\{D\}$	Vector of global displacement
$\{d_e\}$	Vector of displacements associated with element e
d_i^+, d_i^-	Deviation variables
E	Solid modulus
E_i	Modulus of elasticity for element i

$\{F\}$	Vector of applied nodal loads
k	Thermal conductivity
$[K]$	Global stiffness matrix
L	Total length of the element
$\dot{m}_{in-coolingair}$	Mass flowrate of cooling air
N	Total number of element
\dot{Q}	Overall rate of steady state heat transfer
S_b	Stress in i^{th} element
t	Thickness
$T_{hot-inner}$	Inner combustion temperature
$T_{in-coolingair}$	Entry temperature of cooling air
$T_{max-outer}$	Maximum temperature for exterior surface of combustor liner
T_i	Temperature at i^{th} node
T_{melt}	Melting temperature of base material
W_i	Weight or i^{th} objective
v_f	Volume fraction
X	Vector of areas of elements in structural or thermal ground structure and associated topology
X^D	Set of elements in the derivative structure
X^{D-2}	Set of elements in the designed topology in the second design stage
$X_{i,L}$	Lower bounds for the i^{th} design variables

$X_{i,U}$	Upper bounds for the i^{th} design variables
X_v	Set of elements in a ground structure for experiment v
Z	Objective function
α_i	Coefficient of thermal expansion for element i
χ^R	Space of acceptable topologies or possible sets of realized elements
ΔC	Variation in Compliance of structure, associated with dimensional variation
$\Delta_{\mu} C$	Mean Variation in compliance of structure, associated with dimensional and topological variation
ϵ_i	Vector of mechanical strains
ϵ_i^0	Thermal strain
γ_v	Likelihood of Experiment v
ρ_i	Density of i^{th} element for thermal topology design
$\rho_{i,L}$	Lower bounds for density of the i^{th} element
$\rho_{i,U}$	Upper bounds for density of the i^{th} element
σ_C	Standard deviation of compliance, associated with topological variation
σ_Y	Yield strength
μ_C	Mean Compliance, associated with topological variation

SUMMARY

A paradigm shift is underway in which the classical materials *selection* approach in engineering design is being replaced by the *design* of material structure and processing paths on a hierarchy of length scales for specific multifunctional performance requirements. In this dissertation, the focus is on designing materials on *mesoscopic* length scales that are larger than microscopic features but smaller than the macroscopic characteristics of an overall part or system. The mesoscopic *topology*—or geometric arrangement of solid phases and voids within a material or product—is increasingly customizable with rapid prototyping and other manufacturing and materials processing techniques that facilitate tailoring topology with high levels of detail. Fully leveraging these capabilities requires not only computational simulation models but also a *systematic, efficient design method* for exploring, refining, and evaluating product and material topology and other design parameters in order to achieve *multifunctional* performance goals and requirements. The performance requirements for materials are typically derived from larger engineering systems in which they are embedded and often require tradeoffs among multiple criteria associated with disparate physical domains such as heat transfer and structural mechanics. The structures and processing paths of these *multifunctional* materials must be designed to simultaneously balance these multi-physics requirements as much as possible. However, the link between preliminary design specifications and realized multifunctional performance is not deterministic. Deviation from nominal or intended performance can be caused by many sources of variability including manufacturing processes, potential operating environments, simulation models,

and adjustments in design specifications themselves during a multi-stage product development process. Topology and other preliminary specifications for materials and products should be designed to deliver performance that is *robust* or relatively insensitive to this variability.

In this dissertation, the Robust Topological Preliminary Design Exploration Method (RTPDEM) is presented for designing complex multi-scale products and materials concurrently by topologically and parametrically tailoring them for multifunctional performance that is superior to that of standard designs and less sensitive to variations. This systems-based design approach is formulated by establishing and integrating principles and techniques for robust design, multiobjective decision support, topology design, collaborative design, and design space exploration along with approximate and detailed simulation models. A comprehensive robust design method is established for topology design applications. Robust topology design problems are formulated as compromise Decision Support Problems, and guidelines are established for modeling sources of variation in topology design, including variations in dimensions and variations or imperfections in topology. Computational techniques are established for evaluating and minimizing the impact of these sources of variation on the performance of a preliminary topological design. Local Taylor-series based approximations of design sensitivities are introduced for evaluating the impact of small changes in control factors such as dimensions or material properties. Strategic experimentation techniques are established for evaluating the impact of variations in topology that require reanalysis of a design.

Robust topology design methods are used in this dissertation not only to design material topologies that are relatively insensitive to manufacturing-related imperfections but also to systematically and intentionally create topological designs with built-in flexibility for subsequent modification. This flexibility is the foundation for the multi-stage, multifunctional robust topology design method introduced in this dissertation. Because it is very difficult to extend complex topology design techniques to non-structural domains—especially if the phenomena are shape- or scale-dependent, in which case it is also difficult to analyze such phenomena during a structural topology design process—multiple functional domains are treated as multiple stages in a multifunctional topology design process. In the first stage, robust topology design methods are used to explore and generate structural topology that is robust to small changes in the topology itself and the dimensions of its elements. This flexibility is used by a subsequent designer to make small adjustments to the topology and other specifications of a preliminary topological design to enhance performance in an additional functional domain, such as heat transfer, without significant adverse impacts on first-stage structural performance. A modification of the multifunctional design approach involves constructing and sharing approximate, physics-based models of first-stage (structural) performance. To facilitate more extensive changes in topology and other design specifications and potentially more significant enhancement of second-stage performance objectives, the models are utilized by the second-stage designer to evaluate and minimize any associated degradation in first-stage (structural) performance. The multifunctional topology design approach facilitates decomposition and distribution of topology design activities in a manner that is (1) appropriate for highly coupled designs, (2) effective and

computationally efficient compared with over-the-wall (iterative) and fully integrated design approaches, (3) appropriate for leveraging the domain-specific expertise of multiple designers, and (4) conducive to multiple functional analyses and topology design techniques that require different design spaces such as the complex initial ground structures of structural topology design versus simpler initial topologies for thermal design. As part of the approach, topology design techniques are established for thermal applications. The techniques are based on a finite element/finite difference heat transfer analysis approach introduced in this dissertation.

Key aspects of the approach are demonstrated by designing linear cellular alloys—ordered metallic cellular materials with extended prismatic cells—for multifunctional applications. For a microprocessor application, structural heat exchangers are designed that increase rates of heat dissipation by approximately 50% and structural load bearing capabilities substantially relative to conventional heat sinks that occupy equivalent volumetric regions. Also, cellular materials are designed with structural properties that are robust to dimensional changes and topological imperfections such as missing cell walls. Although structural imperfections—or deviations from intended structural characteristics—are observed regularly in cellular materials and in other classes of materials, they have not been considered previously during the design process. Finally, cellular combustor liners are designed to increase operating temperatures and efficiencies and reduce harmful emissions in next-generation gas turbine engines via active cooling and load bearing within topologically and parametrically customized cellular materials. Results from these examples are utilized extensively for validating the RTPDEM and the research hypotheses associated with it.

CHAPTER 1

FOUNDATIONS FOR ESTABLISHING A ROBUST TOPOLOGICAL PRELIMINARY DESIGN EXPLORATION METHOD

The principal goal for this dissertation is to establish a Robust Topological Preliminary Design Exploration Method (RTPDEM) to facilitate the exploration and generation of robust, multifunctional topology and other preliminary design specifications for the mesostructure of prismatic cellular materials, with the potential for broader materials design applications.

The motivation for this research is to establish systematic methods that are suitable for designing materials. As outlined in Section 1.1, *materials design* is an emerging multidisciplinary field in which both science-based tools and engineering systems design methods are utilized to tailor material structures and processing paths to achieve targeted properties, performance, and functionality for specific applications (McDowell, 1998). Because there are numerous classes of materials and several length scales—from atomic scales to macroscopic scales of final parts—for which materials design could be performed, the focus in this dissertation is narrowed to designing a specific class of prismatic cellular materials on mesostructural length scales. *Prismatic cellular materials*, also known as linear cellular alloys (LCAs) are ordered, metallic cellular materials with extended prismatic cells. The multifunctional properties of prismatic cellular materials depend strongly on their mesostructures, including cellular topologies, geometry, dimensions, and other features. *Mesostructural* length scales in this dissertation range from micrometers to millimeters and are larger than microstructural length scales but smaller than the macrostructural characteristics of an overall part or system. The

mesostructures of prismatic cellular materials can be customized during the manufacturing process in order to adjust their properties for particular applications ranging from ultralight structures to heat exchangers to fuel cells.

Several challenges are outlined in Section 1.1 for the design of prismatic cellular material mesostructures. A primary concern is the layout, distribution, or *topology* of solid material within the cellular material. The topological characteristics of prismatic cellular materials (as well as other classes of materials such as composite materials) strongly influence the multifunctional properties and performance of these materials and the engineering components or systems in which they are embedded. Therefore, the focus in this dissertation is on developing design methods that facilitate the exploration of *topology* for materials design applications. However, a complicating factor in the design of any material, including prismatic cellular materials, is the influence on material system performance of uncertainties or variations in model-based predictions, experimental data, operating conditions, processing conditions, and material structure from specimen to specimen. Therefore, another primary focus in this dissertation is on developing *robust design* methods and computational techniques that are appropriate for topology design and facilitate minimization of the impact of variation on material and overall system properties of interest. The property or performance requirements for materials are derived from larger engineering components or systems in which they are embedded. These requirements typically necessitate tradeoffs among multiple criteria, often associated with disparate physical domains such as heat transfer and structural load bearing. *Multifunctional* material structures must be designed that simultaneously balance these multi-physics requirements to the extent possible. Finally, the design

methods developed in this dissertation are intended for the preliminary stages of design. Preliminary design stages take place after physical principles and rough architectures for a system are determined in a conceptual design stage but before the details of a design are finalized in a detailed design stage (Pahl and Beitz, 1996). This is an important contextual detail because it clarifies that the design methods in this dissertation are aimed at exploring a broad range of overall design layout and form (including arrangement, shapes, dimensions, etc.) in order to identify families of preliminary designs that are suitable for detailed design and possible realization.

The materials design motivations for establishing a Robust Topological Preliminary Design Exploration Method (RTPDEM) are discussed in Section 1.1, culminating in a set of requirements for the design method and a primary research question. The frame of reference for developing the RTPDEM is established in Section 1.2. Brief reviews are presented of topology design, multiobjective decision support, and robust design, based on which a set of research questions are posed. The primary research questions, hypotheses, and contributions are discussed in Section 1.3, and a strategy for validating the hypotheses and establishing research contributions is presented in Section 1.4 along with an overview of the dissertation.

1.1 MATERIALS DESIGN—A NEW FRONTIER FOR ENGINEERING SYSTEMS DESIGN

For millennia, the technological capabilities of societies have been linked to available materials so closely that entire eras—the Bronze Age, the Iron Age—have been named for the most advanced engineered materials of the day. Even the modern Information Age owes its name to a revolution in information technology made possible by critical

advances in semiconductors and other materials. Continuing technological advancement of our society is tied closely to our ability to engineer materials that meet the increasingly ambitious requirements of new products.

Despite this fact, we do not *design* materials. Complex new products and systems are currently realized with increasingly sophisticated and effective systems design techniques that have been shown to decrease product development cycle times and increase quality. Like the aircraft illustrated in Figure 1.1, many of these complex systems are realized by concurrently designing the subsystems, components, and parts into which a system is decomposed, as shown in Figure 1.1. However, the design process typically stops at the ‘part’ level—rather than the ‘material’ level—of the system hierarchy illustrated in Figure 1.1. Materials are not typically designed; instead, they are selected from a database of available options (Ashby, 1999), even though the performance of many engineered parts and systems is limited fundamentally by the properties of available, constituent materials. For example, further increases in efficiency and reductions in emissions of the aircraft’s gas turbine engines in Figure 1.1 require high temperature, high strength, structural materials for the engine combustion chambers and turbines. Unfortunately, these combinations of properties are not available from materials in current databases. The inherent difficulty with materials selection is the inability to tailor a material for application-specific requirements—such as those of the engine combustion chamber and turbine—that do not overlap with the properties of catalogued materials. On the other hand, lead times for the development of *new* materials have remained relatively constant and unacceptably long relative to product development cycles for new

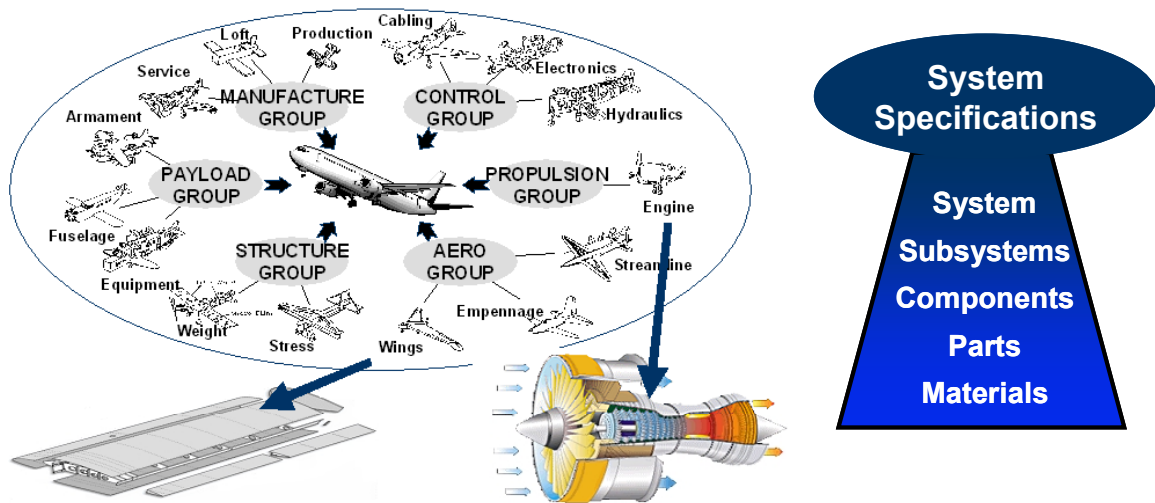


Figure 1.1 – An Aircraft as a Complex, Hierarchical, Multi-scale System

products. The lengthy time frame and expense of new materials development is partially due to the predominantly empirical, trial-and-error approach adopted historically by materials scientists and engineers (McDowell, 1998; Olson, 2000). With this approach, a material is treated as a black box subjected to repeated experiments. Experimental results populate materials databases that are utilized prevalently in engineering design, but design methods are not applied to the ‘material’ level of the hierarchy in Figure 1.1.

A foundational premise for this dissertation (and the field of materials design in general) is that systems design techniques offer the potential for tailoring materials—as well as product systems—for challenging applications. In materials design, we are not limited to *selecting* an available material from a database; instead, we actually *tailor* material structure and processing paths to achieve properties and performance levels that are customized for a particular application. In the materials science and engineering design communities, momentum is building towards materials *design* and away from

exclusively empirical materials development approaches (McDowell, 1998). Materials scientists and engineers facilitate materials design by creating increasingly sophisticated and accurate physics-based models that can be used to support a design process by linking internal structure and processing paths to the properties and performance of materials. In addition, product and systems designers recognize the potential technological breakthroughs that could be achieved by concurrently designing *products and materials*; thereby overcoming the property and performance limitations of currently available materials for a host of applications. For example, one of the major *components* in the aircraft system of Figure 1.1 is the gas turbine engine. Improvements in the efficiency and emissions of the gas turbine engine are limited partially by the *materials* available for engine *parts* such as the combustor liner. Designing the constituent materials offers the potential for alleviating these limitations. However, materials design is challenging. Like large-scale systems, materials are complex, multi-scale, hierarchical systems with phenomena and materials design opportunities manifested on a hierarchy of length and time scales from atomic scales to component length scales, as illustrated in Figure 1.2. In this dissertation, the focus is on mesoscale materials design. In the combustor liner example described in Chapter 7 of this dissertation, the cellular mesostructure of a combustor liner is designed for enhanced multifunctional performance. Further opportunities exist for designing materials on shorter length and time scales—such as continuum, microstructural, and molecular levels—for applications such as the combustor liner. These length and time scales are not investigated explicitly in this dissertation, but it is argued that the design methods established here are

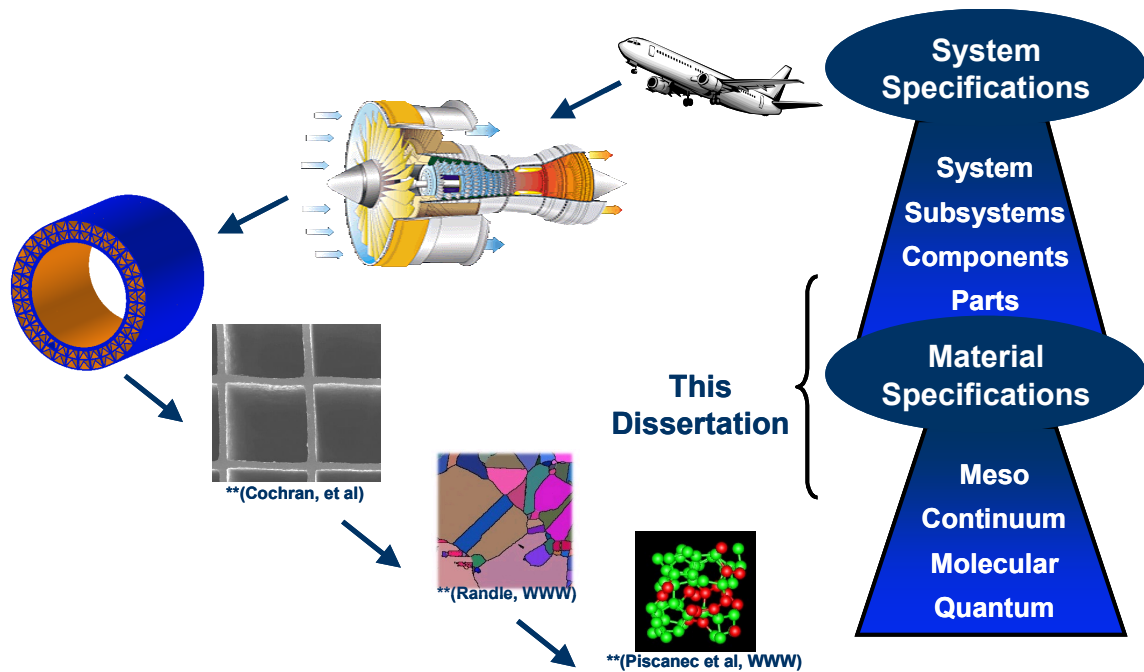


Figure 1.2 – Products and Materials as Complex, Multi-scale, Hierarchical Systems

foundational and extensible for multi-scale materials design applications. In Section 1.1.1, the challenges of multiscale materials design are discussed from a general perspective, and the challenges of designing material mesostructure, specifically, are discussed in Section 1.1.2.

1.1.1 Materials Design Challenges

Materials design efforts rely on continuous development and improvement of predictive models and simulations on a hierarchy of length scales, quantitative representations of structure, and effective archiving, management, and visualization of materials-related information and data. Together, these components provide important *deductive* links within a hierarchy of processing, structure, properties, and performance, as illustrated in Figure 1.3. Such deductive, analytical tools are necessary but not

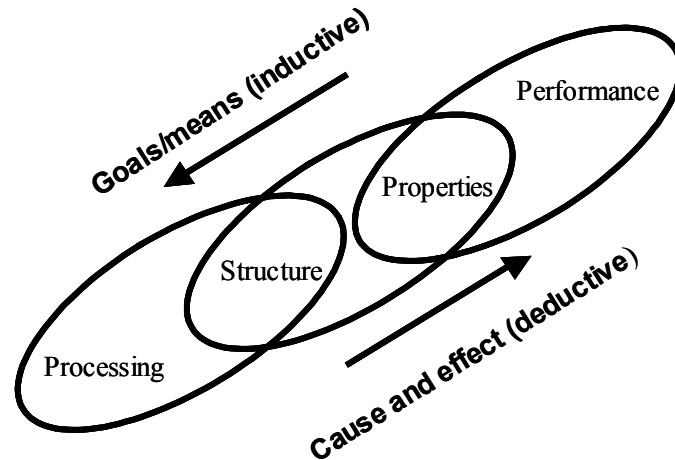


Figure 1.3—Olson’s Hierarchical Concept of ‘Materials by Design’(Olson, 1997)

sufficient for materials design. As proposed by Olson (Olson, 1997) and illustrated in Figure 1.3, materials design is fundamentally an inductive, goal-oriented, *synthesis* activity, aimed at identifying material structures and processing paths that deliver required properties and performance. While Olson’s construct sets an important philosophical foundation on which to support materials design, it delegates practical aspects of the goal-oriented materials design process to the creative will, depth of insight, experience, and knowledge base of the designer. To render the philosophy robust and collaborative, it must be built upon a systems engineering framework. Accordingly, systematic, effective, efficient, *systems-based design methods* are needed for modeling and executing complex, hierarchical materials design processes.

A systems-based design approach is motivated by many of the challenges associated with materials design. For example, materials design is an inherently multi-scale, multifunctional activity. Most applications require materials that satisfy multiple functions—such as structural load bearing, thermal transport, cost, and long-term

stability—and these requirements cannot be defined in isolation from overall system conditions and requirements. These conditions are associated with the operating environment and the component(s) and overall system in which a material is integrated. The material is part of a multi-scale system that includes larger parts, assemblies, and physical systems, as illustrated in Figure 1.2, but materials are hierarchical systems themselves. Desired material properties and performance characteristics often depend on phenomena that operate at different length and time scales, spanning from Angstroms to meters and from picoseconds to years as illustrated in Figure 1.4. A hierarchy of models has been developed and applied to specific length and time scales. Each model is used to inform the formulation of other models on higher length scales that capture the collective behavior of lower length scale subsystems, but it is very difficult to formulate a single model for macroscopic material properties that unifies all of the length scales (McDowell, 1998). For example, first principles models, based on theoretical and solid-state physics, can be used on atomistic and molecular levels to predict structure and properties of ideal designs, but they are too computationally expensive to model real materials with highly heterogeneous structures that strongly influence their macroscopic properties. On the other hand, continuum-based models, based on classical continuum theory, are useful for describing properties at a macroscopic scale relevant to many engineering applications, but they are inappropriate for smaller scale phenomena that require atomistic resolution.

While it is extremely challenging to develop physics-based models that embody relevant process-structure-property relations on different scales for diverse functions, the complexity and restricted domain of application of these models limit their explicit

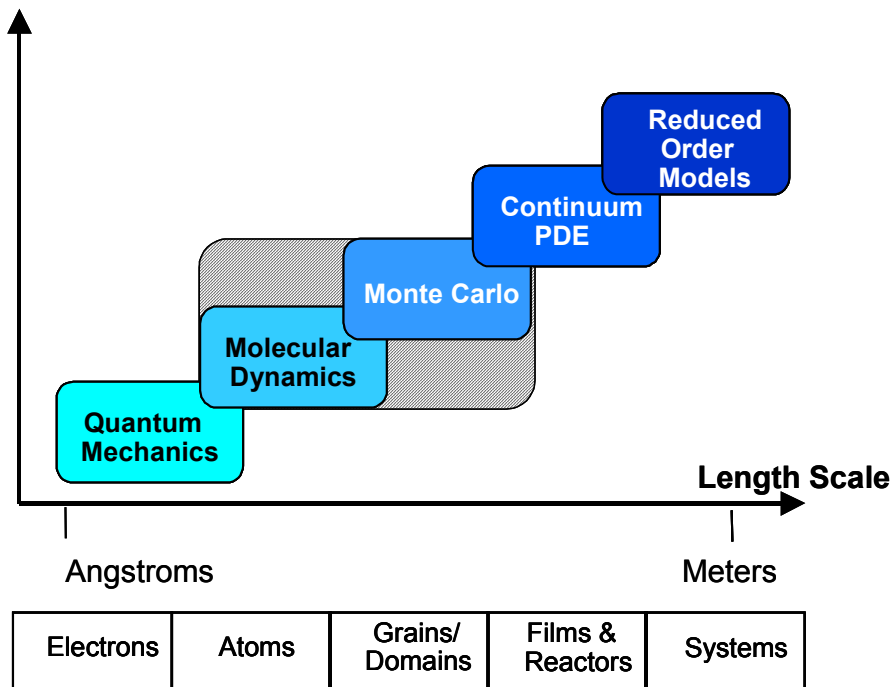


Figure 1.4 – A Hierarchy of Material Length and Time Scales

integration across the length and time scales illustrated in Figure 1.4. Instead, they must be linked in a manner that facilitates exploration of the systems-level design space by a collaborative team of experts. Distributing analysis and synthesis activities also leverages the extensive domain-specific knowledge and expertise of various material and product designers who may be specialized according to length and time scales, classes of materials, and domains of functionality. A fundamental role of each domain-specific expert is to make decisions that involve synthesizing and identifying solution alternatives to achieve desirable tradeoffs between sets of conflicting material property goals. However, material subsystems are interdependent, and the individual decisions associated with them rely on information and solutions generated by other decision-makers at other levels of the hierarchy. In the end, preferable *systems-level* solutions are sought, and they

are not necessarily obtained by ‘optimizing’ each subsystem individually. Therefore, it is critical to establish multi-objective *decision protocols* for individual designers as well as standards, tools, and mathematical techniques for *interfacing* individual decisions and facilitating information flow among multiple experts.

Since materials are complex, hierarchical, heterogeneous systems, it is not reasonable or sufficient to adopt a deterministic approach to materials design. Parameters of a given model are subject to variation associated with variation of material microstructure from specimen to specimen. Furthermore, uncertainty is associated with model-based predictions for several reasons. Models inevitably incorporate assumptions and approximations that impact the precision and accuracy of predictions. Uncertainty may be magnified when a model is utilized near the limits of its intended domain of applicability and when information propagates through a series of models. Also, to facilitate exploration of a broad design space, approximate or surrogate models may be utilized, but fidelity may be sacrificed for computational efficiency. Experimental data for conditioning or validating approximate or detailed models may be sparse, and it may be affected by measurement errors. Also, variation is associated with the structures and morphologies of realized materials due to variations in processing history and other factors. Often, it is expensive or impossible to remove these sources of variability, but their impact on model predictions and final system performance can be profound. Therefore, systems-level design methods need to account for the many sources of variation and facilitate the synthesis of *robust solutions* that are relatively insensitive to them.

There are many more challenges in materials design, as well, including the need for effective information management and computing infrastructure to support collaborative design with heterogeneous software resources. However, it is clear from the present discussion that materials design is a very broad field that is likely to fuel extensive research in materials science and engineering as well as engineering systems design in the coming decades.

1.1.2 The Materials Design Focus of this Dissertation: Mesoscopic Material Structure, Topology, and Prismatic Cellular Materials

Due to the potential breadth of the materials design domain, it is important to narrow the scope of the challenges to be addressed in this dissertation by identifying specific sets of challenges and a specific class of materials to be investigated. *What aspects of materials design are investigated in this dissertation?* In this dissertation, the focus is on designing the mesoscopic structure of materials and, specifically, material topology in the context of the requirements of a larger part or system. As illustrated in Figure 1.2, mesoscopic length scales are intermediate between microscopic length scales at which the microstructure of a material is characterized—including features such as grain and phase structure (Callister, 1994)—and macroscopic length scales on the order of a product or part constructed from the material.

On a mesoscopic length scale, one of the most important characteristics of a material is its topology. Mathematically, *topology* describes the geometric continuity and connectivity of a material space or domain (Christie, 1976; Davis, 2001; Mortenson, 1999). One of the basic entities in the study of topology is a *simple* polyhedron. If it were made of an extremely plastic substance like rubber, a simple polyhedron could be

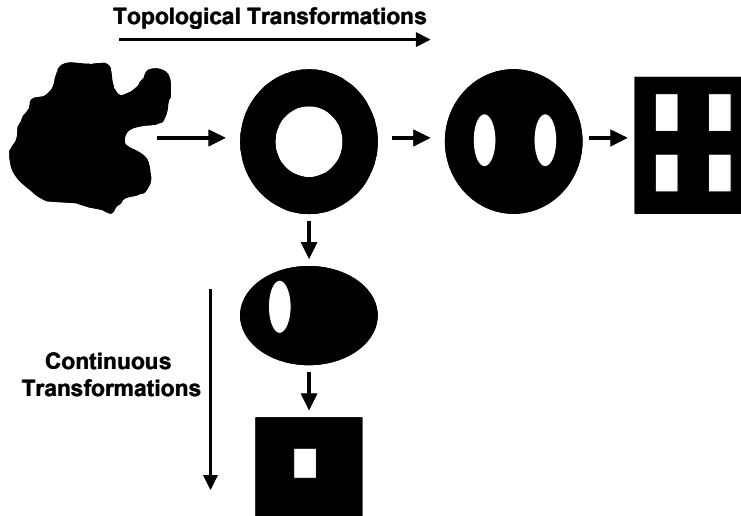


Figure 1.5 – Topological and Continuous Transformations of a Simple Object

deformed to a sphere by bending, twisting, or compressing (without tearing, puncturing, or fusing) (Mortenson, 1999). All simple polyhedra—such as plates, bowls, or bolts—are topologically equivalent, or possess identical topological properties, such as values of the Euler characteristic (Mortenson, 1999).¹ Topologically complex objects—such as a torus, a cup with a handle, or a mechanical washer—can be obtained from a simple topologically non-equivalent parent object by introducing discontinuities or holes via discontinuous deformations such as tearing or fusing of surfaces. Examples of topologically equivalent and non-equivalent objects are illustrated in Figure 1.5. As shown, the shape or dimensions of an object—both interior and exterior surfaces—may be adjusted without changing its topology. However, topological transformations are required to introduce additional discontinuities in the object. Therefore, it is clear that

¹ The Euler characteristic is a topological property associated with the number of holes or discontinuities in an object. For polyhedra, it is typically calculated as the sum of the vertices and faces, minus the sum of the edges.

both topological and continuous properties (e.g., shape and dimensions) are required to characterize a physical object or virtual design. Although the mathematical definition of topology and topological changes is quite strict, its definition is often relaxed in common engineering usage to include not only the number or concentration of discontinuities in a specific domain but also the shape, size, and distribution of those discontinuities. In this dissertation, the notion of topology is most important in the latter, richer, relaxed sense, but topological equivalence or non-equivalence in the strict, mathematical sense is distinguished, as well.

Why is mesoscopic material topology an important aspect of materials design? For what classes of materials and design applications is it important? There are several classes of materials for which mesostructure—mesoscopic topology, in particular—has a very strong influence on properties and performance. Two primary examples are cellular materials and composite materials. Composites are materials in which multiple phases are artificially and strategically combined to provide a better combination of properties than any of the individual phases alone. The multiple phases are chemically dissimilar and separated by distinct interfaces (Callister, 1994). Typically, composites are comprised of a continuous matrix that surrounds a dispersed phase. The topology of the matrix and dispersed phase(s) is important because the properties of composites are functions of the properties of the multiple phases and the topology of the dispersed phase(s) within the matrix—including the size, shape, distribution, and orientation of the dispersed particles or fibers. Two key aspects of composite materials are that they are *artificially* made—rather than naturally occurring—and that their properties depend strongly on their multiphase composition and *topology*.

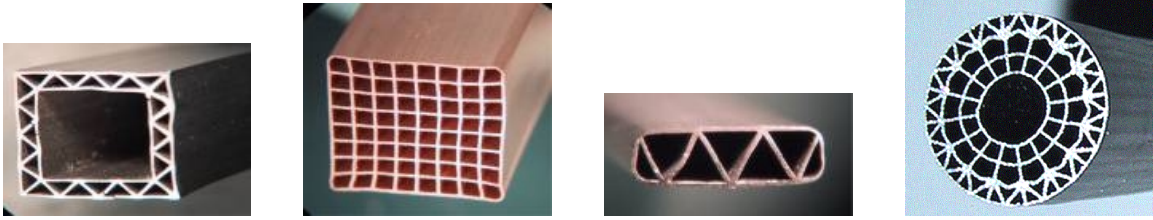


Figure 1.6 – Ordered, Prismatic Cellular Materials

Cellular materials are a special class of composite materials in which the matrix is a solid base material and the dispersed phase is void or empty space. Cellular solids are “made up of an interconnected network of solid struts or plates which form the edges and faces of cells” (Gibson and Ashby, 1997). The two primary categories of cellular materials are stochastic and ordered cellular materials with randomly and regularly organized internal structures, respectively. In this dissertation, the focus is on linear cellular alloys (LCAs)—ordered cellular materials with extended prismatic cells, as illustrated in Figure 1.6 and in the mesostructural level of the system-materials hierarchy in Figure 1.2. LCAs are fabricated by extruding metal oxide powder-based slurries through a die to form a green part. The green part is then exposed to thermal and chemical treatments in a process developed by the Lightweight Structures Group at Georgia Tech (Cochran, et al., 2000). Extruded metallic cellular structures can be produced with nearly arbitrary two-dimensional cellular topologies limited only by paste flow and die manufacturability. Wall thicknesses and cell diameters as small as fifty microns and several hundred microns, respectively, have been manufactured (Church, et al., 2001). Since the manufacturing process enables fabrication of metallic structures with complex in-plane cell topologies that may be tailored to achieve desired

functionality, LCA materials are particularly suitable for multifunctional applications that require not only structural performance but also lightweight thermal or energy absorption capabilities. Certain properties of LCAs, including in-plane stiffness and strength and out-of-plane energy absorption, are superior to those of hexagonal honeycombs or stochastic metallic foams (Evans, et al., 2001; Hayes, et al., 2004), and LCAs are advantageous as heat exchangers due to large surface area density and low pressure drop (Lu, 1999). Several innovative, high-impact applications are envisioned for multifunctional honeycomb materials. For example, stiffened plate elements and multiply layups of LCAs may be designed and manufactured to meet requirements of lightweight structural stiffness, combined with internal damping characteristics achieved by polymer injection into selected cells to attenuate high frequency vibration modes. Traditionally, either passive viscoelastic coatings or active vibration suppression methods are employed. Linear cellular materials may be designed and fabricated as structural heat exchangers that are required to resist bending and membrane forces as structural members while transferring heat away from high heat flux regions, thereby combining functions normally met by structural elements with separate heat exchangers. Structural elements in satellites or wings in hypersonic aircraft could be actively cooled to provide thermal management associated with solar radiation heat flux or supersonic aerodynamic heat generation, respectively.

With the LCA manufacturing process, it is possible to tailor and fabricate nearly arbitrary cellular or partially evacuated structures, with periodic *or* functionally graded topologies. This is an important capability that the LCA fabrication process shares with other emerging manufacturing technologies such as solid freeform fabrication (SFF), also

known as rapid prototyping (RP) (e.g., (Crawford and Beaman, 1999)). SFF technologies embody an additive manufacturing paradigm in which a part is built layer by layer in contrast to conventional manufacturing techniques such as CNC machining in which material is selectively removed from a part. With SFF techniques, such as stereolithography, selective laser sintering, and 3D Printing, it is possible to tailor the *three-dimensional* internal structure of materials and small-scale products and in some cases to fabricate functionally gradient materials in which multiple base materials are blended in a controlled manner to achieve continuous material variation throughout the geometry of a part (e.g., (Kumar, et al., 2004; Rajagopalan, et al., 2001)). There are many other examples in which the mesoscopic topology of a material is customized for a particular application. In many cases the mesoscopic topology of a material (single or multi-phase) is difficult to distinguish from the topology of its parent product because the characteristic length scales of the product are so close to that of the material. Examples include some of the products of SFF or RP processes, MEMS devices, and microprocessors. In these cases, the fabrication of the material and the fabrication of the device occur simultaneously in the same process and the mesoscopic topology of the material *is* the topology of the parent product.

Based on this discussion, it is clear that there are several potential opportunities for *fabricating* customized artificial material topologies. The next logical question is how to *design* material topology to leverage these manufacturing capabilities and to provide a suitable combination of material properties for a particular application.

*What are the challenges involved in **designing** mesoscopic material topologies that are manufacturable and multifunctional?* To answer this question, it is helpful to

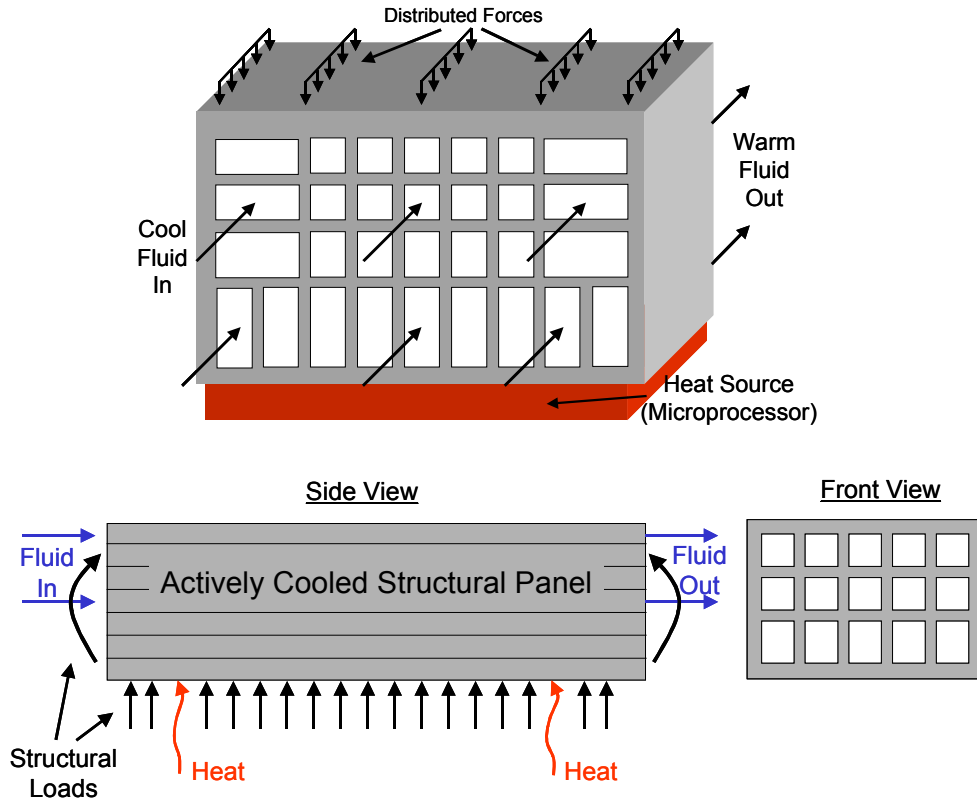


Figure 1.7 – Sample Multifunctional Applications for Prismatic Cellular Materials

consider potential applications such as a structural heat exchanger or an actively cooled structural panel, as illustrated in Figure 1.7. Both structures are *multi-functional*; they are required to have satisfactory performance in more than one domain, including structural, thermal, and impact properties. Thus, a design method for realizing the structures and their constituent materials must support not only *multicriteria* or multiobjective design with a multitude of potentially conflicting objectives, but also *multifunctional* design for which the criteria may be analyzed with multiple domain-specific techniques and software. Due to computational demands and the distributed, heterogeneous nature of software and human expertise, it may not be possible to fully integrate all of the contributing multifunctional analyses associated with the systems-level design.

Multifunctionality is included in the summary of requirements for designing mesoscopic material topology, listed in Table 1.1.

The multifunctional properties of LCAs depend on a hierarchy of length scales, as shown in Figure 1.2, but the focus is on the part and mesoscopic length scales in Figure 1.2 that fall across the continuum and reduced order model levels in Figure 1.4. As with most materials design scenarios, the multiple scales are coupled. Performance requirements flow down from the macroscopic product or system level to lower length scales. Conversely, models at higher length scales (e.g., a structure or product in this case) require property predictions that capture the collective behavior of lower length scale structures (e.g., material mesostructure and microstructure). In this case, important macroscopic properties depend not only on dimensions of the material mesostructures but also on their *topologies* because alternative topologies can significantly impact the structural, thermal, and other properties of a cellular structure. For example, desirable heat transfer topologies may not have acceptable structural characteristics and vice versa. A design approach for material mesostructure must facilitate analysis and exploration of topology—not simply dimensional analysis and synthesis.

In addition, the materials must be manufacturable—in this case, with linear cellular alloy manufacturing techniques. Manufacturability implies constraints on realizable topologies and dimensions as well as expected variation in dimensions, topology (e.g., separated cell walls), and other characteristics like density/porosity or yield strength of the constituent solid material, for example. Many aspects of the operating environment and manufacturing process may not be tightly controlled. This variation may have a large impact on smaller length scales such as material topology if the magnitude of variation is

Design Requirements	Design <i>Method</i> Requirements
<ul style="list-style-type: none"> • Dimensionally <i>and</i> topologically tailored • Multifunctional <ul style="list-style-type: none"> – Constraint satisfaction in multiple domains – Satisfactory trade-offs between multiple goals in multiple domains • Robust or relatively insensitive performance relative to variations in manufacturing and operating conditions, downstream design changes, and other factors. • Manufacturability 	<ul style="list-style-type: none"> • Systematic exploration of flexible and robust, multifunctional, topological, preliminary design specifications. <ul style="list-style-type: none"> – Representation and systematic modification of topology in the context of multifunctional design – Generation of designs with robustness to variation in operating and manufacturing conditions, design parameters, and topology – Flexible exploration of families of multifunctional or multiobjective, compromise solutions – Computationally efficient design exploration – Distributed, multifunctional exploration of topological preliminary designs – Direct applicability for materials design, specifically, mesoscopic topology – Generation of manufacturable designs

large relative to characteristic length scales or if the variation is compounded when a large material domain is considered. It is important to design objects with performance that is robust or relatively insensitive to variations in the environment, the manufacturing process, or other factors. For example, it would not be desirable to design and manufacture a structure with compliance or heat transfer rate that is highly sensitive to small changes in magnitude and direction of applied loads or temperature distribution along its boundaries, respectively. Thus, it is important to search for and identify topological designs that embody desirable tradeoffs between multiple, conflicting objectives, including robustness, or variation in performance due to uncontrolled variation in the environment or design parameters themselves. In summary, we are interested in designing mesoscopic cellular materials from a systems perspective with which we consider the topology, the manufacturing process, and the environment of an

object as a system and consider the performance of the system in multiple domains. A summary list of requirements for robust, multifunctional topological designs and for design methods that facilitate realization of these topological designs is included in Table 1.1.

In this dissertation, the focus is on addressing the *design* challenges summarized in the right side of Table 1.1. The principal challenge is to facilitate efficient, effective design of robust, lightweight, multifunctional structures with complex mesoscopic topologies. Thus, the primary research question is:

Primary Research Question: *How can flexible, robust, multifunctional, topological preliminary design specifications be explored and generated systematically and efficiently?*

To address this challenge, a robust topological preliminary design exploration method (RTPDEM) is presented in this dissertation. As part of the method, robust topology design methods are introduced as well as multifunctional design methods that facilitate distribution of synthesis activities for highly integrated systems such as material topologies. The frame of reference and foundational building blocks for establishing such a method are presented in the next section. A careful review of the available building blocks prompts a number of research questions that are introduced in the next section and summarized and linked with research contributions in Section 1.3.

1.2 FRAME OF REFERENCE

The fundamental building blocks for the RTPDEM are topology design methods, robust design methods, and multi-objective decision support. In this section, each of

these building blocks is discussed in the context of robust, multifunctional topology design for material mesostructures. Based on the discussions, it is clear that the three types of methods are foundational for the RTPDEM, but their limitations motivate a series of research questions that must be addressed in this dissertation in order to achieve the primary goal.

1.2.1 Topology Design

Topology design facilitates strategic distribution of material in an arbitrary domain. During a typical structural design process, the shape and dimensions of an otherwise complete structure of fixed topology are adjusted. In a topology design process, the connectivity and structural architecture of a system is not pre-specified but emerges from the design process itself. Therefore, it is possible to synthesize the external shape and the number and shape of internal boundaries for a material or material phase.

Consider a simple example of a cantilever beam, illustrated in Figure 1.8a. By assigning continuous variables to the height and length of the beam, it is simple to adjust its size parametrically. By modeling its boundary with splines or other parametric curves, it is straightforward to adjust its shape parametrically, as well. With parametric shape and size design, however, a designer is fundamentally limited to adjusting the external shape and dimensions of an object *of fixed topology*. In many cases, it is advantageous—or even necessary—to design the *interior* geometry and dimensions of an object, as well. The load-bearing capacity of the cantilever beam, for example, could be increased—relative to the volume/mass of material utilized in the beam’s construction—by introducing voids in the interior of the beam and thereby creating a truss-like structure as shown in Figure 1.8D and evident in many engineered structures such as bridges.

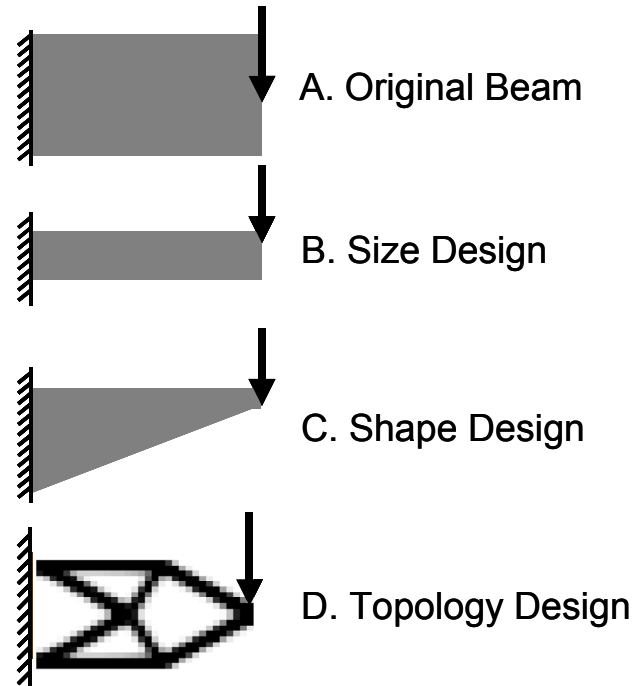


Figure 1.8 – Size, Shape and Topology Design of a Cantilever Beam

However, traditional sizing and shape design cannot change the topology of a structure during the design process; instead, the initial topology is often chosen intuitively or based on previous experience.

Due to the substantial impact of the layout or topology of an object on its behavior, it would be highly beneficial to *design* and tailor topology in pursuit of a satisfactory compromise between various constraints and objectives, rather than selecting or assuming an initial topology that remains unchanged throughout the design process. Fundamentally, one could describe topology via one or more indicator or material distribution functions, $\chi(\mathbf{x})$, that define the portion, Ω^m , of a specified two- or three-dimensional geometric domain, Ω , illustrated in Figure 1.9, that is occupied by a material or phase, m , in terms of a spatial variable, \mathbf{x} , as follows:

$$\chi(\mathbf{x}) = \begin{cases} 1 & \text{if } \mathbf{x} \in \Omega^m \\ 0 & \text{if } \mathbf{x} \in \Omega/\Omega^m \end{cases} \quad 1.1$$

In simple terms, the aim of topology design is to characterize the indicator function by determining the distribution of solid material (or multiple phases of material) within the available domain.

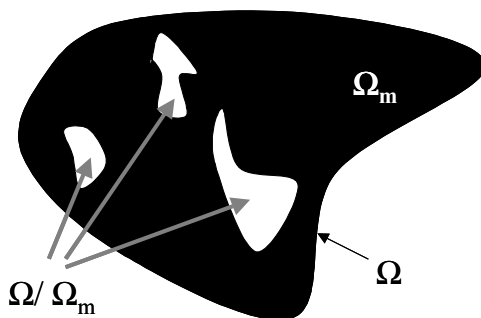


Figure 1.9 – A Binary Approach for Topology Design

There are some intuitive approaches for adjusting the topology of a design and characterizing the indicator function of Equation 1.1, but they are not very useful for efficient computer-aided topology design. For example, holes could be inserted arbitrarily in the domain and then their locations, shapes, and sizes could be adjusted parametrically, but it is difficult to determine *a priori* or to automate the search for the appropriate number of holes and their relative placement in the domain. Another intuitive approach is to discretize the domain into N individual elements and associate a binary variable with each element, similar to the indicator function in Equation 1.1. The

design space associated with such an approach is extremely large, with 2^N possibilities. Even for a relatively small number of elements, the computational resources required for evaluating the properties of each possible combination would be prohibitive. Furthermore, the problem is ill-posed; optimization-based attempts to solve the problem converge toward microstructures with rapid spatial oscillations between solid and void—essentially an infinite number of vanishingly small holes—rather than macroscopic patterns of solid and void with a finite number of macroscopic holes (c.f., (Eschenauer and Olhoff, 2001) for a review).

A number of approaches have been established for designing topology by transforming the ill-posed discrete formulation into a relaxed, continuous representation that can be modified easily and effectively with standard search techniques. Topology design methods include the discrete ground structure-based approach and continuum approaches such as the artificial material model or homogenization-based techniques. In the discrete ground structure-based approach, the domain is discretized with a grid of nodes, and each node is connected to every other node with a basic element in a pattern called a ground structure, as illustrated in Figure 1.10 (c.f., (Kirsch, 1989; Ohsaki and Swan, 2002; Topping, 1984)). Each element in the ground structure is assigned a continuous variable related to its in-plane thickness or cross-sectional area. Elements with vanishing areas during the topology design process are removed from the ground structure at the end of the design process. Elements with larger areas are retained and their relative areas and locations determine the shape and dimensions of the final structure.

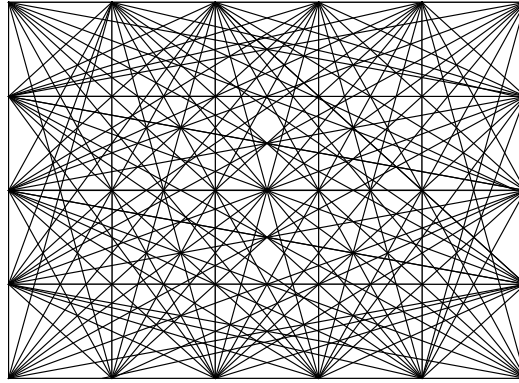


Figure 1.10 – A Ground Structure for Topology Design

In continuum approaches, the ill-posed topology design formulation is relaxed by allowing the density of material at any location to vary continuously across a range of values from 0 (void) to 1 (solid). The domain is typically partitioned into a mesh of finite elements, with the density of each element varying independently. Implicit or explicit penalties are applied during the topology design process to penalize intermediate densities and encourage convergence to macroscopic regions of solid and void. Examples of continuum approaches include the homogenization-based approach (Bendsoe and Kikuchi, 1988) and the SIMP (Solid Isotropic Microstructure with Penalty) (Bendsoe, 1989) approach. In fact, the field of structural topology design became an active area after the seminal work of Bendsoe and Kikuchi (Bendsoe and Kikuchi, 1988) who introduced the homogenization-based approach for topology design. Eschenauer and Olhoff provide a comprehensive review of continuum topology design approaches (Eschenauer and Olhoff, 2001).

While a comprehensive discussion of topology design techniques is undertaken in Chapter 2, the objective in this section is to highlight topology design as a fundamental



Figure 1.11 – Changes in Cantilever Beam Structure as Load Direction Changes

building block for the RTPDEM and to introduce the research gaps that the RTPDEM is intended to fill in order to address the design method requirements outlined in Table 1.1.

What are some of the limitations of current topological design capabilities in the context of materials design? First, robustness of a topology with respect to variations in boundary or operating conditions, material properties, or characteristics of the topology itself (e.g., dimensions or connectivity) are important to consider during a topology design process because they can have significant impacts on the behavior of a specific topology. Furthermore, it is likely that some topologies are more robust to these variations than others. For example, consider the simple cantilever beam design problem again. The topologies illustrated in Figure 1.11 have been designed using the SIMP approach. All conditions are equivalent for each of the designs, except for the direction of the applied load. It is clear that the ‘optimal’ topology changes dramatically from a single solid beam to a truss structure as vertical loading is applied. The message is that the solid beam is not robust to variation in direction of the applied load while truss-like structures are capable of robustly supporting variations in applied loading. The challenge is to identify robust topologies during the design process.

Typically, robustness is not considered during a topology design process, and topology design problems are usually formulated as deterministic optimal design problems with respect to a prescribed loading. In a few cases, authors have addressed the

need for robust topological design approaches by considering multiple loads (e.g., (Diaz and Bendsoe, 1992; Diaz, et al., 1995)), average performance under multiple loads (Christiansen, et al., 2001), reliability (Thampan and Krishnamoorthy, 2001), or worst-case loads among a set of possible loads (Ben-Tal and Nemirovski, 1997; Cherkaev and Cherkaeva, 1999; Kocvara, et al., 2000), and reliability-based approaches (Bae, et al., 2002; Maute and Frangopol, 2003; Sandgren and Cameron, 2002; Thampan and Krishnamoorthy, 2001). However, these are examples of design for mean performance or fail-safe or worst-case design, in which a structure is designed explicitly for worst-case loading, rather than robust design, in which the sensitivity of design performance objectives is minimized with respect to variations in boundary conditions, dimensions, material properties, or other factors. Furthermore, variations in the structure itself—including variations in topology or dimensions—have not been considered. A full review of current progress towards robust topology design is provided in Chapter 2.

When designing material mesostructure, it is clear that variations in dimensions, material properties, and topology must be considered along with variations in operating conditions, such as applied loading. Variations in the material structure itself may be particularly prominent due to the small scale of the application. At such small scales, cellular dimensions, topologies, and base material properties cannot be tightly controlled by novel manufacturing techniques, and associated variations may be larger relative to nominal structural characteristics than for structural design problems at higher length scales. To apply topology design techniques for designing material mesostructures, a comprehensive *robust topology design* approach is needed. Therefore, the following research question is posed,

Research Question 1: *How can flexible and robust topological preliminary design specifications be explored and generated efficiently and effectively?*

Secondly, topological design problems are usually formulated for objectives that are exclusively mechanical/structural rather than multi-functional. Multiple objectives have been considered, but only for structural applications. For example, multiple loads have been considered with a weighted sum approach (Diaz and Bendsoe, 1992; Diaz, et al., 1995); both flexibility and stiffness have been considered for compliant mechanisms (Ananthasuresh, et al., 1994; Frecker, et al., 1999; Frecker, et al., 1997); multiple eigenvalues have been combined into a single weighted scalar objective function for vibration problems (Ma, et al., 1995); and multiple stiffness and eigenfrequencies have been considered using a min-max or normalized multiobjective function (Krog and Olhoff, 1999; Min, et al., 2000). However, in all cases, these multiobjective topological design approaches have considered only structural objectives such as compliance, stiffness, and eigenvalues. To date, multi-physics applications of topology optimization have been limited to coupled field problems in structural analysis in which the interactions of temperature, electric fields, and/or magnetic fields with *structural deformation* are examined for well known applications like piezoelectric or electrothermomagnetic actuators (e.g., (Sigmund, 1998; Sigmund and Torquato, 1997)). However, topology optimization has not been extended to truly multi-functional applications with objectives in multiple domains like elasticity and combined conduction/convection. The reasons are detailed in Chapter 2; for now, it is sufficient to note that many phenomena are strongly dependent on the shape and size of the voids

rather than the structure of the material itself, making it difficult to formulate a well-posed, continuous topology design problem for non-structural phenomena. Furthermore, in many cases it is difficult to *analyze* other phenomena—such as convective heat transfer or catalysis behavior—during a structural topology design process because the topology of the *final*, post-processed design—including the number, configuration, and scale of solid phases and voids—is very different from that of the ground structure or evolving continuum model utilized during topology design.

To design the mesostructures of cellular materials, however, it is important to consider phenomena and objectives in fundamentally different domains in order to address truly multi-functional applications such as actively cooled aircraft skins or gas turbine engine combustor liners. Therefore, the following research question is posed,

Research Question 2: *How can **multifunctional**, topological preliminary design specifications be explored and generated systematically?*

In addressing Research Questions 1 and 2, the first step is to build upon existing techniques for conducting robust design in single- and multi-disciplinary environments.

1.2.2 Robust Design and Multidisciplinary Concept Exploration

Robust design is a method for improving the quality of products and processes by reducing their sensitivity to variations, thereby, reducing the effect of variability without removing its sources (Taguchi, 1986; Taguchi and Clausing, 1990). Typically, in robust design the sensitivity of performance objectives is minimized with respect to variations in boundary conditions, dimensions, material properties, or other factors. Simultaneously,

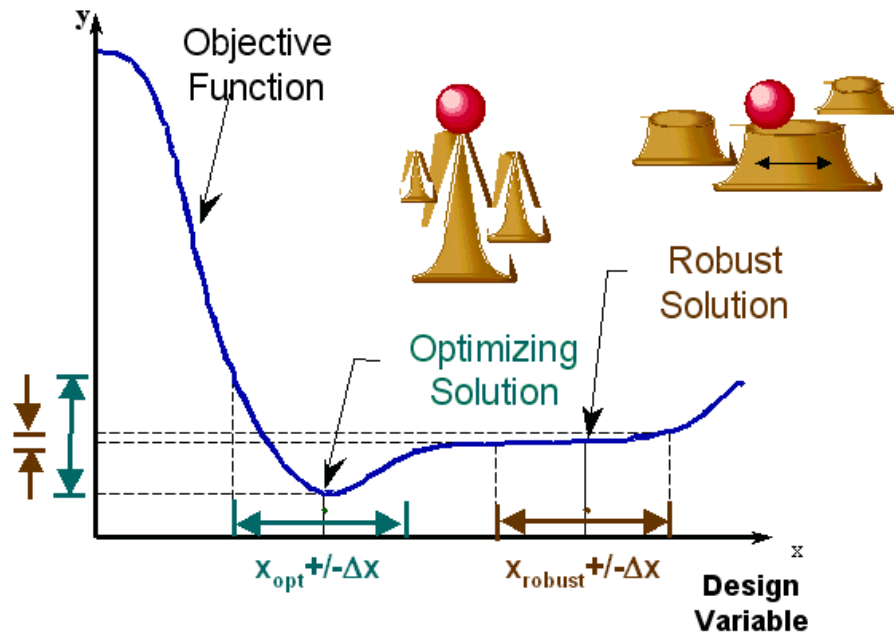


Figure 1.12 – Optimal vs. Robust Solutions (Chen, et al., 1996b)

mean or expected performance is minimized, maximized, or matched with a target. The robust design paradigm is illustrated in Figure 1.12. As shown in the figure, ‘optimal’ designs tend to be optimal for a very limited set of conditions. Robust designs, on the other hand, may offer slightly less superior nominal performance, but the performance is relatively insensitive to changes in conditions.

Although Taguchi’s robust design principles are advocated widely in both industrial and academic settings, his statistical techniques, including orthogonal arrays and signal-to-noise ratio, have been criticized extensively, and improving the statistical methodology has been an active area of research (e.g., (Myers and Montgomery, 1995; Nair, 1992; Tsui, 1992; Tsui, 1996)). During the past decade, a number of researchers have extended robust design methods for a variety of applications in engineering design (e.g., (Cagan and Williams, 1993; Chen, et al., 1996a; Chen, et al., 1996b; Chen and Lewis, 1999;

Mavris, et al., 1999; Otto and Antonsson, 1993a; Otto and Antonsson, 1993b; Parkinson, et al., 1993; Su and Renaud, 1997; Yu and Ishii, 1994)). Typically, the robustness of a design is related to variation in an objective function and constraint(s) caused by variation in environmental conditions or design parameters themselves as well as the feasibility and desirability of a design with respect to constraints and performance targets, respectively, in light of this variation.

Most of the robust design literature is focused on the latter portions of embodiment and detailed design in which dimensions are adjusted to accommodate manufacturing variations; however, there has been some emphasis on infusing robust design techniques in the *earlier stages of design* when decisions are made that profoundly impact product performance and quality. Primarily, this has been achieved by enhancing the robustness of design decisions with respect to subsequent variations in designs themselves. For example, in work that is foundational to our proposed research, Chen and coauthors (Chen, et al., 1996a; Chen, et al., 1996b) use robust design techniques to determine ranged sets of design specifications that are flexible within specified limits. The approach of Chen and coauthors—the Robust Concept Exploration Method (RCEM)—is a domain-independent approach for generating robust, multidisciplinary design solutions. The RCEM facilitates two types of robust design: (1) minimizing performance variation due to uncontrollable noise factors like stochastic operating or boundary conditions (Type I robust design) and (2) minimizing performance sensitivity to downstream changes in a design itself (Type II robust design). In addition, it facilitates the generation of robust design specifications that incorporate considerations from different disciplines (i.e., multifunctional design). Rapid, efficient exploration of multidisciplinary systems is

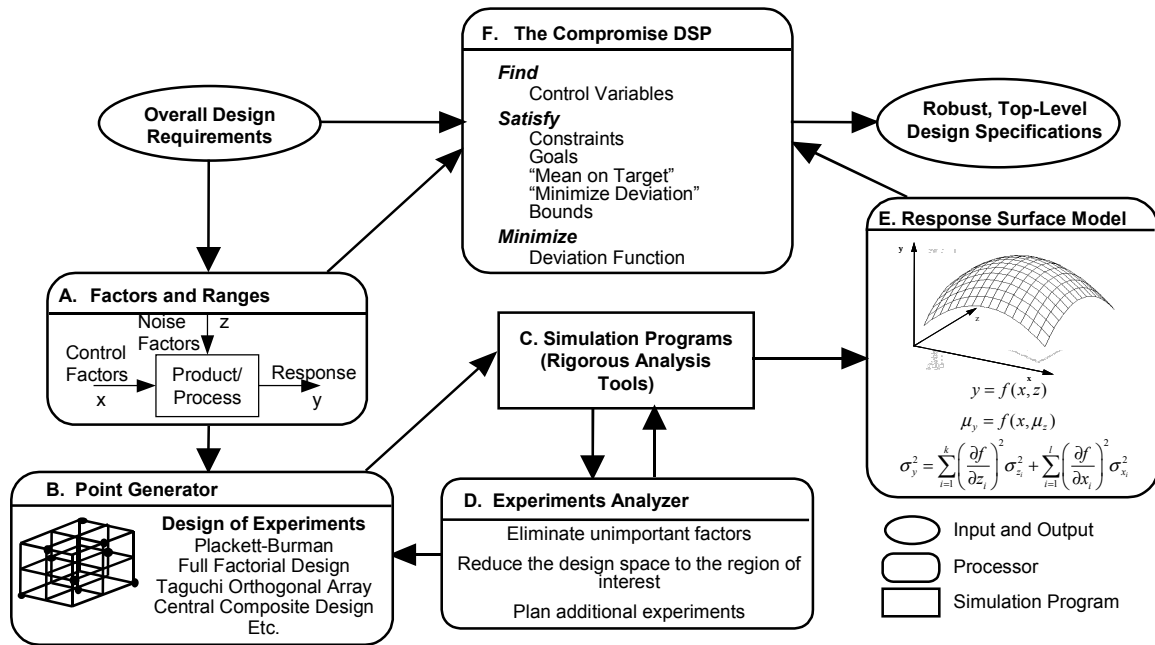


Figure 1.13 – Computing Infrastructure for the Robust Concept Exploration Method (Chen, et al., 1996a)

made possible by integrating statistical experimentation and metamodeling within the RCEM which facilitates replacement of computationally expensive analysis software with fast, efficient, surrogate models. The computational infrastructure for the RCEM is illustrated in Figure 1.13 and discussed in greater detail in Chapter 2.

While the RCEM and related work provide a foundation for performing robust design in the early stages of design, several challenges remain for supporting robust, multifunctional topology design of material mesostructures. First, robust design approaches have *not* been developed or applied specifically for robust *topology* design. In previous applications and extensions of robust design techniques, the existence of a topology or layout for the product or process has been presupposed; the robust design approaches involve specifying design parameters or dimensions rather than design configurations or topologies. It is not straightforward to extend robust design methods to

topology design for several reasons. First, the nature of a topology design process differs from that of a parametric design process. In a topology design process, the layout or configuration of a design changes during the design process. In the ground structure-based and continuum topology design approaches reviewed briefly in the previous section, this effect is manifested by removal of a subset of elements (and their associated parameters) from the final design. Second, there are more sources of variation in topology design, including variations in the topology itself such as imperfect or missing structural elements or joints in a topology; these sources of variation are particularly important in materials design where such variations may be commonplace. Third, whether continuum or ground structure-based approaches are used, there is inevitably a large number of variables. This makes it extremely computationally expensive to utilize experiment-based surrogate models or Monte Carlo analysis for robust design because the data and experiment requirements for both approaches typically grow super-linearly with the number of variables. On the other hand, there is a strong need for robust topology design techniques, motivated by two previously mentioned factors: (1) the topology or layout of a design has a decisive impact on its subsequent performance, and (2) "optimal" topologies tend to be very sensitive to variations in boundary conditions and in the topological designs themselves. Therefore, Research Question 1 arises again:

Research Question 1: How can flexible and robust topological preliminary design specifications be explored and generated efficiently and effectively?

A second challenge associated with developing robust design methods for multifunctional topology design applications is the need to support *multifunctional* or *multidisciplinary* topology design. Although multidisciplinary design is supported by the

RCEM, the approach embodied in the RCEM is not appropriate for robust topology design for two primary reasons. First, the large number of variables in topology design prohibits the use of metamodels in the RCEM. Secondly, the RCEM does not explicitly support distribution of synthesis activities and decisions among multiple decision-makers; instead, it is focused on a single decision-maker. This need for distribution of synthesis activities among multiple designers and/or stages in a robust topology design process is motivated by several factors:

- It is important to leverage the domain-specific expertise of individual designers who typically specialize in analyses on a particular length scale or within a distinct functional domain. Therefore, it is advantageous to preserve their roles in the decision-making and synthesis processes.
- It is computationally intensive to integrate all of the contributing analyses associated with a system-level materials design problem.
- Topology design methods are extremely difficult to implement for non-structural applications. One of the underlying reasons is the difficulty of accommodating shape-dependent phenomena such as convection or impact absorption that rely not only on the distribution of solid material but also on the scale, distribution, shape, and size of voids in the domain. For example, convection boundary conditions for internal flow are functions generally of the scale of the topology and specifically of the size and shape of the voids. These characteristics are typically very different for an evolving continuum topology design model or ground structure and a final design, and the details of the final topology design are unknown until a topology design process converges and appropriate elements are

removed from the design during post-processing procedures. Therefore, it is difficult not only to *design* topology simultaneously for multiple functions but also to *analyze* many aspects of non-structural performance during a structural topology design process. On the other hand, it is possible to design topology for structural objectives in an initial design stage, for example, with built-in flexibility for further modification in a second stage to meet the objectives of other disciplines.

There is, however, an important, complicating factor that makes distributed, multifunctional topology design difficult. Topological structures are typically integrated and multifunctional rather than modular or decomposable. This means that two or more functional categories of behavior are linked to the same integrated structure. A topological structure cannot be decomposed into independent, modular subsystems along functional lines in the way that an aircraft, for example, may be decomposed into structures, controls, and propulsion. Therefore, it is more difficult to distribute multifunctional design activities among domain-specific experts because the structure of the design is integral and hence their design variables are highly coupled.

Although robust design principles and techniques have been developed almost exclusively for a single decision-maker, there have been some efforts to establish and apply robust design principles and techniques for distributed, multidisciplinary synthesis and/or analysis. For example, game theoretic approaches have been combined with robust design approaches to model and coordinate the decisions of distributed designers using protocols (e.g., cooperation, non-cooperation, and Stackelberg leader-follower) and mathematical coordination mechanisms—such as rational reaction sets or best reply

correspondences—in conjunction with generation of robust, *flexible* ranges of design specifications (Chen and Lewis, 1999; Xiao, 2003). Increasingly, probabilistic and robust design techniques are being infused into a number of multidisciplinary design optimization (MDO) approaches that have been proposed for formulating and concurrently solving decomposed or partitioned complex system design problems (c.f., (Lewis and Mistree, 1998; Sobieszczanski-Sobieski and Haftka, 1997), for reviews).² A few authors have focused on considering probabilistic as well as deterministic variables and parameters in an MDO context (eg., (Du and Chen, 2002; Gu and Renaud, 2001)). Other authors have focused on replacing complex, computationally intensive analysis routines with approximate models (e.g., (Giunta, et al., 1997; Koch, et al., 1999; Mavris, et al., 1999)). However, all of these techniques require relatively small numbers of shared variables, a criterion that cannot be met in topology design.

Other approaches have focused on building flexibility into the results of a multi-stage design decision so that subsequent designers have freedom to adjust the design specifications (within limits) without unacceptable sacrifices in performance. For example, Chang and coauthors (Chang and Ward, 1995; Chang, et al., 1994) developed an approach for “conceptual robustness” in which design decisions are robust to variability in the decisions of other team members. Using the RCEM, Chen and coauthors (Chen, et al., 1996a; Chen, et al., 1996b) use robust design techniques to determine ranged sets of design specifications that are flexible within specified limits and, thus,

² Categories of MDO methods include: (1) single level optimization approaches in which analyses are distributed and independently executed while a single optimizer is used to evaluate the results (e.g., simultaneous analysis and design (Haftka, 1985)), and (2) multi-level optimization approaches in which analyses are distributed and subsystems are optimized by subsystem-level and system-level optimizers (e.g., concurrent sub-space optimization (Sobieszczanski-Sobieski, 1988; Wujek, et al., 1996) or collaborative optimization (Kroo, et al., 1994)).

robust to downstream changes in the design. Similarly, Kalsi and coauthors (Kalsi, et al., 2001) use robust design techniques to maintain flexibility between multidisciplinary designers by treating shared variables as noise factors and seeking solutions that are robust to subsequent variations in them for complex, multidisciplinary systems. These approaches seem more promising for robust, multifunctional topology design applications with integral (vs. modular or decomposable) structures, but it is unclear how to apply them effectively for topology design problems in which the number of shared or coupled variables is very large and the topology or layout (and hence the set of coupled variables) is not specified *a priori* and may be noisy or variable itself. Therefore, we are prompted to reiterate Research Question 2:

Research Question 2: *How can multifunctional, topological preliminary design specifications be explored and generated systematically?*

We have arrived at two central research questions from both topology design and robust design perspectives. Underlying both research questions is the need for a multiobjective decision-making approach.

1.2.3 Multiobjective Decision-Making and the Compromise Decision Support Problem

A central challenge in robust, multifunctional topology design is the need to explore designs that balance a set of conflicting objectives. These conflicting objectives may include measures of nominal performance and performance variation or simply multiple performance goals from different functional domains. In either case, it is critical to identify families of designs that embody a range of effective compromises among multiple, conflicting goals. Naturally, a central component of a robust, multifunctional

topology design approach should be a multiobjective decision support model that structures and supports the search for compromise solutions. Therefore, the following research question is posed:

Research Question 3: *How can topology design problems be formulated to facilitate the exploration and generation of families of designs that embody a range of compromises among multiple, conflicting goals involving multifunctional performance and robustness?*

In this dissertation, the compromise Decision Support Problem (DSP) provides a means for mathematically modeling, structuring, and supporting design decisions that involve seeking compromise among multiple conflicting objectives. The compromise DSP is a domain-independent, multiobjective decision model that is a hybrid formulation based on Mathematical Programming and Goal Programming (Mistree, et al., 1993). It is used to determine the values of design variables that satisfy a set of constraints while achieving a set of conflicting goals as closely as possible. The compromise DSP is discussed in detail in Section 2.2. In this dissertation, it is shown that the compromise DSP can be used as a foundational, mathematical construct for structuring the search for families of compromise solutions for materials design problems. The focus in this dissertation is on making consistent compromise decisions in the preliminary design of materials, and specifically, mesostructural topology.

From a broader perspective, the design of robust, multifunctional, material topology—and materials design in general—is a *synthesis* activity in which designers convert information that characterizes the needs and requirements for a material system into knowledge about the material system itself, its behavior, and its structure. In this dissertation, a decision-based design perspective is adopted, anchored in the notion that

the principal role of a designer is to make decisions (Mistree, et al., 1990). From a decision-based perspective, it is not sufficient for a designer to analyze, simulate, experiment, or model. Although these activities are critical to the success of a design process, their primary role in a decision-based design process is to enhance a designer's ability to make decisions. Therefore, in this dissertation, the focus is on both formulating and solving the multiobjective decisions at the heart of materials design in general and robust, multifunctional topology design of material mesostructure, specifically.

1.3 RESEARCH FOCUS, CONTRIBUTIONS, AND STRATEGY

Since the motivation and context for this research are discussed in Sections 1.1 and 1.2, the primary focus, contributions, and strategy for this research activity are presented in this section. The focus is on establishing a method for robust, multifunctional, topology design—based on robust design principles, topology design techniques, and multi-objective decision support—that is suitable for the design of mesoscale material structures as well as broader materials design applications. As presented in Section 1.3.1, the research questions and hypotheses establish context and structure for the research tasks required to achieve the principal goal—establishment of a robust, multifunctional, topology design method. In Section 1.3.2, a set of contributions are presented that summarize the intellectual and pragmatic value of this research. Finally, in Section 1.4, the research strategy is outlined for validating the hypotheses and establishing the contributions.

1.3.1 Fundamental Research Questions and Hypotheses

In this dissertation, the principal goal is to establish a Robust Topological Preliminary Design Exploration Method (RTPDEM) to facilitate the exploration and generation of robust, multifunctional topology and other preliminary design specifications for the mesostructure of prismatic cellular materials, with the potential for broader materials design applications. To establish the RTPDEM, robust design principles and topology design techniques are integrated with the compromise DSP, the multiobjective decision model that anchors the method, as illustrated in Figure 1.14. As documented in Table 1.2, the primary research and secondary research questions follow directly from the principal goal, which embodies the design method requirements identified in Section 1.1.

The primary and secondary research questions are motivated by the need for robust, multifunctional, topology design methods in materials design and by the current state of mutual exclusivity of robust design and topology design methods, as outlined in Sections 1.1 and 1.2, respectively. In robust design applications, the existence of a fixed topology or layout is presupposed, while in topology design applications, factors and parameters are assumed to have deterministic values. Furthermore, topology design methods are typically applied for single-disciplinary, structural applications, limiting their applicability for multifunctional materials design applications.

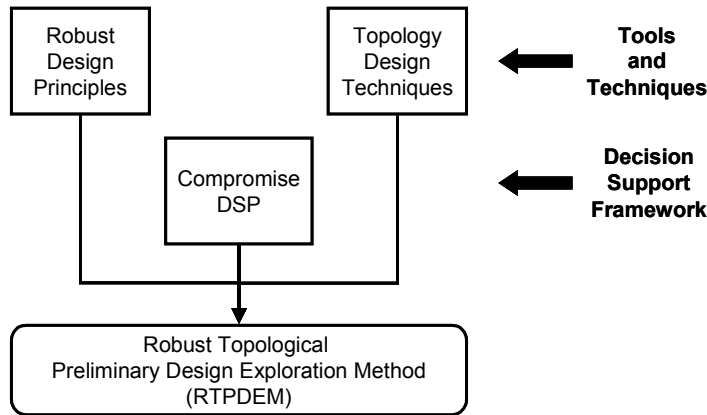


Figure 1.14 – Integration of Robust and Topology Design Tools with the Compromise DSP to Establish the RTPDEM

As outlined in Table 1.2, a set of primary and secondary research hypotheses are motivated directly by the research questions. Together, the research hypotheses define the research tasks that must be investigated and completed successfully to establish a method for robust, multifunctional topology design. The primary hypothesis is derived straightforwardly from the principal research goal, but the secondary hypotheses require further explanation. As discussed in Section 1.2 and illustrated in Figure 1.14, there are three primary components in the RTPDEM: a decision support framework for multiobjective and multifunctional distributed design, robust design methods, and topology design methods. The purpose of Hypothesis 3 is to establish the decision support framework for robust, multifunctional topology design. With Hypotheses 1 and 2, the decision support framework is augmented to support *robust* topology design and *multifunctional*, robust topology design, respectively, by establishing appropriate design methods and computational techniques. Each of the hypotheses are discussed and tested in detail in this dissertation, with the appropriate sections outlined in Section 1.4 for reference.

Table 1.2 – Mapping Requirements to Research Questions and Hypotheses		
Design Method Requirements	Research Questions	Research Hypotheses
<ul style="list-style-type: none"> • Systematic modification of topology. • Generation of robust designs with operating, manufacturing, design parameter, and topological variation • Families of multiobjective, compromise solutions • Generation of manufacturable designs • Computationally efficient design exploration • Distributed, multifunctional exploration of integrated designs • Direct applicability for materials design, specifically mesoscopic topology 	<p>Primary Research Question: How can flexible, robust, multifunctional, topological preliminary designs be explored and generated systematically and efficiently?</p> <p>Secondary Research Questions:</p> <ol style="list-style-type: none"> 1) How can flexible and robust topological preliminary design specifications be explored and generated efficiently and effectively? 2) How can multifunctional, topological preliminary design specifications be explored and generated systematically? 3) How can topology design problems be formulated to facilitate the exploration and generation of families of designs that embody a range of compromises among multiple, conflicting goals involving multifunctional performance and robustness? 	<p>Principal Goal and Primary Research Hypothesis: By integrating robust design principles and topology design techniques with the compromise DSP, a Robust Topological Preliminary Design Exploration Method can be established that facilitates the exploration and generation of robust, multifunctional design specifications—including the topology of a design—in the preliminary stages of design of materials, specifically, material mesostructures for material classes such as prismatic cellular materials.</p> <p>Secondary Research Hypotheses</p> <ol style="list-style-type: none"> 1) Robust design techniques can be established for topology design applications to facilitate the search for robust topological preliminary design specifications. <ul style="list-style-type: none"> 2.1) Statistical experimentation, along with customized models of noise factor and topological variation, can be used to support robust topology design for topological variation. 2.2) Taylor series-based approximations, along with customized models of control factor variation, can be used to support robust topology design for dimensional variation. 2) Generation and communication of flexible topological design specifications, along with approximate physical models, and formulation and solution of multiple compromise DSPs facilitates distributed design exploration of multidisciplinary, integrated, topological systems. 3) The compromise DSP can be used as a mathematical decision model for robust, multifunctional topology design problems to facilitate the consideration of robustness, flexibility, and tradeoffs among multiple objectives.

In Hypothesis 3, the compromise DSP is proposed as a basic template and mathematical model for structuring and supporting decisions in robust, multifunctional topology design. Standard topology design problems are posed as conventional, single-objective, non-linear programming (optimization) problems, which have proven to be effective for pursuing *single* objectives in a deterministic setting. However, in robust, multifunctional design settings, the problem formulation must support exploration of

families of compromise solutions that embody a range of tradeoffs between multiple objectives, including disparate functional requirements and measures of robustness. Also, if multifunctional topology design activities are distributed, it should be possible to formulate and link multiple sub-problems. In Hypothesis 3, it is asserted that the search for multifunctional, flexible, robust solutions to topology design problems can be supported by recasting a standard topology design problem in a compromise DSP formulation.

In Hypothesis 1, it is proposed that a comprehensive robust design method can be established for topology design applications. As noted throughout this chapter, there has been very little overlap between robust design and topology design methods. In topology design problems, the large numbers of variables and the modification of topology (via removal of elements of the design and their associated design variables) make it difficult computationally and conceptually to formulate and implement a robust design method for topology design. As postulated in Hypothesis 1, a comprehensive method is proposed in this dissertation for formulating and solving robust topology design problems. In this approach, a compromise DSP is used to formulate a robust topology design problem, and guidelines and computational techniques are established for evaluating and maximizing the robustness of topology with respect to several types of variation. Two classes of computational techniques are proposed to handle two different categories of variation. For evaluating the impact of small changes in control factors such as element areas or densities or material properties (e.g., solid modulus), local Taylor series-based approximations of design sensitivities are proposed in Hypothesis 1.2. Other sources of variation, such as variations in boundary conditions (e.g., applied loads or displacements)

and variations in topology (e.g., addition or removal of elements or joints), cannot be evaluated effectively with local approximations because they require reanalysis of the structure. For these applications, strategic experiments are proposed in Hypothesis 1.1 for evaluating the impact of variation on responses of interest. For both cases, guidelines for creating models of variation that are appropriate for topology design are proposed.

In Hypothesis 2, robust topology design techniques are proposed for *multifunctional* applications. Topology design techniques are well-established for structural applications, but it can be difficult to extend those techniques to other physical domains, especially if the phenomena are shape dependent, as in heat transfer applications with internal convection, for example. Due to the nature of the topology design process, it is also difficult to analyze such phenomena during a structural topology design process, as mentioned in Section 1.2.2. Therefore, it is proposed that multiple functions be treated as multiple stages in a topology design process. It is proposed that the first stage consist of a full-scale structural topology design process, followed by a more limited topology design process for other functions in the second stage.³ In the first stage, robust topology design methods are used to explore and generate structural topology that is robust to variations in factors such as dimensions, material properties, loading, and the topology itself. This robustness lends flexibility to a subsequent topology design stage for limited adjustment of control and noise factors without significant adverse effects on the structural performance objectives considered in the first stage. However, in order to accommodate broader design changes in the second stage and facilitate a more desirable balance between multifunctional objectives, it is necessary to account for the impact of

³ The second stage is a more limited scale topology design process because it is extremely difficult to conduct non-structural topology design, as discussed in detail in Chapter 2.

these second-stage changes on first-stage performance objectives. Two alternative approaches are proposed and compared in this dissertation:

- (1) Robust, ranged sets of topological preliminary design specifications are generated in an initial structural topology design stage. If the robust topology design methods proposed in Hypothesis 1 are utilized, the specifications may include limited freedom for adjusting both dimensions *and topology*. The robust, ranged sets of topological preliminary design specifications are communicated to a second stage designer who adjusts the design—within the specified ranges—to achieve desired performance in a second functional domain (e.g., heat transfer). In general, models are not provided for the impact of second-stage design changes on first-stage structural design objectives. It is assumed that first-stage design objectives are relatively insensitive to second-stage design changes, provided the changes do not exceed the robust ranges supplied by the first-stage designer.
- (2) Robust, ranged sets of topological preliminary design specifications are generated in the initial structural topology design stage. The specifications are communicated to a second stage designer along with *physics-based* approximate models of the impact of design changes on first-stage structural objectives. These physics-based models should be relatively fast and accurate—such as coarse, low-order finite element models. The physics-based approximate models are valid over a much broader region of the design space than sensitivity-based local approximate models. This provides design freedom for a second-stage designer to make relatively extensive changes to the initial design supplied by the first-stage structural designer. On the other hand, the speed and flexibility of these

approximate models maintains the computational tractability of performing multifunctional analyses. This would not be the case with detailed, computationally intensive physics-based analyses.

The proposed approach is suitable for reducing iteration between stages (although some iteration may be beneficial) and for utilizing distributed computational resources and human expertise effectively. Details of the approach are provided in Chapter 3. In Section 1.4, a strategy is presented for verifying and validating the hypotheses, and an outline is provided of the chapters in which they are justified, elaborated, and verified.

1.3.2 Research Contributions

Research contributions are established by implementing and testing the research hypotheses introduced in the previous section. The **primary research contribution** corresponds to the principal goal, primary research question, and primary research hypothesis. Specifically, **a method is established for robust topological preliminary design exploration that facilitates generation of robust topology and other design specifications to fulfill multiple functional requirements for the preliminary design of material structure—specifically, mesostructural material topology—of prismatic cellular materials and similar classes of materials.**

This method is called the Robust Topological Preliminary Design Exploration Method (RTPDEM). A pictorial summary of the design requirements, foundations, and contributions embodied in the RTPDEM is provided in Figure 1.15. To address the design requirements associated with topology, uncertainty, and multifunctionality (as summarized in Table 1.1), the RTPDEM incorporates not only the capabilities of

conventional topology design, robust design, and multidisciplinary design techniques but also offers novel *design methodology* capabilities for achieving topological robustness and flexibility, and realizing multifunctional topology designs that effectively balance requirements in disparate domains via a multifunctional, robust topology design process suitable for designing highly coupled systems (such as topological designs) in a multi-stage, distributed, collaborative manner. Novel thermal *analysis* and topology design methods are also incorporated within the RTPDEM. Finally, further contributions in the field of *materials design* are associated with applying the RTPDEM for three challenging examples. Contributions in each of the three areas—design methodology, analysis and modeling techniques, and materials design applications—are summarized as follows.

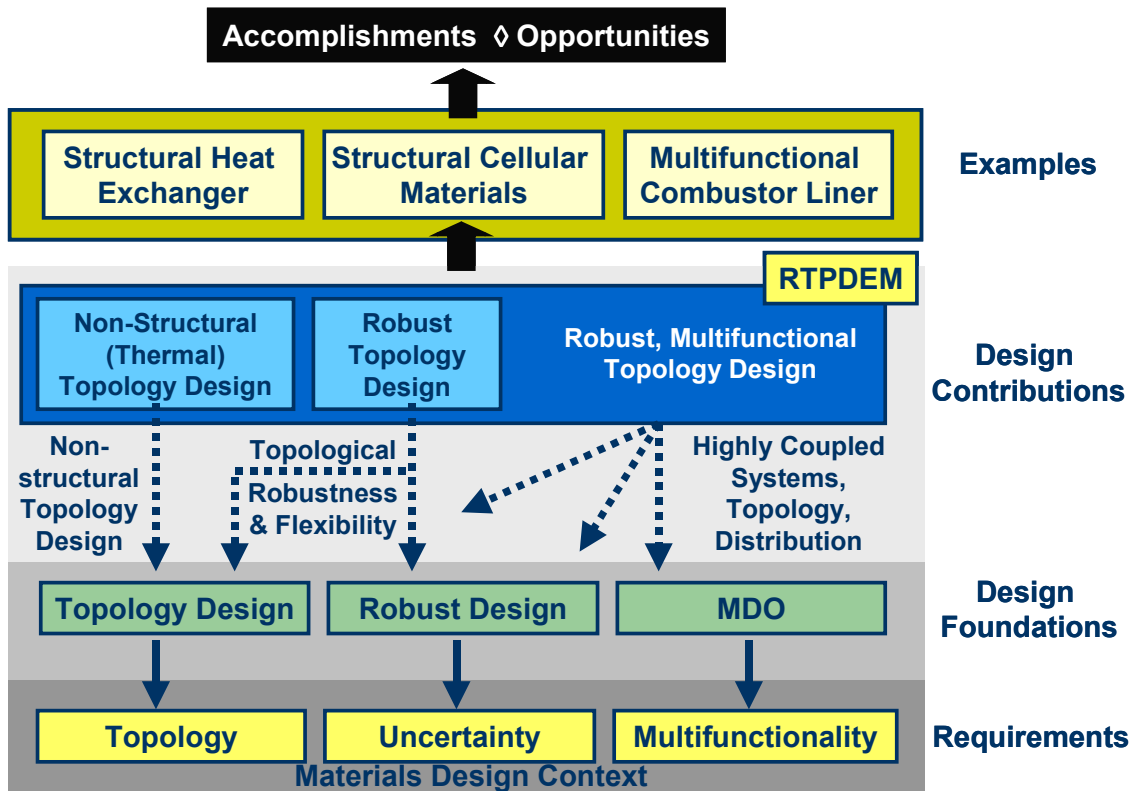


Figure 1.15 – A Summary of Design Requirements, Foundations, Contributions, and Applications of the RTPDEM

The research contributions in the field of *design methodology* are associated with the secondary research questions and hypotheses:

- A flexible, multiobjective decision support model is proposed for robust, multifunctional topology design that facilitates exploration and generation of a *family of topological* designs that embody a *range* of effective compromises among multiple, conflicting goals such as (a) nominal performance and performance variation associated with robust topology design and/or (b) requirements from disparate functional domains such as solid mechanics and heat transfer, that may be associated with distributed decision-makers.
- Guidelines are provided for identifying and modeling sources of variation in topology design—specifically, for materials design applications.
- A comprehensive robust topology design method is established that integrates robust design principles with topology design techniques. The method accommodates variation in boundary conditions, material properties, dimensions, and topology. The method includes mathematical techniques for evaluating *and minimizing* the impact of these sources of variation on overall system performance via robust design of topology and other preliminary design specifications.
- A multifunctional topology design approach is established that facilitates robust topology design for multi-physics applications and highly coupled systems. The method is a distributed, multi-stage topology design approach. In the first stage, robust, flexible designs are generated with full-scale, structural, robust topology design methods. The resulting family of designs is modified for

multifunctionality in a second topology design stage. Two alternative strategies are proposed, applied, and compared for balancing multiple aspects of performance in a multi-stage, distributed topology design process. The strategies differ in the type of information communicated from a lead designer to subsequent designers. Specifically, the options are: (1) communicating exclusively flexible, ranged sets of robust design specifications from stage to stage, with or without local, sensitivity-based approximate models of the impact of subsequent-stage design changes on first-stage (structural) performance and (2) communicating flexible robust design specifications along with approximate physics-based models of first-stage (structural) performance objectives in terms of significant design parameters.

In addition to the contributions in the area of *design methodology*, there are supporting contributions associated with the materials design applications for which the design methods are applied. These supporting contributions fall into two categories: (1) materials design accomplishments, and (2) advances in modeling capabilities. First, the materials design accomplishments:

- Heat exchangers, comprised of prismatic cellular materials, are designed for electronic cooling applications that demonstrate significant improvement over standard finned heat exchangers, in terms of both thermal performance and structural load bearing capabilities. Benchmark studies indicate that the customized cellular heat sinks designed in this dissertation approximately double the total heat transfer rates of conventional microprocessor cooling systems, for example, while offering the capability of supporting structural loads experienced

by portable electronic equipment such as notebook computers. This example is a demonstration of the effectiveness of utilizing a flexible, multiobjective decision support model for exploring and generating a family of multifunctional designs that balance conflicting objectives, in this case, structural and thermal performance requirements.

- Periodic unit cells are designed to meet overall structural elastic requirements that are not achievable with standard cell topologies. It is demonstrated that the unit cell designs are more robust and manufacturable than other designs with similar nominal properties. One non-standard cell topology is introduced in this dissertation, but the robust topology design methods could identify many more for specific applications. This example is a demonstration of the effectiveness and utility of robust topology design methods for materials design applications.
- A combustor liner, comprised of prismatic cellular material, is designed for a gas turbine engine that effectively raises the maximum temperature threshold for gas turbine engine combustor liners by several hundred degrees Celsius—compared with conventional metal alloy-based combustor liners—while simultaneously increasing the efficiency of the engine and reducing harmful NO_x emissions. This is achieved by designing multifunctional cellular materials that simultaneously bear structural loads induced by thermal stresses and combustion pressure while actively cooling themselves via forced air convection through the internal cellular structure. Internal forced convection through the cellular structure reduces the internal temperature of the cellular material to prevent melting and preserve the high-temperature structural properties of the material without requiring

combustion-side film cooling of the combustor liner, thereby enabling higher combustion chamber temperatures, increased efficiency, and reduced emissions. This example is a demonstration of the effectiveness and utility of multifunctional, robust topology design methods that enable strategic utilization of pre-existing alloys to meet otherwise unrealizable design requirements *without* designing a new material composition.

Also, new analysis techniques have been developed as part of the example problems in this dissertation.

- A combined finite difference/finite element heat transfer analysis is established that is relatively fast, accurate, and reconfigurable compared with other heat transfer analysis approaches, such as FLUENT or finite difference approaches. Because it can be quickly reconfigured, it is particularly useful for investigating the effects of topological changes on system performance. Gradients are also calculated for the total rate of heat transfer with respect to thicknesses and depths of elements; thereby, informing a designer or a gradient-based search/optimization algorithm of design changes that are likely to improve the performance of the system. It can be implemented for laminar or turbulent flow conditions.
- An approximate topology design method is established for thermal applications with combined conduction and internal or external convection. The thermal topology design method builds upon the fast, accurate, reconfigurable finite difference/finite element heat transfer analysis technique. An additional technique is introduced for evaluating gradients of thermal performance that

approximate the relative contribution of each element to the thermal performance of the topology. These gradients are used to inform a gradient-based search algorithm that modifies the topology and dimensions to achieve thermal performance goals as closely as possible.

- Several additional analysis models are established that are particularly useful for designing prismatic cellular materials. For example, fast, approximate, finite element models of thermoelastic structural behavior are established, validated, and documented for the combustor liner example. Analytical techniques are established, validated, and documented for evaluating the impact of cellular material imperfections—specifically, tolerances and missing cell walls or joints—on structural performance objectives.

These contributions span a number of research domains. The central contributions are in the area of design methodology, but significant contributions are also demonstrated in materials design applications as well as thermal and structural analysis techniques.

1.4 AN OVERVIEW AND VALIDATION STRATEGY FOR THIS DISSERTATION

The validation and verification strategy for this dissertation is based on the validation square introduced by Pedersen and coauthors (Pedersen, et al., 2000). As noted by Pedersen and coauthors, validation (justification of knowledge claims, in a modeling context) of engineering research has typically been anchored in formal, rigorous, quantitative validation based on logical induction and/or deduction. As long as engineering design is based primarily on mathematical modeling, this approach works well. Engineering design methods, however, rely on subjective statements as well as

mathematical modeling; thus, validation solely by means of logical induction or deduction is problematic. Pedersen and coauthors propose an alternative approach to validation of engineering design methods based on a relativistic notion of epistemology in which “knowledge validation becomes a process of building confidence in its usefulness with respect to a purpose.”

Pedersen and coauthors propose a framework for validating design methods in which the ‘usefulness’ of a design method is associated with whether the method provides design solutions correctly (structural validity) and whether it provides correct design solutions (performance validity). This process of validation is represented in the Validation Square in Figure 1.16. With respect to the square, **theoretical structural validity** involves accepting the individual constructs constituting a method as well as the internal consistency of the assembly of constructs to form an overall method. **Empirical structural validity** includes building confidence in the appropriateness of the example problems chosen for illustrating and verifying the performance of the design method. **Theoretical performance validity** involves building confidence in the generality of the method and accepting that the method is useful beyond the example problems. **Empirical performance validity** includes building confidence in the usefulness of a method using example problems and case studies.

How can this validation framework be implemented in a dissertation? Establishing **theoretical structural validity** involves searching and referencing the literature related to each of the constructs utilized in the design method. In addition, flow charts are often useful for checking the internal consistency of the design method by verifying that there

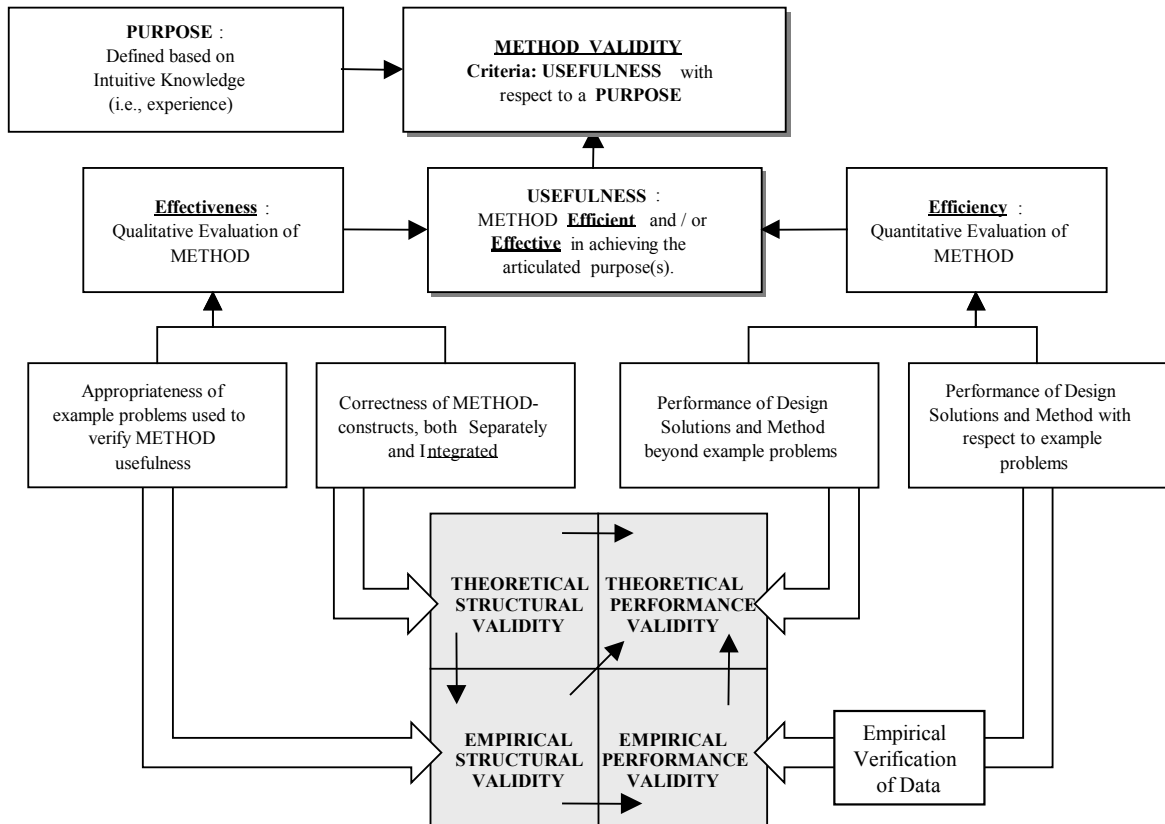


Figure 1.16 – The Validation Square (Pedersen, et al., 2000)

is adequate input for each step and that adequate output is provided for the next step. A list of criteria (see Table 1.1) may be useful for establishing and comparing the theoretical structural validity of methods and constructs with respect to a set of explicit, favorable properties. Establishing **empirical structural validity** consists of documenting that the example problems are similar to the problems for which the methods/constructs are generally accepted, that the example problems represent actual problems for which the method is intended, and that the data associated with the example problems can be used to support a conclusion. **Empirical performance validity** can be established by using representative example problems to evaluate the outcome of the design method in terms of its usefulness. Metrics for usefulness should be related to the degree to which

the method's purpose has been achieved (e.g., reduced cost, reduced time, improved quality). It is also important to establish that the resulting usefulness is, in fact, a result of applying the method. For example, solutions obtained with and without the construct/method can be compared and/or the contribution of each element of the method can be evaluated in turn. An important part of empirical performance validity is **empirical verification** of data used to support empirical performance validation. Empirical verification can be established by demonstrating the accuracy and internal consistency of the data. For example, in optimization exercises, multiple starting points, active constraints and goals, and convergence can be documented to verify that the solution is stationary and robust. For any engineering model, it is important to verify that data obtained from the model represent aspects of the real world that are relevant to the hypotheses in question. The model should react to inputs in an expected manner or in the same way that an actual system would react. **Theoretical performance validity** can be established by showing that the method/construct is useful beyond the example problem(s). This may involve showing that the problems are representative of a general class of problems and that the method is useful for these problems; from this, the general usefulness of the method can be inferred.

In Figure 1.17, an outline of the validation strategy for this thesis is provided. It is arranged according to the quadrants in the validation square, and references are included for chapters and sections in which the validation is documented.

The dissertation is organized as illustrated in Figure 1.18 with the purpose of implementing the validation strategy outlined in Figure 1.17.

Theoretical Structural Validation	
<ul style="list-style-type: none"> • Critical review of literature that is foundational to the Robust Topological Preliminary Design Exploration Method (RTPDEM) proposed in the primary research hypothesis. Topics include robust design, topology design, and multidisciplinary analysis and optimization. • What are the advantages, limitations, and accepted domains of application for available approaches? What are the opportunities for further work? In light of this critical review, do the research tasks and hypotheses represent original, significant contributions? 	Chapter 2
<ul style="list-style-type: none"> • Presentation and discussion of the RTPDEM, including the intellectual and methodological aspects of instantiating each associated hypothesis. • What are the advantages, limitations, and accepted domains of application for the RTPDEM? To what extent does it serve as a foundation for materials design from a theoretical perspective? 	Chapter 3
Empirical Structural Validation	
<ul style="list-style-type: none"> • Identify the materials design significance of the example problems and the need for robust, multifunctional, topological design methods in this context—specifically, the design and analysis of prismatic cellular materials. • Discuss the appropriateness of the example problems in Chapters 5 (Structural Heat Exchanger), 5 (Robust, Structural Unit Cells), and 6 (Multifn Combustor Liner) <ul style="list-style-type: none"> ➤ Document that the example problems are similar enough to problems for which the RTPDEM is accepted theoretically. The characteristics of the proposed domain of application are enumerated in Ch. 3. ➤ Document that the examples are representative of actual problems for which the approach is intended. What are the key characteristics of the examples? ➤ Document that the data associated with the example problems can support a conclusion or conclusions with respect to: <ul style="list-style-type: none"> ▪ Hypothesis 1 (Focus of Ch. 6, also addressed in Ch. 7) ▪ Hypothesis 2 (Focus of Ch. 7) ▪ Hypothesis 3 (Focus of Ch. 5, also addressed in Chs. 6 and 7) 	Chapter 4
Empirical Performance Validation	
<ul style="list-style-type: none"> • Build confidence in the utility of the RTPDEM using the examples. <ul style="list-style-type: none"> ➤ Use the example problems to evaluate the utility of the RTPDEM. <ul style="list-style-type: none"> ▪ Does the compromise DSP-based topology design problem formulation facilitate flexible exploration of robustness and tradeoffs among multiple objectives? ▪ Does the method facilitate exploration and generation of robust, topological design specifications? ▪ Does the method facilitate exploration and generation of robust design specifications (topology and other design parameters) that require distributed, multi-scale, multi-functional analysis and synthesis? ▪ Does the method possess the advantages claimed in Chapters 2 and 3? ➤ Demonstrate that the observed usefulness is linked to applying the method. For example, compare results to those obtained with alternative or conventional methods or to benchmark products. ➤ Verify the empirical data obtained in the experiments (e.g., compare to detailed computer simulations or analytical solutions). • Demonstrate materials design significance and contributions. 	Chapters 5, 6, 7
Theoretical Performance Validation	
<ul style="list-style-type: none"> • Build confidence in the generality and utility of the approach beyond the specific example problems. Argue that the approach is useful for the example problems and that the example problems are representative of general problems. 	Chapter 8

Figure 1.17 -- Validation Strategy for this Dissertation

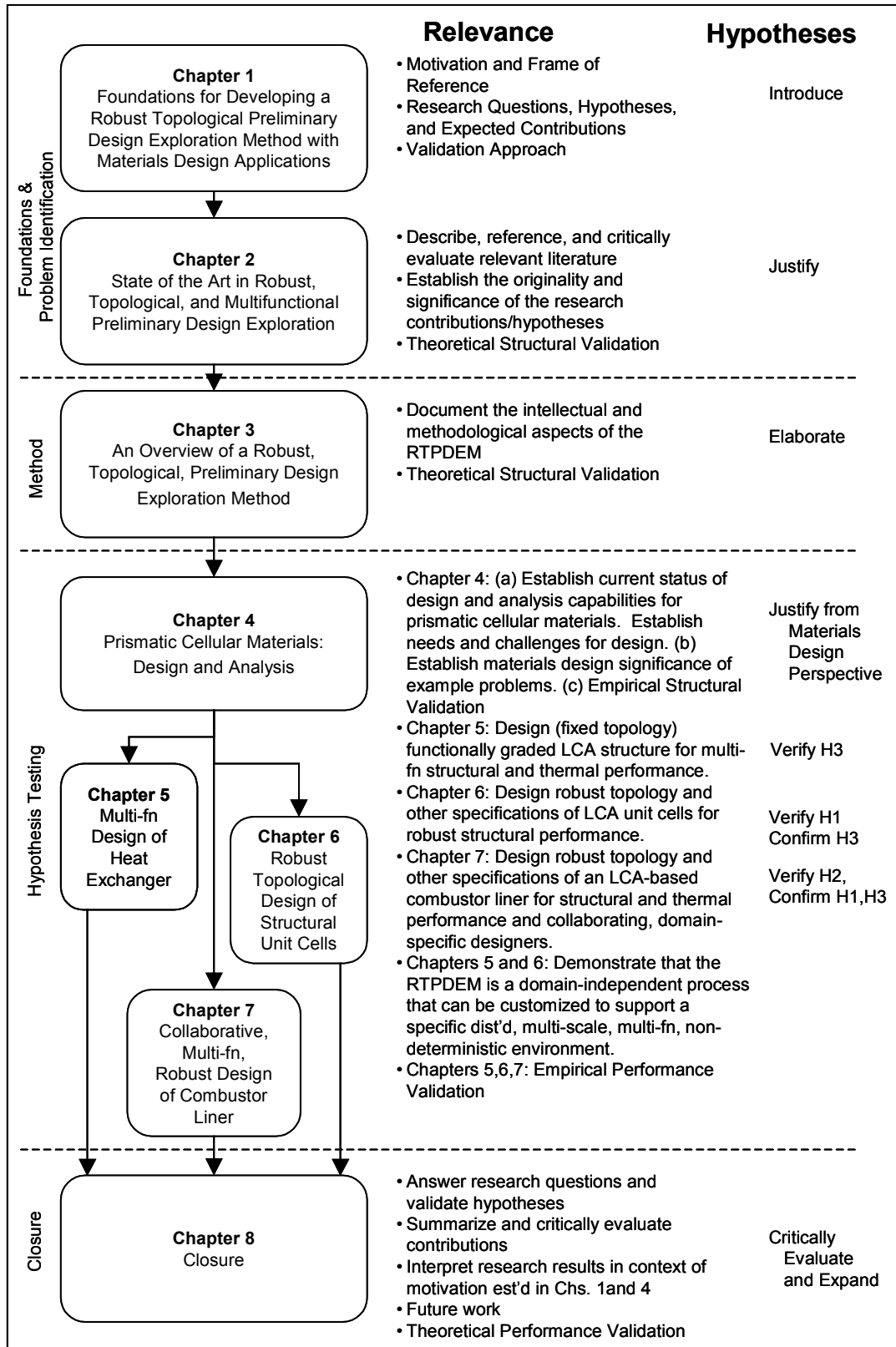


Figure 1.18 – A Dissertation Overview and Roadmap

In Chapter 1, the foundations are established for the Robust Topological Preliminary Design Exploration Method (RTPDEM). The motivation and frame of reference are presented. The principal goal is introduced along with the research questions and hypotheses. The expected contributions are summarized, and a validation strategy is established for the dissertation.

In Chapter 2, the theoretical foundations for the Robust, Topological Preliminary Design Exploration Method (RTPDEM) are introduced and discussed. Those foundations include topology design, robust design, multidisciplinary robust design, and multiobjective decision-making. For theoretical structural validation, relevant literature in each of these research areas is referenced, discussed, and critically evaluated. The purpose is to discuss the availability, strengths, and limitations of methods or constructs that are foundational for the RTPDEM and to identify research opportunities addressed in this dissertation via the RTPDEM.

In Chapter 3, an overview of the RTPDEM is presented. The elements of the RTPDEM are discussed in detail from the perspective of embodying the hypotheses presented in Chapter 1. For theoretical structural validation, emphasis is placed on verifying the internal consistency of the method as well as its originality, advantages, limitations, and accepted domain of application. Advantages, limitations, and originality are discussed in relation to methods and constructs that are available in the literature.

In Chapter 4, an overview of the example problems is provided. The relevance and significance of the example problems is established from a materials design perspective. It is argued that solutions to the example problems constitute significant contributions to the field of materials design and specifically, to the domain of design and analysis of

cellular materials. For empirical structural validation, the appropriateness of each of the examples for validating specific aspects of the RTPDEM is discussed. An experimental plan is presented for each of the examples to document how the examples are used to generate information that can be used to test the hypotheses.

In Chapters 5, 6, and 7, three example problems are presented. For each example, problem statements are provided, and step-by-step implementation of appropriate aspects of the RTPDEM is discussed and documented. The results of the examples are presented, verified, and critically discussed for the purpose of empirical validation of the hypotheses introduced in Chapter 1. The examples of Chapters 5, 6, and 7 are focused primarily on validating Hypotheses 3, 1, and 2, respectively, but Chapters 6 and 7 also confirm Hypothesis 3, and Chapter 7 confirms Hypothesis 1.

In Chapter 5, multifunctional design of structural heat exchangers comprised of cellular materials is presented as an example to illustrate the effectiveness of the compromise DSP for exploring and generating families of material designs that embody a range of compromises between multifunctional goals. Formulation of the compromise DSP for materials design applications is demonstrated in detail along with its use as a flexible template for generating families of solutions.

In Chapter 6, robust design of prismatic cellular materials for structural applications is presented as an example to illustrate the effectiveness of the RTPDEM for robust topology design. Common sources of variation in topology design are modeled, including dimensional and topological variation. Robust topology design methods and computational techniques are demonstrated for evaluating and minimizing the impact of variation on overall material properties and performance in a topology design context.

The effectiveness of the compromise DSP is demonstrated for exploring and generating families of designs with a spectrum of tradeoffs between robustness and nominal performance goals.

In Chapter 7, robust, multifunctional design of gas turbine engine combustor liners is presented as an example to illustrate the effectiveness of the RTPDEM for distributed, robust, multifunctional design of an integrated topological system. Multifunctional topology design is distributed between structural and thermal domains and associated designers. The effectiveness of robust topology design methods is demonstrated for building flexibility into topological preliminary design specifications during a structural topology design process. The flexibility is subsequently used to modify the design in pursuit of thermal objectives. Tradeoffs between multifunctional objectives are supported computationally via (a) generation and communication of flexible topological design specifications and sensitivity information that quantifies the local impact of design parameters on objectives and (b) formulation and solution of a compromise DSP for each functional domain. The effectiveness of robust topology design methods is also demonstrated for minimizing the impact of dimensional, topological, material property, and boundary condition variations on multifunctional performance.

In Chapter 8, the dissertation is summarized and critically reviewed and relevant contributions and avenues for future work are discussed. The advantages and domain of application are discussed for the methods presented in this dissertation, and intellectual contributions are reviewed. For theoretical performance validation, it is argued that the conclusions of this thesis are relevant beyond the two example problems, and potential future applications are discussed. Conditions are identified under which the conclusions

are valid, and limitations of the work are presented explicitly. Recommendations are proposed for future work that would make the approach more effective for the example problems and extend it for a broader range of applications.

CHAPTER 2

ROBUST, MULTIFUNCTIONAL TOPOLOGY DESIGN FOR MATERIALS DESIGN APPLICATIONS: REVIEW OF LITERATURE AND IDENTIFICATION OF RESEARCH OPPORTUNITIES

In this chapter, the theoretical and computational foundations are investigated for establishing a Robust Topological Preliminary Design Exploration Method (RTPDEM). In Chapter 1, the desirable characteristics of the RTPDEM are identified and discussed, as summarized in Table 1.1. In Section 2.1, these characteristics are revisited to establish context for a critical review of the literature in research areas foundational to the RTPDEM. As reviewed in Sections 2.2, 2.3, and 2.4, these research areas include multiobjective decision support, robust design, and topology design. Finally, in Section 2.5, research opportunities are identified by comparing the RTPDEM requirements identified in Section 2.1 with the body of methods, principles, and techniques presented in the literature and reviewed in Sections 2.2 through 2.4.

2.1 DESIGN METHOD REQUIREMENTS FOR THE RTPDEM

Several requirements for the RTPDEM as a design method are listed in Table 1.1. Since the purpose of the literature review is to determine how well these requirements are met with previously existing design methods and techniques, it is important to review these requirements to set the context for the literature review. To make the discussion more concrete, let us refer to a representative application—a structural heat exchanger comprised of prismatic cellular material as illustrated in Figure 1.7. What are the ideal aspects of a *method* for the preliminary design of such a device and its material?

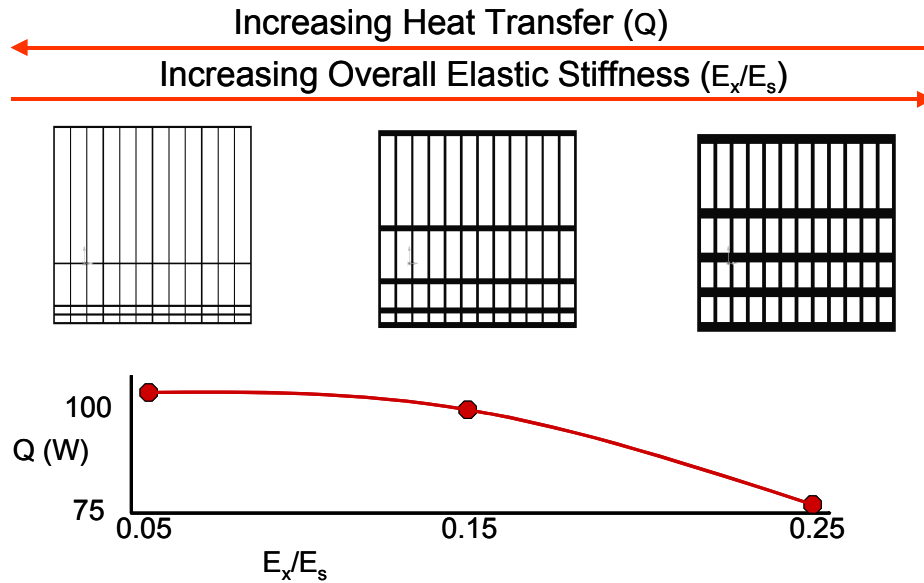


Figure 2.1 – A Family of Structural Heat Exchangers, Exhibiting a Range of Multiobjective Tradeoffs

The method should facilitate exploration and generation of families of multifunctional or multiobjective compromise solutions. Typically, materials design applications involve multiple objectives or goals that must be considered simultaneously during the design process.¹ As in the structural heat exchanger, multiple goals are often associated with different aspects of functionality such as maximizing total rates of steady state heat transfer and maximizing overall structural stiffness. Often, the goals are in conflict with one another such that design parameter settings that most closely achieve one goal differ from those for another goal. Consequently, families of compromise solutions are often available that embody a range of tradeoffs between conflicting goals. A family of structural heat exchanger designs is illustrated in Figure 2.1 along with a plot

¹ In this dissertation, goals are distinguished from constraints by the rigidity associated with them. Goals are *soft* requirements to be minimized, maximized, or target-matched as much as possible. Constraints are *hard* requirements that must be met for feasibility. A design method should facilitate satisfaction of constraints that ensure the feasibility of a design.

of the tradeoffs exhibited by the designs in terms of overall structural elastic stiffness (normalized by base material properties) and total rates of steady state heat transfer. The details of the designs are provided in Chapter 5, but it is clear from this figure that a family of compromise solutions may exhibit a broad range of multi-dimensional performance and that designs that perform as well as possible in one functional dimension may perform poorly in another. In the preliminary stages of design, it is desirable to generate these families of solutions to provide insight into the design problem that cannot be obtained from a single solution and to preserve design freedom (in the form of *multiple* concepts) for subsequent design stages. Furthermore, by explicitly considering multiple goals during a design process, a designer guards against the likelihood of obtaining uni-dimensional designs that perform well from one functional perspective but poorly from others. Finally, multifunctional design activities are often distributed among multiple experts with their own domain-specific knowledge, models, and computing resources. Distributed design can enhance concurrency and design process efficiency, but it is challenging to integrate these activities in pursuit of system-level objectives.

The method should facilitate systematic modification of topology. In materials design, particularly on mesoscopic scales, the arrangement or layout of material is critically important, and its impact on performance is often more profound than subsequent dimensional changes in a design. Rather than simply selecting or intuitively guessing an appropriate topology, it is important to systematically explore topology just as a designer would explore dimensions or other design parameters. However, topology design is more general than size and shape design in which a designer modifies the

dimensions or shape and dimensions with a priori specified topology. It is also more general than *selection* approaches in which topology and material are selected from a database of available options. Because topology design involves systematically exploring layout, shape, dimensions, and material distribution, it allows a designer to systematically explore a much broader class of design solutions with increased design freedom. In the case of the structural heat exchanger, changes in topology are essential for tailoring multifunctional performance. Fixed topology design severely restricts the space of available options and performance capabilities. Topology design is also necessary for leveraging the capabilities of the cellular material manufacturing process.

The method should facilitate consideration and maximization of robustness and flexibility with respect to many sources of variation. In this dissertation, *optimal* solutions are assumed to be chimeras—impossible, fanciful, and illusive aspirations. Optimal solutions are guaranteed to be superior to other solutions *only* under the strict conditions assumed during the design process. In reality, everything is subject to change and uncertainty, from the accuracy of a behavioral model, to the evolutionary and iterative changes in design parameters over the course of a design process (a particularly important concern in preliminary design stages), to the manufacturing and operating conditions in which it is fabricated and used by a customer. With these changes and uncertainties, the ‘optimal’ solution usually deviates from its superior performance and often fails to satisfy minimum requirements for feasibility. Instead, we seek robust solutions that are relatively insensitive to variations in operating and manufacturing conditions, design parameters, and topology and also *flexible* for accommodating changes in design parameters during the design process. In the preliminary design of a structural

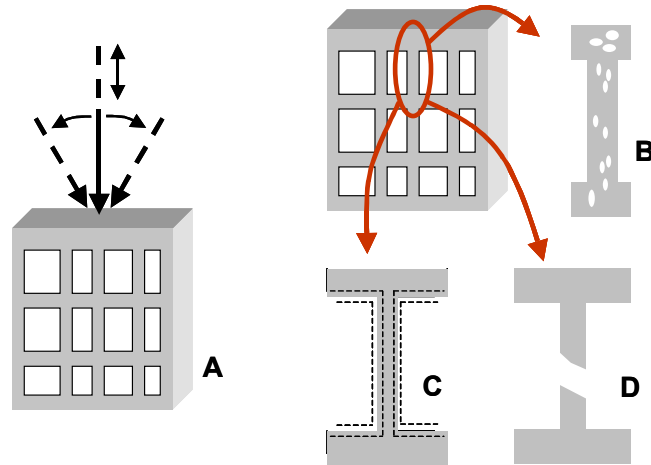


Figure 2.2 – Potential Sources of Performance Variation in a Prismatic Cellular Material. Examples include: (a) stochastic operating conditions such as applied loading, (b) porosity in base material, (c) dimensional tolerances, and (d) cracked or missing cell walls or joints.

heat exchanger, comprised of cellular materials, we are concerned with manufacturing-related variations in dimensions, material properties, and topology (e.g., cell wall cracks and missing joints), as well as changes in operating conditions such as applied loading, as illustrated in Figure 2.2.

Finally, since topology design is a preliminary design activity, a designer should expect changes to be made to the preliminary design in subsequent stages of design. Therefore, it is desirable to design flexibility and robustness into the design to accommodate these changes and variations. For example, consider the simplified design illustrated in Figure 2.3. In a multi-stage design process, a fixed design requires iterative redesign to accommodate changes. If the design is flexible—represented by the geometric ranges between the overlapping regions—any design within the ranged set of possibility satisfies relevant goals and objectives. As the design progresses toward the final stages of design, each designer has the freedom to adjust the design within the

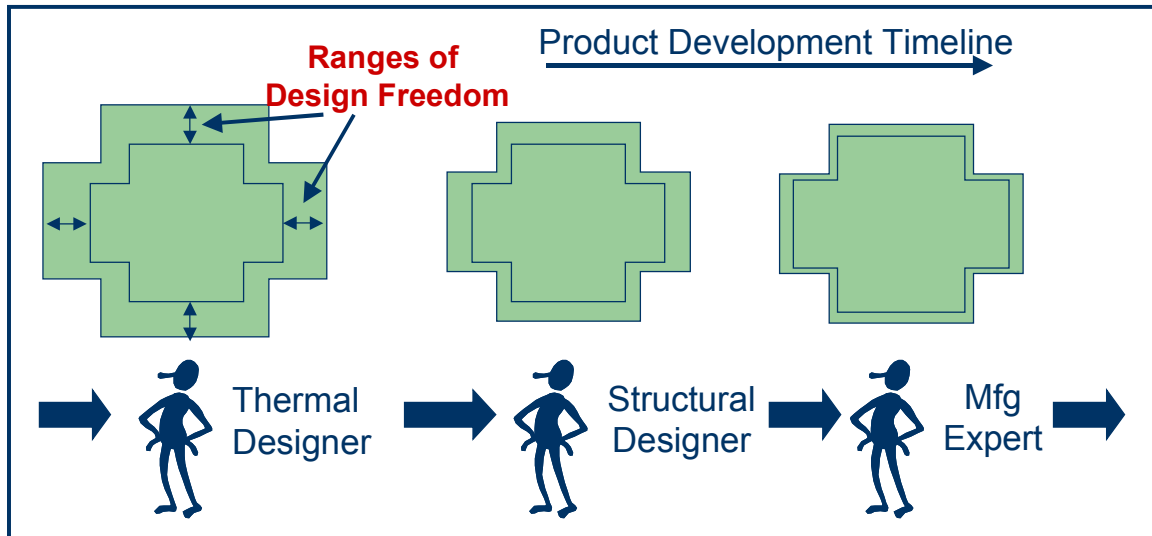


Figure 2.3 – Flexibility in Preliminary Design Specifications

specified ranges in order to satisfy his/her design objectives. Flexibility is gradually reduced until the design specifications are fixed and design freedom is closed.

The method should facilitate systematic, efficient, and effective design. *Webster's* defines a method as "...a regular, orderly procedure or way of teaching, investigating, etc...." (Guralnik, 1973) In other words, the method should establish a procedure, accompanied by tools and computational techniques, for investigating appropriate designs that meet a set of requirements. Therefore, it should help a designer avoid *ad hoc* approaches that involve trying different options in a disorganized manner, often involving many trials that overlook better solutions. In other words, the method should be prescriptive, by providing guidelines for the design process itself as well as for the attributes that a resulting design should have (Finger and Dixon, 1989). If it is executed correctly in a context for which it is accepted, the RTPDEM should be **effective** for facilitating the identification of superior solutions, relative to other feasible solutions to

the design problem. (Of course, it must also establish a set of criteria by which solutions are compared and superiority established.) It should be more **efficient** than exhaustively searching a feasible design space in search of a superior solution. Efficiency may derive from both strategic, informed direction of the search process and use of relatively accurate, computationally efficient, approximate models instead of detailed models whenever possible.

In Sections 2.2, 2.3, and 2.4, the research areas most closely related to these design method requirements are reviewed, namely, multiobjective decision support, topology design, and robust design. The design method requirements discussed in this section are revisited in Section 2.5 in which research opportunities are identified.

2.2 MULTIOBJECTIVE DECISION SUPPORT AND THE COMPROMISE DSP

The first requirement for a method is that it should facilitate exploration and generation of families of multiobjective or multifunctional compromise solutions. This requirement is driven by the fact that designers often must balance conflicting objectives in materials design applications in order to obtain viable solutions. For example, in the structural heat exchanger example, a designer must seek a compromise between maximizing overall elastic stiffness and maximizing total rates of steady state heat transfer—requirements that place very different demands on the structure or form of the device. The challenge is to identify values of design parameters—which describe the structure or form of a design and possibly its environment—that yield preferred compromise solutions with respect to the set of objectives.

In its most general form, a conventional mathematical programming problem is formulated as follows:

$$\text{Minimize} \quad f(\mathbf{x}) \quad (2.1)$$

$$\text{Subject to} \quad \mathbf{g}(\mathbf{x}) \leq 0 \quad (2.2)$$

$$\mathbf{h}(\mathbf{x}) = 0 \quad (2.3)$$

$$\mathbf{x}_L \leq \mathbf{x} \leq \mathbf{x}_U \quad (2.4)$$

where $f(\mathbf{x})$ is a function to be minimized, $\mathbf{g}(\mathbf{x})$ and $\mathbf{h}(\mathbf{x})$ are vectors of inequality and equality constraints, respectively, and \mathbf{x}_L and \mathbf{x}_U are vectors of lower and upper bounds for the vector of design variables, \mathbf{x} . When multiple objectives are considered, the objective function effectively becomes a vector, as well, and Equation 2.1 must be expressed as follows:

$$\text{Minimize} \quad \mathbf{f} = [f_1(\mathbf{x}), f_2(\mathbf{x}), \dots, f_n(\mathbf{x})] \quad (2.5)$$

By placing different relative values or priorities on the individual objectives, it is possible to obtain many solutions to the multiobjective problem. The range of compromise solutions is often called a Pareto set, curve, or frontier. Individual solutions or members of the Pareto set are called Pareto solutions or points. A Pareto solution is one that is not dominated by any other solution in the feasible design space (defined by the set of constraints and bounds). A non-dominated or Pareto solution is one for which no other *feasible* solution yields preferred values for *all* objectives. In other words, it is impossible to locate another feasible solution that improves one or more objectives without worsening the values of other objectives. The concept of a Pareto solution and Pareto set is borrowed from economics and named for the economist Vilfredo Pareto who defined an allocation of resources as Pareto efficient if it is impossible to identify another

allocation that makes some people better off without making others worse off (Pareto, 1909).

Design solutions are rarely judged on the basis of a single criterion; instead, their value is determined by how well they balance multiple criteria associated with cost, performance, environmental impact, robustness, and other categories. Therefore, it is reasonable to pursue a balance between these multiple criteria or objectives during the design process itself. Accordingly, many techniques have been proposed for generating Pareto sets of solutions and for determining the most preferable multiobjective solution. One of the most straightforward techniques is the weighted sum approach. A weighted sum formulation of an objective function, Z , is expressed as a linear, additive combination of the multiple objectives:

$$Z = \sum_{i=1}^m w_i f_i \quad (2.6)$$

where w_i is the weight for the i^{th} objective, f_i , and m is the number of objectives. The weighted sum formulation is straightforward and easy to implement. By varying the weights, it is possible to generate a family of Pareto solutions to the multiobjective design problem posed in Equations 2.2 through 2.5. However, it has been shown that many Pareto solutions may be overlooked (i.e., it is not possible to identify all Pareto solutions) with a weighted sum formulation if the problem is non-convex (Koski, 1985). Also, if a single multiobjective solution is sought, it is difficult to determine *a priori* an appropriate set of weights that yield a preferable compromise solution that does not overemphasize one or more objectives relative to other objectives.

Messac (1996; 1996) has proposed a physical programming formulation to remedy the latter limitation. With the physical programming approach, a designer expresses his preferences for each objective through various degrees of desirability from unacceptable to ideal. Based on these preferences, sets of weights are determined automatically for each objective, with each weight valid over a specified range of objective function values, to form a convex, piecewise linear merit function for each objective. With physical programming formulations, solutions that achieve tolerable or desirable values for all criteria are preferred over solutions that achieve ideal values of some objectives at the expense of extremely poor values of other objectives. However, like the simple weighted sum approach, the physical programming formulation still suffers from inability to identify a full range of Pareto solutions (because it is based on a linear weighted sum formulation). Furthermore, many designers object to the use of semantic preference levels that are central to the physical programming formulation.

The weighted sum approach is a special case of compromise programming (Yu and Leitmann, 1974; Zeleny, 1973) in which a multiobjective function is expressed as the distance between objective values, $f(\mathbf{x})$, for a particular solution and a set of ideal or utopian objective values, f^* , as follows:

$$Z = \left\{ \sum_{i=1}^m \left(w_i (f_i(\mathbf{x}) - f_i^*) \right)^p \right\}^{1/p} \quad (2.7)$$

where p is a positive integer. If p equals one and the ideal objective values have null values, the compromise programming formulation reduces to the weighted sum formulation. If p equals two, the Euclidean formulation is established. The Tchebycheff formulation is obtained by setting p equal to infinity:

$$Z = \min \max_{i=1, \dots, m} \{w_i(f_i(\mathbf{x}) - f_i^*)\} \quad (2.8)$$

The Tchebycheff formulation has been shown to be much more effective for generating an entire Pareto set of options, even for non-convex problems, than the weighted sum formulation (c.f., (Bowman, 1976)) and has been used to generate a Pareto frontier for bi-objective robust design problems that involve tradeoffs between nominal performance and robustness (Chen, et al., 1999b). The standard min-max formulation in engineering optimization is a special case of Equation 2.8 in which the ideal or utopia objective values are assigned null values and the weights are removed by assigning values of unity to all of them. Although compromise programming formulations have been shown to be effective for generating Pareto sets of solutions for multiobjective problems, they have the disadvantage of requiring ideal or utopian solutions within the problem formulation. In strictly keeping with the compromise programming approach, an ideal or utopian point must be identified *separately* for *each* objective by minimizing/maximizing the objective over the feasible solution space. This is an expensive requirement, and its cost grows with the number of objectives.

There are many other multiobjective formulations. For example, utility theory has been shown to be a mathematically rigorous, domain independent approach for multiobjective decision-making (Keeney and Raiffa, 1976; von Neumann and Morgenstern, 1947). A decision-maker's preferences are explicitly assessed and modeled as utility functions that are valid for conditions of risk and uncertainty as well as tradeoffs among multiple attributes. As long as a decision-maker's preferences obey a set of axioms, it can be proven mathematically that his/her preferred alternative—and therefore the rational choice—is the one with the highest expected utility. Although utility theory

is a theoretically sound approach for identifying compromise solutions, especially when uncertainty is associated with the objectives, the associated informational demands on a decision-maker are very high (c.f., (Fernandez, 2002; Seepersad, 2001) for discussions). Among other demands, utility theory requires a decision-maker to assign probabilities to *every* possible outcome or set of objective function values and to know *a priori* exactly what his/her preferences are for combinations of multiple objectives. The latter requirement is particularly prohibitive in the early stages of design when a designer may be using multiobjective searches to discover or explore the potential range of compromise solutions for a specific problem; a designer may not know what he/she wants until he/she ascertains what is *possible*.

Another mathematical construct for modeling multiple objectives in engineering design applications is the compromise Decision Support Problem (DSP) (c.f. (Mistree, et al., 1993a)). The compromise DSP is a hybrid formulation based on mathematical programming and goal programming. The focus of goal programming is to establish goals for each objective and to achieve each of the goals as closely as possible (Charnes and Cooper, 1961). The corresponding mathematical formulation is similar to compromise programming, but ideal or utopian objective function values are replaced with goals or targets established by a designer. For each objective, an achievement function, $A_i(\mathbf{x})$, represents the value of the objective as a function of a set of design variables, \mathbf{x} , and a goal or target value, G_i , is established for each objective. Deviation variables, d_i^- and d_i^+ , represent the extent to which an objective underachieves or overachieves its target or goal, as follows:

$$A_i(\mathbf{x}) + d_i^- - d_i^+ = G_i \quad (2.9)$$

The overall objective function is expressed as a function of the deviation variables as follows:

$$Z = f(d_i^-, d_i^+) \quad (2.10)$$

$i=1, \dots, m$

As expressed in Equation 2.10, the objective function in goal programming is exclusively a function of the deviation variables that measure the extent to which conflicting goals are achieved. The objective function could take many forms, the simplest of which is the weighted sum formulation:

$$Z = \sum_{i=1}^m (w_i^+ d_i^+ + w_i^- d_i^-) \quad (2.11)$$

Restrictions are placed on the deviation variables to limit them to positive values and ensure that only one deviation variable is positively valued at any specific point in the design space:

$$d_i^- \geq 0; d_i^+ \geq 0; d_i^- \cdot d_i^+ = 0 \quad (2.12)$$

Although strict formulations of goal programming do not support equality or inequality constraints, these constraints are supported in the compromise DSP with formulations borrowed from mathematical programming:

$$g_i(\mathbf{x}) \geq 0, \quad i = 1, \dots, p \quad (2.13)$$

$$h_i(\mathbf{x}) = 0, \quad i = 1, \dots, q \quad (2.14)$$

where p and q are the numbers of inequality and equality constraints, respectively. Bounds are also specified on the set of design variables that describe the form of potential solutions:

$$x_{i,\min} \leq x_i \leq x_{i,\max}, \quad i = 1, \dots, n \quad (2.15)$$

where n is the number of design variables and $x_{i,L}$ and $x_{i,U}$ are the lower and upper bounds, respectively, for the i^{th} design variable.

The objective function formulation and constraints borrowed from goal programming and mathematical programming, respectively, are unified with other constructs into a single decision support construct—the compromise DSP, as illustrated in Figure 2.4. The compromise DSP is used to determine the values of design variables that satisfy a set of constraints and bounds and achieve a set of conflicting, multifunctional goals as closely as possible. As in goal programming formulations, the deviation function is formulated as a function of deviation variables that measure the extent to which multiple goals are achieved. The compromise DSP differs from goal programming, however, because it is tailored to handle common engineering design situations in which physical limitations are manifested as system constraints (mostly inequalities) and bounds on the system variables. In traditional mathematical programming, the objective function typically represents a *single* goal, by which the desirability of a design solution is measured. All other characteristics of a design are modeled as hard constraints. On the other hand, the compromise DSP is more flexible than traditional mathematical programming because it accommodates multiple constraints *and* objectives, as well as both quantitative information and information—such as bounds and assumptions—that may be based on a designer’s judgment and experience (Marston, et al., 2000). In the compromise DSP, multiple goals have been considered conventionally by formulating the deviation function either with Archimedean weightings or preemptively (lexicographically) (Mistree, et al., 1993a). An Archimedean formulation is illustrated in Figure 2.4.

Given		
An alternative to be improved through modification		
Assumptions used to model the domain of interest		
The system parameters:		
n	number of system variables	
p+q	number of system constraints	
p	equality constraints	
q	inequality constraints	
m	number of system goals	
$C_i(\mathbf{X})$	Capability of the system	
$D_i(\mathbf{X})$	Demand to the system	
$g_i(\mathbf{X})$	System constraint function	
$g_i(\mathbf{X}) = C_i(\mathbf{X}) - D_i(\mathbf{X})$		
Find		
X_i	System Variables	$i = 1, \dots, n$
d_i^+, d_i^-	Deviation Variables	$i = 1, \dots, m$
Satisfy		
System Constraints (linear, nonlinear)		
$g_i(\mathbf{X}) = 0$		$i = 1, \dots, p$
$g_i(\mathbf{X}) \geq 0$		$i = p+1, \dots, p+q$
System Goals (linear, nonlinear)		
$A_i(\mathbf{X}) + d_i^- - d_i^+ = G_i$		$i = 1, \dots, m$
Bounds		
$X_{i,\min} \leq X_i \leq X_{i,\max}$		$i = 1, \dots, n$
$d_i^+, d_i^- \geq 0$		$i = 1, \dots, m$
$d_i^+ \cdot d_i^- = 0$		$i = 1, \dots, m$
Minimize		
Deviation Function: Archimedean formulation		
$Z = \sum_i W_i (d_i^+, d_i^-)$		
		$i = 1, \dots, m$

Figure 2.4 – Mathematical Formulation of the Compromise DSP (Mistree, et al., 1993b)

The conceptual basis of the compromise DSP is to minimize the difference between that which is desired (the goal, G_i) and that which can be achieved ($A_i(x)$) for *multiple* goals. The underlying philosophy of the compromise DSP and its goal programming foundations is similar to the concept of *satisficing* solutions and bounded rationality proposed by Simon (Simon, 1983; Simon, 1996). According to Simon’s theory of

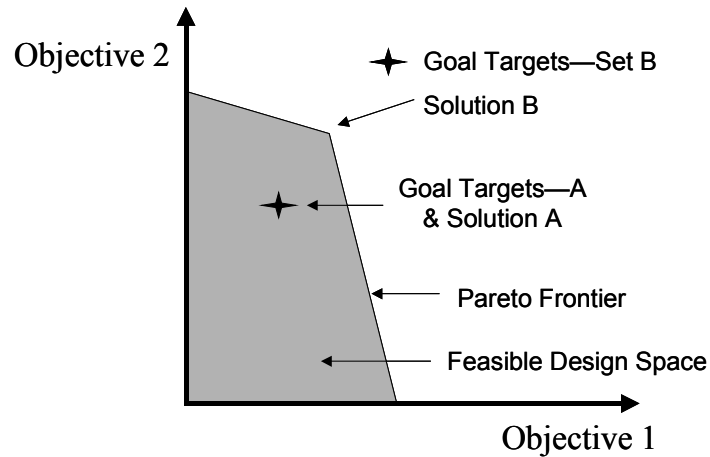


Figure 2.5 – Pareto Solutions and Goal Targets in the Compromise DSP

bounded rationality, decision-makers are not omniscient and recognize that search is expensive. Consequently, they establish targets or thresholds and accept solutions that meet or exceed these targets as ‘good enough’ or *satisficing*. The thresholds are similar to the goal values specified in goal programming and the compromise DSP.

Simon proposed a Nobel Prize-winning perspective with which to view human decision-making in a variety of contexts. It has very important consequences in an engineering design setting. For example, if the goal target values established by a designer for the compromise DSP are easily achieved, solution of the compromise DSP may produce solutions that are dominated (in the Pareto sense) by other feasible solutions. Suppose that two objectives are being balanced, as illustrated in Figure 2.5, and constraints limit achievement of the pair of objectives to the shaded feasible design space bounded by a Pareto frontier. If established goals are easily achieved (i.e., within the Pareto frontier) as with set A in Figure 2.5, then solution of the compromise DSP will satisfy the goals exactly, despite the fact that other feasible solutions dominate the targeted solution. Other solutions are feasible and offer preferred levels of *all* objectives.

This is a common criticism of goal programming formulations—that they often deliver solutions that are inferior to other feasible Pareto solutions. However, this is not an inherent limitation of the compromise DSP formulation. *Satisficing* designs—such as solution A in Figure 2.5—may actually be *preferable* to solutions on the Pareto frontier, especially in the early stages of design. As design parameters and conditions change, satisficing solutions are more likely to remain acceptable than Pareto solutions because satisficing solutions do not reside on the frontier of the feasible space and are therefore less likely to violate critical constraints as soon as design parameter values change. In the early stages of design, it is typical for assumptions and preliminary design parameter values to shift. As a result, ‘optimal’ designs may no longer be optimal; in fact, they may be infeasible. The flexibility built into satisficing solutions is particularly important for coupled, distributed design problems in which collaborating designers need this flexibility for adjusting design parameters without rendering the design unacceptable to other designers. The capabilities of the compromise DSP—coupled with robust design methods—for supporting collaborative design via exploration and generation of flexible solutions is discussed in further detail in Section 3.4.2. It is argued that flexible, satisficing solutions may be regarded as preferable rather than inferior to optimal solutions in some contexts. However, if Pareto solutions are sought, they are obtainable with the compromise DSP formulation. The enabling strategy is to set goal target values sufficiently high as with set B in Figure 2.5. In fact, it is easy to determine whether targets have been set sufficiently high because all of the deviation variables will have positive values.

In addition to facilitating the search for *either* flexible, satisficing solutions or Pareto solutions, the compromise DSP has additional capabilities that make it the construct of choice in this dissertation for modeling multiobjective decisions in materials design. For example, once a compromise DSP is formulated for a particular problem, it is possible to generate families of related designs by changing goal target values, weights, and/or design variable bounds *without* reformulating the problem. Unlike conventional single-objective optimization, a designer is not forced to choose a single objective and arbitrarily constrain other objectives. Instead, a designer can explore a range of tradeoffs between multiple conflicting objectives. Those objectives may include multiple measures of nominal performance (e.g., mass, heat transfer rates, effective stiffness) as well as measures of performance variation, induced by many sources of variation or uncertainty. Furthermore, the compromise DSP has been successfully utilized for designing many types of engineering systems, and its library of overall objective function formulations has been expanded to include physical programming (Hernandez, et al., 2001), Bayesian (Vadde, et al., 1994), fuzzy (Zhou, et al., 1992), and utility theory formulations (Seepersad, 2001) for specific contexts. Since the compromise DSP has been previously developed and utilized, the contribution in this dissertation is in demonstrating that it can be used for materials design applications, specifically, mesoscale materials design involving robust, multifunctional topology design for which a flexible, multiobjective decision support construct is needed. This need is established in the following sections.

2.3 TOPOLOGY DESIGN

The second design method requirement identified for the RTPDEM in Section 2.1 is the representation and modification of topology. This is a significant challenge for a design method and requires capabilities for addressing a much broader class of problems than those for which multiobjective formulations, robust design methods, and other design tools are typically applied. Usually, these approaches are applied for modifying or refining designs for which a topology has been specified *a priori*. For example, in size and shape design applications, the dimensions and/or shape of a design are modified or synthesized, but it is assumed that the topology of the design is specified *a priori* and cannot be adjusted during the design process. (Revisit Figure 1.8 for a pictorial representation of size, shape, and topology design.) In other cases, such as some types of configuration design, a library of fixed topology designs are available from which to choose, but topology is not varied during the design process. Parametric representations can be established relatively easily for size and shape design; examples include dimensions or parametric curves that can be adjusted parametrically during an iterative design (optimization) process. On the other hand, it is not obvious how to parametrically adjust the topology of a design since changes in topology involve changes in connectivity, continuity, or material distribution/layout of a design. Topology design modifications necessarily entail changes in the number and nature of size and shape parameters required for characterizing the form or structure of a design. Fundamentally, in topology design, the connectivity of a design is not assumed *a priori*. Instead, the central focus of topology design is on simultaneously optimizing both the external shape

and the number and shape of internal boundaries with respect to a specified design objective for a given 2D or 3D domain and associated boundary conditions (Eschenauer and Olhoff, 2001). Topology design is typically conducted in the early stages of design to find ‘optimal’ concepts for further detailed design. The generation or identification of topology is particularly important due to the profound influence of topology on the subsequent performance of a design.

Scientists and engineers have investigated techniques for the optimal design of topology for at least a century.² As early as 1904, Michell (1904) investigated the form of thin truss structures for minimum mass. Rozvany and Prager extended this work for the design of optimal grillage systems—*discrete* structures comprised of beams (Rozvany, 1972) and optimal layout theory for low volume fraction *discrete* or grid-like structures (Rozvany and Prager, 1976). Discrete topology design optimization became an active research area in the 1960s and 1970s with the widespread application of computers for engineering design applications. Rozvany then formulated generalized shape optimization for *continuum* structures with higher volume fraction (Rozvany, et al., 1992). Topology optimization of continuum structures became an extremely active area of research with the introduction of a homogenization method by Bendsoe and Kikuchi (1989; 1988).

The general challenge addressed by topology design optimization techniques is the problem of material distribution in a specified domain, Ω (Bendsoe, 1995). As shown in Figure 2.6, the known quantities are the applied boundary conditions—including loads,

² The influence of shape on the strength and other characteristics of natural and artificial bodies was investigated much earlier. An example is the work of Galileo on a “theory of bodies with equal strength” in the seventeenth century.

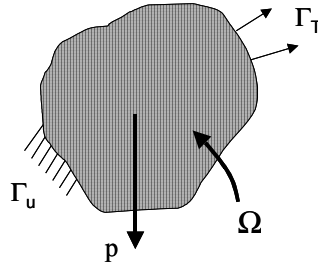


Figure 2.6 – A Design Domain for Topology Optimization

tractions, Γ_T , or body forces, p , and support conditions or displacements, Γ_u —the volume or area of the domain, and possibly the locations, shapes, and sizes of prescribed holes. The topology, shape, and physical size of the structure occupying the domain are unknown. The objective is to distribute material such that a set of constraints is satisfied and objectives are minimized or maximized. An obvious approach for topology design would be to discretize the domain into a grid of finite elements (similar to the grid pictured in Figure 2.6). Topology would be modified by discretely adding or removing elements from the grid. Three characteristics of this approach make it intractable: (1) for a domain of reasonable size and a grid fine enough to yield high-fidelity final topologies, the number of elements and associated design variables is extremely large, (2) the problem is inherently discrete in nature with 2^n possibilities where n is the number of discrete elements, and (3) the problem is ill-posed and results in lack of convergence or rapid oscillation between regions of solid and void if solved directly. Even if the resulting design problem were not ill-posed, it would be a binary design problem with very large numbers of variables. Exhaustive search would be prohibitive, given that analysis of the properties of a candidate design requires non-trivial computational

resources, and mixed integer optimization algorithms are not likely to be effective with such large numbers of variables and associated computational requirements.

Topology design techniques address this challenge by introducing continuous variables for each element that serve to relax the problem and facilitate solution of well-posed problems with a variety of optimization techniques. As discussed in the historical overview, these topology design techniques can be divided into two broad categories: (1) continuum methods in which the domain of interest is modeled as a continuum, and (2) discrete methods in which the topological domain is modeled with discrete elements (e.g., truss, beam, or frame finite elements).

In discrete topology design optimization, the domain is modeled as a finite system of pin-jointed truss elements or rigidly-jointed frame elements rather than as a solid continuum (for reviews, see (Kirsch, 1989a; Ohsaki and Swan, 2002; Topping, 1984)). The origins of discrete topology optimization approaches are usually attributed to the 1904 work of Michell (1904) on determining minimum-weight designs for a planar truss that transmits a specified load without exceeding limits on the axial stresses in the bars. Michell trusses are impractical, however, because they typically contain an infinite number of bars. Dorn (1964) overcame these limitations by introducing a ground structure that consists of a grid of points that represent joints, supports, and loading locations. The points are connected by potential members. A sample ground structure with highly connected nodes is illustrated in Figure 2.7. In ground structure-based topology optimization, the connectivity of the elements is designed—a process which includes modifying topological, sizing, and sometimes geometrical variables that specify

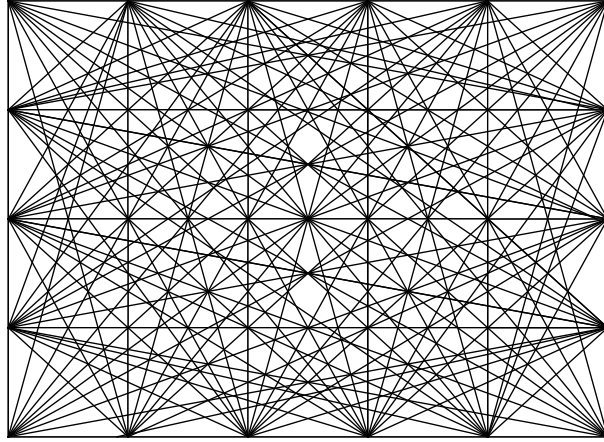


Figure 2.7 – A Highly Connected Ground Structure

element connectivity and spatial arrangement, cross-sectional dimensions of elements, and nodal coordinates, respectively.

In discrete topology optimization, the challenge is to determine the optimal connectivity (via elements) of a pre-determined set of nodes and elements for specified loading conditions. Usually, the objective involves minimizing the weight of the structure, constraints are placed on cross-sectional areas of elements, forces or stresses in elements, and other criteria. The topology optimization problem could be posed as a mixed-integer problem with 0-1 binary design variables representing the absence or existence of each element and continuous design variables representing the cross-sectional areas of each element. Such problems can be solved with computational methods such as genetic algorithms or simulated annealing (e.g., (Hajela and Lee, 1995; Topping, et al., 1996)), but the computational cost of excessive analysis can be prohibitive, and the quality of resulting topologies can be poor. Typically, the discrete topology design optimization problem is posed as a nonlinear programming problem as follows (Ohsaki and Swan, 2002):

$$\text{Minimize} \quad V = \sum_{i=1}^m A_i L_i \quad (2.16)$$

$$\text{Subject to:} \quad g_j \leq 0, \quad (j=1,2,\dots,n) \quad (2.16a)$$

$$A_i \geq 0, \quad (i=1,2,\dots,m) \quad (2.16b)$$

where A_i and L_i refer to the cross-sectional area and length of the i^{th} member (when there are m members), V is the total volume of the structure, and g_j are inequality constraints. The continuous variables are the cross-sectional areas, A_i , of each element. Mathematical programming methods such as sequential linear programming, the method of modified feasible directions, and sequential quadratic programming may be applied to Equations 2.16 to determine optimal or superior solutions in an iterative manner. The objective function usually represents the cost or weight of the structure.³ The constraints may be either behavioral—imposing limits on stresses, displacements, buckling, etc.—or geometrical—restricting cross-sectional dimensions, numbers and directions of elements, etc.

How is topology modified via the ground structure-based discrete topology optimization formulation? Typically, members with vanishing cross-sectional areas are removed from the optimized design to obtain the final topology. However, there are several important issues that arise when solving Equations 2.16 to determine the topology of a structure. First, notice that cross-sectional areas of elements are permitted to converge to zero in Equations 2.16. This may cause computational instability during the optimization process because it is possible to have a node with one or zero members connected to it, or in the case of truss-based ground structures, two colinear elements

³ Optimality criteria methods are also used, but they restrict the problem formulation more severely than nonlinear programming approaches. For example, it is difficult to accommodate large numbers of constraints with optimality criteria methods.

connected only by a hinge (with no other members connected to it). Both of these scenarios create computational problems when the displacements at the relevant, under-constrained nodes are evaluated with finite element analysis. To prevent these computational problems, a very small lower bound, A_l , on element cross sectional areas is specified. Elements with areas that converge to the lower bound should be removed from the final structure, after the optimization cycle is complete.

In topology design, seemingly simple analyses can be complicated tremendously by the fact that elements are eventually removed from a ground structure after the optimization process has converged. A designer is interested in the characteristics of the final structure (after unnecessary elements have been removed) rather than those of the ground structure before elements have been removed. The primary challenge in topology design is to simulate the impact of element removal on the behavior of a structure (without actually removing any of the elements from the structure). In discrete topology design approaches, elements to be removed are identified by their extremely small (lower bound) areas as the design optimization process converges. As elements areas converge to extremely small lower bounds, their impact on elastic structural responses such as compliance and displacement becomes negligible. However, despite their extremely small areas, the elements could be contributing to other phenomena such as buckling prevention for nearby elements, and the state of stress in the elements could be very high. However, it is meaningless to apply stress constraints and other restrictions to elements that are eventually removed, nor should the elements be permitted to contribute substantially to the performance of the structure. Whenever an analysis is performed during a topology design optimization process, it is extremely important for it to be

formulated such that the *final* structure meets requirements and objectives; i.e., the analysis must not be overly dependent on elements that are later removed. Two phenomena that illustrate this challenge in discrete topology design are stress and buckling constraints.

Stress constraints are applied for a discrete topology design formulation by modifying Equations 2.16 as follows (Ohsaki and Swan, 2002):

$$\text{Minimize} \quad V = \sum_{i=1}^m A_i L_i \quad (2.17)$$

$$\text{Subject to:} \quad \sigma_i^L \leq \sigma_i^k \leq \sigma_i^U, \text{ for } A_i > 0 \quad (2.17a)$$

$$(i = 1, 2, \dots, m; k = 1, 2, \dots, f) \quad (2.17b)$$

$$A_i \geq 0, (i = 1, 2, \dots, m) \quad (2.17c)$$

where f is the number of loading conditions and the condition, $A_i > 0$, indicates that the stress constraints should be relaxed at $A_i = 0$. The constraints must be relaxed because two types of difficulties arise when element cross-sectional areas approach their lower bounds (i.e., zero or a very small value). One concern is that constraints do not need to be satisfied by elements that are going to be removed from the topology (i.e., elements with cross-sectional areas that have approached the lower bound). Elements with cross-sectional areas above the lower bound *do* need to satisfy all of the constraints. Hence, there is a discontinuity in the constraints. Secondly, the stress in an element cannot be calculated directly from the force, N_i , and cross-sectional area of element i as follows:

$$\sigma_i^k = \frac{N_i^k}{A_i} \quad (2.18)$$

if the lower bound on cross-sectional area is zero or a very small value. A well-posed calculation of the stress in an element is obtained by calculating the strain, e_i , in element i from axial deformation, d_i (obtained from nodal displacements) as follows:

$$\sigma_i^k = E e_i^k = E \frac{d_i^k}{L_i} \quad (2.19)$$

where E is the elastic modulus. A relaxed stress constraint formulation is formulated as follows (Cheng and Guo, 1997):

$$(\sigma_i^L - \sigma_i^k) A_i \leq \varepsilon \quad (2.20)$$

$$(\sigma_i^k - \sigma_i^U) A_i \leq \varepsilon \quad (2.21)$$

$$A_i \geq \varepsilon^2 \quad (2.22)$$

where ε has a sufficiently small positive value. Using this formulation, there is no discontinuity in stress constraints as the cross-sectional area of an element approaches an arbitrarily small lower bound.

Local buckling constraints are often included, as well, but successful implementation is difficult. The Euler buckling stress replaces the lower bound on stress, σ_i^L , in Equations 2.16 with the following relation:

$$\sigma_i^L = \sigma_i^{buckling} = \frac{-\pi^2 E_i I_i}{l_i^2} \quad (2.23)$$

where E_i , I_i , and l_i are the elastic modulus, moment of inertia, and node-to-node length of the i^{th} element, and the element is assumed to have two pin-jointed ends. Local buckling constraints can prevent the existence of slender members in the final topology, if it is derived from pin-jointed truss structures. Buckling constraints are very difficult to impose, however, because the characteristic length for buckling depends partially on the

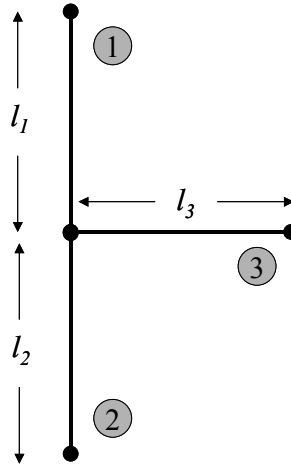


Figure 2.8 – Local Buckling Analysis in Discrete Topology Optimization

status of neighboring elements (Rozvany, 1996). Suppose three members meet at a node in an initial ground structure, as shown in Figure 2.8. For analysis purposes, one would assume that the characteristic length of each member is equivalent to the node-to-node length of the element (e.g., l_1 for element 1). If the cross-sectional area of member three converges to its lower bound during the design process, it is removed from the final topology. Then, two problems arise. First, the solution becomes unstable if the two elements are joined at a hinge joint. Second, the actual characteristic buckling length is equivalent to the sum of the element lengths (i.e., $l_1 + l_2$), rather than the length of an individual element, and the actual critical buckling load is lower, implying that the critical buckling load may be exceeded by the final topology of the structure. It is not practical to cancel or remove joints systematically in a ground structure, however, because one would have to redesign the structure for every possible discrete combination of joint removals—a computationally expensive task. System stability constraints and imperfections in the ground structure have been introduced to prevent unstable optimal

solutions, but they sometimes lead to nonoptimal solutions, as well (Rozvany, 1996). Thus, local buckling constraints should be used with caution.

Another important issue in the solution of Equations 2.16 is the global quality of the final solution. Although mathematical programming algorithms are applied to Equations 2.16, it is very difficult to identify a globally optimal solution and local optima are often encountered due to the nonlinear, nonconvex nature of objectives and/or constraints in many problem formulations. If enough joints and members are included in a ground structure, it is generally true that the layout is not necessarily unique; rather, multiple layouts yield identical or similar objective function values. The quality of the solution may be assessed by comparing its associated objective function value with a lower bound value obtained by relaxing or neglecting some of the problem constraints, such as compatibility conditions or stress constraints, and solving a simplified linear programming problem (Kirsch, 1989b).

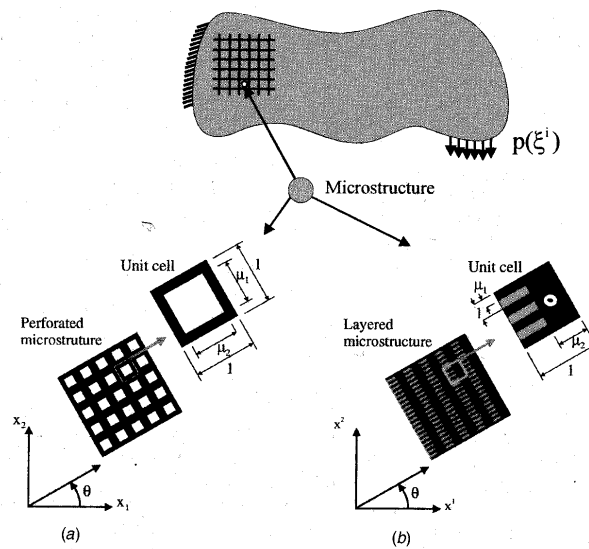


Figure 2.9 – Perforated and Layered Microstructure Material Models (from (Eschenauer and Olhoff, 2001))

In *continuum* topology design approaches, a structure is modeled as a solid continuum of variable topology, and spatially distributed design variables are used to vary the material distribution in a structure. Essentially, the material at any point x in a domain is permitted to partially occupy the point via formulations based on composite materials or mixtures. The *partial* occupation of a point can be described via a number of material arrangements. For example, in the homogenization approach, material is modeled with a periodic, porous microstructure that permits continuous variation of the density and orientation of each element or cell, as shown in Figure 2.9. In fact, continuum topology design optimization has been an active area of research since the seminal papers by Bendsoe and Kikuchi (1988) and Bendsoe (1989) who introduced the homogenization approach. Other material models for continuum topology design include two-dimensional and three-dimensional layered microstructures in which two different isotropic materials are stacked in alternate layers (e.g., (Bendsoe, 1989)), as shown in Figure 2.9. Also, mixing rule formulations have been proposed in which effective properties are evaluated with mixing rules rather than microstructure descriptions and homogenization techniques. An example is the artificial material model (Bendsoe, 1989) in which the design domain is partitioned into a grid of finite elements. The elasticity tensor of each element, E_{ijkl} , and the volume of a structure are given by (Eschenauer and Olhoff, 2001):

$$E_{ijkl}(x) = \rho(x)^p E_{ijkl}^0 \quad \text{Volume} = \int_{\Omega} \rho(x) dx \quad (2.24)$$

where $\rho(x)$ is a density function, E^0 is the elasticity tensor for a solid isotropic material, and p is a constant greater than one that penalizes intermediate material densities since at

such densities, the material has diminished properties relative to a reference material at the same cost in terms of weight. In all of these material models, an interpolation is established between pure void and pure solid material behavior.

As noted previously with respect to Figure 2.6, continuum topology design optimization begins with a spatial domain, Ω , a set of boundary conditions, and an initial material layout. The performance of the structure is evaluated with respect to any of several criteria, including stiffness, compliance, eigenvalues, critical buckling loads, ultimate strength, and non-performance based measures such as weight, volume fraction, or total perimeter of solid material. The performance criteria are evaluated using a low-order finite element discretization of the domain, usually with bilinear two-dimensional plate or shell elements or trilinear three-dimensional elements. Using one of the described approaches, material is arranged or distributed in the domain to satisfy constraints and maximize or minimize specified objectives.

A sample cantilever beam, designed with the artificial material model, is illustrated in Figure 2.10. As evident from comparisons of Figure 2.10 with some of the designs illustrated in Chapter 6, the nature of final solutions is very different from those derived

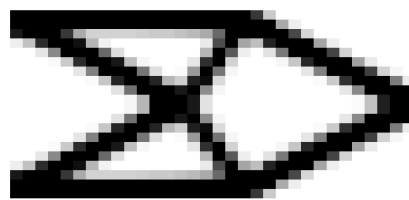


Figure 2.10 – A Cantilever Beam Designed with the Artificial Material or SIMP Topology Optimization Approach

from discrete approaches because the domain is modeled as a solid continuum. In the final design, the material arrangements must be interpreted or post-processed into an object with clearly defined boundaries that may not resemble a system of discrete members with well-defined members as in discrete topology design. This is sometimes difficult if large regions of grey, partially dense regions exist in the final design. In practice, several difficulties have been encountered in continuum-based approaches, including the presence of checkerboard (alternating solid and void) patterns that are not physically realizable. Filters, perimeter control techniques, and other methods are typically applied to prevent the emergence of checkerboards and reduce the mesh-dependence of final solutions. In general, many locally optimal solutions exist for most topology design problems.

What are the relative strengths and weaknesses of the continuum and discrete topology design approaches? Discrete topology design approaches are relatively straightforward to implement. The design variables are simply the areas or thicknesses of the beam or truss elements that connect the grid of nodes. After the design optimization process is complete, the structure is post-processed by removing elements with areas near the lower bound value. A similar step is performed in continuum approaches in which a threshold is established to distinguish or filter solid areas from empty or void areas. For example, in the artificial material model, elements with a density above the threshold are considered solid and those below are considered void. During the design optimization process, filtering is not necessary for distinguishing solid and empty areas in discrete topology design approaches. The edges of the elements establish the solid boundaries. In continuum approaches, the boundary between solid and void is not clearly demarcated

during the design optimization process. As can be seen in the gray areas of Figure 2.10, there are typically regions of intermediate status that cannot be labeled solid or void without a filtering process. The capability of distinguishing the precise boundaries of solid material *during* the design optimization process may be important for several reasons. For example, it may be necessary to set limits on feature sizes such as maximum dimensions, angles, or shapes for manufacturing reasons. Also, it may be necessary to consider variability in element or solid material dimensions or random failure of members within a large structure. These things are difficult to consider during design optimization with continuum approaches because it is not possible to demarcate clearly the boundary of solid material during the design optimization process. This feature of continuum topology design approaches also makes it difficult to consider any shape-dependent boundary conditions and phenomena that cannot be expressed exclusively as functions of a continuous spatial distribution of material but require identification and assessment of the boundaries, shape, and critical dimensions of solid material. For example, convective boundary conditions associated with internal forced convection are functions of the shape and size of holes in the structure, and of course, the boundaries of holes are difficult to discern and emerge actively during a continuum-based topology design process. Buckling is another shape-dependent phenomenon that requires knowledge of the precise length and cross-sectional geometry of a material segment—as well as loading and end conditions—which are difficult to determine during a continuum-based topology design process. It is also difficult to apply stress constraints during a continuum-based topology design process because the final size and shape of the cross-sectional areas of parts of a structure are unknown. Continuum topology design really

only tells a designer where elements should be positioned and approximately what position, shape, and size they should have. Usually, other considerations are addressed in post-processing when dimensions may be adjusted for stress constraints, manufacturing considerations, and other issues. With discrete topology design approaches, it is possible to consider shape-dependent phenomena during the topology design process since the boundaries of solid material are clearly and inherently demarcated.

While post-optimization filtering is common for both categories of approaches, the structures that are obtained may be quite different in nature. With discrete approaches, the geometry of the final structure can be obtained directly from the topological model with the exception of some smoothing that may be needed at the joints where elements typically overlap. Structures achieved with continuum approaches tend to have jagged boundaries, as can be seen in Figure 2.10. Interpretation and curve- and surface-fitting are required to render a solid model of the structure in a CAD application and then analyze the properties of the structure with a CAE package such as ANSYS or FLUENT. Therefore, with continuum-based approaches, a substantial amount of design is required during post-processing. There is no guarantee that post-processing changes to an ‘optimal’ design will not negate the relative benefits—relative to ad-hoc or previously available designs—obtained by performing topology design.

Unrealistic or unstable solutions are obtained sometimes from both continuum and discrete approaches. In discrete approaches, too many members may be removed resulting in unstable, mechanism-like motion (with truss-based rather than frame-based ground structures) or lack of connectivity between elements. Lack of connectivity may manifest itself as an element with a free end, unconnected to other elements and

performing no function. In continuum-based approaches, it is common to find unrealistic checkerboard patterns of elements with nearly full and nearly zero density. In other words, the solution often tends toward a design with a very large number of small holes rather than a few macroscopic holes, and this is undesirable for further analysis and manufacturing. Perimeter bounds, local filtering, and constraints on material density gradients are some of the techniques that have been used to avoid these problems by preventing rapid oscillations in the density of the material in the structure (Eschenauer and Olhoff, 2001).

While discrete topology design approaches require less post-processing and are more suitable for analysis of shape-dependent phenomena, there are some associated limitations. For example, topology designs may depend strongly on the initial ground structure. Important features of the ground structure include the number and location of nodes and the initial placement of elements and associated connectivity of nodes. These features determine the mesh density as well as the space of potential solutions; a solution must be a subset of the initial ground structure. Generally, a large number of initial elements and nodes are needed in the initial ground structure to achieve a high-fidelity, high quality final design. It is very difficult to *add* elements or nodes during a design optimization process. For example, Reddy and Cagan (1995) suggested a formal grammar for modifying a truss by subtraction *and* *addition* of elements. However, it is very difficult to achieve high-quality solutions (with performance that meets or exceeds that of other feasible solutions) with their approach, and the required stochastic algorithms lead to a very large number of iterations and resulting computational inefficiency relative to standard approaches.

For reasons established in the previous discussion, discrete topology design approaches are utilized in this dissertation. Because discrete topology design approaches clearly demarcate regions of solid and void during the topology design process, they facilitate the consideration of manufacturing and multifunctional criteria during the topology design process. Also, discrete approaches do not require significant post-processing of resulting designs, making it easier to transfer design specifications between simulations without building or rebuilding a geometric model. Although continuum topology design approaches are not investigated explicitly in this dissertation, it is anticipated that many of the methods proposed in this dissertation and validated via application of discrete topology design methods are also applicable for continuum topology design methods. This issue is revisited in Chapter 8. Unfortunately, in their present form, topology design approaches do not address all of the design method requirements identified in Section 2.1.

What are some of the limitations of current topological design capabilities in the context of materials design? In their present form, how well-suited are topology design techniques for addressing the materials design challenges outlined in Section 2.1 and in Chapter 1? Topology design techniques have been applied for designing materials with prescribed elastic and thermoelastic macroscopic properties. Sigmund (1994; 1995) uses both discrete and continuum topology design methods for tailoring the constitutive tensors (i.e., elastic properties) of materials in two dimensions. Periodic base or unit cells are designed for minimum mass and constrained constitutive parameters (i.e., elements of the constitutive tensor that relates stress and strain in a linearly elastic solid). Materials with extreme elastic properties, such as negative Poisson's ratio are also obtained.

Sigmund and Torquato (1997) design materials with extreme thermoelastic properties, including maximum thermal expansion (e.g., thermal actuators) and negative isotropic thermal expansion. Their approach is a three-phase topology design method that distributes a void phase and two material phases with different but positive thermal expansion coefficients. Similarly, Sigmund (2000) uses a continuum topology design approach to design two-phase composite materials with extreme bulk moduli. Hyun and Torquato (2002) design two-dimensional cellular solids for optimal effective bulk and shear moduli and effective conductivity.

The work of Sigmund, Torquato, and Hyun suggests that topology design methods can be applied not only for designing large-scale structures but also for designing material microstructures with tailored elastic and thermoelastic properties; however, several requirements are associated with materials design that are not necessarily important for larger-scale structural applications. Some of these design method requirements are identified in Section 2.1 and in Tables 1.1 and 1.2. Specifically, design methods are required to facilitate not only topology design but also robust design and multifunctional design. For example, even small-scale changes in dimensions or topology of a material can have a significant impact on its properties and performance because the material structure itself is manifested on a small scale; whereas small dimensional tolerances may have a negligible impact on the properties of a large-scale bridge, for example. Furthermore, materials design applications are inherently multifunctional with a material being required to function in multiple physical domains in almost all applications. In the structural problems for which topology design methods have primarily been developed and applied, the focus is almost exclusively on structural

properties. Very little work has been done to merge topology design techniques with robust design and multidisciplinary design methods, as proposed for the RTPDEM, and establishing robust, multifunctional topology design methods is a challenging objective. In the following sections, progress towards robust topology and multifunctional topology design methods is reviewed, and limitations of previous approaches are identified.

2.3.1 Robust Topology Design

Topological design problems are usually formulated as optimal design problems with respect to a prescribed loading. Important factors like loading and boundary conditions, material properties, and dimensions are expressed as deterministic, single-valued parameters. Resulting topologies are ‘optimal’ only for the specific parameter values assumed during the optimization process. An important question to ask is: *what happens to the performance of a specific design when critical parameter values change?* In other words, *how sensitive is an ‘optimal’ design to the conditions for which it was optimized?* *If the conditions change, would the design specifications change as well, and would the performance of the original design degrade when exposed to the varied conditions?* For example, as illustrated in Figure 2.11, the design specifications of a cantilever beam change considerably when the direction of the applied load changes. The structures in Figure 2.11 were obtained with a topology design optimization algorithm based on the



Figure 2.11 – Changes in Cantilever Beam Structure as Load Direction Changes

artificial material model with all parameters held constant from scenario to scenario except the direction of the applied loading. As can be seen in the difference between structures A, B, and C in Figure 2.11, very small changes in loading direction can cause significant changes in topology. In other cases, such as structures C, D, and E in Figure 2.11, small changes in loading direction change the size and shape of elements of a structure but not its topology in a strict, mathematical sense.⁴ One of the reasons for the changing design specifications in Figure 2.11 is that a design's nominal performance—defined as its behavior in response to nominal parameter values—is often very different in magnitude from its performance when critical parameter values are changed. For example, the structure designed for only horizontal or coincident loads (i.e., structure A in Figure 2.11) seems to be very sensitive to small changes in loading direction because its topology changes dramatically from structure A to B when a small vertical load is applied in addition to the horizontal load. Often, alternative designs differ in both nominal performance and performance sensitivity in response to parameter deviations. Sometimes, a design can be identified with performance that is less sensitive to variations from nominal parameter values than the design that is 'optimized' for nominal parameter values. For example, as the direction of applied load changes, the topology of structure E in Figure 2.11 remains relatively stable compared with structure D which has been designed for a slightly different loading direction. On the other hand, structure A exhibits dramatic changes in topology compared with structure B. The cantilever beam (E in

⁴ In a strict mathematical sense, topology is defined as the connectivity of a structure; therefore topology changes only when the number of holes or discontinuities in a structure changes. In less strict technical applications, the term topology is used to refer to the number, shape and size of internal holes and the shape and location of external boundaries of a structure. In the latter sense, all of the structures in Figure 6 have different topologies, but in the strict mathematical sense, only structures A, B, and C have different topologies with structures C, D, and E exhibiting equivalent topology.

Figure 2.11) designed for vertical loads appears to be less sensitive to changes in applied loading direction than the structure (A) designed for purely horizontal loads. However, in most cases, a reduction in sensitivity is not achieved without a compromise in nominal performance. For example, if nominal loads are expected in the horizontal direction with small fluctuations in direction, structure E may be less sensitive to loading direction variations, but structure A is obviously stiffer in response to strictly horizontal nominal loads than other structures with equivalent mass of material. Therefore, if deviations are expected in design parameters, it is important to consider not only nominal performance but also performance variation or sensitivity *during the topology design process*. Robust topology design methods are needed that facilitate the search for designs that embody preferable tradeoffs between nominal performance (which may be minimized, maximized, or target-matched) and performance variation or sensitivity.

In recent topology design research, authors have noted that both the structure and performance of ‘optimal’ topology designs tend to be sensitive to assumed conditions for applied loading. In response, they have considered multiple potential loading conditions and designed topologies for either average or worst-case performance requirements (e.g., (Ben-Tal and Nemirovski, 1997; Cherkaev and Cherkaeva, 1999; Christiansen, et al., 2001; Diaz and Bendsoe, 1992; Diaz, et al., 1995; Kocvara, et al., 2000)). In these cases, a design is typically subjected to a finite set of potential loading scenarios, the performance of the structure is assessed for each scenario, and an objective function is evaluated either as a weighted sum of performance functions for each loading scenario or as a minimum performance function for all loading scenarios for average or worst-case formulations, respectively. The worst-case formulation is closely related to reliability-

based approaches that have been applied in topology design (Bae, et al., 2002; Maute and Frangopol, 2003; Thampan and Krishnamoorthy, 2001) in which the objective is either to minimize or to constrain the probability that a performance value is larger or smaller than a target value when loading conditions or material properties are stochastic. In investigations of both multiple loads and reliability, authors generally find that stochastic variations in loading conditions have a significant impact on the ‘optimum’ structural topology with redundancy, stability, member thicknesses, and structural weight generally increased.

As will be discussed in Section 2.4, average and worst-case formulations are very different from robust design approaches, in which a balance is sought between achieving mean performance requirements and minimizing the *sensitivity* of design performance with respect to variations in boundary conditions, dimensions, material properties, or other factors. When topology is designed for average performance, the sensitivity or variation in performance is not explicitly considered; therefore, a resulting design may have desirable average performance but suffer severe performance degradations due to small changes in design parameters. When worst-case or reliability-based approaches are utilized, emphasis is entirely on extreme or worst-case values of performance without regard for mean performance or for the tradeoffs between improving mean performance and reducing the variation between mean and extreme values of performance. Reliability-based design for a specific risk or reliability level may be appropriate for hard constraints that cannot be violated without risk of catastrophic failure. On the other hand, *objectives* are conceptualized as soft constraints with associated target values that are desirable to achieve but not absolutely required. Since extreme objective function values

are usually undesirable but not catastrophic, it is important to focus on the nominal or expected performance of a design along with variations from the nominal value—two factors that are considered in robust design approaches.

The critical question is *how can robust designs be identified or generated during a topology design process?* Considering robustness or sensitivity to variation (along with nominal performance) *during* the design process itself is very important. As illustrated with respect to the cantilever beam examples in Figure 2.11, designs with significantly different structures may have similar nominal performance but vastly different sensitivities to variation in boundary conditions, material properties, and other factors. The objective of a robust design process is to identify robust designs that are likely to sustain greater variations from nominal design parameter values without significant variation in performance when compared with non-robust designs because robust designs have been designed with both nominal performance and performance variation in mind.

A preliminary investigation of robust topology design has been reported by Sandgren and Cameron (2002). Their investigation was limited to Type I sources of variability in loading conditions and material properties, and their approach was highly computationally intensive—relying on genetic algorithms nested with nonlinear programming algorithms for optimization and Monte Carlo analysis for each evaluation of the objective function to approximate the output distribution. They considered robustness by formulating constraints as functions of nominal values and standard deviations for each constraint. However, they did not consider the robustness of objectives; this makes their approach a *partial* implementation of robust design.

While Sandgren and Cameron's approach represents a significant departure from previously proposed average, worst-case, and reliability-based approaches for topology design, several challenges remain unanswered. Many of the challenges are associated with the unique difficulties of topology design and can be mapped from the desirable characteristics for a comprehensive robust topology design approach:

(1) A robust topology design approach should accommodate both Type I and Type II robust design. Type I sources of variation include boundary and loading conditions (magnitudes and directions) and material properties. Type II sources of variation include the size, shape, and topology of a structure. For example, in materials design applications, dimensions and shapes of regions of a solid material (or phase) are likely to be induced by materials processing or fabrication. It is also possible that variations from nominal, intended topology will be observed; for example, missing or broken cell walls or joints in a prismatic cellular material. Since the primary focus of topology design is to determine the connectivity of material, it is important to consider the status and potential variation of this connectivity in light of potentially broken members or missing joints between members. The latter phenomenon is labeled topological variability in this dissertation. Type II robust design has not been considered in a topology design setting, and topological variability has not been considered in the robust design literature at all. Since topology is determined in the early conceptual stages of design, it is extremely important to consider all of these sources of variability during topology design so that the resulting structure meets performance requirements despite deviations from its nominal structure during latter stages of design or during fabrication and processing.

Furthermore, it is important to formulate robust design *objectives* as well as constraints for topology design—something that has not appeared in the topology design literature.

(2) A robust topology design approach should be computationally tractable and efficient. To pursue robust topology designs, it is necessary to evaluate the sensitivity or variation of objectives and constraints for each iteration of the design process and to incorporate those measures into the objective and constraint functions. Evaluating response variation involves propagating or transmitting variation from its sources to the responses themselves. Several possible ways of accomplishing this are suggested in Section 2.4. A unique challenge in topology design is its combination of (a) large numbers of variables, and (b) non-negligible computational times per iteration. These factors make it very difficult to use either surrogate models (which require experimental data points that grow exponentially in number with the number of design variables or parameters) or Monte Carlo analysis and similar methods that require large numbers of function evaluations to assess the distribution of responses. Sandgren and Cameron (2002) used Monte Carlo analyses, but the extensive computational times associated with this approach may prohibit its use for relatively large structures. In the robust topology design approach introduced in Chapter 3, analytical gradients are used whenever possible to reduce this effect.

(3) In topology design, unlike other applications of robust design methods, some variables are eventually turned ‘off’ and their associated elements or regions of material are removed from the final topology. This is accomplished typically by allowing the area or density of an element to approach a very small positive value (nearly zero) that serves as a lower bound on the design variables during the iterative design process. After the

search or optimization algorithm has converged to a solution, the elements with areas or densities between the lower bound and a very small threshold value are removed from the topology. This process is successful because an element's contribution to the performance of the entire structure becomes negligible as its area or density vanishes. Similarly, in robust design, an element's contribution to the overall variation in performance of a structure should become negligible as its area or density vanishes. In other words, an element's contribution to a total objective function—including nominal performance and performance variation components—should approach zero as its density or area vanishes. Otherwise, there would be a large, undesirable change in performance of a topology upon removal of the appropriate elements. Although robust design methods tend to yield overdesigned structures, this tendency cannot prevent the smooth removal of elements and the corresponding changes in topology that are the focus of topology design methods.

A comprehensive robust topology design approach—the RTPDEM—is introduced in Chapter 3 to address these challenges fully. The RTPDEM simultaneously addresses the need for multifunctional topology design established in the next section.

2.3.2 Multifunctional Topology Design

In addition to topology and robust design, the design method requirements for the RTPDEM include the need for multifunctional design. In a truly *multifunctional* application, objectives are pursued in multiple physical domains, such as heat transfer and structural mechanics. Topology design and optimization techniques have been developed primarily by the solid mechanics community, and objectives have been limited mostly to structural considerations such as compliance, eigenvalues, and deformation. To

date, multi-physics applications of topology optimization have not been truly multifunctional. They have been limited to coupled field problems in structural analysis in which the interactions of temperature, electric fields, and/or magnetic fields with deformation are examined for applications such as piezoelectric or electrothermomagnetic actuators (c.f., (Sigmund, 1998; Sigmund and Torquato, 1997)) or thermoelastic materials (Sigmund and Torquato, 1997). In the field of thermal design, Li and coauthors (2000; 1999) have extended topology design methods—namely, the Evolutionary Structural Optimization approach—for topology design for steady state heat conduction with multiple heat sources. In this approach, a structure is subjected to finite element thermal analysis, and small regions that do not contribute substantially to heat conduction, as evidenced by relatively low heat flux density, are removed.

Topology design and optimization methods have the potential for facilitating the search for *globally* superior designs characterized by nearly arbitrary topology, shape, and dimensions. However, to date the approaches have not been extended for truly multifunctional applications of interest such as linear elasticity combined with conjugate (conduction and convection) heat transfer in a general case involving internal or external convection and conduction along with other multifunctional objectives. Consideration of multifunctionality is likely to increase the scale, complexity, and computational expense of a topology design problem. It is not only difficult (if not ineffective or infeasible) to apply structural topology design techniques directly for many other physical phenomena but also practically impossible to *analyze* other phenomena—such as convective heat transfer or catalysis behavior—during a structural topology design process. There are two related reasons for this difficulty. First, many phenomena—such as convective heat

transfer and catalysis—are dependent on the shape and size of the *voids* rather than the structure of the material itself. These phenomena are not easily homogenized, and it is therefore difficult to formulate a well-posed topology design problem using existing continuum or discrete topology design approaches. Secondly, the topology of the *final*, post-processed topology design—including the number, configuration, and scale of solid phases and voids—is very different from that of the ground structure or evolving continuum model utilized during topology design. Analyzing the heat transfer characteristics of the ground structure in Figure 2.7, for example, with a plethora of small-scale voids would be meaningless if the final structure retains only a small fraction of the elements and therefore only a few, relatively large voids or passageways for convective fluid. When elements are removed from a topology at the *end* of a topology design process, the size and scale of the voids increases, and this is a critical factor in the heat transfer characteristics of the design to the extent that the heat transfer characteristics of a final topology design may be unrecognizable from the results of a ground structure-based analysis.

To illuminate the difficulty of establishing a truly multifunctional topology design approach, consider a characteristic heat sink application involving conjugate heat transfer with conduction and internal forced convection. As illustrated in Figure 2.12, the heat exchanger domain is limited to a volume with dimensions W by D by H . The mechanism for heat dissipation is forced convection via cooling fluid which flows into the heat sink at a constant ambient temperature, T_{in} . The challenge is to transfer heat away from a high temperature heat source such as a microprocessor. The structure of the heat sink interior is entirely unspecified, as represented by the hatched interior region in Figure 2.12.

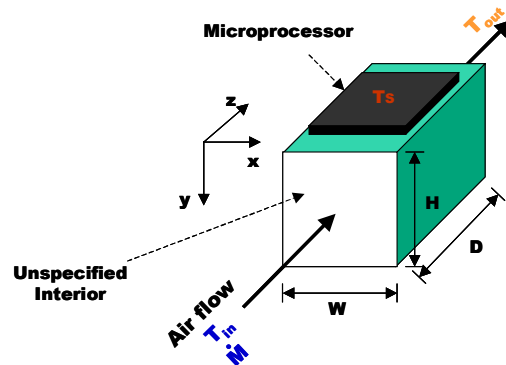


Figure 2.12 – Sample Heat Sink

During the multifunctional topology design process, the distribution of material within the heat sink needs to be determined. This task involves specifying the shape, number, dimensions, and connectivity of heat transfer surfaces or walls within the space that maximize the rate of heat dissipation (and fulfill other multifunctional objectives such as overall structural stiffness, volume fraction, etc.).

It is impossible to apply structural topology design techniques directly to this example for several reasons. First, boundary conditions must be specified for solid heat sink material for any surface that is exposed to the convective fluid medium. For internal forced convection, several types of information are required in order to specify these boundary conditions: (1) the precise location of the boundaries or surfaces at which fluid and solid meet, (2) the geometry of the convective passageway, (3) properties of the fluid within the convective passageway such as density, viscosity, and specific heat—all of which are temperature dependent—and (4) flow conditions. A common aspect of continuum topology optimization approaches is the presence of partially dense regions in the design domain throughout the optimization process. As a result, it is difficult (sometimes even at the end of the optimization process) to clearly separate solid and void

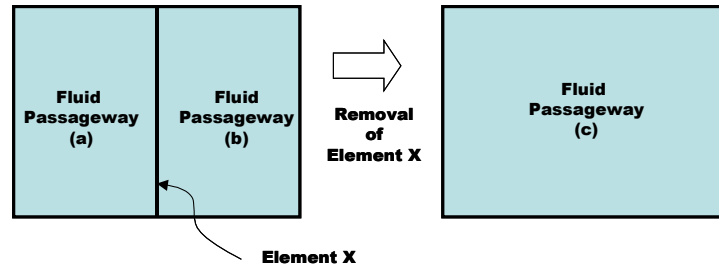


Figure 2.13 – Effect of Wall Removal on the Geometry of a Fluid Passageway

(which would be occupied by convective fluid in this case) due to the presence of partially dense regions. Therefore, it would be difficult to apply shape-dependent convective boundary conditions to the interior voids in an evolving structure, and it is unclear how one would specify fluid flow properties in partially dense elements. Ground structure-based discrete topology design approaches do not pose this problem because the solid and void/fluid regions are always clearly demarcated; however, there are other challenges associated with applying these techniques. Typically, in structural applications, boundary conditions are specified a priori and do not vary with adjustments to the topology itself during the optimization process. For heat sink applications, boundary conditions for thermal elements (of solid material) change as the topology changes. Changes in topology or shape within a heat sink impact the geometry of neighboring fluid passageways. Geometry changes in a passageway influence the associated convective coefficients and mean temperature of the fluid medium. These factors directly influence the boundary conditions for the thermal elements that partition the heat sink domain; thus, the boundary conditions are not static but depend on the shape, size, relative location, and number of interior voids. Furthermore, these changes in boundary conditions are not continuous. As illustrated in Figure 2.13, removing a wall

invokes a discrete change in boundary conditions due to the associated discrete change in hydraulic diameter and associated properties. Therefore, it is not sufficient to perform topology design exclusively by allowing the cross-sectional areas of elements to approach a very small lower limit. Regardless of the lower limit on cross-sectional area, the element will always separate its two neighboring fluid passageways. When the associated elements are actually removed from the structure (after the optimization cycle is completed), the properties and performance of the structure may change significantly. Therefore, it is desirable to anticipate these changes in a way that can inform the design/optimization process.

Two types of foundational constructs are needed to facilitate truly multifunctional topology design. First, as mentioned in the previous paragraphs, a technique is required (for each functional analysis) of anticipating and/or parameterizing the contribution of each topological element to overall functional performance. In structural topology design applications, density or area/thickness variables serve this role. However, this parameterization is not sufficient for many other applications, such as conjugate heat transfer with shape- and topology-dependent boundary conditions and other complicating factors. If topology design problems are parameterized differently for different functional domains, it may be necessary to perform multifunctional topology design in multiple topology design stages (associated with different functionalities) or by iteratively cycling through multiple design stages. This challenge is revisited in Section 2.4.4.

Second, a foundational construct is needed for structuring and supporting the multiobjective decisions that are central to multifunctional topology design. In structural

topology design applications, multiple objectives have been modeled with a weighted sum formulation (c.f., (Diaz and Bendsoe, 1992; Diaz, et al., 1995; Frecker, et al., 1997)), a min-max formulation (Krog and Olhoff, 1999), a norm or compromise programming formulation (Chen and Wu, 1998; Ma, et al., 1995; Min, et al., 2000), or by combining multiple objectives into a single overall metric (c.f. (Frecker, et al., 1999; Saxena and Ananthasuresh, 2000)).

When coupling topology design with multifunctional and robust design requirements, a designer is faced with a much more complicated task of balancing conflicting objectives in two dimensions. First, compromises must be achieved between multiple objectives associated with multiple functional aspects of performance. Second, nominal performance must be balanced with robustness for each objective. This has not been demonstrated for topology design applications. A flexible, domain-independent, multiobjective decision support construct is needed to fulfill this role. In Section 2.2, it is argued that the compromise DSP has these characteristics. By building upon its mathematical and goal programming foundations, the compromise DSP facilitates identification of design variable values that satisfy a set of constraints and bounds and achieve a set of conflicting goals as closely as possible. It offers flexibility for (1) considering multiple goals, including measures of robustness, along with hard constraints (2) incorporating engineering judgment in the problem formulation in the form of constraints, bounds, and assumptions, (3) utilizing alternative objective function formulations such as the preemptive, Archimedean, physical programming, and utility theory formulations, according to the characteristics of the problem, and (4) adjusting weights, target values, and any other objective function parameters for generating

families of compromise solutions. Therefore, the compromise DSP is proposed in Hypothesis 3 as a mathematical construct for modeling and supporting multifunctional, robust topology design decisions.

2.4 ROBUST DESIGN AND ROBUST CONCEPT EXPLORATION

One of the research opportunities identified in Section 2.3 is the need for a comprehensive robust topology design method that is suitable for multifunctional applications. In this section, robust design methods, principles, and techniques are reviewed as a partial foundation for establishing such a method. The foundations for robust design in theory and practice are based on the philosophy of Genichi Taguchi, a Japanese industrial consultant. These foundations are reviewed in Section 2.4.1. During the last two decades, significant industrial and academic attention has been devoted to applying Taguchi's robust design philosophy for engineering design applications. As a result, many robust design methods and techniques have been proposed for improving the effectiveness and applicability of robust design for a wide variety of applications, including those involving computer simulation and experimentation. These approaches are reviewed in Section 2.4.2. Many of these approaches are focused on detailed design applications for products or processes with relatively mature design specifications that are 'tweaked' to increase robustness. Furthermore, it is implicitly assumed that all relevant aspects of a system are designed simultaneously by a single designer or decision-maker; distribution, concurrency, or decomposition of design activities for complex systems or multidisciplinary applications is not typically considered for robust design. However, these assumptions are not appropriate for the design context established in this dissertation, as highlighted in Section 2.1. Accordingly, robust design for the early stages

of design is reviewed in Section 2.4.3 and multidisciplinary robust design is discussed in Section 2.4.4. Finally, research opportunities in robust design for multifunctional topology and materials design applications are presented in Section 2.5.

2.4.1 The Taguchi Approach for Robust Design

Robust design is a method for improving the quality of products and processes by reducing their sensitivity to variations, thereby, reducing the effects of variability without removing its sources (Taguchi, 1986; Taguchi and Clausing, 1990). A robust design is a product or process that can be exposed to variations—in the manufacturing process and environment, in customer operating and usage conditions, or in the design specifications themselves—without suffering unacceptable performance degradations. The collection of design principles and methods known as robust design is founded on the philosophy of a Japanese industrial consultant, Genichi Taguchi, who proposed that product design is a more cost-conscious and effective way to realize robust, high-quality products than by tightly controlling manufacturing processes.

Instead of measuring quality via tolerance ranges—a common practice in industry—Taguchi proposed a Quality Loss Function in which the quality loss, L , is proportional to the square of the deviation of performance, y , from a target value, T , as illustrated in Figure 2.14.

$$L = k(y - T)^2 \quad (2.25)$$

As shown in the figure, any deviation from target performance results in a quality loss. The Quality Loss Function represents Taguchi's philosophy of striving to deliver on-target products and processes rather than those that barely satisfy a corporate limit or tolerance level (as illustrated in Figure 2.14). From Taguchi's perspective, tolerance

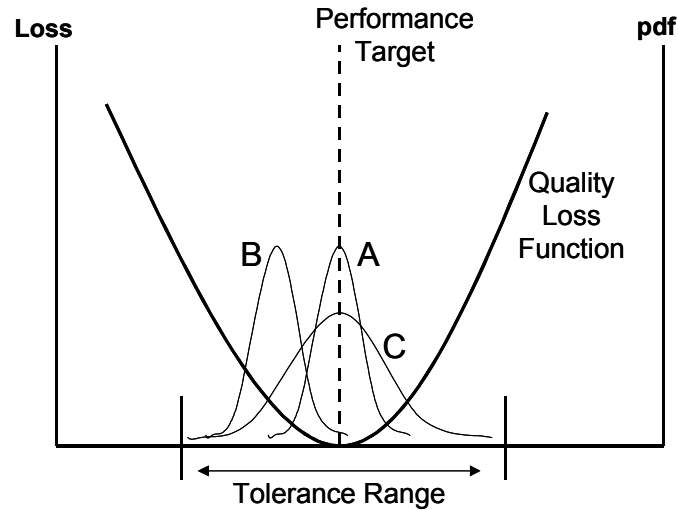


Figure 2.14 – Taguchi’s Quality Loss Function

design—which involves tightening tolerances on product or process parameters—is expensive and should be utilized only when robustness cannot be ‘designed into’ a product or process by selecting parameter levels that are least sensitive to variations. Robust design occurs during the parameter design stage that precedes tolerance design but follows the system design in which a preliminary layout is specified for the product or process. Taguchi notes that too many tolerance-driven engineers skip directly from system design to tolerance design and ignore the critically important parameter design stage.

Taguchi’s robust design approach for parameter design involves clearly separating *control factors*—design parameters that can be controlled easily—from *noise factors*—design parameters that are difficult or impossible to control. Designed experiments, based on orthogonal arrays, are conducted in control and noise factors to evaluate the effect of control factors on nominal response values and sensitivity of responses to variations in noise factors. The overall quality of alternative designs is compared via

signal to noise ratios that combine measures of the mean response and the standard deviation. Product or process designs, characterized by specific levels of control factors, are selected that maximize the signal to noise ratio. The intent is to minimize performance deviations from target values while simultaneously bringing mean performance on target. By this measure, a designer would search for solutions such as Product A in Figure 2.14 which offers both on-target performance and minimal standard deviation, compared with Products B and C, respectively, and therefore lower quality loss.

In robust design, it is important to take advantage of interactions and nonlinear relationships between control and noise factors to dampen the effect of noise factors and thus reduce variation in the response(s). This effect is illustrated in Figure 2.15. As shown in the figure, control factor settings are chosen to minimize the sensitivity of a design to fluctuations in noise factors. Similarly, if control factors are expected to

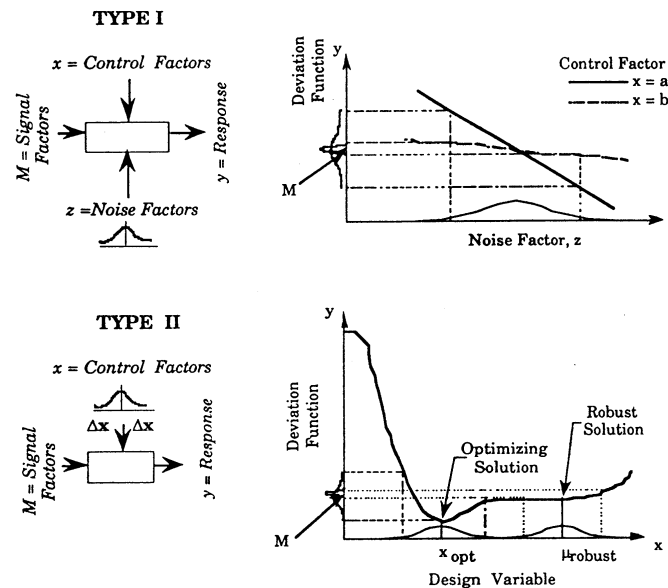


Figure 2.15 – Robust Design for Variations in Noise Factors and Control Factors (Chen, et al., 1996b)

fluctuate, control factor settings are chosen that minimize the sensitivity of overall system performance to control factor variation. As shown in Figure 2.15, compromises must be made typically between mean performance and performance variation. Robust solutions may not be ‘optimal;’ conversely, optimal decisions are rarely robust.

Undoubtedly, Taguchi initiated a paradigm shift in engineering design towards considering quality, robustness and variability earlier in the design process rather than exclusively in the final, detailed stages of design when tolerances are specified. He also encouraged designers to design quality into products and processes rather than imposing it during the manufacturing process. Quality engineering that focuses exclusively on tolerancing has proven to be a very expensive approach relative to robust design. Precision manufacturing is costly. As a result of Taguchi’s influence, statistical methods are more commonly used during the design process to consider the non-deterministic nature of many factors and assumptions in a systematic, mathematical manner. The alternative is to impose high factors of safety to ensure that a design can accommodate any potential variability. However, products with large factors of safety are often heavier, more expensive, and less attractive than their robustly designed counterparts. Overall, the potential benefits of implementing a robust design approach include increased customer satisfaction with products that exhibit consistently high rather than marginal quality, and decreased cost of re-work and replacement of defective products.

From this discussion, it is evident that Taguchi’s robust design philosophy is appropriate as a partial foundation for a comprehensive, robust topology design method for multifunctional applications. However, it is still unclear how the robust design philosophy could be implemented for engineering design applications. Due to the

intellectual and practical appeal of Taguchi's robust design philosophy, researchers and practitioners have been actively establishing and improving the methods and techniques needed to implement robust design for engineering applications. Important criticisms and extensions are reviewed in the following section.

2.4.2 Improvements and Extensions of Taguchi's Robust Design Methodology for Engineering Design Applications

Although Taguchi's robust design principles are advocated widely in industrial and academic settings, his statistical techniques, including orthogonal arrays and signal-to-noise ratio, have been criticized extensively, and improving the statistical methodology has been an active area of research (e.g., (Myers and Montgomery, 1995; Nair, 1992; Tsui, 1992; Tsui, 1996)). In the panel discussion reported by Nair (1992), practitioners and researchers—including Genichi Taguchi's son Shin Taguchi—discuss Taguchi's robust design methodology, the underlying engineering principles and philosophy, and alternative statistical techniques for implementing it. Some of the panelists suggest replacing Taguchi's orthogonal array experimental design—which requires an unnecessarily large number of experiments—with other standard experimental designs that utilize a single array for both noise and control factors, a concept promoted by Welch and coauthors (1990), Shoemaker and coauthors (1991), and Tsui (1992), among others. The panelists also suggest modeling the mean response and variability directly or via statistical data transformations (c.f., (Box, 1988; Tsui, 1992; Vining and Myers, 1990)), rather than modeling the signal to noise ratio—a practice that discards useful information about the response (particularly by confounding mean response with variance information). The panelists have many other suggestions, including the use of response

surfaces and other methodologies for modeling the relationship between the response and the control and noise factors (c.f., (Welch, et al., 1990)).

When robust design methods are used in engineering design applications, analytical models or computer simulations are typically available (in place of or in addition to physical experiments) for evaluating the relationship between system response and input factors. In this context, a number of researchers advocate nonlinear programming approaches for robust design. Ramakrishnan and Rao (1996) formulate a robust design problem based on Taguchi's quality loss function, using statistical concepts and nonlinear programming. They consider variations in both control and noise factors. Cagan and Williams (1993) establish first-order necessary conditions for robust optimality based on measures of the flatness and curvature of the objective relative to local variations in design variables. Michelena and Agogino (1994) introduce an approach whereby monotonicity analysis is used for solving N-type (i.e., nominal performance values are preferred) robust design problems. Sundaresan and coauthors (1995) introduce a sensitivity index for formulating a nonlinear objective function for robust design.

Since constraints are typically an important aspect of a nonlinear programming problem, several authors have investigated the formulation of constraints for robust design applications. Parkinson and coauthors (1993) coined the term 'feasibility robustness' for designs that continue to satisfy constraints and remain within a feasible design space despite variations in control or noise factors. They proposed worst case, Taylor series-based and linear statistical analysis approaches for calculating the magnitude of variation that is transmitted from control and noise factors to constraints. Yu and Ishii (1998) propose a manufacturing variation pattern approach for adjusting

constraints to account for correlated manufacturing-induced variations. Otto and Antonsson (1993) adopt a constrained optimization approach for robust design, with a modified version of Taguchi's signal-to-noise ratio as the objective function. Du and Chen (2000) review several approaches for maintaining feasibility robustness and introduce a most probable point (MPP) based approach that offers accuracy similar to Monte Carlo based approaches with fewer computations.

In work that is foundational to the robust topology design method proposed in this dissertation, Chen and coauthors (1996b) and Bras and Mistree (1993) formulate a robust design problem as a multiobjective decision using the compromise DSP. Both control and noise factors are considered as potential sources of variation, and constraints are modeled in a worst-case formulation to ensure feasibility robustness. Separate goals of bringing the mean on target and minimizing variation (for each design objective) are included in a goal programming formulation of the objective function. This provides flexibility for achieving compromises among multiple performance objectives and between mean values and variations for all objectives. This capability is very important for robust, multifunctional topology design for which it may be necessary to explore trade-offs between different aspects of performance associated with different functions. Trade-offs may also need to be negotiated between nominal performance and robustness as well as between different types of robustness (i.e., robustness to noise factor variation, control factor variation, and topological variation). The flexibility to consider tradeoffs is not supported by traditional single-objective mathematical programming approaches, advocated widely in topology design and broader engineering design settings; nor is it supported by collapsing mean and variation measures into signal-to-noise ratios or loss

functions. In more recent work, Chen and coauthors have extended the approach to include alternative formulations of the objective function, such as compromise programming (Chen, et al., 1999b) and physical programming (Chen, et al., 2000). In this dissertation, the approach needs to be extended to accommodate multifunctional topology design problems and associated sources of variation with the characteristics described in Section 2.1. This research opportunity is discussed further in Section 2.5.

Once a robust design problem has been formulated, it must be solved. Solution of a robust design problem is distinguished by the need to evaluate not only a nominal value for each response but also the variation of each response due to control or noise factor variation. If a response, y , is a function of control factors, \mathbf{x} , and noise factors, \mathbf{z} :

$$y = f(\mathbf{x}, \mathbf{z}) \quad (2.26)$$

where the function, f , could be a detailed simulation model, a surrogate model, or a physical system, the challenge is to estimate the expected value, μ_y , and variance, σ_y^2 of the response. There are many techniques for transmitting or propagating variation from input factors to responses, and each technique has strengths and limitations. Monte Carlo analysis is a simulation-based approach that requires a very large number of experiments (Liu, 2001). It is typically very accurate for approximating the distribution of a response, *provided* that probability distributions are available for the input factors. On the other hand, it is very computationally expensive, especially if there are large numbers of variables or if computationally expensive simulations are needed for evaluating each experimental data point. If only a moderate number of experimental points are computationally affordable, a variety of space-filling experimental designs are available such as Latin Hypercube designs (Koehler and Owen, 1996; McKay, et al., 1979). If

only a few experimental points can be afforded, sparser experimental designs such as fractional factorials or orthogonal arrays are available (e.g., (Myers and Montgomery, 1995)). Whereas these experimental designs require fewer experimental points, they do not provide approximations of the distribution of a response, but they do provide estimates of the range(s) of response(s). All of these experimental techniques can be used in two ways: (1) to provide estimates of the variation or distribution in responses at a particular design point or (2) to construct surrogate models of the response that can then be used in place of a computationally expensive simulation model for evaluating mean responses and variations (c.f., (Chen, et al., 1996b; Mavris, et al., 1999; Welch, et al., 1990)). They all suffer from the problem of size identified by Koch and coauthors (1999) in which the number of experiments becomes prohibitively large (given the computational expense of most engineering simulations) as the number of input factors or design variables increases. This characteristic is very important for topology design applications in which there are large numbers of variables and non-negligible computational requirements. Although experiments may be appropriate for evaluating the impact of variation in noise factors (which may be relatively few in number), they are not likely to be computationally attractive for evaluating the impact of variation in factors such as local material properties or design variables, which usually number in the hundreds or thousands.

An alternative means for propagating variation is by Taylor series expansions (c.f., (Phadke, 1989)). A first order Taylor series expansion, for example, can be used to relate variation in response, Δy , to variation in a noise factor, Δz , or a control factor, Δx , as follows:

$$\Delta y = \sum_{i=1}^k \left| \frac{\partial f}{\partial x_i} \Delta x_i \right| + \sum_{i=1}^m \left| \frac{\partial f}{\partial z_i} \Delta z_i \right| \quad (2.27)$$

where the variation could represent a tolerance range or a multiple of the standard deviation. Higher order Taylor series expansions can also be formulated to provide better approximation of the variation in response, but higher order expansions also require higher order partial derivatives of the response function with respect to control and noise factors. Taylor series expansions are relatively accurate for small magnitudes of variation in control or noise factors but lose their accuracy for large variations or highly nonlinear functions, f . A Taylor series expansion requires evaluation of the partial derivative or *sensitivity* of the response function with respect to changes in control or noise factors. If analytical expressions are available for the sensitivities, this can be a computationally attractive and relatively accurate approach (c.f., (Bisgaard and Ankenman, 1995)), even for large numbers of control and noise factors. Otherwise, the sensitivities can be estimated using finite differencing techniques, automatic differentiation (a feature built into some computer programming languages), and other advanced techniques such as perturbation analysis and likelihood ratio methods (c.f., (Andradottir, 1998)), but these techniques can diminish the computational attractiveness and accuracy of the approach. Sensitivity-based approaches have been proposed for modeling constraints (c.f., (Parkinson, et al., 1993; Phadke, 1989)) and objectives (c.f., (Belegundu and Zhang, 1992; Su and Renaud, 1997)) in robust design. Because analytical expressions, derived from finite element formulations, are typically available in topology design applications, a Taylor series expansion is promising for propagating variation in control factors in robust topology design.

Robust design and reliability-based design share some of the same computational techniques, but they have different philosophies and do not achieve the same end effects in general. In reliability-based design, the focus is on ensuring that designs do not fail, according to a specified criterion (e.g., probability of failure per manufactured unit). Precise characterizations of performance distributions are required for failure analysis to evaluate the probability of failure, but emphasis is placed on minimizing this probability (or achieving a target value for it) rather than minimizing performance variation. In reliability design, the focus is entirely on bringing the worst-case design within a critical constraint. Essentially, reliable designs are *optimal* for a set of worst-case conditions rather than for nominal conditions. On the other hand, in robust design the focus is on achieving goals for mean performance as closely as possible and minimizing the sensitivity of this performance to multiple sources of variation. Solutions obtained with robust design techniques are *robust* for a range of conditions rather than *optimal* for a worst-case set of conditions. The philosophies are very different. In the author's opinion, reliability-based design is more appropriate for handling critical constraints while robust design is more appropriate for goals and objectives with flexible target values that are achieved as closely as possible.

Although robust design has been applied for a variety of engineering applications, most of the work is focused on the detailed stages of design. It is assumed that a preliminary design—with concrete layout and preliminary design specifications—has already been determined. Robust design methods are applied to adjust a design slightly to make its performance more robust to manufacturing variations, but exploration of a broad design space and significant adaptations or variations in a system are typically not

undertaken or facilitated. To support the primary research focus of this dissertation, robust design techniques are needed for the early stages of design when preliminary design specifications—including the layout or topology of a system—are determined.

2.4.3 Robustness in the Early Stages of Multidisciplinary Design

Whereas most of the robust design literature is focused on the latter portions of embodiment and detailed design in which dimensions are adjusted to accommodate manufacturing variations, there has been some emphasis on infusing robust design techniques in the earlier stages of design when decisions are made that profoundly impact product performance and quality. Primarily, this has been achieved by enhancing the robustness of design decisions with respect to subsequent variations in designs themselves.

For example, Chang and Ward (1995; 1994) facilitate simultaneous, distributed design by encouraging designers to make conceptually robust decisions that are relatively insensitive to variations in the decisions of other designers regarding shared parameters that impact both designers' decisions. Chang and Ward model these shared parameters as noise factors. Distributed designers make decisions that are robust to variations in the shared parameters, and communicate not only the resulting robust designs to other designers, but also marginal loss functions that model the quality loss imposed on the design if other designers adjust levels of the shared parameters. Ward and coauthors (1995) argue that developing and communicating robust ranges or sets of designs independently and concurrently—also known as set-based concurrent engineering—helps Toyota engineers design and make high-quality cars cheaply.

Ben-Haim (2001) provides an information-gap approach for making robust design decisions in settings—such as the early stages of design—that are characterized by severe lack of information and highly unstructured uncertainty (i.e., uncertainty for which probability distributions or likelihoods are not available). The robustness of a design is defined as the greatest level or range of variation that the design can accommodate while satisfying a minimal set of requirements. Elishakoff and coauthors (1994) apply this notion of bounded uncertainty for structural design in which the worst value of an objective function is minimized and the worst value of a constraint function must satisfy the constraint limit. They use an approach called anti-optimization to find the worst combination of factors within a specified bounded region of uncertainty. Although Ben-Haim uses the term *robustness*, this approach is essentially a variation of reliability design that does not require probability distributions.⁵ Its lack of reliance on probability distributions makes it useful for the early stages of design when such probabilistic information may not be reliably available, but it does not support *robust* design in which tradeoffs are sought between bringing the mean or nominal value of an objective on target and minimizing variation during a search process. In essence a solution obtained with robust design methods is *robust* with respect to a range of conditions rather than *optimal* for worst-case conditions.

In work that is foundational to our proposed research, Chen and coauthors (1996a; 1996b) use robust design techniques to determine ranged sets of preliminary design specifications that are both robust and flexible. They formulate their domain-independent, systematic approach—the Robust Concept Exploration Method (RCEM)—by integrating statistical experimentation and approximate models, robust design

⁵ Reliability design is distinguished from robust design in Section 2.4.2.

techniques, multidisciplinary analyses, and multiobjective decisions. The computing infrastructure of the RCEM is illustrated in Figure 2.16. As shown in the figure, design parameters are classified in stage A as noise factors, control factors, or responses. Statistical experiments are designed in stage B, and the results of the experiments are analyzed in stage D, based on data obtained from rigorous analysis models (stage C). Typically, experimentation is performed sequentially to explore and narrow the design space and to identify important factors for each response. In stage E, metamodels or surrogate models are constructed for each response. Multiobjective robust design decisions are modeled as compromise Decision Support Problems (DSPs) in stage F, and they are solved using the surrogate or response surface models directly rather than the computationally expensive analysis models.

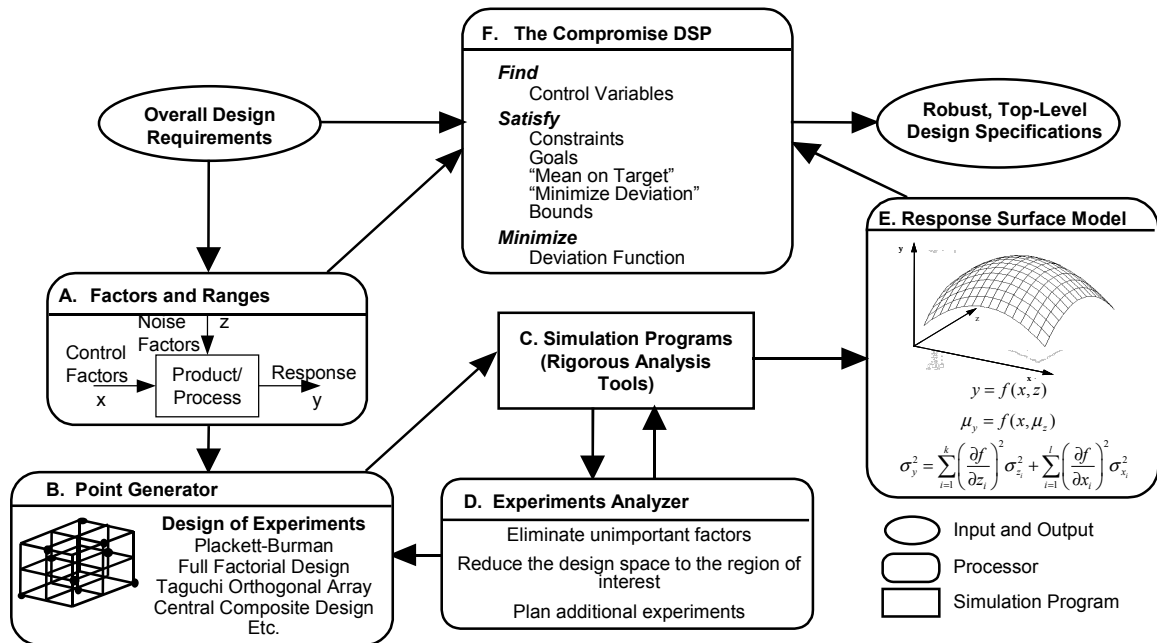


Figure 2.16 – Computing Infrastructure for the Robust Concept Exploration Method (Chen, et al., 1996a)

RCEM has been employed successfully for a simple structural problem and design of a solar powered irrigation system (Chen, 1995), a High Speed Civil Transport (HSCT) (Chen, et al., 1996a), and a General Aviation Aircraft (Simpson, et al., 1996). In addition, RCEM has been extended to facilitate the design of complex, hierarchical systems (Koch, 1997) and product platforms (Simpson, et al., 2001).

RCEM has several characteristics that make it particularly useful for the early stages of design. First, it facilitates exploration and generation of designs that are both robust and flexible via Type I and Type II robust design. With Type I robust design methods, preliminary designs are generated that are robust to noise factors. Therefore, it is possible to minimize variations in performance caused by variations in manufacturing or operating environments or variations in assumptions about the settings of influential design parameters (with values that may change during the product realization process). With Type II robust design methods, it is possible to minimize variations in performance caused by variations in control factors or design variables themselves. This capability facilitates considering the effect of downstream design changes early in the design process. If performance is relatively insensitive to changes in design variables within bounded ranges, then the ranged set of design specifications embody flexibility for downstream designers to adjust them without significantly degrading the performance for which they were originally designed.

Within the RCEM framework, the compromise DSP is used as a multiobjective decision model for determining the values of design variables that satisfy a set of constraints and balance a set of conflicting goals, including bringing the mean on target and minimizing variation associated with each performance parameter. In this setting,

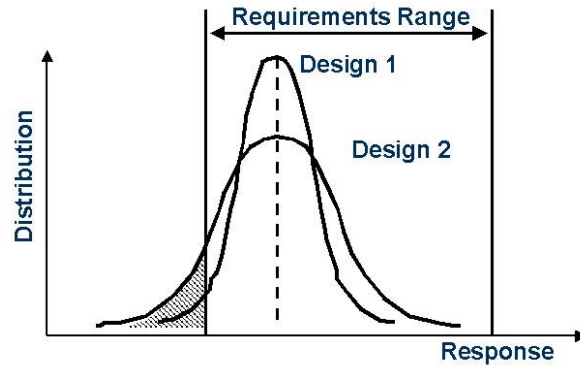


Figure 2.17 – Comparing Two Designs with Respect to a Range of Requirements

the compromise DSP is particularly flexible. Families of robust designs can be generated by changing the priority levels or weights of goals or by changing the target values for design requirements—none of which require reformulation of the compromise DSP.

There are some cases in the early stages of design when requirements themselves are uncertain and most appropriately expressed as a range (i.e., smaller than a lower limit, larger than an upper limit, or between lower and upper limits) rather than a target value, as shown in Figure 2.17. In these cases, it may not be appropriate to bring the mean on target and minimize variation. Instead, it may be necessary to measure the extent to which a range or distribution of design performance (induced by a range of design specifications) satisfies a ranged set of design requirements. The design capability indices are a set of metrics that are based on process capability indices and designed especially for assessing the capability of a ranged set of design specifications for satisfying a ranged set of design requirements. The design capability indices are incorporated as goals in the compromise DSP within the RCEM framework. The details are described by Chen and coauthors (1999a). In further work, Chen and Yuan (1999) introduced a design preference index that allows a designer to specify varying degrees of

desirability for ranged sets of performance, rather than specifying precise target values or limits for a range of requirements beyond which designs are considered worthless.

In addition to facilitating the generation of robust, flexible, ranged sets of design specifications, the RCEM framework also facilitates exploration of a broad design space in a concurrent, multidisciplinary design environment during the early stages of design. By replacing computationally expensive simulation models with fast analysis models—built as experiment-based metamodels—some of the computational difficulties of performing probability-based robust design are alleviated. The metamodels allow exploration of broader regions of the design space with limited computational resources. Both response surface and kriging approaches for metamodeling have been considered within the RCEM framework (Simpson, et al., 1998). The response surface approach has been augmented with artificial neural networks, as well (Varadarajan, et al., 2000). Chen and coauthors (1999b) also construct an approximate function—labeled quality utility—for the Pareto efficient frontier to facilitate exploration of alternative robust design solutions for bi-objective problems involving bringing the mean on target and minimizing variation.

Utilization of fast metamodels also allows integration of multidisciplinary analyses across disciplines, thereby facilitating multidisciplinary design. As in the RCEM, response surface models are constructed by other authors (e.g., (Koch, et al., 1999; Mavris, et al., 1999)) to model system level objectives and constraints and to replace disciplinary-specific, computationally intense analysis tools in an integrated, systems-level, multidisciplinary design process. However, the cost associated with constructing a high-fidelity surrogate model for a broad design space can be prohibitive, especially

when there are large numbers of variables. Alternatively, a number of multidisciplinary design approaches have been developed for distributing design activities among multiple designers and/or sub-level design problems. Since multidisciplinary design is an important focus in this dissertation, robust design methods for distributed, multidisciplinary applications are reviewed in the next section.

Unfortunately, the conceptual or early-stage robust design methods reviewed in this section have many of the same limitations of other robust design methods reviewed in Section 2.4.2. One of the fundamental assumptions is that the topology or layout of a design is known *before* robust design methods are applied. In this dissertation, the objective is to apply robust design methods *concurrently* with topology design methods. This is not a simple task. As noted in Section 2.3, there are typically large numbers of variables, coupled with non-negligible computational requirements, in a topology design problem. This makes it difficult to apply the statistical experimentation and surrogate modeling techniques used by other authors to transmit variation in conceptual or early-stage applications. Monte Carlo analysis is also computationally expensive in this context. Therefore, transmitting variation in a topology design problem is a challenge.

Furthermore, topology design problems are fundamentally different from the parametric design problems considered in robust design applications to date. Topology is modified by adding or removing elements—and their associated design variables or control factors—from an initial topology. Therefore, the set of design variables is modified during the topology design process. This is typically accomplished by allowing design variables—such as element thicknesses in discrete topology design or element densities in continuum-based topology design—to approach an extremely small value, far

below the manufacturable or realizable limit. Therefore, modeling variation in control factors in topology design needs significant thought and attention.

Finally, to realize topology designs that are flexible and robust with respect to downstream changes, it is important to consider potential topological variations, in addition to variations in control and noise factors (such as applied loads, dimensions, and material properties). Topological variations could include downstream design changes in the topology to achieve multifunctional requirements more closely or to enhance manufacturability or stochastic imperfections in topology induced by the manufacturing process. Since a topology design process has a broad impact on the layout of a final design, it is reasonable for a robust topology design process to facilitate designing a broader range of flexibility into the product, including flexibility for accommodating variations in *topology* in addition to dimensions and other properties and conditions.

Since one of the primary objectives in this dissertation is to facilitate *multifunctional*, robust topology design, recent advances in robust design methodology for multidisciplinary design applications are reviewed in the next section.

2.4.4 Robust Design for Multidisciplinary Applications

To reduce the computational cost of multidisciplinary design and to leverage distributed designer expertise, analysis models, and computing resources, multidisciplinary synthesis or design activities may be decomposed and distributed among multiple designers or design teams, each of whom bring discipline-specific expertise to the design process.⁶ Whereas design freedom is preserved for tailoring

⁶ The computational expense of solving an integrated multidisciplinary systems design problem can be prohibitively high when conventional analysis and optimization algorithms are used, as well. The computational burden of analysis and synthesis (optimization) tends to increase super-linearly with the numbers of parameters and analysis codes, making the cost of integrated, systems-level multidisciplinary

performance in each discipline, the effects of interactions between multiple disciplines (or designers) on system-level performance must be considered in multidisciplinary design. Comprehensive reviews of deterministic multidisciplinary design optimization are available in the literature (c.f., (Kroo, 1997; Sobieszczanski-Sobieski and Haftka, 1997)) and are not repeated in this review. Here, the focus is on *robust* design methods for multidisciplinary applications, of which there are only a few examples.

In terms of a general approach for robust, multidisciplinary design, Chang and Ward (1995; 1994) facilitate concurrent or simultaneous robust design via generation and communication of ranged sets of specifications, coupled with quality loss functions. In similar work, Kalsi and coauthors (2001) treat shared variables as noise factors in complex, multidisciplinary systems design performed by multiple designers. Each designer searches for solutions that are robust to changes in shared variables by other designers. Coupled or shared variables are modeled as noise factors with uniform probability distributions within bounds specified by the designers based on a pattern search of their design spaces. A lead designer solves his/her disciplinary design problem for solutions that are robust with respect to the coupled noise factors. This preliminary solution is communicated to a secondary designer who solves his/her design problem and selects specific values of the coupled or shared variables within the ranges (i.e. uniform probability distributions) specified initially. This approach can accommodate two-way interactions between designers, in contrast to the predominantly one-way dependencies implied by Chen and coauthors and Chang, Ward, and coauthors.

design greater than the sum of the individual costs of disciplinary analysis and synthesis (optimization) (c.f., (Sobieszczanski-Sobieski and Haftka, 1997)). Furthermore, integrated, systems-level, multidisciplinary design problems must be solved centrally by a single decision-maker—an approach that does not leverage the disciplinary expertise and computing resources distributed among individual members of a multidisciplinary design team.

Chen and Lewis (1999) couple robust design methods with game theory protocols for modeling interactions and enhancing flexibility in multidisciplinary design processes involving multiple designers. According to Stackelberg game theoretic protocol, two designers are designated as a leader and a follower. A rational reaction set (RRS) is formulated to serve as a prediction of the follower's behavior in response to the leader's decision. Specifically, the RRS is a response surface model of the values of the follower's shared variables (i.e., variables controlled by the follower but also required by the leader) as a function of possible values for the leader's shared variables. The leader solves his/her design problem using the RRS and his/her own analysis models and generates robust design solutions that include ranged sets of values for the shared variables. Finally, the follower selects values of the shared variables from within the ranges specified by the leader and solves his/her design problem. In a notable extension of this work, Xiao (2003) uses design capability indices and game theory protocols to facilitate flexible, robust, interactive decision-making among multiple, distributed designers.

Both Kalsi and coauthors and Chen and Lewis demonstrate that the robust design methods improve the follower's design performance in exchange for relatively small sacrifices in the leader's design performance. The approach of Kalsi and coauthors does not require RRS's, which can be computationally expensive to develop and may not be very accurate. On the other hand, their approach relies on identifying mutually satisfactory ranges for coupled or shared variables *a priori*—a task that may require some iterative communication among designers.

In addition to game theory, there are many other approaches for multidisciplinary design, such as collaborative optimization and concurrent subspace optimization (c.f., (Kroo, 1997; Sobieszczanski-Sobieski and Haftka, 1997) for reviews). A limited amount of work has been done to infuse uncertainty analysis within these approaches. Gu and coauthors (2001; 2000) develop numerical techniques for transmitting uncertainty through multidisciplinary system analyses using first-order sensitivity analyses to determine ranges of output values. The uncertainty information is used to maintain feasibility robustness for a multidisciplinary system. Du and Chen (Du and Chen, 2002) use Taylor series expansions combined with local and global sensitivity analyses for uncertainty analysis in multidisciplinary design. Their approach accommodates probabilistic representations of uncertain parameters as well as model parameter and structure uncertainty.

There are two crucial characteristics of multidisciplinary *topology* design problems that make it difficult to apply the robust, multidisciplinary design methods discussed in this section. First, a fundamental assumption behind multidisciplinary design methods is that a system-level design problem can be decomposed into multiple, nearly independent sub-problems, usually associated with different disciplines. Simon (1996) describes decomposable and *nearly* decomposable systems as systems made up of subsystems between which there are negligible interactions and weak but non-negligible interactions, respectively. In this sense, electrical and structural subsystems in an aircraft, for example, are nearly decomposable and subject to multidisciplinary design methods. Each discipline has its own design variables and responses, but there are a *few* coupled or *shared* parameters that both disciplines require, as shown in the left side of Figure 2.18.

As the extent and strength of interactions between subsystems or disciplines increases, it becomes more and more difficult to partition the system into subsystems. The number of coupled or shared parameters typically increases, and the potential benefits of distributed, multidisciplinary design diminish because each subsystem design problem becomes essentially a system-level design problem due to the strength and extent of dependencies with other subsystems.

Multidisciplinary topology design problems are not decomposable *at all*. The designs are highly coupled or integral in the sense that all aspects of performance are controlled by the same *shared* variables, including topology, shape, and dimensions, as shown in the right side of Figure 2.18. The objective is to find a *single* topology or layout of material for a geometric domain that performs multiple functions. In order to influence or tailor one aspect of performance, it is necessary to modify topology, shape, and/or dimensions that strongly influence other aspects of performance, as well. It is not possible to partition the design space into relatively independent subsystems. In this dissertation, the design of topology for multiple aspects of performance (in distinct disciplines such as thermal, structural, or electrical) is called *multifunctional* design to distinguish it from multidisciplinary design, for which the body of multidisciplinary design methods are directly applicable. In multifunctional design, complex systems or products that are integral—not decomposable—are designed for multi-physics aspects of performance.

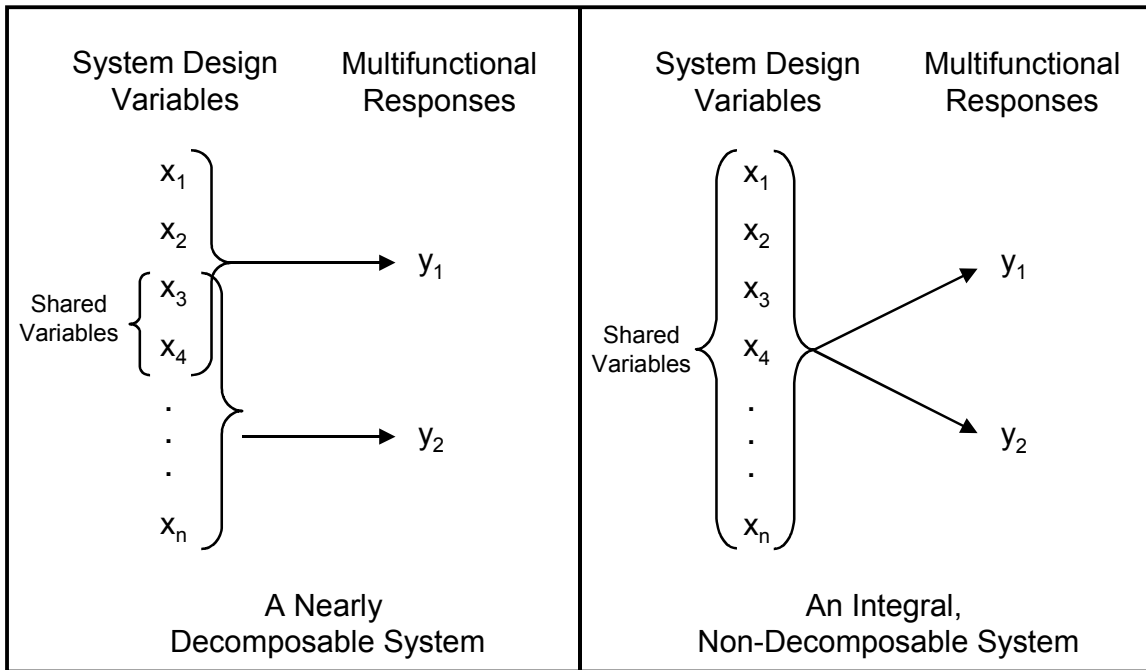


Figure 2.18 – Decomposable vs. Integral Systems

Since concurrent, distributed multifunctional design is not a viable option, the remaining options are to (1) design the topology in a single-stage, integrated robust design process in which all of the multifunctional requirements are considered simultaneously, or (2) design the topology in a sequential manner for each physical function (e.g., structural topology design followed by thermal topology design), treating *all* of the design variables as coupled parameters that must be robust and flexible for downstream design changes. As noted in Section 2.3, it is very difficult to consider true multi-functional objectives in a full-scale, single-stage, topology design process. Therefore, a multifunctional, robust topology design approach is proposed in Chapter 3 that is based primarily on the latter option, with full-scale structural topology design in an initial design stage, followed by topology design for other functions in latter stages and

an option to consider multi-physics requirements simultaneously in the latter stages in a limited multifunctional topology design process. Details are provided in Chapter 3.

2.5 RESEARCH OPPORTUNITIES

The primary purpose of the literature review is to identify research opportunities relevant to the focus of this dissertation. In this section, these research opportunities are summarized with the goal of establishing the originality and significance of the primary and secondary research questions and hypotheses. Therefore, the research opportunities are organized by research question.

2.5.1 Research Question 1: Robust Topology Design

As established in Sections 2.3.1 and 2.4.3, a comprehensive robust topology design method has not been established in the literature. In documented applications of robust design methodology, even for the early stages of design, the physical topology or layout of a system is determined *a priori*. Conversely, topology design methods have been established almost exclusively for deterministic contexts in which potential variations in material properties, applied loads, structural dimensions, and other factors are not considered. As discussed in Section 2.3.1, the most closely related work involves designing for worst-case loading and worst-case stress and displacement constraints (i.e., feasibility robustness).

Addressing these research opportunities is expected to be a challenging task—not simply a straightforward, direct application of robust design methods. One of the fundamental challenges in robust topology design lies in *framing* the problem by identifying critical issues and establishing a methodological and computational framework for defining and solving robust topology design problems. Also, many

characteristics of topology design problems make them challenging applications for robust design methods. As discussed in Section 2.3.1, these features include large numbers of variables, non-negligible computational requirements, and the ‘on/off’ nature of variables that facilitates topological modification. (The on/off nature of variables in topology design essentially means that the size of the variable set is reduced as a result of the topology design process.) These features make it difficult to model sources of variation in topology design because topology is changing as a result of the design process and because design variables have very small lower bounds that exceed realizable or manufacturable limits. It is also difficult to propagate this variation from its sources to relevant responses because computational demands and large numbers of variables make both Monte Carlo approaches and statistically designed experiments extremely computationally expensive.

What is needed is a comprehensive approach for robust topology design. Since topology has a profound effect on the overall performance of a design, it is important to ensure that the topology is robust to potential fluctuations and changes. Ideally, a robust topology design method should facilitate robust topology design for several sources of variation, including Type I sources such as boundary, loading, and operating conditions and material properties and Type II sources such as stochastic dimensions and topology (e.g., stochastic variations in the connectivity of material such as cracks). Type II sources of variation have not been considered in topology design—even in a worst-case scenario—and topological variation has not been considered in robust design applications at all. Guidelines are needed for modeling these sources of variation. Also, methods are required for transmitting this variation from its sources to objective and constraint

functions where measures of response variation are needed for assessing the robustness of performance. Multiobjective decision support constructs are needed for modeling robust topology design decisions and balancing multiple objectives associated with nominal performance and robustness of several, possibly multifunctional, performance criteria. This issue is addressed with respect to Research Question 3. Topology design typically precedes detailed and other latter stages of design; therefore, it is also a suitable point for using robust design techniques to design flexibility into the topology and general structure of a design. The flexibility is intended to accommodate subsequent changes in design specifications to fulfill additional requirements or meet changing objectives without requiring iterative redesign of the structure. The robust topology design method needs to be computationally tractable and efficient despite the large numbers of variables and non-negligible computational times inherent in topology design.

2.5.2 Research Question 2: Multifunctional Topology Design

As established in Section 2.3.2, multifunctional topology design capabilities are currently limited primarily to coupled field problems in structural design in which the effects of thermal, electrical, and magnetic fields on the state of mechanical stress and deformation in a body are considered with a few applications in thermal conduction as well. Truly *multifunctional* topology design applications—in which objectives are pursued in multiple physical domains such as heat transfer and structural mechanics—have not been considered.

Coupling structural topology design with topology design for other physical phenomena is likely to increase the scale and complexity of the topology design process, placing additional demands on computational resources. Also, as discussed in Section

2.3.2, structural topology design techniques do not apply straightforwardly to other physical domains. Therefore, it may be necessary to parameterize topology design problems differently when designing for different aspects of functionality. These computational challenges, coupled with the advantages of leveraging the knowledge of disciplinary experts, leads to the conclusion that multifunctional topology design processes may need to be divided among distributed disciplinary experts and computing resources. However, as discussed in Section 2.4.4, topology design spaces are highly coupled and integral⁷ rather than decomposable like many multidisciplinary systems such as aircraft. All of the multidisciplinary design (and multidisciplinary robust design) techniques, including game theory, have been established and applied for concurrent, distributed design of decomposable (or nearly decomposable) systems. Concurrent, distributed design, partitioned along functional lines, is not a viable option because all of the structural variables are linked and because a topology design process necessarily involves topological modifications that could not be made concurrently by separate designers. Therefore, alternative or expanded robust design techniques for integral, multifunctional applications are needed that may involve sequential distribution of design activities.

In order to facilitate multifunctional topology design, techniques are needed for topology design in each physical domain under consideration. These techniques must include parameterized quantifications of the relative contribution of topological elements or regions to the overall functional performance of a structure. These parameterized quantifications are needed to avoid ‘trial-and-error’ approaches to topology design that

⁷ *Integral* implies that all aspects of performance are controlled by the same structural variables, including size, shape, and topology.

are rarely effective for exploring a broad set of possible designs and are inevitably computationally intractable. Second, a multiobjective decision support construct is needed to facilitate the complicated task of balancing conflicting objectives in multiple functional domains, along with robustness objectives. Third, a theoretical and computational framework is needed for facilitating multifunctional design of integral topology designs. It must facilitate achievement of system-level objectives as well as effective use of distributed human and computing resources. Each designer needs to account for the impact of his/her design decisions on the decisions and objectives of other designers. Whereas relevant mathematical models (e.g., game theory) have been established for decomposable multidisciplinary systems, multifunctional topology design adds two new challenges: (1) modification of topology, and (2) integral or highly coupled systems that are not decomposable.

2.5.3 Research Question 3: Compromise DSP for Multifunctional, Robust Topology Design

A common thread in the previous discussions is the need for flexible, domain-independent, multiobjective decision support for both robust topology design and multifunctional topology design. Such an approach is needed for balancing conflicting objectives that include multiple measures of functional performance and robustness. To date, several multiobjective formulations have been applied for considering multiple loads or objectives in structural topology design, including weighted sum, compromise programming, and min-max formulations. However, it is argued in Section 2.2 that none of these approaches have all of the advantageous characteristics of the compromise DSP for multifunctional, robust topology design applications. Those characteristics include flexibility for (1) considering multiple goals *and* hard constraints, (2) leveraging

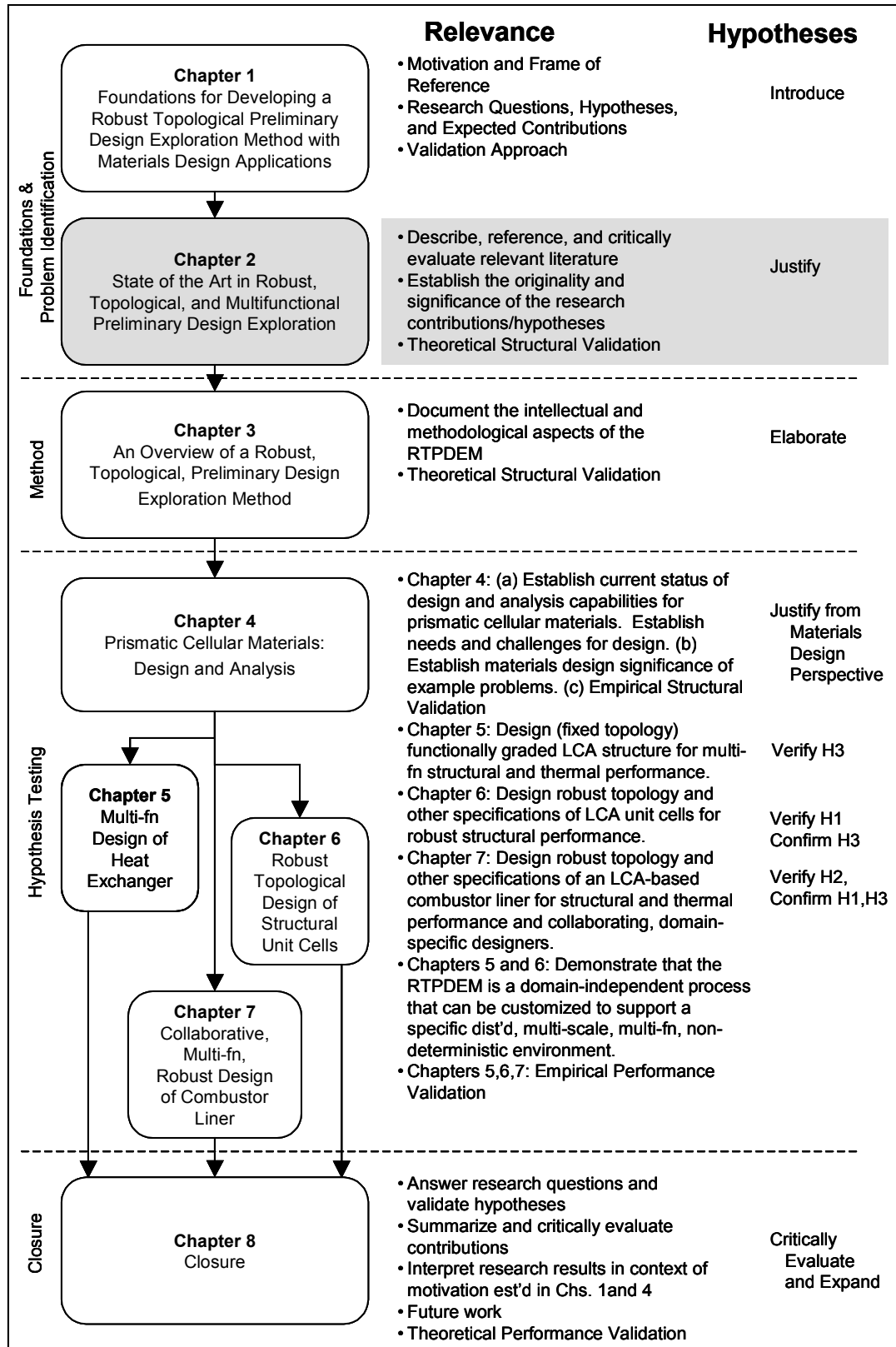


Figure 2.19 – Dissertation Roadmap

engineering judgment into the design problem formulation, (3) utilizing alternative objective function formulations such as preemptive, Archimedean, and utility theory formulations, and (4) adjusting weights *and* target values along with bounds and other parameters to facilitate exploration and generation of a family of multifunctional design solutions. In this dissertation, the compromise DSP is utilized as a foundational multiobjective decision support construct for the RTPDEM.

2.6 CHAPTER SYNOPSIS

As shown in Figure 2.19, the primary role of the discussions in this chapter has been to justify the research questions and hypotheses proposed in this dissertation by establishing their originality, significance, and theoretical structural validity in the context of relevant literature. In this chapter, the relevant literature has been reviewed critically in the areas of robust design, topology design, and multidisciplinary and multiobjective decision-making and design. The capabilities and limitations of available approaches have been discussed. Based on the critical review of the literature, a set of research opportunities have been identified and discussed in Section 2.5. The research opportunities have been organized according to the research questions and hypotheses in order to highlight the potential for original, significant research contributions represented by each research hypothesis. The next step is to discuss the implementation of the proposed research hypotheses in the form of the Robust Topological Preliminary Design Exploration Method presented in Chapter 3.

CHAPTER 3

AN OVERVIEW OF THE ROBUST TOPOLOGICAL PRELIMINARY DESIGN EXPLORATION METHOD

A Robust Topological Preliminary Design Exploration Method is presented in this chapter as a systematic approach for exploring and generating robust, multifunctional topology and other preliminary design specifications for materials design applications. The method includes a comprehensive approach for considering robustness and flexibility in topology design. It also includes multidisciplinary robust design methods for linking distributed design phases—associated with multiple disciplines, designers, or length/time scales—via generation and communication of flexible ranges of topological preliminary design specifications and approximate, quantitative models of performance. As part of the multidisciplinary approach, topology design techniques are established for multifunctional applications that include both structural and thermal phenomena.

The Robust Topological Preliminary Design Exploration Method (RTPDEM) is developed based on a set of research hypotheses introduced in Chapter 1. The relationship between the method and the three primary research hypotheses is summarized in Section 3.2, following a brief contextual overview of the method in Section 3.1. The details, benefits, and uniqueness of the RTPDEM are discussed in Sections 3.3 and 3.4. The core of the RTPDEM is a robust topology design method presented in Section 3.3 that addresses Hypotheses 1 and 3. As described in Section 3.4, those robust topology design foundations are expanded for supporting *multifunctional* topology design and addressing Hypothesis 2. A thermal analysis and topology design approach is presented in Section 3.5 for extending topology design techniques beyond the

structural domain. Finally, in Section 3.6, the advantages, limitations, and appropriate domain of applicability for the RTPDEM are discussed to validate the structure of the method. Empirical validation of the RTPDEM is implemented with a series of cellular materials design examples in Chapters 5, 6, and 7, and the strategy for empirical validation is discussed in Chapter 4.

3.1 AN INTRODUCTION TO THE ROBUST TOPOLOGICAL PRELIMINARY DESIGN EXPLORATION METHOD

A robust topology design method is established for systematic exploration and identification of concepts, defined by topology and other preliminary design parameters, with properties that are robust or relatively insensitive to variations in factors such as manufacturing or operating conditions or design specifications themselves. In this section, a general overview is given of the method established for formulating and solving a robust topology design problem. As outlined in Figure 3.1, the robust topology design process facilitates transformation of a set of overall design requirements into a set of robust specifications for a preliminary design or concept. The transformation is performed in three phases.

3.1.1 Phase I: Formulate a Robust Topology Design Space

First, the robust design space is formulated by explicitly describing the form, behavior, and requirements of a design with a set of design parameters. The design space is not a specific solution of a design problem but a template or domain in which potential solutions may lie. Important parameters are identified but specific values are not yet assigned to them. Parameters include (1) design variables and exogenous or fixed factors that describe the *form* or structure of a system and its environment, (2) performance-

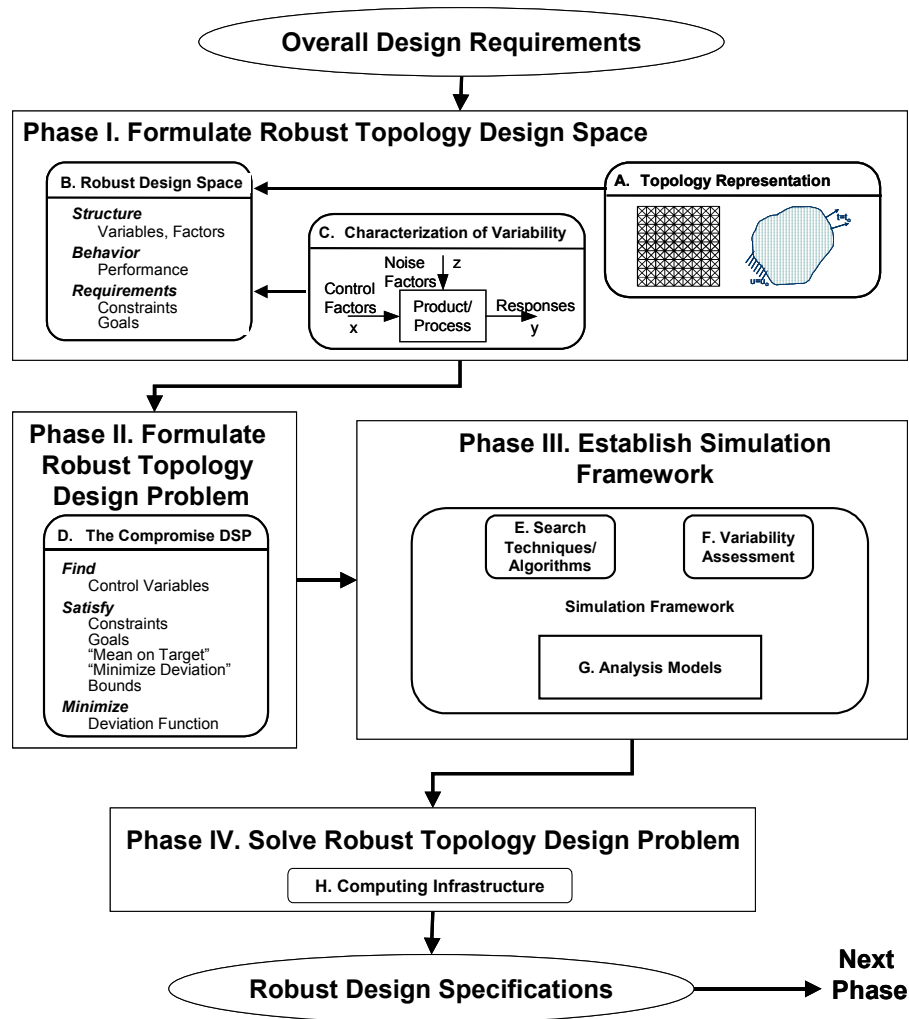


Figure 3.1 – Steps of the Robust Topological Preliminary Design Exploration Method

related attributes that describe the *behavior* of a system, and (3) performance- or form-related *requirements* by which the quality of a design is evaluated. A subset of parameters represents the design topology in such a way that it can be modified systematically during the design process. For example, topology-related parameters may include the numbers, locations, and dimensions of elements associated with a ground structure, as introduced in Chapter 2. Finally, potential sources of variation among the

design parameters are identified and characterized with tolerance ranges or statistical distributions.

3.1.2 Phase II: Formulate a Robust Topology Design Problem

In Phase II, the robust topology design problem is formulated as a compromise Decision Support Problem. The compromise DSP is customized for structuring and supporting the robust topology design exploration process. It is a flexible, mathematical, multiobjective decision model that accommodates multiple goals associated with nominal performance and performance variation and facilitates rapid exploration of multiple design scenarios and the impact of changing priorities on design specifications.

3.1.3 Phase III: Establish Simulation Framework

Finally, the decision support problem formulated in Phase II is solved using a simulation infrastructure that includes search algorithms, variability propagation/transmission techniques, and analysis tools. Analysis tools are required, of course, to evaluate the behavior, properties, or performance of a system as a function of its form. However, analysis tools are typically deterministic, and variability assessment techniques are required to evaluate the variation in performance associated with variation in inputs to the analysis. Typical variability assessment techniques include Monte Carlo analysis, Latin hypercube sampling, statistically designed experiments such as orthogonal arrays and factorial designs, and Taylor series-based analytical methods. Finally, search algorithms are used to explore the design space and identify regions of the robust topology design space that satisfy rigid requirements and meet conflicting goals as closely as possible, according to the decision support problem formulation. Search algorithms may include gradient-based algorithms such as sequential quadratic

programming, exploratory algorithms such as simulated annealing or genetic algorithms, exhaustive search procedures, experimental sampling, or other techniques. Together, variability assessment techniques, analysis models, and search algorithms comprise the simulation infrastructure. While the robust topology compromise DSP guides the design exploration process, the simulation infrastructure supplies quantitative information about the design space—including the relationship between responses and design variable values and factor variation and the location of preferable regions of the design space—that informs the decision-maker solving the compromise DSP.

3.1.4 Phase IV: Solve the Robust Topology Design Problem

Finally, all of the components of the RTPDEM are embodied in a computer infrastructure that is used to solve the problem. The outcome of the solution process is a set of robust design specifications that may be passed along to another designer or phase of product development.

3.2 THE RESEARCH HYPOTHESES AND THEIR RELATIONSHIP WITH THE ROBUST TOPOLOGICAL PRELIMINARY DESIGN EXPLORATION METHOD

The Robust Topological Preliminary Design Exploration Method, summarized briefly in Section 3.1, serves as the methodological context for investigating the research hypotheses of this dissertation. Specifically, the research hypotheses are embodied in the RTPDEM as illustrated in Figure 3.2.

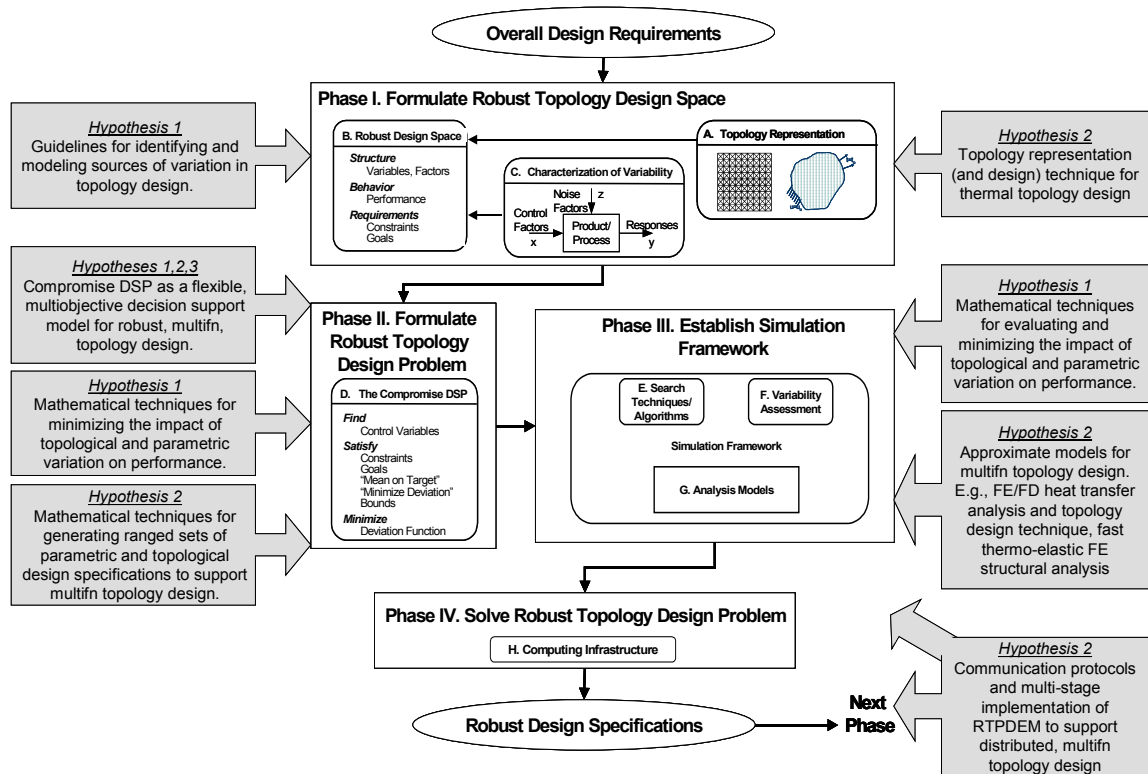


Figure 3.2 – Relationship Between the Research Hypotheses and the RTPDEM

Hypothesis 3

As illustrated in Figures 3.1 and 3.2, the compromise DSP is used in Phase II of the RTPDEM as the mathematical decision model for robust, multifunctional topology design problems. It is intended to facilitate the consideration of robustness, flexibility, and tradeoffs among multiple objectives. In Section 3.3, formulation of a compromise DSP is described for robust topology design problems in which nominal performance is considered along with sensitivity of performance to dimensional and topological variation. In Section 3.4, formulation of compromise DSP's is described for multiple designers in a multi-stage, distributed, topology design process for multifunctional applications.

Hypothesis 1

Robust topology design with the RTPDEM is described in Section 3.3. In summary, Hypothesis 1 is embodied in each phase of the RTPDEM, as illustrated in Figure 3.2. In the first phase, guidelines are provided for identifying and modeling sources of variation in topology design. These sources include tolerances, topological imperfections (e.g., missing cell walls or joints), material property variations, and other sources. In Phases II and III, mathematical techniques and decisions support protocols are devised for evaluating and minimizing the impact of topological and parametric variation on multifunctional performance. The compromise DSP is utilized as a mathematical decision support model for robust topology design.

Hypothesis 2

Multifunctional topology design with the RTPDEM is described in Section 3.4. In general, the entire RTPDEM is implemented multiple times by individual designers in a multi-designer, multi-stage, multifunctional topology design process. Communication protocols are established to support distributed, multifunctional topology design via generation and communication of robust ranged sets of design specifications and potential topologies. These ranged sets of topological and parametric design specifications are generated using the mathematical techniques for robust topology design proposed in Hypothesis 1. The compromise DSP is utilized as a decision support model for each designer. To facilitate non-structural topology design, thermal topology analysis and design techniques are proposed and described in Section 3.5. To facilitate broader exploration of a multifunctional topology design space, it is proposed that approximate behavioral models be created and communicated from one domain-specific designer to

another. Several approximate models are introduced in this dissertation including the finite element/finite difference heat transfer analysis model described in Section 3.5.

3.3 ADDRESSING HYPOTHESIS I – ESTABLISHING ROBUST DESIGN METHODS FOR TOPOLOGY DESIGN

The Robust Topological Preliminary Design Exploration Method (RTPDEM)—introduced in Section 3.1—embodies a comprehensive method for robust topology design, as described in this section. It is comprehensive because many sources of variation can be considered during a topology design process and because methods are established for efficiently assessing and minimizing the impact of this variation on important behavioral responses in a topology design context. Robust topology design methods are established in this section for addressing three sources of variation encountered in topology design:

- *noise factors* such as applied loads or material properties,
- *control factors* such as the dimensions of individual elements of a topology,
- and *topology* itself, corresponding to geometric connectivity.

Robust topology design methods involve reconceptualization of the design spaces, problem formulations, and simulation-based solution procedures typically utilized in standard topology design approaches. These changes are embodied in each step of the Robust Topological Preliminary Design Exploration Method (RTPDEM) introduced in Section 3.1. Specifically, variations in topology design parameters—including noise factors, control factors, and topology itself—must be identified and characterized mathematically as part of the robust topology design space in Phase 1 of the RTPDEM. A standard topology design problem must be reformulated as a compromise Decision

Support Problem to facilitate multiobjective, robust topology design in Phase 2 of the RTPDEM. Finally, in Phases 1, 2, and 3 of the RTPDEM, Types I, II, and T robust topology design methods must be introduced for assessing and minimizing the impact of variability in noise factors, control factors, and topology, respectively, on responses of interest.

In this section, the aspects of the RTPDEM that facilitate robust topology design are highlighted and described in detail. The section is organized according to the steps of the RTPDEM, thus providing a step-by-step method for performing robust topology design.

3.3.1 Phase 1: Formulate a Robust Topology Design Space

In the first phase of the RTPDEM shown in Figure 3.3, the robust topology design space is formulated by identifying important structural and behavioral parameters, including those required for representing and modifying topology, and by characterizing the potential sources of variation as well as the responses affected by them.

Phase I-A: Topology Representation

In Phase IA, **topology** is **represented** with a set of clearly defined continuous parameters that can be adjusted with standard search techniques. The set of parameters is defined according to the conventions of a standard topology design approach and includes element areas in ground structure-based approaches, for example, or element densities in an artificial material model. The parameters define the domain of potential topologies of a material or physical artifact and comprise a portion of the overall design space.

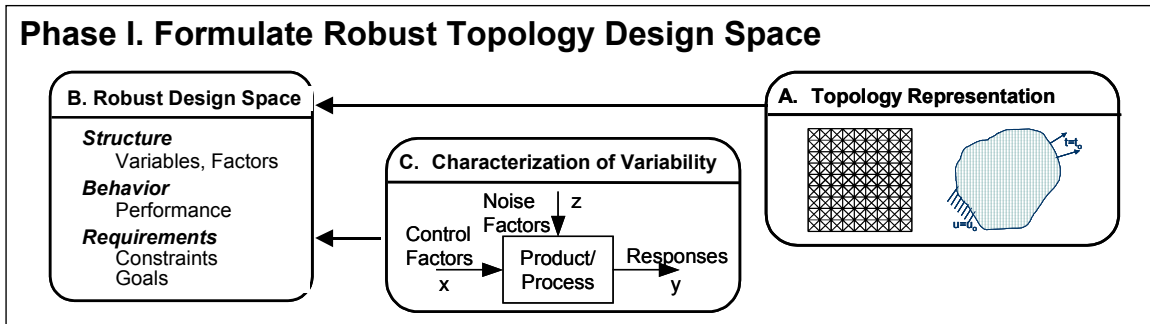


Figure 3.3—Phase I of the RTPDEM

In this dissertation, a discrete ground truss structure approach is utilized for **representing and modifying topology** (as reviewed in (Burns, 2002; Rozvany, 2001)) in Phase IA. In the ground structure approach, the domain is discretized with a grid of nodes, as illustrated in Figure 3.4. Every pair of nodes is connected with a one-dimensional finite element. Boundary conditions, such as displacements and loads, are applied at some of the nodes, as illustrated in Figure 3.4. The union of all potential elements, nodes, and boundary conditions is the ground structure. The finite elements are typically truss elements with two degrees of freedom per element or frame elements with six degrees of freedom per element (four in translation and two in rotation). The length of each element is fixed by the distance between adjacent nodes. Each element is assumed to possess unit depth in the out-of-plane direction and continuously variable thickness or cross-sectional area (defined as the product of thickness and unit depth), as illustrated in Figure 3.4. The area, X_i , of each element, i , is a design variable, and the collection of design variables is an n -dimensional vector, \mathbf{X} , with n defined by the number of elements in the ground structure.

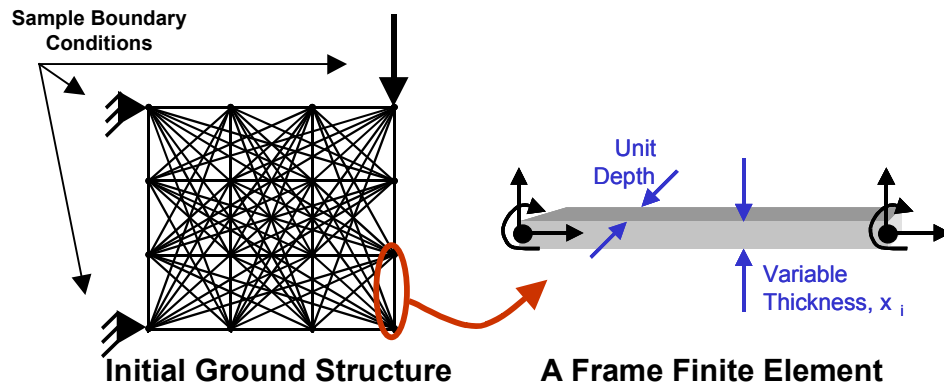


Figure 3.4 -- A Ground Structure for Topology Design

Phase I-B: Identification of Design Parameters

In Phase I-B of the RTPDEM in Figure 3.3, the entire set of design requirements and structural and behavioral design parameters is identified. In addition to the vector of design variables, several additional parameters are required to describe the topological design space and the form of the design itself. These parameters are called fixed factors and include the number and location of nodes and elements in the initial ground structure; boundary conditions (e.g., magnitude, direction, and point of application of loads and specified displacements); size and shape of the geometric domain in which topology is arranged; and material properties. Behavioral responses of interest may include compliance, stress, volume fraction or weight, and others. Requirements may include limits on mass, constraints on maximum stress, and goals for minimizing compliance or matching targets for stiffness, and others.

Phase I-C: Identification and Quantitative Modeling of Sources of Variation

In standard topology design formulations, all of the parameters—including design variables, fixed factors, and responses—are assumed to be deterministic with precise

point values assigned to them. In robust topology design, this assumption is relaxed, and deviations or fluctuations in design parameters are considered explicitly during a topology design process. Accordingly, in Phase I-C, **potential sources of variation are identified** among the set of design parameters, **and** the design parameter variation is **modeled quantitatively**.

Topology design parameters are classified here as control factors, noise factors, fixed factors, and responses in the robust design terminology introduced in Chapter 2. Responses—such as compliance, stress, and volume fraction or weight—characterize the performance of the system and enter the constraint and objectives included in most decision formulations. Response values are influenced by control factors that are systematically adjusted during the design process and by fixed factors that are assumed to have constant values during the design process. Control factors are typically known as design variables and include element areas in topology design.

In many cases, the precise values of fixed factors—such as material properties and magnitudes and directions of applied loading or displacement—cannot be known *a priori*. The values of these factors fluctuate from one environment to another and from time to time, and these fluctuations may cause concept performance to deviate from its nominal value. These stochastic parameters are labeled *noise factors* and distinguished from *fixed factors* with values that remain relatively stable by assumption. As an example of a noise factor, the magnitude and direction of an applied load may vary in a stochastic environment as shown in Figure 3.5a, and variation in applied loads has been shown to have a significant effect on the layout of an optimum topology (e.g., (Sandgren and Cameron, 2002)). The implication is that load fluctuations cause significant

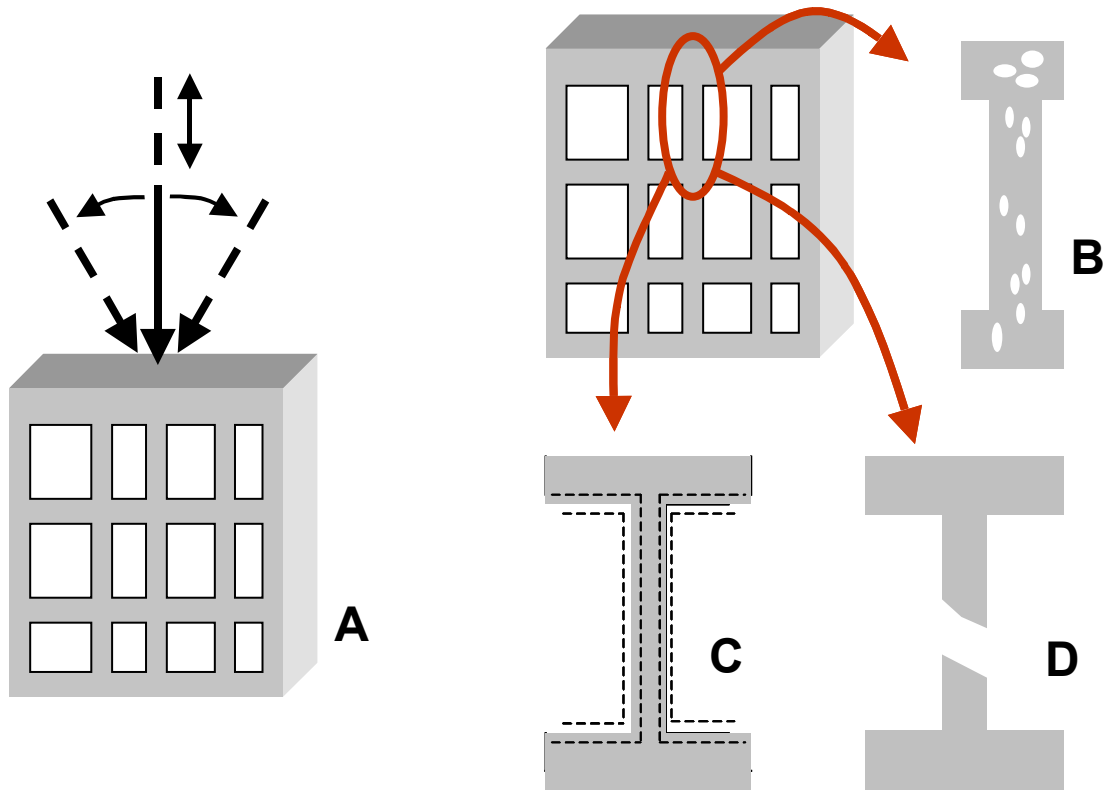


Figure 3.5 – Potential Sources of Variation in Topology Design

performance deviation that could be lessened by selecting a more robust topology. Other potential noise factors in topology design include nodal locations, size and shape of the topological domain, and magnitudes and directions of applied displacements. Also, material properties could be influenced by a host of stochastic processing-related phenomena such as porosity illustrated in Figure 3.5b.

As shown in Figure 3.5c, it is also possible for control factors—element areas in topology design—to deviate from nominal values as a result of fabrication-related noise or tolerances or due to subsequent changes in the factor values during the design process. Another type of control factor variation, called *topological variation*, occurs when the topological properties of a design are non-deterministic. With topological variation,

geometric connectivity may be altered uncontrollably by tearing or fusing of connective links or surfaces. An example is illustrated in Figure 3.5d in which an element of the original topology is severed, changing the number of isolated holes or discontinuities in the structure and therefore its topological properties.

Fluctuations in factors may be more influential in materials design applications than in large-scale structural applications. Materials are designed and fabricated or processed on smaller length scales where processing-related factors may be more difficult to control. Also, on smaller length scales, even small fluctuations may be large relative to the nominal value of a factor. For example a 50 μm tolerance on a 250 μm element is quite large relative to a similar tolerance on a 10 cm (or 10,000 μm) element.

Variation in noise and control factors should be quantified as accurately as possible to enable quantitative assessment of its impact on response values. Here, the vectors of control factors and noise factors are designated X and p , respectively. Each factor that fluctuates is characterized further with a nominal value and a deviation, as follows:

$$X_i \pm \delta X_i; P_i \pm \delta P_i \quad (3.1)$$

If statistical information is available for the factor, then it is a *probabilistic parameter*.

The mean (μ) and standard deviation (σ) may be substituted for nominal values and deviations, respectively, as follows for a normal or uniform distribution:

$$\mu_{X_i} \pm k\sigma_{X_i}; \mu_{P_i} \pm k\sigma_{P_i} \quad (3.2)$$

where k is a multiple of the standard deviation. If statistical distributions are not available, then the factor is classified as a *flexible parameter*. A flexible parameter may assume any value within a specified range or interval. Probabilities are not assigned to specific values with the interval; instead, values are assumed to cluster within the

specified ranges. Ranges of values may be specified when insufficient data is available for estimating a statistical distribution or when a designer intends to specify ranges of values rather than precise point values for control factors. For flexible control or noise factors, tolerance ranges (ΔX or ΔP) may serve as deviation estimates, as follows:

$$X_i \pm \Delta X_i; P_i \pm \Delta P_i \quad (3.3)$$

In the early stages of design, ranges of values associated with sets of possible solutions and conditions are common, and measurement-based, probabilistic information is scarce; thus, the latter formulation may be more appropriate for robust topology design.

Noise factor variation can be modeled straightforwardly, in the form of Equations 3.2 or 3.3. The noise factor designation, P , is replaced with a specific factor such as the solid modulus of elasticity, E , the magnitude of an applied load, L , or the direction of an applied load, θ .

Quantitatively modeling *control factor variations* is difficult in ground structure-based robust topology design applications because some elements—and their corresponding control factors—are eventually removed from an initial topology. Control factors effectively switch from ‘on/active’ to ‘off/removed’ unlike typical robust design problems in which control factors are always active and influential. In ground structure-based approaches, topology modification is achieved by permitting control factor values to range from an upper bound, X_U , to an extremely small lower bound, X_L , during an iterative search process, as depicted in Figure 3.6. The ratio of upper to lower bound values, X_U/X_L , is typically on the order of 10^4 or larger. The large ratio is needed to simulate removal of elements from the initial topology. Element removal—and therefore topology modification—is based on the assumption that elements with extremely small

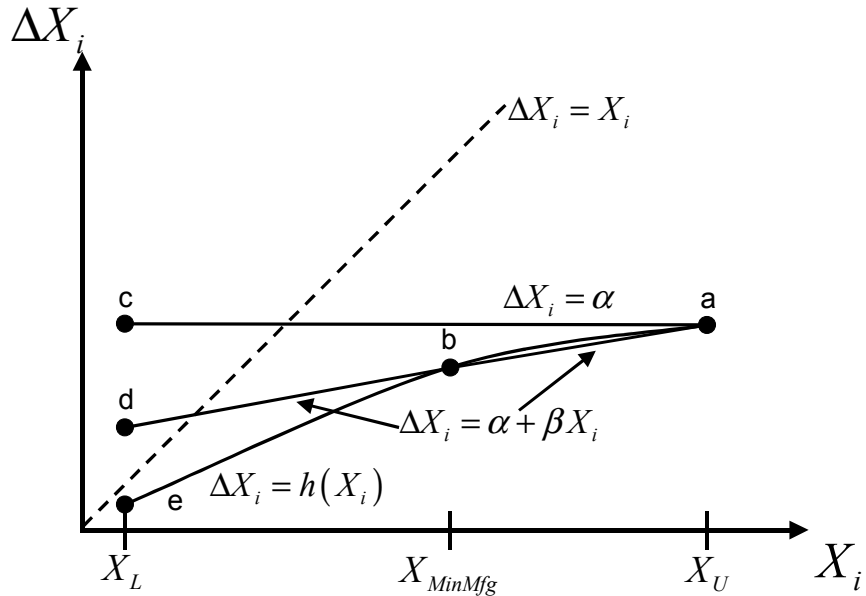


Figure 3.6—Relating Nominal Control Factor Values and Control Factor Tolerance Ranges

areas (relative to neighboring elements) have little impact on the performance of the overall structure. Therefore, after the iterative search process converges, elements with areas near the lower bound are removed from the initial topology. Utilization of continuous element areas with extremely small lower bounds relaxes the original, discrete topology modification problem (with elements that are either ‘on/active’ or ‘off/removed’)—making it amenable to continuous search techniques.

As a result of the large range of control factor values, special restrictions must be applied to models of control factor variation. Typically, models of control factor variation are created for realizable regions of the design space—delimited, for example by manufacturing limitations. It is likely that the minimum manufacturable area, X_{MinMfg} , is much larger than X_L , as shown in Figure 3.6, and tolerance or statistical distribution data is available only over the range, $X_{MinMfg} \leq X_i \leq X_U$. However, during the iterative

search process, control factors will be assigned values smaller than X_{MinMfg} and as small as X_L . Although topology elements with areas this small can not be manufactured, it is necessary to assign extremely small values to some element areas during the iterative search process to simulate the removal of elements. To estimate tolerance ranges for element areas less than X_{MinMfg} , we assume that a function, $\Delta X_i = h(X_i)$, is constructed to quantify the tolerance range, ΔX_i , as a function of the nominal area, X_i , of element i . Preliminarily, one might apply a constant tolerance function, $\Delta X_i = h(X_i) = \alpha$, based on a single data point, or a linear tolerance function, $\Delta X_i = h(X_i) = \alpha + \beta X_i$, based on two data points, as represented by \overline{ac} and \overline{abd} , respectively, in Figure 3.6. Both formulations are inappropriate for robust topology design, however, because tolerance ranges are larger than nominal values in regions near the lower bound in Figure 3.6; i.e., the tolerance range for small nominal areas includes clearly inadmissible negative values of element areas. Another option is to assign tolerance values for the manufacturable interval, $X_{MinMfg} \leq X \leq X_U$, and assume zero tolerance values for smaller nominal areas. However, over the range, $X_L \leq X \leq X_U$, h would not be continuous due to the discontinuity at X_{MinMfg} . This would introduce discontinuities in robust design constraints and objectives which include not only nominal response values but also response ranges, calculated as continuous functions¹ of ΔX_i as discussed in the following section. Since it is desirable to preserve continuity in a topology design problem so that gradient-based search algorithms are effective, the function h (where $\Delta X_i = h(X_i)$) should be a continuous function with values greater than the nominal area, $\Delta X_i = h(X_i) \geq X_i$ over

¹ In a worst case formulation, reviewed in Section 2.2.

the range, $X_L \leq X \leq X_U$. The sample function, h , represented by curve abe in Figure 3.6, is an example of such a function that also interpolates two known data points (a and b).

Models for Topological Variation

Models for *topological variation* are necessarily different from models for control and noise factor variation because variations in topology involve changes in the set of control factors that describe the topology during the topology design process. An initial ground structure can be thought of as a complete set of all of the elements (arranged in a specific pattern) that may be included in any derivative structure. *Derivative structures* include a full or partial subset of the elements in the initial ground structure, arranged geometrically according to the configuration of the initial ground structure. Derivative structures may have unique topologies that are created by removing elements from the initial ground structure during a topology design process. The control factors for an initial ground structure can be expressed as a set, \mathbf{X}^G , with size, N^G , determined by the number of elements in the nominal ground structure:

$$\mathbf{X}^G = \{X_1, X_2, \dots, X_{N^G}\} \quad (3.4)$$

For example, for the initial ground structure illustrated at the top of Figure 3.7, there are 36 independent control factors—one for each element in the structure, with an independent element connecting each pair of nodes. At the conclusion of a topology design process, some of the elements in the initial ground structure are removed to modify the topology, and only N^D elements are retained for the derivative structure. For example, the derived structure in Figure 3.7 includes a subset of twelve elements (labeled I through $I2$ in the figure) from the initial ground structure. The control factors for the derivative structure can be expressed as a set, \mathbf{X}^D , with size, N^D ,

$$\mathbf{X}^D : \mathbf{X}^D \subseteq \mathbf{X}^G, |\mathbf{X}^D| = N^D, N^D \leq N^G \quad (3.5)$$

During a series of subsequent design stages and a processing or fabrication stage, the derived structure is transformed into a physical artifact. As shown in the bottom row of Figure 3.7, a physical realization of a derived structure may not be topologically identical to it. There could be multiple reasons for this. First, the topology of the derived structure may be changed during subsequent stages of the design process to accommodate design requirements. Also, topology-related imperfections may be introduced by stochastic fabrication or processing environments. These changes are unpredictable *a priori* and give rise to *topological variation*. In this dissertation, topological variation includes unintended topological changes to a structure that occur *after* its topology has been designed and specified. The topological changes refer to removal of one or more elements or one or more nodes/joints in the intended topology, as illustrated in the bottom row of Figure 3.7. ‘Removal’ is a general term that refers to both extraction of an element or node during subsequent design stages and cracked/severed/missing elements and joints that cannot contribute to the performance of the overall structure. In Figure 3.7, the structures illustrate removal of element 6, removal of elements 6 and 7, and removal of node *e* (which makes elements 4, 6, 7, and 9 inactive). In this dissertation, topological changes involving physical relocation (i.e., translation, rotation) of elements in a structure are not considered.

Due to topological variation, a physically realized structure includes only a subset, \mathbf{X}^R , of the control factors and associated elements in a derived structure:

$$\mathbf{X}^R : \mathbf{X}^R \subseteq \mathbf{X}^D, N^R \leq N^D \quad (3.6)$$

where N^R is the number of elements in the realized structure. Although the transformation from an initial ground structure to a derived structure occurs deterministically through a topology design process, the difference between a derived structure and a physically realized structure cannot be known *a priori*. The difference between the set of control factors in the derived and realized structures is the set of missing elements, \mathbf{X}^M , where

$$\mathbf{X}^D / \mathbf{X}^R = \mathbf{X}^M \quad (3.7)$$

Neither the number of missing elements, N^M , nor their identities, \mathbf{X}^M , are known *a priori*. Therefore, there is a chance that one or more of the elements designated for the *derived* structure will not be present or active in the realized structure. During a topology design process, when an initial ground structure is transformed into a derived structure, a designer should account for the likelihood that an element is actually realized if it is included in the derived structure. The probability that an individual element, X_i , is a member of the set of missing elements, \mathbf{X}^M , if the element is a member of the derived structure, \mathbf{X}^D , is expressed as:

$$P(X_i \in \mathbf{X}^M | X_i \in \mathbf{X}^D) \quad (3.8)$$

It is possible that more than one element specified for the derived structure is missing from the final realized structure. If the probabilities that element i and element j are missing from the realized structure are independent, then the probability that *both* element i and element j are missing from the realized structure is:

$$\begin{aligned} P\left(\left(X_i \in \mathbf{X}^M | X_i \in \mathbf{X}^D\right) \cap \left(X_j \in \mathbf{X}^M | X_j \in \mathbf{X}^D\right)\right) = \\ P\left(X_i \in \mathbf{X}^M | X_i \in \mathbf{X}^D\right) \bullet P\left(X_j \in \mathbf{X}^M | X_j \in \mathbf{X}^D\right) \end{aligned} \quad (3.9)$$

Equation 3.9 can be extrapolated straightforwardly for outcomes in which more than two elements are missing from the realized structure. In Equations 3.8 and 3.9, each element may have a unique probability of being missing or removed; however, it is important to note that assigning a relatively higher probability of being missing to a particular elements effectively biases the topology design process towards removal of the element from the initial ground structure. Clearly, if there is a relatively strong chance that a particular element will be missing from a realized structure, it would be beneficial—in terms of potential variation from nominal performance—to avoid including the element in the derived structure. In this dissertation, all elements are assumed to have equal probabilities of being missing from a realized structure in the event that they are included in a derived structure.

Similarly, the possibility of a missing or removed node can be considered during the topology design process. The number of nodes in the initial ground structure, derived structure, and realized structure are specified as C^G , C^D , and C^R , respectively, and the set of nodes in the initial ground structure, derived structure, and realized structure are designated \mathbf{R}^G , \mathbf{R}^D , and \mathbf{R}^R , respectively:

$$\mathbf{R}^G = \{R_1, R_2, \dots, R_{C^G}\} \quad (3.10)$$

$$\mathbf{R}^D : \mathbf{R}^D \subseteq \mathbf{R}^G, |\mathbf{R}^D| = C^D, C^D \leq C^G \quad (3.11)$$

$$\mathbf{R}^R : \mathbf{R}^R \subseteq \mathbf{R}^D, C^R \leq C^D \quad (3.12)$$

The probability that one node is missing from a realized structure is:

$$P(R_i \in \mathbf{R}^M | R_i \in \mathbf{R}^D) \quad (3.13)$$

where \mathbf{R}^M is the set of missing nodes, based on the derived structure as follows:

$$\mathbf{R}^D \cap \mathbf{R}^R = \mathbf{R}^M \quad (3.14)$$

The probability that two nodes are missing simultaneously is specified as follows:

$$\begin{aligned} P\left(\left(R_i \in \mathbf{R}^M \mid R_i \in \mathbf{R}^D\right) \cap \left(R_j \in \mathbf{R}^M \mid R_j \in \mathbf{R}^D\right)\right) = \\ P\left(R_i \in \mathbf{R}^M \mid R_i \in \mathbf{R}^D\right) \bullet P\left(R_j \in \mathbf{R}^M \mid R_j \in \mathbf{R}^D\right) \end{aligned} \quad (3.15)$$

where the previous relationship is based on the assumption that the probability of a missing node is independent of the probability of another missing node. When a node is missing, all of the elements connected to the node are inactive or effectively missing as well. Since each element joints two distinct nodes, removal of either node implies that the element is inactive or effectively missing. If there is a chance of a missing node, there is automatically a chance of one or more missing elements. By specifying probabilities of missing nodes, the two sources of variation are separated. The probability of encountering one or more severed elements with intact nodes, as depicted in the lower left and lower center of Figure 3.7, respectively, should be specified via Equations 3.8 and 3.9, independently of the probability that an element is inactive because one of its nodes has been removed, as specified via Equations 3.13 and 3.15 and depicted in the lower right of Figure 3.7.

The quantitative model of topological variation in Equations 3.8, 3.9, 3.13, and 3.15 captures the probability of missing elements or nodes with respect to the *derived* structure rather than the *initial* ground structure. It must be used *during* a topology design process, however, when all of the elements and nodes in an *initial* ground structure are active and none of the elements or nodes have yet been removed to reduce it to a *derived* structure. A topological variation model of this type is appropriate for use during a topology design process because a topology designer is not interested in fabricating an *initial* ground

structure; nor is he/she interested in the likelihood of missing elements or nodes from the initial ground structure if it were fabricated in its entirety. Instead, he/she must account for the possibility that an element(s) or node(s) is missing from a realized structure, *if and only if* the element or node is retained for a derived structure. The model of Equations 3.8, 3.9, 3.13, and 3.15 quantifies this information and can be used—in conjunction with the decision formulation and simulation infrastructure described in the following sections—to design derived structures that are robust to topological variation.

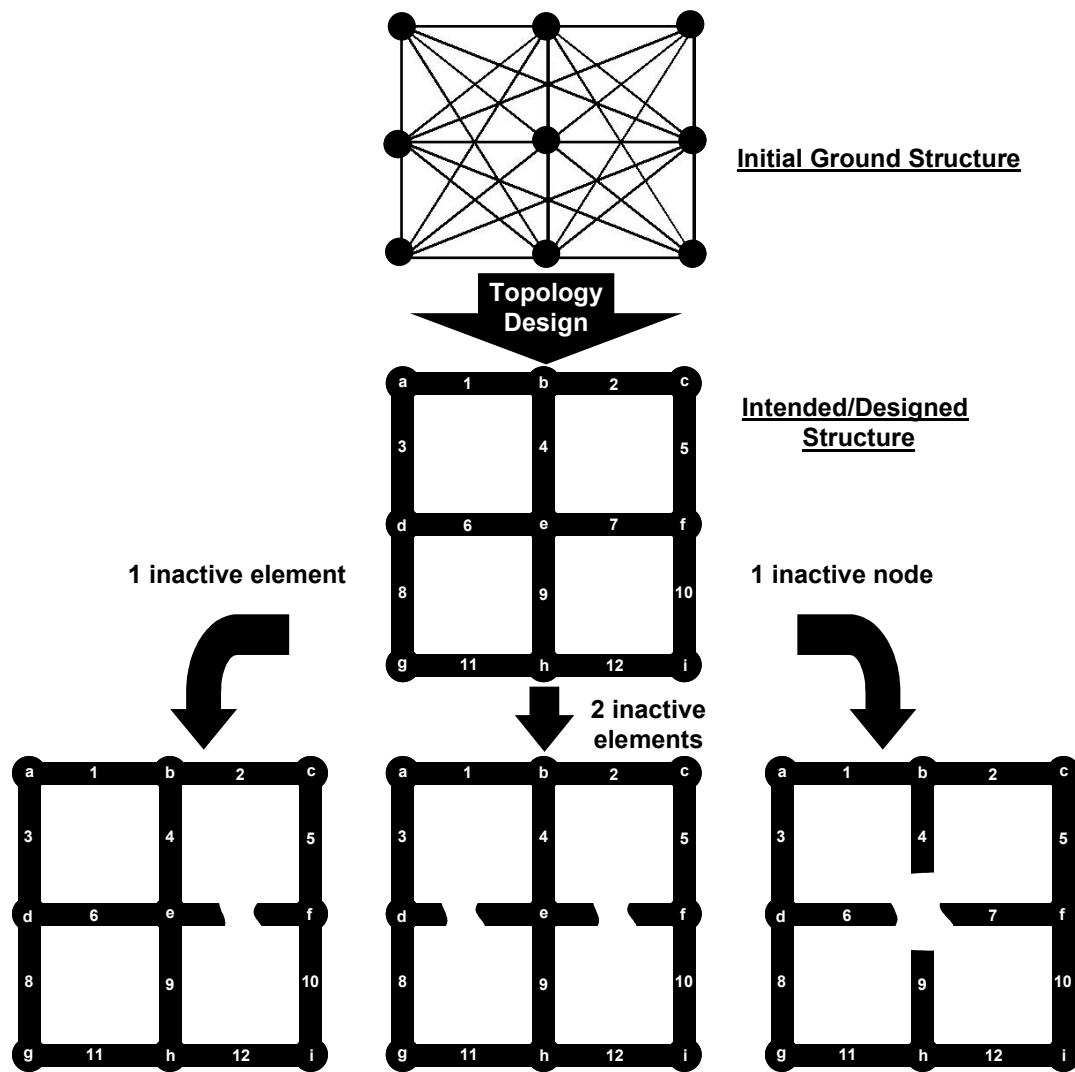


Figure 3.7—Examples of Topological Variation

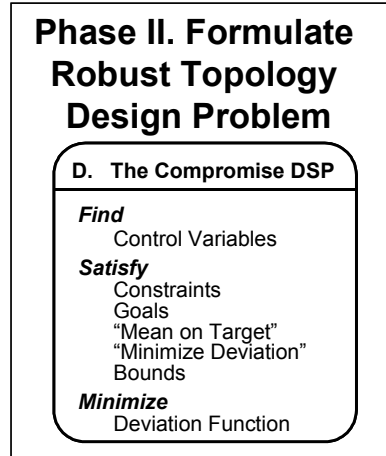


Figure 3.8 – Phase 2 of the RTPDEM: Formulating a Robust Topology Design Problem

3.3.2 Phase 2: Formulate a Robust Topology Design Problem

In Phase 2 of the RTPDEM illustrated in Figure 3.8, the variability information described in the previous section must be incorporated within a robust topology design problem formulation. A standard, ground structure-based topology design problem can be formulated as a non-linear programming problem as follows:

$$\mathbf{Find} \quad X_i \quad i = 1, \dots, n \quad (3.16)$$

$$\mathbf{Satisfy} \quad g_i(\mathbf{X}) \leq 0 \quad i = 1, \dots, p \quad (3.17)$$

$$X_L \leq X_i \leq X_U \quad i = 1, \dots, n \quad (3.18)$$

$$\mathbf{Minimize} \quad f(\mathbf{X}) = [f_1(\mathbf{X}), \dots, f_m(\mathbf{X})] \quad (3.19)$$

where $f_i(\mathbf{X})$ and $g_i(\mathbf{X})$ are objective and constraint functions, respectively; X_L and X_U are upper and lower bound values for element areas; and n , m , and p are the number of design variables, objectives, and constraints, respectively. In this standard topology design problem formulation, all of the design variables and responses (i.e., objectives and

constraints) are assumed to be deterministic. As discussed in the previous section, however, variation is expected in design parameters, including design variables and other factors, and these variations are expected to induce deviations in system responses. In robust design, these deviations are minimized while nominal responses are shifted to meet critical performance requirements. To carry out robust design, the standard topology design formulation in Equations 3.16-3.19 must be reformulated as a robust topology design problem to accommodate: (1) mathematical models of variation in design parameters as discussed in Phase 1, (2) estimates of induced response variation, (3) constraint formulations that account for variation in constraint functions, (4) and robust design metrics that facilitate not only meeting critical performance requirements but also minimizing ranges or distributions of performance for multiple objectives. These issues are addressed systematically by formulating a compromise decision support problem for robust topology design. Reasons for utilizing the compromise DSP, in particular, are provided in Section 2.2 and are not repeated here.

As presented in Figure 3.9, the compromise decision support problem for robust topology design facilitates the search for nominal values of system variables, \mathbf{X} , that satisfy a set of constraints, $\mathbf{g}(\mathbf{X}, \mathbf{P})$, and achieve a set of conflicting goals, $\mathbf{A}(\mathbf{X}, \mathbf{P})$, to the extent possible. It is based on the compromise Decision Support Problem (DSP), a multiobjective mathematical decision model that is a hybrid formulation based on mathematical programming and goal programming (Mistree, et al., 1993). A detailed description of the compromise DSP is available in Chapter 2 and in the literature (e.g., (Mistree, et al., 1993; Mistree, et al., 1990)); therefore, we limit our discussion here to customizing and utilizing the compromise DSP for robust topology design.

Given			
An alternative to be improved through modification			
Assumptions used to model the domain of interest			
The system parameters:			
	n	number of system variables	
	q	number of system constraints	
	m	number of system goals	
	c	number of nodes in initial ground structure	
$g_i(\mathbf{X}, \mathbf{P})$		System constraint function	
$A_i(\mathbf{X}, \mathbf{P})$		Goal achievement function	
P_i		Noise factor	
$P(X_i \in \mathbf{X}^M X_i \in \mathbf{X}^D)$		Topological variation in control factors	
			$i = 1, \dots, n$ Eq. (3.8)
$P(R_i \in \mathbf{R}^M R_i \in \mathbf{R}^D)$		Topological variation in nodes	
			$i = 1, \dots, c$ Eq. (3.13)
$\delta \mathbf{P} = h_p(\mathbf{X}, \mathbf{P})$		Noise factor variation function	Eq. (3.20)
$\delta \mathbf{X} = h_x(\mathbf{X}, \mathbf{P})$		Control factor variation function	Eq. (3.21)
$\delta g_i(\mathbf{X}, \mathbf{P})$		Constraint variation function	Eq. (3.22)
$\delta A_i(\mathbf{X}, \mathbf{P})$		Goal variation function	Eq. (3.23)
Find			
X_i		Control factors (Nominal Values)	$i = 1, \dots, n$
d_i^+, d_i^-		Deviation Variables	$i = 1, \dots, 2m$
Satisfy			
System Constraints			
	$g_i(\mathbf{X}, \mathbf{P}) - \delta g_i(\mathbf{X}, \mathbf{P}) \geq 0$		$i = 1, \dots, q$ Eq. (3.24)
System Goals			
	$A_i(\mathbf{X}, \mathbf{P}) + d_i^- - d_i^+ = G_i$		$i = 1, \dots, m$ Eq. (3.25)
	$\delta A_i(\mathbf{X}, \mathbf{P}) + d_i^- - d_i^+ = G_i$		$i = m+1, \dots, 2m$ Eq. (3.26)
Bounds			
	$X_{i,L} \leq X_i \leq X_{i,U}$		$i = 1, \dots, n$ Eq. (3.27)
	$d_i^+, d_i^- \geq 0$		$i = 1, \dots, 2m$ Eq. (3.28)
	$d_i^+ \cdot d_i^- = 0$		$i = 1, \dots, 2m$ Eq. (3.29)
Minimize			
Objective Function: Archimedean formulation			
	$Z = \sum_i w_i (d_i^+, d_i^-)$		$i = 1, \dots, 2m$ Eq. (3.30)

Figure 3.9 –Decision Support Problem Formulation for Robust Topology Design

As in the standard topology design formulation of Equations (3.16-3.19), constraints ($\mathbf{g}(\mathbf{X}, \mathbf{P})$)—criteria that *must* be met by all feasible designs—are distinguished from goals ($\mathbf{A}(\mathbf{X}, \mathbf{P})$) that are minimized, maximized, or matched with respect to target values. As reported in the *Given* section of the compromise DSP, both constraints and goals are assumed to be functions of control and noise factors, and the functions are assumed to be available in closed form or as part of a simulation model. Variation functions, $\delta\mathbf{X} = h_x(\mathbf{X}, \mathbf{P})$ and $\delta\mathbf{P} = h_p(\mathbf{X}, \mathbf{P})$, are assumed to be available for each of the control factors (also known as system variables) and noise factors, respectively.² The variation functions could be tolerance ranges or statistical distributions, as indicated in Equations 3.3 and 3.2, respectively. Also, models of topological variation for nodes (Equations 3.13 and 3.15) and/or elements (Equations 3.8 and 3.9) are assumed to be available. Based on nominal values, \mathbf{X} and \mathbf{P} , and specified variations, $\delta\mathbf{X}$ and $\delta\mathbf{P}$, for control and noise factors, respectively, and models of topological variation, it is possible to approximate nominal values and variations for responses, designated as $g_i(\mathbf{X}, \mathbf{P})$ and $\delta g_i(\mathbf{X}, \mathbf{P})$ for constraint functions and $A_i(\mathbf{X}, \mathbf{P})$ and $\delta A_i(\mathbf{X}, \mathbf{P})$ for goal achievement functions. Techniques for propagating variation from control and noise factors to constraint or goal functions for robust topology design are discussed as part of Phase 3.

The nominal values of independent system variables, \mathbf{X} , can be adjusted as required to change the behavior of the system. In robust topology design, the independent system variables are the nominal values of element areas. Each variable has associated continuous and topological variation, defined as a function of nominal variable values,

² If a system variable, X_i , is not expected to exhibit variation, one can assume that ΔX_i is equivalent to zero.

that leads to ranges of values for system constraints and goals, $\delta\mathbf{g}(\mathbf{X}, \mathbf{P})$ and $\delta\mathbf{A}(\mathbf{X}, \mathbf{P})$, respectively. To ensure that an entire range of system constraint function values satisfies a constraint limit, constraints are expressed in a worst-case formulation (Parkinson, et al., 1993) as shown in Equation 3.24 in Figure 3.9.

Variations in system goal values, $\delta\mathbf{A}(\mathbf{X}, \mathbf{P})$, are minimized. Simultaneously, nominal goal values, $\mathbf{A}(\mathbf{X}, \mathbf{P})$, are minimized, maximized, or matched with respect to a target, depending on the goal. Tradeoffs are to be expected between the two aspirations. Therefore, for each goal achievement function, $\mathbf{A}(\mathbf{X}, \mathbf{P})$, two system goals are included in the decision support problem—Equation 3.26 in Figure 3.9 for minimizing the variation in goal achievement and Equation 3.25 in Figure 3.9 for minimizing, maximizing, or target-matching the nominal value of goal achievement, respectively. In each equation, G_i , represents the target value for the goal. In Equation 3.26, the target may be zero or a very small value while the target value in Equation 3.25 is the desired value for $\mathbf{A}(\mathbf{X}, \mathbf{P})$. As in goal programming formulations, deviation variables, d_i^+ and d_i^- , measure the difference between a goal target value and the actual level of achievement of a goal. Two deviation variables are utilized for each goal function and two constraints are applied to the deviation variables (Equations 3.28 and 3.29) to guarantee that the deviation variables assume only positive or zero values—greatly simplifying application of a solution algorithm.

The aim of the objective function, Z , in Equation 3.30 is to minimize the difference between that which is desired (the goal, G_i) and that which can be achieved ($A_i(\mathbf{X}, \mathbf{P})$) for *multiple goals*. The objective function is expressed in terms of deviation variables and

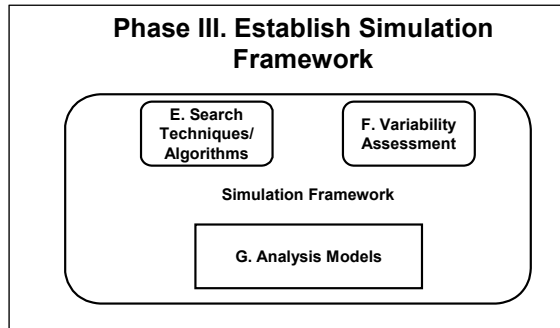


Figure 3.10 – Phase 3 of the RTPDEM: Solving a Robust Topology Design Problem

measures the extent to which multiple goals are achieved. In the compromise DSP, multiple goals have been considered conventionally by formulating the deviation function in several ways, including with Archimedean weightings (Mistree, et al., 1993) as illustrated in Figure 3.9.

3.3.3 Phase 3: Establish Simulation Framework

In Phase 3 of the RTPDEM, illustrated in Figure 3.10, a simulation framework is established for solving the robust topology design problem. A simulation framework for a robust topology design problem includes:

- Topology modification techniques for determining which aspects of an initial topology (established in Phase I) are retained in the derived topology,
- Analysis models for evaluating the behavior of proposed solutions,
- Variability assessment techniques for estimating the impact of variation in control and noise factors and topology on responses of interest, and
- Search algorithms for exploring the design space.

Several aspects of topology design problems have strong impacts on the formulation of a simulation framework; they are reviewed before proceeding to describe each

component of a simulation framework. First, there are large numbers of system variables in topology design problems. In a full ground structure, every pair of nodes is connected with an element, and there is one system variable per element. For a full ground structure with r nodes, there are $n = \frac{1}{2}r(r-1)$ system variables. Secondly, each system variable necessarily has a very broad range of possible values with the ratio of upper and lower bound values, X_U/X_L , typically on the order of 10^4 or larger. Thirdly, computational times are non-negligible. A detailed analysis is required to evaluate the performance of each candidate solution proposed by a search algorithm. Examples of analysis models include finite element analysis, computational fluid dynamics analysis, and cost models. The models may be embedded in commercial software (e.g., ANSYS or FLUENT) or in customized, user-generated software written in languages such as C, FORTRAN, or BASIC or in simulation environments such as MATLAB. Finally, both the standard topology design problem in Equations 3.16 through 3.19 and the robust topology design formulation in Figure 3.9 are nonlinear.

Search Algorithms

Several classes of search algorithms have been utilized for topology design including optimality criteria methods, gradient-based mathematical programming algorithms, and exploratory methods such as genetic algorithms or simulated annealing algorithms. Gradient-based, non-linear mathematical programming methods—such as sequential quadratic programming or sequential linear programming—are used here for several reasons. They are more flexible than optimality criteria methods for handling complex problem formulations. For problems with large numbers of continuous variables and non-negligible computational times, gradient-based algorithms tend to be more efficient

than exploratory algorithms because exploratory algorithms often require large numbers of iterations and function evaluations for such problems before arriving at a solution (which may be of poor quality). On the other hand, the efficiency and effectiveness of gradient-based search algorithms in topology design depends partially on the availability of analytical gradients—expressions for the partial derivatives of constraint and goal functions with respect to the vector of design variables. Finite differencing schemes are available for approximating these gradients. However, analytical expressions are utilized in typical topology design applications and in this dissertation because they can be derived from the finite element-based analysis utilized in topology design and tend to be much less computationally expensive. The computational savings is compounded by the fact that gradients can be utilized for Taylor series-based estimates of response variation for robust design as described in this section—thereby avoiding computationally expensive Monte Carlo simulations or other types of sampling.

Several categories of gradient-based algorithms are available for topology design applications. To support establishment of the RTPDEM, the performance of three commonly utilized algorithms—SLP, SQP, and the method of moving asymptotes (MMA)—was compared for a common topology design problem (Fernandez, 2003). The common topology design problem was based on the cantilever beam design problem and the 99-line MATLAB code introduced by Sigmund for compliance minimization via the SIMP topology design approach (Sigmund, 2001). The MMA algorithm was provided by Krister Svanberg (1987) for MATLAB applications, and the SLP and SQP algorithms were incorporated as functions within MATLAB (2001). In a side-by-side comparison, the MMA and SLP algorithms required much less computational time for convergence to

feasible solutions than the SQP algorithm, partially due to the large number of function evaluations and computationally expensive Hessian evaluations required by the SQP algorithm. The SLP algorithm was faster than the MMA algorithm for problems with large numbers of variables, but it required significant user interaction for setup and calibration of parameters, especially bounds on design variables, to prevent divergence, primarily due to the tendency of SLP to push design variable values alternately between upper and lower extrema or bounds. In contrast, the MMA algorithm required very little user interaction—aside from appropriately scaling the magnitudes of function values and gradients—and tends to converge quickly and smoothly for the sample problem. Therefore, the MMA algorithm is utilized for the examples in this dissertation.

When gradient-based search algorithms are applied to the robust topology design problem formulation of Figure 3.9, analytical gradient expressions are needed for the nominal values *and variations* of the constraint and goal achievement functions in Equations 3.10, 3.11, and 3.12. Therefore, the partial derivatives of response *variations* must be formulated and calculated for robust topology design; only the partial derivatives of nominal responses are used in standard topology design formulations. Although search algorithms, combined with analysis codes and analytical gradients derived from them, are sufficient for solving the standard topology design problem in Equations 3.1 through 3.4, solution of the robust topology design problem formulation in Figure 3.9 also requires approximations of response variations as well as expressions for the gradient of response variations with respect to the vector of design variables.

Variability Assessment

Monte Carlo analysis, statistically designed experiments, and analytical Taylor series expansion are three common techniques for evaluating variation in responses (i.e., $\delta\mathbf{g}$ and $\delta\mathbf{A}$) due to variation in control or noise factors, $\delta\mathbf{X}$, $\delta\mathbf{P}$. Monte Carlo analysis provides a relatively accurate approximation of the statistical distribution of responses, but it requires a large number of system evaluations for *each* iteration of a search algorithm. Statistically designed experiments—such as fractional factorial, Latin Hypercube, orthogonal array, or other designs—can also be used to sample the domain of noise and control factors and approximate the nominal value and variation of responses. Although statistically designed experiments generally require fewer system evaluations than Monte Carlo simulations, the number of experiments grows (nonlinearly, in many cases) with the number of control and noise factors. The large numbers of system evaluations required by both approaches make them costly for robust topology design with large numbers of control factors and non-negligible computational times for system analysis. The techniques proposed in this dissertation for transmitting variation in robust topology design are based on Taylor series expansion for propagating control and/or noise factor variation and customized experiments for transmitting topology variation.

For robust topology design, we use a Taylor series expansion to transmit variation from control (or noise) factors to responses (i.e., constraint and goal achievement functions). The nominal response value is calculated by setting all factors at their nominal values. Variation in the i^{th} constraint or goal achievement function, respectively, is calculated with a Taylor series expansion as follows:

$$\Delta g_i = \sum_{j=1}^n \left| \frac{\partial g_i}{\partial X_j} \Delta X_j \right|_{\mathbf{x}} \quad (3.31)$$

$$\Delta A_i = \sum_{j=1}^n \left| \frac{\partial A_i}{\partial X_j} \Delta X_j \right|_{\mathbf{x}} \quad (3.32)$$

where the right-hand sides of Equations (3.31) and (3.32) are evaluated at nominal control factor values. The approximate tolerance ranges are utilized for the constraint and goal formulations in Equations (3.24) and (3.26) in the robust topology design formulation of Figure 3.9. This approach is also known as a worst case analysis, introduced by Parkinson and coauthors (1993) because fluctuations are assumed to occur simultaneously in a worst-case combination. It is most accurate for small tolerances and weak or negligible interactions among the factors that fluctuate. Tolerance ranges, rather than statistical distributions, are assigned to relevant control and/or noise factors.

Analytical Taylor series-based methods have several advantages in robust topology design. Because gradient-based mathematical programming algorithms are utilized with analytical gradient expressions, the gradient information required in Equations (3.31) and (3.32) is already available. Therefore, evaluation of Equations (3.31) and (3.32) is computationally inexpensive. However, derivatives of the constraint and goal achievement function tolerances (i.e., Equations (3.31) and (3.32)) are needed in order to implement gradient-based search algorithms for the robust topology design formulation in Figure 3.9. In other words, a gradient-based search algorithm requires partial derivatives of Equations (3.24), (3.25), and (3.26), respectively, in Figure 3.9 with respect to each control factor, X_j , as follows:

$$\frac{\partial}{\partial X_j}(g_i(\mathbf{X}, \mathbf{P}) - \Delta g_i(\mathbf{X}, \mathbf{P})) = \frac{\partial g_i(\mathbf{X}, \mathbf{P})}{\partial X_j} - \frac{\partial(\Delta g_i(\mathbf{X}, \mathbf{P}))}{\partial X_j}; \quad (3.33)$$

$$i = 1, \dots, p; j = 1, \dots, n$$

$$\frac{\partial}{\partial X_j}(d_i^- - d_i^+) = \frac{\partial}{\partial X_j}(G_i - A_i(\mathbf{X}, \mathbf{P})) = -\frac{\partial A_i(\mathbf{X}, \mathbf{P})}{\partial X_j}; i = 1, \dots, m; j = 1, \dots, n \quad (3.34)$$

$$\frac{\partial}{\partial X_j}(d_i^- - d_i^+) = \frac{\partial}{\partial X_j}(G_i - \Delta A_i(\mathbf{X}, \mathbf{P})) = -\frac{\partial(\Delta A_i(\mathbf{X}, \mathbf{P}))}{\partial X_j}; \quad (3.35)$$

$$i = 1, \dots, m; j = 1, \dots, n$$

where the derivatives in Equations (3.34) and (3.35) are evaluated in terms of the deviation variables which enter the objective function in Equation (3.30). In Equations (3.33-3.35), the partial derivatives of nominal constraint and goal achievement functions are calculated for standard topology design problems, but the partial derivatives of their ranges are required specifically for the robust topology design problem. They can be derived directly from the Taylor series expansion used to calculate the ranges, as follows:

$$\frac{\partial}{\partial X_j}(\Delta g_i(\mathbf{X}, \mathbf{P})) = \frac{\partial}{\partial X_j} \left(\sum_{k=1}^n \left| \frac{\partial g_i}{\partial X_k} \Delta X_k \right|_{\mathbf{X}} \right) \quad (3.36)$$

$$\frac{\partial}{\partial X_j}(\Delta A_i(\mathbf{X}, \mathbf{P})) = \frac{\partial}{\partial X_j} \left(\sum_{k=1}^n \left| \frac{\partial A_i}{\partial X_k} \Delta X_k \right|_{\mathbf{X}} \right) \quad (3.37)$$

The details of the calculations of Equations (3.33-3.37) are specific to particular goal and constraint functions and are addressed specifically for the examples in Chapters 6 and 7.

Variability Assessment for Topological Variation

As noted in the Phase I discussion, topological variation is associated with elements or nodes intended for the final topology but missing from a realized structure. This type of variation cannot be modeled as a continuous function of control or noise factor values;

instead, it is captured as the probability that a particular element or node is missing from a realized structure, even though it was specified as part of a derived structure:

$$P(X_i \in \mathbf{X}^M | X_i \in \mathbf{X}^D) \quad (3.8)$$

$$P(R_i \in \mathbf{R}^M | R_i \in \mathbf{R}^D) \quad (3.13)$$

Topological variation is discrete in nature because the number of control factors decreases when an element or node is removed or missing from a structure. Taylor series-based approximations are valid for small changes in continuous factors when all other conditions are fixed, including the number and identity of control factors. Therefore, they cannot be used to evaluate the impact of a missing node or element on responses of interest. Instead, discrete experiments are required to evaluate the impact of potential variations in the realized topology.

The purpose of conducting experiments for topological variation is to evaluate the mean and standard deviation of each goal and constraint function, which are random variables due to the presence of topological variability. If a total of V experiments are conducted to simulate topological variability, the mean and standard deviation of a goal function, $A_i(\mathbf{X}, \mathbf{P})$, is calculated as follows:

$$\mu_{A_i} = \sum_{v=1}^V \gamma_v A_i(\mathbf{X}_v, \mathbf{P}_v) \quad (3.38)$$

$$\sigma_{A_i}^2 = \sum_{v=1}^V \gamma_v \left(A_i(\mathbf{X}_v, \mathbf{P}_v) - \mu_{A_i} \right)^2 \quad (3.39)$$

where γ_v is the probability of experiment v , \mathbf{X}_v and \mathbf{P}_v are vectors of control factors and noise factors, respectively, and their values for experiment v , and $A_i(\mathbf{X}_v, \mathbf{P}_v)$ is the nominal value of a goal function if control factor variation is present. Note that the number of

control factors will change from experiment to experiment due to topological variation. If several experiments are conducted, a goal range, calculated according to Equation 3.32, is likely to have different values for each experiment. An average value for a goal range is calculated as follows:

$$\Delta_{\mu} A_i = \sum_{v=1}^V \gamma_v \Delta A_i(\mathbf{X}_v, \mathbf{P}_v) \quad (3.40)$$

Expressions for the mean and standard deviation of a constraint function are obtained straightforwardly by substituting a constraint function, $g_i(\mathbf{X}_v, \mathbf{P}_v)$, for the goal function in Equations 3.38 and 3.39. Since the gradients of Equations 3.24, 3.25, and 3.26 are required by gradient-based search algorithms, the partial derivatives of Equations 3.38 and 3.39 must be calculated with respect to each control factor in turn:

$$\frac{\partial \mu_{A_i}}{\partial X_j} = \begin{cases} \sum_{v=1}^V \gamma_v \frac{\partial A_i(\mathbf{X}_v, \mathbf{P}_v)}{\partial X_j} & \text{if } X_j \in \mathbf{X}_v \\ 0 & \text{if } X_j \notin \mathbf{X}_v \end{cases} \quad (3.41)$$

$$\frac{\partial \sigma_{A_i}}{\partial X_j} = \begin{cases} \frac{\sum_{k=1}^V \gamma_v (A_i(\mathbf{X}_v, \mathbf{P}_v) - \mu_{A_i}) \left(\frac{\partial A_i(\mathbf{X}_v, \mathbf{P}_v)}{\partial X_j} - \frac{\partial \mu_{A_i}}{\partial X_j} \right)}{\sigma_{A_i}} & \text{if } X_j \in \mathbf{X}_v \\ 0 & \text{if } X_j \notin \mathbf{X}_v \end{cases} \quad (3.42)$$

$$\frac{\partial (\Delta_{\mu} A_i)}{\partial X_j} = \begin{cases} \sum_{v=1}^V \gamma_v \frac{\partial \Delta A_i(\mathbf{X}_v, \mathbf{P}_v)}{\partial X_j} & \text{if } X_j \in \mathbf{X}_k \\ 0 & \text{if } X_j \notin \mathbf{X}_k \end{cases} \quad (3.43)$$

Notice that the partial derivative with respect to an element, X_j , is calculated only if the element is included in the structure for the v^{th} experiment.

The next logical step is to determine the number of experiments, V , and the details of each experiment. The number of required experiments is equivalent to the number of

topological permutations associated with topological variation. Using basic set theoretic principles, the number of possible permutations of a structure (induced by topological variation) can be calculated. The number of possible permutations is shown to be very high, even for a small structure, resulting in potentially prohibitive computational costs of experimentation. Based partially on information obtained from the topological variation models, a strategy is proposed for limiting the number of permutations and associated experiments.

If elements or nodes are randomly removed from a structure, there are many possible permutations of the structure to consider. Each permutation is a potential experiment in Equations 3.38 – 3.43. To begin, consider an initial ground structure of N elements from which several elements are randomly missing, leaving only k elements in a realized structure. The set of elements remaining in the realized structure is a subset of the set of elements, \mathbf{X}^N , defined for the initial ground structure. Formally, if k elements are present in a realized structure, a sample space, \mathcal{S}^k , can be defined of possible combinations, \mathbf{X}^k , of N elements, selected k at a time:

$$\mathcal{S}^k \equiv \{ \mathbf{X}^k \mid \mathbf{X}^k \subseteq \mathbf{X}^N, |\mathbf{X}^k| = k, k \leq N \} \quad (3.44)$$

For example, if one element is missing at random from the initial ground structure of N elements, then the sample space, \mathcal{S}^{N-1} , includes N possible unique permutations or combinations, \mathbf{X}^{N-1} , of $N-1$ total elements. Members of \mathcal{S}^{N-1} , which are permutations of \mathbf{X}^{N-1} , include:

$$\{X_2, X_3, \dots, X_N\}, \{X_1, X_3, \dots, X_N\}, \dots \{X_1, X_2, \dots, X_{N-1}\} \quad (3.45)$$

The number of members in a sample space, \mathcal{S}^k , is equivalent to the number of possible permutations of an initial ground structure (and the number of experiments in Equations

3.38-3.43) if k elements are embodied at random from the set of N initial elements. It is calculated as a function of the number of elements in the nominal/initial ground structure, N , and the number of elements remaining in the realized structure, k :

$$\binom{N}{k} = \frac{N!}{k!(N-k)!} \quad (3.46)$$

In a full ground structure, one element connects each pair of nodes in the structure. The total number of elements in the full ground structure, N , is calculated as a function of the number of nodes, R , as follows:

$$N = \frac{R}{2}(R-1) \quad (3.47)$$

For example, in the initial ground structure of Figure 3.7, there are 9 nodes and 36 elements. If the one element is randomly missing, there are 35 possible permutations of the realized 35-element structure. Similarly, if two elements are missing randomly, there are $\frac{35!}{33!(35-33)!} = 595$ possible permutations of the realized structure. Furthermore, this

is a relatively simple structure with only 9 nodes and 36 elements; most structures have a much larger number of nodes and elements.

It is possible to account for randomly missing nodes in a similar manner. The number of nodes in the initial ground structure and the realized structure are designated, R and j , respectively, and the set of nodes in the initial ground structure is expressed as \mathbf{R}^D :

$$\mathbf{R}^D = \{R_1, R_2, \dots, R_D\} \quad (3.48)$$

Due to topological variation, the number of nodes in a realized structure, j , may be less than the number of nodes in the initial ground structure, D . A sample space, \mathcal{S}^j , can be defined of possible combinations, \mathbf{R}^j , of D nodes, selected j at a time:

$$\mathbf{S}^j \equiv \{ \mathbf{R}^j : \mathbf{R}^j \subseteq \mathbf{R}^D, |\mathbf{R}^j| = j, j \leq D \} \quad (3.49)$$

The number of possible combinations of missing nodes in a sample space is calculated according to Equation 3.46 with N and k replaced with D and j , respectively. When a node is missing, all of the elements connected to the node become inactive. Since each element joints two distinct nodes, removal of either node implies that the element becomes inactive.

Since the number of nodes in a structure is always much less than the number of elements, according to Equation 3.47, the number of permutations of missing nodes is much less than the number of permutations of missing elements. For example, for the initial ground structure of Figure 3.7 with 9 nodes, the number of possible permutations of realized structures with one or two missing nodes is 9 and 36, respectively—much less than the 35 and 595 possible permutations of structures with one or two missing elements, respectively.

The number of possible combinations of missing elements or nodes is important because evaluation of each combination requires a separate finite element analysis of the structure. The structural behavior of a ground structure is evaluated typically with a finite element model that is constructed specifically for that particular ground structure. Whenever the topology of a structure changes, through addition or removal of an element or node, for example, a revised finite element model must be formulated and solved. Reformulation involves adjusting stiffness matrices and/or nodal displacements to accommodate the reduced number of elements and/or nodes. Re-solution of the finite element model involves numerically solving for relevant forces and displacements. Since a modified finite element model must be formulated and solved for each topological

change in a structure, the computational costs of analysis are multiplied directly by the number of topological changes considered during the topology design process (i.e., by the number of possible permutations). Typically in topology design, a finite element model of a structure is solved only once per iteration. This is true also for the Taylor series-based evaluations of the impact of continuous control and noise factor variations on responses. Since formulation and solution of a finite element model is typically the most computationally intensive portion of a topology design iteration, it is important to estimate and, if possible, limit the number of required experiments and associated finite element analyses.

There are two primary ways to limit the number of permutations and associated experiments and finite element analyses. First, if missing elements are considered, one could limit the maximum number of missing elements to be considered in an experiment. In other words, one could assign a large lower bound on the value of k , the number of elements in a realized structure. For example, a restriction such as $k \geq N-1$ in Equations 3.44 and 3.46 would drastically reduce the number of permutations and experiments, even for a small ground structure since the number of permutations increases nonlinearly with the quantity, $N - k$. A justification for this assumption is that there may be an extremely small chance of encountering more than one or two missing elements. For example, suppose that the probability of encountering one missing element in a realized structure is 3%. Then the probability of encountering two missing elements simultaneously is 0.09% (i.e., $0.03 * 0.03 = 0.0009$) if one assumes that the probabilities are independent. It is even less likely that three or more elements are missing simultaneously for a structure. Furthermore, for most structures, a 3% failure rate is

probably relatively high; otherwise, this may not be a viable option for limiting the number of experiments. Of course, by limiting the number of missing elements considered in topological variability experiments, one does ignore the potentially catastrophic (although highly unlikely) event of encountering a large number of missing elements. This would be a very important point for reliability analysis in which the probability of failure is the main concern, but it is not as important for robust design applications with a primary focus on minimizing performance variation or standard deviation (on which a catastrophic event with extremely small probability has very little effect). Nevertheless, the tradeoff must be considered.

A second strategy for reducing the number of permutations and experiments is to consider missing nodes rather than missing elements. As discussed previously, the number of permutations of structures with missing nodes is always less than that for missing elements, assuming that a full or partial ground structure is being considered. Furthermore, one could limit the maximum number of nodes missing in any experiment, in the manner discussed above for missing elements. By systematically removing each node in a series of experiments, each element is guaranteed to be removed twice. The drawback is that elements are always removed in groups, defined by all of the elements attached to a particular node. This implies that one is always considering a relatively worst-case event of multiple element removal. However, the benefit is that topological variability can be considered with a minimum number of experimental analyses of the structure.

It is worth noting that an invalid approach to limiting the number of permutations would be to designate a subset of elements or nodes as permanent, with no possibility of

Phase IV. Solve Robust Topology Design Problem

H. Computing Infrastructure

Figure 3.11 – Phase 4 of the RTPDEM: Solving the Robust Topology Design Problem

random removal. The remaining subset of elements or nodes would be assigned positive probabilities of random removal. Unless this is actually the case in practice, such an assumption would bias the topology design process away from nodes and elements with a chance of being missing from a realized structure.

3.3.4 Phase 4: Solving the Robust Topology Design Problem

With the simulation infrastructure proposed for Phase 3, coupled with the robust topology design problem formulation of Figure 3.9, it is possible to explore and generate solutions for a robust topology design problem characterized by large numbers of variables, broad ranges of system variable values, a nonlinear problem formulation, and variation in control factors, noise factors, or topology. In order to carry out this method, a step-by-step computing process and supporting infrastructure are required.

The computing infrastructure for the RTPDEM is represented in Figure 3.12. As shown in the figure, a robust topology design process begins with a set of overall design requirements. Based on these requirements, a robust design space is formulated which includes both a means for representing topology so that it can be modified during the design process and quantitative characterization of the relevant sources of variability. A designer formulates a compromise DSP for robust topology design based on the robust design space and his/her judgment and knowledge of the problem. The compromise DSP is solved with a simulation framework that includes a search algorithm, variability assessment techniques, and analysis models.

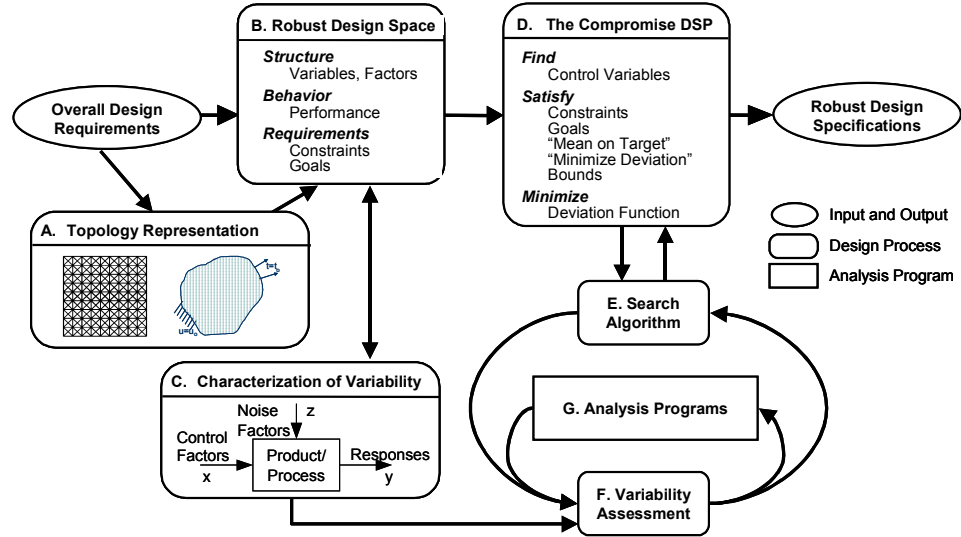


Figure 3.12 – Computing Infrastructure for the RTPDEM

A more detailed description of the solution process is useful for supporting practical implementation of the method. As shown in Figure 3.13, the solution process begins after the robust design space and compromise DSP have been formulated. The first step is to assign values to some of the parameters in the compromise DSP. The parameters include targets and weights for each goal, bounds on the system variables, and limits for each constraint. A starting point is specified by assigning values to the control factors that satisfy the bounds and constraints in the compromise DSP.

If topological or boundary condition variability is present, repeated reanalysis of the structure is required to evaluate the effect of the variation on system responses. A set of discrete experiments is specified with experimental points selected to cover the range of interest for boundary conditions or the sample space of possible topological permutations for topological variability. For each of the experimental points, the nominal performance

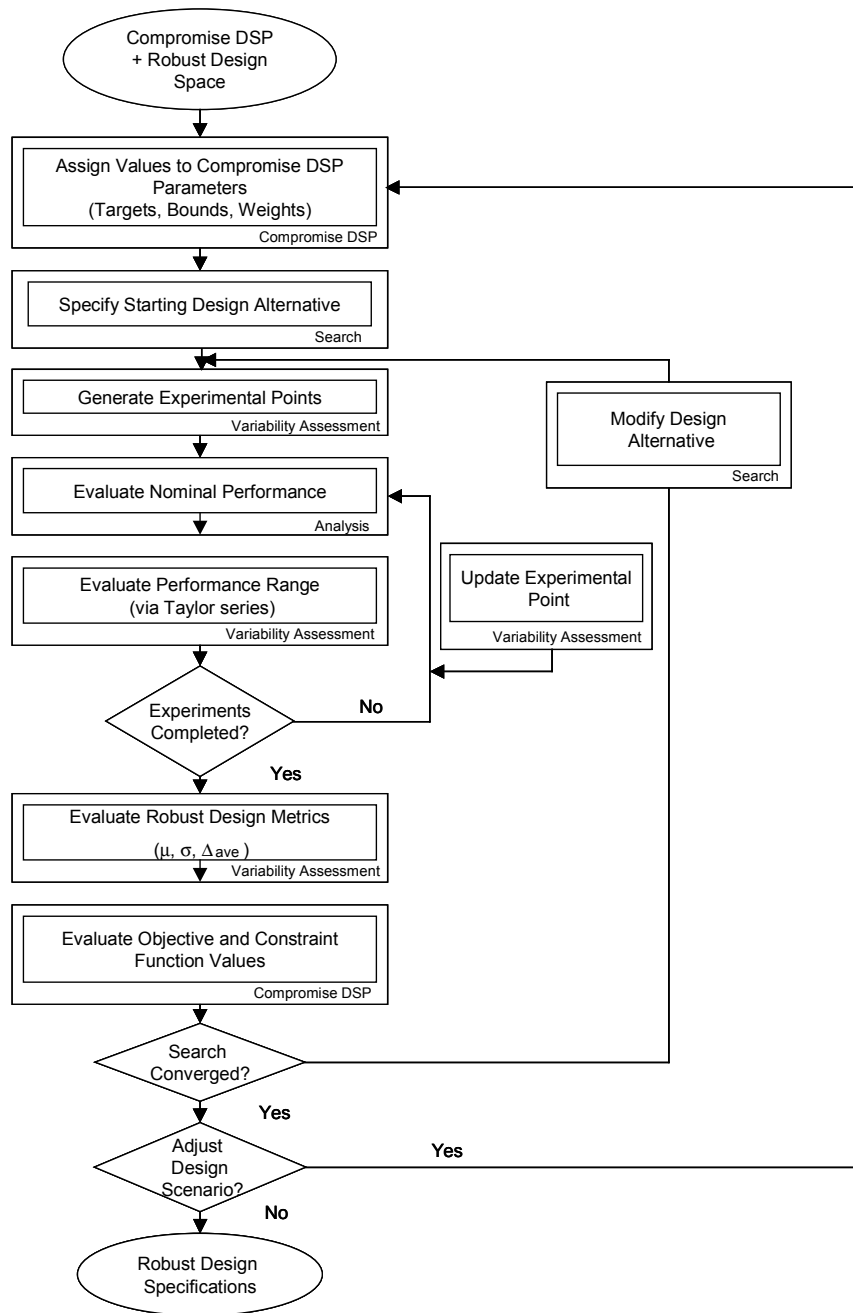


Figure 3.13 – A Closer Look at the Solution Process for the RTPDEM

of the structure is analyzed as a function of the nominal (intended) values of control and noise factors. Also, the range of performance, associated with small continuous changes in control or noise factors, is evaluated with Taylor series-based methods as specified in Equations 3.31 and 3.32.

After the set of experiments is completed, robust design metrics are evaluated for the current design alternative, according to Equations 3.38 – 3.40, for the mean value, standard deviation, and average range of each goal and constraint function. Based on the values of these metrics, the values and gradients of the constraint and objective functions in the compromise DSP are calculated for input to a search algorithm. (Gradients of the objective and constraint functions are calculated according to Equations 3.33-3.37 and 3.41-3.43 and supplied to the search algorithm.) If the iterative search process has not converged, according to a specified metric such as the change in the objective function value, the design alternative is modified by the search algorithm. Modifications involve adjustments to control factor values that are intended to improve the feasibility and/or objective function value of the alternative. Control factor changes are determined partially by the gradient or sensitivity values transferred to the search algorithm.

If the iterative search process has converged, the designer has an option to adjust the design scenario. Utilizing the flexibility of the compromise DSP, a designer may modify weights or target values for each goal, bounds on the control factors, and/or limits for each constraint. By modifying the design scenario, a designer can explore a design space more thoroughly and generate a family or Pareto set of solutions, perhaps with very different characteristics and tradeoffs among multiple goals. Repetition of the design process with alternative sets of parameters in the compromise DSP and/or different

starting points is recommended for verification and validation of resulting design specifications.

3.4 ADDRESSING HYPOTHESIS II—MULTIDISCIPLINARY ROBUST TOPOLOGY DESIGN

The RTPDEM is a foundational method for *multifunctional* topology design in addition to the single-function, single-designer context for which the RTPDEM is described in Section 3.3. Multifunctional applications involve multiple collaborating designers associated with distinct domains such as alternative length and time scales, distinct functionalities, and other divisions of perspective. As discussed in Section 3.4.1, it is typically necessary to sequence and distribute multifunctional topology design activities, even though the decisions made by one functional designer may strongly influence both the decisions of other functional designers and their ability to meet functional goals. As described in Section 3.4.2, the RTPDEM can be used as a foundation for a multifunctional topology design process that is multi-stage, hierarchical, or distributed in nature. As illustrated in Figure 3.14, two options are proposed for integrating multi-stage implementations of the RTPDEM in order to facilitate the pursuit of a satisfactory balance or compromise among multifunctional objectives. First, the RTPDEM can be used by a leading designer to generate flexible, robust ranges of topological preliminary design specifications for a functional domain that are communicated to a subsequent designer who implements the RTPDEM again for another functional domain. The flexible ranges of topological preliminary design specifications generated by the leading designer provide limited but substantial freedom for subsequent designers to adjust the specifications without significantly diminishing design

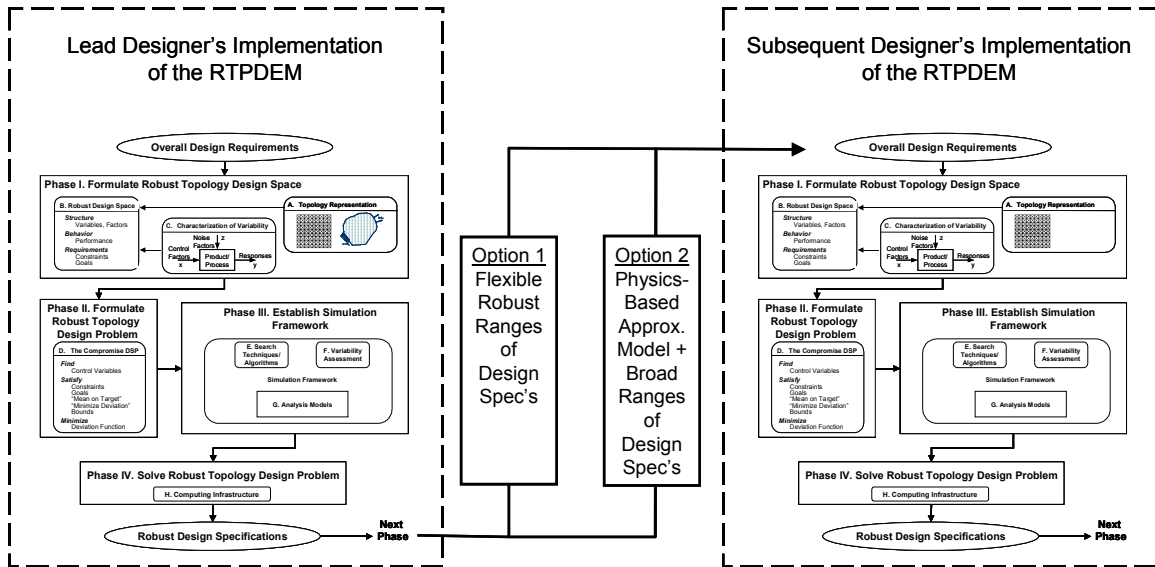


Figure 3.14 – A Multifunctional, Multi-stage Implementation of the RTPDEM

performance in the leading designer's domain (since the *robust* design specifications exhibit performance that is relatively insensitive to changes in the design specifications themselves). This option is called the *range-based* approach. As a second option, it is also possible for a leading designer to communicate approximate, physics-based models of his/her functional domain to subsequent designers, thereby enhancing a subsequent designer's ability to evaluate the impact of changes in design specifications on objectives and constraints in the leading designer's domain. As a result, it is possible for a leading designer to communicate very broad ranges of topological preliminary design specifications, supplying a subsequent designer with greater freedom for changing the design specifications. This option is called the *model-based* approach. Before describing these options in Section 3.4.2, it is necessary to outline the basic motivations, assumptions, and concepts underlying a multifunctional, robust topology design problem.

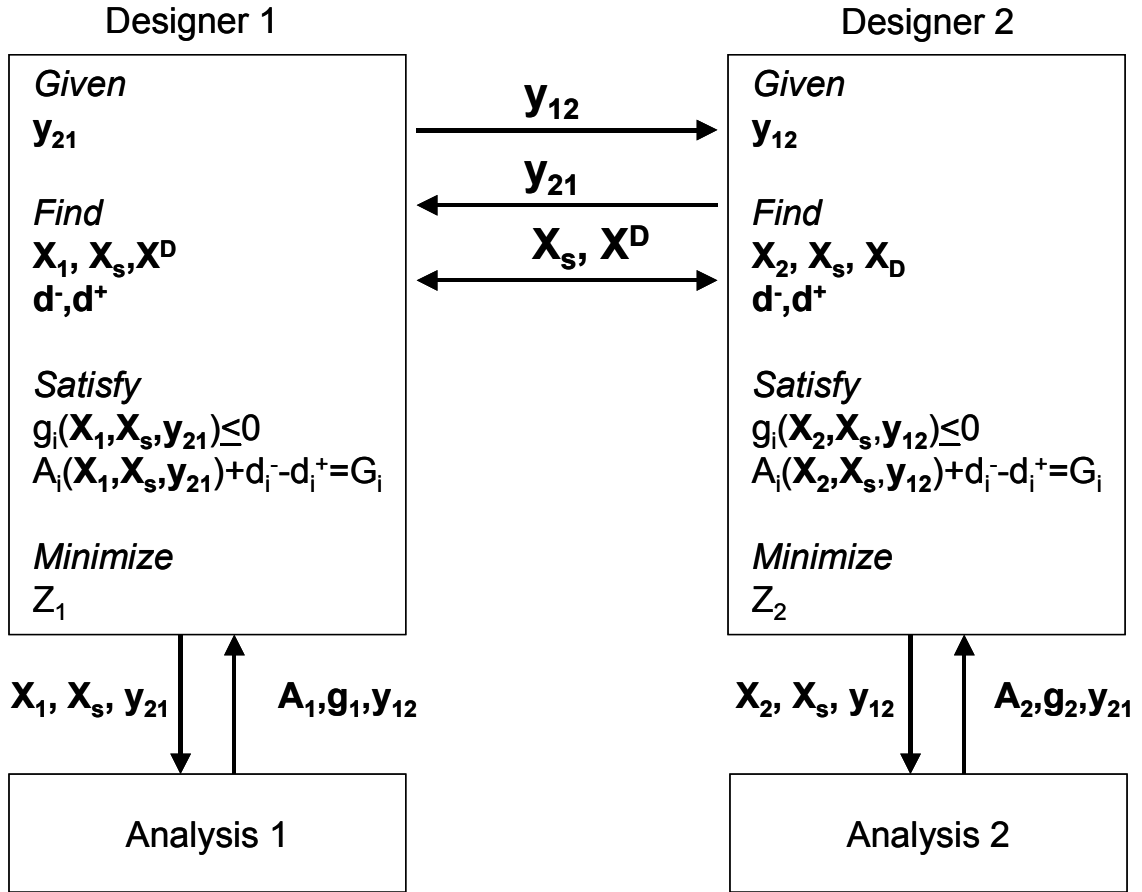


Figure 3.15 – A General Multifunctional Topology Design Problem Formulation

3.4.1 Basic Assumptions and Motivation for Multidisciplinary Robust Topology Design

The most basic requirement for a multifunctional topology design problem is the need to achieve a satisfactory balance or compromise among multiple objectives associated with different functional domains. A dual domain topology design problem formulation is illustrated in Figure 3.15. For simplicity, the emphasis in Figure 3.15 is on the problem formulation, and other aspects of the RTPDEM such as formulation of the robust topology design space have been omitted. As shown in Figure 3.15, it is assumed that there are at least two functional domains and that it is possible to formulate a robust

topology design space and a robust topology design problem for each functional domain and to solve each domain-specific problem with appropriate domain-specific analysis models. Each functional domain is associated with a designer in charge of formulating and solving a domain-specific compromise DSP.³ Specifically, the i^{th} designer is responsible for determining the values of control variables, \mathbf{X}_i and \mathbf{X}_s , that satisfy a set of constraints, $g_i(\mathbf{X}_i, \mathbf{X}_s, \mathbf{y}_{ij})$, and achieve a set of conflicting, domain-specific goals, $A_i(\mathbf{X}_i, \mathbf{X}_s, \mathbf{y}_{ij})$, as closely as possible.⁴ For each designer, the control variables are divided into two groups: (1) independent control variables, \mathbf{X}_i , that influence behavior in only the i^{th} functional domain and are controlled by only the i^{th} individual designer and (2) shared variables, \mathbf{X}_s , that strongly influence behavior in both functional domains and are controlled ideally by both designers. In addition, some of the responses or dependent variables of functional domain, i , may serve as inputs to the analyses of functional domain, j , and these behavior parameters are labeled \mathbf{y}_{ij} . An example of such coupled variables is a temperature distribution in a multifunctional, thermo-structural design process in which the temperature distribution is determined during thermal analysis and required as input for thermoelastic structural analysis.

In this general multifunctional design context, the domain-specific decisions are coupled. Specifically, it is clear that the goals and constraints in both functional domains are influenced by a common set of variables, \mathbf{X}_s and \mathbf{y}_{ij} , and a common topology, X_D , that are shared between designers. As a result, conflicts may arise. For example, it is unlikely that the values of shared variables, \mathbf{X}_s , that satisfy the first designer's constraints

³ It is possible for a single designer to negotiate solutions for multiple functional domains, but it is assumed here that a different designer, with domain-specific expertise, is associated with each decision.

⁴ The designer is also responsible for determining the set of control factors and associated elements, \mathbf{X}^D , that are retained in the initial ground structure.

and minimize his/her objective function, Z_1 , also satisfy the second designer's constraints and minimize his/her objective function, Z_2 . If so, the multifunctional goals are contradictory, and a satisfactory balance or compromise solution must be obtained in terms of the shared control variables, X_s , and coupled behavioral variables, y_{ij} . Therefore, the question becomes: *How can the domain-specific designers together determine the values of their shared and coupled variables so that resulting solutions exhibit a satisfactory balance or compromise among multifunctional goals?*

An obvious solution to this dilemma is to fully integrate the multifunctional design activities, govern them with a single multifunctional compromise DSP, and combine or sequence the analyses appropriately. However, there are many reasons not to do this, such as:

- *Significantly different design spaces.* It may not be possible to design or analyze for multiple functions simultaneously because different analyses and problem formulations may require different design spaces. This is particularly important in multifunctional topology design, for example. As discussed in Section 2.3.2, the topology design techniques established for structural applications do not apply straightforwardly to other physical domains, especially domains such as heat transfer for which boundary conditions depend strongly on the size, shape, and location of voids within a structure. While structural topology design may be carried out quite comprehensively with large numbers of variables and potential elements, topology design for other functions (such as heat transfer) must be more limited in scope with more realistic initial topologies and more modest changes in topology. Structural topology design may begin with a very complex ground structure with large numbers

of interconnected elements and associated design variables and reduce it to a simpler structure with favorable structural properties; on the other hand, other functional domains may require a more limited or simpler topology with which to begin. In fact, as discussed in Section 2.3.2, it may not be possible even to *analyze* behavior in functional domains such as heat transfer (with internal convection) in a meaningful way during a structural topology design process. The heat transfer characteristics of a ground structure or continuum model with a plethora of small-scale voids (such as the ground structure illustrated in Figure 2.7) would be totally unrepresentative of the heat transfer characteristics of the final topology that is likely to have only a few elements and larger-scale voids with very different heat transfer characteristics. Rather than eliminating structural topology design for complex initial topologies, it is more reasonable to conduct structural topology design for a complex initial ground structure and follow it with topology design for other functions that leverages or builds upon the topologically simpler outcome of the structural topology design process.

- *Computational tractability.*

- (1) Different analyses may have very different computational intensities, and thus require different amounts of computational time. For example, simulation A for one functional domain may be much faster than simulation B for a second functional domain. By virtue of its speed, it is much more suitable for exploring a large design space while simulation B is really best suited for only a few confirmatory runs. Exploring a design space with both simulations simultaneously (i.e., running both analyses to

support each experiment or optimization iteration) requires an extraordinary amount of time and prohibits broad exploration of a design space. If the objective is to identify regions that are suitable for both physical perspectives, it is more efficient to use the faster simulation to identify regions of the design space that are acceptable for the first domain and then use the detailed, computationally intensive simulation in a second design phase to analyze for the second functional perspective only in those regions.

(2) The number of required iterations of a given optimization algorithm typically grows super-linearly with the number of variables, and in some cases, its ability to find a globally superior solution diminishes. If a system with a large number of variables can be partitioned into subsystems with fewer variables, the computational time required for optimization can be reduced.

- *Distributed computing resources.* Proprietary software may be required to reside at different locations where it is utilized by designated experts. In many cases, it may be possible to share *only* final results or designs but *not* simulation software or intermediate data.
- *Distributed human resources and domain-specific expertise.* A systems-level multifunctional design process may involve several domain-specific experts with specialized knowledge and expertise. If the design problem is integrated totally into a systems-level problem, opportunities are reduced or eliminated for these experts to make decisions and use their seasoned judgment to review intermediate and final

results. In a cutting edge design process, it is rarely possible to utilize ‘black box’ simulations that can be utilized over large regions of a design space without user monitoring and modification. An expert can critically evaluate a resulting design and negotiate the capabilities and limitations of simulation software, correcting or updating it for more accurate results.

For these and other reasons, it may not be possible or reasonable to integrate fully a multifunctional design process and formulate and solve a single compromise DSP.

An alternative solution is to separate the functional domains as illustrated in Figure 3.15. Then, the challenge involves determining the most effective communications protocol between the two designers; i.e., what type of information is communicated and in what sequence. One option is an ‘over the wall’ approach in which the activities are partitioned completely and a lead designer communicates a fixed design to the subsequent designer. Unfortunately, a fixed design does not offer the subsequent designer any freedom for adjusting the design to meet his/her domain-specific objectives and constraints without blindly—and most likely adversely—affecting the initial designer’s intentions and domain-specific performance. Significant iteration between the designers is likely to result. In topology design, this problem is compounded by the highly integral nature of the problem—as discussed in Section 2.4.4—and the large number of shared variables associated with that. This makes it extremely difficult for a subsequent designer to make even small changes to a design because those changes affect not only performance in his/her functional domain but also performance in the initial designer’s functional domain.

An alternative to the fully integrated and ‘over-the-wall’ approaches is needed. The challenge for such an approach is to preserve design freedom for each designer (both a lead designer and subsequent designers) to modify a design to achieve satisfactory levels of performance for each functional domain. In the next section, two related approaches are proposed for performing multifunctional topology design in a multi-stage, distributed manner.

3.4.2 A Multi-Stage Robust Design Approach for Multifunctional Topology Design

A multi-stage, multifunctional topology design approach is proposed in this section that is anchored partially in robust design principles and methods. The challenge that lingers from the discussion in Section 3.4.1 is that of partitioning or distributing topology design activities among multiple domain-specific designers and design processes while simultaneously reducing the adverse impact of the decisions made by a designer on the capabilities of subsequent designers to meet objectives for other functional domains. One way to address this challenge is to build flexibility into the solutions that are communicated from one stage to another. Flexibility is achieved by utilizing the robust topology design methods introduced in Section 3.3 to generate designs that are relatively insensitive to changes in the design specifications themselves, including dimensions and topology. These flexible solutions are communicated to subsequent designers as ranges of design specifications rather than fixed, point solutions. Because the flexible solutions are generated with robust design methods, subsequent designers can modify them within the specified ranges without significantly impacting performance in the lead designer’s domain. This increased flexibility for subsequent modification of an intermediate solution reduces the adverse impact of upstream decisions on the ability of subsequent

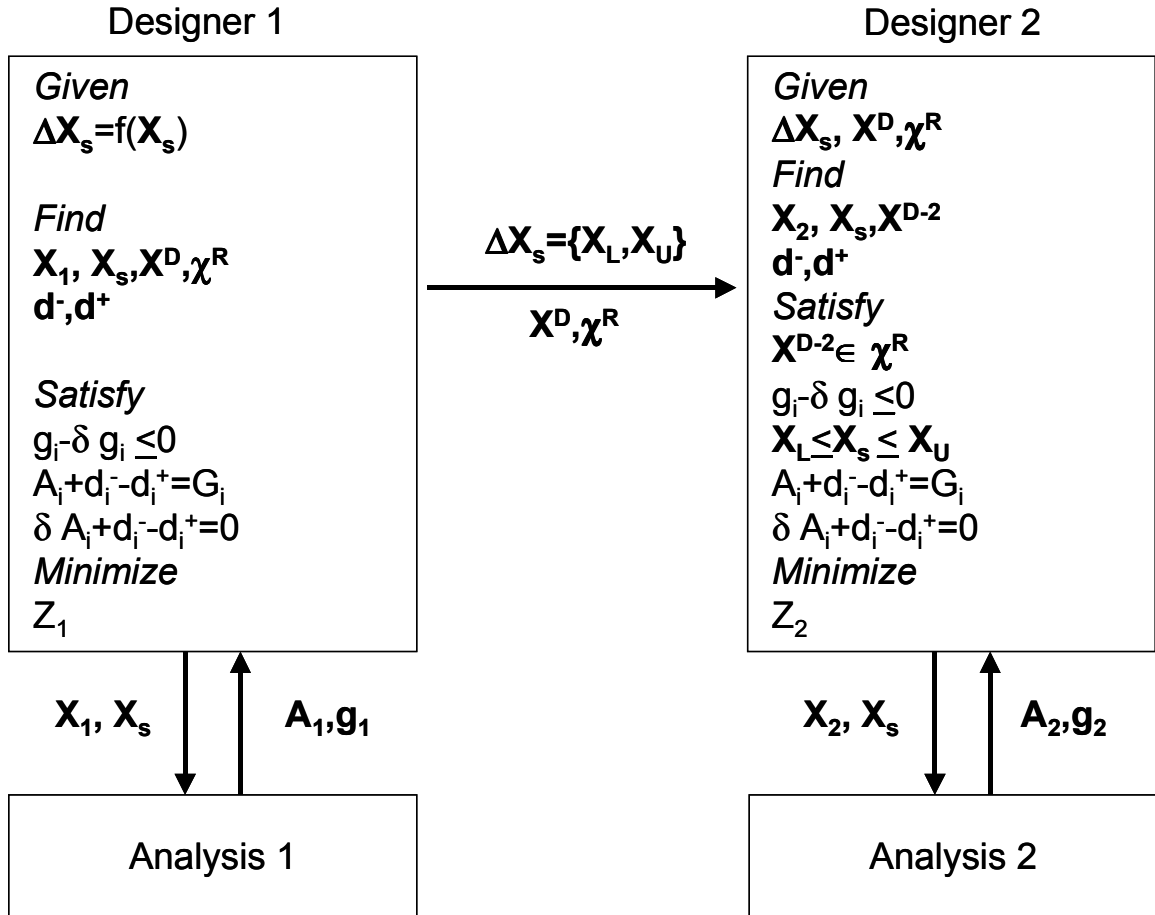


Figure 3.16 – Multistage, Multifunctional Topology Design via Communication of Ranges of Design Specifications

designers to meet additional functional requirements and thereby makes it possible to reach a better balance among multifunctional objectives.

The multi-stage, multifunctional topology design approach is illustrated in greater detail in Figures 3.14 and 3.16. As shown in Figure 3.14, the approach is based on implementing the RTPDEM repeatedly—once for each functional domain. A closer look at the problem formulation is provided in Figure 3.16. As shown in the figure, the lead designer formulates and solves a robust topology design problem. The outcome is a designed nominal topology that consists of a subset, X^D , of the set of control factors and

associated elements in the parent ground structure, \mathbf{X}^G . The space of possible sets of realized elements, \mathcal{X}^R , must also be determined and communicated to subsequent designers. The space of possible sets of realized elements indicates which elements may be added to or removed from the designed topology in subsequent design stages, effectively embodying a range or set of potential topologies that can be explored by subsequent designers. As indicated in the right side of Figure 3.16, subsequent designed topologies (e.g., \mathbf{X}^{D-2}) are members of the space of potential realized topologies, \mathcal{X}^R . The parametric design specifications (i.e., the element dimensions) are expressed as ranges of values, $\Delta\mathbf{X}_s$, for each element in the designed nominal topology. The ranges should be specified for all shared variables; otherwise, the shared variables must remain fixed. Subsequent designers are free to adjust the values of these variables within the specified ranges (i.e., if $\Delta\mathbf{X}_s = \{X_L, X_U\}$, then $X_L \leq X^s \leq X_U$).

A simple example is illustrated in Figure 3.17. Using robust design techniques, the structural designer in Figure 3.17 generates a flexible initial design with built-in freedom for subsequent modifications. Any design within the specified robust ranges is guaranteed to satisfy at least a minimum level of structural performance capabilities. Subsequent designers—such as the thermal designer and the manufacturing expert indicated in Figure 3.17—can make adjustments to the design within the specified robust ranges without fear of violating those structural performance capabilities. Also, using the robust *topology* design techniques proposed in Section 3.3, the structural designer can generate an initial design with built-in freedom for subsequent dimensional *and topological* modifications. As shown in Figure 3.18, robust topology designs are accompanied by robust ranges of design specifications and robust sets of possible topologies. For the simple design in

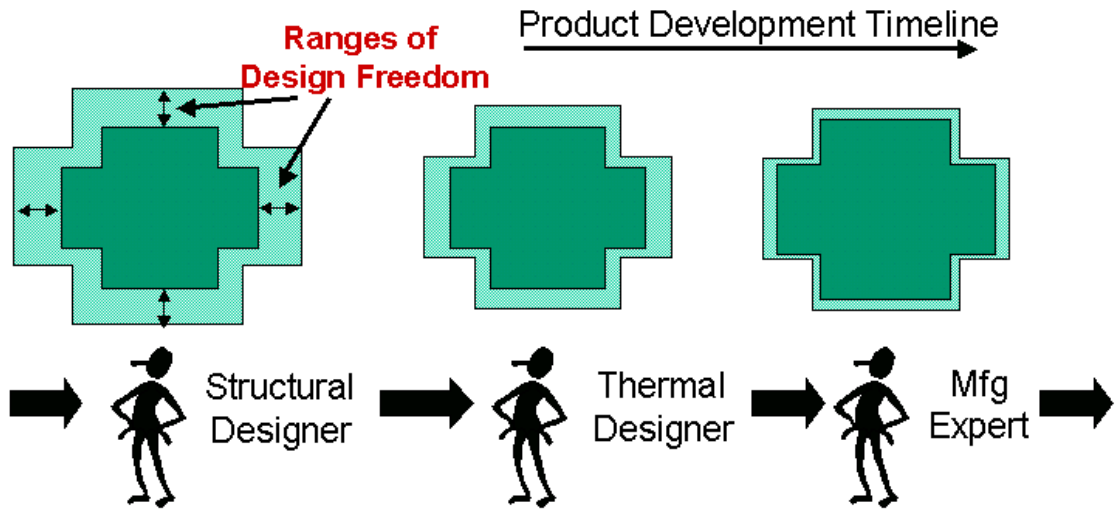


Figure 3.17 – Communicating Robust Ranges of Design Specifications

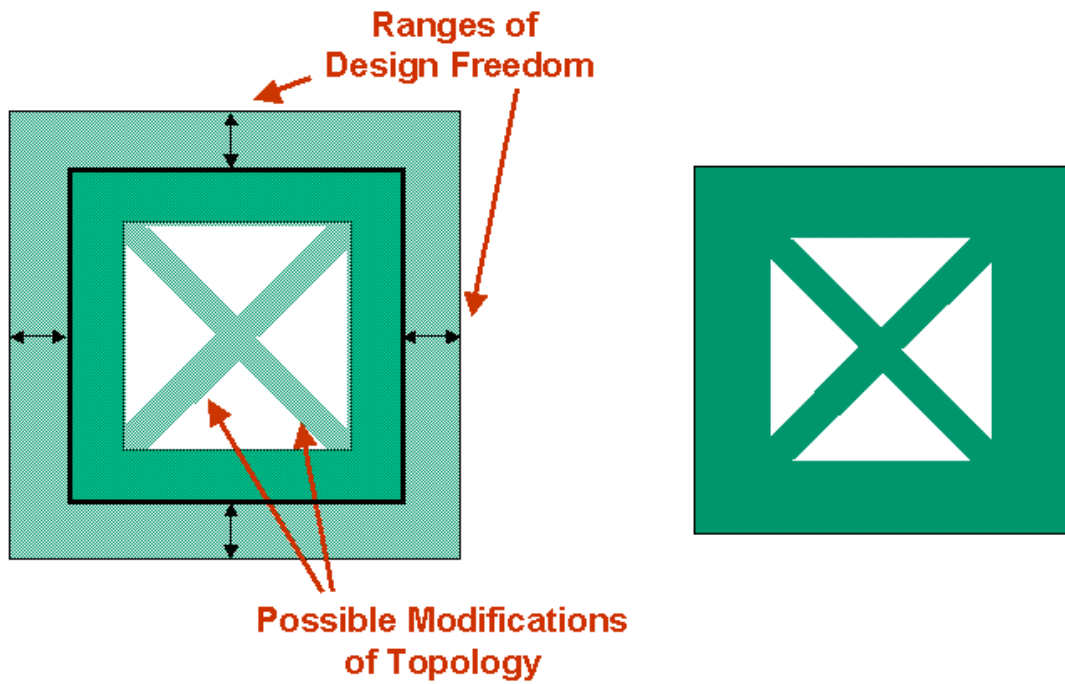


Figure 3.18 – Communicating Robust Ranges of Design Specifications and Robust Sets of Possible Topologies

Figure 3.18, subsequent designers can make dimensional adjustments within the specified robust ranges or topological adjustments within the space of possible topologies. In this case the space of possible topologies includes the nominal (hollow square) topology and the nominal topology with diagonal cross-members. The diagonal cross members are not part of the nominal topology, but they are part of the space of *potential* realized topologies. Because the robust ranges of design specifications and robust sets of possible topologies are generated with robust topology design techniques, subsequent designers can make changes within the ranges or sets while continuing to satisfy structural performance requirements or goals.

An initial designer who generates robust ranges of design specifications—as opposed to fixed, point solutions—may sacrifice some performance in his own domain in exchange for enhancing the robustness of the solution and the extent of the design specification ranges. Such tradeoffs are a typical phenomenon in robust design processes. In return, iteration among the disciplines is minimized, and freedom is preserved for subsequent designers to adjust the design specifications to satisfy their own objectives—thereby identifying compromise solutions that balance multi-functional objectives in a way that is satisfactory to all associated designers.

There is an important potential limitation of this approach. Specifically, subsequent designers may be unable to identify feasible or satisfactory solutions within the range of design solutions generated by an upstream designer. In this case, costly and time-consuming design iteration may be required to identify alternative design regions that are satisfactory for all designers and their respective functional domains. Another option is to broaden the scope for making changes to an initial design in subsequent design phases.

To make more extensive changes to a design, designers need to evaluate the impact of those changes on the objectives and constraints considered by previous domain-specific designers. They need to check for continued multifunctional feasibility of a design. They also need to modify the design in such a way that it achieves their own domain-specific objectives while maintaining satisfactory levels of performance for objectives considered by previous designers. Essentially, they need behavior simulation models of previously considered functional domains that they can use to evaluate the impact of their design changes on the domain-specific objectives of previous designers.

A second multi-stage, multifunctional topology design approach—and an alternative to the approach presented previously in this section—involves communicating approximate, physics-based models of behavior in a functional domain along with the robust, ranged sets of design specifications. As shown in Figure 3.19, the multifunctional topology design problem is formulated similarly to the previous formulation in Figure 3.16. As in the previous formulation, robust ranged sets of design specifications are communicated from one domain-specific designer to another. In contrast with the previous formulation, approximate behavioral models are communicated along with the robust, ranged sets of design specifications. The subsequent designer has the freedom to adjust the design within the ranges specified by the lead designer without evaluating the impact on the previous designer's performance objectives. However, if the subsequent designer cannot satisfy constraints and achieve satisfactory levels of goals for his/her domain, he/she may utilize the approximate behavioral models to support more extensive changes in design specifications. The approximate behavioral models support broader

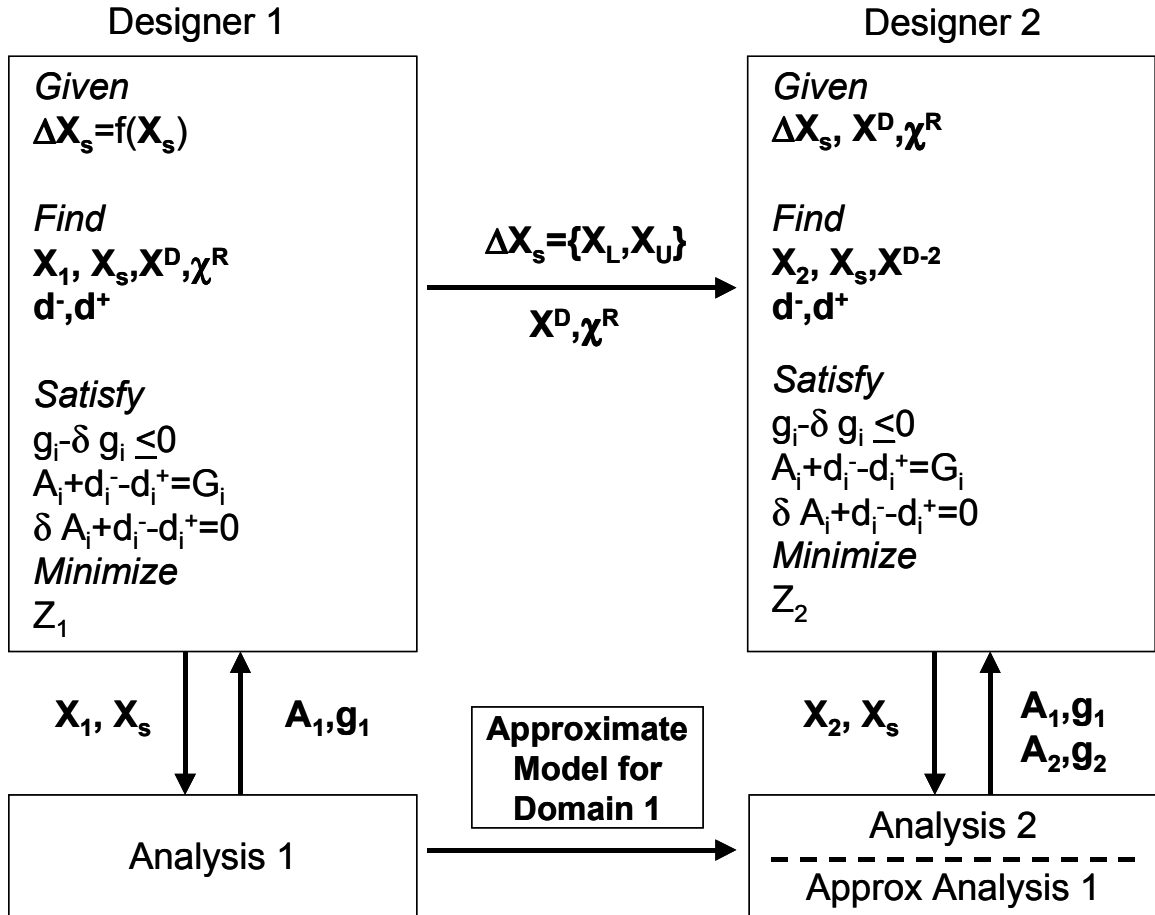


Figure 3.19 – Multi-stage, Multifunctional Robust Topology Design via Communication of Ranged Sets of Design Specifications and Physics-Based Approximate Models

changes because they allow the designer to evaluate and minimize the negative impact of these changes on the objectives of the previous designer. The physics-based models relax restrictions on changes for subsequent designers without requiring extensive iteration among the designers.

Approximate behavioral models differ from the metamodels or surrogate models that have been used to support non-topological design in multiobjective and robust design contexts (e.g., (Chen, et al., 1996; Mavris, et al., 1999)). Surrogate models are typically best-fit models based on data generated by computer or physical experiments. Examples

include response surfaces and kriging models (c.f., (Chen, et al., 2003)). While they are intended to approximate trends in the available data, they are not based on physical principles directly. As noted in Section 2.4.3, surrogate models are difficult to apply to topology design problems because it becomes extremely computationally expensive to generate the data required to build the models when the number of variables is large as it is in topology design. Examples of *physics-based approximate models* include low-order finite element models of structural phenomena or finite difference models of heat transfer phenomena. The models are approximate because they can be executed relatively quickly, compared with detailed computational fluid dynamics models or high-order commercial finite element models, for example. They are physics-based because they are derived directly from physical principles (e.g., the first-law heat or energy equation), but they are based on simplifying assumptions (e.g., finite difference approximations) that make them both faster and more approximate than more detailed models. Physics-based approximate models are advantageous in multifunctional design situations because they reduce the computational expense—relative to surrogate models (with large data gathering requirements) or more detailed physics-based models (with large computational resource and time requirements)—of considering objectives from multiple functional domains simultaneously. In addition, they tend to be relatively accurate compared with surrogate models.

There are several favorable characteristics for these approximate models to have. They should be as adaptable, fast, and accurate over as broad a range of the design space as possible. Faster approximate models imply lower computational costs for multidisciplinary analyses, but speed is usually balanced with accuracy. Accuracy of an

approximate model over a broad range of the design space provides more design freedom for a second stage designer to adjust the design specifications. Finally, an adaptable approximate model can be reconfigured easily to accommodate topology changes. In addition, the approximate behavioral models need to be generated by a designer with expertise in the specific domain and communicated to and utilized by designers with expertise in other domains. Therefore, they need to be relatively straightforward to use, and the assumptions and limits of applicability should be clearly specified (and communicated). Furthermore, they need to be compatible—to the extent possible—with the topological and parametric representations of the design that are utilized by subsequent designers. In addition to generating and communicating robust ranges of design specifications, it is important for designers in different functional domains to utilize compatible representations of topology so that control variables in one functional domain can be paired or at least translated directly to variables in another functional domain. For example, if structural topology design is followed by thermal design, it is useful to utilize the designed structural topology along with element labels and dimensions directly as a starting point for the thermal design process.

In summary, two alternative approaches have been presented for multi-stage, multifunctional robust topology design. The first alternative is based exclusively on generating and communicating robust ranged sets of specifications to subsequent designers. The second alternative involves communicating approximate behavioral models along with the ranged sets of specifications. While the second approach increases the computational burden, it also broadens the scope for changes by a subsequent designer and increases the likelihood of identifying a satisfactory compromise solution.

The two multifunctional topology design approaches are applied and compared in the combustor liner example of Chapter 7. As noted throughout this section, each stage in a multifunctional topology design process is anticipated to include both topological and parametric design activities, with a different domain or function represented in each stage. Two functional domains—structural and thermal—are represented in the examples in this dissertation. While structural topology design methods have been discussed throughout the dissertation thus far, thermal topology design methods are relatively undeveloped. In the following section, a thermal topology design approach is presented and discussed.

3.5 EXTENDING TOPOLOGY DESIGN TECHNIQUES BEYOND THE STRUCTURAL DOMAIN—A THERMAL TOPOLOGY DESIGN APPROACH

Whereas topology is designed typically for structural applications alone, the multifunctional topology design approach described in the previous section is intended to facilitate topological preliminary design for multiple domains of functionality. This is important because the internal structure or topology of multifunctional, multi-scale, natural and artificial systems typically has a strong impact on behavior from *multiple* functional perspectives. Trabecular bones, for example, are porous cellular solids comprised of a network of strands called trabeculae. The trabeculae continuously adapt themselves and their architecture or arrangement in response to changes in the mechanical environment, thereby increasing the stiffness and fracture resistance of the bone (e.g., (Judex, et al., 2003; Keaveny, 2001; Silva and Gibson, 1997)). Internal structure is critical for flow systems such as the lungs, vascular tissues, trees, and rivers

that organize themselves to facilitate flow between a central location—a heart or a river delta, for example—and a finite volume (Bejan, 2000). In artificial engineering systems, topology is equally important. Composite materials are tailored for superior stiffness, ambient and high-temperature strength, and other properties by tailoring not only the concentration and size of multiple material phases but also their shape, distribution, and orientation (Callister, 1994). A compliant mechanism achieves its mobility from the combined flexibility of its members; output motion and force is a function of material properties as well as numbers, sizes, and connectivity relations of members (e.g., (Frecker, et al., 1997)).

In the examples in this dissertation, the focus is on designing mesoscopic topology for prismatic cellular materials for multifunctional structural and *thermal* requirements. One of the reasons for this focus is the desirable structural and thermal properties of prismatic cellular materials, along with the challenging thermostructural applications for which prismatic cellular materials are strategically applicable.

To perform multifunctional structural and thermal topology design, both structural and thermal topology design methods are required. Whereas structural topology design approaches are relatively well-developed in the literature (at least for deterministic applications, rather than robust design applications) as reviewed in Chapter 2, systematic thermal topology design methods are virtually non-existent. Although thermal performance—often manifested as heat transfer away from regions of high heat flux—is a critical aspect of many multifunctional applications ranging from MEMS devices to large-scale industrial processes, heat exchangers and heat sinks have been designed conventionally by selecting from commercially available options to meet a set of

requirements. Increasingly, techniques are being introduced for customizing heat exchangers via spacing and dimensional tailoring. Beyond parametric variation, however, it is still difficult to systematically explore and tailor complex *topology*—defined as the layout or internal structure of a heat exchanger—despite the fact that topology strongly influences thermal performance. Since manufacturing freedom is increasingly available for fabricating heat exchangers with complex internal geometries, it is important to design the internal structures of these devices. For certain classes of materials such as prismatic cellular materials, it is also possible to tailor the mesoscopic topology of the materials specifically for thermal performance by introducing voids or passageways for cooling fluids. However, systematic ways are needed for identifying and synthesizing mesoscopic topologies and material layouts with desirable thermal properties.

In this section, a thermal topology design approach is presented for analyzing and designing mesoscopic material topology for heat exchanger or heat sink applications. The approach is based on an initial thermal ground structure comprised of thermal finite elements and boundary conditions. The ground structure is analyzed with a hybrid finite element/finite difference (FE/FD) approach for approximating the temperature distribution in the heat exchanger, the total rate of steady state heat transfer, and pressure losses. Each finite element is characterized by a thickness variable that facilitates adjustment of the size of each element and the contribution of the element to overall thermal performance. The thermal ground structure—along with the finite element/finite difference analysis approach and gradients that are derived from it—are coupled with gradient-based optimization algorithms for exploring the topology and dimensions of a heat exchanger. The FE/FD approach is relatively fast and accurate, compared with

alternatives for detailed thermal analysis such as FLUENT. Also, it is easily reconfigurable to accommodate various initial, intermediate, and final thermal topologies. In Chapter 7, the approach is used along with structural topology design methods in a multi-stage, multifunctional topology design process to tailor the thermal and structural performance of a combustor liner for a jet engine application. Validation and verification of the approach is also discussed in Chapter 7 and associated appendices. The thermal topology design approach is presented in Section 3.5.2, following a discussion of some of the critical design issues and conventional thermal design approaches in Section 3.5.1.

3.5.1 Critical Design Issues and Conventional Design Approaches for Thermal Topology and Parametric Design

The focus of the thermal topology design approach is on designing the internal structure or topology of material systems for thermal applications, in which they function as compact heat exchangers that transfer heat between two entities at different temperatures via conduction and forced internal convection. As noted by several authors, the design of a heat exchange system involves tailoring many parameters such as the dimensions, spacing, and profiles of fins and walls; solid material properties; and the geometric layout of the fluid flow and the solid walls or heat transfer surfaces (e.g., (Bejan, 1993; Fraas, 1989; Lee, 1995)). These characteristics—along with important operating conditions and restraints such as ambient fluid temperature, maximum heat sink size, and the composition and cross-sectional geometry of incoming flow—impact heat transfer rates, pressure drop, maximum temperatures, cost, manufacturability, and a number of other important design objectives and constraints.

To examine some of the critical design issues, let us consider the heat sink illustrated in Figure 3.20. It is representative of a section of prismatic cellular material. As shown

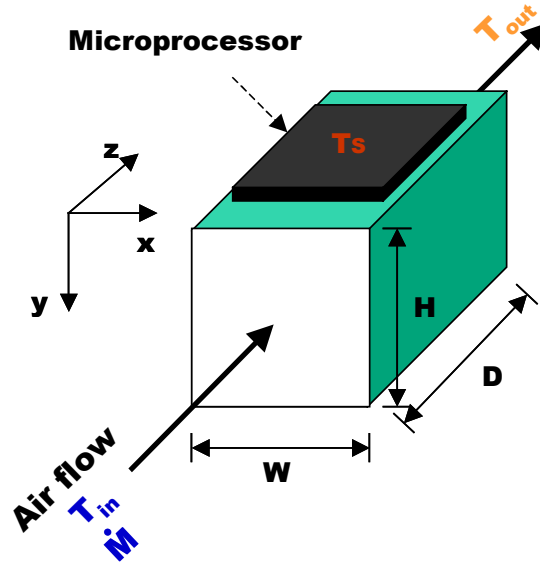


Figure 3.20 –Heat Sink Example

in the figure, the available space for the cellular heat exchanger is limited to a volume with dimensions W by D by H . The mechanism for heat dissipation is conduction and forced convection via cooling fluid which flows into the heat sink at a constant ambient temperature, T_{in} , and total mass flowrate, \dot{M} . The heat sink is attached to a heat generation source—a microprocessor, for example—that maintains the top surface at a constant temperature, T_s . At the beginning of the design process, the structure of the heat sink interior is unspecified, as represented by the open interior region in the figure. During the design process, the distribution of material within the heat sink needs to be determined. This task involves specifying the shape, number, dimensions, and connectivity of heat transfer surfaces or walls within the space that maximize the rate of heat dissipation. Simultaneously, other important objectives and constraints must be

satisfied, including maximum and minimum relative density of the structure, maximum pressure drop, and manufacturability constraints.

The design task is challenging because there are complex interactions between many of the variables and parameters. For example, suppose a designer specifies a single row of rectangular passages, each with height H , in the heat exchanger. Increasing the density of passages or cell walls—and therefore the ratio of heat transfer surface area to volume—appears to be a sensible strategy for enhancing overall heat transfer performance. However, for a constant flowrate, the mean outlet temperature of the cooling fluid approaches the temperature of the heat source as the wall spacing decreases; therefore, an increase in volumetric flowrate may be required to realize an improvement in heat dissipation. Typically, the volumetric flowrate is constant or linked to pressure drop for a specific fan. As the number of heat transfer surfaces increases, hydraulic diameters decrease, pressure drops within individual cells increase, and the overall rate of heat dissipation may diminish. For laminar and turbulent flow, the Nusselt number, heat transfer coefficient, and friction factor for each channel are functions of hydraulic diameter and cross-sectional geometry. Thus, the shape and size of each passage or duct influence its heat transfer characteristics.

The influence of internal structure or topology on thermal performance is evidenced by recent studies of heat sinks comprised of two-dimensional cellular metals. Two-dimensional or prismatic cellular materials have complex and variable cross-sectional cellular arrangements that are extended along an axis perpendicular to the cross-section, as shown in Figure 3.21. Evans and coauthors (Evans, et al., 2001; Gu, et al., 2001)

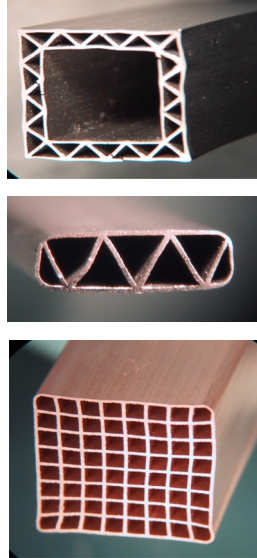


Figure 3.21 – Examples of Linear Cellular Alloys

analyzed the heat dissipation capacity of standard square, triangular, and hexagonal cell topologies for forced convection in compact heat exchangers under steady state, laminar flow conditions. For specified relative densities, the authors found that hexagonal cells offer the highest ratio of total heat transfer rate to pumping power required to force fluid through the cellular structure, followed by square and then triangular cells. Triangular cells exhibit higher heat dissipation capacities than other cells, but they are accompanied by even higher pressure drops. Prismatic cellular materials are advantageous from a thermal perspective due to high surface area to volume ratios, low pressure drop, and extensive freedom for topology adjustment. Via a thermo-chemical extrusion fabrication process developed at Georgia Tech, for example, prismatic cellular materials can be produced with nearly arbitrary two-dimensional topologies, metallic base materials, and wall thicknesses as small as fifty microns (Cochran, et al., 2000). The success of this process demonstrates that it is possible to fabricate prismatic cellular materials that are

tailored for multifunctional applications.⁵ Therefore, it is important to develop design methods that facilitate multifunctional tailoring and strategically leverage the manufacturing freedom that is available.

Since the structure or topology of a heat sink strongly influences its thermal performance and topologically tailored materials can be fabricated via techniques such as the Georgia Tech extrusion process, we are motivated to design the internal structure of these materials. By design, we refer to the systematic exploration of topology, dimensions, and other design variables to identify superior solutions that satisfy a set of constraints and achieve one or more objectives as closely as possible. Currently, heat exchanger designers in industry and academia address some but not all of these challenges. Conventionally, heat exchangers are designed by *selecting* a heat exchanger—including geometry, material, surface type, size, and fluids—from commercially available options to meet a set of design requirements (e.g., (Fraas, 1989; Kraus and Bar-Cohen, 1995)). However, if commercially available assets do not satisfy the design requirements, it may be desirable to customize a heat sink. Several authors have reported techniques for optimally spacing identical heat dissipating fins or heat generating plates in a fixed volume under free convection or laminar or turbulent forced convection (e.g., (Bar-Cohen and Iyengar, 2003; Bejan and Morega, 1994; Knight, et al., 1991)). Recent work on design and optimization of heat exchangers and heat sinks has focused on a thermodynamic approach of entropy generation minimization pioneered by Bejan (1995). This approach has been used for fin spacing as well (e.g., (Culham and Muzychka, 2001)). More recently, it has been utilized to move beyond spacing to spatial

⁵ Further descriptions of prismatic cellular materials and the associated design challenges are provided in Chapter 4.

layout via the constructal method (Bejan, 2000). The constructal method has been employed to generate architectures for heat exchangers, conduction paths, and other applications involving flow between a point and a finite area or volume. The resulting architecture is modular, hierarchical, and constructed in a series of steps beginning with the smallest elemental area. The shape of the elemental area for a heat exchanger is optimized to pack the maximum possible heat transfer rate into a fixed volume (Bejan, 2002). Then, the elemental area is fixed and assembled hierarchically into larger and larger constructs. At each stage or scale, the shape of the assembly is optimized to fill the fixed volume effectively. The end result is a tree-like structure that is more complex than simple linear spacings of fins, plates, or channels. Because the constructal method proceeds from the smallest elemental construct to larger assemblies (rather than breaking a large volume into successively smaller pieces), it is deterministic and has enabled the prediction of flow patterns and organization in natural systems (Bejan, 2000). A large measure of topological and spatial design freedom is sacrificed, however, due to the requirement of fixed elemental constructs combined in a strictly hierarchical sequence. With its emphasis on local, substage optima, the approach does not necessarily provide global optima, and it relies heavily on the assumption of a homogeneous space for which a single, fixed elemental area is appropriate.

Using topology design and optimization techniques, material can be distributed relatively *arbitrarily* within a fixed volume. The objective is to minimize or maximize one or more objectives via strategic distribution of material, subject to constraints that often include a limit on the fraction of the volume allocated to material versus non-occupied or void space. As reviewed in Section 2.3, topology design and optimization

approaches have the potential for facilitating the search for *globally* superior designs characterized by nearly arbitrary topology, shape, and dimensions. However, to date the approaches have not been extended for truly multi-functional applications of interest such as conjugate (conduction and convection) heat transfer in general cases involving internal or external convection and conduction along with other multifunctional objectives.

In the next section, a thermal topology design method—derived from structural topology design and optimization approaches—is presented for synthesizing the internal structure and dimensions of a heat sink that transfers heat away from high heat flux regions via conduction and forced internal convection. In Chapter 7, the effectiveness of the approach is demonstrated by designing heat sinks comprised of prismatic cellular materials.

3.5.2 Thermal Topology Design Approach

A heat sink design process begins with a general performance scenario and a set of basic design requirements. As illustrated in the representative heat sink of Figure 3.20, heat is transferred via forced convection from a region of high heat flux at an elevated temperature, T_s , to a fluid entering the heat sink at a lower temperature, T_{in} . The high heat flux region includes the entire top surface of the structure, and the remaining three sides of the structure are insulated. Fluid flow is assumed to be turbulent and fully developed. Geometrically, the volume available for fluid flow is fixed with dimensions W , D , and H , as illustrated in Figure 3.20. The challenge is to distribute solid material or position thermal elements strategically within the interior of the heat sink to maximize the total rate of steady state heat transfer while satisfying constraints on the total volume

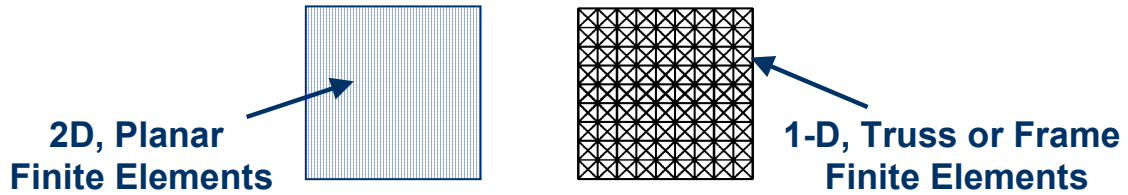


Figure 3.22 – Discretizations for Continuous (Left) and Discrete (Right) Topology Optimization Approaches

of solid material (which is required to be significantly less than the total volume of the heat sink) and the overall pressure drop.

The thermal topology design approach proposed here is rooted in a discrete structural topology optimization approaches based on ground structures. In structural topology optimization approaches, the geometry and response fields within the entire admissible design domain are represented by a fixed finite element mesh. In continuum approaches (such as homogenization and SIMP), the finite element mesh is typically a uniform, rectangular partitioning of space for two-dimensional applications. In discrete approaches, the space is partitioned by a system of frame or truss elements joined at nodes; the union of nodes, elements, and applied boundary conditions is called a ground structure as shown in Figure 3.22. In both types of approaches, continuous variables—orientations and densities for continuum approaches or element cross-sectional areas for discrete approaches—are assigned to each finite element for representation and adjustment of its contribution to the properties of the overall structure. In the ground structure-based discrete approach, elements are effectively removed as their cross-sectional areas approach a very small lower limit during the optimization cycle. It is possible to adjust the topology, geometry, and dimensions of a structure with the ground

structure-based discrete approach by including both cross-sectional element areas and nodal locations as design variables.

The characteristics of heat sink applications make it impossible to apply structural topology design techniques directly. The associated challenges illuminate the difficulty of the task and justify our choice of discrete rather than continuum topology design techniques as the foundation for our thermal topology design approach. First, boundary conditions must be specified for solid heat sink material for any surface that is exposed to the convective fluid medium. For internal forced convection, several types of information are required in order to specify these boundary conditions: (1) the precise location of the boundaries or surfaces at which fluid and solid meet, (2) the geometry of the convective passageway, (3) properties of the fluid within the convective passageway such as density, viscosity, and specific heat, and (4) flow conditions. A central mechanism of continuum topology optimization approaches is the presence of partially dense regions in the design domain throughout the optimization process. As a result, it is difficult (sometimes even at the end of the optimization process) to clearly separate solid and void (which would be occupied by convective fluid in this case) due to the presence of partially dense regions. Therefore, it would be difficult to apply shape-dependent convective boundary conditions to the interior voids in an evolving structure, and it is unclear how one would specify fluid flow properties in partially dense elements. Ground structure-based discrete topology design approaches do not pose this problem because the solid and void/fluid regions are always clearly demarcated; however, there are other challenges associated with applying these techniques. Typically, in structural applications, boundary conditions are specified a priori and do not vary with adjustments

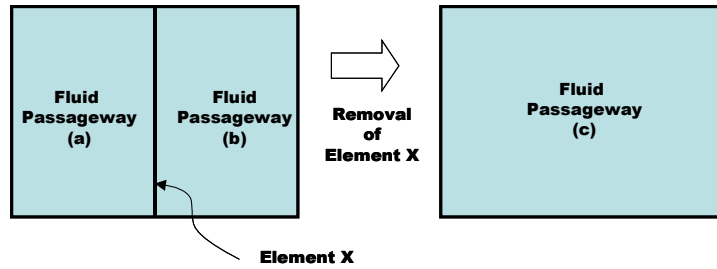


Figure 3.23 – Effect of Wall Removal on the Geometry of a Fluid Passageway

to the topology itself during the optimization process. For heat sink applications, boundary conditions for thermal elements (of solid material) change as the topology changes. Changes in topology or shape within a heat sink impact the geometry of neighboring fluid passageways. Geometry changes in a passageway influence the associated convective coefficients and mean temperature of the fluid medium. These factors directly influence the boundary conditions for the thermal elements that partition the heat sink domain; thus, the boundary conditions are not static but depend on the shape, size, relative location, and number of interior voids. Furthermore, these changes in boundary conditions are not continuous. As illustrated in Figure 3.23, removing a wall invokes a discrete change in boundary conditions due to the associated discrete change in hydraulic diameter and associated properties. Therefore, it is not sufficient to perform topology design exclusively by allowing the cross-sectional areas of elements to approach a very small lower limit; regardless of the lower limit on cross-sectional area, the element will always separate its two neighboring fluid passageways. When the associated elements are actually removed from the structure (after the optimization cycle is completed), the properties and performance of the structure may change significantly. Therefore, it is desirable to anticipate these changes in a way that can inform the

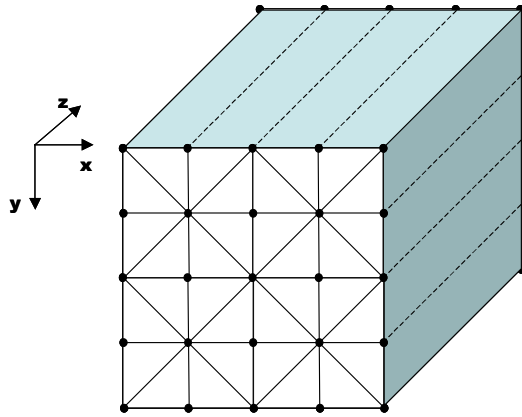


Figure 3.24 – A Sample Thermal Ground Structure

design/optimization process. We have accomplished this by establishing a thermal topology design approach that relies on a ground structure in which each thermal element is described and modified by both a cross-sectional area variable and a density variable.

Thermal Ground Structure

The thermal ground structure is a collection of nodes connected by *thermal topology elements*. As illustrated in Figure 3.24, nodes and thermal topology elements—represented by dots and connecting solid lines in the x-y plane—are arranged in an initial ground structure pattern. A designer may begin with an arbitrary ground structure as long as elements are connected only at nodal locations and do not overlap. The ground structure in Figure 3.24 is a representative example. The ground structure is extended in the z direction to represent the three-dimensional heat sink. Each thermal topology element is three-dimensional with a transverse thickness, length from node to node in the x-y plane, and depth in the z direction. Each thermal topology element, m , has two associated variables: (1) thickness, t_m , for adjusting the size of the geometric space allocated to the element, and (2) density, ρ_m , for adjusting the extent to which the element

occupies its allocated space and separates the two neighboring fluid passages. The thickness corresponds to the actual transverse thickness of an element (i.e., the perpendicular distance between its two lateral surfaces). The density is a continuous variable that interpolates between a fully solid state in which the thermal topology element behaves as a normal element with the designated length, depth, and thickness and a fully void state in which the element effectively disappears. In a zero-density void state, an element does not conduct heat or separate its neighboring fluid passageways. By adjusting the densities of the elements, it is possible to simulate addition or removal of each element independently. Computationally, this is achieved by linking the density of an element to its depth in the z -direction. To illustrate how this interpolation is performed, it is necessary to describe the approach for analyzing the heat transfer performance of the structure.

Thermal Analysis of the Ground Structure

Heat transfer analysis is performed using a hybrid finite element/finite difference approach for approximating the temperature distribution in the heat sink and the total rate of steady state heat transfer from the heat sink to the fluid flowing through the passageways. Both the thermal behavior of the structural material and the changing properties of the fluid are modeled. As shown in Figure 3.25, the ground structure representation of the heat sink is divided into n slices at regular intervals in the z -direction. As in finite difference approaches, the slices are analyzed one at a time. Each fluid passageway is also sliced into n fluid cells of equal length, as shown in Figure 3.25. Each thermal topology element is sliced into n corresponding components, each of which is modeled as a plane, linear, rectangular finite element.

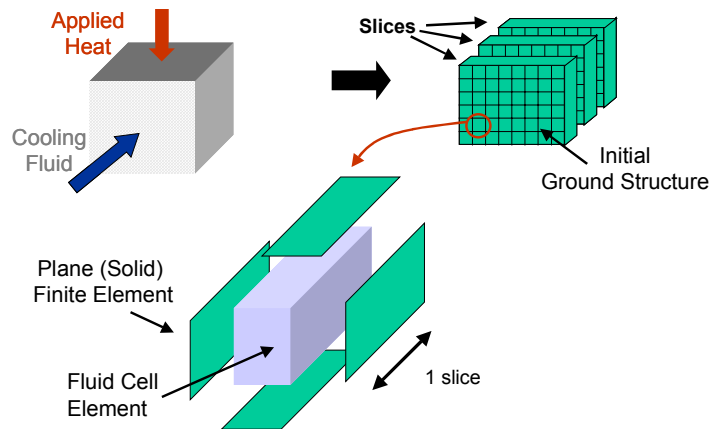


Figure 3.25 – Finite Element Analysis of a Thermal Ground Structure

A schematic diagram of a plane, linear, rectangular finite element is provided in Figure 3.26. The element can be used to model heat flow in a plane of unit thickness, as shown in Figure 3.26, including internal heat conduction and generation in a physical domain Ω , convective heat transfer on lateral surfaces, S_1 and S_2 , and conduction, convection, and applied heat flux along its boundaries, Γ . As indicated in Figure 3.26, the element has sides a and b and four nodes with one degree of freedom per node (i.e., temperature). We assume that the heat sink walls are thin and the temperature gradient through the thickness of a wall in the \bar{z} direction in Figure 3.26 is negligible. This allows us to model the walls as plane, linear rectangular elements and affords considerable computational savings compared with three-dimensional elements. The thermal conductivity, k_s , is assigned a constant value in all elements, and it is normalized to account for the thickness of the element/wall. For convective conditions, we assume that each finite element has a constant surface temperature equivalent to the average of its nodal temperatures. Heat conduction in the z -direction is assumed to be negligible. Each

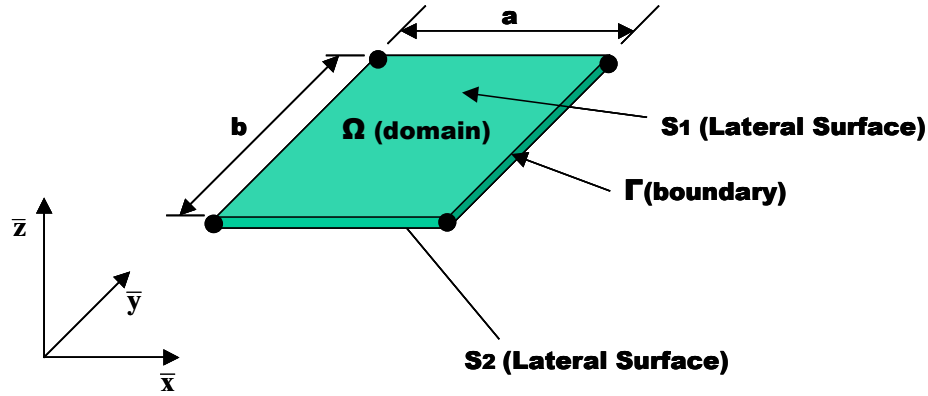


Figure 3.26 – A Plane, Linear, Rectangular Finite Element

slice of a thermal topology element is modeled with a single finite element in this work. Depending on the cell geometry, it may be necessary to use multiple finite elements in each element slice.

The finite element model for the solid walls of the heat sink can be derived from the governing equation for steady state heat transfer in a two-dimensional plane system:

$$f(x, y) + \frac{\partial}{\partial x} \left(k_x \frac{\partial T}{\partial x} \right) + \frac{\partial}{\partial y} \left(k_y \frac{\partial T}{\partial y} \right) + \beta_1(x, y)(T_{\infty_1} - T) + \beta_2(x, y)(T_{\infty_2} - T) = 0 \quad (3.50)$$

where T is the temperature in degrees K, k_x and k_y are the thermal conductivities of the material in W/m-K in the x and y directions respectively, f is the internal heat generation per unit volume in W/m³, β_1 and β_2 are the convective heat transfer coefficients for lateral surfaces, S_1 and S_2 , respectively, and T_{∞_1} and T_{∞_2} are the ambient temperatures of the surrounding fluid medium on each lateral surface. The natural conditions along the boundary, Γ , are a balance of energy transfer across the boundary due to conduction and/or convection (i.e., Newton's Law of Cooling) (Incropera and DeWitt, 1996):

$$k_x \frac{\partial T}{\partial x} n_x + k_y \frac{\partial T}{\partial y} n_y + \beta_\Gamma (T - T_{\infty_\Gamma}) = \hat{q}_n \quad (3.51)$$

where β_Γ and T_{∞_Γ} are the convective heat transfer coefficient and the ambient temperature of the fluid medium along the boundary, Γ , of the solid domain, Ω , and \hat{q}_n is the heat flux specified along the boundary. The weak form of Equations (3.50) and (3.51) is:

$$0 = \int_{\Omega^e} \left[k_x \frac{\partial w}{\partial x} \frac{\partial T}{\partial x} + k_y \frac{\partial w}{\partial y} \frac{\partial T}{\partial y} - wf - w\beta_1 (T_{\infty_1} - T) - w\beta_2 (T_{\infty_2} - T) \right] dx dy \quad (3.52)$$

$$- \oint_{\Gamma^e} w \left[\hat{q}_n - \beta_\Gamma (T - T_{\infty_\Gamma}) \right] ds$$

where w is the weight function and the superscript e refers to element e . The finite element model is derived from Equation (3.52) by replacing w with finite element approximation functions, ψ_i^e , and T with a finite element approximation:

$$T = \sum_{j=1}^n T_j^e \psi_j^e(x, y) \quad (3.53)$$

The finite element model has the following form:

$$\sum_{j=1}^n (K_{ij}^e + H_{ij}^e) T_j^e = F_i^e + P_i^e \quad (3.54)$$

where:

$$K_{ij}^e = \int_0^b \int_0^a \left[k_x \frac{\partial \psi_i}{\partial x} \frac{\partial \psi_j}{\partial x} + k_y \frac{\partial \psi_i}{\partial y} \frac{\partial \psi_j}{\partial y} \right] dx dy \quad (3.55)$$

$$H_{ij}^e = \oint_{\Gamma^e} \beta_\Gamma^e \psi_i \psi_j ds + \beta_1^e \int_{\Omega^e} \psi_i \psi_j dx dy + \beta_2^e \int_{\Omega^e} \psi_i \psi_j dx dy \quad (3.56)$$

$$F_i^e = \int_{\Omega^e} f \psi_i dx dy + \oint_{\Gamma^e} q_n^e \psi_i ds \quad (3.57)$$

$$P_i^e = \oint_{\Gamma^e} \beta_\Gamma^e \psi_i T_{\infty_\Gamma} ds + \int_{\Omega^e} (\beta_1^e \psi_i T_{\infty_1} + \beta_2^e \psi_i T_{\infty_2}) dx dy \quad (3.58)$$

$$\psi_1 = \left(1 - \frac{\bar{x}}{a}\right) \left(1 - \frac{\bar{y}}{b}\right), \psi_2 = \left(\frac{\bar{x}}{a}\right) \left(1 - \frac{\bar{y}}{b}\right), \psi_3 = \left(\frac{\bar{x}}{a}\right) \left(\frac{\bar{y}}{b}\right), \psi_4 = \left(1 - \frac{\bar{x}}{a}\right) \left(\frac{\bar{y}}{b}\right) \quad (3.59)$$

and \bar{x} and \bar{y} are local or element coordinates. In this case, there is no internal heat generation, and the material is assumed to be isotropic. Also, convective heat transfer takes place along the lateral surfaces of the elements but not along their boundaries where either essential or natural boundary conditions are specified (i.e., temperature or heat flux). In these equations, both β_1 and β_2 may be functions of \bar{x} and \bar{y} if only portions of the lateral surfaces of an element are exposed to the surrounding convective fluid medium, for example. If β_1 and β_2 are constants along their respective surfaces, and all of the previous assumptions are considered, the finite element equations reduce to the following in matrix form:

$$[K^e + H^e]\{T^e\} = [F^e] + [P^e] \quad (3.60)$$

where

$$[K^e] = \frac{k_{solid}}{6} \begin{bmatrix} 2\left(\frac{a}{b} + \frac{b}{a}\right) & \left(\frac{a}{b} - \frac{2b}{a}\right) & \left(\frac{-a}{b} - \frac{b}{a}\right) & \left(\frac{-2a}{b} + \frac{b}{a}\right) \\ \left(\frac{a}{b} - \frac{2b}{a}\right) & 2\left(\frac{a}{b} + \frac{b}{a}\right) & \left(\frac{-2a}{b} + \frac{b}{a}\right) & \left(\frac{-a}{b} - \frac{b}{a}\right) \\ \left(\frac{-a}{b} - \frac{b}{a}\right) & \left(\frac{-2a}{b} + \frac{b}{a}\right) & 2\left(\frac{a}{b} + \frac{b}{a}\right) & \left(\frac{a}{b} - \frac{2b}{a}\right) \\ \left(\frac{-2a}{b} + \frac{b}{a}\right) & \left(\frac{-a}{b} - \frac{b}{a}\right) & \left(\frac{a}{b} - \frac{2b}{a}\right) & 2\left(\frac{a}{b} + \frac{b}{a}\right) \end{bmatrix} \quad (3.61)$$

$$[H^e] = \frac{ab(\beta_1 + \beta_2)}{9} \begin{bmatrix} 1 & \frac{1}{2} & \frac{1}{4} & \frac{1}{2} \\ \frac{1}{2} & 1 & \frac{1}{2} & \frac{1}{4} \\ \frac{1}{4} & \frac{1}{2} & 1 & \frac{1}{2} \\ \frac{1}{2} & \frac{1}{4} & \frac{1}{2} & 1 \end{bmatrix} \quad (3.62)$$

$$[F^e] = \frac{ab\hat{q}_n}{4} \begin{bmatrix} 1 \\ 1 \\ 1 \\ 1 \end{bmatrix} = 0 \quad (3.63)$$

$$[P^e] = (\beta_1 T_{\infty_1} + \beta_2 T_{\infty_2}) \left(\frac{ab}{4} \right) \begin{bmatrix} 1 \\ 1 \\ 1 \\ 1 \end{bmatrix} \quad (3.64)$$

By applying appropriate boundary conditions and assembling the element equations (Equation (3.60)), a finite element model of the heat sink walls is formulated. The global finite element model is solved for the unknown temperature distribution in the walls. To determine appropriate boundary conditions for the heat sink walls and evaluate the total rate of steady state heat transfer for the system, the properties of the convective fluid must be evaluated.

Fluid elements are used to model the convective fluid (air) flowing through the interior passageways of the heat sink. The fluid element is used to approximate the temperature of the cooling fluid in each duct and to determine the convective coefficients for the finite element model of the solid walls. As shown in Figure 3.25, the cross-sectional geometry and area of a fluid cell and hence its hydraulic diameter depend on the arrangement and thicknesses of its neighboring solid elements, and the length in the z-

direction depends on the length of a slice (or on the number of slices used to segment a heat sink of specified depth, D). Fully developed turbulent flow is assumed in each fluid cell. The temperature in each incremental fluid cell is assumed to be constant, and the fluid temperature difference in a fluid cell from inlet to exit is assumed to be very small. Fluid properties for each incremental fluid cell are evaluated at the inlet temperature based on curve fits to tabulated data available in handbooks or textbooks (e.g., (Incropera and DeWitt, 1996)). The inlet fluid temperature, T_{in} , is assumed constant over the entire cross-section. The mass flowrate of air is determined with a momentum balance calculation (Hodge, 1999) in which the pressure head is equalized for each cell. The pressure drop, ΔP , across the heat sink is calculated with the Darcy-Weisbach formula, which is equivalent to the pressure head multiplied by the fluid density (Incropera and DeWitt, 1996):

$$\Delta P_i = f_i \frac{\rho_{inlet} L_i V_i^2}{D_{H_i} 2} \quad (3.65)$$

where f_i , ρ_{inlet} , L_i , D_{H_i} , and V_i are the Darcy friction factor, mean fluid density at the heat sink inlet, total passage length, hydraulic diameter, and mean fluid velocity, respectively, for the i^{th} fluid cell. For turbulent flow, the Darcy friction factor, f , and the Nusselt number, Nu , are functions of Reynolds number and Prandtl number, Pr (Incropera and DeWitt, 1996):

$$f_i = (0.790 \ln(Re_{D_i}) - 1.64)^{-2} \quad (3.66)$$

$$Nu_{D_i} = \frac{(f_i/8)(Re_{D_i} - 1000) Pr_i}{1 + 12.7(f_i/8)^{1/2} (Pr_i^{2/3} - 1)} \quad (3.67)$$

The Nusselt number is used to calculate the convective coefficient, β_i , for the fluid cell as follows (Incropera and DeWitt, 1996):

$$Nu_{D_i} = \frac{\beta_i D_{H_i}}{k_i} \quad (3.68)$$

where k_i is the conductivity of the fluid medium. The convective coefficient for the i^{th} incremental fluid cell can be used to calculate the change in mean fluid temperature between the entrance (T_{in_i}) and the outlet (T_{out_i}) as a function of the surface area of the incremental fluid cell, A_{s_i} , mean wall temperature of the solid material enclosing the fluid cell, T_{wall_i} , mass flowrate of fluid in the incremental fluid cell, \dot{m}_i , and the specific heat of the fluid, c_{p_i} , evaluated at T_{in_i} :

$$T_{out_i} = T_{wall_i} - (T_{wall_i} - T_{in_i}) \exp(-\beta_i A_{s_i} / \dot{m}_i c_{p_i}) \quad (3.69)$$

The mean wall temperature is obtained by solving Equation 3.54 for the nodal temperatures in the heat sink. We assume that the outlet temperature of an incremental fluid cell becomes the inlet temperature of the fluid cell in the next slice. The rate of steady state heat transfer, \dot{Q}_i , from heat sink walls to a fluid cell is calculated as follows:

$$\dot{Q}_i = \dot{m}_i c_{p_i} (T_{in_i} - T_{out_i}) \quad (3.70)$$

The *total* rate of steady state heat transfer, \dot{Q} , is obtained by summing the contributions from each cell, I , for each incremental slice, j , of the structure:

$$\dot{Q} = \sum_j \sum_i \dot{Q}_i^j \quad (3.71)$$

It is also important to calculate the volume fraction of solid material in the heat sink. In some cases, it may be useful to constrain the volume fraction below a specified limit.

For example, prismatic cellular structures are more easily manufactured if their volume fractions are below approximately 0.25 (i.e., 25% solid material). The volume fraction is calculated as follows:

$$vf = \frac{\sum_{m=1}^{\# \text{ walls}} t_m l_m d_m}{WHD} \quad (3.72)$$

where t_m , l_m , and d_m are the in-plane thickness, length, and depth of a cell wall, as illustrated in Figure 3.25, and W and H are the total width and height of the heat sink, as illustrated in Figure 3.20.

Although the approach is based on a series of first-order approximations, it has been shown to be relatively accurate by comparison with FLUENT simulations of equivalent heat sinks. A detailed report on validation and verification of the FE/FD model and its parametric and topological design capabilities is provided in Chapter 7. As reported in Chapter 7, the MATLAB-based simulations agree with the FLUENT simulations within about 10%. It is significant to note that the MATLAB-based simulations run in approximately 1 minute on a Pentium IV processor with 1 GB of RAM while the FLUENT simulations require at least 1 day on the same computer. Furthermore, the MATLAB-based simulations are self-reconfigurable for representing alternative ground structures and real-time modifications to the heat sink geometry while similar changes in FLUENT require regenerating a solid model, remeshing it, and re-importing the model into FLUENT—a relatively time-consuming process. Thus, when compared with commercially available software, the finite element/finite difference technique is fast, reconfigurable, and relatively accurate.

Thermal Topology Design

The purpose of establishing thermal ground structures and finite element/finite difference analysis techniques is to facilitate thermal topology design of heat exchangers. The design objective is to determine the topology and thicknesses of thermal topology elements that maximize the total rate of steady state heat transfer and satisfy constraints on the fluid pressure drop and the volume fraction of solid material. As defined previously, the variables for each element, m , are the thickness, t_m , and the density, ρ_m .

Using the relations described previously, it is possible to calculate the properties of interest for an initial ground structure, including total rate of steady state heat transfer (Equation (3.71)), pressure drop (Equation (3.65)), and the volume fraction of solid material (Equation (3.72)). By appropriately modifying the hydraulic diameters of the fluid passageways and the transverse thicknesses of the heat sink walls, it is also possible to calculate the properties for a range of element thicknesses, varied simultaneously or independently for all of the thermal topology elements. Also, because the MATLAB-based heat transfer analysis is easily reconfigurable for different heat sink topologies, it is also possible to accommodate the removal of one or more thermal topology elements from the initial thermal ground structure. When a thermal topology element is removed, the hydraulic diameter of the surviving neighboring cell is adjusted automatically to reflect its merger with the other fluid cell that borders the removed thermal topology element, and the global finite element model is adjusted by eliminating the contribution of the removed element. The fluid cell models are relatively accurate for fluid passageways with convex, non-circular cross-sections when hydraulic diameter is used to

calculate friction and heat transfer coefficients although accuracy tends to diminish as corners become sharper (Kakac, et al., 1987).

To perform thermal topology design, we need to search the design space efficiently and effectively. In this case, the design space is represented by the initial ground structure and the variables—thickness and density—associated with each thermal topology element. To search this design space, we have several options. Since each element can be removed, the number of possible ground structure subsets is 2^n where n is the number of elements in the initial ground structure. In addition, the thickness of each element is permitted to vary. In the context of non-trivial computational times for each analysis of the structure, an exhaustive search would be computationally prohibitive for all but the simplest initial ground structures. Optimization algorithm options include gradient-based techniques such as sequential quadratic programming and sequential linear programming and exploratory techniques such as genetic algorithms and simulated annealing. Exploratory algorithms do not require analytical or numerical gradient information, but they have been found to yield solutions of poor quality in topology design problems and sometimes require a large number of design analyses (Eschenauer and Olhoff, 2001). Gradient-based algorithms tend to be more efficient and effective in topology design problems because they make use of gradient information and converge to superior solutions. Since there are large numbers of variables in topology design problems, however, it is extremely inefficient to calculate gradients numerically, and analytical gradients are needed.

Two categories of analytical gradients are needed—partial derivatives of each response with respect to the thickness and partial derivatives with respect to the density

of each thermal topology element. The partial derivative of the rate of steady state heat transfer, \dot{Q}_i , in cell i with respect to the thickness, t_m , of element m is calculated as follows:

$$\frac{\partial \dot{Q}_i}{\partial t_m} = \frac{\partial \dot{m}_i}{\partial t_m} [c_{p_i} (T_{in_i} - T_{out_i})] - \frac{\partial T_{out_i}}{\partial t_m} (\dot{m}_i c_{p_i}) \quad (3.73)$$

assuming that $\frac{\partial T_{in_i}}{\partial t_m}$ and $\frac{\partial c_{p_i}}{\partial t_m}$ are negligible. The partial derivative of the *total* rate of steady state heat transfer with respect to the thickness, t_m , of element m is the sum of contributions from each cell, i , for each incremental slice, j , of the structure:

$$\partial \dot{Q} / \partial t_m = \sum \sum (\partial \dot{Q}_i^j / \partial t_m) \quad (3.74)$$

Several partial derivatives are required to evaluate Equation (3.73) for each fluid cell. To calculate the partial derivative of the rate of steady state heat transfer in cell i with respect to the thickness of element m , several additional partial derivatives are required. First, we assume that $\frac{\partial \dot{m}_i}{\partial t_m}$ is approximately proportional to $\frac{\partial A_i}{\partial t_m}$ where A_i is the cross-sectional area of fluid cell i :

$$\frac{\partial \dot{m}_i}{\partial t_m} \cong V_i \rho_{inlet} \frac{\partial A_i}{\partial t_m} \quad (3.75)$$

The second unknown component of Equation (3.73) is calculated by differentiating Equation (3.69) with respect to t_m :

$$\begin{aligned} \frac{\partial T_{out_i}}{\partial t_m} = & \frac{\partial T_{wall_i}}{\partial t_m} \left(1 - \exp(-\beta_i A_{s_i} / \dot{m}_i c_{p_i}) \right) - \\ & (T_{wall_i} - T_{in_i}) \exp(-\beta_i A_{s_i} / \dot{m}_i c_{p_i}) \left(\partial(-\beta_i A_{s_i} / \dot{m}_i c_{p_i}) / \partial t_m \right) \end{aligned} \quad (3.76)$$

where

$$\frac{\partial \left(\frac{-\beta_i A_{s_i}}{\dot{m}_i c_{p_i}} \right)}{\partial t_m} = \frac{-\beta_i \frac{\partial A_{s_i}}{\partial t_m} - \frac{\partial \beta_i}{\partial t_m} A_{s_i}}{\dot{m}_i c_{p_i}} + \frac{\beta_i A_{s_i} c_{p_i} \frac{\partial \dot{m}}{\partial t_m}}{(\dot{m}_i c_{p_i})^2} \quad (3.77)$$

The constituent derivatives in Equations (3.76) and (3.77) are calculated as follows:

$$\frac{\partial \beta_i}{\partial t_m} = \frac{D_{H_i} k_i \frac{\partial Nu_i}{\partial t_m} - Nu_i k_i \frac{\partial D_{H_i}}{\partial t_m}}{D_{H_i}^2} \quad (3.78)$$

$$\frac{\partial Nu_i}{\partial t_m} = \frac{\partial}{\partial t_m} \left[\frac{(f_i/8)(Re_{D_i} - 1000) Pr_i}{1 + 12.7(f_i/8)^{1/2} (Pr_i^{2/3} - 1)} \right] \quad (3.79)$$

$$\frac{\partial f_i}{\partial t_m} = \frac{-1.58}{Re_{D_i}} \left(0.790 \ln(Re_{D_i}) - 1.64 \right)^{-3} \left[\left(\frac{\rho_i V_i}{\mu_i} \right) \frac{\partial D_{H_i}}{\partial t_m} + \left(\frac{\rho_i D_{H_i}}{\mu_i} \right) \frac{\partial V_i}{\partial t_m} \right] \quad (3.80)$$

$$\frac{\partial Re_{D_i}}{\partial t_m} = \frac{\rho_i}{\mu_i} \left(\frac{\partial V_i}{\partial t_m} + \frac{\partial D_{H_i}}{\partial t_m} \right) \quad (3.81)$$

and

$$\frac{\partial T_{wall_i}}{\partial t_m} = \frac{\sum_{n \in \Phi} \frac{\partial T_n}{\partial t_m}}{N_\Phi} \quad (3.82)$$

where Φ is the set of nodes that define the surface surrounding incremental fluid cell i and N_Φ is the number of nodes in the set Φ and the partial derivative of nodal temperature with respect to element thickness is derived from Equation (3.54) as follows :

$$\left(K_{yz,m} + H_{yz,m} \right) T_z + \left(K_{yz} + H_{yz} \right) T_{z,m} = P_{y,m} \quad (3.83)$$

where K , H , T , and P refer to global matrices. Equation (3.83) is expressed in indicial notation in which $P_{y,m}$ indicates $\frac{\partial P_y}{\partial t_m}$. The partial derivatives of the stiffness matrices are

derived directly from Equations (3.55) through (3.59) with substitution of previous

equations that are provided. In the above equations, the partial derivatives $\frac{\partial Pr_i}{\partial t_m}$ and $\frac{\partial \mu_i}{\partial t_m}$ are assumed to be negligible. The partial derivatives $\frac{\partial A_{s_i}}{\partial t_m}$, $\frac{\partial D_{H_i}}{\partial t_m}$, and $\frac{\partial V_i}{\partial t_m}$ are derived straightforwardly from cell geometry.

Conceptually, a change in the thickness of an element implies a change in the hydraulic diameter, cross-sectional area, and wetted perimeter of each of the neighboring fluid cells. Since the total mass flowrate is divided among the cells via a momentum balance, a change in the cross-sectional area of one cell impacts the mass flowrate distribution among the cells and the common velocity of the fluid in each cell. Consequently, the convective coefficient changes in each cell. Also, the finite element model for the associated cell wall is affected by the increased thickness via changes in the normalized thermal conductivity of the cell wall and the convective coefficients for each neighboring fluid cell. This contributes to changes in the temperature distribution in the walls of the heat sink. Finally, all of these factors contribute to a change in the outlet temperature of the fluid for each incremental fluid cell and a corresponding change in the total rate of steady state heat transfer.

The partial derivative of the rate of steady state heat transfer, \dot{Q}_i , in cell i with respect to the density, ρ_m , of thermal topology element m is more difficult to calculate. The purpose of the density variable is to simulate the removal of a thermal topology element. Therefore, as the density decreases, the contribution of the thermal topology element to the overall performance of the heat sink should diminish. One way to accomplish this is to relate the density, ρ_m , of a thermal topology element to its length, d_m , in the z-direction in Figure 3.20, as follows:

$$d_m = \rho_m^p D \quad (3.84)$$

where p is a penalization power greater than one and D is the overall depth of the heat sink as shown in Figure 3.20. By adjusting the density of a thermal topology element, we effectively control the portion of allocated volume that a thermal topology element actually occupies. Decreasing the density of a thermal topology element continuously decreases its contribution to the global finite element model and its role as a barrier and convective surface between the two neighboring fluid cells. The penalization power is used to force the topology design toward limiting values of density near zero (void) and one (solid). It penalizes intermediate densities because those densities contribute less to the total heat transfer rate of a heat sink than a non-penalized reference element (with depth $\rho_m D$) but at the same cost in terms of the volume fraction of solid material which is calculated according to Equation (3.72). The partial derivative of the rate of steady state heat transfer in cell i , \dot{Q}_i , with respect to the density, ρ_m , of thermal topology element m is calculated as follows:

$$\frac{\partial \dot{Q}_i}{\partial \rho_m} = \frac{\partial \dot{Q}_i}{\partial d_m} \frac{\partial d_m}{\partial \rho_m} \quad (3.85)$$

where

$$\frac{\partial d_m}{\partial \rho_m} = pD(\rho_m^{p-1}) \quad (3.86)$$

and $\frac{\partial \dot{Q}_i}{\partial d_m}$ is approximated as follows:

$$\frac{\partial \dot{Q}_i}{\partial d_m} \cong \frac{\dot{Q}_{i_j} + \dot{Q}_{k_j} - \dot{Q}_{(i \cup k)_j}}{\Delta d_m} \quad (3.87)$$

where Δd_m is the length of a single slice of the structure, \dot{Q}_{i_j} is the total rate of steady state heat transfer in the i^{th} cell in the j^{th} slice. Thermal topology element m separates cells i and k in slice j . If it were removed from the slice by decreasing its length Δd_m , the two cells would be joined with a total rate of steady state heat transfer of $\dot{Q}_{(i \cup k)_j}$. The slice under consideration is always the last full slice (i.e., the rearmost slice in the direction of fluid flow) occupied by the thermal topology element m . Therefore, calculation of the partial derivative of the total rate of steady state heat transfer with respect to the density of each element is based ultimately on a finite difference approximation. The difference approximation is based on removal of the element from a single slice (i.e., the last slice fully occupied by an element). This is computationally cheaper than basing them on removal of the element from every slice in the structure. It may not be as accurate, however, because temperature profiles of the fluid and solid change throughout the structure; therefore, by basing the difference approximations on a single slice, the result is essentially a local snapshot of the effect of reducing the density of an element. If temperature gradients are significant throughout the structure in the z -direction, it may be necessary to consider slices in other locations in the structure rather than just the slice nearest the back of the structure. It is important to note that partially dense elements are not physically realizable, but in final designs, density thresholds are established for post-processing and penalization powers are employed during the optimization process to segregate the elements into those that remain and those that must be removed.

Empirical Validation and Verification

The thermal topology design approach and the FE/FD heat transfer model on which it is based are utilized for the actively cooled combustor liner example in Chapter 7. In that context, the accuracy of the FE/FD model is evaluated by comparison with the results of FLUENT simulations for identical combustor liner configurations. The accuracy and effectiveness of the thermal topology design approach are also evaluated systematically before being utilized for the example.

3.6 THEORETICAL STRUCTURAL VALIDATION FOR THE RTPDEM

The thermal topology design approach described in Section 3.5 is utilized as part of the RTPDEM for multifunctional applications as described in Section 3.4. The RTPDEM is intended to facilitate robust, multifunctional, systematic exploration of topology and other preliminary design specifications. In this section, the theoretical structural validity of the RTPDEM is investigated by exploring the advantages, disadvantages, and accepted domain of application of the RTPDEM. From a theoretical perspective, it is possible to establish the internal consistency of a method and identify explicitly the favorable and unfavorable properties of the method for particular application domains. Empirical studies are required to establish the usefulness and effectiveness of the method. A strategy for empirical validation of the method is provided in Chapter 4 where appropriate materials design applications are discussed in the context of the method.

The theoretical advantages and limitations of the RTPDEM are summarized in Table 3.1, organized according to research hypotheses. Generally, the RTPDEM enables application of robust design methods in the early, conceptual stages of a design process. Taguchi separated the design process into three stages: concept design, parameter design,

and tolerance design (Phadke, 1989). In concept design, the architecture or layout of a product or process is determined. Parameter design involves characterizing the product or process by specifying values for relevant design parameters. In the detail design stage, the details of a design are finalized, including tolerances and manufacturing specifications. Taguchi and other practitioners of robust design focus on robust design methods for the parameter design stages when robustness can be designed *into* a product by specifying design parameter values that bring mean performance on target and reduce performance variation without removing the sources of that variation. This is more effective and less expensive in many cases than reducing variation in the tolerance design stages by more expensive means such as tightening manufacturing tolerances or specifying higher-grade materials or components. However, Taguchi and other practitioners of robust design have not addressed the potential for synthesizing robust architectures or layouts of products or processes during the concept design stages. This is difficult to achieve because product or process layout is not easily parameterized—a requirement for using robust design methods. However, it is clear that the layout or architecture of a product or process has a profound impact on its performance; therefore, it is reasonable to assume that it may have a strong impact on the potential robustness of performance as well. If alternative layouts offer similar nominal performance but

Table 3.1 – Theoretical Capabilities and Limitations of the RTPDEM

Capabilities and Advantages
<p><i>Hypothesis 1</i></p> <ul style="list-style-type: none"> • Apply robust design methods for the conceptual design stage, which occurs before the Taguchi’s parameter and detailed design stages. • Formulate a robust design problem for topology and other preliminary design specifications using a compromise DSP. The compromise DSP provides flexibility—via modification of weights, targets, bounds, objective function formulations, etc.—for exploring a conceptual design space and generating families of robust compromise solutions. • Synthesize <i>topology</i> and other preliminary design specifications that are robust to (a) parametric noise and (b) topological noise. • Build flexibility into topology and other preliminary design specifications to accommodate adjustments in (a) parametric and (b) topological characteristics of a concept without requiring costly iterative analysis or synthesis. • Solve a robust topology design problem (formulated as a compromise DSP) efficiently with standard gradient-based mathematical programming techniques, coupled with Taylor series- and experiment-based assessment of performance variation. <p><i>Hypothesis 2</i></p> <ul style="list-style-type: none"> • Facilitate distribution of topological preliminary design activities across multiple design stages, associated with different functional perspectives and possibly different designers. Simultaneously, reduce iteration and facilitate compromise among multifunctional objectives via communication of ranged sets of topological preliminary design specifications, with or without approximate behavioral models. • Generation and communication of ranged sets of topological preliminary design specifications facilitates non-iterative collaboration among multiple designers because subsequent designers can adjust design specifications—within the specified parametric ranges and set of potential topologies—to meet their own functional objectives without violating satisfactory performance levels of previous designers. • Generation and communication of approximate behavioral models broadens the scope for non-iterative collaboration among multiple designers. Subsequent designers can adjust design specifications extensively by utilizing their own simulation models coupled with the approximate behavioral models of other domains to evaluate the impact of design changes on their own performance objectives and those of previous designers, respectively. The approximate behavioral models are intended to be fast, relatively accurate, and topologically adaptable to reduce the computational burden associated with them. • Facilitate distributed, multi-stage design for highly coupled, <i>integral</i>, multifunctional products. Distribution of topological preliminary design activities is accomplished via generation and communication of ranged sets of specifications and approximate behavioral models. This approach does not require decomposability or near-decomposability of a system, but accommodates highly coupled systems with larger proportions of shared variables. • Allow designers with expertise in an area to make decisions in that area. • Distribute synthesis activities to avoid computational intractability and extensive interaction. • Support multifunctional topology design for different functional domains with different topological design spaces.
Limitations and Disadvantages
<p><i>Hypothesis 1</i></p> <ul style="list-style-type: none"> • Robust topology design methods are limited to applications for which discrete or continuum topology design approaches can be applied and/or new topology design techniques can be established. • The RTPDEM is applicable for synthesis of topology and other continuous design parameters of <i>integral</i> structures but not for configuration-based or modular design. • Increased computational time and resources are associated with solving robust design problems, compared with standard design problems, but the expense is likely to be balanced by fewer overall design iterations and enhanced quality of a final product. • The compromise DSP—in the form utilized in this dissertation—does not necessarily identify Pareto solutions. • The RTPDEM is presented in this dissertation in the context of discrete ground structure-based topology design approaches. Some modifications are required in order to use it with continuum topology design approaches. • Some potential sources of conceptual and topological variability are not considered in this dissertation, such as imprecision in analysis models, variability in the nodal positions and element lengths in an initial ground structure, and variation in the size and shape of the domain occupied by an initial ground structure. <p><i>Hypothesis 2</i></p> <ul style="list-style-type: none"> • Although the RTPDEM facilitates balancing multifunctional objectives, it does not guarantee the identification of Pareto solutions. If all functions, designers, and stages could be considered simultaneously in a fully integrated design process, it is likely that improved solutions would be identified. However, a fully integrated design process is not a reasonable option for the reasons cited in Section 3.4. • The design freedom of subsequent designers is restricted. If subsequent designers operate with the ranged sets of design specifications, they are limited to the specified parametric ranges and space of potential topological changes. If they choose to utilize approximate behavioral models, the scope for changes is broadened at the cost of creating and repeatedly executing the approximate model. • More information must be generated and communicated among designers. If approximate models are utilized, the models must be created and verified.

different potentials for performance robustness, it is worthwhile to apply robust design methods during concept design stages if possible.

The RTPDEM is intended to extend robust design methods into the conceptual stages of design via robust topology design methods. Using topology design methods, it is possible to synthesize the layout or distribution of material in a design, including the number and shape of internal voids or regions of different material phases—an activity within the realm of concept design. By establishing robust design techniques for topology design applications, it is possible to synthesize topologies and other preliminary design specifications (e.g., dimensions) that are robust to parametric or topological noise. Parametric noise is associated with design parameters such as dimensions, material properties, or magnitudes of applied loads. Topological noise is non-parametric in nature and associated with changes in topology such as removal of elements or joints of a topology.

There are two categories of benefits obtained from robust topology design capabilities. First, robust topology designs can tolerate topological or parametric noise during the fabrication process without significant deviation from expected performance or expensive reductions in manufacturing tolerances. Secondly, the designs have built-in flexibility for accommodating changes in parameters (such as dimensions, material properties, etc.) or topology itself. As a result, the topology should not have to be redesigned when small changes are made to the design in later design stages. This flexibility is useful for multifunctional topology design applications. As noted in Chapter 2, it is sometimes difficult to formulate and solve a topology design problem for non-structural applications. Initial application of the RTPDEM is predicated on the ability to

formulate a well-posed topology design problem—a requirement that may limit the extent to which multiple domains of functionality can be considered. However, with robust topology design methods, it is possible to design a concept in two or more stages and thereby tailor a design for multifunctional performance. In the first stage, the topology is designed for structural performance targets, using robust topology design techniques and assuming topological and parametric variation. In subsequent stages, the built-in flexibility in topology and other conceptual design parameters is utilized to adjust the design to fulfill other performance requirements (e.g., thermal targets or manufacturability goals).

As recorded in Hypothesis 2, the RTPDEM is created for such multifunctional applications. The RTPDEM is intended to facilitate distribution of multifunctional topological preliminary design activities across multiple design stages that may be associated with different functional perspectives and possibly different designers. This is accomplished via generation and communication of ranged sets of topological preliminary design specifications.⁶ Non-iterative collaboration is enhanced because subsequent designers can adjust the design specifications within the specified sets and ranges to meet their own functional objectives without violating satisfactory performance levels of previous designers and requiring costly iteration and redesign. If necessary, the scope for non-iterative collaboration can be broadened by creating and communicating approximate behavioral models. Subsequent designers can adjust design specifications more extensively by utilizing their own simulation models coupled with the approximate behavioral models of other domains to evaluate the impact of design changes on their

⁶ The ranged sets of topological preliminary design specifications include robust ranges of design parameters such as dimensions along with spaces of potential topologies which indicate the scope for adjustment of a nominal topology via addition or removal of specified topological elements.

own performance objectives and those of previous designers, respectively. The approximate behavioral models are intended to be fast, relatively accurate, and topologically adaptable. The approach is designed to reduce the level of costly iteration that accompanies sequential, ‘over-the-wall’ approaches while avoiding the computational intractability and other disadvantages of fully integrated approaches. The approach (with or without approximate behavioral models) is suitable for highly coupled, integral, multifunctional products, as defined in Section 2.4.4, and it accommodates utilization of different topological design spaces for structural versus other domains. It is also designed to allocate decisions to designers with appropriate expertise in the domain.

By formulating a robust topological preliminary design problem as a compromise DSP, it is possible to explore a conceptual design space comprehensively and generate families of robust compromise solutions. The key enabling feature of the compromise DSP is its flexibility. Typically, only a single compromise DSP needs to be formulated for the problem. After the compromise DSP is formulated, weights and targets can be adjusted to shift emphasis among multiple goals or to modify the aspiration space (defined by goal targets). Design variable bounds and constraint limits can be adjusted to shift the boundaries of the feasible design space. In addition, it is possible to change the objective function formulation with possible formulations including Archimedean, preemptive, and utility-based. Together, these changes make it possible to generate families of solutions that embody a range of tradeoffs between multiple goals. For example, as greater weights and/or more ambitious target values are assigned to performance variation goals relative to nominal performance goals, more robust designs can be obtained. It is not necessary to reformulate the compromise DSP in order to make

these changes; it is sufficient to change the values of appropriate constants. This contrasts with single-objective mathematical programming approaches that accommodate only one objective, and standard weighted sum multiobjective optimization formulations that utilize weights but not targets for each objective. Targets are extremely important in the compromise DSP because they allow a designer to specify aspiration or target levels for each goal. Improvements in goal values beyond a target value do not improve an objective function; therefore, a solver concentrates on improving other goal values at that point. This respects a designer's preferences for levels of performance beyond which he/she is indifferent and prevents skewed compromise solutions with exceptionally high/low (i.e., beyond target) goal values for some goals while other goal values remain in unacceptable ranges. However, a designer should keep in mind that the compromise DSP does not *necessarily* facilitate the identification of Pareto efficient solutions as discussed in Section 2.2. If one or more target values have been met by a specific solution, it is possible for another solution to exist in the feasible design space for which the values of one or more goal values (specifically, the goals that have reached their target values) are improved without worsening any other goal values. However, these solutions would not be distinguished from one another because the objective function does not reward goal values that exceed target values. It is possible to avoid this problem by setting sufficiently ambitious target values for each goal. On the other hand, these satisficing or nearly Pareto efficient solutions may be preferred for their robustness to changing design parameters and for their flexibility for subsequent modification, as discussed in Section 2.2. In fact, robust design solutions—as generated with the RTPDEM for general and distributed multifunctional applications—are rarely equivalent

to the Pareto efficient solutions obtained for deterministic, non-robust problem formulations because some measure of nominal performance is often sacrificed for increased robustness.

With respect to solving a compromise DSP for robust topology design, the nature of the problem formulation has a strong impact on the ease with which it is solved and the computational tools required to solve it. Both discrete ground structure-based and continuum topology design approaches are formulated to be continuous and smooth⁷ (in terms of constraints and objectives) with respect to system variables over the entire range of system variable values. The robust topology design problem formulation presented in this chapter is also continuous and smooth with respect to system variables. Control factor or system variable tolerances are smooth, continuous functions of system variable values (which translates into smooth, continuous values of related performance variation according to Equations 3.31 and 3.32 since gradients are also continuous). To assess the impact of topological variability, a number of experiments are conducted with different topologies. For each experiment the constraints and objectives are continuous and smooth with respect to system variables, and the overall constraints and objectives are smooth, continuous functions of the results of the individual experiments. Since the experiments are consistent from iteration to iteration, the overall problem formulation is smooth and continuous. Gradient-based mathematical programming algorithms (e.g., sequential quadratic programming) are efficient and effective for nonlinear problems with continuous gradients. This is extremely important for topology design for two reasons. First, discontinuous problems necessitate the use of exploratory algorithms (e.g., genetic

⁷ A smooth function is C^1 continuous such that its partial derivative with respect to each system variable is continuous.

algorithms) that require large numbers of iterations and thus numerous expensive analyses. Also, discontinuities in the problem formulation could prevent the algorithm from exploring the entire design space and converging to near-lower bound variable values for appropriate elements. Extremely small variable values are particularly significant because the corresponding elements are later removed from the topology.

There are some obvious computational disadvantages to solving robust topology design problems relative to standard design problems. The computational time associated with assessing the impact of variation on performance parameters can be substantial. Special attention was devoted in the RTPDEM to minimizing the computational burden by using readily available gradients of performance with respect to design variables for Type II robust topology design, for example. Nevertheless, the computational costs may be significantly higher for solving robust design problems. The computational cost is estimated for the example problems in Chapters 6 and 7. The increased expense of formulating and solving a robust design problem is balanced by the enhanced quality of the final product. Also, manufacturing costs may be reduced and costly iterative redesign may be avoided via robust design because the performance of robust designs is less sensitive to small stochastic or intentional variations in a design.

The RTPDEM is applicable for the synthesis of topology and other continuous conceptual design parameters for *integral* structures but not for configuration-based or modular design. Integral structures fulfill multiple functions with a single part or with very few parts; modular structures fulfill multiple functions through a combination of discrete, distinct modules or parts, for which there may be a one-to-one mapping between modules and functions (Pahl and Beitz, 1996; Ulrich, 1995). The integral parts designed

with the RTPDEM are likely to be modules or discrete parts of a larger system; however, other configuration or systems design methods are needed to complement the RTPDEM and support design of the larger system.

There are also some limitations to the multifunctional aspects of the RTPDEM. Although the RTPDEM facilitates balancing multifunctional objectives, it does not guarantee the identification of Pareto solutions. In other words, there are likely to be better available solutions to the problem. For example, if all functions, designers, and stages could be considered simultaneously in a fully integrated design process, it is likely that improved solutions would be identified. However, a fully integrated design process is not a reasonable option for the reasons cited in Section 3.4. The design freedom of subsequent (i.e., non-lead) designers is restricted. If subsequent designers operate within the ranged sets of design specifications, they are limited to the specified parametric ranges and space of potential topological changes. If they choose to utilize approximate behavioral models, the scope for changes is broadened at the cost of creating and repeatedly executing the approximate model. In the end, both lead designers and subsequent designers are somewhat restricted in their ability to make design changes and satisfy their own performance objectives. The lead designer must trade off nominal performance for performance robustness in order to generate ranges and sets of design specifications that are as broad as possible. Subsequent designers must make relatively modest changes (or broader changes with the assistance of approximate behavioral models) to a pre-determined design.

The domain of application includes prismatic cellular materials, but it is also potentially much broader. The RTPDEM is particularly appropriate for novel

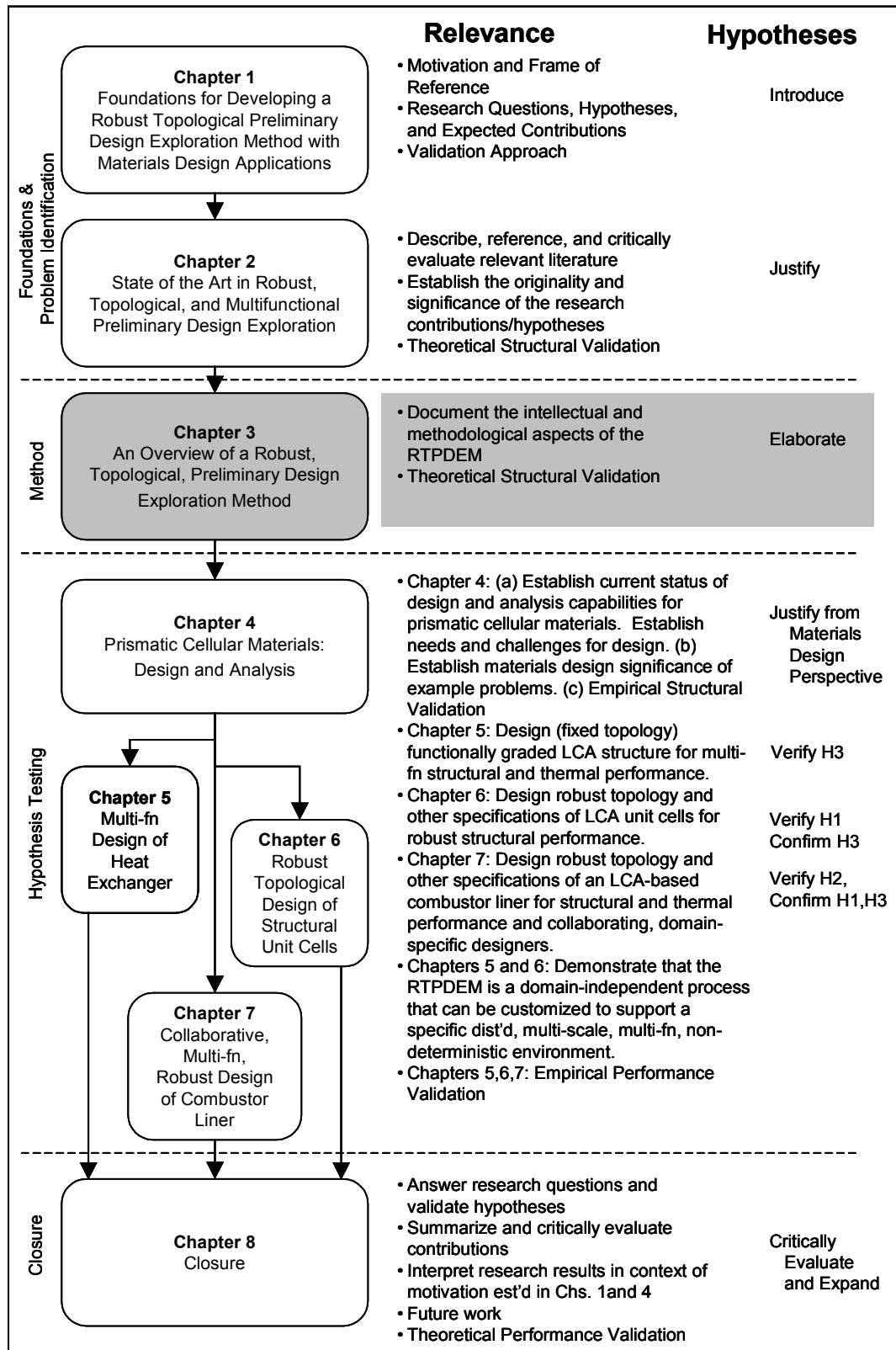


Figure 3.27 – Dissertation Roadmap

manufacturing techniques and smaller scale applications such as cellular materials fabrication, solid freeform fabrication or rapid prototyping or rapid manufacturing techniques, and MEMS fabrication. In these applications, levels of variability may be significant relative to nominal or intended outcomes, and it is sometimes difficult to control this variation. Using the RTPDEM, it may be possible to achieve functional prototypes from emerging, small-scale, or cutting-edge manufacturing technologies. The ability to consider topological variation and to tailor the topology of a material is particularly important for many emerging manufacturing techniques such as solid freeform fabrication and cellular materials fabrication. These fabrication techniques facilitate topological tailoring of a design in two or three dimensions, and in many cases they can create internal voids and functionally gradient material distributions. On the other hand, variation can be significant in important factors such as dimensions, material properties (directionally dependent or anisotropic material properties, porosity, etc.), and topology (e.g., cracked or weak regions of a structure). Using the RTPDEM, a designer can account for these phenomena during the design process. In addition, the topology and other preliminary design specifications can be generated to balance the multifunctional requirements of challenging applications.

3.7 CHAPTER SYNOPSIS

In this chapter the Robust Topological Preliminary Design Exploration Method (RTPDEM) has been introduced, described, and evaluated. As described in Section 3.2, the RTPDEM is the proposed embodiment of the research hypotheses introduced in Chapter 1. The research hypotheses—and therefore the RTPDEM—directly respond to the research opportunities identified via a critical review of the literature in Chapter 2.

The theoretical and methodological aspects of the RTPDEM are documented in Sections 3.3, 3.4, and 3.5 so that it can be applied directly to the examples in Chapters 5, 6, and 7. Theoretical structural validation for the RTPDEM is documented in Section 3.6 in which the advantages, limitations, and appropriate domain of application for the RTPDEM are discussed. As shown in Figure 3.28, the next step is to identify appropriate example problems for empirically validating the RTPDEM. In this dissertation, the example problems involve multifunctional, robust design of prismatic cellular materials. In the next chapter, these examples are briefly reviewed. Their relevance and appropriateness are established for empirically validating the research hypotheses and for challenging, advancing, and demonstrating systematic materials design capabilities.

CHAPTER 4

DESIGN OF PRISMATIC CELLULAR MATERIALS

The need for materials design methods is the motivating factor for the development of the RTPDEM. The materials design domain is potentially very broad, spanning length and time scales from the quantum level to the macroscopic scales of an overall part or system and spanning a broad range of material classes from alloys to ceramics to polymers, but in this dissertation, the focus is narrowed to the design of material mesostructures and specifically, mesostructural topology for prismatic cellular materials and similar classes of materials. The prismatic cellular materials illustrated in Figure 1.6 have several characteristics that make them promising for structural and multifunctional applications. To a significant extent, these properties can be tailored by modifying the topology, shape, and dimensions of their prismatic cells—aspects of the internal structure that may be customized with state-of-the-art manufacturing techniques. Significant progress has been made in characterizing the properties of prismatic cellular materials for structural, thermal, and other types of applications. However, very few advancements have been made in establishing systematic methods for *designing* these materials, despite the fact that extrusion-based fabrication techniques are now available with manufacturing freedom for accommodating complex cellular topologies. Critical design needs include capabilities for systematically tailoring cellular materials for multifunctional requirements and for minimizing the impact of variation—from processing factors or other sources—on the realized properties and performance of the materials. In this dissertation, it is proposed that these needs can be addressed by applying the RTPDEM for the design of prismatic cellular materials. In Section 4.1, relevant literature and

current state-of-the-art techniques in design, analysis, and fabrication of prismatic cellular materials are reviewed, and the need is established for the RTPDEM in a prismatic cellular materials design context.

In Section 4.2, three example applications of prismatic cellular materials are briefly reviewed: (1) a structural heat exchanger, (2) robust structural materials, and (3) a gas turbine engine combustor liner. These examples are documented in detail in Chapters 5, 6, and 7, respectively. In this chapter, the salient features of each example are discussed, including its relevance to materials design goals and its role in validating the research hypotheses. It is argued that the examples are appropriate for validating the RTPDEM, representative of challenging materials design applications, and suitable for demonstrating the advancements in materials design capabilities embodied in the RTPDEM.

4.1 DESIGN, ANALYSIS, AND FABRICATION OF PRISMATIC CELLULAR MATERIALS

Prismatic cellular materials have been used in a variety of structural applications from sandwich panel cores in aerospace applications and shock-absorbing landing gear for the Apollo 11 landing module to ceramic catalytic converters (Gibson and Ashby, 1997). The advantage of prismatic cellular materials in structural applications is their superior specific properties¹, including high stiffness and yield strength at relatively low densities and high energy absorption capacities for many crash or blast amelioration scenarios due to large compressive strains at relatively constant, pre-densification stress levels (Evans, et al., 1999; Gibson and Ashby, 1997; Hayes, et al., 2004). From recent efforts to analyze the structural properties of this class of materials (e.g., (Evans, et al., 1999;

¹ The term *specific* refers to property values per unit mass.

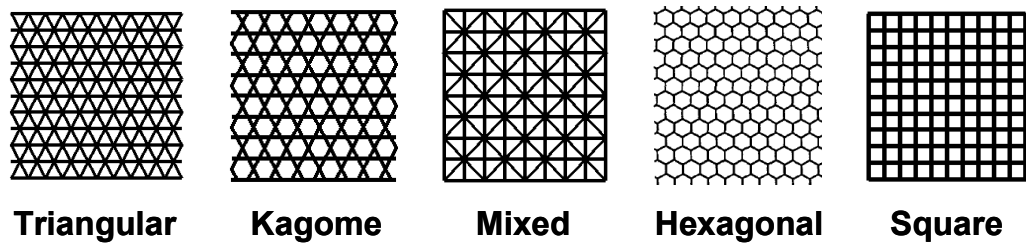


Figure 4.1 – Standard Cell Topologies for Prismatic Cellular Materials

Gibson and Ashby, 1997; Hayes, et al., 2004; Torquato, et al., 1998)), it is clear that their significant in-plane structural properties, including elastic properties and initial buckling strengths, depend strongly on the relative density of the cells and properties of the cell wall material. Also, cell shape and topology have a significant influence on properties and performance, and several standard cell topologies are common in the literature, including square, rectangular, hexagonal, triangular, mixed, and kagome cells, as shown in Figure 4.1. For example, for equivalent relative densities, triangular cells have higher in-plane elastic stiffness and plastic buckling strength than hexagonal cells; hexagonal cells, in turn, have higher stiffness and plastic strength in shear than square cells but lower values in compression (Hayes, et al., 2004). Thus, there is reason to believe that designing the topology, shape, and dimensions of prismatic cellular materials will have a significant impact on their properties.

During the design process, it is important to consider the available means of fabricating specified designs. Fabrication methods impact the freedom afforded a designer for adjusting the internal structure of a cellular material and introduce variability into the realized structures that trigger deviations from expected performance. In the past, most metallic prismatic cellular materials were comprised of hexagonal cells because they could be easily manufactured via stamping and bonding/welding processes.

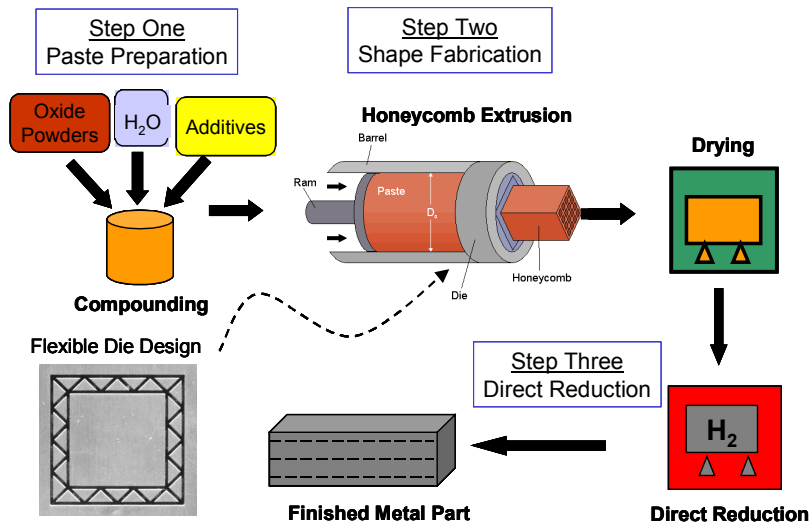


Figure 4.2 – The Prismatic Cellular Materials Fabrication Process at Georgia Tech (Diagram Courtesy of the Lightweight Structures Group at Georgia Tech)

Today, it is possible to fabricate metallic or ceramic prismatic cellular materials via a two-step process involving extrusion and thermochemical treatment (Cochran, et al., 2000), as illustrated in Figure 4.2. Powder-based ceramic pastes are extruded through a micro-machined die that can be customized to adjust the in-plane topology and dimensions of the material. Cell and cell wall dimensions and arrangements are limited only by paste flow and die manufacturability in a process that is much more flexible than traditional stamping. For metallic materials, the green part is reduced in a hydrogen atmosphere, chemically reducing metal oxides to metals. Then, the green part is sintered at elevated temperatures and various heat treatments are applied to the alloy parts. Several alloys have been manufactured this way, including maraging steels, nickel alloys, and copper alloys. Using similar extrusion processes, without hydrogen reduction, it is possible to manufacture ceramic cellular materials such as those used in catalytic converters.

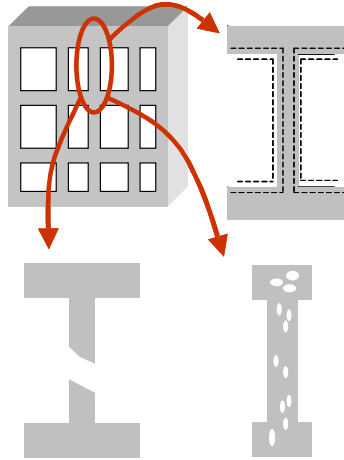


Figure 4.3 – Examples of Processing-Related Variations in Prismatic Cellular Materials. Clockwise from Upper Left: Dimensional Tolerances, Porosity, Cracked Cell Walls

While the thermochemical extrusion process offers valuable topological freedom for tailoring metallic or ceramic prismatic cellular materials, it also introduces imperfections in the final parts. As illustrated in Figure 4.3, possible imperfections include tolerances or dimensional variation, curved or wrinkled cell walls, cracked or missing cell walls or joints, and variations in porosity and other properties of the cell wall material. For example, the porosity of sintered materials has been found to influence several characteristics including conductivity, strength, and elastic moduli, and analytical relationships have been proposed for each of the properties as a function of porosity (Bocchini, 1986). Variations in cell shape have been simulated by comparing the responses of Voronoi honeycombs (generated from a random set of points or nodes separated by a minimum distance) and periodic, hexagonal honeycombs to applied compressive stress. While variations in shape do not affect the elastic moduli significantly, elastic buckling and plastic yield strength can be reduced by 25% or more due to higher bending moments and increased stress in relatively long struts (Gibson and

Ashby, 1997; Silva, et al., 1995). Both elastic moduli and plastic compressive strength of periodic hexagonal and non-uniform Voronoi prismatic cellular materials decrease significantly (30% or more) if just 5% of cell walls are missing and degrade completely if 35% or more of cell walls are missing. Also, it has been shown that triangular cell honeycombs are more resistant to cell wall defects than square or hexagonal cell honeycombs in terms of compressive strength and elastic moduli for defect rates of 5% or more (Wang and McDowell, 2004). In general, we can conclude that cell topology, shape, dimensions, and imperfections have a significant impact on mechanical properties of interest. Therefore, it would be advantageous to be able to design the topology, shape, and dimensions of cells and cell walls of prismatic cellular material for realistic fabrication environments in which imperfections are introduced within the cellular structure.

While significant effort has been devoted to analyzing the properties of prismatic cellular materials (e.g., (Gibson and Ashby, 1997)), relatively little attention has been paid to designing them in a systematic manner. Most of the design-oriented analytical work so far has been directed towards developing relationships between density and cellular dimensions and properties of interest for pre-specified cellular topologies such as hexagonal cells (e.g., (Gibson and Ashby, 1997; Hayes, et al., 2004)). Non-dimensional indices have also been created that combine measures of heat transfer and structural performance for the purpose of comparing the performance of alternative standard triangular, square, and hexagonal cellular topologies for a range of relative density or weight (Evans, et al., 2001; Gu, et al., 2001). While these indices are useful for visualizing trends between performance and one or two design parameters, their use is

limited in design because they necessarily embody specific trade-offs between multiple performance measures that cannot be adjusted. Furthermore, the focus has been on selecting from among a pre-determined set of standard cellular topologies—square, triangular, and hexagonal—rather than systematically exploring and designing cellular topology, arrangement, and dimensions for desired performance.

When designing prismatic cellular materials, it is important to explore cell topology, cell dimensions (e.g., functionally graded cells with varying ratios of cell width to cell length), cell wall dimensions throughout the structure (e.g., gradations of cell walls in various directions or independent adjustment of cell wall thickness throughout a structure), and potential imperfections or variation in the cells and cell walls. Furthermore, it is important to consider the impact of these parameters—along with boundary conditions—on several aspects of performance that are of interest for a particular application. In notable research towards this goal, periodic and functionally graded arrangements of prismatic cellular materials have been explored systematically for thermal (Kumar and McDowell, 2002) and multifunctional (Seepersad, et al., 2004) performance, but these efforts have been limited to prescribing geometric parameters for cellular materials with fixed topology of rectangular cells. Topology optimization techniques have been applied to obtain composite or single-phase material structures with prescribed effective properties without imposing an underlying geometry or topology of the material phase(s) (c.f., (Hyun and Torquato, 2001; Neves, et al., 2000; Neves, et al., 2002; Sigmund, 1994; Sigmund, 1995; Sigmund, 2000; Sigmund and Torquato, 1997; Sigmund and Torquato, 1999)). As demonstrated by these authors, topology design methods are valuable for developing novel cellular structures with specific functional

characteristics. However, to date, only strictly periodic cellular topologies have been designed for structural applications. The effect of variation in design parameters—including variation in boundary conditions, imperfections, and functional grading of a fixed cellular topology—on performance has not been considered in a topology design process. If variation were considered, it should be possible to generate robust topology design specifications with performance that is relatively insensitive to known sources of variation in the material structure itself (induced by manufacturing variability or extended use) and its operating environment. Furthermore, objectives for cellular topology design have been limited to the structural domain (e.g., stiffness, strength, displacement)—with the exception of thermal conductivity—and have not been extended to the array of objectives that characterize the promising multifunctional applications of prismatic cellular materials.

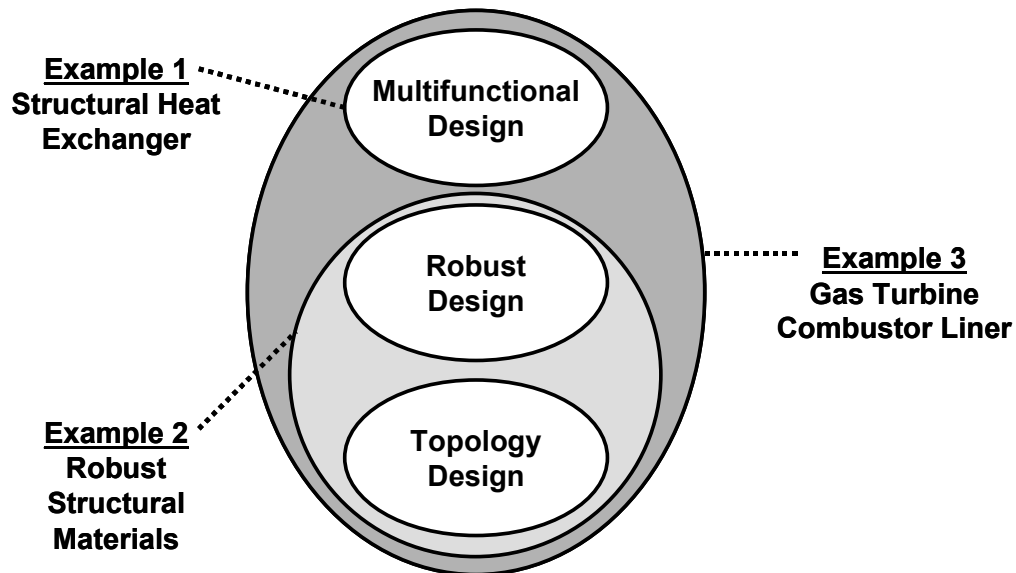


Figure 4.4 – Design Method Requirements as Motivated by Prismatic Cellular Materials Design. Via Three Examples, Application of the RTPDEM is Demonstrated for these Design Method Requirements.

What is needed is a systematic design method that facilitates simultaneous explicit exploration of multifunctional properties and requirements, topology, and robustness. Therefore, there is a clear need for a method such as the RTPDEM which is intended to fulfill this role. The design needs are summarized graphically in Figure 4.4. With respect to Figure 4.4, it is important to note the lack of pre-existing systematic design methods for addressing these capabilities. Although robust design and topology design methods have been researched actively, there has been very little effort devoted to establishing systematic design methods that can accommodate simultaneous exploration of robustness *and* topology, as noted in Chapter 2. Similarly, multifunctional topology design capabilities are extremely limited as are extensions of robust design principles for distributed, multifunctional applications with multiple experts or decision-makers. These capabilities are established with the RTPDEM. As shown in Figure 4.4, three examples of prismatic cellular materials design are planned to demonstrate the effectiveness of the RTPDEM for addressing this combination of design capabilities. The examples are reviewed in the next section.

4.2 EXAMPLES OF PRISMATIC CELLULAR MATERIALS DESIGN

In the preceding section, three major categories of design method requirements are identified, specifically:

- Multifunctional design methods are needed for systematically exploring and generating materials design specifications that effectively balance multiple conflicting objectives or requirements—associated with one or more functional domains. The required domain-specific expertise and analysis models may be distributed and difficult to integrate within a single designer and a single analysis model.

- Robust design methods are needed to reduce the sensitivity of material performance and properties to variations in structure, processing, and operating conditions from specimen to specimen. The link between material structure and other design specifications and multifunctional properties and performance is not deterministic. Treating it deterministically may result in significant quality losses and sacrifices in performance.
- Finally, robust, multifunctional design methods must be applied for exploring material *topology* as well as shape and dimensions. Topology design methods are needed that are appropriate for materials and can be merged with robust and multifunctional design methods.

The RTPDEM is intended to fill these gaps in materials design capabilities. To demonstrate and validate the RTPDEM's capabilities for addressing many of the challenges facing materials designers, three examples are planned. The examples are introduced in Section 4.2.1, and their materials design relevance is discussed. In Section 4.2.2, the appropriateness of the examples for empirically validating the RTPDEM and each of the associated research hypotheses is discussed.

4.2.1 Overview and Materials Design Relevance of Three Prismatic Cellular Materials Design Examples

The relationship between the examples and the materials design capabilities they are intended to demonstrate is summarized in Table 4.1. Different materials design capabilities of the RTPDEM are emphasized with each example. (The role of the examples for validating the research hypotheses is discussed in Section 4.2.2.)

In the first example, prismatic cellular materials are designed for a structural heat exchanger application. As indicated in Table 4.1, the primary focus of the example is

Table 4.1 – Materials Design Capabilities Demonstrated in Each Example			
	Example 1 Structural Heat Exchanger	Example 2 Robust Structural Materials	Example 3 Combustor Liners
Multifunctional Design Exploration			
Single Domain		✓	
Multiple Domains	✓		✓
Distributed Multifunctional Synthesis			✓
Robust Design Exploration			
Variation in control factors		✓	✓
Variation in topology		✓	✓
Variation in material properties		✓	
Variation in operating conditions			✓
Robust design methods to support distributed, multifunctional design			✓
Topology Design			
Structural		✓	
Multifunctional (Structural and Thermal)			✓
Coupled with robust design methods		✓	✓
Distributed			✓

demonstration of multifunctional design. A structural heat exchanger is designed for an application that requires both overall structural stiffness and high total rates of steady state heat transfer, achieved via forced convection with air flowing through the prismatic cells. Families of multifunctional designs are generated that embody a range of compromises between the disparate structural and thermal objectives. Cell and cell wall dimensions and aspect ratios are designed for fixed rectangular cell topologies. Potential variation in design factors is not considered. From a materials design perspective, the example demonstrates the effectiveness of utilizing multiobjective decision protocols for exploring and generating families of materials designs that balance multiple performance requirements.

In the second example, robust prismatic cellular materials are designed for structural applications. As indicated in Table 4.1, the primary focus of the example is

demonstration of *robust* topology design for materials design applications. In this example, prismatic cellular materials are designed for structural applications that require tailored elastic properties. The components of the constitutive tensor that quantify the relationship between states of stress and strain in a material are multiple objectives in the design exploration process. The topology, shape, and dimensions of cells are designed for prismatic cellular materials that meet a set of elastic property requirements as closely as possible. Variations in cellular topology and dimensions are considered along with variation in the properties of the bulk material comprising the cell walls. The example demonstrates the effectiveness of robust topology design methods for tailoring the properties of prismatic cellular materials and minimizing their sensitivity to potential variation from several sources.

In the third example, multifunctional prismatic cellular materials are designed for combustor liners of gas turbine engines. As indicated in Table 4.1, the primary focus of the example is demonstration of *multifunctional* robust topology design techniques. While both robust topology design and multifunctional design for non-topology applications are demonstrated in the first two examples, the stakes are raised in this example to include *multifunctional, distributed* design of the *topology*, shape, and dimensions of a combustor liner comprised entirely of metallic prismatic cellular material. The cellular combustor liner is designed to withstand structural loadings due to the pressure of the combustion reactions. Since structural properties of the bulk material are diminished at high temperatures, the cellular combustor liner is also designed for high rates of heat dissipation via convection from the walls to turbulent cooling air flowing through its cells. The topology, shape and dimensions are designed in a two-stage,

distributed process with structural design followed by thermal design. Robust topology design techniques are utilized in the initial structural design phase to build in both robustness and flexibility for modifications to the initial design in the second, thermal design stage. Variations in dimensions, topology, and boundary conditions are considered during both stages of design. The example demonstrates the effectiveness of distributed, multifunctional, robust topology design methods for tailoring the properties of prismatic cellular materials for multifunctional applications.

The examples in this dissertation are designed to not only provide evidence for the effectiveness of the design methods proposed in this dissertation (i.e., the RTPDEM), but also to substantiate some of the potential benefits of pursuing materials design in general. For example, the resulting structural heat exchanger designs are intended to demonstrate significant performance improvements over conventional designs for microprocessor heat sinks and other similar applications. In the second example, cellular topologies are designed for target properties that are not achievable with standard cellular topologies; furthermore, the resulting designs are targeted to be more robust to topological, dimensional, and other sources of variation than other local minima with similar nominal performance. In the final example, one of the objectives is to demonstrate that strategic materials design can have a significant impact on a materials-limited application. With very limited success, materials scientists have spent decades investigating new materials, such as ceramic matrix composites, to raise the internal temperature and pressure thresholds over conventional alloy-based combustor liners. One of the objectives here is to demonstrate that a previously developed and characterized microstructure can be distributed strategically on mesoscopic and macroscopic scales, via a systematic

materials design process, to enhance its performance in a demanding application. In this case, the bulk, parent material is utilized within a prismatic cellular material arrangement—designed with the RTPDEM—to withstand higher combustion temperatures and pressures and thereby reduce emissions from the gas turbine, *without* requiring expensive, time-consuming development of a new alloy or bulk material.

In the present discussion, evidence is provided for the empirical structural validity of the RTPDEM in this dissertation. Specifically, the present discussion supports the argument that the examples are representative of *actual* materials design examples for which the RTPDEM is developed and intended. As noted in this section, the examples cover the range of design challenges identified for prismatic cellular materials (and many other materials design applications as well). Also, the examples are undertaken in response to ambitious, overall design requirements that cannot be achieved with standard, non-customized designs but require customized solutions that challenge the effectiveness and efficiency of the proposed design methods (i.e., RTPDEM).

4.2.2 The Role of the Examples in Validating the Research Hypotheses

The second significant aspect of empirical structural validation involves verifying that the examples can be used to validate the research hypotheses upon which the RTPDEM is founded. Three research hypotheses are proposed in Section 1.3. Specific aspects of the examples are designed to demonstrate and validate empirically each of the hypotheses.

Hypothesis 1

In the first research hypothesis, it is proposed that robust design methods can be established for topology design applications to facilitate the search for robust topological preliminary design specifications. Specifically, it is proposed that statistical

experimentation, along with customized models of noise factor and topological variation, can be used to support robust topology design for variable topology and boundary conditions. Taylor series-based approximations, along with customized models of control factor variation, are proposed for robust topology design for control factor or dimensional variation. The compromise DSP is used to model robust topology design decisions, and the decision support problems are solved with gradient-based search algorithms. The hypotheses are implemented and tested via several features of the example problems.

In Example 2, the application of robust topology design methods is illustrated for a structural application.

- Topological variation is modeled in terms of sets of potential permutations of an initial ground structure.
- Dimensional variation is modeled according to the special requirements of topology design, discussed in Section 3.3. Dimensional variation is modeled as an increasing function of nominal element dimensions with magnitudes that are less than or equal to the nominal dimensions over the entire range of dimensions (from a lower limit near zero to an upper limit).
- The use of systematic experiments is illustrated for evaluating the impact of topological variation on structural properties.
- The use of Taylor series-based techniques is illustrated for evaluating the impact of dimensional variation on structural properties.
- The use of gradient-based solution algorithms is illustrated for solving a compromise DSP for robust topology design.

In Example 3, the application of robust topology design methods is illustrated for a multifunctional application with both thermal and structural requirements.

- Robust topology design methods are used to explore and establish topological preliminary design specifications for an entire structure comprised of prismatic cellular materials. The topological specifications are designed to be robust to variations in the material itself, including tolerances and topological imperfections. All of the items illustrated in Example 2 for robust topology design are also illustrated in Example 3.
- Robust design methods are utilized to facilitate multi-stage, multifunctional topology design. In the first stage of a two-stage topology design process, robust topology design methods are utilized to generate topological preliminary design specifications with structural performance that is robust to dimensional and topological changes within specified, limited ranges. Both the flexible, robust topological design and the associated ranges of potential design parameter values are communicated to a second-stage designer who uses the design freedom to adjust the topology and other parameters of the design for thermal performance objectives.

Hypothesis 2

In the second research hypothesis, it is proposed that distributed design exploration of multifunctional topological systems can be facilitated by generation and communication of flexible topological design specifications, along with physics-based approximate models, and formulation and solution of multiple compromise DSPs. The hypothesis is implemented and tested via several features of the third example problem.

In Example 3, a multi-stage, robust topology design process is demonstrated. Robust structural topology design is performed in the first stage followed by thermal topology and parametric design in the second stage. Structural topology design is performed first because it is possible to explore a much broader range of topologies with structural topology design techniques than with thermal topology design methods.

- In the first stage, robust topology design methods are used to generate flexible design specifications that are robust to changes in the structure of the design itself, including dimensional changes and topological changes or imperfections. These robust, flexible topological design specifications are communicated to the second design stage along with either (1) physics-based approximate models of the first-stage (structural) objectives that can be used by the second-stage designer to evaluate the impact of second-stage design changes on first-stage (structural) objectives in addition to the thermal objectives with which he/she is primarily concerned, or (2) no additional information beyond acceptable ranges for which the robust design specifications are valid.
- The advantages and limitations of the three alternative methods are compared by applying them to a common combustor liner example problem. This enables comparison of the computational efficiency of the three approaches as well as their relative effectiveness for achieving balance or compromise among multifunctional objectives.

Hypothesis 3

In the third research hypothesis, it is proposed that the compromise DSP can be used as a mathematical decision model for robust, multifunctional topology design problems to

facilitate consideration of robustness, flexibility, and tradeoffs among multiple objectives. The hypothesis is implemented and tested via several features of the example problems.

In Example 1, a compromise DSP is formulated for a multifunctional materials design problem with multiple objectives, multiple domains of functionality, and design specifications that include the aspect ratio and dimensions (but not the topology) of the prismatic cellular material. The compromise DSP is used as a flexible decision support template for generating a family of compromise solutions; specifically, the weights and target values for each goal are adjusted to achieve a range of tradeoffs between the multiple objectives. This formulation is not supported by conventional, single-objective, mathematical programming (with only a single objective) or goal programming alone (with multiple goals or objectives but no constraints).

In Example 2, the use of the compromise DSP is demonstrated as a mathematical model for robust topology design problems with objectives that include nominal elastic properties and variations in elastic properties due to topological and dimensional noise. The design specifications include the *topology* and dimensions of the cellular material. The use of the compromise DSP is illustrated for generating a family of robust topology designs that embody a range of tradeoffs between nominal performance, robustness with respect to topological variation, and robustness with respect to dimensional variation.

In Example 3, the use of multiple compromise DSP's is demonstrated to facilitate multi-stage, multifunctional, robust topology design. In the initial topology design stage, a compromise DSP is formulated and solved for generating robust topology design specifications that are later modified in a subsequent topology design stage associated with another functional domain. The second-stage topology design problem is also

formulated as a compromise DSP to facilitate balancing multifunctional objectives and to accommodate the ranged sets of design specifications received from previous design stages.

Analysis Techniques

In addition to the formal research hypotheses, new analysis techniques are introduced in this dissertation. They are demonstrated and validated via the example problems, as follows:

- Finite Difference/Finite Element Heat Transfer Analysis: In Example 3, the details of the finite difference/finite element heat transfer analysis technique are discussed. Its use is illustrated for modeling and analysis of forced convection heat transfer within the combustor liner. The extent to which it is fast, accurate, and reconfigurable is demonstrated by comparing its performance with finite difference techniques and commercially available FLUENT software.
- Thermal Topology Design with the Finite Difference/Finite Element Heat Transfer Model: In Example 3, the effectiveness of the finite element/finite difference heat transfer model for facilitating topological and parametric design for thermal applications is illustrated. The model is configured with built-in gradient calculations of the partial derivative of the total rate of heat transfer with respect to the thickness and depth of each element. The gradients are used to support gradient-based search algorithms for dimensional and topological tailoring. In Example 3, the accuracy of the gradients is investigated along with their effectiveness for guiding gradient-based search algorithms for tailoring topology and parametric design specifications to meet performance requirements and objectives as closely as possible.

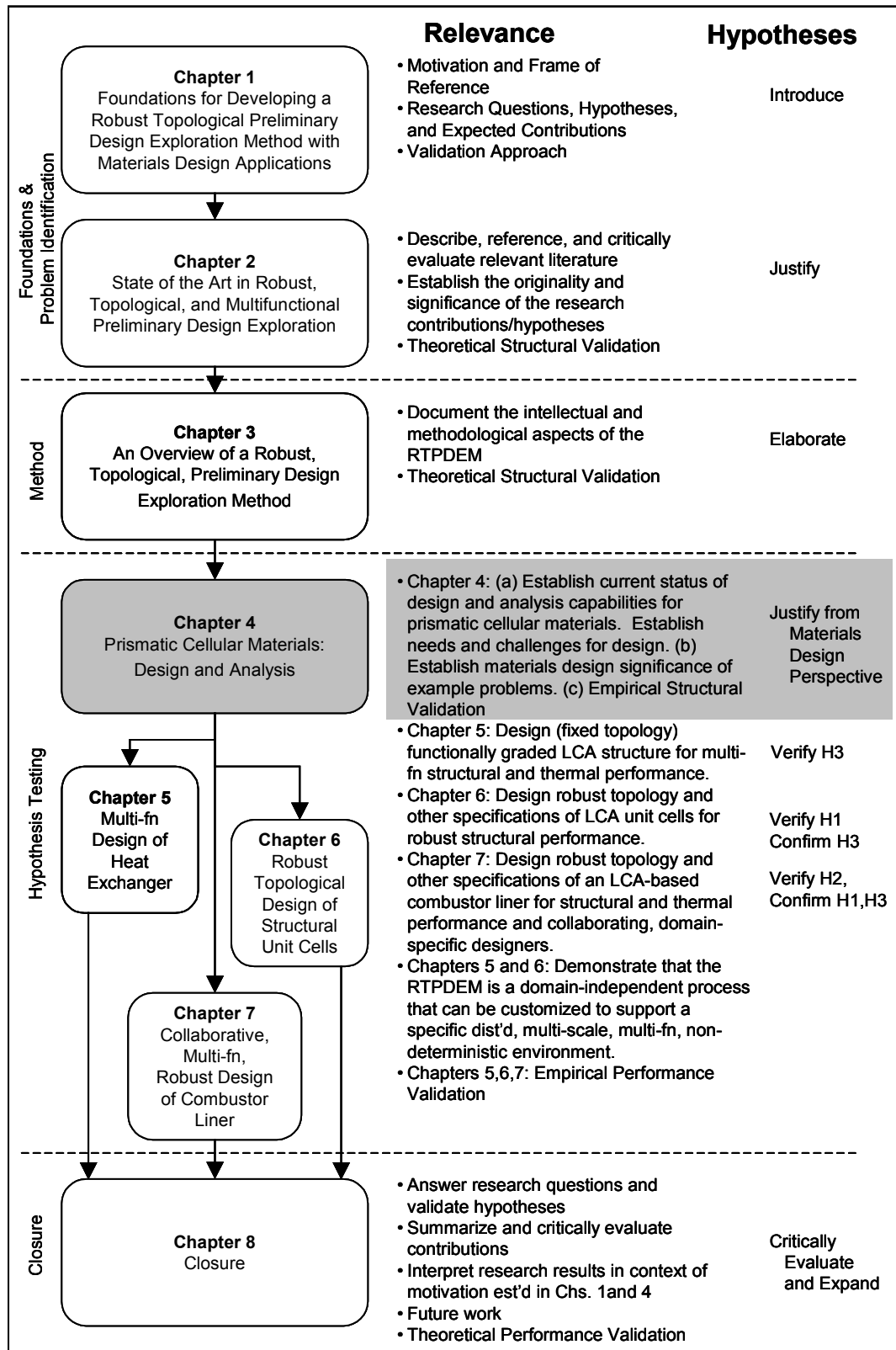


Figure 4.5 – Dissertation Roadmap

- Other Analysis Models: In Example 3, fast finite element analysis models for evaluating and designing the thermoelastic structural behavior of prismatic cellular materials are demonstrated and validated. In Example 2, analytical techniques are demonstrated and validated for evaluating the impact of dimensional variations and topological imperfections on the structural performance of prismatic cellular materials.

4.3 CHAPTER SYNOPSIS

As highlighted in Figure 4.5, prismatic cellular materials are introduced as the class of materials for which the RTPDEM is applied in this dissertation. By reviewing current state-of-the-art techniques in design, analysis, and fabrication of prismatic cellular materials, a set of design method requirements and gaps in design capabilities for prismatic cellular materials are identified. These requirements and gaps in design capabilities justify the hypotheses posed in Chapter 1. Three prismatic cellular materials design examples are outlined. For the purposes of empirical structural validation, it is argued that they are representative of significant materials design challenges and that they are appropriate for empirically validating the research hypotheses embodied in the RTPDEM. In the following chapters, the three prismatic cellular materials design examples are presented, and the results are critically reviewed as a means of testing the effectiveness of the RTPDEM and the validity of the research hypotheses.

CHAPTER 5

MULTIFUNCTIONAL DESIGN OF PRISMATIC CELLULAR MATERIALS FOR STRUCTURAL HEAT EXCHANGERS

One of the foundational constructs in the Robust Topological Preliminary Design Exploration Method (RTPDEM) is the compromise Decision Support Problem (DSP). As proposed in Hypothesis 3, the role of the compromise DSP within the RTPDEM is to facilitate synthesis of a *family* of material designs that satisfy constraints and bounds and embody a *range* of effective compromises among multiple, conflicting goals such as overall structural elastic stiffness and total heat transfer rate. In the early stages of design, it is particularly important to generate such a family of materials design concepts that represents the scope of a multifunctional design space and offers distinct alternatives for further design and analysis.

In the structural heat exchanger example described in this chapter, the RTPDEM is applied for designing functionally graded, two-dimensional cellular structures with desirable structural and thermal capabilities. The compromise DSP—coupled with efficient, flexible, structural and thermal analysis models—facilitates design of a *family* of multi-functional structures. Periodic, functionally graded, and multi-objective structures are designed and compared. Trade-offs between total heat transfer rates and overall structural elastic stiffness are demonstrated. In this example, modifications of the cellular structure are limited to parametric adjustments of cell dimensions and cell wall thickness, along with discrete adjustments in the number of cells. The topology of the cells is fixed and rectangular, and variations in operating conditions and material structure from specimen to specimen are not considered. Topology design and robust

design aspects of the RTPDEM are reserved for the examples in Chapters 6 and 7. In this chapter, the focus is on parametric design of multifunctional cellular material structures as a means of demonstrating the utility of the compromise DSP as a foundational construct for the RTPDEM that facilitates balancing multiple objectives and multiple functional requirements in materials design applications.

5.1 AN OVERVIEW OF MULTIFUNCTIONAL DESIGN OF CELLULAR STRUCTURAL HEAT EXCHANGERS

Low density, prismatic cellular materials have a combination of properties that make them suitable for multifunctional or multi-physics applications that involve combinations of domains, such as ultralight load-bearing, energy absorption, and heat transfer. In this example, non-uniform, graded cell structures are designed to achieve superior thermal and structural performance. Specifically, families of structural heat exchangers are designed for a representative electronic cooling application that demands satisfactory performance in two distinct physical domains: (1) overall rate of steady state heat transfer and (2) overall structural elastic stiffness.

A sample structural heat exchanger—comprised of prismatic cellular materials with graded, rectangular, cells—is illustrated in Figure 5.1. The device is intended for a representative electronic cooling application in which it is required to dissipate heat and support structural loads. The overall performance objective is to transfer as much heat as possible from the heat source, maintained at an elevated temperature, T_s , to cooling air that flows through the cellular structure with a fixed entry temperature, T_{in} , and a variable total mass flow rate \dot{M} linked to the pressure drop of the air. In addition, the device should satisfy minimum targets for overall elastic stiffness in the x- and y-directions

(principal in-plane directions) in Figure 5.1. These objectives are tailored by varying the number and aspect ratios¹ of cells within the device and by varying the cell wall dimensions. Cell topology is assumed to be fixed and rectangular. Finally, the device must be manufacturable; therefore, fabrication-related restrictions are placed on the space of possible cellular structures, including constraints on minimum cell wall thickness and maximum aspect ratios of cells.

For this example, the RTPDEM is utilized as a general multifunctional design approach that integrates multiobjective decision-making with multi-physics analysis tools of structural and heat transfer performance. Approximate analysis models for heat transfer and elastic stiffness are utilized to analyze designs efficiently. Robustness and topology design are not considered in this example. Instead, the focus is to demonstrate the basic effectiveness of the RTPDEM for facilitating multifunctional materials design in a deterministic, parametric design context. The capabilities of the RTPDEM (and the

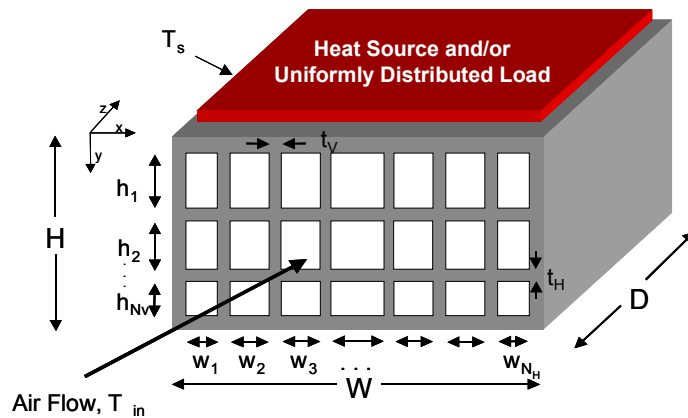


Figure 5.1 – Compact, Forced Convection Heat Exchanger with Graded, Rectangular, Prismatic, Cellular Materials

¹An aspect ratio is the ratio of height to width of a cell or cell wall.

compromise DSP) for facilitating *robust, topology* design of multifunctional cellular materials are investigated empirically in Chapters 6 and 7. Specifically, the focus in this chapter is on the compromise DSP as a foundational basis for the RTPDEM and an important resource for implementing multifunctional materials design. In this example, the compromise DSP is demonstrated to be an effective mathematical decision model for exploration and generation of families of designs that embody a range of compromises among multiple, conflicting goals for multifunctional materials design problems. This is an important capability for *multifunctional* materials design in which multiple, conflicting goals are simultaneously pursued and balanced. The intention is to supersede conventional, materials design development efforts that concentrate primarily on a single functional objective, ignore other functional aspects of performance, and generate new materials with deficiencies in terms of overall, multifunctional design requirements.

5.2 VALIDATION AND VERIFICATION WITH THE EXAMPLE

The structural heat exchanger example is intended to (1) demonstrate the effectiveness of the RTPDEM and, specifically, the compromise DSP as a foundational construct for multifunctional materials design applications, and (2) provide evidence for the validity of Hypothesis 3. Whereas the former item is discussed in Chapter 4 and Section 5.5, the role of the structural heat exchanger example for empirical structural and performance validation of Hypothesis 3 is discussed in this section.² Since robustness and topology design are not considered in this example, the focus is on the compromise DSP as a central basis for the RTPDEM, enabling multifunctional design via flexible, multiobjective, mathematical decision support, as proposed in Hypothesis 3.

² The role of this example—together with the structural unit cell and combustor liner examples in Chapters 6 and 7—for theoretical performance validation of all of the hypotheses is discussed in Chapter 8.

5.2.1 Empirical Structural Validation

Empirical structural validation of Hypothesis 3 involves documenting that the example is similar to problems for which the compromise DSP is intended, that the example is similar to *actual* problems for which the compromise DSP may be applied, and that the data associated with the example can be used to support the hypothesis.

Is this example similar to the problems for which the compromise DSP is intended?

The structural heat exchanger example has characteristics that qualify it as an intended application for the compromise DSP within the RTPDEM:

- Multiple, conflicting objectives from different functional domains must be balanced in order to achieve families of compromise solutions. The objectives include total rates of steady state heat transfer and overall structural elastic stiffness, for which separate analyses are required. Constraints and bounds are also associated with manufacturing considerations.
- It is possible to identify baseline designs—derived from standard square, triangular, hexagonal and similar cell topologies—but significant performance improvements can be obtained by parametrically modifying the standard designs.³ Manufacturing freedom is available for adjusting cell wall aspect ratios and dimensions, with some restrictions such as minimum cell wall thicknesses.

Is this example representative of an actual problem for which the compromise DSP may be applied? The example is representative of preliminary design exploration for multifunctional materials design in a parametric, deterministic context. Approximate

³ Further performance improvements can be obtained by modifying cell topology, as well, as demonstrated in Chapters 6 and 7.

models are utilized for structural and thermal analysis (with the structural analysis model much more simplified than the thermal model). Such fast analysis models are appropriate in *preliminary* design activities in which it is desirable to explore a broad design space and identify families of solutions or superior regions of the design space. Detailed, computationally expensive models tend to be more accurate but prohibitively costly for extensive design exploration. Instead, they are used to calibrate the approximate thermal and structural models. Manufacturability is considered in the form of constraints on internal structure such as cell wall thickness and cell aspect ratios. Therefore, it is the author's opinion that the example accurately reflects an actual multifunctional materials design problem in which property-structure and structure-property relations are explored to synthesize material mesostructure that satisfies multiple performance-related objectives and can be fabricated. However, many phenomena have not been considered that could have a significant impact on the acceptability of a cellular material's multifunctional performance for the structural heat exchanger example. Examples include buckling and yielding. Structural variables do not include the topology of the material in a systematic manner or manufacturing-induced variations in the cellular structure; nor are microstructural or smaller length- and time-scale phenomena considered with respect to the base material in the cell walls. Variations in the material structure and operating conditions, along with systematic topology design, are reserved for Chapters 6 and 7.

Can the data from this example be used to support conclusions with respect to Hypothesis 3? For the structural heat exchanger example, data is obtained for the values of design variables and responses—including objectives and constraints—for

multifunctional cellular materials designs obtained by formulating and solving a compromise DSP. The data associated with these multifunctional designs can be compared with data obtained from single objective formulations and from heuristic designs (e.g., reasonable starting points or initial guesses). The data can be used to show that the compromise DSP effectively supports the search for families of compromise solutions. Data from the search/optimization process—such as convergence plots, sensitivity analysis, results associated with multiple starting points, etc.—can be used to verify that compromise DSP solutions obtained with search/optimization algorithms accurately reflect the capabilities of the compromise DSP for identifying satisfactory multifunctional designs that are superior to most other feasible designs. Data is not generated for robustness or flexibility objectives, and topology is not modeled or modified. Therefore, the data from this example cannot be used to support the effectiveness of the RTPDEM (within which the compromise DSP is utilized) for robust design or topology design.

5.2.2 Empirical Performance Validation

The structural heat exchanger example also enables empirical performance validation of Hypothesis 3. This is achieved by (1) evaluating the outcomes of the method (i.e. the compromise DSP as it is utilized within the RTPDEM) with respect to its intended purposes, (2) demonstrating that the effectiveness of the method is linked to its application, and (3) verifying the accuracy and internal consistency of the empirical data generated in the example and used for validation.

How can the outcomes of the design method be evaluated with respect to its stated purpose? Is the observed effectiveness of the method linked to its application? A two-

stage approach is planned to investigate the effectiveness of the compromise DSP for supporting the search for multifunctional material designs that balance conflicting objectives. As outlined in Table 5.1, conventional single objective optimization techniques are utilized in the first stage to generate prismatic cellular materials designs for the thermal conditions and requirements identified in Section 5.3. By exploring different numbers of cells, preliminary material layouts (i.e., numbers and arrangements of cells) are obtained that are modified for multiple objectives in the second stage. Also, single-objective solutions are obtained for comparison with multi-objective solutions from the second stage. The second stage involves using the compromise DSP to design multifunctional prismatic cellular materials for the structural heat exchanger requirements and conditions identified in Section 5.3. Families of compromise designs are generated by varying targets and other parameters in the compromise DSP, effectively utilizing the compromise DSP as a template for identifying sets of options that embody a range of tradeoffs between multiple, conflicting objectives. Successful completion of the second stage demonstrates that the compromise DSP *can* be used to support multiobjective

Table 5.1 – Experimental Plan and Outline	
Description	Purpose
Stage 1: Design single objective prismatic cellular materials for the thermal conditions and requirements identified in Section 5.3. Use these designs for comparison with the results of Stage 2.	Obtain baseline, preliminary layouts (i.e., numbers and arrangements of cells) for prismatic cellular materials that are refined in Stage 2. Obtain single-objective solutions for comparison with multi-objective compromise solutions obtained in Stage 2.
Stage 2: Design multifunctional prismatic cellular materials for the conditions and requirements identified in Section 5.3. Use the compromise DSP to support associated multiobjective decisions involving structural and thermal objectives and as a focal point for integrating associated multifunctional analyses. Compare with the results of Stage 1.	Demonstrate that the compromise DSP can be used to design prismatic cellular materials for desired multi-functionality. Demonstrate that the multifunctional materials designs obtained with the compromise DSP balance multiple objectives more effectively than designs obtained in Stage 1 with conventional, single objective techniques or heuristic designs based on unmodified standard cellular topologies.

decision-making for multifunctional materials design applications. Comparison of Stage 2 designs with the families of designs obtained in Stage 1 is intended to clearly link the *effectiveness* of the compromise DSP with the capability of systematically obtaining satisfactory compromise solutions.

How is the accuracy and internal consistency of the example results verified? The analysis models are compared with the results of detailed FLUENT simulations and theoretical structural models. The quality of the solutions obtained with search/optimization algorithms is verified by utilizing multiple starting points for search/optimization cycles, restarting each search/optimization cycle from the results of the previous cycle until no further design improvements are observed, and monitoring the design variable, constraint, and objective function values during the iterative cycles for smooth convergence. With respect to multifunctional designs, it is important to look for distinct improvements in objective function values, compared with starting points. Tradeoffs between multiple objectives should be evident among a family of designs, and the trends in objective values should follow the emphasis placed on each objective via target values and weights in the compromise DSP formulation.

5.3 INSTANTIATING THE DESIGN APPROACH FOR THIS EXAMPLE

Structural heat exchangers are designed by utilizing the general procedure of the RTPDEM.⁴ As described in Chapter 3, the RTPDEM is implemented in four phases, beginning with formulation of a design space.

⁴ Since robustness and systematic topology design are not considered in this example, aspects of the RTPDEM associated with robust design and topology design are omitted from the implementation described in this chapter.

5.3.1 Implementing Phase 1 of the RTPDEM: Formulating a Design Space

In Phase 1 of the RTPDEM, influential design parameters are identified, topology is represented for subsequent modification, and variation is characterized from many sources. Since stochastic variation and systematic topology design, are not considered in this example, Phase 1 reduces to identifying the influential design parameters, including design variables, fixed factors, assumptions, and responses. These parameters are summarized in Table 5.2.

The representative structural heat exchanger illustrated in Figure 5.1 has fixed overall width (W), depth (D), and height (H) of 25 mm, 75 mm, and 25 mm, respectively. It is insulated on the left, right, and bottom sides and is subjected to a heat source at constant temperature, T_s , on the top face. The mechanism for heat dissipation is forced convection via air with entry temperature, T_{in} , and total mass flow rate \dot{M} . The flow rate is variable, but it is linked to the available pressure head through a representative characteristic fan

Table 5.2 – Summary of Design Parameters for the Structural Heat Exchanger Example	
Fixed Factors	
$T_s = 373$ K	Temperature of heat source
$T_{in} = 293$ K	Temperature of air at inlet
\dot{M}	Flowrate of air, tied to pressure drop via fan curve (Figure 5.2)
$k_s = 363$ W/m-K	Thermal conductivity of solid base material
$W = 25$ mm	Overall width of device
$D = 75$ mm	Overall depth of device
$H = 25$ mm	Overall height of device
Design Variables	
h_i	Height of the i^{th} row of cells
w_i	Width of the i^{th} column of cells
N_H	Number of columns of cells
N_V	Number of rows of cells
t_v	Thickness of vertical cell walls
t_H	Thickness of horizontal cell walls
Responses	
\dot{Q}	Overall rate of steady state heat transfer
\tilde{E}_x / E_s	Overall structural elastic stiffness in x-direction, relative to the solid modulus of the base material
\tilde{E}_y / E_s	Overall structural elastic stiffness in y-direction, relative to the solid modulus of the base material

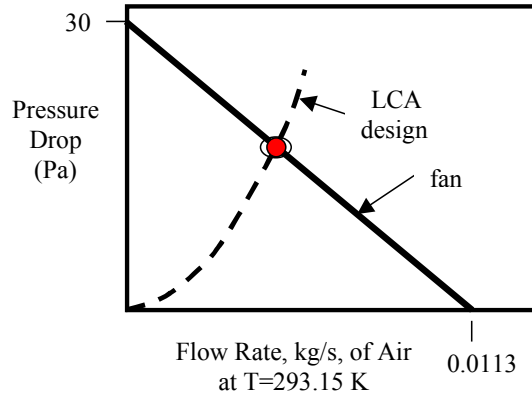


Figure 5.2—Characteristic Fan Curve

curve, illustrated in Figure 5.2. Steady state, incompressible laminar flow is assumed. The solid material in the device is copper. The thermal conductivity, k_s , of copper samples fabricated with the thermo-chemical extrusion process has been measured to be 363 W/m-K (Church, et al., 2001).

For this example, the prismatic cellular structure is comprised exclusively of rectangular cells, but the size, shape (i.e., aspect ratio), and number of cells are permitted to vary in a graded manner. In a graded structure, each row of cells may assume a different height, h_i , and each column a different width, w_i . The only restriction on cell height and width is that the cells must fit within the external dimensions with sufficient remaining space for vertical cell walls of variable thickness, t_V , and horizontal walls of variable thickness, t_H . The numbers of cells in the horizontal and vertical directions are designated N_H and N_V , respectively.

5.3.2 Implementing Phase 2 of the RTPDEM: Formulating a Compromise DSP for Prismatic Cellular Materials Design for a Structural Heat Exchanger

A compromise DSP is formulated for the structural heat exchanger example, as shown in Figure 5.3. As formulated in Figure 5.3, the objective is to determine the values of a set of design variables that satisfy a set of constraints and achieve a set of potentially conflicting goals as closely as possible for a specified set of boundary conditions and dimensions (Table 5.2). The design variables include the numbers of cells in the horizontal and vertical directions, N_H and N_V , the thickness of horizontal and vertical cell

Given	
Thermal and Structural Analysis Algorithms (Section 5.3.3)	
Boundary Conditions (Table 5.2)	
Find	
$N_H, N_V, t_H, t_V, \dot{M}, h_1, h_2, \dots, h_{N_V}$	
Satisfy	
<i>Constraints:</i>	
Fan Curve (Figure 5.2): $\Delta P \leq 30 - (2663.35 * \dot{M})$ Eq. 5.1	
$Re \leq 2300$	
$wN_H + t_V(N_H + 1) = W$	Eq. 5.2
$\sum_{i=1}^{N_V} h_i + t_H(N_V + 1) = H$	Eq. 5.3
<i>System Goals:</i>	
$\frac{\dot{Q}_{total}}{\dot{Q}_{total-target}} + d_1^- - d_1^+ = 1$	Eq. 5.4
$\frac{\tilde{E}_y / E_s}{(\tilde{E}_y / E_s)_{target}} + d_3^- - d_3^+ = 1$	Eq. 5.6
$\frac{\tilde{E}_x / E_s}{(\tilde{E}_x / E_s)_{target}} + d_2^- - d_2^+ = 1$	Eq. 5.5
<i>Bounds on Design Variables:</i>	
Common	Heat transfer & Elastic stiffness
$2 \leq N_H \leq 16$	$0.00025 \text{ m} \leq h_i \leq 0.022 \text{ m}$
$2 \leq N_V \leq 16$	$0.00015 \text{ m} \leq t_H \leq 0.002 \text{ m}$
$d_1^+, d_1^- \geq 0$	$0.00015 \text{ m} \leq t_V \leq 0.002 \text{ m}$
$d_1^+ \cdot d_1^- = 0$	$0.0005 \text{ kg/s} \leq \dot{M} \leq 0.003 \text{ kg/s}$
Minimize	
$Z = W_1 d_1^- + W_2 d_2^- + W_3 d_3^-$ Eqn. 5.7	
(See Table 5.4 for weights and target values for each design scenario.)	

Figure 5.3 – Compromise DSP Formulated for Structural Heat Exchanger Design

walls, t_H and t_V , the internal height of each row of cells, h_i , and the total mass flow rate, \dot{M} . Each column of cells is assumed to have identical internal width, w , which is a dependent variable that is a function of the total width, W , of the structure and the variable thickness of the vertical cell walls, t_V , according to Equation 5.2 in Figure 5.3. Compatibility constraints on the design include restrictions (Equations 5.2 and 5.3 in Figure 5.3) that ensure that the cells and cell walls fit together and occupy the overall dimensions of the structure. Pressure drop and mass flowrate are related according to the fan curve of Figure 5.2, expressed as Equation 5.1, and laminar flow is enforced in each cellular passageway. Together, the design variables and the set of inviolable constraints and bounds define the design space of feasible, potential solutions.

Within the feasible design space, preferred solutions achieve a set of potentially conflicting, multifunctional goals as closely as possible. For this design, there are three goals, all of which are maximized: total rate of steady state heat transfer, \dot{Q}_{total} (Equation 5.4), and overall structural elastic stiffness in the horizontal and vertical directions, \tilde{E}_x / E_s and \tilde{E}_y / E_s , expressed as fractions of the elastic modulus of the solid cell wall material, E_s (Equations 5.5 and 5.6). Deviation variables d_i^- and d_i^+ measure the extent to which each goal, i , achieves an ambitious target value (e.g. $\dot{Q}_{total-target}$ in Figure 5.3) in Equations 5.4-5.6. The deviation variables for all goals are combined into an objective function, which measures the extent to which multiple goals are achieved. Note that this approach differs from classical single-objective optimization with imposed constraints. In Figure 5.3, the objective function is expressed in Equation 5.7 as a weighted sum of relevant deviation variables, although other formulations are possible (Mistree, et al.,

1993). The weights and target values for each goal are recorded along with the results in Section 5.4. After the problem is formulated, it must be solved using appropriate domain-specific analyses and software codes coupled with solution or search algorithms, as described in Section 5.3.3.

5.3.3 Implementing Phase 3 of the RTPDEM: Analysis Models and Simulation Infrastructure for Prismatic Cellular Material Design for a Structural Heat Exchanger

A simulation infrastructure is needed for solving the compromise DSP of Figure 5.3 by searching the design space and evaluating the thermal and structural properties of alternative material designs. As illustrated in Figure 5.4, the simulation infrastructure for this example is anchored in the compromise DSP. The compromise DSP is solved using solution algorithms that are paired with appropriate domain-specific analysis models. In this example, the focus is on designing prismatic cellular materials that meet requirements for both heat transfer rate and elastic stiffness. Two sets of analysis codes are required for the thermal and structural domains of analysis. The thermal and structural analysis models are user-developed Fortran and Basic computer programs. Commercial design integration software (i.e., iSIGHT) is used to integrate the disparate analysis codes with search algorithms governed by the compromise DSP formulation.

In the remainder of this section, brief reviews are provided of (1) a finite difference approach for quickly evaluating thermal performance in terms of total rates of steady state heat transfer, and (2) a simplified model for determining overall structural elastic stiffness. Although the thermal and structural models presented in this section are less accurate than commercially available structural and thermal/fluids analysis programs such as ANSYS and FLUENT, they are also more computationally efficient. Therefore,

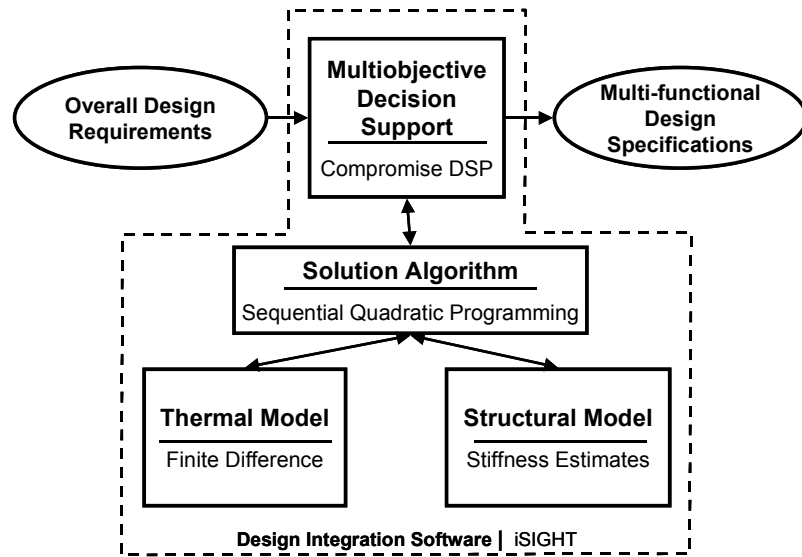


Figure 5.4 – Multifunctional Design Approach

they are more suitable for broad exploration of a preliminary design space, whereas more accurate, detailed models are used for validation of the fast analysis models and resulting designs.

Finite Difference Heat Transfer Analysis

The finite difference method is a numerical technique for solving the three-dimensional steady state heat transfer equations—Fourier's law (conduction), Newton's law of cooling (convection), and an energy balance for the internal flow—associated with the sample prismatic cellular heat exchanger shown in Figure 5.1 (Incropera and DeWitt, 1996). Complete details of the formulation and validation are provided by Dempsey and coauthors (Dempsey, 2002; Seepersad, et al., 2004). The prismatic cellular material is discretized spatially using a set of nodal points located distances Δx and Δy apart in a cross section in the x-y plane, as shown in Figure 5.5. Cross-sections are repeated at regular intervals, Δl , along the length of the prismatic cellular material in the

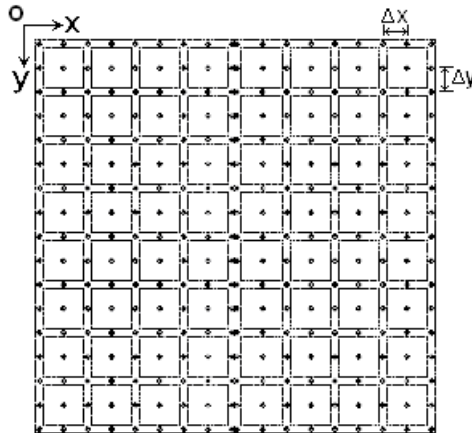


Figure 5.5 – FD Nodal Placement on a Typical Cross-Section of Cellular Material (Seepersad, et al., 2004)

z-direction in Figure 5.1. A uniform temperature is designated for the fluid in each incremental length, Δl , of a cell and for each cell wall segment between nodes. Nodal spacing is dictated by cell sizes as graded cell dimensions may vary within a cross-section. By evaluating the energy balance for each node and utilizing central difference approximations with second order accuracy, a linear system of algebraic equations is constructed and then solved to obtain the temperature at each node. The exit temperature, T_{exit_i} , of the fluid in each cell, i , can be used to calculate the total rate of steady state heat transfer, \dot{Q}_{total} , by a summation over all of the cells:

$$\dot{Q}_{total} = \sum_i^{n \text{ cells}} \dot{m}_{cell_i} c_p (T_{exit_i} - T_{in}) \quad (5.8)$$

where \dot{m}_{cell_i} , T_{in} , and c_p are the mass flow rate in cell i , inlet fluid temperature, and specific heat of the fluid, respectively. The finite difference heat transfer analysis has been validated with physical experiments, analytical solutions, and FLUENT CFD

simulations for both uniform and dimensionally graded cell configurations (Dempsey, 2002; Seepersad, et al., 2004).

Estimates of Overall Structural Elastic Stiffness

Several authors have reported in-plane elastic properties and initial buckling loads for two-dimensional cellular materials with periodic hexagonal, square, rectangular, or triangular topologies (Gibson and Ashby, 1997; Gu, et al., 2001; Hayes, et al., 2004; Torquato, et al., 1998). These analytical estimates are not appropriate, however, for the *non*-periodic rectangular cell structures explored in this example. Here, we outline a simplified approach for assessing the overall structural elastic stiffness of such non-periodic, rectangular, prismatic, cellular materials.

When a prismatic cellular material with non-periodic rectangular cells is loaded along one of the coordinate axes in Figure 5.5, elastic deformation occurs due to axial extension or compression of the cell walls. If the loading is axial, and there are no imperfections in the structure, there is no bending contribution to the deformation in this particular loading configuration. Thus, the overall structural elastic stiffness in the x-direction (\tilde{E}_x) or y-direction (\tilde{E}_y) is approximated as the fraction of the total structural width (W) or height (H), respectively, occupied by cell walls, i.e.,

$$\tilde{E}_x / E_s \cong \frac{t_h(N_v + 1)}{H} \quad (5.9)$$

$$\tilde{E}_y / E_s \cong \frac{t_v(N_h + 1)}{W} \quad (5.10)$$

where E_s is the elastic modulus of the isotropic solid cell wall material.

5.4 PRESENTATION AND DISCUSSION OF STRUCTURAL HEAT EXCHANGER DESIGNS

Functionally graded LCA heat exchangers with desirable structural and thermal properties are designed for the boundary conditions listed in Table 5.2. Design is guided with the use of the compromise DSP in Figure 5.3. Given a set of boundary conditions and techniques for analyzing non-periodic LCA heat exchangers, the objective is to find the values of the set of design variables that satisfy the set of constraints and bounds and achieve the targets for one or more goals as closely as possible. Design solutions are achieved using iSIGHT (2003) design automation and exploration software, coupled with the finite difference algorithms and analytical expressions described in Section 5.3. The solution process is mapped in Figure 5.6.

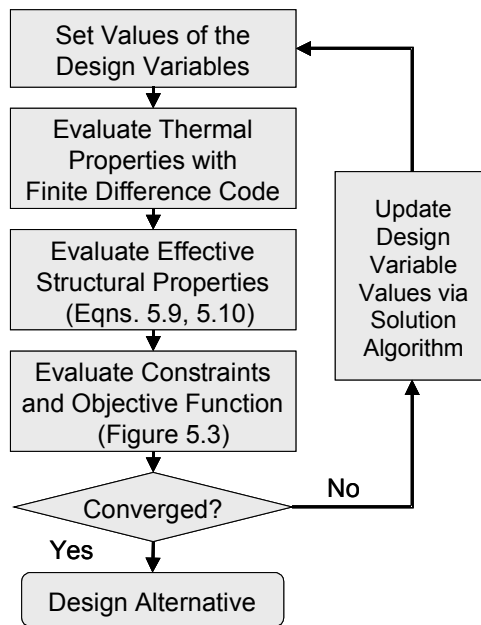


Figure 5.6 – Solution Process

Stage	Design Variables	Design Objective(s)	Outcome
1A	$N_H, N_V, t_H, t_V, \dot{M}$ (h and w are dependent variables)	Maximize Q_{total}	Determine the appropriate shape and number of cells .
1B	$t_H, t_V, \dot{M}, h_1, h_2, \dots, h_{N_V}$ (w_1, w_2, \dots, w_{N_H} are uniform and dependent variables) (fix N_H, N_V)	Maximize Q_{total}	Determine functionally graded designs for a single objective , for number of cells determined in Stage 1a.
2	$t_H, t_V, \dot{M}, h_1, h_2, \dots, h_{N_V}$ (w_1, w_2, \dots, w_{N_H} are uniform and dependent variables) (fix N_H, N_V)	Maximize Q_{total} , \tilde{E}_x / E_s , \tilde{E}_y / E_s	Determine functionally graded designs that satisfy multiple objectives , for number of cells determined in Stage 1a.

A two-stage design approach is employed, as outlined in Tables 5.1 and 5.3. In the first stage, single-objective designs are generated—as preliminary layouts and for comparison with the multifunctional solutions obtained in the second stage—by maximizing *only* the total rate of steady state heat transfer. In the second stage, multifunctional prismatic cellular materials are designed for both thermal and structural performance objectives. The first design stage is implemented in two parts—Stage 1A and Stage 1B—to facilitate management of design freedom, development of intuition with respect to desirable solutions, and exploration of the design space. In Stage 1A, preliminary layouts are explored for the cellular material in light of an established set of performance requirements. In this case, the process involves preliminary exploration and selection of the shape and number of cells from a finite set of feasible alternatives based on available quantitative and qualitative information. In Chapters 6 and 7, this role is

fulfilled by topology design techniques within the RTPDEM. The outcome of this phase is a concept that embodies the basic geometry, arrangement, and topology of the material. In Stage 1B, single-objective designs are obtained based on the configurations identified in Stage 1A. These designs represent the outcomes of a single-objective optimization process and are used to highlight the difference between ‘optimized,’ single-objective designs and the multifunctional compromise designs obtained with the compromise DSP. In Stage 2, multifunctional designs are generated, starting from the preliminary layouts identified in Stage 1A. Influential design variables—such as dimensions—are modified systematically to satisfy constraints and explore trade-offs among a set of multifunctional objectives. The outcome of Stage 2 is a family or Pareto set of designs—based on a common concept—that embodies a range of multifunctional performance. Such a two-stage design approach is particularly pragmatic when concepts with a broad range of shapes and sizes or fundamentally different cell configurations or topologies—such as standard square, triangular, or hexagonal cell shapes, or arbitrary shapes and arrangements obtained with topology optimization techniques—are identified, evaluated, and filtered in Stage 1 and then refined for superior multi-functional performance in Stage 2. Results from the first and second stages are recorded in Sections 5.4.1 and 5.4.2, respectively.

5.4.1 Designing Baseline Prismatic Materials for the Structural Heat Exchanger Application

Stage 1A. In Stage 1A, the general layout of the cellular heat exchanger is determined, including the shape and approximate size of the cells. Since the primary objective is to maximize the rate of steady state heat transfer for laminar flow within the cells, rectangular cell topologies are chosen because they exhibit higher Nusselt numbers

than other standard topologies (Incropera and DeWitt, 1996). The layout of the material is characterized more completely by exploring and comparing a range of feasible cell counts, sizes, and aspect ratios for superior steady state heat transfer rates for the specified boundary conditions. As a preliminary exploration of the design space, the numbers of cells in the horizontal and vertical directions are varied while the cells are assumed to be periodic with equivalent widths and equivalent heights. The thickness of the vertical cell walls (t_V) and the thickness of the horizontal cell walls (t_H) are also varied, along with total mass flowrate (\dot{M}) (which is tied to the pressure drop via the fan curve of Figure 5.2). Two solution techniques may be used in Phase 1: (1) exploratory solution algorithms (e.g., simulated annealing, genetic algorithm) that accommodate both discrete and continuous variables with t_H , t_V , \dot{M} , and N_H and N_V as design variables, or (2) gradient-based solution algorithms (e.g., sequential quadratic programming) that accommodate only continuous variables and must be employed repeatedly for fixed values of N_H and N_V , with t_H , t_V , and \dot{M} as design variables. The latter approach is employed in this case.⁵ Validation of design solutions is discussed in Section 5.4.3.

An LCA structure with periodic, rectangular cells is designed for each combination of rows and columns depicted in Figure 5.7. The ordinate axis in Figure 5.7 represents maximum achievable total heat transfer rates for each configuration. As shown in Figure 5.7, it is advantageous, from a thermal perspective, to employ a relatively large number of columns of cells and a small number of cell rows. The 14 by 2 and 14 by 3 configurations have the largest heat transfer rates and are utilized as preliminary layouts

⁵ Based on preliminary trials for this example, the latter approach tends to be more time-consuming but leads to better solutions. The former approach generated solutions that were clearly inferior with respect to overall objectives. (Note that the strengths and limitations of these two techniques are associated with the solution algorithms rather than the design approach itself.)

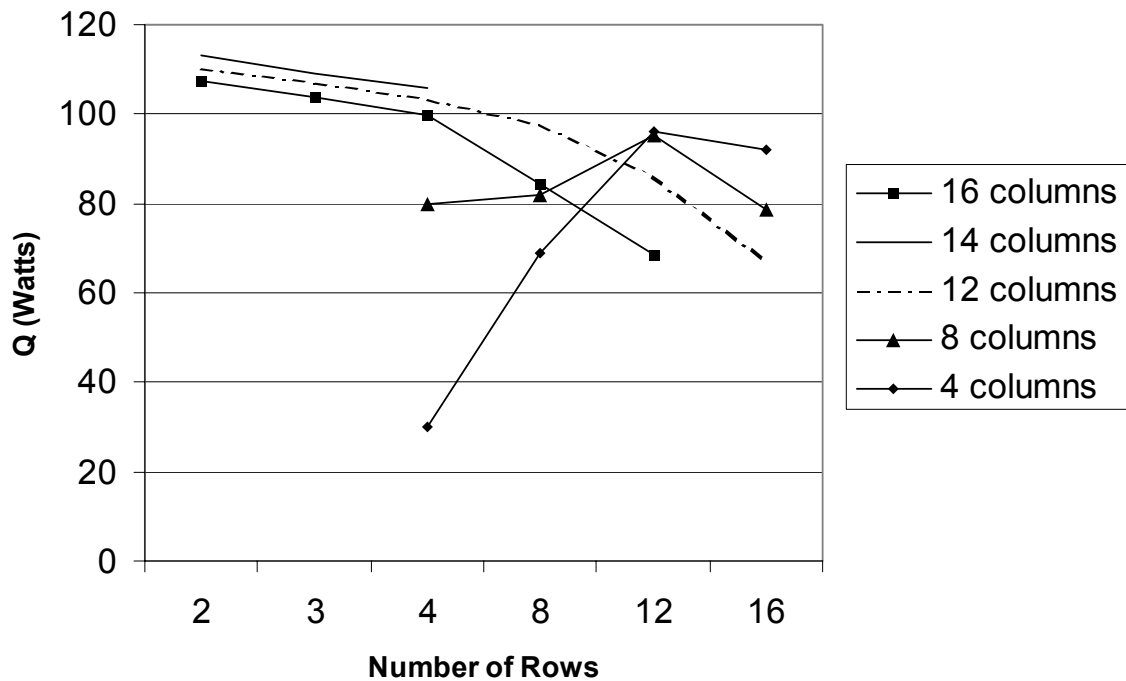


Figure 5.7 – Total Heat Transfer Rate for Periodic Rectangular Cell LCAs with Various Numbers of Rows and Columns

in Stages 1B and 2. Designs with periodic rectangular cells for 14 by 2 and 14 by 3 configurations are illustrated in Tables 5.4A and 5.4E. It is important to note that these results may be sensitive to the stated boundary conditions and dimensions. Alternative numbers of rows and columns may be appropriate for other boundary conditions, dimensions, or cell shapes. Only rectangular cells are investigated here due to their superior heat transfer properties in the laminar flow regime (Incropera and DeWitt, 1996).

Table 5.4 – Example Prismatic Cellular Material Designs for the Structural Heat Exchanger Application

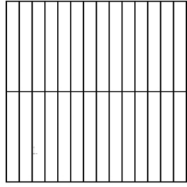
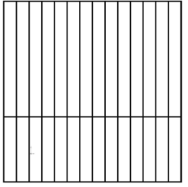
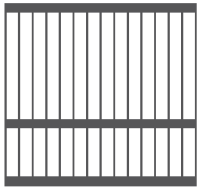
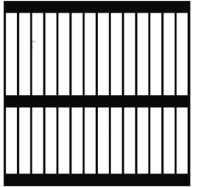
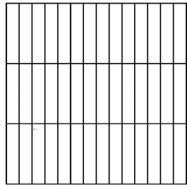
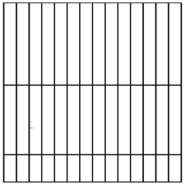


14 columns x 2 rows--Heat Transfer and Elastic Stiffness			
<p>A. Stage 1A Single Objective Uniform cell heights</p> 	<p>B. Stage 1B Single Objective Graded cell heights</p> 	<p>C. Stage 2 Multifunctional design</p> 	<p>D. Stage 2 Multifunctional Design</p> 
<p>Weights and Targets: $W = \{1.0, 0, 0\}$ $\dot{Q}_{total-target} \gg \dot{Q}_{total}$</p> <p>Design Variable Values: $h = 12.26$ mm $w = 1.59$ mm $t_v = 0.18$ mm $t_H = 0.16$ mm</p> <p>Goal Values: $\tilde{E}_x / E_s = 0.02$ $\tilde{E}_y / E_s = 0.11$ $\dot{Q}_{total} = 112.99$ W</p>	<p>Weights and Targets: $W = \{1.0, 0, 0\}$ $\dot{Q}_{total-target} \gg \dot{Q}_{total}$</p> <p>Design Variable Values: $h = 15.73, 8.79$ mm $w = 1.59$ mm $t_v = 0.18$ mm $t_H = 0.16$ mm</p> <p>Goal Values: $\tilde{E}_x / E_s = 0.02$ $\tilde{E}_y / E_s = 0.11$ $\dot{Q}_{total} = 113.13$ W</p>	<p>Weights and Targets: $W = \{0.5, 0.25, 0.25\}$ $\dot{Q}_{total-target} = 110$ W $(\tilde{E} / E_s)_{target} = 0.15$</p> <p>Design Variable Values: $h = 14.65, 6.6$ mm $w = 1.50$ mm $t_v = 0.27$ mm $t_H = 1.25$ mm</p> <p>Goal Values: $\tilde{E}_x / E_s = 0.16$ $\tilde{E}_y / E_s = 0.15$ $\dot{Q}_{total} = 96.8$ W</p>	<p>Weights and Targets: $W = \{0.5, 0.25, 0.25\}$ $\dot{Q}_{total-target} = 110$ W $(\tilde{E} / E_s)_{target} = 0.20$</p> <p>Design Variable Values: $h = 11.10, 9.01$ mm $w = 1.48$ mm $t_v = 0.28$ mm $t_H = 1.63$ mm</p> <p>Goal Values: $\tilde{E}_x / E_s = 0.17$ $\tilde{E}_y / E_s = 0.20$ $\dot{Q}_{total} = 91.62$ W</p>

TABLE CONTINUED ON NEXT PAGE

TABLE 5.4 CONTINUED

14 columns x 3 rows—Heat Transfer and Elastic Stiffness			
<p>E. Stage 1A Single Objective Uniform cell heights</p> 	<p>F. Stage 1B Single Objective Graded cell heights</p> 	<p>G. Stage 2 Multifunctional design</p> 	<p>H. Stage 2 Multifunctional Design</p> 
<p>Weights and Targets: $W = \{1.0, 0, 0\}$ $\dot{Q}_{total-target} \gg \dot{Q}_{total}$</p>	<p>Weights and Targets: $W = \{1.0, 0, 0\}$ $\dot{Q}_{total-target} \gg \dot{Q}_{total}$</p>	<p>Weights and Targets: $W = \{0.5, 0.25, 0.25\}$ $\dot{Q}_{total-target} = 110 \text{ W}$ $(\dot{E} / E_s)_{target} = 0.15$</p>	<p>Weights and Targets: $W = \{0.5, 0.25, 0.25\}$ $\dot{Q}_{total-target} = 110 \text{ W}$ $(\dot{E} / E_s)_{target} = 0.20$</p>
<p>Design Variable Values: $h = 8.13 \text{ mm}$ $w = 1.60 \text{ mm}$ $t_v = 0.17 \text{ mm}$ $t_H = 0.15 \text{ mm}$</p>	<p>Design Variable Values: $h = 11.30, 9.50, 3.64 \text{ mm}$ $w = 1.60 \text{ mm}$ $t_v = 0.17 \text{ mm}$ $t_H = 0.15 \text{ mm}$</p>	<p>Design Variable Values: $h = 10.3, 5.92, 5.13 \text{ mm}$ $w = 1.52 \text{ mm}$ $t_v = 0.25 \text{ mm}$ $t_H = 0.92 \text{ mm}$</p>	<p>Design Variable Values: $h = 9.10, 6.55, 4.51 \text{ mm}$ $w = 1.48 \text{ mm}$ $t_v = 0.28 \text{ mm}$ $t_H = 1.21 \text{ mm}$</p>
<p>Goal Values: $\tilde{E}_x / E_s = 0.02$ $\tilde{E}_y / E_s = 0.11$ $\dot{Q}_{total} = 109.15 \text{ W}$</p>	<p>Goal Values: $\tilde{E}_x / E_s = 0.02$ $\tilde{E}_y / E_s = 0.11$ $\dot{Q}_{total} = 109.91 \text{ W}$</p>	<p>Goal Values: $\tilde{E}_x / E_s = 0.15$ $\tilde{E}_y / E_s = 0.15$ $\dot{Q}_{total} = 90.01 \text{ W}$</p>	<p>Goal Values: $\tilde{E}_x / E_s = 0.17$ $\tilde{E}_y / E_s = 0.19$ $\dot{Q}_{total} = 88.47 \text{ W}$</p>

Stage 1B. In Stage 1B, graded cell structures are designed to maximize the total rate of steady state heat transfer (Q_{total}). Specifically, graded cells are designed by permitting the height of each row of cells to vary independently. By allocating *fractions* of available height to each cell, rather than basic dimensions, we ensure that the sum of cell dimensions and wall thicknesses does not exceed the height of the structure. Wall thicknesses and total mass flowrate are variable. Uniform cell widths are maintained across the structure because graded cell widths appear to have relatively small effects on satisfying the objectives for these boundary conditions. Gradient-based solution algorithms (specifically, sequential quadratic programming) are employed in this phase since all variables are continuous.

The outcome of Stage 1B is a set of graded LCA designs that maximize heat transfer for each of the promising cell configurations identified in Stage 1A. The resulting designs are shown in Tables 5.4B and 5.4F. As shown in Tables 5.4B and 5.4F, cells at the top of the structure (near the heat source where cell wall temperatures are higher) tend to elongate to facilitate heat transfer. Cell walls tend to be thin for both periodic and graded designs, since the solid material is high conductivity copper. The overall structural elastic stiffness in the x-direction is especially low for these designs due to thin, sparse horizontal cell walls. A slight improvement in total heat transfer is realized by grading the cells. It is likely that the benefits of graded cells would be enhanced by increased temperature gradients within the structure (e.g., due to a higher temperature heat source or a lower temperature, non-insulated bottom surface).

5.4.2 Designing Multifunctional Prismatic Cellular Materials for the Structural Heat Exchanger Application

Stage 2: Finally, in Stage 2, graded structures are designed to maximize a combination of total heat transfer (Q_{total}) and overall structural elastic stiffness in the x- and y-directions (\tilde{E}_x/E_s and \tilde{E}_y/E_s , respectively). This is a *multi-objective* design exercise in which the objective function in Figure 5.3 is utilized with weights of 0.5, 0.25, and 0.25 for Q_{total} , \tilde{E}_x/E_s , and \tilde{E}_y/E_s , respectively. The aim is to minimize a weighted sum of underachievements (d_i^-) for each goal (i.e., a weighted sum of the normalized differences between the actual value of each performance parameter and the target value for the parameter, provided that actual performance does not exceed the target value). If performance exceeds a target value, this overachievement is not considered in the objective function. The target values for each objective ($(Q_{total-target})$, $(\tilde{E}_x/E_s)_{target}$, and

$(\tilde{E}_y / E_s)_{target}$ are adjusted to facilitate the exploration of a range of design capabilities. For example, by setting an ambitious target for total heat transfer rate (110 W) and achievable target values for overall structural elastic stiffness (0.05, 0.1, 0.15, 0.2, 0.25, and 0.3, expressed as fractions of the elastic modulus of solid material, E_s), a family of designs are generated that exhibit a range of tradeoffs between thermal and structural performance.

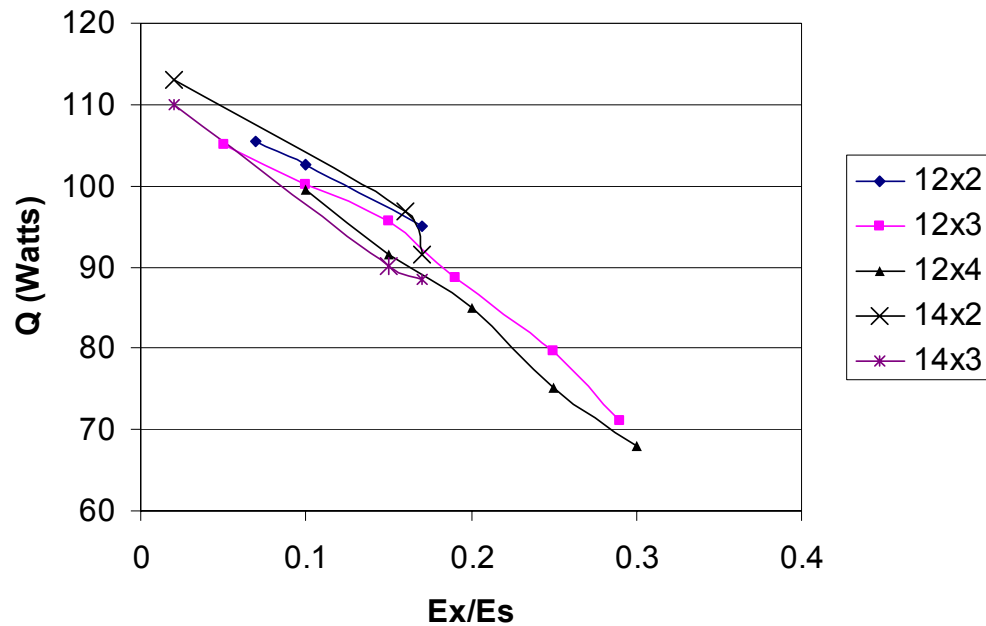


Figure 5.8 – Tradeoffs Between Total Heat Transfer and Effectiveness Stiffness for 12x2, 12x3, and 12x4 LCA Structures

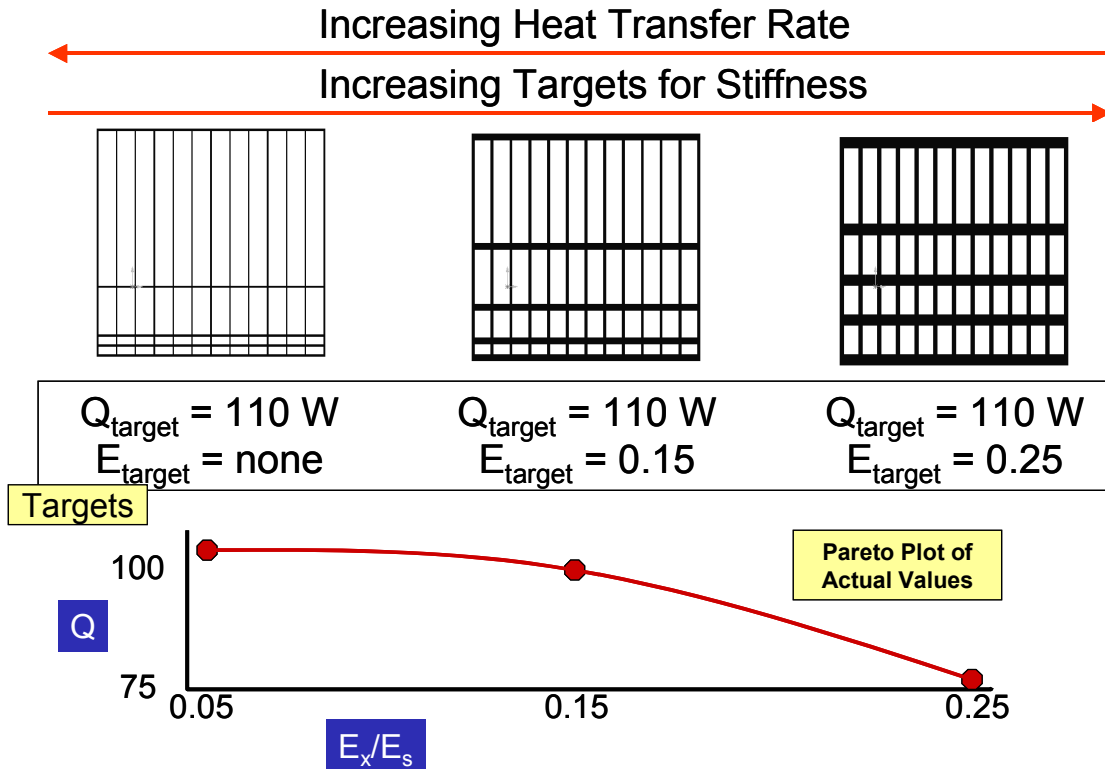


Figure 5.9 – Illustration of Multifunctional Tradeoffs for Prismatic Cellular Material Designs with 12x4 Cells

Achievable tradeoffs between total heat transfer rate and overall structural elastic stiffness are illustrated in Figure 5.8 for 12 by 2, 12 by 3, 12 by 4, 14 by 2, and 14 by 3 cell configurations, and a plot of achievable tradeoffs between heat transfer rate and overall structural elastic stiffness is illustrated in Figure 5.9. Sample multi-objective designs with 14 by 2 and 14 by 3 cells are illustrated in Tables 5.4C, 5.4D, 5.4G, and 5.4H. It is apparent that the multifunctional designs have much thicker walls in order to achieve higher overall structural elastic stiffness. The multi-objective designs also have lower total heat transfer rates than the other designs. With smaller cell sizes and larger cell wall thicknesses in the multi-objective designs, a portion of the total heat transfer rate is sacrificed to achieve higher elastic stiffness. As the aspect ratio of cell wall thickness

to cell dimension increases, it also becomes easier to manufacture the cells. As a rule of thumb, aspect ratios of 0.08 and above are manufacturable with current techniques. Only the multifunctional designs in Table 5.4 strictly meet this criterion. Although it is feasible to manufacture these functionally graded cellular materials with the LCA manufacturing process, it is important to note that formalisms for design of functionally graded, two-dimensional cellular materials have not been previously presented.

5.4.3 Verification and Validation of Resulting Designs

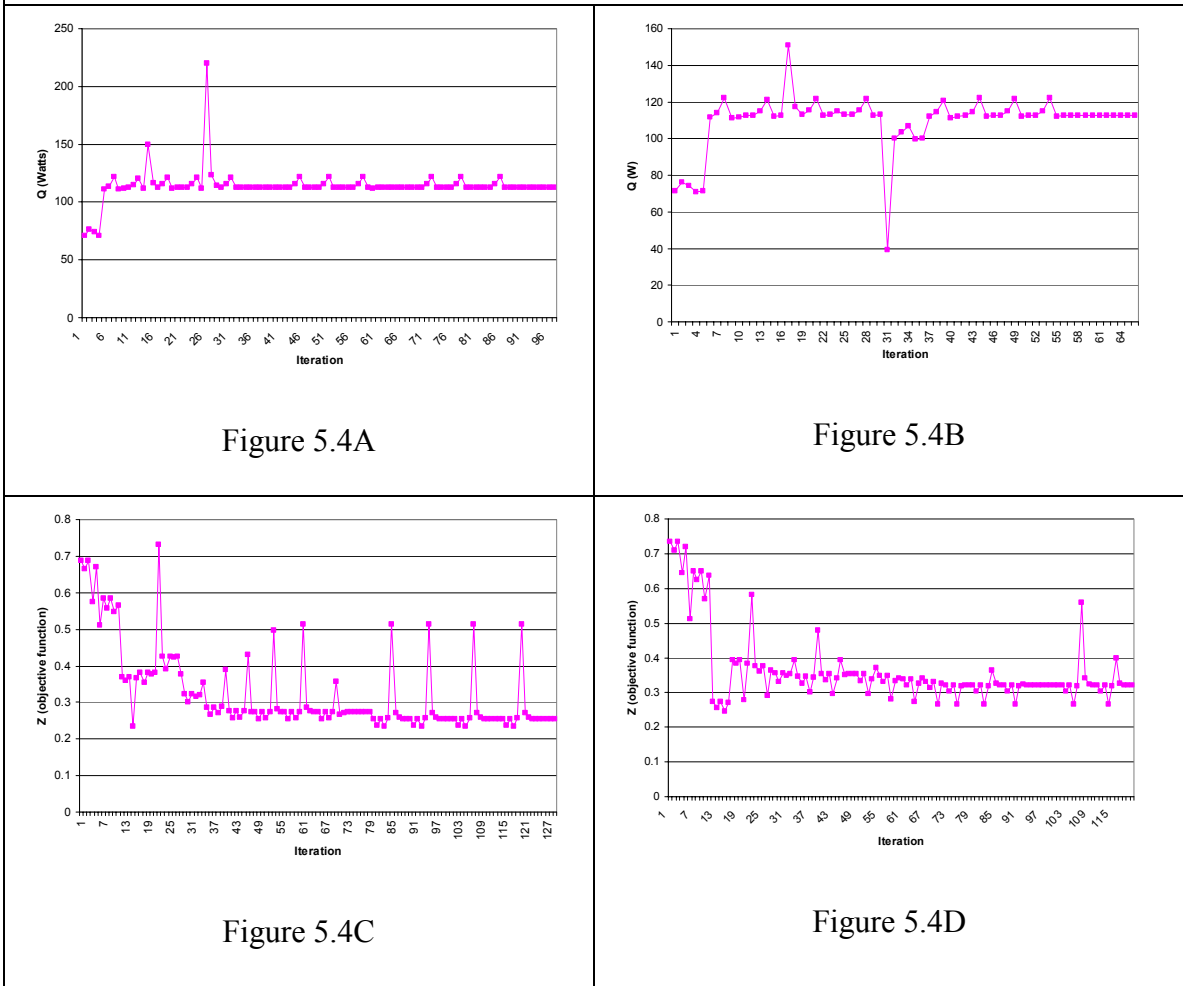
The design solutions are verified in several ways. During each iterative design process, the objective function is monitored for smooth convergence to a final value. Convergence plots for the 14 by 2 designs from Table 5.4 are illustrated in Table 5.5. Since the designs in Tables 5.4A and 5.4B are based on single objective design, the values for the single objective—the total rate of steady state heat transfer—are plotted against the iteration number in the first row of Table 5.5. In the second row of Table 5.5, the objective function (Z) value (Equation 5.7 in Figure 5.3) is plotted versus the iteration number because a multiobjective compromise DSP formulation is used to guide the design process. In all cases, convergence is relatively smooth. Most of the spikes represent infeasible designs that are rejected by the solver. Some of the spikes are associated with restarting the search/optimization algorithm for each design. Utilizing multiple sequential starting points is another verification strategy for this example. After an algorithm converges to a solution, the converged solution is utilized as the starting point for another search/optimization cycle, and the process continues until no further improvements are obtained in the solution. Convergence plots for the 14 by 3 designs are similar to those reported for the 14 by 2 designs in Table 5.5. The convergence plots

also document the relative improvement of final solutions, compared with initial starting points. In the first row, the objective is to maximize the plotted total rate of steady state heat transfer, and approximately 60-70% improvements are observed. In the second row, the objective is to minimize the objective function, for which 60-65% improvements are observed.

Another way to verify new designs is to compare them with previously obtained designs or closely related multifunctional designs. For example, the single-objective graded-cell designs in Table 5.4B and 5.4F can be compared with the single-objective uniform-cell designs in Table 5.4A and 5.4E. As a check on the quality of the graded-cell designs, the overall rate of steady state heat transfer for the graded-cell designs should be at least as high as the rate for the uniform cell designs. This is observed in Table 5.4. Similarly, it is expected that multifunctional designs embody tradeoffs between multiple objectives. As increasing weights or targets are specified for overall structural elastic stiffness, it is expected that the overall structural elastic stiffness of a multifunctional design will increase at the expense of decreasing heat transfer rates. This is observed by comparing the consistent tradeoffs embodied by the designs in Table 5.4 B, C, and D for the 14 by 2 cell configuration and the designs in Table 5.4 F, G, and H for the 14 by 3 cell configuration.

Finally, the relative accuracy of the structural and thermal analysis models are verified for the design region of interest. Details of the thermal model verification are provided by Dempsey and coauthors (Dempsey, 2002; Seepersad, et al., 2004) by comparing the performance of the finite difference analysis with results from physical experiments and detailed FLUENT analysis. The finite difference algorithm agrees with

Table 5.5 – Convergence Plots for 14 x 2 Designs in Table 5.4



FLUENT results within approximately 15% for the region of interest. The structural analyses are based on self-evident theoretical assumptions and are acknowledged to be extremely simplified, approximate models; therefore, no additional verification is supplied.

5.5 CRITICAL DISCUSSION OF THE EXAMPLE RESULTS

The results of the structural heat exchanger example support the utility of the compromise DSP as a foundational construct for multifunctional materials design, as

proposed in Hypothesis 3. By formulating a compromise DSP and adjusting weights and target values in the goal and objective functions, it is possible to generate a family or Pareto set of multifunctional materials designs that exhibit a range of tradeoff values between multiple objectives. As documented in Table 5.4 and Figures 5.8 and 5.9, the cellular material designs demonstrate a range of tradeoffs between structural and thermal properties for both the 14 by 2 and 14 by 3 cellular structures. These tradeoffs are evident in the documented performance of the designs and manifested in the actual mesostructures of the materials. For the first and second columns of results—for which only heat transfer is maximized—cell walls tend to be very thin, resulting in high overall rates of steady state heat transfer but low overall structural elastic stiffness. The multifunctional designs in the third and fourth columns of Table 5.4 have thicker walls in order to achieve higher overall elastic structural stiffness. With smaller cell sizes and larger cell wall thicknesses in the multifunctional designs, a portion of the total heat transfer rate is sacrificed to achieve higher stiffness. Cells near the top of the structure—where the heat source is located—tend to elongate to facilitate heat transfer.

The compromise DSP facilitates generation of these families of multifunctional designs in several ways. First, the compromise DSP provides structure for a multiobjective decision in terms of design variables, constraints, bounds, and multiple goals. Once it is formulated, the compromise DSP serves as a flexible decision template, enabling generation of a family of related designs via changes in goal target values, weights, and/or design variable bounds *without* reformulating the problem. All of the designs in Table 5.4 are obtained from a single compromise DSP by changing target values and weights and by omitting or retaining structural goals in the overall objective

function. (Of course, the number of cells was adjusted as well.) Unlike conventional single-objective optimization, a designer is not forced to choose a single objective and arbitrarily constrain other objectives. Instead, freedom is provided for seeking an unconstrained balance between multiple conflicting objectives. The multifunctional balances achieved by solving the compromise DSP are evident in the range of performance capabilities demonstrated by the sets of designs in Table 5.4. For this application, adjustment of target values is shown to be particularly effective for adjusting and controlling the precise balance between conflicting objectives.

In summary, the compromise DSP is shown to be an effective decision support construct for multifunctional materials design that facilitates the synthesis of a *family* of designs that satisfy constraints and bounds and embody a *range* of effective compromises among multiple, conflicting goals such as overall structural elastic stiffness and total heat transfer rate. In the early stages of design, it is particularly important to generate such a family of concepts that represents the scope of the multi-functional design space and offers distinct alternatives for further design and analysis. The design approach itself is independent of functional domain; thus, it is possible to balance goals and requirements from alternative functional perspectives—such as acoustics, electromagnetism, or economics—in addition to heat transfer and solid mechanics, as well as other considerations such as robustness and flexibility, as demonstrated in Chapters 6 and 7.

There are limitations to the compromise DSP and its application in this example. First, as discussed in Chapter 2, there is no guarantee that solutions obtained with the compromise DSP are Pareto efficient. Therefore, it is theoretically possible for solutions to exist that improve on one objective without worsening the other objective, in

comparison with the multifunctional designs reported in Table 5.4. For example, target values and weights for overall structural elastic stiffness are adjusted to generate the multifunctional designs illustrated in Figures 5.8 and 5.9 and Table 5.4. As illustrated, this approach is effective for generating designs with a range of multifunctional capabilities. Because the objective function in the compromise DSP does not reward improvement in goal values beyond their target values, alternative designs could exist that improve on the overall structural elastic stiffness of the design in Table 5.4G, for example, (which exactly meets its target values for overall structural elastic stiffness) without worsening its thermal performance. In this case, however, it is likely that any further improvements in overall structural elastic stiffness will be accompanied by decreases in thermal performance, based on the trends observed in the example. Furthermore, in such preliminary design contexts, the intention is not to *optimize* but to explore the space of possible solutions and uncover a range of possible compromise solutions, and the compromise DSP has proven especially useful for these situations.

Another observation from this example is the value of utilizing computationally efficient approximate models in the preliminary stages of design. FLUENT models, for example, could be used in place of fast finite difference models. The FLUENT models would require hours of simulation time, compared with the seconds required to run a finite difference simulation. Also, three-dimensional solid models must be rebuilt for each design modification in FLUENT—an activity that typically requires extensive human intervention and person hours. With approximate models, it is possible to rapidly explore large regions of a design space and identify promising regions that can be explored subsequently with more accurate, detailed models. When using approximate

models, the challenge is to verify that they are accurate enough to identify superior regions of the design space and to ensure that design exploration is confined to regions for which the models are valid.

With respect to the field of materials design, results from the heat exchanger example help demonstrate the value of using systems-based design methods for identifying promising multifunctional material mesostructures and for improving baseline material designs. The evidence indicates that the performance of systematically designed materials typically exceeds that of heuristically generated designs or conventional designs for similar applications. *In fact, the total rates of steady state heat transfer for the heat exchangers presented in this chapter are approximately double the rates exhibited by 2003-2004 era heat sinks with equivalent 'footprints' or volumes for desktop computer microprocessors.⁶ In addition, the heat exchangers provide structural load-bearing capability for devices such as notebook computers or other portable electronics.*

In this example, there is additional evidence of the value of systems-based design methods for materials design applications. For example, it is possible to generate families of designs that represent the *scope* of possible solutions to a design problem rather than constraining oneself to random guesses or limited modifications of previous designs. In this example, multiobjective decision protocols are coupled with analysis models of structure-property relations to identify structures that offer desirable properties. Process-structure relations are included as constraints in the multiobjective decision problem formulation.

⁶ Actual heat transfer rates for the heat sinks used by microprocessor manufacturers are proprietary; therefore, actual numbers are not reported here.

In more comprehensive materials design problems, process-structure relations could be included as additional analysis models, additional design stages in a sequence of design stages, or as data-driven empirical constraints and objectives. Future materials design problems also need to consider many other objectives that are not modeled in this example, including those from other functional domains and from other length and time scales. For example, the impact of porosity and microstructural phenomena on the properties and performance of the base material in the cell walls is an important consideration in this example. In addition, materials design is inherently hierarchical and complex. Models and relations are approximate in many cases and agreement between their predictions and observed properties and performance are subject to variation from specimen to specimen due to many factors including stochastic processing conditions. Therefore, robustness is an important factor to consider, as addressed in the examples of Chapters 6 and 7. Finally, the preliminary layout for the structural heat exchanger designs is *selected* from a library of standard cell topologies (rectangular, square, triangular, etc.) and the number of cells is searched exhaustively. In other words, the topology is *not* designed together with the dimensions and other parameters of the cellular material. As discussed in Chapter 4, evidence suggests that such a simplification may have a strong impact on design performance, especially when multiple objectives must be balanced. Therefore, topology design is emphasized in the examples in Chapters 6 and 7.

5.6 CHAPTER SYNOPSIS

In the structural heat exchanger example presented in this chapter, functionally graded prismatic cellular materials have been designed for multifunctional structural and

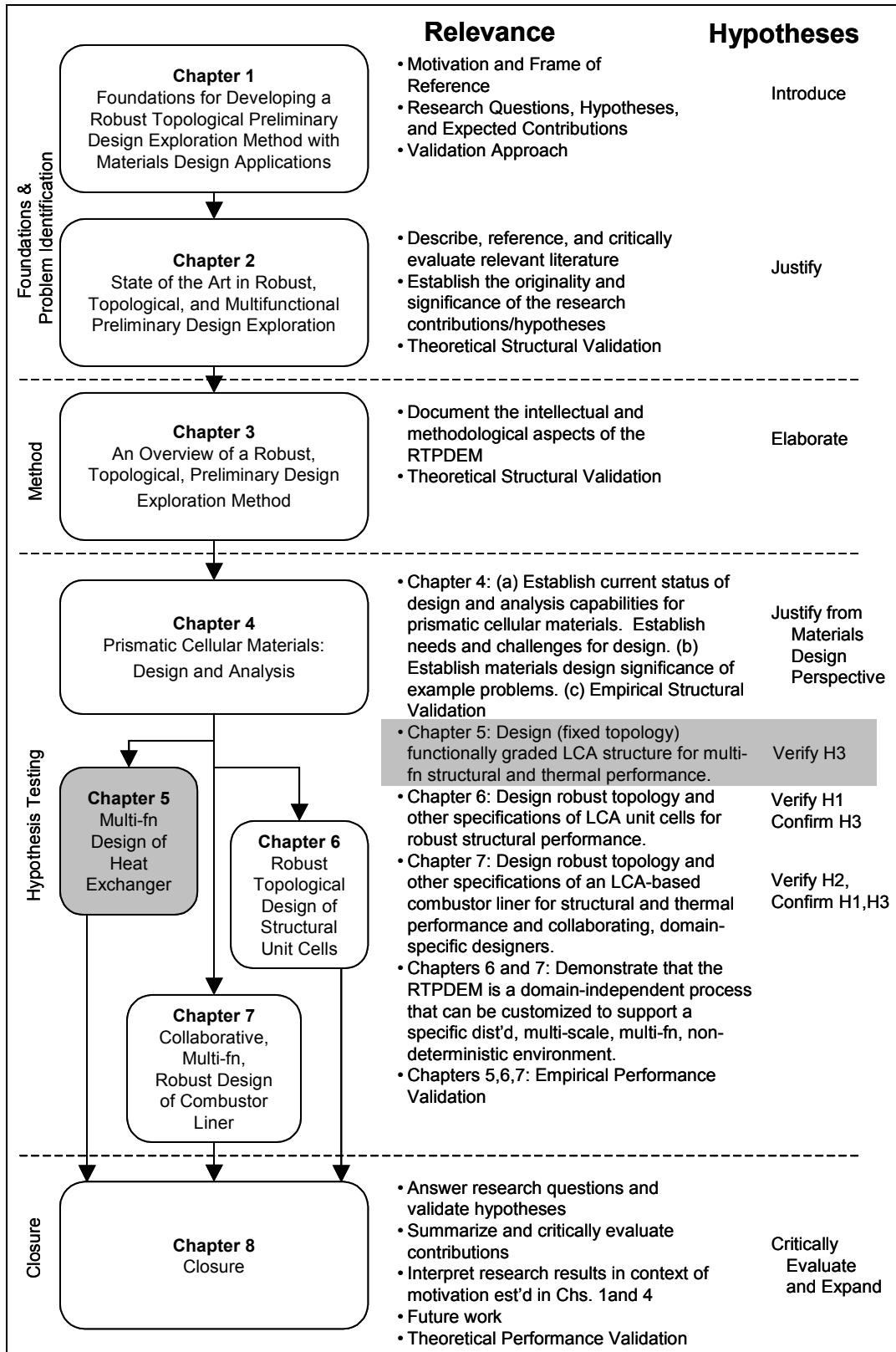


Figure 5.10 – Dissertation Roadmap

thermal performance. The results of the example have been utilized to demonstrate the utility of the compromise DSP—as part of the RTPDEM—as a mathematical, multiobjective decision model for materials design applications that involve balancing multifunctional objectives. It has been used to generate a family of designs that embody a range of tradeoffs between multiple conflicting objectives and represent the scope of possible designs that may serve as starting points for subsequent detailed design activities. The results demonstrate the utility of systems-based approaches for materials design applications—doubling the total rate of steady state heat transfer of conventional microprocessor heat sinks while simultaneously providing load-bearing capabilities. Evidence has been provided for affirmative empirical structural and performance validation of Hypothesis 3. Further evidence for Hypothesis 3 is provided in the examples presented in Chapters 6 and 7. Specifically, the compromise DSP is utilized as part of the RTPDEM for effectively balancing multiple objectives that include robustness and flexibility in the context of exploring and generating robust topology designs in defense of Hypothesis 1 in Chapter 6 and robust multifunctional topology designs in support of Hypothesis 2 in Chapter 7.

CHAPTER 6

ROBUST TOPOLOGY DESIGN OF PRISMATIC CELLULAR MATERIALS FOR STRUCTURAL APPLICATIONS

With the Robust Topological Preliminary Design Exploration Method, it is possible to synthesize topology and other preliminary design specifications that are robust to variations in topology, dimensions, operating and boundary conditions, and other factors. In this chapter, this capability is demonstrated by using the RTPDEM to design the mesoscopic topology, shape, and dimensions of periodic unit cells of a prismatic cellular material for a structural application. Topological and dimensional variations are considered and their effects minimized with the robust topology design methods within the RTPDEM. The results of this example support the hypothesis that the RTPDEM effectively facilitates *robust* topology design (i.e., Hypothesis 1) for prismatic cellular materials and other applications with similar characteristics. The results of this example demonstrate that it is important not only to tailor systematically the topology, shape, and dimensions of cellular materials for targeted performance, but also to consider robustness of performance during the topology design process. Also, the results of this example provide secondary support for Hypothesis 3 that the compromise DSP is an effective construct for structuring and supporting multiobjective robust topology design decisions. Finally, the results of this example represent a contribution to the field of materials design because the robustness of cellular material performance has not been considered as an objective during a topology or parametric design process despite the fact that variations in cellular materials are known to impact their properties.

6.1 AN OVERVIEW OF ROBUST TOPOLOGY DESIGN OF STRUCTURAL UNIT CELLS

The focus of this example is to demonstrate the effectiveness of the RTPDEM for tailoring the internal mesostructure of a prismatic cellular material, including cellular topology, shape, and cell wall dimensions. The design objective is to achieve a set of structural performance requirements as closely as possible, despite significant topological and parametric variation induced by the manufacturing process. A list of requirements for the cellular material in this example is provided in Table 6.1 and clarified in this section.

To establish context for this example, suppose that a novel load-bearing structure is under development with critical material-related requirements that include relatively low mass combined with targeted elastic stiffness properties. To fulfill these demands, the structural designers have chosen to use prismatic cellular materials for their advantages in these areas. The structural requirements of low mass and targeted elastic stiffness properties can be translated into the cellular materials domain as constraints on the volume fraction of base material and targets for effective elastic structural stiffness of the

Table 6.1 – Requirements for Prismatic Cellular Materials for a Structural Application
<ul style="list-style-type: none"> • Low volume fraction (no more than 20%) • Targeted effective elastic stiffness, C_{ij} <ul style="list-style-type: none"> ○ Case 1: $C_{11-target} = C_{22-target} = 0.1$ ○ Case 2: $C_{11-target} = 0.035$; $C_{22-target} = 0.085$; $C_{33-target} = 0.045$ • Minimum variation in effective elastic stiffness due to manufacturing-induced topological and parametric noise • Meet manufacturing constraints <ul style="list-style-type: none"> ○ Minimum wall thickness of 50 μm ○ Maximum cell wall aspect ratio (cell wall length:thickness) of 8:1 ○ Maximum of 8 cell walls meeting at a single joint ○ Maximum volume fraction of 30%

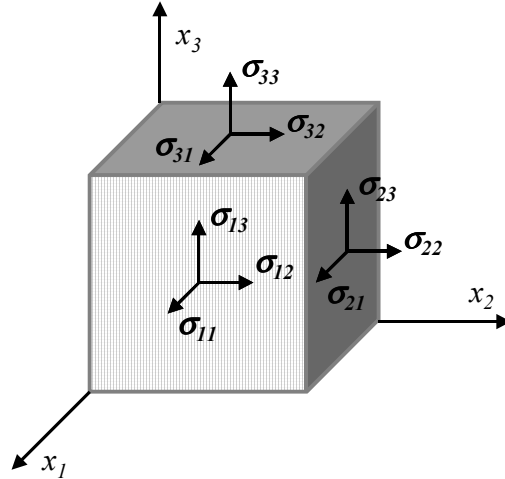


Figure 6.1 – Stress Tensor at a Point in an LCA Structure

material. The volume fraction, v_f , is the percentage of available space occupied by base material. Effective elastic structural properties, C_{ij} , characterize a cellular material's deformation in response to applied stress or structural loading. The properties are 'effective' because they are measured typically as a fraction of the corresponding properties for a fully dense piece of base material.

The elastic properties of a cellular material can be expressed as a tensor of elastic constants that relate stress to strain. At any point in an LCA structure, the applied stresses can be expressed as a tensor with nine components, as illustrated in Figure 6.1. The material deforms when it is subjected to normal or shear stresses, as represented by $(\sigma_{11}, \sigma_{22}, \sigma_{33})$ and $(\sigma_{12}, \sigma_{13}, \sigma_{21}, \sigma_{23}, \sigma_{31}, \sigma_{32})$, respectively, in Figure 6.1. If the deformed LCA recovers its original form when the loading is removed and if there is a perfectly proportional relationship between the internal state of mechanical stress induced by the loads and the state of strain, the behavior is linearly elastic. The constitutive equation for a linear elastic solid describes the macroscopic behavior of a homogeneous,

linearly elastic material and relates stress, σ , and strain, ε , via a tensor of elastic constants, C , according to the constitutive law (Malvern, 1969):

$$\{\sigma\} = [C]\{\varepsilon\} \quad (6.1)$$

A cellular material with three mutually orthogonal planes of symmetry is orthotropic. When two of the principal axes (labeled x_1 and x_2 in Figure 6.1) of the orthotropic cellular material are aligned with planes of symmetry and a state of plane strain is assumed parallel to the plane of the axes, the constitutive law can be expressed in 2D as

$$\begin{Bmatrix} \sigma_{11} \\ \sigma_{22} \\ \sigma_{12} \end{Bmatrix} = \begin{Bmatrix} \sigma_1 \\ \sigma_2 \\ \sigma_3 \end{Bmatrix} = \begin{bmatrix} C_{11} & C_{12} & 0 \\ C_{12} & C_{22} & 0 \\ 0 & 0 & C_{33} \end{bmatrix} \begin{Bmatrix} \varepsilon_1 \\ \varepsilon_2 \\ \varepsilon_3 \end{Bmatrix} \quad \text{where} \quad \begin{Bmatrix} \varepsilon_1 \\ \varepsilon_2 \\ \varepsilon_3 \end{Bmatrix} = \begin{Bmatrix} \varepsilon_{11} \\ \varepsilon_{22} \\ \varepsilon_{12} \end{Bmatrix} \quad (6.2)$$

where C_{ij} represents the four independent elastic constants.

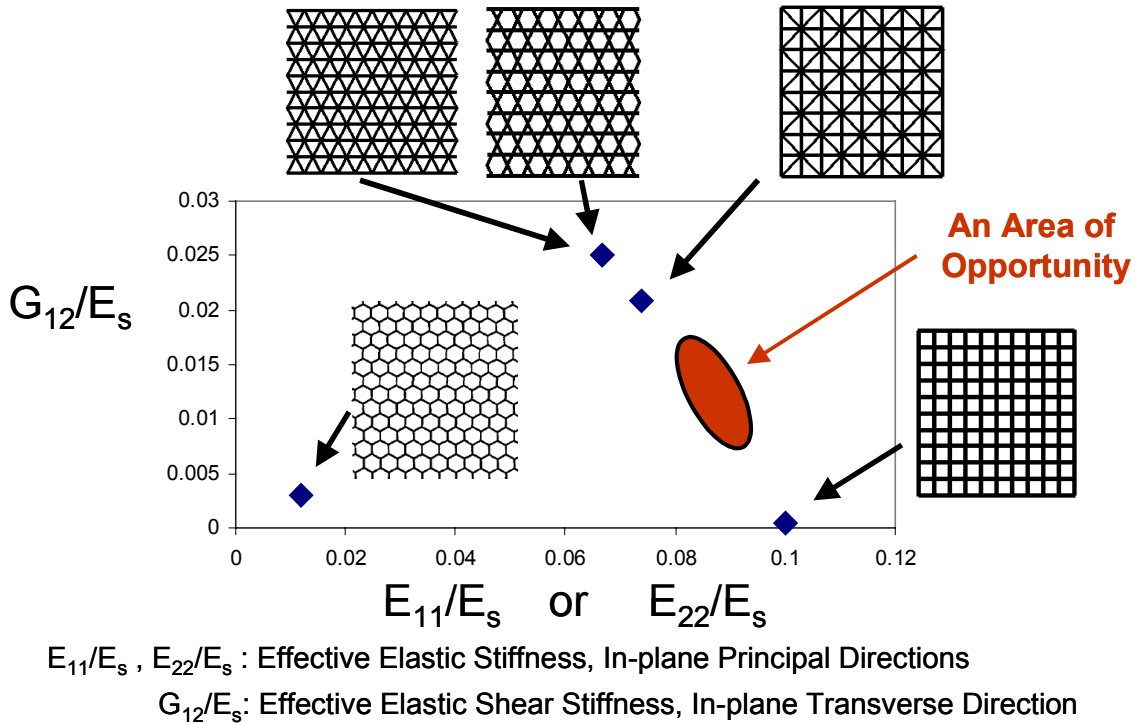


Figure 6.2 – Effective Elastic Properties of Standard Cellular Topologies

In this example, we seek to tailor these independent elastic constants—and therefore the quantified linear elastic behavior—of an LCA by modifying the spatial arrangement, connectivity, and dimensions of the cells and cell walls within the material.¹ Such topological and dimensional changes in the cellular structure of an LCA are required to adjust the elastic properties appreciably. In fact, as illustrated in Figure 6.2, a relatively limited set of effective elastic properties is obtainable with standard cell topologies. To construct Figure 6.2, a consistent relative density of 20% is assumed for all standard topologies. (Larger or smaller relative densities generally move the data points farther away or closer to the origin, respectively.) The properties are the effective elastic stiffness in the principal (horizontal and vertical) in-plane directions, plotted on the x-axis, and effective shear stiffness, plotted on the y-axis. A plot of this nature—similar to an Ashby plot—is useful for identifying areas of opportunity for the development of new materials that offer properties that are unobtainable with current materials. One such area of opportunity is highlighted in Figure 6.2; another corresponds to the effective elastic property requirements for this example, as listed in Table 6.1. This is a good example of *materials design*, in which customized materials are synthesized to fulfill functions that standard materials cannot fulfill.

It is not sufficient to simply *design* a novel prismatic cellular material; the material must be manufactured as well. Therefore, an important requirement for the example is the manufacturability of the prismatic cellular material designs. As indicated in Table

¹ Rather than designing an entire piece of cellular material in this example, we design a unit cell which can be periodically repeated, similar to the squares on a checkerboard, to form a piece of LCA material with elastic properties equivalent to those of the unit cell.

6.1, manufacturability implies minimum cell wall dimensions and aspect ratios, maximum relative densities, and approximate limits on the number of cell walls at any single joint. Also, the fabrication process is stochastic which complicates the design of the materials. If the manufacturing and product development processes could be controlled perfectly, there would be a deterministic relationship between the specified topology and dimensions for an LCA structure or unit cell and its performance. However, when designing LCAs, we must be concerned with several sources of manufacturing variation, including stochastic properties of the cell wall material (e.g., porosity, yield strength, thermal conductivity, etc.), integrity of the cellular structure (e.g., cracks, defects, corrugated extruded surfaces), as well as changing operating environments and dimensional variation during the latter stages of product development and during the manufacturing process. Variations in these factors induce variation in the elastic performance of the LCA. In this example, we quantify the effect on elastic properties of variation in the solid modulus of the cell wall material, dimensional variation during the manufacturing process, and topological noise in the form of cell wall cracks (i.e., severed cell walls). The effect is manifested as variation in performance responses, including the elastic constants in the constitutive law and the volume fraction. In this case, performance variation is undesirable, but it is difficult to remove the sources of variation. Instead, we seek to reduce the impact of the cited variations on the performance of the LCA.

In the example documented in this chapter, the RTPDEM is demonstrated to be an effective systematic method for facilitating *robust* design of *topology, shape, and dimensions* of periodic prismatic cellular materials. As shown throughout the chapter,

consideration of variation during the design process has a significant impact on not only the design process but also the nature of resulting cellular topologies, shapes, and dimensions.

6.2 VALIDATION AND VERIFICATION WITH THE EXAMPLE

It is important for this example to fulfill two roles, namely (1) to demonstrate that the proposed design methods advance the state-of-the-art in materials design capabilities, and (2) to provide direct evidence to support validation of one or more of the hypotheses posed in Chapter 1. While both items are discussed in Chapters 4 and 8, the latter is discussed in greater detail in this section. Specifically, there are three aspects of validation, as outlined in Chapter 1, that are relevant to this example: empirical structural validation, empirical performance validation, and theoretical performance validation. The first two aspects of validation are covered here. Empirical performance validation is revisited in Section 6.5, and theoretical performance validation is reserved for the concluding chapter. The primary focus of this example is on validation of Hypothesis 1, but it also serves as a validating example for Hypothesis 3, which is the primary focus of the structural heat exchanger example of Chapter 5.

6.2.1 Empirical Structural Validation

To support the *empirical structural validation* of Hypothesis 1, it is important to document that the example is similar to problems for which the RTPDEM is intended, that the example is similar to *actual* problems for which the RTPDEM may be applied, and that the data associated with the example can be used to support the research hypotheses posed in Chapter 1.

Is this example similar to problems for which the RTPDEM is intended? As discussed in the previous section and in Chapter 4, the present example has several characteristics that qualify it as an intended application for RTPDEM, including:

- (a) motivation to tailor the topology, shape, and dimensions of a design because those characteristics strongly influence performance,
- (b) freedom to adjust the topology, shape, and dimensions of a design and manufacture the resulting topologically tailored design, and
- (c) rationale for modeling variability in the structure itself and its boundary conditions because it causes significant performance variation—the nature and/or magnitude of which is influenced by the topology of the structure, and
- (d) a need for balancing multiple objectives (associated with multiple measures of nominal performance and robustness) to achieve families of compromise solutions.

The only characteristic that the present example does not have is non-structural or multifunctional requirements—a characteristic that is included in the combustor liner example of Chapter 7.

Is this example representative of an actual problem for which the RTPDEM may be applied? Care has been taken to ensure that the problem is modeled accurately and realistically with respect to potential industrial-strength applications, but some simplifying assumptions have been made to expedite the design process without significantly sacrificing accuracy or realism in the author's judgment. For example, the accuracy of the finite element model has been compared positively with theoretical results. Its accuracy especially in shear could be improved by adding more elements and

perhaps by using Timoshenko beam elements rather than Euler-Bernoulli beam elements, but the corresponding cost would be high in terms of iterative design time. The objectives and constraints—elastic constants, volume fraction, and maximum stress—are realistic for most practical applications of cellular materials. In-plane strength and out-of-plane mechanical properties may also be important but are not considered. The sources of variability—missing cell walls, porosity, and tolerances—have been chosen to reflect the primary imperfections reported in the literature and experienced with the LCA manufacturing process. Curved or corrugated cell walls are also present, but their effects are difficult to model with a coarse finite element mesh. The manufacturability of the final designs is considered via formulation of the topological and dimensional design space, specification of minimum cell wall thickness and maximum numbers of elements emanating from a single joint, and explicit consideration and accommodation (via robust design techniques) of the variability and imperfections introduced during the manufacturing process. Altogether, it is the author’s opinion that the example reflects the range of challenges involved in designing cellular materials for actual applications.

Can the data from this example be used to support conclusions with respect to Hypotheses 1 and 3? The hard data generated in this example includes estimates for performance and performance variation/ranges for prismatic cellular material designs generated using RTPDEM. This data can be compared with the performance of designs generated with deterministic design approaches (i.e., ignoring robustness and variability) to determine whether considering variation and robustness during the design process actually improves the robustness of the final design. The results can also be compared with the performance of designs with standard topologies (with and without dimensional

tailoring) to determine whether RTPDEM is effective at topologically tailoring designs for desired/superior performance. The data is useful for comparing the effectiveness of RTPDEM in comparison with the best designs obtained with previously existing, state-of-the-art design approaches. Finally, data is generated for multiple goals and constraints for families of compromise solutions. The data can be used to evaluate the effectiveness of the compromise DSP as a multiobjective decision support construct for robust topology design.

6.2.2 Empirical Performance Validation

To support the *empirical performance validation* of Hypothesis 1, it is important to build confidence in the usefulness of the method by evaluating the outcomes of the method with respect to its stated purposes, demonstrating that the observed effectiveness of the method is linked to its application, and verifying the accuracy and internal consistency of the empirical data generated for the example.

How can the outcomes of the method be evaluated with respect to its stated purpose? Is the observed effectiveness of the method linked to its application? A three-stage design approach is planned to investigate the effectiveness of the RTPDEM with respect to its intended functionality. As shown in Table 6.2, the first stage involves using the RTPDEM to design a prismatic cellular material for the boundary and initial conditions, goals, and constraints identified in Section 6.3. The first stage is implemented in two sub-stages: (A) robust topology design for dimensional variation and (B) robust topology design for dimensional and topological variation. If this stage is completed successfully, it is reasonable to conclude that the RTPDEM *can* be used as a theoretical and computational infrastructure for designing topology, shape, and dimensions for desired

Description	Purpose
<p>Stage 1: Design <i>robust</i> prismatic cellular material topology, shape, and dimensions for the conditions identified in Section 6.3.</p> <p>Stage 1B: Design <i>robust</i> prismatic cellular materials for dimensional variation.</p> <p>Stage 1B: Design <i>robust</i> prismatic cellular materials for topological and dimensional variation.</p>	<p>Demonstrate that the RTPDEM can be used to design robust topology, shape, and dimensions for desired functionality.</p>
<p>Stage 2: Design prismatic cellular material topology, shape, and dimensions deterministically (without considering variation) for the conditions identified in Section 6.3. Compare with results of Stage 1.</p>	<p>Demonstrate that the RTPDEM facilitates the generation of <i>robust</i> topologies that are less sensitive to variation than designs obtained typically with standard topology design optimization techniques.</p>
<p>Stage 3: Compare results of Stage 1 with standard topology designs. Verify numerical results of analysis and synthesis.</p>	<p>Demonstrate that the RTPDEM facilitates topological tailoring of designs with customized performance relative to standard designs. Verify the accuracy of numerical results generated for all stages.</p>

functionality. The next question involves its *effectiveness* for this purpose. In the second stage, prismatic cellular material topology, shape, and dimensions are designed *deterministically* (without robust design techniques and without considering variation or imperfections). Then, the performance ranges of the first stage designs are compared with those of the second stage designs subject to equivalent sources of variability. This stage is designed to demonstrate that the RTPDEM facilitates the generation of *robust* topologies that are not obtained typically with standard topological design methods. Finally, in the third stage, standard cellular topologies (e.g., square, triangle, and hexagonal) are compared with the results of the first two stages. This is intended to demonstrate that the RTPDEM facilitates topological tailoring of designs with performance that exceeds that of heuristically generated designs. Also in the third stage, the numerical results of analysis and synthesis are verified in several ways, as described in the following paragraph.

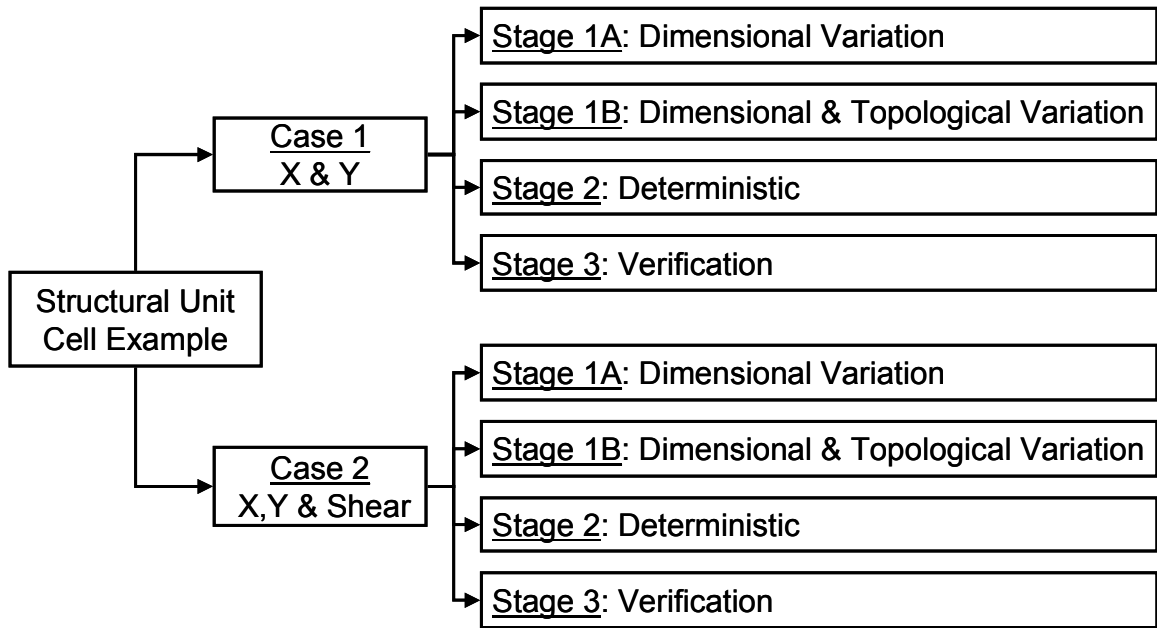


Figure 6.3 – Outline of Examples in this Chapter

How is the accuracy and internal consistency of the example results verified as part of Stage 3 in Table 6.2? First, each of the approximate analysis models is verified. The FE analysis and gradient-based transmission of variation are compared with theoretical and worst-case analyses, respectively. The accuracy of the variability analysis (for missing cell walls, porosity, and tolerances) is compared with worst-case analyses. The formulation of the topology design problem is verified by investigating the mesh or ground structure sensitivity of the final designs. The sensitivity of the results to assumptions regarding the magnitude of variability is also investigated. The optimization results are verified to confirm that superior solutions have been obtained. Several techniques are utilized including multiple starting points, starting points based on the results of the preceding optimization, and monitoring of design variable, constraint, and objective function values for smooth convergence and a well-posed formulation.

Each of the three experimental stages is conducted for two cases outlined in Figure 6.3. In the first case, effective elastic stiffness is tailored in the two in-plane principal directions (x - and y -directions, corresponding to 1^{st} and 2^{nd} principal directions, respectively, in Figure 6.1 and the C_{11} and C_{22} components of the constitutive tensor in Equation 6.2). In the second case, effective elastic stiffness is tailored in the two principal directions and in shear (corresponding to C_{11} , C_{22} , and C_{33} , respectively in Equation 6.2).

6.3 INSTANTIATING THE ROBUST TOPOLOGICAL PRELIMINARY DESIGN EXPLORATION METHOD AS THE DESIGN APPROACH FOR THIS EXAMPLE

The RTPDEM is introduced and described in detail in Chapter 3. In this section, its step-by-step application is described for designing prismatic cellular materials that fulfill the requirements outlined in the previous section.

6.3.1 Implementing Phase 1 of the RTPDEM: Formulating the Robust Topology Design Space for Cellular Materials Design

Formulating the robust topology design space is the first phase of the RTPDEM, according to Figure 3.1. The phase involves identifying influential design parameters, devising a scheme for representing and modifying topology, and characterizing variability in design parameters. The initial topology design space for a single unit cell is modeled as a ground structure as shown in Figure 6.4a. The ground structure is populated with frame finite elements that are a superposition of bar and Euler-Bernoulli beam elements, with six degrees of freedom per element (four displacement and two rotation) (cf. (Reddy, 1993)). Frame finite elements are employed instead of truss finite elements because they more closely approximate the behavior of low volume fraction

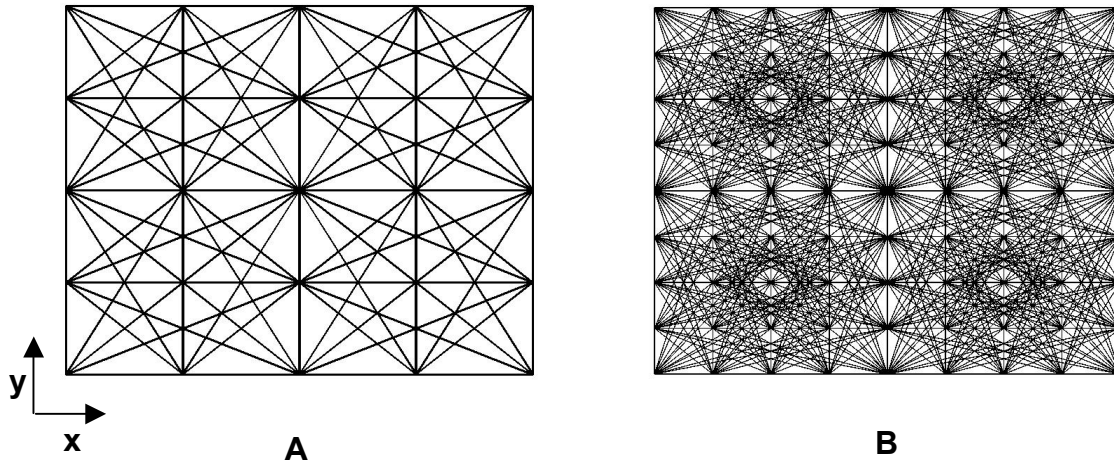


Figure 6.4 – Initial Ground Structures for Cellular Material Topology Design

unit cells under shear loading conditions. Two planes of symmetry, aligned with the principal horizontal and vertical axes, are applied to the structure to impose orthotropy. The planes of symmetry divide the ground structure into four quadrants, each of which is modeled with a full ground structure with all of the nodes connected directly to one another. The entire ground structure has 25 nodes (5×5) and 132 finite elements in total. However, only one quadrant of nodes and elements is active—a total of 9 nodes and 36 elements—and the design parameters for the active quadrant are mirrored into the other three quadrants. Because topology design results can be dependent on the initial ground structure, the designs obtained with the 25 node ground structure in Figure 6.4a are validated by comparison with designs obtained from the 81 node ground structure, comprised of 1160 elements, as shown in Figure 6.4b. In this example, each unit cell is assumed to be a 1 cm square.

Based on the ground structures introduced in Figure 6.4, the design variables are the cross-sectional areas of each element in the ground structure. Bounds on the design variables are broad, with the lower bound at least five orders of magnitude smaller than

the upper bound to facilitate topology design. Elements with areas that converge to values near the lower bound contribute very little to the properties of the unit cell and are removed from the structure after the iterative search process. Post-optimization removal of elements and adjustment of element areas constitute modification of the internal topology, shape, and dimensions of the unit cell. Other design parameters include responses and fixed factors. The details of the initial ground structure—including numbers and locations of nodes and elements, applied boundary conditions, and material properties—are assumed to remain constant during the design process. Responses include the volume fraction, v_f , of solid material in the unit cell and the elastic constants, C_{ij} , as defined in Equation 6.2.

As mentioned in Chapter 3, there are many potential noise factors or sources of uncertainty in a topology design problem of this nature. In this example, we consider dimensional variation in the cross-sectional areas of each element. This variation could be induced by manufacturing variation or by adjustments in the design during subsequent design stages. The relationship between the nominal cross-sectional area (X_e) of an element e and the variation in area (ΔX_e) is modeled as follows:

$$\Delta X_e = X_e - \alpha_1 X_e^{\alpha_2} \quad (6.3)$$

where α_1 and α_2 are constants with values of 0.502 and 1.085, respectively, and X_e is measured in μm . The model has the desirable properties outlined in Section 3.3.1, including smoothness and a guarantee that $\Delta X_e \leq X_e$ for all bounded values of X_e (specifically, in this example, $0.01 \mu\text{m} \leq X_e \leq 1000 \mu\text{m}$). The model is consistent with manufacturing observations that suggest that tolerance values begin at approximately 15

μm for a $50 \mu\text{m}$ wall thickness—the minimum realizable cell wall thickness with present manufacturing techniques—and gradually approach 10% tolerances for larger dimensions (e.g., $\Delta X_e \cong 100 \mu\text{m}$ for $X_e = 1000 \mu\text{m}$).

Topological variability is also considered in this example. Specifically, the possibility of *one* randomly missing or removed node is considered. The probability that a particular node, R_i , is missing from a realized structure, assuming that the node is specified as part of the derived structure is expressed with Equation 3.13:

$$P(R_i \in \mathbf{R}^M | R_i \in \mathbf{R}^D) \quad (3.13)$$

where \mathbf{R}^D is the set of nodes included in the derived or designed structure (as a subset of the set of nodes in the ground structure) and \mathbf{R}^M is the set of nodes missing from the realized structure. In the examples in this chapter, this probability is assumed to be 1%. In other words, it is assumed that there is a 1% chance that any specific node will be missing or removed from the intended structure. Therefore, the probability that all of the nodes are realized if they are all included in the derived structure is

$$\left[1 - P(R_i \in \mathbf{R}^M | R_i \in \mathbf{R}^D)\right]^{C^G} \quad (6.4)$$

where C^G is the number of nodes in the initial ground structure. For the initial ground structure in Figure 6.4a, there are 9 nodes in a single quadrant.² If one assumes that all nodes are included in the derived structure, the probability that the structure is intact is approximately 91% or $(1 - 0.01)^9$, and the probability that at least one element is missing from the realized structure is approximately 9%. As discussed in Section 3.3.3, the possibility of two or more nodes missing simultaneously from a realized structure is not

² Recall that orthotropic symmetry is imposed on the ground structure in Figure 4.3, with only one quadrant of active nodes and elements that are mirrored into the other three quadrants.

considered in order to limit the number of independent structural analyses required during each design iteration. Although this may seem to be a small probability for stochastic node removal, one must remember that this is specified for a unit cell rather than an entire structure. The probability that a node is missing from an entire structure, composed of many unit cells, is much higher.

The actual probability of a missing node or joint is difficult to specify for the LCA manufacturing process. It depends partially on the specific topology and dimensions of the cells, the base material, and extrusion conditions such as die design, paste viscosity, extrusion speed, and other factors. Therefore, a representative probability has been assigned for this example. Its magnitude may impact the nature of the results (e.g., the magnitude of performance variation), but it does not affect the design approach.

Variations in material properties are considered as well. Specifically, the solid modulus of elasticity is assumed to vary by as much as 20% from its nominal value. This variation may stem from porosity that remains in the structure after it is post-processed. Porosity is known to have a significant effect on the solid modulus, as well as other properties such as thermal conductivity and yield strength. Bocchini (1986) proposed the following relation between the Young's modulus of a fully dense material, E_o , and the Young's modulus of a sintered material, E_s , with porosity, P ,

$$E_s = E_o (1 - P)^{3.4} \quad (6.5)$$

From this equation, one can conclude that porosity values on the order of 95%—typical for the LCA manufacturing process—degrade the solid modulus of elasticity by approximately 15%. Therefore, it is not unreasonable to investigate a reduction in the solid modulus of elasticity by as much as 20%.

	Stage 1A	Stage 1B	Stage 2
Fixed Factors	<ul style="list-style-type: none"> Initial ground structure (Fig. 6.4), boundary conditions, material properties 	<ul style="list-style-type: none"> Initial ground structure (Fig. 6.4), boundary conditions 	<ul style="list-style-type: none"> Initial ground structure (Fig. 6.4), boundary conditions, material properties
Sources of Variation	<ul style="list-style-type: none"> Dimensional variation 	<ul style="list-style-type: none"> Dimensional variation Topological variation Material property variation 	<ul style="list-style-type: none"> No variation
Design Variables	<ul style="list-style-type: none"> \mathbf{X}, Vector of areas of elements in ground structure 	<ul style="list-style-type: none"> \mathbf{X}, Vector of areas of elements in ground structure 	<ul style="list-style-type: none"> \mathbf{X}, Vector of areas of elements in ground structure
Behavioral Responses	<ul style="list-style-type: none"> v_f, Volume fraction nominal value C_{ij}, Elastic constant nominal values ΔC_{ij}, Elastic constant variation due to dimensional variation 	<ul style="list-style-type: none"> v_f, Volume fraction nominal value C_{ij}, Elastic constant nominal values ΔC_{ij}, Elastic constant variation due to dimensional and material property variation $\sigma_{C_{ij}}$, Elastic constant std deviation due to topological variation 	<ul style="list-style-type: none"> v_f, Volume fraction C_{ij}, Elastic constants

Several categories of variation are not considered in this chapter. For example, one could consider variation in nodal locations in the ground structure. This would simulate variation in the relative length of elements, as opposed to variations in element thicknesses, as modeled previously. Secondly, variation in boundary conditions is usually very important. This could include changes in the magnitude or direction of applied loads or displacements. Since unit cells—rather than complete structures—are designed in this example, periodic boundary conditions are applied in the analysis, and variations in boundary conditions are not considered.

In Table 6.3, a summary is provided of the design parameters—design variables, fixed factors, and behavioral responses—and sources of variation considered in each of the design stages outlined in Table 6.2. In Table 6.3, it is noted that the responses of interest include the variation in elastic constants induced by variation in dimensions, material properties, and topology. The technique for evaluating variations and nominal values of elastic constants is discussed in Section 6.3.3, but first the design parameters are

organized within compromise DSP's that support design exploration for each of the example stages.

6.3.2 Implementing Phase 2 of the RTPDEM: Formulating the Robust Topology Design Problem for Cellular Materials Design

To implement Phase 2 of the RTPDEM, a compromise decision support problem must be formulated for this example. Because the present example is implemented in three stages (as outlined in Tables 6.2 and 6.3 and Figure 6.3), the generic decision support problem presented in Figure 3.9 is instantiated separately for Stages 1A, 1B, and 2 in Figures 6.5, 6.6, and 6.7, respectively. The separate compromise DSP formulations are required because different goals and assumptions are associated with each stage, as outlined in Table 6.3. For each stage, the goals include achieving target values for nominal values of elastic constants, C_{11} , C_{22} , and C_{33} . For Stage 2, they are the only goals because variation is not considered. For Stages 1A and 1B, dimensional variation is considered in element areas or cell wall thicknesses. Therefore, models of dimensional variation and its impact on elastic constants are assumed, and the set of goals includes minimizing ranges of elastic constant values that are associated with dimensional variation and signified by ΔC_{11} , ΔC_{22} , and ΔC_{33} . In Stage 1B, topological variation is considered, as well. Since the impact of topological variation is investigated with a series of experiments that correspond to possible permutations of the initial ground structure, associated variations in elastic constants are based on standard deviations of elastic constant data for the set of experiments and represented as $\sigma_{C_{11}}$, $\sigma_{C_{22}}$, $\sigma_{C_{33}}$. These goals

are minimized in Stage 1B along with goals for elastic constant variation associated with dimensional and material property deviations, $\Delta_{\mu}C_{11}$, $\Delta_{\mu}C_{22}$, and $\Delta_{\mu}C_{33}$.³

The compromise DSP's in Figures 6.5, 6.6, and 6.7 are formulated for Stages 1A, 1B, and 2 of the example, respectively. Each compromise DSP formulation supports the two cases identified in Section 6.1 and Figure 6.3.⁴ The aim of the robust topology design process is to find the values of the cross-sectional areas of elements within an initial ground structure that satisfy a set of bounds on their nominal values and a volume fraction constraint and achieve a set of goals as closely as possible. (Elements with cross-sectional areas near the lower bound are subsequently removed from the ground structure in a post-processing step.) For each goal, a set of deviation variables— d_i^- , d_i^+ —are assigned that measure the extent to which target values are achieved for each goal. Elastic constant variation and standard deviation goals are normalized by elastic constant target values in the goal formulations to normalize the values of deviation variables. The objective function, Z , represents a weighted sum of distances or deviations (d_i^- and d_i^+) from each of the target values, and it is minimized.

The compromise DSP's formulated in Figures 6.5, 6.6, and 6.7 are used to structure the search for solutions to this example. To solve the problem, specific goal target values, constraint limits, design variable bounds, and objective function weights are required, as outlined in Table 6.4. The values for constraints and goals in Table 6.4 are expressed as fractions of the properties of a completely solid unit cell with full density and no

³ These goals are subscripted with a μ to signify that the elastic constant ranges are mean values for the set of topological variation experiments.

⁴ In Case 1, the elastic constants C_{11} and C_{22} in Equation 6.2 are tailored to achieve preferred effective elastic stiffness for the cellular material in the horizontal (x) and vertical (y) in-plane principal directions. In Case 2, the elastic constants C_{11} , C_{22} , and C_{33} are tailored for preferred effective elastic stiffness in the principal directions and in shear.

Given

Assumptions used to model the domain of interest, including an initial ground structure.

System constraint function: $v_f(\mathbf{X})$, defined in Equation 6.17

System goal achievement functions: $C_{ij}(\mathbf{X})$, defined in Equation 6.16

Tolerance range function: $\Delta\mathbf{X}$, defined in Equation 6.3

Goal variation function for dimensional variation: $\Delta C_{ij}(\mathbf{X})$, defined in Equation 6.18

Goal target values, design variable bounds, and weights for each case, as defined in Table 6.4

Find

X_i	Element Areas (Nominal Values)	$i = 1, \dots, N$
d_i^-, d_i^+	Deviation Variables	$i = 1, \dots, 6$

Satisfy*Constraint*

$$v_f \leq v_{f\text{-limit}} \quad \text{see Equation 6.17}$$

Goals

Cases 1 and 2:

$$C_{11} + d_1^- - d_1^+ = C_{11\text{-target}} \quad \text{see Equation 6.16}$$

$$\frac{\Delta C_{11}}{C_{11\text{-target}}} + d_2^- - d_2^+ = \Delta C_{11\text{-target}} \quad \text{see Equation 6.18}$$

$$C_{22} + d_3^- - d_3^+ = C_{22\text{-target}} \quad \text{see Equation 6.16}$$

$$\frac{\Delta C_{22}}{C_{22\text{-target}}} + d_4^- - d_4^+ = \Delta C_{22\text{-target}} \quad \text{see Equation 6.18}$$

Case 2 only:

$$C_{33} + d_5^- - d_5^+ = C_{33\text{-target}} \quad \text{see Equation 6.16}$$

$$\frac{\Delta C_{33}}{C_{33\text{-target}}} + d_6^- - d_6^+ = \Delta C_{33\text{-target}} \quad \text{see Equation 6.18}$$

Bounds

$$X_{i,L} \leq X_i \leq X_{i,U} \quad i = 1, \dots, N$$

$$d_i^- \bullet d_i^+ = 0 \quad i = 1, \dots, 6$$

$$d_i^-, d_i^+ \geq 0 \quad i = 1, \dots, 6$$

Minimize

$$\text{Case 1: } Z = W_1 d_1^- + W_2 d_2^+ + W_3 d_3^- + W_4 d_4^+ \quad (\text{Equation 6.6})$$

$$\text{Case 2: } Z = W_1 d_1^- + W_2 d_2^+ + W_3 d_3^- + W_4 d_4^+ + W_5 d_5^- + W_6 d_6^+ \quad (\text{Equation 6.7})$$

Figure 6.5 – Decision Support Problem for Robust Topology Design of Unit Cells with Dimensional Variation Only (Stage 1A)

Given

Assumptions used to model the domain of interest, including an initial ground structure.

System constraint function: $v_f(\mathbf{X})$, defined in Equation 6.17

Mean system goal achievement function: $\mu_{C_{ij}}$, defined in Equations 6.21 and 6.16

Tolerance range function: $\Delta\mathbf{X}$, defined in Equation 6.3

Mean goal variation function for dimensional variation: $\Delta_\mu C_{ij}(\mathbf{X})$, defined in Equations 6.18 and 6.23

Goal variation function for topological variation: $\sigma_{C_{ij}}(\mathbf{X})$, defined in Equation 6.22

Goal target values, design variable bounds, and weights for each case, as defined in Table 6.4

Find

X_i	Element Areas (Nominal Values)	$i = 1, \dots, N$
d_i^-, d_i^+	Deviation Variables	$i = 1, \dots, 9$

Satisfy*Constraint*

$$v_f \leq v_{f\text{-limit}} \quad \text{see Equation 6.17}$$

Goals

Cases 1 and 2:

$$\mu_{C11} + d_1^- - d_1^+ = \mu_{C11\text{-target}} \quad \text{see Equation 6.21}$$

$$\frac{\Delta_\mu C_{11}}{\mu_{C11\text{-target}}} + d_2^- - d_2^+ = \Delta_\mu C_{11\text{-target}} \quad \text{see Equation 6.23}$$

$$\frac{\sigma_{C11}}{\mu_{C11\text{-target}}} + d_3^- - d_3^+ = \sigma_{C11\text{-target}} \quad \text{see Equation 6.22}$$

$$\mu_{C22} + d_4^- - d_4^+ = \mu_{C22\text{-target}} \quad \text{see Equation 6.21}$$

$$\frac{\Delta_\mu C_{22}}{\mu_{C22\text{-target}}} + d_5^- - d_5^+ = \Delta_\mu C_{22\text{-target}} \quad \text{see Equation 6.23}$$

$$\frac{\sigma_{C22}}{\mu_{C22\text{-target}}} + d_6^- - d_6^+ = \sigma_{C22\text{-target}} \quad \text{see Equation 6.22}$$

Case 2 only:

$$\mu_{C33} + d_7^- - d_7^+ = \mu_{C33\text{-target}} \quad \text{see Equation 6.21}$$

$$\frac{\Delta_\mu C_{33}}{\mu_{C33\text{-target}}} + d_8^- - d_8^+ = \Delta_\mu C_{33\text{-target}} \quad \text{see Equation 6.23}$$

$$\frac{\sigma_{C33}}{\mu_{C33\text{-target}}} + d_9^- - d_9^+ = \sigma_{C33\text{-target}} \quad \text{see Equation 6.22}$$

Bounds

$$X_{i,L} \leq X_i \leq X_{i,U} \quad i = 1, \dots, N$$

$$d_i^- \cdot d_i^+ = 0; \quad d_i^-, d_i^+ \geq 0 \quad i = 1, \dots, 9$$

Minimize

$$\text{Case 1: } Z = W_1 d_1^- + W_2 d_2^+ + W_3 d_3^+ + W_4 d_4^- + W_5 d_5^+ + W_6 d_6^+ \quad (\text{Equation 6.8})$$

$$\text{Case 2: } Z = W_1 d_1^- + W_2 d_2^+ + W_3 d_3^+ + W_4 d_4^- + W_5 d_5^+ + W_6 d_6^+ + W_7 d_7^- + W_8 d_8^+ + W_9 d_9^+ \quad (\text{Equation 6.9})$$

Figure 6.6 – Decision Support Problem for Robust Topology Design of Unit Cells with Topological and Dimensional Variation (Stage 1B)

Given

Assumptions used to model the domain of interest, including an initial ground structure.

System constraint function: $v_f(\mathbf{X})$, defined in Equation 6.17

System goal achievement functions: $C_{ij}(\mathbf{X})$, defined in Equation 6.16

No tolerance range function

Goal target values, design variable bounds, and weights for each case, as defined in Table 6.4

Find

X_i	Element Areas (Nominal Values)	$i = 1, \dots, N$
d_i^-, d_i^+	Deviation Variables	$i = 1, \dots, 3$

Satisfy*Constraint*

$$v_f \leq v_{f\text{-limit}} \quad \text{see Equation 6.17}$$

Goals

Cases 1 and 2:

$$C_{11} + d_1^- - d_1^+ = C_{11\text{-target}} \quad \text{see Equation 6.16}$$

$$C_{22} + d_2^- - d_2^+ = C_{22\text{-target}} \quad \text{see Equation 6.16}$$

Case 2 only:

$$C_{33} + d_3^- - d_3^+ = C_{33\text{-target}} \quad \text{see Equation 6.16}$$

Bounds

$$X_{i,L} \leq X_i \leq X_{i,U} \quad i = 1, \dots, N$$

$$d_i^- \cdot d_i^+ = 0 \quad i = 1, \dots, 3$$

$$d_i^-, d_i^+ \geq 0 \quad i = 1, \dots, 3$$

Minimize

$$\text{Case 1: } Z = W_1 d_1^- + W_2 d_2^+ \quad (\text{Equation 6.10})$$

$$\text{Case 2: } Z = W_1 d_1^- + W_2 d_2^+ + W_3 d_3^- \quad (\text{Equation 6.11})$$

Figure 6.7 – Decision Support Problem for Deterministic Topology Design of Unit Cells (Stage 2)

Table 6.4 – Goal Target Values, Constraint Limits, Design Variable Bounds, and Weights						
	Phase 1A		Phase 1B		Phase 2	
	Case 1	Case 2	Case 1	Case 2	Case 1	Case 2
Volume Fraction, v_f -limit	0.2	0.2	0.2	0.2	0.2	0.2
Elastic Constant, C_{11} -target (Horizontal Principal Direction)	0.1	0.035	--	--	0.1	0.035
Elastic Constant, C_{22} -target (Vertical Principal Direction)	0.1	0.09	--	--	0.1	0.09
Elastic Constant, C_{33} -target (Shear Direction)	NA	0.045	--	--	NA	0.045
Mean Elastic Constant, μ_{C11} -target (Horizontal Principal Direction)	--	--	0.1	0.035	--	--
Mean Elastic Constant, μ_{C22} -target (Vertical Principal Direction)	--	--	0.1	0.09	--	--
Mean Elastic Constant, μ_{C33} -target (Shear Direction)	--	--	NA	0.045	--	--
Variation of Elastic Constants (Dimensional) ΔC_{11} -target, ΔC_{22} -target, ΔC_{33} -target	0	0	--	--	--	--
Mean Variation of Elastic Constants (Dimensional) $\Delta_{\mu} C_{11}$ -target, $\Delta_{\mu} C_{22}$ -target, $\Delta_{\mu} C_{33}$ -target	--	--	0	0	--	--
Variation of Elastic Constants (Topological), σC_{11} -target, σC_{22} -target, σC_{33} -target	--	--	0	0	--	--
Upper Bound for Nominal Design Variable Value, $X_{i,U}$	1000 μm	250 μm	1000 μm	250 μm	1000 μm	250 μm
Lower Bound for Nominal Design Variable Value, $X_{i,L}$	0.01 μm	0.01 μm	0.01 μm	0.01 μm	0.01 μm	0.01 μm
Weights, W_i	0.25	0.17	Example- Specific	Example- Specific	0.5	0.33

unoccupied space. As reviewed in the following section, analysis models and simulation infrastructure are needed for relating the design variable values to nominal values and ranges of responses and for solving the decision support problem via exploration of the design space.

6.3.3 Implementing Phase 3 of the RTPDEM: Analysis Models and Simulation Infrastructure for Cellular Materials Design

To implement Phase 3 of the RTPDEM in Figure 3.1, a simulation infrastructure is established for solving a compromise DSP for robust topology design. As shown in Figure 3.1, the simulation infrastructure is assembled in three stages: (E) search

algorithms, (F) variability assessment techniques, and (G) analysis models. In this section, we review each of these stages for the present example.

The **analysis model** for this example is a finite element-based homogenization approach that is used to obtain the macroscopic (continuum) constitutive properties of the material in Equation 6.2 in terms of its periodic cellular mesostructure.⁵ The approach is similar to that utilized by Sigmund (1994; 1995), Neves and coauthors (2000), and others. The homogenization approach is applied to a representative volume element (RVE) that statistically represents the mesoscopic heterogeneities of the material. In this case, the RVE is a periodically repeating unit cell of the honeycomb material. If the RVE or unit cell is represented in Equation 6.2 by an equivalent homogeneous, linearly elastic solid characterized by an homogenized tensor of elastic constants $[C^H]$, the homogenized elastic constants can be calculated using energy considerations. Specifically, the elastic strain energy of a unit cell characterized by an homogenized upper bound tensor of elastic constants $[C^H]$ subjected to a test strain field $\{\varepsilon^0\}$ is equivalent to the average elastic energy integrated over the mesostructure (unit cell) volume subjected to an equivalent test strain field, i.e.,

$$\frac{1}{2}\{\varepsilon^0\}^T [C^H] \{\varepsilon^0\} = \frac{1}{2A_u} \int_{A_u} \left(\{\varepsilon^0\} + \{\delta\varepsilon\} \right)^T [C] \left(\{\varepsilon^0\} + \{\delta\varepsilon\} \right) dA \quad (6.12)$$

where $[C]$ is the local tensor of elastic constants at each point in the mesostructure, A_u is the area of the unit cell, $\{\varepsilon\}$ is the local strain in the mesostructure, and $\{\delta\varepsilon\} = \{\varepsilon\} - \{\varepsilon^0\}$ is the local strain perturbation from uniform test strain at each point in the mesostructure

⁵ *Mesosopic* length scales are intermediate between *microscopic* length scales, which apply to characteristics like gradients of chemical composition and microstructure (e.g., grain boundaries, dislocations, crystal structure), and *macroscopic* length scales, much greater than the characteristic lengths of heterogeneities, at which homogeneous continuum models are valid.

(Nemat-Nasser and Hori, 1999). By subjecting the unit cell to each of three uniform test strain fields, corresponding to $\{\epsilon^0\}_1 = \{1,0,0\}$, $\{\epsilon^0\}_2 = \{0,1,0\}$, and $\{\epsilon^0\}_3 = \{0,0,1\}$, all the elements of $[C^H]$ can be calculated. To facilitate evaluation of the right side of Equation 6.12 for complex mesoscopic topologies, the unit cell is discretized into beam finite elements according to the ground structure shown in Figure 6.4, and the induced strain is calculated using standard finite element equations and boundary information pertaining to each of these uniform strain fields via

$$[K]\{D^i\} = \{F^{\epsilon^0}\}_i \quad (6.13)$$

for a unit cell, where $\{F^{\epsilon^0}\}_i$ is the vector of nodal loads that induce the initial strain field $\{\epsilon^0\}_i$, $[K]$ is the global stiffness matrix compiled from N element stiffness matrices $[k_e]$, and $\{D^i\}$ is the vector of global displacements. The strain energy of a finite element can be calculated as follows (Cook, et al., 1989):

$$U_e = \frac{1}{2} \{d_e\}^T [k_e] \{d_e\} \quad (6.14)$$

where $\{d_e\}$ is the vector of displacements associated with element e and $[k_e]$ is the stiffness matrix for element e . The stiffness matrix for a frame element may be obtained from standard finite element textbooks (Reddy, 1993). The average strain energy integrated over the mesostructure volume can be approximated based on finite element results, i.e.,

$$\bar{U} = \frac{1}{2} \sum_{e=1}^N \frac{1}{A_e} \{d_e\}^T [k_e] \{d_e\} \quad (6.15)$$

where A_e is the in-plane area of element e . Making use of the property of unit applied test strains with Equations 6.12-6.15, the homogenized elastic constants can be calculated based on finite element results, i.e.,

$$[C_{ij}^H] = \sum_{e=1}^N \left(\frac{1}{A_e} \right) \{d_e^i\}^T [k_e] \{d_e^j\} \quad (6.16)$$

where $\{d_e^i\}$ is the vector of displacements associated with element e due to induced strain field $\{\epsilon^i\}$. To obtain these displacement vectors, the ground structure finite element model is subjected to each of the three test strains discussed previously, and periodic boundary conditions are applied to the unit cell to simulate the periodic nature of the cellular material (cf. (van der Sluis, et al., 2000)).

Finally, it is important to calculate the remaining response in the compromise DSP's—the portion of a unit cell occupied by solid material. The volume fraction can be calculated simply as

$$v_f = \frac{1}{A_U} \sum_{e=1}^N X_e L_e \quad (6.17)$$

where A_U is the area of the entire unit cell domain, X_e is the nominal in-plane thickness (or out-of-plane cross-sectional area) of element e , and L_e is the length of element e .

Once the analysis model has been established, the next step in establishing the simulation infrastructure is to devise techniques for **variability assessment**. Specifically, the parameters in Equations 6.12-6.17 represent nominal values, but the compromise DSP formulations for Stage 1 in Figures 6.5 and 6.6 also require an estimate of the range of elastic constant values, ΔC_{ij} , induced by variation in control factor values, $\Delta \mathbf{X}$, as well as the standard deviation of elastic constant values, σ_{Cij} , associated with topological noise. As described in Chapter 3, a Taylor series expansion is utilized to evaluate

response ranges associated with dimensional variation, and it is applied to elastic constants as follows:

$$\Delta C_{ij} = \sum_{e=1}^N \left| \frac{\partial C_{ij}}{\partial X_e} \Delta X_e \right| \quad (6.18)$$

To evaluate Equation 6.18, the partial derivative of an elastic constant with respect to element area must be calculated as follows, for unit cell boundary conditions, assuming that the prescribed displacements are constant:

$$\frac{\partial C_{ij}}{\partial X_e} = \{d_e^i\}^T \frac{\partial [k_e]}{\partial X_e} \{d_e^i\} \quad (6.19)$$

Here, d_e^i is the portion of the global displacement vector relevant to element e due to prescribed test strain $\{\mathcal{E}^i\}_i$, and k_e is the stiffness matrix for element e .

As discussed in Section 6.3.1, it is assumed that any *single* node may be missing randomly from the initial ground structure of Figure 6.4. As reviewed in Section 3.3.3, a sample space, \mathcal{S}^j , can be defined of possible combinations, \mathbf{R}^j , of D nodes, selected j at a time:

$$\mathcal{S}^j \equiv \{ \mathbf{R}^j : \mathbf{R}^j \subseteq \mathbf{R}^D, |\mathbf{R}^j| = j, j \leq D \} \quad (3.49)$$

In this case, there are nine nodes (i.e., $D = 9$) in a single quadrant of the ground structure in Figure 6.4A.⁶ Since j equals eight when one node is missing, the sample space of nodes, $\mathcal{S}^{j=8}$ includes nine permutations, $\mathbf{R}^{j=8}$, or possible combinations of the nine nodes, selected eight at a time, namely:

$$(R_2, R_3, \dots, R_9), (R_1, R_3, \dots, R_9), \dots, (R_1, R_2, \dots, R_8) \quad (6.20)$$

⁶ There are twenty-five nodes in a single quadrant of the ground structure in Figure 4.4B. This ground structure is utilized for verification and validation in Stage 3 of this example. For brevity, the present discussion is referred to Figure 4.4A only.

where R_1 is the first node, R_2 is the second node, and so on. Therefore, a total of $V=10$ experiments must be conducted to simulate topological variation. Nine experiments simulate each of the missing nodes and one experiment simulates the intact ground structure. For each experiment, a distinct node is removed from the first quadrant of the initial ground structure along with all of the elements attached to the node. The mean and standard deviation of an elastic constant are calculated as follows based on Equations 3.38 and 3.39:

$$\mu_{C_{ij}} = \sum_{v=1}^V \gamma_v C_{ij}(\mathbf{X}_v) \quad (6.21)$$

$$\sigma_{C_{ij}}^2 = \sum_{v=1}^V \gamma_v (C_{ij}(\mathbf{X}_v) - \mu_{C_{ij}})^2 \quad (6.22)$$

where \mathbf{X}_v is the vector of design variables for permutation or Experiment v ,⁷ and γ_v is the likelihood of Experiment v . As discussed in Section 6.3.1, the likelihood of an intact structure is assumed to be approximately 91% in this case, and the likelihood of a missing node is assumed to be approximately 1% for each node. Since the ranges of elastic constant values associated with dimensional variation are likely to have different values for each experiment, the mean value for an elastic constant range is calculated as follows, based on Equation 3.40:

$$\Delta_{\mu} C_{ij} = \sum_{v=1}^V \gamma_v \Delta C_{ij}(\mathbf{X}_v) \quad (6.23)$$

Equations 6.20 through 6.22 complete the formulation of a variability assessment technique for evaluating the impact of dimensional and topological variation on elastic constant values.

⁷ The vector of design variables changes for each experiment because a different node is removed in each experiment along with the elements that are connected to it.

Since the methods for evaluating nominal response values and response variation have now been instantiated for this example, the next step is to describe the **search technique** for numerically exploring the design space in order to identify design variable values that simultaneously satisfy constraints and bounds and minimize a compromise DSP objective function. In this example, the Method of Moving Asymptotes (MMA) (Svanberg, 1987) algorithm—a gradient-based nonlinear programming algorithm—is used. For each design iteration, the MMA algorithm accepts as input the objective function value, Z , calculated according to Equations 6.6 through 6.11, design variable bounds, and a volume fraction constraint value (calculated as the difference between the volume fraction limit and the nominal volume fraction value), as well as partial derivatives of the constraint and objective functions. The MMA algorithm returns updated values for the element areas. When the MMA algorithm converges, some element areas are near their lower bound values. In a post-processing step, these elements are removed from the ground structure; thereby modifying the topology.

Gradient-based algorithms use gradients of constraint and objective functions to move strategically from point to point in the design space, converging upon a final solution. As mentioned in Chapter 3, gradient-based algorithms are more efficient if the gradients of constraint and objective functions are obtained analytically rather than via numerical methods such as forward or central differencing. Therefore, partial derivatives are required for volume fraction, nominal and mean elastic constant values, and elastic constant ranges and standard deviations with respect to the design variables, \mathbf{X} , because those parameters enter the constraint and goal functions of the compromise DSP

formulation. The derivative of the volume fraction with respect to each design variable is obtained readily from Equation 6.17 as follows:

$$\frac{\partial v_f}{\partial X_e} = \frac{L_e}{A_u} \quad (6.24)$$

where A_u is the total area of the unit cell. The partial derivative of the nominal value of an elastic constant is calculated according to Equation 6.19. The first derivative of the variation in an elastic constant is obtained from Equations 6.3, 6.16, 6.18, and 6.19 as follows:

$$\frac{\partial(\Delta C_{ij})}{\partial X_e} = \frac{\partial}{\partial X_e} \left(\sum_{m=1}^N \left| \frac{\partial C_{ij}}{\partial X_m} \Delta X_m \right| \right) = \frac{\partial^2 C_{ij}}{\partial X_e^2} \Delta X_e + \frac{\partial C_{ij}}{\partial X_e} \frac{\partial \Delta X_e}{\partial X_e} \quad (6.25)$$

The quantities on the right-hand side of Equation 6.25 are uniformly positive over the region of interest in this example (thus, the absolute value signs have been removed). The second derivative of constitutive parameter C_{ij} is required for Equation 6.25, and it is calculated as follows:

$$\frac{\partial^2 C_{ij}}{\partial A_e^2} = \{d_e^i\}^T \frac{\partial^2 [k_e]}{\partial A_e^2} \{d_e^j\} \quad (6.26)$$

assuming that prescribed displacements are held fixed.

If topological variation is considered, the partial derivatives of Equations 6.21, 6.22, and 6.23, must be calculated as follows, based on Equations 3.41, 3.42, 3.43, 6.18, and 6.25:

$$\frac{\partial \mu_{C_{ij}}}{\partial X_j} = \begin{cases} \sum_{v=1}^V \gamma_v \frac{\partial C_{ij}(\mathbf{X}_v)}{\partial X_j} & \text{if } X_j \in \mathbf{X}_v \\ 0 & \text{if } X_j \notin \mathbf{X}_v \end{cases} \quad (6.27)$$

$$\frac{\partial \sigma_{Cij}}{\partial X_j} = \frac{\sum_{k=1}^V \gamma_v (C_{ij}(\mathbf{X}_v) - \mu_{Cij}) \left(\frac{\partial C_{ij}(\mathbf{X}_v)}{\partial X_j} - \frac{\partial \mu_{Cij}}{\partial X_j} \right)}{\sigma_{Cij}} \quad \text{if } X_j \in \mathbf{X}_v \quad (6.28)$$

$$0 \quad \text{if } X_j \notin \mathbf{X}_v$$

$$\frac{\partial (\Delta_\mu C_{ij})}{\partial X_j} = \sum_{v=1}^V \gamma_v \frac{\partial \Delta C_{ij}(\mathbf{X}_v)}{\partial X_j} \quad \text{if } X_j \in \mathbf{X}_k \quad (6.29)$$

$$0 \quad \text{if } X_j \notin \mathbf{X}_k$$

This completes the formulation of the simulation infrastructure in Phase 3 of the RTPDEM for the structural unit cell example. The next phase of the RTPDEM involves solving it for this example, according to the solution process outlined in Figure 3.13. The results for each of the stages and cases outlined in Figure 6.3 are presented in the next section.

6.4 PRESENTATION AND DISCUSSION OF ROBUST CELLULAR MATERIAL DESIGNS

In this section, cellular materials design results are presented and discussed for all of the design stages identified in Figure 6.3. The designs are obtained by exercising the robust topology design method presented in Chapter 3 and customized for this application in Section 6.3.

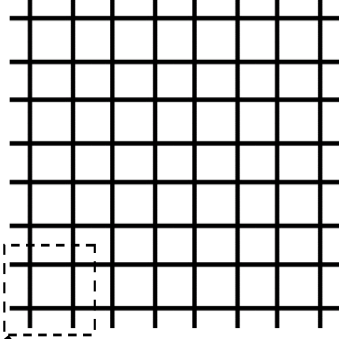
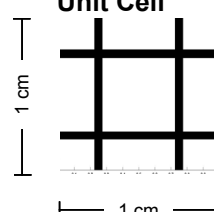
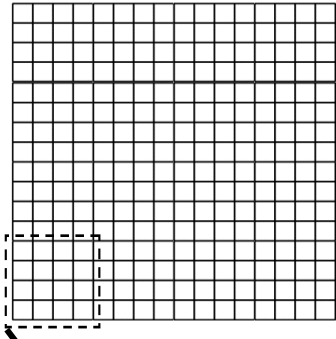
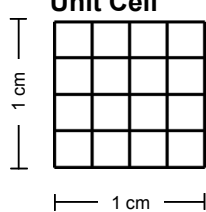
6.4.1 Results for Robust Topology Design for Dimensional Variation—Experimental Stage 1A for Design Cases 1 and 2

The first stage of the experimental plan—Stage 1A—involves designing cellular materials that offer robust elastic constants in the presence of dimensional variation or tolerances in the cell walls. Sample cellular materials designs are presented in Tables 6.5 and 6.6 for two cases. In the first case, documented in Table 6.5, a cellular material is designed for effective elastic stiffness in the horizontal and vertical principal directions.

In the second case, documented in Table 6.6, effective elastic stiffness in shear is considered along with the principal directions. In each table, a robust design and a non-robust design are presented. The robust designs are the results of Stage 1A experiments, obtained by solving the associated compromise DSP in Figure 6.5. The non-robust designs are products of Stage 2 of the experimental plan in Figure 6.3. They are generated for comparison purposes by solving the compromise DSP in Figure 6.7. For the non-robust designs, the tolerances on element areas are assumed to be zero (i.e., $\Delta X = 0$ in Equation 6.3) and therefore variation in elastic constants is not considered; this is the primary difference between the non-robust and robust topology design problem formulations. Relevant target values, constraint limits, design variable bounds, and weights are documented in Table 6.4 for each design stage and case. The initial ground structure for the unit cell is illustrated in Figure 6.4A.

Diagrams of resulting cellular materials designs are presented in Tables 6.5 and 6.6 along with quantitative evaluations of material properties obtained via the design process. The diagrams represent the final converged materials designs. After the search algorithm converges, elements with cross-sectional areas near the lower bound are removed from the initial ground structure. The remaining elements are rendered as solid lines in a diagram, and the thicknesses of the lines reflect the relative magnitudes of the cross-sectional areas of the elements. The outcome of a design process is a unit cell that is periodically repeated to construct a material segment.

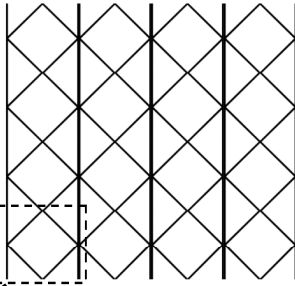
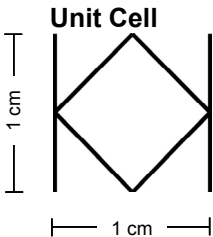
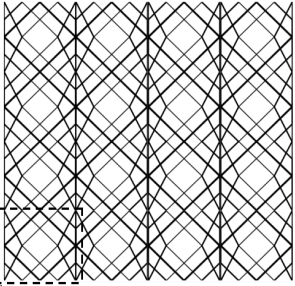
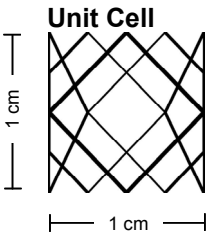
In the bottom row of Tables 6.5 and 6.6, nominal values for constraints and goals and ranges of goal values (associated with dimensional variation) are presented for robust and non-robust designs. For non-robust designs, the ranges of goal values are not included in

Table 6.5 – Robust vs. Non-Robust Periodic Unit Cell Designs for Effective Stiffness in Both Principal Directions, Considering Dimensional Variation Only (Comparison of Stages 1A and 2 Results for Case 1)	
Robust Design for Dimensional Variation	Non-Robust Design
<p style="text-align: center;">Material</p>  <p style="text-align: center;">Unit Cell</p> 	<p style="text-align: center;">Material</p>  <p style="text-align: center;">Unit Cell</p> 
<p style="text-align: center;">Design Performance</p> $C_{11} = 0.10 \pm 0.015$ $C_{22} = 0.10 \pm 0.015$	<p style="text-align: center;">Design Performance</p> $C_{11} = 0.099 \pm 0.021^*$ $C_{22} = 0.099 \pm 0.021^*$ * (40% higher than robust design) ⁸

goal or objective functions during the design process but are calculated *a posteriori* for comparison purposes by utilizing the same element area tolerances assumed for the robust designs (i.e., Equation 6.3). All values in Tables 6.5 and 6.6 are normalized by the value of the Young's modulus of the solid material.

⁸ ΔC_{11} and ΔC_{22} are calculated for comparison, *a posteriori*. They were not calculated during non-robust design.

A comparison of the cellular material diagrams reveals topological differences between the results of the two cases and between the robust and non-robust topologies for each case. The two designs illustrated in each table are topologically non-equivalent. Although each design has a 20% volume fraction of solid material, the connectivity and configuration of the material is different in each design. Continuous deformations such as stretching and bending (without fusing and tearing) would have been insufficient to

Table 6.6 – Robust vs. Non-Robust Periodic Unit Cell Designs for Effective Stiffness in Both Principal Directions and in Shear, Considering Dimensional Variation Only (Comparison of Stages 1A and 2 Results for Case 2)	
Robust Design for Dimensional Variation	Non-Robust Design
<p style="text-align: center;">Material</p>  <p style="text-align: center;">Unit Cell</p> 	<p style="text-align: center;">Material</p>  <p style="text-align: center;">Unit Cell</p> 
<p style="text-align: center;">Design Performance</p> <p> $C_{11} = 0.035 \pm 0.007$ $C_{22} = 0.094 \pm 0.020$ $C_{33} = 0.049 \pm 0.010$ </p>	<p style="text-align: center;">Design Performance</p> <p> $C_{11} = 0.031 \pm 0.008^*$ $C_{22} = 0.085 \pm 0.020^{**}$ $C_{33} = 0.042 \pm 0.011^{***}$ </p> <p> [*] (14% higher than robust design)⁹ ^{**} (identical to robust design) ^{***} (10% higher than robust design) </p>

⁹ ΔC_{11} , ΔC_{22} , and ΔC_{33} are calculated for comparison. They were not calculated during non-robust design.

transform any one of the robust designs into its corresponding non-robust design or vice versa. These changes in topological properties would not have been feasible during the design process without topology design methods such as the ground structure-based technique.

For Case 1, the observed rectangular grid patterns in Table 6.5 are expected outcomes because they maximize effective elastic stiffness in the principal in-plane directions—the two components of the constitutive tensor targeted in this example. However, the rectangular cell designs of Table 6.5 have very poor effective elastic shear stiffness. When effective elastic shear stiffness is considered for Case 2, diagonal elements are present in the final topology (as illustrated in Table 6.6) to increase the shear stiffness of the design. It is interesting to observe that the cell topologies of Case 2 (Table 6.6) are significantly different from any of the standard cell topologies discussed in the literature for prismatic cellular materials (e.g., square, triangular, hexagonal, kagome, etc.; c.f. (Hayes, et al., 2004)). A novel cellular topology is expected for this example because the standard cell topologies cannot meet the combination of effective elastic stiffness targets specified for this material. This is a good example of *materials design* in which material structure is tailored to achieve a desired set of properties that are unattainable with available material assets.

A comparison of the robust and non-robust topologies for each example yields important insights into the effectiveness of the robust topology design method. For each example, it is clear that the robust and non-robust topologies have similar nominal effective elastic stiffness, but the variation in performance induced by element area tolerances is up to 40% higher for non-robust designs. This provides evidence for the

relative insensitivity of *robust* design performance to control factor variation as well as the effectiveness of the robust topology design method in generating relatively robust topologies. The fact that robust and non-robust designs for each case exhibit similar nominal elastic constant values indicates that the designs represent alternative local minima to the materials design problem posed in Figures 6.5 and 6.7. In fact, by adjusting weights, starting points, and other convergence parameters for the non-robust designs, it is possible to obtain additional topologically distinct local minima. It is clear that the robust designs have simpler topologies with fewer elements and voids per unit cell than the non-robust, standard topologies. The robustness of a cellular structure with respect to element area tolerances is largely a function of the number of elements in the structure. In many cases, as with the rectangular grid designs in Table 6.5, it is possible to achieve identical or nearly identical nominal performance with either large numbers of thin elements or small numbers of relatively thick elements. The latter category of designs yields lower overall performance variation if the ratio of element area tolerances to nominal element area values decreases with increasing nominal element areas. On the other hand, if tolerances were strictly proportional to nominal element areas, then the induced performance variation would be equivalent for the two designs in Table 6.5 and other similar designs. However, in most cases, tolerances are not necessarily proportional to nominal dimensions; instead, they may be decreasing as a percentage of the nominal dimension as the nominal dimension increases. This is especially true when tolerances are more difficult to maintain for smaller dimensions, as in this example. This behavior is embodied in the tolerance function in Equation 6.3, which is increasing and concave in

nominal values of element area so that the ratio of tolerances to nominal values of element areas is monotonically decreasing over the region of interest.

6.4.2 Results for Robust Topology Design for Dimensional and Topological Variation—Experimental Stage 1B for Design Cases 1 and 2

Stage 1B of the experimental plan involves designing cellular materials with targeted elastic constants that are robust to both dimensional *and topological* variation. Sample

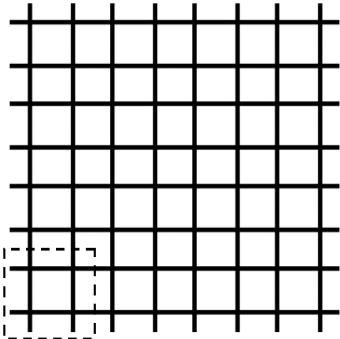
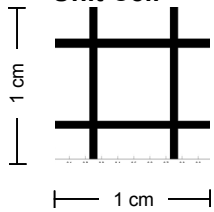
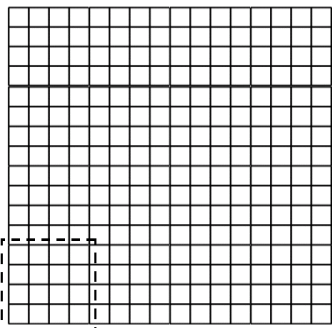
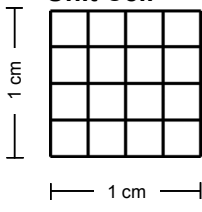
Table 6.7 – Robust vs. Non-Robust Periodic Unit Cell Designs for Effective Stiffness in Both Principal Directions, Considering Topological and Dimensional Variation (Comparison of Stages 1A, 1B, and 2 Results for Case 1 with 5x5 Node Ground Structure, Fig 6.4A)	
Robust Design for Dimensional Variation	Non-Robust Design And Robust Design for Topological Variation
<p style="text-align: center;">Material</p>  <p style="text-align: center;">Unit Cell</p> 	<p style="text-align: center;">Material</p>  <p style="text-align: center;">Unit Cell</p> 
<p style="text-align: center;">Design Performance</p> $\mu_{C11} = 0.098$ $\mu_{C22} = 0.098$ $\Delta_{\mu}C_{11} = 0.015$ $\Delta_{\mu}C_{22} = 0.015$ $\sigma_{C11} = 0.0140$ $\sigma_{C22} = 0.0140$	<p style="text-align: center;">Design Performance</p> $\mu_{C11} = 0.098$ $\mu_{C22} = 0.098$ $\Delta_{\mu}C_{11} = 0.021$ $\Delta_{\mu}C_{22} = 0.021$ $\sigma_{C11} = 0.0082$ $\sigma_{C22} = 0.0082$

Table 6.8 – Robust vs. Non-Robust Periodic Unit Cell Designs for Effective Stiffness in Principal Directions, Considering Topological and Dimensional Variation (Comparison of Stages 1A, 1B, and 2 Results for Case 1 with 9x9 Node Ground Structure, Fig 6.4B)		
Robust Design for Dimensional Variation	Robust Design for Dimensional and Topological Variation	Non-Robust Design and Robust Design for Topological Variation
<p style="text-align: center;">Material</p> <p style="text-align: center;">Unit Cell</p> <p style="text-align: center;">1 cm 1 cm</p>	<p style="text-align: center;">Material</p> <p style="text-align: center;">Unit Cell</p> <p style="text-align: center;">1 cm 1 cm</p>	<p style="text-align: center;">Material</p> <p style="text-align: center;">Unit Cell</p> <p style="text-align: center;">1 cm 1 cm</p>
<p style="text-align: center;">Design Performance</p> <p style="text-align: center;"> $C_{11} = 0.098$ $C_{22} = 0.098$ $\Delta_{\mu} C_{11} = 0.014$ $\Delta_{\mu} C_{22} = 0.014$ $\sigma_{C_{11}} = 0.014$ $\sigma_{C_{22}} = 0.014$ </p>	<p style="text-align: center;">Design Performance</p> <p style="text-align: center;"> $\mu_{C_{11}} = 0.098$ $\mu_{C_{22}} = 0.098$ $\Delta_{\mu} C_{11} = 0.019$ $\Delta_{\mu} C_{22} = 0.018$ $\sigma_{C_{11}} = 0.0098$ $\sigma_{C_{22}} = 0.0090$ </p>	<p style="text-align: center;">Design Performance</p> <p style="text-align: center;"> $\mu_{C_{11}} = 0.099$ $\mu_{C_{22}} = 0.099$ $\Delta_{\mu} C_{11} = 0.025$ $\Delta_{\mu} C_{22} = 0.025$ $\sigma_{C_{11}} = 0.0062$ $\sigma_{C_{22}} = 0.0062$ </p>

cellular materials designs are presented in Tables 6.7 and 6.8 for Case 1 (targeted elastic constants in principal directions) and in Table 6.9 for Case 2 (i.e., targeted elastic constants in principal directions and in shear). The robust designs for topological variation are products of the Stage 1B experiments, and therefore designed specifically for topological robustness by solving the compromise DSP of Figure 6.6. In each table, the non-robust designs and robust designs for dimensional variation are products of the Stage 2 and Stage 1A experiments, respectively, and are reported in this section for

comparison. Relevant target values, constraint limits, design variable bounds, and weights for each design are documented in Table 6.4.

Since topological noise is considered here, quantitative evaluations of material properties are reported in the style of Equations 6.21 through 6.23 that accommodate experiments for assessing the impact of topological noise on material properties. As discussed in Section 6.3 in relation to Equations 6.21 through 6.23, an experiment is conducted for each potential topological permutation, and the permutations in this case include an intact ground structure and ground structures with each of the active nodes missing in turn. Therefore, for each design, mean elastic constant values, $\mu_{C_{ij}}$, are reported that reflect the weighted average of elastic constant values for the set of topological experiments. Similarly, elastic constant ranges, $\Delta_{\mu}C_{ij}$ —induced by dimensional variation—are also reported as mean values for the entire set of experiments. The new piece of information is the standard deviation of elastic constants, $\sigma_{C_{ij}}$; it quantifies the spread in elastic constant values relative to their mean values for the potential topological imperfections represented by the set of topological experiments.¹⁰

During a robust topology design process, the goals—as modeled in the compromise DSP of Figure 6.6—include bringing mean elastic constant values on target and minimizing the mean elastic constant ranges and standard deviations. To investigate the impact of topological noise on robust topology design results, let us begin by reviewing the results for targeted elastic stiffness in principal directions (i.e., Case 1) in Tables 6.7 and 6.8. The only difference between the two sets of results is the initial ground structure; the results in Tables 6.7 and 6.8 are based on the 5x5 node and 9x9 node

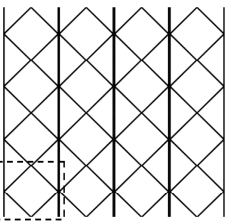
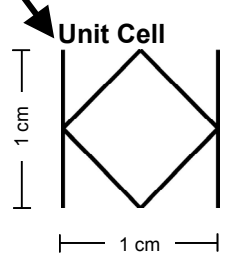
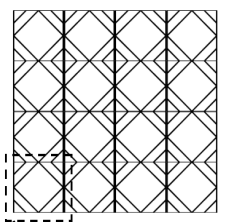
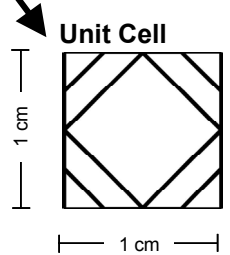
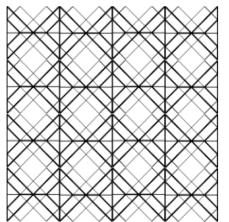
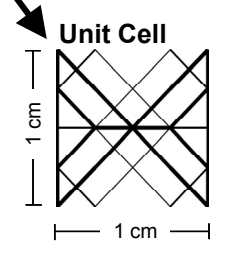
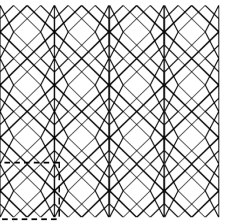
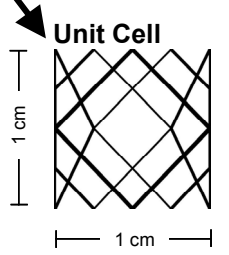
¹⁰ These quantities were calculated *a posteriori* for the non-robust designs and dimensionally robust designs.

ground structures, respectively, in Figure 6.4. First, observe that all of the designs are variations of a grid pattern. This is to be expected when stiffness is considered in only the orthogonal, in-plane principal directions with no consideration of shear stiffness or Poisson's ratio. The primary geometric difference between the designs is that they accomplish the same elastic constant goals with different numbers of elements—i.e., a few thick orthogonal elements, a large number of thinner orthogonal elements, or something in between. This is confirmed by the mean values of elastic constants, which are nearly identical for all of the designs in Tables 6.7 and 6.8. From the previous section, we know that there are often a number of local minima for a topology design problem, and all of these designs are clearly local minima.

The differences between the designs lie in the elastic constant ranges and standard deviations. Local minima with an abundance of thinner elements impose higher elastic constant ranges relative to more efficient designs with fewer thicker elements because tolerances tend to be relatively high (as a percentage of element thickness/area) for thinner elements. Therefore, the impact of tolerances on elastic constant ranges increases with the number of elements in a final topology, and simple topologies are preferred for robust design for dimensional variation. This is reflected in the mean elastic constant ranges, which are smaller for simpler topologies with fewer elements and voids for a given domain.

A converse conclusion is reached when one considers topological noise and its impact on elastic constant variation, namely, the standard deviations of elastic constant values reported in the tables. In this case, the simpler topologies have much higher standard deviations of elastic constant values than the more complex topologies. This conclusion

is intuitively related to the mechanics of the problem. When experiments are conducted to simulate the impact on performance of topological noise, the possibility is considered of missing each node (or element) in turn, and standard deviations are derived from the resulting experimental values of performance. In relatively simple topologies such as the dimensionally robust topologies in the left-most columns in Tables 6.7 and 6.8, only a few elements are available for providing stiffness or carrying structural loads. If one or more of the elements fail, there are few ‘back-up’ elements to provide some measure of stiffness. In more complex topologies such as the non-robust designs in the right-most columns of Tables 6.7 and 6.8, there are many more elements. The failure of any single element or node has a much smaller impact on the stiffness of the overall structure. In fact, this effect is so strong that the non-robust design in Table 6.7 is also the robust design if both topological and dimensional noise are considered. If dimensional variation were not considered, the non-robust topology in Table 6.7 would be the dominant design, offering on-target nominal performance and minimal deviation due to topological noise. It is also evident that there is a clear tradeoff between robustness to topological noise and robustness to dimensional variation, with designs performing well with respect to one criterion performing poorly with respect to the other. This is also evident for the designs in Table 6.8, based on the 9x9 node initial ground structure. In this case, it is easier to discern a family of designs, embodying tradeoffs between robustness to dimensional variation and robustness to topological variation. If relatively large weight is placed on the impact of dimensional variation (measured as elastic constant ranges), the left-most robust design for dimensional variation is preferred. Conversely, if relatively large weight is placed on the impact of topological variation (measured as standard deviations

Table 6.9 – Robust vs. Non-Robust Periodic Unit Cell Designs for Effective Stiffness in Principal Directions and Shear, Considering Topological and Dimensional Variation (Comparison of Stages 1A, 1B, and 2 Results for Case 2)			
Robust Design for Dimensional Variation	Robust Design for Dimensional and Topological Variation	Robust Design for Dimensional and Topological Variation	Non-Robust Design
<p>Material</p>  <p>Unit Cell</p> 	<p>Material</p>  <p>Unit Cell</p> 	<p>Material</p>  <p>Unit Cell</p> 	<p>Material</p>  <p>Unit Cell</p> 
<p>Design Performance</p> <p> $\mu_{C11} = 0.033$ $\mu_{C22} = 0.096$ $\mu_{C33} = 0.045$ $\Delta_{\mu}C_{11} = 0.0067$ $\Delta_{\mu}C_{22} = 0.021$ $\Delta_{\mu}C_{33} = 0.0096$ $\sigma_{C11} = 0.0049$ $\sigma_{C22} = 0.0122$ $\sigma_{C33} = 0.0071$ $Z = 0.2846^*$ </p>	<p>Design Performance</p> <p> $\mu_{C11} = 0.055$ $\mu_{C22} = 0.082$ $\mu_{C33} = 0.027$ $\Delta_{\mu}C_{11} = 0.013$ $\Delta_{\mu}C_{22} = 0.017$ $\Delta_{\mu}C_{33} = 0.0075$ $\sigma_{C11} = 0.0069$ $\sigma_{C22} = 0.0101$ $\sigma_{C33} = 0.0068$ $Z = 0.2645^*$ </p>	<p>Design Performance</p> <p> $\mu_{C11} = 0.051$ $\mu_{C22} = 0.078$ $\mu_{C33} = 0.030$ $\Delta_{\mu}C_{11} = 0.012$ $\Delta_{\mu}C_{22} = 0.018$ $\Delta_{\mu}C_{33} = 0.0095$ $\sigma_{C11} = 0.0057$ $\sigma_{C22} = 0.009$ $\sigma_{C33} = 0.0035$ $Z = 0.2911$ </p>	<p>Design Performance</p> <p> $\mu_{C11} = 0.030$ $\mu_{C22} = 0.094$ $\mu_{C33} = 0.039$ $\Delta_{\mu}C_{11} = 0.0076$ $\Delta_{\mu}C_{22} = 0.022$ $\Delta_{\mu}C_{33} = 0.0097$ $\sigma_{C11} = 0.0038$ $\sigma_{C22} = 0.0127$ $\sigma_{C33} = 0.0071$ $Z = 0.3680^*$ </p>

of elastic constants), the preferred design is the right-most design (which is both the non-robust design and the robust design for topological variation). For intermediate weights or for relatively equal weights on topologically- and dimensionally-induced performance variation, intermediate designs are preferred such as the dimensionally and topologically robust design reported in the center column of Table 6.8.

Similar conclusions can be drawn from the Case 2 designs tailored for elastic stiffness in both principal directions and shear and reported in Table 6.9. Two dimensionally and

topologically robust designs are presented in the middle columns of Table 6.9. They are generated by coupling the topological and dimensional robust design techniques to generate the robust designs reported in the middle columns (i.e., both elastic constant ranges induced by dimensional variation and standard deviations induced by topological noise are included in the objective function for these designs). These designs can be compared with non-robust designs and dimensionally robust designs (designed for dimensional variation alone), presented in the fourth and first columns of Table 6.9, respectively. The tradeoffs are subtler in this case. The dimensionally and topologically robust designs in the middle columns improve the standard deviations *and* mean ranges for two of the elastic constants (those governing the vertical principal direction, C_{22} , and shear, C_{33}) relative to the non-robust and dimensionally robust designs. These improvements are accompanied by tradeoffs, however, in the off-target nature of the mean elastic constant values and in the increased topologically- and dimensionally-related variation in the elastic stiffness in the horizontal principal direction, C_{11} . Visually, one can notice that the sensitivity to topological variation of the dimensionally and topologically robust designs (in the middle columns) is reduced by introducing additional, redundant, diagonal and horizontal elements. These additional elements reduce the impact of random removal of a node or element on elastic constant values.

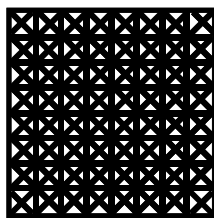
6.4.3 Verification of Results—Experimental Stage 3

Before using the results of this section to validate the effectiveness of the RTPDEM, the data presented in the tables must be verified. Several techniques are utilized here to verify different aspects of the data. First, the numerical performance of the analysis models are validated by comparing analysis-based estimates of effective elastic stiffness

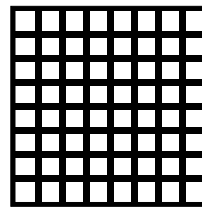
	Mixed Cells (Fig. 10)		Square Cells (Fig. 10)	
	C_{11}, C_{22}	C_{33} (shear)	C_{11}, C_{22}	C_{33} (shear)
Theoretical (Hayes, et al., 2004)	3.1E-3	8.74E-4	1.2E-03	9.3E-10
Calculated	3.3E-3	8.70E-4	1.2E-03	2.5E-09

with theoretical results available in the literature for standard cell designs. The accuracy of the frame finite element model for simulating the mean values of elastic constants for cellular materials has been confirmed by comparing results calculated with the finite element model with theoretical results reported by Hayes and coauthors (Hayes, et al., 2004) for standard unit cell topologies. In Table 6.10, comparisons are reported for the square and mixed cell designs illustrated in Figure 6.8.

As shown in Table 6.10, the finite element-based calculations agree very closely with the theoretical values. The disparities in shear stiffness estimates for square cells are due to the extremely small magnitude of the shear stiffness, round-off error in the calculations, and the use of Euler-Bernoulli beam elements and associated interpolation functions; the results reported by Hayes and coauthors (2004) are exact.



Periodic Mixed
Triangular Cells

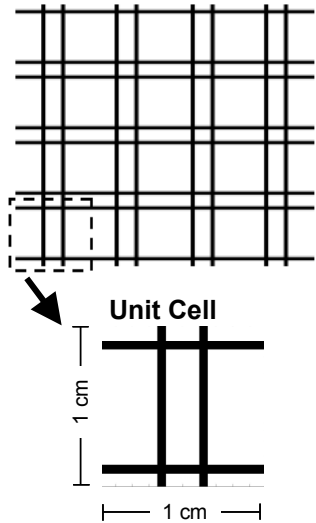
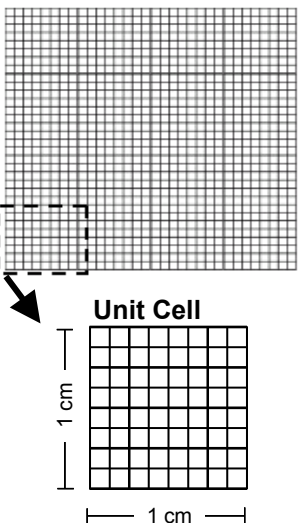


Periodic
Square Cells

Figure 6.8 – Examples of Standard Periodically Repeating Unit Cells

Secondly, since performance range estimates are based on an approximate Taylor series model, the accuracy of the finite element simulations and Taylor series model for calculating the variation in elastic constants due to dimensional tolerances was verified by comparing reported values for each solution with worst-case analyses. For each of the designs, dimensions were increased and then decreased systematically by the maximum tolerance value in Equation 6.3 and the resulting worst-case ranges of performance were compared with the ranges estimated by the Taylor series model in Equation 6.18. Because the magnitude of the tolerance ranges is small and because the finite element models are not highly nonlinear in element areas for these examples, the finite element-based Taylor series calculation approximates the worst-case variation with errors of less than 3% for this example.

Thirdly, it is known that the results of discrete topology design approaches can be sensitive to the choice of initial ground structure mesh. Specifically, when topological design is conducted with finite element analysis, it is recognized generally that the number and arrangement of the finite elements—characterized as the finite element mesh—can impact the final topology significantly. We need to determine whether the nature of our conclusions changes if the number of nodes and elements in the initial ground structure is adjusted. The designs reported in Tables 6.5, 6.6, 6.7, and 6.9 are based on the 5 x 5 node initial ground structure illustrated in Figure 6.4A. Since coarsening this mesh (i.e., reducing the number of nodes and elements) would prohibit the formation of many basic cell structures, we chose instead to refine the size of the

Table 6.11 – Robust vs. Non-Robust Periodic Unit Cell Designs for Effective Stiffness in Both Principal Directions (9 x 9 nodal mesh)	
Robust Design for Dimensional Variation	Non-Robust Design
<p style="text-align: center;">Material</p>  <p style="text-align: center;">Unit Cell</p> <p style="text-align: center;">1 cm 1 cm</p>	<p style="text-align: center;">Material</p>  <p style="text-align: center;">Unit Cell</p> <p style="text-align: center;">1 cm 1 cm</p>
<p style="text-align: center;">Design Performance</p> <p style="text-align: center;"> $C_{11} = 0.10$ $C_{22} = 0.10$ $\Delta C_{11} = 0.015$ $\Delta C_{22} = 0.015$ </p>	<p style="text-align: center;">Design Performance</p> <p style="text-align: center;"> $C_{11} = 0.10$ $C_{22} = 0.10$ $\Delta C_{11} = 0.028$ $\Delta C_{22} = 0.028$ </p>

ground structure to a mesh of 9 x 9 nodes and associated elements. Sample robust and non-robust designs obtained with the 9 x 9 mesh are illustrated in Table 6.11 for the first design case of targeted elastic constants in both principal directions.¹¹ The designs and numerical values reported in Tables 6.11, derived from a 9 x 9 node initial ground structure, can be compared with corresponding results in Tables 6.5, derived from a 5 x 5 node initial ground structure. The values for goal targets and constraints are identical for the two sets of designs. It is apparent that the topology for the two robust designs is

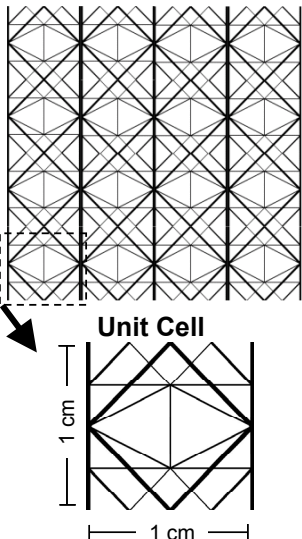
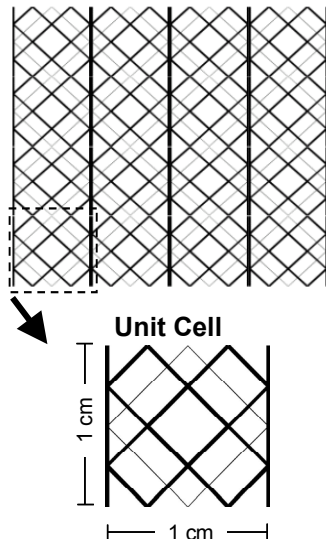
¹¹ The designs reported in Table 6.11 are identical to those in Table 6.8, but they are reported here without topological variation data for direct comparison with Table 6.5.

similar, with both unit cell designs including two vertical and two horizontal cell walls. Both nominal performance and performance variation, ΔC_{ij} , are identical for the two robust designs. These observations lead us to conclude that the robust topology design method is effective for *different* mesh sizes. Important information is also obtained from the non-robust designs in Tables 6.5 and 6.11. In both Tables 6.5 and 6.11, performance variation is greater for non-robust designs than for robust designs, but the difference is even greater for the 9 x 9 node designs in Table 6.11. Both of the non-robust unit cell topologies include the maximum numbers of horizontal and vertical cell walls (i.e., 5 x 5 for Table 6.5 and 9 x 9 for Table 6.11). This result is expected since robustness is not considered in these designs and there is no incentive for a search algorithm to eliminate any of the vertical or horizontal cell walls. Since there are greater numbers of thinner cell walls in the 9 x 9 node non-robust structure, its performance sensitivity to dimensional variation can be expected to be larger than other designs, and specifically, robust designs derived from the same or different initial ground structures. Therefore, there is evidence that the benefits of considering robustness during topology design may increase as the topological design space becomes more complex and finely discretized.

Similar results are valid for the second design case of targeted elastic constants in both principal directions and shear. The robust design for the 9 x 9 node initial ground structure is identical in topology to the dimensionally robust design reported in the left-most columns of Tables 6.6 and 6.9, based on the 5 x 5 node initial ground structure. This re-confirms that the robust topology design method is effective for different initial ground structures. It is interesting to note that it is very difficult to obtain reasonable, candidate topologies with the 9 x 9 node and larger mesh sizes using standard topology

design techniques (i.e., *without* the robust topology design methods). In many cases, the resulting topologies are disconnected or converge to off-target values of elastic constants. The relative success at obtaining robust topology designs can be attributed to the influence of the robust topology design methods, which act as penalty functions to encourage convergence to crisp, simple topologies. Others have noted the need for penalty functions in complex, multiobjective topology design scenarios with ground structures (e.g., (Frecker, et al., 1997)). As the mesh size grows, this behavior becomes more and more important.

Finally, it is important to verify that the search algorithms are converging to designs that are superior to other designs in the feasible design space. There are several ways to build confidence in the quality of the results. First, an outcome can be compared with other local minima, obtained by changing influential parameters in the decision formulation or search process such as starting points, weights, design variable bounds, goal target values, and other parameters. In topology design, it is difficult to adjust starting points; a uniform distribution of material among all of the elements in the initial ground structure is applied as a typical starting point to enhance convergence. However, goal weights, design variable bounds, and search algorithm parameters can be adjusted to obtain different local minima, and this strategy has been adopted for this example. For Case 2 (with targeted elastic constants in the principal directions and in shear), several additional local minima have been obtained, in addition to those documented in Tables 6.6 and 6.9. Two examples are included in Table 6.12. By generating a family of solutions, a designer creates a library of designs with which a newly generated design can be compared. In multiobjective, multifunctional design situations, Pareto sets of designs

Table 6.12 – Additional Local Minima for Unit Cell Designs for Design Case 2 (Effective Stiffness in Both Principal Directions and in Shear) (5 x 5 nodal mesh)	
Material 	Material 
Design Performance $C_{11} = 0.053$ $C_{22} = 0.082$ $C_{33} = 0.034$ $\Delta C_{11} = 0.013$ $\Delta C_{22} = 0.020$ $\Delta C_{33} = 0.0087$ $\sigma_{C11} = 0.0058$ $\sigma_{C22} = 0.0094$ $\sigma_{C33} = 0.0053$	Design Performance $C_{11} = 0.029$ $C_{22} = 0.093$ $C_{33} = 0.038$ $\Delta C_{11} = 0.0081$ $\Delta C_{22} = 0.0213$ $\Delta C_{33} = 0.0099$ $\sigma_{C11} = 0.0058$ $\sigma_{C22} = 0.013$ $\sigma_{C33} = 0.0081$

can be obtained, representing different tradeoffs between multiple objectives. Pareto solutions are compromise solutions for which it is impossible to improve one or more objectives without worsening at least one other objective.¹² In other words, other feasible solutions should be inferior to a Pareto solution with respect to at least one criterion of interest. A library of Pareto solutions is very useful for comparison purposes. If a new

¹² The potential for achieving Pareto efficient and non-Pareto efficient solutions for a compromise DSP is discussed in Section 2.2.

design is dominated by another design in the library with respect to *all* of the criteria of interest, then it is clearly not a superior design. It is also useful to assess the tradeoffs between a new design and other archived designs. If tolerance-induced performance ranges are weighted heavily during the design process, then the resulting designs should not be dominated by other designs with respect to performance ranges. This thought process was applied to all of the designs documented in this section. Only non-robust designs are dominated by other designs (e.g., in Table 6.6). Otherwise, compromises among the multiple objectives are evident from design to design. Designs tend to be superior to other documented designs with respect to the criteria that are emphasized in a particular design process. For example, the third design in Table 6.9 dominates most other designs with respect to standard deviations of elastic constants—criteria that are weighted heavily during its design process. Many other similar observations can be made.

A second way to build confidence in the quality of the results is to compare the results with known theoretical optima for simple problems. For Case 1 (targeted elastic stiffness in the horizontal and vertical principal directions), the results reported in Table 6.5 are theoretical optima. Any design with vertical cell walls that occupy 10% of the width of the unit cell and horizontal cell walls that occupy 10% of the height of the structure is theoretically capable of achieving the elastic constant targets of 0.1 and 0.1 in the horizontal and vertical directions, respectively. Due to the tolerance stack-up phenomenon discussed previously, a minimum number of cell walls is necessary for a robust design and a maximum of cell walls is necessary for an extremely non-robust

design. This corresponds to the designs in Table 6.5.¹³ Therefore, we can declare conclusively that the robust topology design algorithm has identified a globally robust design for this case. For designs that are robust to dimensional *and* topological variation, a compromise is expected between a topologically non-robust simple topology and a topologically robust but dimensionally non-robust complex topology (e.g., the robust and non-robust designs, respectively, in Table 6.5). The weights determine where the compromise solution lies. This phenomenon was observed with the dimensionally and topologically robust designs for Cases 1 and 2. For Case 2 (targeted elastic stiffness in the horizontal and vertical principal directions and in shear), there is no previously established theoretical optimum because none of the standard cell topologies provide the effective elastic stiffness properties sought in Case 2, as documented in Table 6.1 and Figure 6.2. The results reported in Tables 6.6 and 6.9 support the conclusion that the RTPDEM is effective for customizing cell topology to achieve material properties that are unobtainable with standard cell topologies.

A third way to build confidence in the quality of the results is to monitor the convergence behavior of the objective function and the activity of the constraints during every solution process. For all of the designs reported in this section, the volume fraction constraint was active. Convergence plots for the objective function are reported in Table 6.13 for the designs presented in Tables 6.5 through 6.9. As shown, convergence for each of the cases is relatively smooth, but there are some ‘peaks,’ most of which are associated with continuous element removal (i.e., element areas converging to their lower bounds) or with temporary divergence of the search algorithm. In the last plot, some of the early

¹³ Note that the minimum number of cell walls in a unit cell is two horizontal and two vertical cell walls due to the orthotropic symmetry imposed on the design process; i.e., one quadrant is designed and then mirrored to the other three quadrants.

objective function values are lower than the final converged value because designs were infeasible during the early iterations.

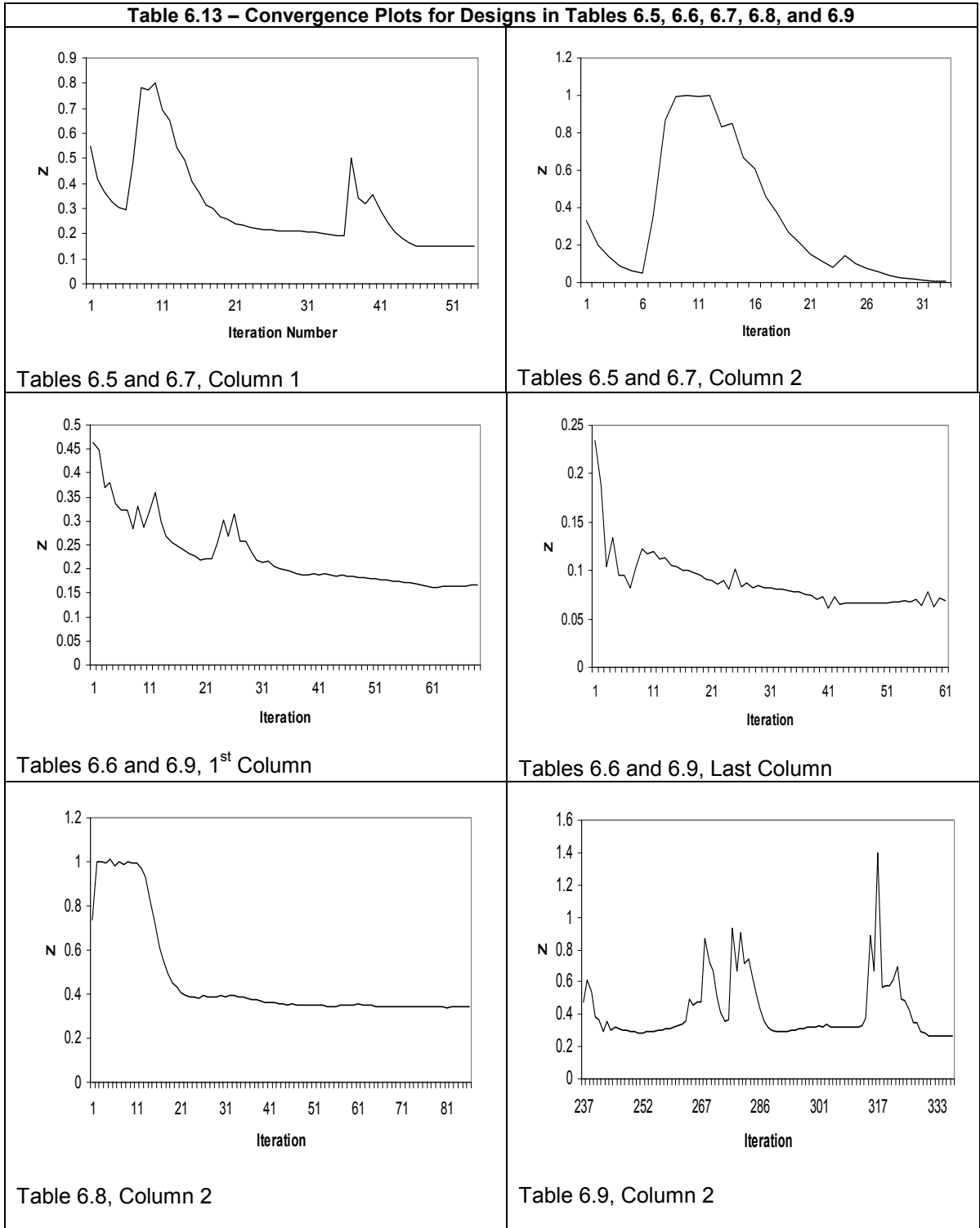


Table 6.13 -- Continued

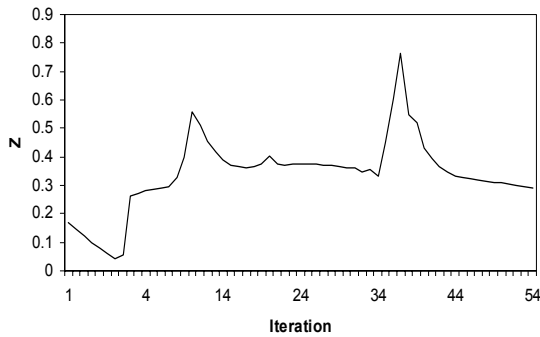


Table 6.9, Column 3

6.5 CRITICAL DISCUSSION OF THE RESULTS

The results of this example problem prompt many insights into the effectiveness, advantages, and limitations of the RTPDEM and its usefulness for materials design applications. First, the present example provides evidence that the RTPDEM is an effective method for robust topology design for both dimensional and topological variation as proposed in Hypothesis 1. Evidence is generated primarily by comparing robust topology designs—obtained with the RTPDEM—with benchmark designs obtained with standard topology design techniques. For dimensionally robust design, the evidence indicates that the robust topology designs exhibit smaller performance ranges than standard, non-robust designs exposed to identical levels of dimensional variation. On the other hand, nominal performance is not compromised. This indicates that robust topology design methods facilitate the search for *robust* local minima for problems for which there may be many local minima. Topologically, the dimensionally robust designs tend to have simpler, less complex topologies that appear to be easier to fabricate, as well. As shown in this example, the simple topologies designed for dimensional robustness are not necessarily very robust to topological noise. In fact, non-robust,

deterministic designs tend to be less sensitive to topological noise because they retain more elements within a more highly connected topology. Example evidence suggests that coupling robust topology design methods for dimensional and topological variation yields topologies that offer a compromise between the simpler topologies with superior robustness to dimensional variation and the more complex topologies with low levels of robustness to dimensional variation but high levels of robustness to topological noise. Therefore, the evidence supports both Hypothesis 1.1 and Hypothesis 1.2.

The example also provides evidence for Hypothesis 3 that the compromise DSP is a flexible, effective mathematical decision model for robust topology design applications. By changing objective function formulations and weights in the compromise DSP, a family of designs is generated for each of the design cases. The ability to generate a family of designs for any particular application is important both for providing a range of options from which to choose (based on manufacturability or other criteria) and also for verifying the quality of newly generated results. The flexibility of the compromise DSP makes that possible.

Based on experiences with this example, it is also possible to comment on the operational behavior and characteristics of the RTPDEM. As mentioned in the previous section, the RTPDEM seems to act as a penalty function, encouraging convergence to crisp topologies with two clearly defined groups of elements: (1) prominent, thick elements that remain in the structure and (2) extremely thin elements that are removed from the structure with little impact on its performance. This characteristic of the RTPDEM approach also makes it easier to obtain reasonable topologies from various mesh sizes, as evidenced by comparisons based on the 5x5 and 9x9 node initial ground

structures. On the other hand, the results of non-robust, standard topology design methods seem to be more dependent on the initial ground structure and may be increasingly difficult to obtain for denser initial ground structures. Convergence tended to be smooth and relatively fast with the RTPDEM; a large number of extra runs were not required, compared with standard topology design methods.

Although some sacrifice is required in terms of increased computational time, the effect appears to be minimal for the RTPDEM for this example. First, consider the computational expense of robust topology design for dimensional variation. For these examples, computational times are 5 to 10% longer per iteration than with standard topology design methods but much less than the computational times required for Monte Carlo simulation or other experiment-based approaches for propagating variation from input factors to responses. The increased computational time relative to standard topology design approaches is attributable to the calculation of Equations 6.18, and 6.25 through 6.29 for each iteration. (Recall that Equations 6.19 and 6.24 are standard calculations for non-robust and robust topology design because they are needed for the gradient-based search algorithm.) However, Equations 6.18, 6.25, and 6.26 do not require modification and re-solution of the finite element equations—a particularly time-consuming aspect of the computations—since they rely on displacement information that is calculated by default for nominal factor values. On the other hand, if Monte Carlo or experiment-based approaches were utilized, the control and/or noise factor levels would be adjusted multiple times for each Monte Carlo simulation or experimental point, requiring corresponding finite element re-analysis. Furthermore, these experiments would be repeated during *each* iteration of the search algorithm, and the computational

expense would be compounded by the large number of system variables. Secondly, the number of iterations required for robust topology design is usually less than the number required for standard topology design, and the robust topology design algorithm's capability for identifying high-quality solutions is less sensitive to details such as the number of elements in the ground structure. Effectively, the tolerance function (Equation 6.3) and the performance variation goals in the decision support problem act as penalty functions that encourage convergence of element areas to their lower or upper bounds. Finally, since a continuous model of control factor variation is assumed with the desirable properties outlined in Section 3.3—even for extremely small, non-manufacturable element areas—the robust topology design problem is smooth and continuous over the entire range of element areas, including extremely small values that signal eventual removal of an element from the ground structure in post-processing operations.

When topological variation is considered, all of the above advantages are still applicable, but the computational time is increased significantly. Each permutation of the initial ground structure¹⁴ requires a separate finite element re-analysis, and the full suite of permutations or topological noise experiments must be conducted during each design iteration. In this example, computational expense was limited by restricting topological permutations to include only one missing node. The number of permutations and hence the computational expense would be increased by considering more permutations as a result of (a) an initial ground structure with more nodes and elements, (b) a need to consider two or more missing nodes and all of the associated topological permutations, or (c) simulation of missing elements rather than missing nodes (since there are far more

¹⁴ A permutation is associated with each of the topological noise experiments conducted to evaluate the impact of topological noise on performance variation.

elements than nodes and many more combinations of missing elements to consider). The computational cost of re-analysis may be reduced with techniques that have been introduced in the literature (e.g.,(Kirsch and Papalambros, 2001)); however, these techniques have not been implemented in this example and provide opportunities for future investigation.

In addition to increased computational time, other drawbacks and limitations of the RTPDEM have been identified with this example. The convergence behavior of the RTPDEM—as well as standard topology design techniques—is very sensitive to the choice of initial conditions, including design variable bounds, weights, initial ground structure, etc. Quite a bit of effort is required to investigate different sets of initial conditions before the search process converges to a reasonable design. Also, with increasing numbers of goals (as in the second design case), it seems to become increasingly difficult to identify balanced designs with near-target or satisfactory performance with respect to all or most of the criteria. This is symptomatic of the weighted sum objective function utilized in this example. Unlike maximin, utility-based, or physical programming approaches, it is not formulated to place higher importance on improving the poorest performing goals. However, it is a simple, straightforward approach that is a linear function of the objectives and provides ample flexibility for exploring different weighting scenarios in order to generate families of compromise solutions.

It is also important to recognize the domain limitations of the present example. Although the examples are multiobjective in nature, they are not multifunctional. Only structural criteria are considered in this example. Furthermore, several important

structural factors have not been considered in this example, including stress constraints and buckling resistance. In addition, several potential sources of variation have not been considered including loading variation, imprecision in analysis models, variability in nodal positions and element lengths in an initial ground structure, and variation in the size and shape of the domain occupied by an initial ground structure. The example also has a relatively small initial topological domain. Based on the effectiveness of the RTPDEM for the 9 x 9 node initial ground structure, there are some indications that it is effective for larger domains, but more work is needed to confirm this conclusion. Finally, only discrete topology design approaches are utilized in this chapter (and in the rest of the dissertation); continuum topology design approaches have not been investigated in the context of robustness.

Despite its inherent, domain-specific limitations, the present example has important *materials design implications*. As discussed in Chapter 4, the RTPDEM is used in this example to design topologies for cellular materials with explicit consideration of the variations and imperfections observed in fabricated prismatic cellular materials. Although research has indicated that these imperfections impact the performance of cellular materials significantly, no work has been done on *designing* the material topology to minimize their impact on overall structural performance. It appears that the robust topology design methods are effective not only for minimizing the sensitivity of material mesostructures to dimensional and topological variation but also for adjusting the complexity or simplicity of the resulting topologies, a feature that may prove useful for customizing materials for applications such as catalysis that require complex structures or considerations such as manufacturability that require simplicity.

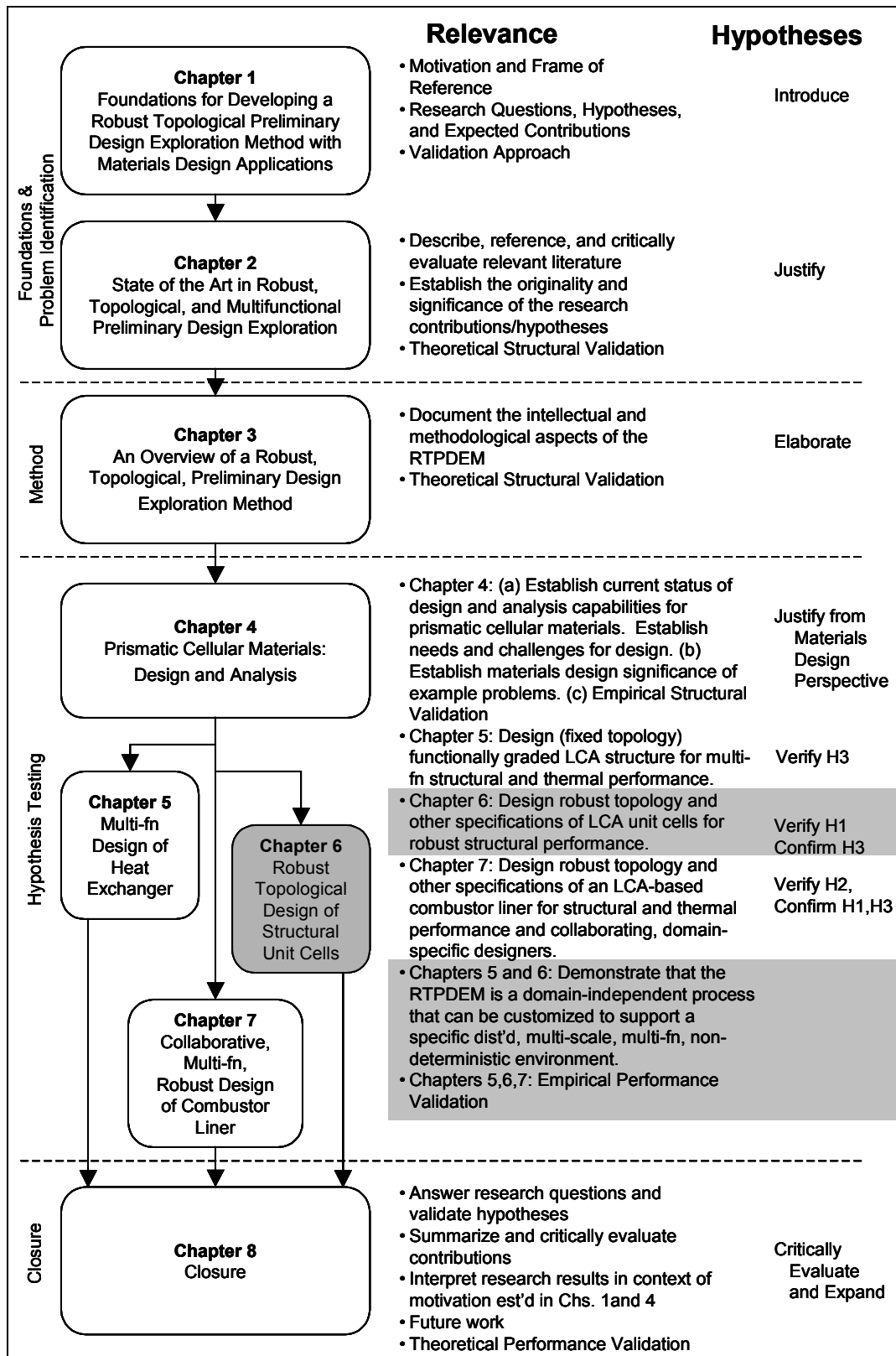


Figure 6.9 – Dissertation Roadmap

Furthermore, in this example, the RTPDEM is used to identify a *new standard cellular topology* that meets requirements that are beyond the scope of other standard cellular topologies, as illustrated in Figure 6.2. It is anticipated that the RTPDEM can be used to design additional cellular topologies for specific requirements, including robustness considerations. Furthermore, it is rare to find a truly multiobjective materials design

approach that facilitates the search for compromise solutions rather than solutions that are predominantly single objective in nature. Finally, the RTPDEM is symbolic of a systematic approach to materials design that is requirements-driven, structured, and exploratory in nature, in contrast to ad hoc approaches based exclusively on empiricism or serendipitous discovery.

6.6 CHAPTER SYNOPSIS

In this example, unit cells of prismatic cellular materials are designed for structural performance that is robust to variations in dimensions and imperfections in topology. Using the RTPDEM, *robustness* is *designed into* cellular topologies that are demonstrated to be less sensitive to variations and imperfections than designs obtained with standard, non-robust topology design methods. The RTPDEM is used to generate a family of robust designs with a range of tradeoffs between nominal structural performance and variations in performance due to tolerances and topological imperfections. The families of designs range from simple topologies with relatively low sensitivity to dimensional variation (and potential ease of fabrication) to complex topologies with built-in redundancy for robustness to topological imperfections such as missing or damaged joints or elements/walls. Furthermore, a new standard cellular topology is designed to

meet structural requirements that are not satisfied by standard cellular topologies. As illustrated in Figure 6.9, the example results verify the effectiveness of the RTPDEM for robust topology design and of the compromise DSP for mathematically modeling robust topology design decisions, as proposed in Hypotheses 1 and 3, respectively. Whereas the emphasis of the combustor liner example of Chapter 7 is on multifunctional topology design and Hypothesis 2, further evidence is also provided for Hypotheses 1 and 3.

CHAPTER 7

MULTIFUNCTIONAL, ROBUST TOPOLOGY DESIGN OF COMBUSTOR LINERS

Using the RTPDEM, it is possible to synthesize topology and other preliminary design specifications for materials with properties that are both multifunctional and robust. In this chapter, this capability is demonstrated by designing the mesoscopic topology and dimensions of prismatic cellular materials for a combustor liner within a next-generation gas turbine engine. The multifunctional topology design process is divided into two stages corresponding to the structural and thermal functional domains that are important in combustor liner design. Using robust topology design methods, topological and parametric flexibility is designed into a material during an initial structural topology design phase. This flexibility is utilized in a subsequent thermal design stage to adjust the topology and dimensions of the material, thereby improving its thermal performance. Approximate structural models are also created by the structural designer and shared with the thermal designer to enable evaluation of both structural and thermal performance by the thermal designer and, consequently, broader changes to the preliminary material specifications proposed by the structural designer.

The results of this example are used to support the proposition that systems-based materials design methods—such as the RTPDEM—are crucial ingredients in materials design efforts. Via the combustor liner example, it is demonstrated that systematic design methods are effective for meeting the requirements of advanced, materials-limited applications that have challenged materials scientists for decades. In this case, the RTPDEM is utilized to synthesize cellular-based combustor liners that promise to

inexpensively reduce the emissions and increase the efficiency of gas turbine engines. This is accomplished by designing actively- and internally-cooled cellular materials that can withstand the temperatures and pressures of next-generation combustion chambers while eliminating the need for emissions-inducing air cooling that is required for the combustion-side surfaces of conventional solid metallic combustor liners. The example is also used to demonstrate the effectiveness of the thermal topology and parametric design approach introduced in Section 3.5. Finally, the results of this example are primarily used to support the hypothesis that the RTPDEM effectively facilitates multifunctional robust topology design as proposed in Hypothesis 2.

7.1 AN OVERVIEW OF MULTIFUNCTIONAL, ROBUST TOPOLOGY DESIGN OF COMBUSTOR LINERS

The purpose of this example is two-fold. First, it is intended to demonstrate the effectiveness of the RTPDEM for tailoring the mesostructure of a prismatic cellular material—including cellular topology and dimensions—for a *multifunctional* application in which structural and thermal properties and performance are required along with manufacturability and robustness. Second, it is intended to demonstrate that the RTPDEM—as a representative systematic design method—can be utilized effectively for designing materials that meet the requirements of challenging applications more closely and with shorter development times than materials derived solely by trial-and-error methods. In this example, the focus is on an application that has been challenging materials scientists for decades—the need for high-temperature materials for gas turbine engine applications.

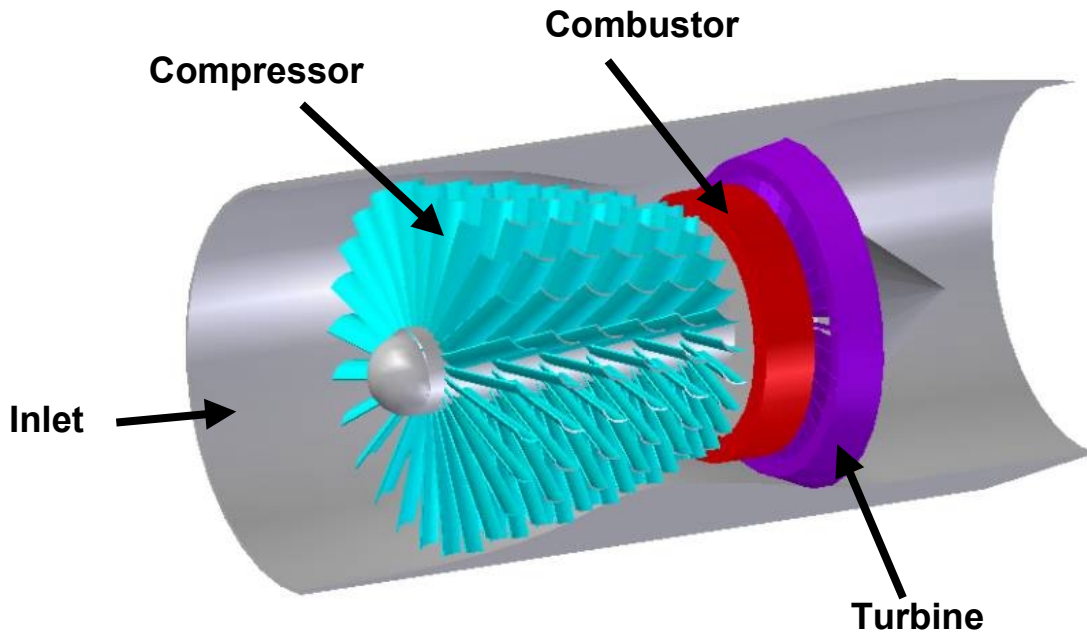


Figure 7.1 – A Schematic of a Gas Turbine Engine

Gas turbine engines are very demanding environments for their constituent materials because of the high temperatures and pressures created by combustion reactions. As shown in Figure 7.1, a gas turbine engine has three primary components: a compressor, a combustion chamber, and a turbine. Air enters the compressor where it is pressurized and fed into a combustion system at very high speeds. In the combustor, the air is mixed with fuel, and the mixture is burned. Hot combustion gases expand through the turbine blades, providing power for the compressor and other auxiliary equipment (including electricity generators in the case of power plants) before exiting the engine. In jet engines, the outlet is formed into a nozzle for generating thrust via expanding combustion gases.

Temperatures in the combustion chamber typically reach 1500 K and may approach 2000 K or more in next-generation engines. This temperature approaches or exceeds the

melting point of most metal alloys and superalloys used in gas turbine engine applications. For example, the nickel-based superalloys used in many gas turbine combustors and turbines demonstrate melting points as high as 1600 to 1700 K with significant diminishment of structural properties at much lower temperatures. Two strategies have been proposed for accommodating the extreme temperatures and pressures within the combustion chamber. The first strategy is to provide a coating of cool air to shield the combustor liner and turbine blades from the hot combustion gases (c.f., (Bailey, et al., 2002)). This strategy is effective for reducing the surface temperature of the combustor liner and turbine blades and enabling utilization of conventional alloys and superalloys, but the increased flow of cool air in the combustion chamber reduces the efficiency of the engine and increases emissions of NO_x and other harmful pollutants (c.f., (Bailey, et al., 2002; Dimiduk and Perepezko, 2003)). The second strategy is to develop entirely new materials such as ceramic matrix composites that can withstand the high temperatures and pressures directly with little or no air cooling. The ceramic matrix composite (CMC) is one of the most widely studied classes of materials under development for high temperature structural applications such as gas turbine engines. CMC's have an attractive combination of high melting temperature (greater than 3000 C), low coefficient of thermal expansion, and relatively high strength and stiffness for a broad range of temperatures (c.f., (Buckley, 1998; Tiegs and Wang, 1995)). However, after decades (and millions of dollars) of research and development, they continue to suffer from poor interlaminar properties and most importantly, poor oxidation resistance.

In this example, a novel approach is proposed that relies on strategic *materials design* rather than expensive, lengthy, empirical, trial-and-error materials development efforts. The proposed approach involves utilizing actively cooled prismatic cellular materials as combustor liners. The active cooling is achieved via forced convection with atmospheric air *within* the cells of the prismatic cellular materials, where the air is separated from the combustion chamber and does not reduce energy efficiency or increase NO_x emissions. A Mo-Si-B alloy is proposed as the base material for the prismatic cellular material. It is possible to fabricate Mo-Si-B materials with the thermochemical LCA manufacturing process described in Chapter 4 (c.f., (Schneibel, et al., 2001; Summers, et al., 2000)), and Mo-Si-B alloys have properties that are favorable for high temperature structural applications. Recent studies have determined that Mo-Si-B alloys have a very high melting point (greater than 2000° C), high thermal conductivity (50 to 112 W/m-K), low coefficients of thermal expansion (6E-6 m/m-K), low density (5-7% lower than single-crystal Ni alloys), very good oxidation resistance,¹ and high yield strengths ranging from 1500 MPa at 25° C to 400 MPa at 1370° C (c.f., (Dimiduk and Perepezko, 2003; Schneibel, et al., 2001)). These properties exceed those of most alloys and superalloys currently used for combustor liner applications.

Using the RTPDEM, the topology and dimensions of the prismatic cellular material are designed to maximize heat transfer rates and lower temperatures throughout the structure. Coupled with a thin ceramic thermal barrier on the combustion side of the combustor liner, the temperature gradients induced by active cooling in the cells are intended to lower temperatures in the material sufficiently to eliminate the need for

¹ Several alloys form protective scales of SiO₂ (B) that prohibit oxidation at high temperatures.

combustion-side air cooling (as required by conventional alloys and superalloys) and enable the use of intermetallic materials (e.g., Mo-Si-B alloys) with lower melting temperatures and better corrosion resistance than ceramic matrix composites. Simultaneously, the cellular topology is designed to withstand the high pressures of the combustion reaction coupled with mechanical stresses induced by thermal expansion at high temperatures. By strategically designing the cellular topology with the RTPDEM, it is anticipated that a balance of structural and thermal properties can be obtained that meet or exceed the requirements of next-generation jet engines without requiring combustion-side cooling or further structural support.

In this example, *multifunctional* prismatic cellular materials are designed for a combustor liner application with the requirements and conditions outlined in Tables 7.1 and 7.2, respectively. In the schematic in Table 7.2, combustion occurs inside the cylinder. The walls of the cylinder are comprised of prismatic cellular materials with cells aligned with the axis of the combustor liner. Cooling air flows along the axis of the combustor liner within the walls. No cooling air is permitted to serve as a thermal barrier on the combustion-side surface of the combustor liner, but a thin ceramic thermal barrier is permitted to shield the material from peak combustion temperatures. Temperatures within the prismatic cellular material are lowered via convective heat transfer to the cooling air. Therefore, design requirements include maximizing the total rate of steady state heat transfer to the cooling air, which effectively lowers the temperature in the walls of the cellular material. In addition, the combustor liner is subjected to interior pressure from the combustion chamber. The prismatic cellular material in the combustor liner must support the interior pressure and withstand the stresses of thermal expansion

Table 7.1 – Requirements for Prismatic Cellular Materials for a Combustor Liner Application	
Structural	<ul style="list-style-type: none"> • Minimize compliance • Stress \leq yield strength at local temperature of material • No further structural reinforcement of material, except flexible supports for securing the outer surface of the combustor liner
Thermal	<ul style="list-style-type: none"> • Maximize overall rate of steady state heat transfer • Minimize temperature throughout cellular combustor liner (linked with previous requirement via convective heat transfer mechanism) • No combustion-side air cooling of combustor liner • Thin ceramic thermal barrier permitted on combustion-side surface
Geometry	<ul style="list-style-type: none"> • Accommodate the spatial restrictions listed in Table 7.2
Manufacturing	<ul style="list-style-type: none"> • Minimum wall thickness of 50 μm. • Maximum cell wall aspect ratio (cell wall length to thickness ratio) of 8:1 • Maximum of 8 cell walls meeting at a single joint • Maximum volume fraction of approximately 30%
Robustness	<ul style="list-style-type: none"> • Minimize the impact of processing and operating variations on the properties and performance of the cellular material

without yielding. Of course, thermal stresses increase with the local temperature of the material; therefore thermal and structural objectives and requirements are interdependent. Finally, the cellular material must be robust and manufacturable, according to the specifications listed in Table 7.1.

With the combustor liner example documented in this chapter, the RTPDEM is demonstrated to be an effective systematic method for facilitating *multifunctional*, robust design of the topology and dimensions of prismatic cellular materials. Using the RTPDEM, prismatic cellular materials are designed for the combustor liner in two stages—an initial structural topology design stage followed by a predominantly thermal topology design stage. In each stage, the topology and dimensions of the material are modified systematically in pursuit of the objectives and requirements outlined in Table

Table 7.2 – Conditions for a Combustor Liner Application	
$P^*_{\text{gauge}} = P_{\text{inner}} - P_{\text{outer}}$ (interior pressure)	100 MPa
$T_{\text{hot-inner}}$ (inner combustion temperature)	2000 K
$T_{\text{max-outer}}$ (outer temperature)	500 – 600 K (goal)
D (diameter)	12.7 cm
t (thickness)	2 cm
L (length of segment)	5 cm
$T_{\text{in-cooling air}}$ (entry temperature of cooling air)	300 K
$\dot{m}_{\text{in-cooling air}}$ (mass flowrate of cooling air)	0.015 kg/s
Material	Mo-Si-B Alloy (Base)
k (thermal conductivity)	100 W/m-K
CTE (coefficient of thermal expansion)	6E-6 m/m-K
σ_Y (yield strength)	1500 MPa (300 K), 400 MPa (1650 K)
E (solid modulus)	327 Gpa
T_{melt} (melting temperature of base material)	2273 K or higher
Inner Lining on Combustion Side	Ceramic, thickness to be determined

7.1 for the conditions detailed in Table 7.2. During the structural topology design process, the material is designed to minimize overall compliance and prevent yielding due to mechanical loading and thermal expansion. In the thermal topology design process, the topology and dimensions of the material are designed to maximize the overall rate of steady state heat transfer and thereby reduce temperatures within the material relative to combustion chamber temperatures. The thermal topology design approach described in Chapter 3 is demonstrated to be effective for thermal topology and parametric design, with limitations that are clearly specified. Alternative techniques for

separating and integrating a multifunctional topology design process are investigated, and comparative studies and critical analysis of the techniques are reported. In general, the RTPDEM is shown to be an efficient and useful approach that yields cellular material designs that achieve structural and thermal constraints and objectives much more closely than standard topologies or heuristically (i.e., trial-and-error) generated designs. Furthermore, the cellular combustor liners are demonstrated to be promising alternatives to combustor liners comprised of conventional alloys, superalloys, or advanced ceramic matrix composite materials. This serves as evidence for the potential advantages of replacing or augmenting empirical, trial-and-error materials development methods with systematic design approaches such as the RTPDEM. A detailed experimental plan and procedure for designing cellular materials for the combustor liner is described in Sections 7.2 and 7.3.

7.2 VALIDATION AND VERIFICATION WITH THE EXAMPLE

The combustor liner example is intended to provide evidence for the validity of Hypotheses 2 by demonstrating that the proposed RTPDEM is an effective and efficient systematic method for designing materials—specifically, multifunctional, robust, material mesostructures—that meet the requirements of challenging applications. The materials design significance of this example is discussed in Chapter 4 and revisited in Section 7.5. In this section, empirical structural validation is discussed and an experimental plan and outline is presented for empirical performance validation. The example serves primarily as validation for Hypothesis 2 but also provides evidence confirming Hypotheses 1 and 3, which are the foci of the examples in Chapters 6 and 5, respectively.

7.2.1 Empirical Structural Validation

Empirical structural validation of Hypothesis 2 and confirmation of Hypotheses 1 and 3 involves documenting that the example is similar to problems for which the RTPDEM is intended, that the example is similar to *actual* problems for which the RTPDEM may be applied, and that the data associated with the example can be used to support the hypotheses. Since the focus of the combustor liner example is on *multifunctional* robust topology design, the focus in this discussion is on the multifunctional characteristics of the example.

Is this example similar to the problems for which the RTPDEM is intended? The combustor liner has several characteristics that qualify it as a suitable application of the RTPDEM, including:

- A need for balancing multiple objectives in requirements associated with different functional domains, i.e., structural and thermal. The objectives include overall rates of steady state heat transfer and the structural compliance and stress distribution in the structure due to applied structural loading and thermal expansion.
- A need to separate topology and preliminary design activities along disciplinary lines associated with multiple domains of functionality for an integral design. As discussed in Chapter 3, it is not possible to fully integrate structural topology design with thermal design or other disciplinary design problems that depend on the exact shape, location, number, and size of the voids or holes in the topology.² In addition, the design is *integral* rather than decomposable or nearly decomposable as discussed in Chapters 2 and 3. Its internal structure cannot be decomposed easily into

² In other cases, it may be necessary to separate design activities to leverage distributed computing resources or knowledge/expertise and to avoid solving massive design problems that are computationally intractable without partitioning.

- independent modules or subsystems associated with independent, disciplinary decision-makers; instead, multiple decision-makers must operate on a common internal structure (i.e., topology, dimensions, base material, etc.) that influences all aspects of functionality. In other words, the disciplinary sub-problems are highly coupled, but the associated design processes cannot be integrated. Therefore, it is necessary in this example to perform distributed, multi-stage topology and preliminary design, thereby testing the strategies proposed in Chapter 3 for mathematically integrating the design decisions of multiple disciplinary experts.
- Motivation to tailor the topology and dimensions of a design because those features strongly influence multifunctional performance. The impact of topology on the properties and performance of prismatic cellular materials is documented in Chapter 4. As demonstrated with the results of this example, ideal structural topologies and preliminary design specifications are not likely to be ideal for thermal applications and vice versa. Therefore, compromise designs are required that test the effectiveness of the RTPDEM for multifunctional applications.
 - Freedom to adjust the topology and dimensions of a design and manufacture the resulting topologically tailored design. The LCA manufacturing process affords significant manufacturing freedom for tailoring not only the base material but also its in-plane topology. This makes it worthwhile to design the topology and dimensions of the prismatic cellular materials. However, the process has its associated limits—such as minimum cell wall thicknesses and maximum cell wall aspect ratios—that must be not be violated by proposed designs.

- Rationale for modeling variability in the structure itself and its boundary conditions because it causes significant performance variation—the nature and/or magnitude of which is influenced by the topology of the structure. Potential sources of variation are discussed in Chapter 4 for prismatic cellular materials.

Is this example representative of an actual problem for which the RTPDEM may be applied? In many ways, the combustor liner example is representative of the challenging applications for which systematic materials design methods—such as the RTPDEM—are intended. Materials scientists and engineers have been investigating alternative composites, alloys, superalloys, and intermetallics for high temperature structural applications for decades, expending millions of dollars in research and development efforts. However, current materials still fail to meet all of the objectives and requirements for combustor liner applications. This example is both challenging and timely with the current interest in reducing emissions from gas turbine and jet engines and the need for higher temperatures and pressures in next-generation engines. In summary, the example represents a demanding topic of current interest to materials scientists that has significant potential for highlighting the benefits of utilizing systematic design methods for materials design applications. Furthermore, as discussed in previous paragraphs, the combustor liner has characteristics that identify it as a potential RTPDEM application.

In addition, care has been taken to ensure that the thermal and structural models utilized in the example are fast enough to facilitate design space exploration but accurate enough to adequately predict the properties and performance of proposed designs for the preliminary stages of an actual, industrial-strength design process. The accuracy of the

structural finite element model has been compared with results obtained from ANSYS finite element simulations for stress distributions and displacements in prismatic cellular materials in combustor liner contexts. The accuracy of the thermal finite element/finite difference model has been compared with results obtained from FLUENT simulations for overall rates of steady state heat transfer and temperature distributions in prismatic cellular materials in a combustor liner context. Manufacturability is considered during the design process in order to eliminate designs that cannot be fabricated. Finally, the conditions listed in Table 7.2 are representative of a next-generation jet engine application, and those conditions are applied uniformly during the design process. Therefore, it is the author's opinion that the example accurately reflects an actual multifunctional materials design problem in which process-structure and structure-property relations are explored to synthesize material (meso)structure that satisfies challenging multifunctional requirements including manufacturability. On the other hand, simplifications and assumptions have been made in the interest of design process efficiency and clarity of the example. For example, both structural and thermal finite element models are relatively coarse compared with ANSYS or FLUENT models. The specific assumptions embodied in the models are discussed in Section 7.3. More detailed, computationally expensive models—such as those built and analyzed in a FLUENT or ANSYS analysis—tend to be more accurate but prohibitively costly for design space exploration. Instead, they are used to calibrate the approximate thermal and structure finite element models. Several structural and thermal phenomena have not been modeled that could have an impact on the acceptability of the prismatic cellular material's performance in the combustor liner application. Examples include buckling

and structural fatigue from thermal cycling associated with engine start-up and shut-down. Additional thermal phenomena include the pressure drop of fluid flowing through each cell (although extremely high pressure heads can be expected in jet engine applications) and a detailed accounting of entry effects.

Can the data from this example be used to support conclusions with respect to the hypotheses? The data generated in this example includes estimates for thermal and structural performance and performance variation/ranges for prismatic cellular material designs generated with the RTPDEM. This data is generated for each of several alternative multifunctional topology design approaches, and the numerical results from each approach are compared. The numerical performance estimates for designs obtained with the RTPDEM are also compared with the performance of standard or heuristic (i.e., ‘best guess’) topologies to determine whether the RTPDEM is effective for topologically and dimensionally tailoring prismatic cellular material designs for desirable multifunctional performance. Finally, numerical property and performance estimates can be compared with publicly available data for conventional combustor liner materials and designs.

7.2.2 Empirical Performance Validation

The combustor liner example also facilitates empirical performance validation of Hypothesis 2. This is achieved by (1) evaluating the outcomes of the RTPDEM with respect to its intended purposes, (2) demonstrating that the effectiveness of the method is linked to its application, and (3) verifying the accuracy and internal consistency of the empirical data generated in the example and used for validation.

Description	Purpose
<p>Stage 1: Design multifunctional cellular material topology and dimensions for the combustor liner conditions identified in Tables 7.1 and 7.2, using each of the alternative multifunctional topology design approaches identified in Section 3.4.</p> <p>Stage 1A: First, design robust, flexible ranges of structural topology and dimensions. Then, perform thermal topology and dimensional design within the ranges established by the structural designer.</p> <p>Stage 1B: First, design robust, flexible ranges of structural topology and dimensions. Then, perform thermal topology and dimensional design. Use fast/approximate structural analysis models provided by the structural designer to simultaneously evaluate structural performance during the thermal design.</p>	<p>Demonstrate that the RTPDEM can be used to design robust, <i>multifunctional</i>, topology and dimensions for desired functionality. Compare alternative multifunctional topology design approaches and extract recommendations and insights regarding their effectiveness and computational cost.</p>
<p>Stage 2: Design a prismatic cellular material combustor liner heuristically. Compare with results of Stage 1.</p>	<p>Demonstrate that the RTPDEM facilitates achievement of multifunctional properties and multiobjective compromises beyond those obtained typically with standard or heuristically generated designs.</p>
<p>Stage 3: Research the high temperature structural properties of current combustor liner materials. Compare with results of Stage 1.</p>	<p>Demonstrate the benefits of utilizing systematic materials design approaches—such as the RTPDEM—in place of empirical, trial-and-error materials development methods.</p>

How can the outcome of the method be evaluated with respect to its stated purpose?

Is the observed effectiveness of the method linked to its application? A three-stage design approach is planned to investigate the effectiveness of the RTPDEM with respect to *multifunctional* topology design. As shown in Table 7.3, the first stage involves using the RTPDEM to design prismatic cellular materials using two different multifunctional design approaches. The first experimental stage is implemented in two sub-stages that correspond to the two alternative multifunctional design approaches. Details of the alternative approaches are provided in Sections 3.4 and 6.3 and are not repeated here. Results from the alternative approaches are compared with one another and with the requirements and objectives established in Tables 7.1 and 7.2. Recommendations and insights are extracted with respect to the relative effectiveness and computational cost of

the approaches. If the first experimental stage is completed successfully, it is reasonable to conclude that the RTPDEM *can* be used as a theoretical and computational infrastructure for designing *multifunctional* topology, shape, and dimensions. The second experimental stage is designed to demonstrate its *effectiveness* for this purpose. In the second experimental stage, the performance of a heuristically generated cellular design (i.e., a design that seems reasonable, based on the characteristics of the problem, but is not systematically designed) is evaluated for the combustor liner application. The purpose of the second stage is to demonstrate that the RTPDEM facilitates the exploration and generation of multifunctional topological designs with properties that cannot be obtained typically with standard, non-customized, or heuristically generated designs. Finally, in the third experimental stage, the performance of the prismatic cellular material combustor liners obtained in Stage 1 is compared with the properties and performance of conventional combustor liners. The purpose of this experimental stage is to demonstrate the benefits of utilizing systematic materials design approaches—such as the RTPDEM—in place of empirical, trial-and-error materials development methods.

How is the accuracy and internal consistency of the example results verified? First, the structural and thermal analysis models are validated by comparison with detailed FLUENT and ANSYS analyses. The formulation of the structural and thermal topology design problems are validated by investigating the mesh or ground structure sensitivity of the final designs. The sensitivity of the results is investigated with respect to certain assumptions such as the stiffness of supports for the outside of the combustor liner. The optimization results are validated to confirm that superior solutions are obtained. Several techniques are utilized including multiple starting points and assumptions, comparison

with families of alternative designs, and monitoring of design variable, constraint, and objective function values for smooth convergence.

7.3 INSTANTIATING THE ROBUST TOPOLOGICAL PRELIMINARY DESIGN EXPLORATION METHOD AS THE DESIGN APPROACH FOR THIS EXAMPLE

The RTPDEM is introduced and described in detail in Chapter 3, with the general method described in Section 3.3 and multi-stage implementation for multifunctional applications described in Section 3.4. In this section, the RTPDEM is applied, step-by-step, for the design of multifunctional prismatic cellular materials for a combustor liner application with the requirements outlined in Section 7.1. As described in Section 3.5, the multifunctional topology design process is implemented in two stages in this example. The first stage is a structural topology design stage followed by second-stage thermal design. Implementation details for both stages are discussed in this section. In Sections 7.3.1 through 7.3.3 the details of Phases 1 through 3, respectively, of the RTPDEM are discussed. In Section 7.3.4, verification and validation of the structural and thermal simulation infrastructure is discussed in the context of the combustor liner example problem. In Section 7.3.5, implementation of the RTPDEM for two-stage, multifunctional topology design is discussed.

7.3.1 Implementing Phase 1 of the RTPDEM: Formulating a Robust Multifunctional Topology Design Space for A Cellular Combustor Liner

Formulating a multifunctional robust topology design space is the first phase of the RTPDEM for multifunctional applications, as outlined in Figures 3.1 and 3.14. The phase involves identifying and characterizing influential design parameters and devising a scheme for representing and modifying topology. In a *multifunctional* topology design

process, it is also important to ensure that coupled parameters have common or easily translatable representations so that designs can be communicated easily between stages and/or designers, as discussed in Section 3.4.

The initial topology design space for structural design is modeled as a ground structure as shown in Figure 7.2. The geometric domain represented in Figure 7.2 is a 1/32 fraction slice of the entire symmetric cylindrical combustor liner. In other words, a total of 32 of these symmetrically arranged structures are repeated symmetrically to complete the entire combustor liner. The inner and outer radii of the combustor liner are assumed to be 4.35 and 6.35 cm, respectively, as noted in Table 7.2. The ground structure is populated with frame finite elements that are a superposition of bar and Euler-Bernoulli beam elements, with six degrees of freedom per element (Reddy, 1993). Frame elements have been found to approximate the behavior of low volume fraction unit cells more closely than truss elements, especially under shear loading conditions. As pictured, the ground structure has a plane of symmetry through its center and aligned with a radius of the combustor liner. The entire ground structure has 9 nodes and 27 elements, with an element connecting each pair of nodes in either symmetric half of the ground structure.

Based on the ground structure introduced in Figure 7.2, the design variables for structural topology design are the cross-sectional areas of each element in the ground structure. Bounds on the design variables should be broad, with the lower bound several orders of magnitude smaller than the upper bound to facilitate topology design. Elements with areas that converge to values near the lower bound contribute very little to the structural properties of the combustor liner and are removed from the ground structure after the iterative search process. Elements with relatively large areas remain in the

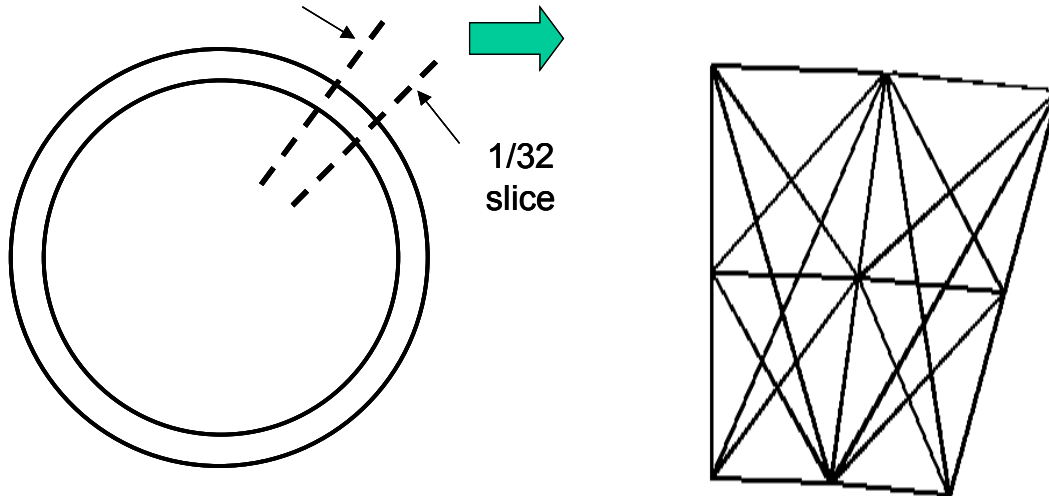


Figure 7.2 – Initial Ground Structure for Structural Topology Design. The Illustrated Domain is a 1/32 Fraction Slice of the Entire Cylindrical Combustor Liner.

structure with their associated dimensions, as determined during the search process. Post-optimization removal of elements and adjustment of element areas constitute modification of the internal topology, shape, and dimensions of the combustor liner. Additional iterative search/optimization cycles are conducted for the modified ground structure.

According to the multi-stage, multifunctional implementation of the RTPDEM, the ground structure for thermal design necessarily depends on the outcome of the structural design stage because the thermal designer begins the thermal design process with the preliminary design supplied by the structural designer. Based on the preliminary structural design, the thermal designer may modify the topology by adding or removing elements from it. For this reason, the thermal designer may superimpose a thermal ground structure on the preliminary structural design. A sample standard thermal ground structure is illustrated in Figure 7.3. The location of the nodes—and therefore the placement of elements—in the sample ground structure is adjusted to accommodate the

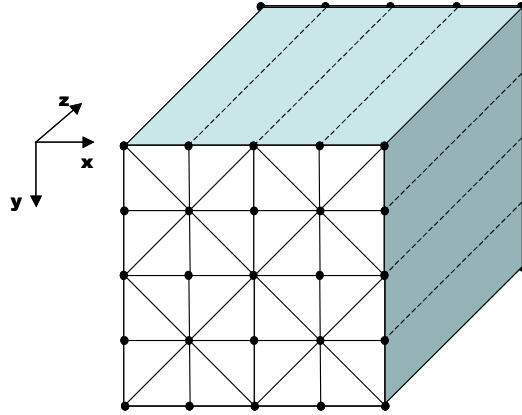


Figure 7.3 – A Sample Standard Ground Structure for Thermal Topology Design

topology determined in the first-stage structural topology design process. Details are provided for this specific example in Section 7.4.

The fixed factors, responses, and sources of variation for structural design for the first experimental stage of Table 7.3 are recorded in Table 7.4. Details for the second and third experimental stages are left for the verification and validation of results in Section 7.4. As indicated in Table 7.4, the details of the initial ground structure—including numbers and locations of nodes and elements, applied boundary conditions, and material properties—are assumed to remain fixed without deviations. Structural responses include the compliance of the structure—a measure of the overall deformation of the structure—and the stress in each element in the ground structure. Thermal responses include the total rate of steady state heat transfer for the 1/32 slice, and the temperature distribution in the structure. The volume fraction—or percentage of area or volume occupied by solid base material—is an important response for manufacturing purposes.

Table 7.4 – Summary of Design Parameters for Combustor Liner Example	
Fixed Factors	<ul style="list-style-type: none"> • Initial ground structure, Figures 7.2 and 7.3. • Boundary and operating conditions, Table 7.2
Sources of Variation	<ul style="list-style-type: none"> • Dimensional Variation • Topological Variation (missing nodes/elements)
Design Variables	<ul style="list-style-type: none"> • \mathbf{X}, vector of areas of elements in structural or thermal ground structure and associated topology • ρ_i, density of i^{th} element for thermal topology design
Responses	<ul style="list-style-type: none"> • v_f, volume fraction of solid material • \dot{Q}, total rate of steady state heat transfer • T_{i_s}, temperature at i^{th} node • C, compliance of overall structure • ΔC, variation in compliance of structure, associated with dimensional variation • $\Delta_{\mu} C$, mean variation in compliance of structure, associated with dimensional and topological variation • μ_C, mean compliance, associated with topological variation • σ_C, standard deviation of compliance, associated with topological variation • S_i, stress in i^{th} element

In this example, both dimensional and topological variation are considered. The relationship between the nominal cross-sectional area, X_i , of an element i and the variation in element area, ΔX_i , is modeled according to Equation 6.3. Similarly, topological variation is modeled as described in Section 6.3.1.

7.3.2 Implementing Phase 2 of the RTPDEM: Formulating the Robust Multifunctional Topology Design Problem for a Cellular Combustor Liner

In Phase 2 of the RTPDEM, the generic compromise DSP formulation for robust topology design in Figure 3.9 is instantiated separately for the structural and thermal domains. The compromise DSP for structural design is documented in Figure 7.4. It is identical for experimental Stages 1A and 1B in Table 7.3. As documented in the compromise DSP of Figure 7.4, the structural topology designer seeks to identify a satisfactory topology, defined by the set of constituent elements, \mathbf{X}^D , and the nominal

area of each element, X_i . Also, the structural designer indirectly identifies the acceptable ranges for each element area, ΔX_i , and the space of acceptable realized topologies, χ^R , as described in Section 3.4. The ranges are derived from the tolerance range function defined in Equation 6.3 and quantify the range of changes in element areas that a subsequent (thermal) designer can make without adversely affecting structural performance because the structural topology is designed to be robust to these changes. The space of possible sets of elements in the realized topology, χ^R , is also derived from the robust topology design process. It documents the possible topologies (i.e., the identities of the elements in each of a set of possible topologies) from which a subsequent (thermal) designer can select. It specifies the variations from nominal topology (i.e., addition or removal of elements) for which the performance of the structural topology is designed to be relatively robust. In summary, the structural topology designer identifies a nominal topology, X^D , a space of acceptable topologies, χ^R , and values of the design variables, X_i , that satisfy a set of constraints and achieve a set of goals as closely as possible. Constraints are applied to the total volume fraction in the structure and the stress in each element in the topology. The goals include minimizing the mean overall compliance of the structure, μ_c , minimizing the mean variation in compliance due to dimensional tolerances, $\Delta_\mu C$, and minimizing the standard deviation in compliance due to topological variation, σ_c . Weights, constraint limits, goal targets, and design variable bounds are documented in Table 7.5.

The compromise DSP for thermal design is documented in Figures 7.5 and 7.6 for experimental Stages 1A and 1B, respectively, of Table 7.3. The separate compromise DSP formulations are required because different goals, constraints, and assumptions are

required for experimental Stages 1A and 1B for the thermal designer, who follows the leading structural designer and accepts ranged sets of design specifications from him/her. In both Stage 1A and Stage 1B, the thermal designer identifies the values of element areas, X_i , and densities, ρ_i , along with the identities of the set of elements in the final thermal topology, \mathcal{X}^{D-2} . As defined in Section 3.5, the densities are used in thermal topology design to simulate addition or removal of elements. (Further details of their use are provided in Sections 7.3.3 and 7.4.) In both Stage 1A and Stage 1B, the volume fraction of the final structure is constrained, and the goal is to maximize the total rate of steady state heat transfer in the combustor liner, thereby lowering the temperature within the solid material.

Experimental Stages 1A and 1B correspond to the range-based and model-based multi-stage, multifunctional topology design approaches identified in Section 3.4. The thermal designer makes changes of very different scope to the structural topology in these two approaches, and this is reflected in the compromise DSP's for the range-based Stage 1A and model-based Stage 1B in Figures 7.5 and 7.6, respectively. In range-based Stage 1A, the thermal designer modifies the design generated by the structural designer, within the dimensional ranges and set of potential topologies supplied by the structural designer. As shown in the compromise DSP in Figure 7.5, changes in element areas are limited to the ranges specified by the structural designer and modified topologies are required to remain within the space of possible topologies, \mathcal{X}^R , specified by the structural designer. In model-based Stage 1B, the thermal designer utilizes an approximate physics-based model supplied by the structural designer for making broader changes to the design. As

Given

Assumptions for modeling the structural domain in the combustor liner example. See Section 7.3.3 for assumptions within the analysis model. See Table 7.2 for assumptions regarding boundary and operating conditions.

An initial ground structure for structural topology design. See Section 7.3.1.

System constraint functions:

v_f , volume fraction, defined in Equation 7.11

S_i , mechanical stress in the i^{th} element, defined in Equation 7.7

Tolerance range function for element dimensions:

$\Delta\mathbf{X}$, defined in Equation 6.3

System goal achievement functions:

C , overall compliance of the 1/32 fraction slice of the combustor liner, defined in Equation 7.6

$\Delta C(\mathbf{X})$, defined in Equation 7.12

$\Delta_\mu C(\mathbf{X})$, defined in Equation 7.17

$\sigma_C(\mathbf{X})$, defined in Equation 7.16

Goal target values, design variable bounds, constraint limits, and weights, as defined in Table 7.5

Find

X_i Element areas (Nominal Values) $i = 1, \dots, N$

\mathbf{X}^{D} Set of elements in the nominal designed topology

\mathbf{X}^{R} Space of acceptable topologies (after modification in the second (thermal) design stage)

Satisfy

Constraints

$v_f \leq v_{f\text{-limit}}$ See Equation 7.11

$S_i \leq S_{i\text{-limit}}$ See Equation 7.7

Goals

$\mu_C + d_1^- - d_1^+ = \mu_{C\text{-target}}$ see Equation 7.15

$\frac{\Delta_\mu C}{\mu_{C\text{-target}}} + d_2^- - d_2^+ = \Delta_\mu C_{\text{target}}$ see Equation 7.17

$\frac{\sigma_C}{\mu_{C\text{-target}}} + d_3^- - d_3^+ = \sigma_{C\text{-target}}$ see Equation 7.16

Bounds

$X_{i,L} \leq X_i \leq X_{i,U}$ $i = 1, \dots, N$

$d_i^- \bullet d_i^+ = 0$; $d_i^-, d_i^+ \geq 0$ $i = 1, \dots, 3$

Minimize

$Z = W_1 d_1^+ + W_2 d_2^+ + W_3 d_3^+$ (Equation 7.1)

Figure 7.4 – Compromise DSP for Robust Topology Design by the Structural Designer in the Combustor Liner Example

Given

Assumptions for modeling the thermal domain in the combustor liner example. See Section 7.3.3 for assumptions within the analysis model. See Table 7.2 for assumptions regarding boundary and operating conditions.

An initial ground structure for thermal topology design. See Section 7.3.1.

System constraint functions:

v_f , volume fraction, defined in Equation 7.11

System goal achievement function:

\dot{Q} , total rate of steady state heat transfer for the 1/32 fraction slice of the combustor liner, defined in Equation 3.71

Goal target values, design variable bounds, constraint limits, and weights, as defined in Table 7.5

Robust ranges of design specifications, ΔX_s , and space of acceptable topologies, \mathcal{X}^R , communicated from the first-stage structural designer

Find

X_i Element areas (Nominal Values) $i = 1, \dots, N$

$\mathbf{X}^{\mathcal{D}-2}$ Set of elements in the designed topology

ρ_i Density of i^{th} element for thermal topology design $i = 1, \dots, N$

Satisfy

Constraints

$v_f \leq v_{f\text{-limit}}$ See Equation 7.11
 $\mathbf{X}^{\mathcal{D}-2} \in \mathcal{X}^R$

Goals

$\dot{Q} + d_1^- - d_1^+ = \dot{Q}_{\text{target}}$ see Equation 3.71

Bounds

$X_{i,L} \leq X_i \leq X_{i,U}$, ($X_{i,L}$ and $X_{i,U}$ specified within ΔX_i) $i = 1, \dots, N$

$\rho_{i,L} \leq \rho_i \leq \rho_{i,U}$ $i = 1, \dots, N$

$d_i^- \cdot d_i^+ = 0$; $d_i^-, d_i^+ \geq 0$ $i = 1$

Minimize

$Z = W_1 d_1^-$ (Equation 7.2)

Figure 7.5 – Compromise DSP for Thermal Topology Design for Range-Based, Multi-Stage, Multifunctional Topology Design for Stage 1A of the Combustor Liner Example

Given

Assumptions for modeling the thermal domain in the combustor liner example. See Section 7.3.3 for assumptions within the analysis model. See Table 7.2 for assumptions regarding boundary and operating conditions.

An initial ground structure for thermal topology design. See Section 7.3.1.

System constraint functions:

v_f , volume fraction, defined in Equation 7.11

S_i , mechanical stress in the i^{th} element, defined in Equation 7.7

System goal achievement function:

\dot{Q} , total rate of steady state heat transfer for the 1/32 fraction slice of the combustor liner, defined in Equation 3.71

C , overall compliance of the 1/32 fraction slice of the combustor liner, defined in Equation 7.6

Goal target values, design variable bounds, constraint limits, and weights, as defined in Table 7.5

Robust ranges of design specifications, ΔX_s , and space of acceptable topologies, \mathcal{X}^R , communicated from the first-stage structural designer

Approximate structural model, communicated from the first-stage structural designer, $C = f(\mathbf{X})$

Find

X_i Element areas (Nominal Values) $i = 1, \dots, N$

\mathbf{X}^{D-2} Set of elements in the designed topology

ρ_i Density of i^{th} element for thermal topology design $i = 1, \dots, N$

Satisfy*Constraints*

$v_f \leq v_{f-limit}$ See Equation 7.11

$S_i \leq S_{i-limit}$ See Equation 7.7

Goals

$\dot{Q} + d_1^- - d_1^+ = \dot{Q}_{target}$ see Equation 3.71

$C + d_2^- - d_2^+ = C_{target}$ see Equation 7.6

Bounds

$X_{i,L} \leq X_i \leq X_{i,U}$ $i = 1, \dots, N$

$\rho_{i,L} \leq \rho_i \leq \rho_{i,U}$ $i = 1, \dots, N$

$d_i^- \bullet d_i^+ = 0; d_i^-, d_i^+ \geq 0$ $i = 1, 2$

Minimize

$Z = W_1 d_1^- + W_2 d_2^+$ (Equation 7.3)

Figure 7.6 – Compromise DSP for Thermal Topology Design for Model-Based, Multi-stage, Multifunctional Topology Design for Stage 1B of the Combustor Liner Example

Table 7.5 – Goal Targets, Design Variable Bounds, Constraint Limits, and Weights for Combustor Liner Design				
	Constraint Limits	Design Variable Bounds	Goal Targets	Goal Weights
Robust Structural Design; Table 7.11	$v_f = 0.2$ $S_i = 600 \text{ MPa}$	$0.00001 \text{ m} \leq X_i \leq 0.0045 \text{ m}$	$\mu_C = 2$ $\Delta_\mu C(\mathbf{X}) = 0$ $\sigma_C(\mathbf{X}) = 0$	$W(\mu_C) = 0.33$ $W(\Delta_\mu C(\mathbf{X})) = 0.33$ $W(\sigma_C(\mathbf{X})) = 0.33$
Non-robust Structural Design; Table 7.12	$v_f = 0.2$ $S_i = 600 \text{ MPa}$	$0.00001 \text{ m} \leq X_i \leq 0.005 \text{ m}$	$C = 2$	$W(c) = 1$
Range-Based Stage 1A Thermal Design; Tables 7.13 and 7.14	$v_f = 0.47^*$	See Tables 7.13 and 7.14	$\dot{Q} = 10,000 \text{ W}$	$W(\dot{Q}) = 1$
Model-Based Stage 1B Thermal Design; Tables 7.15 and 7.16 (Right-Side Design)	$v_f = 0.51^*$ $S_i = 600 \text{ MPa}$	See Table 7.15	$\dot{Q} = 10,000 \text{ W}$ $C = 200$	$W(\dot{Q}) = 1$ $W(C) = 0$
Model-Based Stage 1B Thermal Design; Table 7.16 (Center Design)	$v_f = 0.51^*$ $S_i = 600 \text{ MPa}$	See Table 7.15	$\dot{Q} = 10,000 \text{ W}$ $C = 200$	$W(\dot{Q}) = 0.5$ $W(C) = 0.5$
	<i>*actual value is approximately 50% of this value due to element overlap in the thermal ground structure</i>			

reflected in the compromise DSP for model-based Stage 1B thermal topology design in Figure 7.6, the thermal designer begins with the design determined by the structural designer, but he/she is not limited to the ranges of specifications and set of possible topologies determined by the structural designer. The thermal designer has the freedom to make broader adjustments to the design. In return, the thermal designer uses the approximate structural model, $C = f(\mathbf{X})$, supplied by the structural designer to evaluate the impact of those changes on the structural responses of overall compliance and stress distribution in the structure. (The approximate structural model is described in Section 7.3.3.) Stress constraints and a compliance goal are added in the problem formulation. Weights, constraint limits, goal targets, and design variable bounds are documented in Table 7.5 for thermal topology design for experimental Stages 1A and 1B.

7.3.3 Implementing Phase 3 of the RTPDEM: Analysis Models and Simulation Infrastructure for a Cellular Combustor Liner

In Phase 3 of the RTPDEM in Figure 3.1, a simulation infrastructure is established for solving the compromise DSP's for structural and thermal topology design. As documented in Figure 3.1, a simulation infrastructure has three components: (E) search algorithms, (F) variability assessment techniques, and (G) analysis models. In this section, each of these components is reviewed for both structural and thermal domains.

Analysis Model for Structural Design

The **analysis model for structural design** is based on a finite element model of the structure. Each individual element in the initial ground structure illustrated in Figure 7.2 is modeled as a one-dimensional frame finite element with two nodes and six degrees of freedom—two displacement degrees of freedom per node and one rotational degree of freedom per node. The stiffness matrix for a frame element, k_e , may be obtained from a standard finite element textbook (Cook, et al., 1989; Reddy, 1993). The displacement at each node of the ground structure can be obtained by solving the global system of finite element equations for the system:

$$[K]\{D\} = \{F\} + \{F^{th}\} \quad (7.4)$$

where $\{D\}$ is the vector of global displacements, $\{F\}$ is the vector of applied nodal loads, and $[K]$ is the global stiffness matrix compiled from N element stiffness matrices, k_e . The vector of loads that account for thermal heating of the element are calculated for a frame element as follows:

$$F_i^{th} = \alpha_i E_i X_i T_i \begin{bmatrix} -1 \\ 0 \\ 0 \\ 1 \\ 0 \\ 0 \end{bmatrix} \quad (7.5)$$

were α_i , E_i , X_i , and T_i are the coefficient of thermal expansion, modulus of elasticity, area, and average temperature, respectively, for element i .

The boundary conditions for structural analysis are illustrated in Figure 7.7. Symmetric boundary conditions are applied to the left and right sides of the 1/32 slice in Figure 7.2 to simulate the symmetry of the entire structure. A pressure of 100 MPa is applied to the inner combustion edge of the structure. Each node on the outer surface of the structure is supported by springs. Spring-like supports are simulated by placing

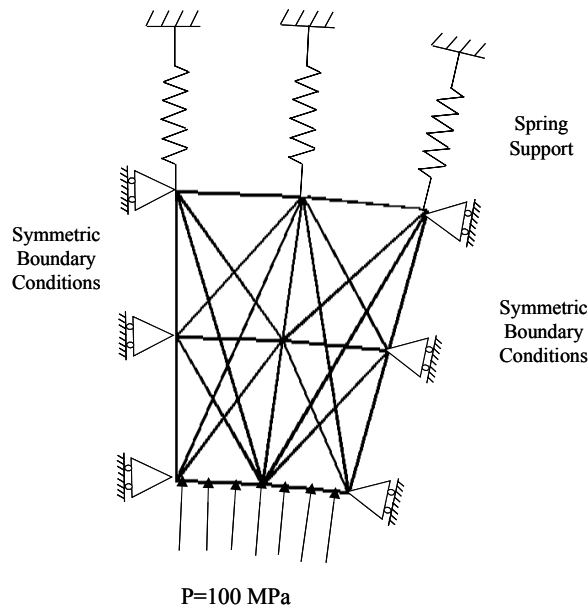


Figure 7.7 – Boundary Conditions for Structural Topology Design

‘artificial’ elements at each outer node. Each artificial element is assumed to have a node-to-node length of 1 cm, a thickness or area of 100 μm (smaller than the remaining elements in the structure), and a modulus of elasticity equivalent to the solid material in the rest of the structure (327 GPa for Mo-Si-B). One end of each artificial element is fixed and the other end is attached to the structure to serve as a spring, as illustrated in Figure 7.7.

The overall compliance of the structure is calculated as follows:

$$C = \sum_{e=1}^N \{d_e\}^T [k_e] \{d_e\} \quad (7.6)$$

where $\{d_e\}$ is the vector of displacements associated with element e due to applied loads and N is the total number of elements.

The stress in each element is calculated as follows (Cook, et al., 1989):

$$S_i = [E_i] (\{\varepsilon_i\} - \{\varepsilon_i^o\}) \quad (7.7)$$

where ε_i is the vector of mechanical strains produced by displacements of the nodes, calculated as follows:

$$\{\varepsilon_i\} = [B_i] \{d_i\} \quad (7.8)$$

where the strain-displacement matrix, $[B_i]$, is calculated for a frame element as follows:

$$[B_i] = \begin{bmatrix} -\frac{1}{L} & \frac{-6}{L^2} + \frac{12x}{L^3} & \frac{-4}{L} + \frac{6x}{L^2} & \frac{1}{L} & \frac{6}{L^2} - \frac{12x}{L^3} & \frac{-2}{L} + \frac{6x}{L^2} \end{bmatrix} \quad (7.9)$$

where x is the distance along the length of the element, and L is the total length of the element. Thermal strains are accounted for in Equation 7.7 by ε_i^o , calculated for a frame element as follows:

$$\{\boldsymbol{\varepsilon}_i^o\} = \alpha_i T_i \begin{bmatrix} -1 \\ 0 \\ 0 \\ 1 \\ 0 \\ 0 \end{bmatrix} \quad (7.10)$$

where T_i is the average temperature in element i , and α is the coefficient of thermal expansion.

Finally, the volume fraction of solid material is calculated as follows:

$$v_f = \frac{1}{A_T} \sum_{e=1}^N X_e L_e \quad (7.11)$$

where A_T is the total area of the combustor liner slice under consideration and L_e is the length of an element.

Analysis Model for Thermal Design

The **analysis model for thermal design** is presented in Section 3.5. The total rate of steady state heat transfer is calculated according to Equation 3.71. The temperatures throughout the structure are calculated by solving the global form of Equation 3.60. The thickness of an element is denoted as t_i in Section 3.5 and X_i in this chapter. The boundary conditions for thermal analysis and design are listed in Table 7.2 and illustrated in Figure 7.8. As shown, a symmetric slice of the combustor liner is modeled. Three sides are assumed to be insulated, and the inner surface is exposed to the combustion chamber at a temperature of 2000 K. The conditions of the cooling fluid (air) that is forced through the cross section are listed in Table 7.2.

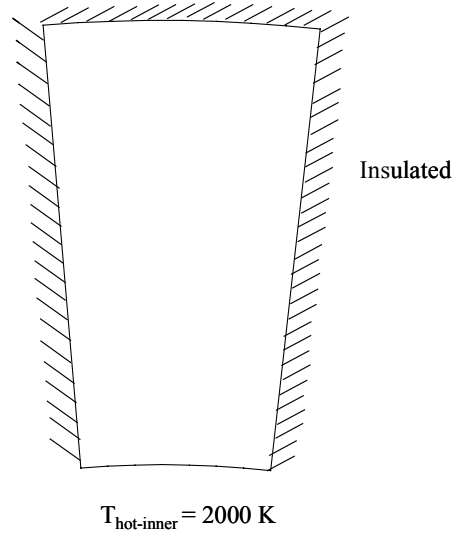


Figure 7.8 – Boundary Conditions for Thermal Topology Analysis and Design

Variability Assessment

Once the analysis model has been established, the next step in establishing the simulation infrastructure is to devise techniques for **variability assessment**. Specifically, the values in Equations 7.4 through 7.11 represent nominal values, but the compromise DSP for structural topology design in Figure 7.5 requires an estimate of the range of compliance, ΔC , induced by variation in control factors, $\Delta \mathbf{X}$, and the standard deviation of compliance, σ_c , due to topological variation. As described in Chapter 3, a Taylor series expansion is utilized to evaluate the response ranges associated with dimensional variation, and it is applied to compliance as follows:

$$\Delta C = \sum_{e=1}^N \left| \frac{\partial C}{\partial X_e} \Delta X_e \right| \quad (7.12)$$

To evaluate Equation 7.12, the partial derivative of compliance with respect to an element area must be calculated as follows, for the specified boundary conditions, assuming that the prescribed loads and displacements are constant:

$$\frac{\partial C}{\partial X_e} = -\{d_e\}^T \frac{\partial [k_e]}{\partial X_e} \{d_e\} + 2\{d_e\}^T \frac{F_i^{th}}{X_i} \quad (7.13)$$

in which it is assumed that the second derivative of compliance with respect to element area is negligible.

As discussed in Section 6.3.1 with respect to topological variation, it is assumed that any *single* node may be missing randomly from the initial ground structure of Figure 7.2. As reviewed in Section 3.3.3, a sample space, \mathcal{S}^j , can be defined of possible combinations, \mathbf{R}^j , of D nodes, selected j at a time:

$$\mathcal{S}^j \equiv \{ \mathbf{R}^j : \mathbf{R}^j \subseteq \mathbf{R}^D, |\mathbf{R}^j| = j, j \leq D \} \quad (3.49)$$

In this case, there are nine nodes (i.e., $D = 9$) in a single slice (1/32 fraction) of the ground structure in Figure 7.2. Since j equals eight when one node is missing, the sample space of nodes, $\mathcal{S}^{j=8}$ includes nine permutations, $\mathbf{R}^{j=8}$, or possible combinations of the nine nodes, selected eight at a time, namely:

$$(R_2, R_3, \dots, R_9), (R_1, R_3, \dots, R_9), \dots, (R_1, R_2, \dots, R_8) \quad (7.14)$$

where R_1 is the first node, R_2 is the second node, and so on. Therefore, a total of $V=10$ experiments must be conducted to simulate topological variation. Nine experiments simulate each of the missing nodes, and one experiment simulates the intact ground structure. For each experiment, a distinct node is removed from the first quadrant of the initial ground structure along with all of the elements attached to the node. The mean and standard deviation of compliance are calculated as follows based on Equations 3.38 and 3.39:

$$\mu_C = \sum_{v=1}^V \gamma_v C(\mathbf{X}_v) \quad (7.15)$$

$$\sigma_C^2 = \sum_{v=1}^V \gamma_v (C(\mathbf{X}_v) - \mu_C)^2 \quad (7.16)$$

where \mathbf{X}_v is the vector of design variables for permutation or Experiment v ,³ and γ_v is the likelihood of Experiment v . As discussed in Section 6.3.1, the likelihood of an intact structure is assumed to be approximately 91% in this case, and the likelihood of a missing node is assumed to be approximately 1% for each node. Since the range of compliance values associated with dimensional variation is likely to have different values for each experiment, the mean value for the range of compliance is calculated as follows, based on Equation 3.40:

$$\Delta_\mu C = \sum_{v=1}^V \gamma_v \Delta C(\mathbf{X}_v) \quad (7.17)$$

Equations 7.12 through 7.17 complete the formulation of a variability assessment technique for evaluating the impact of dimensional and topological variation on overall structural compliance. Since robust design is performed only in the first (structural) design stage, variability assessment techniques are not reported for the thermal domain.

Search Technique

Since the methods for evaluating nominal response values and response variation have now been instantiated for this example, the next step is to describe the **search technique** for numerically exploring the design space in order to identify design variable values that simultaneously satisfy constraints and bounds and minimize a compromise DSP objective function. In this example, the Method of Moving Asymptotes (MMA) (Svanberg, 1987) algorithm—a gradient-based nonlinear programming algorithm—is used. For each design iteration, the MMA algorithm accepts as input the objective

³ The vector of design variables changes for each experiment because a different node is removed in each experiment along with the elements that are connected to it.

function value, Z , calculated according to Equations 7.1 through 7.3, design variable bounds, and volume fraction and stress constraint function values, as well as partial derivatives of the constraint and objective functions. The MMA algorithm returns updated values for the element areas. When the MMA algorithm converges, some element areas are near their lower bound values. In a post-processing step, these elements are removed from the ground structure; thereby modifying the topology.

Gradient-based algorithms use gradients of constraint and objective functions to move strategically from point to point in the design space, converging upon a final solution. As mentioned in Chapter 3, gradient-based algorithms are more efficient if the gradients of constraint and objective functions are obtained analytically rather than via numerical methods such as forward or central differencing. Therefore, partial derivatives are required for volume fraction, stress, nominal and mean compliance, and compliance ranges and standard deviations with respect to the design variables, \mathbf{X} , because those parameters enter the constraint and goal functions of the compromise DSP formulation. The derivative of the volume fraction with respect to each design variable is obtained from Equation 7.11 as follows:

$$\frac{\partial v_f}{\partial X_e} = \frac{L_e}{A_r} \quad (7.18)$$

The partial derivative of the nominal value of compliance is calculated according to Equation 7.13. The first derivative of the variation in compliance is obtained from Equations 6.3, 7.6, 7.12, and 7.13 as follows:

$$\frac{\partial(\Delta C)}{\partial X_e} = \frac{\partial}{\partial X_e} \left(\sum_{m=1}^N \left| \frac{\partial C}{\partial X_m} \Delta X_m \right| \right) = \frac{\partial^2 C}{\partial X_e^2} \Delta X_e + \frac{\partial C}{\partial X_e} \frac{\partial \Delta X_e}{\partial X_e} \quad (7.19)$$

The quantities on the right-hand side of Equation 7.19 are uniformly positive over the region of interest in this example (thus, the absolute value signs have been removed). The second derivative of compliance is required for Equation 7.19, and it is calculated as follows:

$$\frac{\partial^2 C_{ij}}{\partial A_e^2} = \{d^i\}^T \frac{\partial^2 [k_e]}{\partial A_e^2} \{d^j\} \quad (7.20)$$

assuming that prescribed displacements and loads are fixed.

If topological variation is considered, the partial derivatives of Equations 7.15, 7.16, and 7.17, must be calculated as follows, based on Equations 3.41, 3.42, 3.43, 7.12, 7.13, and 7.19:

$$\frac{\partial \mu_C}{\partial X_j} = \begin{cases} \sum_{v=1}^V \gamma_v \frac{\partial C(\mathbf{X}_v)}{\partial X_j} & \text{if } X_j \in \mathbf{X}_v \\ 0 & \text{if } X_j \notin \mathbf{X}_v \end{cases} \quad (7.21)$$

$$\frac{\partial \sigma_C}{\partial X_j} = \begin{cases} \frac{\sum_{k=1}^V \gamma_v (C(\mathbf{X}_v) - \mu_C) \left(\frac{\partial C(\mathbf{X}_v)}{\partial X_j} - \frac{\partial \mu_C}{\partial X_j} \right)}{\sigma_C} & \text{if } X_j \in \mathbf{X}_v \\ 0 & \text{if } X_j \notin \mathbf{X}_v \end{cases} \quad (7.22)$$

$$\frac{\partial (\Delta_\mu C)}{\partial X_j} = \begin{cases} \sum_{v=1}^V \gamma_v \frac{\partial \Delta C(\mathbf{X}_v)}{\partial X_j} & \text{if } X_j \in \mathbf{X}_k \\ 0 & \text{if } X_j \notin \mathbf{X}_k \end{cases} \quad (7.23)$$

The partial derivatives of the total rate of steady state heat transfer with respect to element areas, X_i , and element densities, ρ_i are reported in Section 3.5 in Equations 3.74, 3.85, and accompanying equations and are not repeated here.

This completes the formulation of the simulation infrastructure for Phase 3 of the RTPDEM for the combustor liner example. Phase 4 of the RTPDEM involves solving

the combustor liner example problem. Before the RTPDEM can be used to solve the combustor liner example problem, it must be configured for a multi-stage, multifunctional implementation, as discussed in general in Section 3.4 and described for this example in the following section.

7.3.4 Verification and Validation of the Structural and Thermal Simulations for the Combustor Liner Example Problem

Before utilizing the thermal and structural analysis models and related variability assessment and search techniques, it is important to verify that they accurately model the structural and thermal behavior of the combustor liner for the specified conditions. In the following sections, the accuracy, speed, and other characteristics of the structural and thermal simulations are discussed.

Verification and Validation of Structural Simulations

The finite element-based simulation model for the structural domain is validated by comparing its stress and displacement predictions with those of ANSYS for equivalent conditions and cellular mesostructures. The cellular mesostructure is illustrated in Figure 7.9. As shown in the figure, it is a symmetric slice from a cylindrical combustor liner, and represents 1/32 (or 11.25 degrees) of the entire cylindrical combustor liner. The boundary conditions for the validation exercises are identical to those reported in Table 7.2 and Figure 7.7. As illustrated in Figure 7.7, symmetric boundary conditions are applied to two sides of the structure. A uniform pressure of 100 MPa is applied to the inner, combustion-side boundary, and the outer boundary is either free of constraints, fixed, or supported with springs as illustrated in Figure 7.7 and described in Section 7.3.3, depending on the scenario. The solid material is assumed to be a Mo-Si-B alloy with a solid modulus of 327 GPa, a Poisson's ratio of 0.27, a coefficient of thermal

expansion of $6E-6$ m/m-K, and a yield strength of 1500 MPa and 400 MPa at 300 K and 1640 K, respectively.

An ANSYS model is constructed for the structure illustrated in Figure 7.9. The ANSYS finite element model is comprised of 8-node quadrilateral elements with at least three elements through the in-plane thickness of each cell wall. Simultaneously, a simplified finite element model of the structure in Figure 7.9 is constructed according to the description in Sections 7.3.1 and 7.3.3. The approximate finite element model is illustrated in Figure 7.10 in which the elements and nodes are labeled numerically along with the radius of the combustor liner at several locations.

For the purposes of validation, stress distributions and displacements are compared from the approximate structural model and the ANSYS model for free expansion, fixed displacement, and spring boundary conditions along the outer surface of the combustor liner. Thermal expansion is not considered in this scenario. The stress values for each element in the left symmetric half of Figure 7.10 are listed in Table 7.6 for both ANSYS and the approximate structural model. The stresses are reported in MPa. The ANSYS stress values are based on plots of von Mises stress approximately averaged over the element in question. From the data in Table 7.6, it is apparent that the approximate FE model predictions of stress agree with the ANSYS models within approximately 10-20% for most elements. The approximate FE model estimates of *displacement* at each node also agree with the ANSYS model within approximately 10%.

When elevated temperatures and thermal expansion are considered in the finite element analyses, stress levels increase approximately by an order of magnitude if displacements are fixed along the outer ring. Extremely high stresses for thermal

expansion conditions are alleviated when the structure is supported with springs instead of fully fixed supports. When spring supports are introduced, the stresses in the element range from approximately 150 MPa to 450 MPa—well within the allowable stress limits for the Mo-Si-B alloy, even at elevated temperatures.

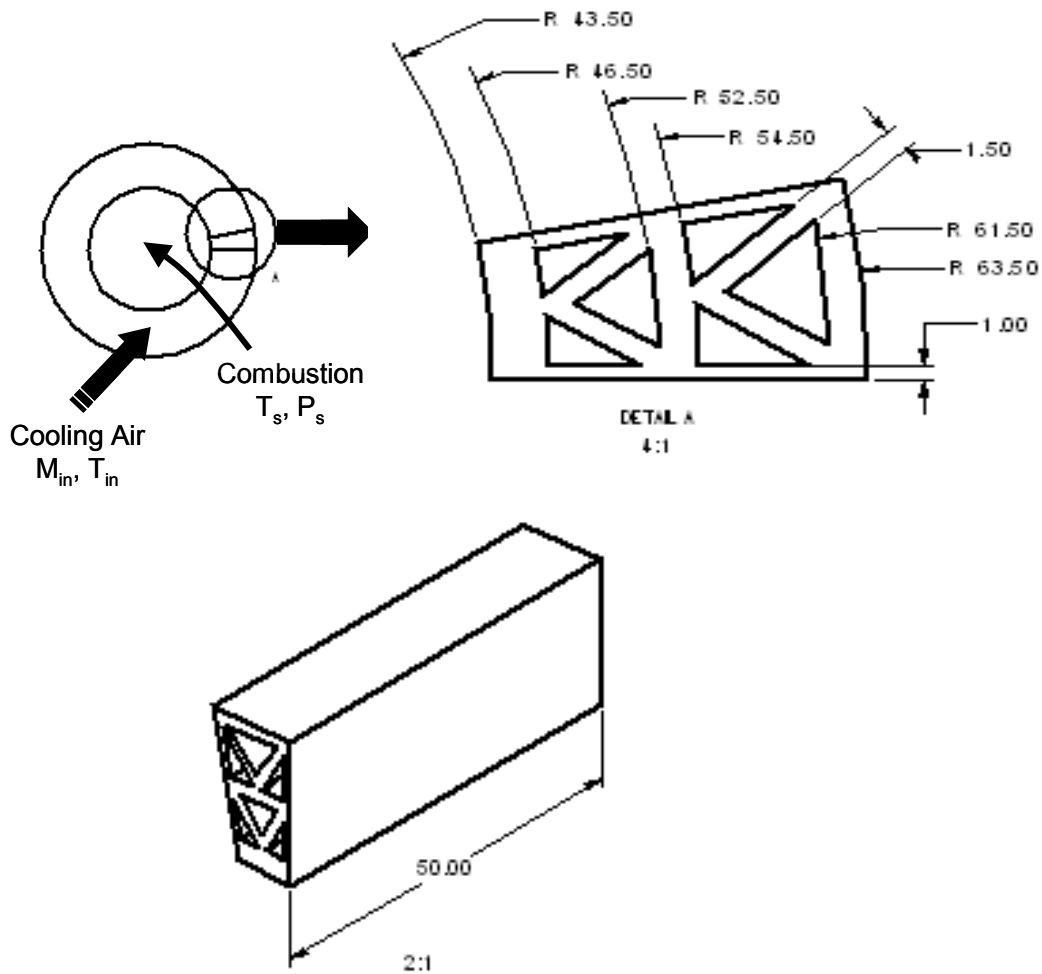


Figure 7.9 – Details of Cellular Heat Exchanger Structure for FE/FD Algorithm Validation with FLUENT (All dimensions in millimeters.)

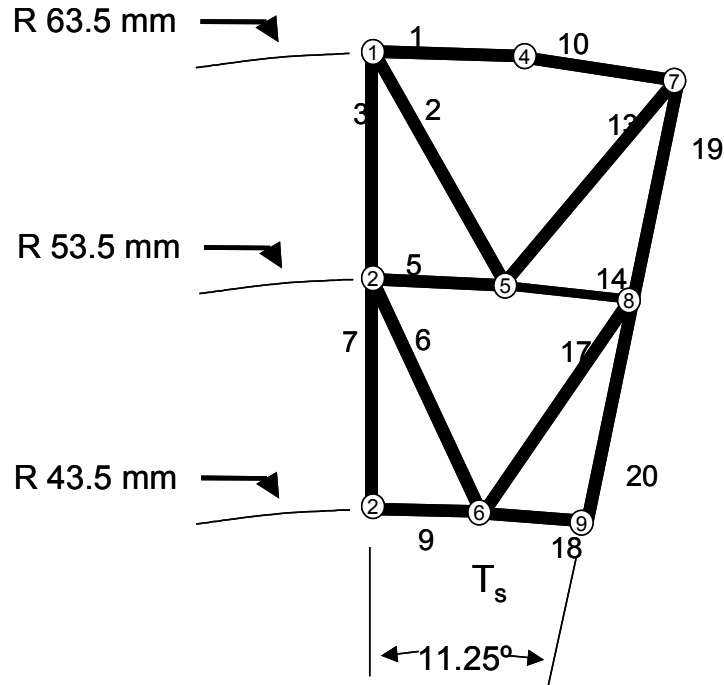


Figure 7.10 – Schematic of the Approximate Structural Finite Element Model

Based on these investigations, it is reasonable to conclude that the approximate FE model is relatively accurate for predicting the stress distribution and nodal displacements within the cellular structure of a combustor liner. It is also relatively fast, analyzing the sample structure in less than one second, compared with ANSYS which requires 5 to 10 seconds per analysis and minutes to hours of model preparation time. The approximate FE model is also easily reconfigurable. Whereas the ANSYS model requires regeneration of a 3D solid model to accommodate any parametric or topological changes in a structure, the FE model can be instantaneously reconfigured to change element dimensions or to add or remove elements from the structure. This feature is extremely important for supporting design exploration activities in which many unique sets of design specifications must be evaluated.

Element	Free Expansion on Outer Ring		Fixed Displacement on Outer Ring		Spring Supports on Outer Ring (Fig. 7.7)	
	ANSYS	Approx FE	ANSYS	Approx FE	ANSYS	Approx FE
1	300	371	10	0	220	234
2	30	36	85	84	10	7
3	100	119	285	315	160	183
5	400	439	85	40	275	331
6	60	20	125	156	50	65
7	150	146	245	212	200	168
9	500	549	100	122	380	455

Verification and Validation of Thermal Simulations

The finite element/finite difference simulation model for the thermal domain is validated by comparing its temperature and heat transfer predictions with those of FLUENT for equivalent conditions and cellular mesostructures. The representative cellular mesostructure is illustrated in Figure 7.9. As shown in the figure, it is a symmetric slice from a cylindrical combustor liner, and represents 1/32 (or 11.25 degrees) of the entire combustor liner. The boundary and operating conditions for validation exercises are recorded in Table 7.7. The heat source is applied on the inner (combustion) surface of the structure with a fixed temperature, T_s , of 2000 K. The other three sides are insulated. (Insulating the radial sides is required for symmetric boundary conditions.) Air with an inlet temperature, T_{in} , of 300 K and a mass flowrate, \dot{M} , of 0.015 kg/s is forced through the cellular passageways. The base material for the cellular structure is assumed to be a Mo-Si-B alloy with constant thermal conductivity, k , of 100 W/mK.

A FLUENT model is constructed and analyzed for the structure illustrated in Figure 7.9 and the conditions recorded in Table 7.7. A k- ϵ turbulence model is applied for the

Table 7.7 – Boundary and Operating Conditions for Validation of FE/FD Algorithm with FLUENT	
T_s	2000 K
T_{in}	300 K
\dot{M}	0.015 kg/s
k	100 W/mK
L	0.05 m

flow conditions inside the cells, and steady state conditions are assumed. As part of a mesh convergence study, total rates of steady state heat transfer for the structure are recorded for three different mesh densities. For the mid-level mesh density, two to eight three-dimensional elements are included through the thickness of each wall and twenty along the length of the structure.⁴ The results are recorded in Figure 7.11 in which the mesh density is measured by the total number of elements in the FLUENT model of the structure. As illustrated in Figure 7.11, the FLUENT estimate of the total rate of steady state heat transfer appears to have converged for the mid-level mesh density because further increases in mesh density (i.e., increases in the number of elements) do not impact the heat transfer estimate significantly. Therefore, results from the mid-level model are utilized for comparison with results from the FE/FD algorithm.

A FE/FD model is constructed and analyzed for the same structure and the same conditions utilized for the FLUENT simulations. The in-plane finite element discretization of the structure is illustrated in Figure 7.12. As illustrated in Figure 7.12, the inner surface of the combustor liner is maintained at the source temperature recorded in Table 7.7, and the other three sides are assumed insulated. (The radial sides of the slice are insulated to simulate symmetric boundary conditions.) Each circle represents a

⁴ For the high mesh density, five to seventeen elements are included through the thickness of each wall and thirty along the length of the structure. For the low-level mesh density, only one element is present through the thickness of each cell wall and twenty along the length of the structure.

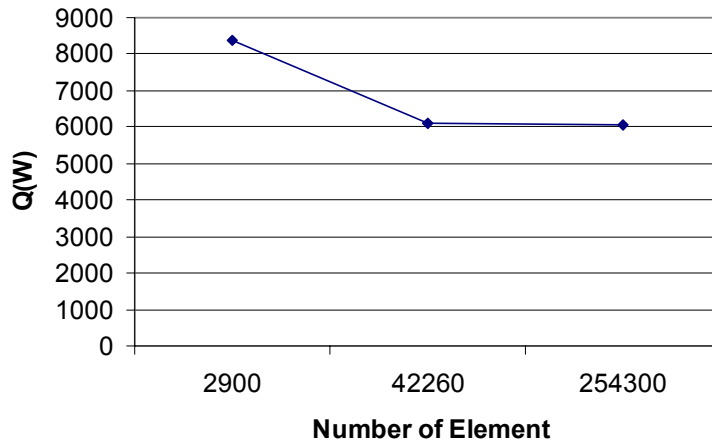


Figure 7.11 – Mesh Convergence Study for FLUENT Analysis

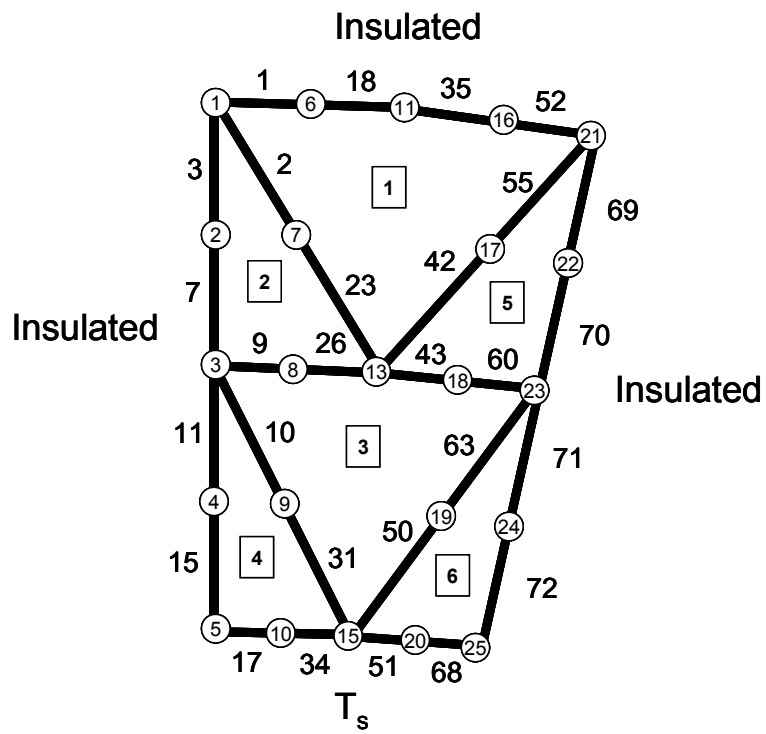


Figure 7.12 – Finite Element Discretization for Thermal Analysis of the Cellular Mesostructure Illustrated in Figure 7.9

node with its numerical label indicated within the circle. Each fluid passageway is labeled with a number enclosed in a square and assigned a cross-sectional area equivalent to that of the FLUENT model for comparison purposes. Each black line represents the edge of a 2-D finite element. Each 2-D finite element extends an increment, Δz , along the length of the cellular heat exchanger (as described in Section 3.5), with the magnitude of the increment determined by the number of slices, n_{slices} , into which the length, L , of the heat exchanger is divided, as described in Section 3.5. Also, artificial elements are used to account for (out of plane) conduction through the thickness of elements 17, 34, 51, and 68 (i.e., the elements comprising the inner ring).⁵ A mesh convergence study is conducted for the FE/FD model by estimating the total rate of steady state heat transfer for several different mesh densities. In this case, mesh density is measured by the number of slices, n_{slices} , into which the length of the structure is divided. A plot of the number of slices n_{slices} , versus the total rate of steady state heat transfer, Q , is illustrated in Figure 7.13. As shown in Figure 7.13, the rate of change of heat transfer rate with respect to the number of slices diminishes after approximately 100 slices. (In other words, further increases in the number of slices would increase the accuracy of the

⁵ Planar 2-D elements model in-plane conduction and convection but cannot model out-of-plane conduction. For a 2D planar element, temperature may vary in the plane of an element, but the temperature is assumed to be constant and uniform through the thickness of an element and the wall it models. Whereas this assumption has negligible impact for thin walls/elements or for minor temperature differences between two faces of a wall/element, it can have significant impact for thick walls with alternate faces exposed to significantly different temperature fields. For example, elements 17, 34, 51, and 68 in Figure 3—which form the interior wall of the cellular heat exchanger—cannot model temperature gradients *through* the wall. However, the interior wall is relatively thick (3 mm) and is exposed to 2000 K combustion temperatures on one side and 300 K cooling fluid on the other side. Whereas the FE/FD model assumes that the interior wall temperature is 2000 K on the combustion side *and* the fluid side, the FLUENT model accounts for conduction through the wall and estimates the fluid-side temperature of the wall at 1650 to 1850 K. To account for this shortcoming in the FE/FD model, artificial elements are added at nodes 5, 10, 15, 20, and 25 to account for conduction through the inner ring. These elements are 2D planar elements with their planes oriented parallel with radii of the combustor liner, as described in Section 3.5, with dimensions governed by the thickness and node-to-node width and depth of elements 17, 34, 51, and 68.

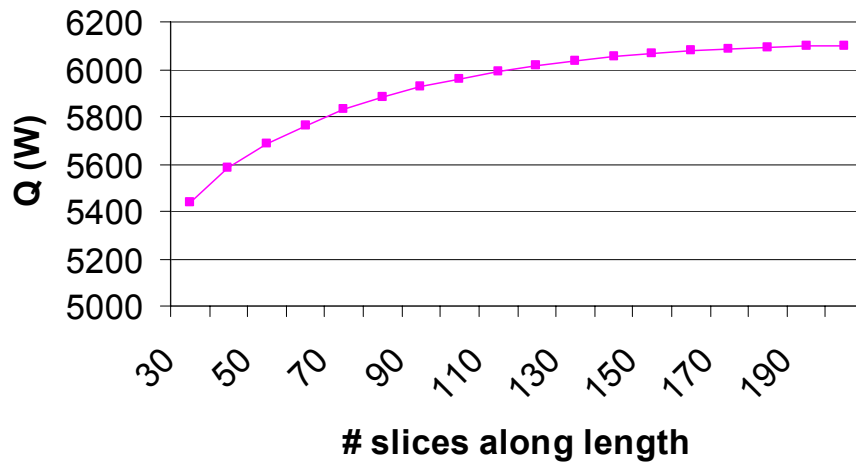


Figure 7.13 – Mesh Convergence Plot for the FE/FD Algorithm

predictions marginally but not enough to compensate for the increased computational time associated with the additional slices.) Therefore, the results of FE/FD analyses with 100 slices are utilized for comparison with FLUENT results.

Detailed FLUENT and FE/FD results are recorded in Tables 7.8 and 7.9. The FLUENT data is derived from the mid-level mesh density reported in Figure 7.11. The FE/FD results are derived from an FE/FD model with 100 slices, the element configuration illustrated in Figure 7.12, and fluid passageway areas and wall dimensions equivalent to those of the FLUENT model. In the first row of Table 7.8, total rates of

	FLUENT	FE/FD	% difference
Q (W)	5514	5960	+8.1
<i>Outlet Fluid Temperatures</i>			
T_1 (K)	548	473	-13.7
T_2	668	586	-12.3
T_3	680	750	+10.3
T_4	975	1086	+11.4
T_5	672	586	-12.8
T_6	969	1086	+12.1

Table 7.9 – Comparison of FLUENT and FE/FD Results for Cell Wall Temperature Distribution				
<i>Structural Temperatures</i>	FLUENT		FE/FD ($T_s = T_{fluid\ side} = 2000\ K$)	
	Inlet	Outlet	Inlet	Outlet
T_1 (K)	800	1000	585	789
T_2	900	1200	695	908
T_3	1000	1350	873	1095
T_4	1500	1600	1236	1418
T_5 (fluid side)	1850	1850	1759	1818
T_5 (combustion side)	2000	2000	2000	2000
T_6	800	800	574	774
T_7	850	1000	606	812
T_8	1000	1300	789	1009
T_9	1400	1500	1176	1358
T_{10} (fluid side)	1850	1850	1790	1840
T_{10} (combustion side)	2000	2000	2000	2000
T_{11}	800	1000	570	770
T_{13}	1000	1300	722	937
T_{15} (fluid side)	1650	1800	1720	1785
T_{15} (combustion side)	2000	2000	2000	2000
T_{16}	800	1000	574	775
T_{17}	850	1000	606	812
T_{18}	1000	1350	789	1008
T_{19}	1400	1500	1176	1358
T_{20} (fluid side)	1850	1850	1789	1839
T_{20} (combustion side)	2000	2000	2000	2000
T_{21}	800	1000	637	789
T_{22}	900	1200	770	911
T_{23}	1000	1350	978	1096
T_{24}	1500	1600	1401	1422
T_{25} (fluid side)	1850	1850	1759	1817
T_{25} (combustion side)	2000	2000	2000	2000

steady state heat transfer are reported. In remaining rows, temperatures are reported for the fluid at the outlet of each fluid passageway. In Table 7.9, temperatures are reported for each of the nodal locations in the structure illustrated in Figure 7.12 for both inlet and outlet cross-sections.⁶ Two temperature points are recorded for nodes 5, 10, 15, 20, and 25—the temperature on the heated, combustion side and the temperature on the cooler fluid side. As shown in Table 7.9, the temperatures agree within 25% or less for each nodal location. As shown in Table 7.8, the total rate of steady state heat transfer for the FE/FD model agrees with the FLUENT results within 8%.

To validate the FE/FD model for a broader range of conditions, the source temperature is varied from 2000 K to 1500 K to 1000 K and FLUENT and FE/FD analyses are conducted for the structure at each new temperature. All assumptions and conditions (mass flowrate, dimensions, etc.) are consistent for each temperature trial. The total rates of steady state heat transfer for the FE/FD and FLUENT analyses are recorded in Figure 7.14. Based on the data in Figure 7.14, it is clear that the FE/FD model agrees with the FLUENT results within less than 10% over the range of temperatures.

With respect to the accuracy of the FE/FD model compared with the FLUENT model, the conclusion is that the FE/FD model predictions of total rates of steady state heat transfer and fluid outlet temperatures are accurate within approximately 10%. The difference between the FE/FD results and the FLUENT results is attributed to the coarseness of the finite element mesh for the FE/FD model and the approximate correlations for estimating convective heat transfer coefficients, fluid temperatures, and fluid properties in the FE/FD model.

⁶ Temperatures from the FLUENT model are estimated based on contour plots of temperature.

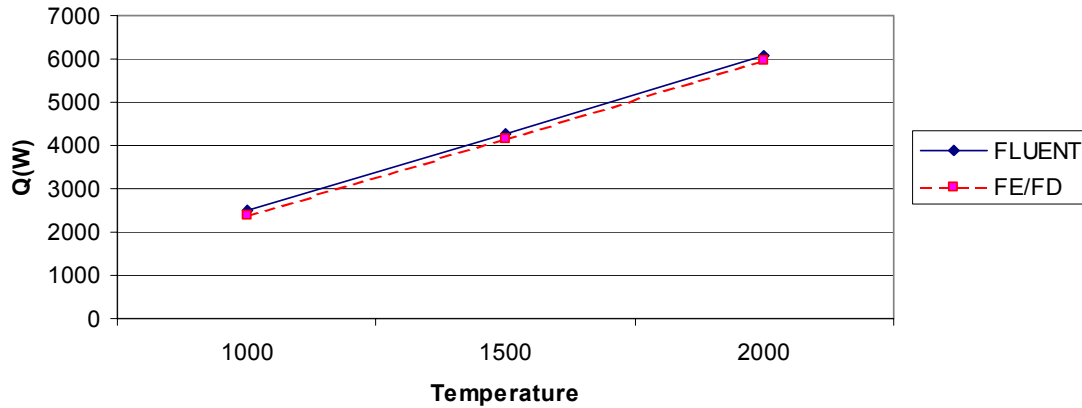


Figure 7.14 – Comparison of FLUENT and FE/FD Predictions of Heat Transfer for a Range of Source Temperatures

In addition to evaluating the accuracy of the FE/FD approximate model relative to the FLUENT model, it is important to evaluate its speed and reconfigurability for design purposes. The FLUENT model requires approximately 3 hours to converge for the mid-level mesh density reported in Figure 7.11. In contrast, the FE/FD model requires approximately 1.5 minutes. *The FE/FD approximate thermal model is approximately two orders of magnitude faster than the FLUENT model and yields results that are accurate within 10% of the FLUENT model with respect to total rates of steady state heat transfer.* It is also important to note that the FE/FD model is much more easily reconfigured for parametric and topological design changes than the FLUENT model. FLUENT models require recreation of a 3D solid model for each parametric or topological change in a model. The FE/FD model can be adjusted instantaneously during the design process.

Finally, since the FE/FD model is intended to support parametric and topology design and is introduced in this dissertation without prior utilization, it is important to validate

its performance in support of parametric and topology design for thermal performance. These aspects of validation are documented in Appendix A. As described in the appendix, the FE/FD approximate model has been shown to be effective for identifying changes in dimensions and limited changes in topology that improve the overall thermal performance of an initial structure.

Since the design spaces, problem formulations, and analysis models have been presented (and the analysis models validated) for both structural and thermal topology design, all of the components of the RTPDEM for each domain have been introduced. The next step is to weave the components together into a multi-stage, multifunctional topology design process, as described in the following section.

7.3.5 Multifunctional Design with the RTPDEM

The multi-stage, multifunctional implementation of the RTPDEM is organized according to Figure 3.14, with Options 1 and 2 in Figure 3.14 corresponding to range-based Stage 1A and model-based Stage 1B in Table 7.3. The decisions for range-based Stage 1A are organized according to Figure 3.16 with Designers 1 and 2 corresponding to the structural and thermal designers, respectively. As illustrated in Figure 7.15, the structural designer implements the RTPDEM process for the structural domain and communicates ranges of element area values and a space of possible topologies to the thermal designer. The thermal designer then implements the RTPDEM to improve the thermal performance of the design but makes changes to the structural design *only* within the dimensional ranges and sets of topologies specified by the structural designer.

The decisions for model-based Stage 1B are organized according to Figure 3.19 with Designers 1 and 2 corresponding to the structural and thermal designers, respectively. As

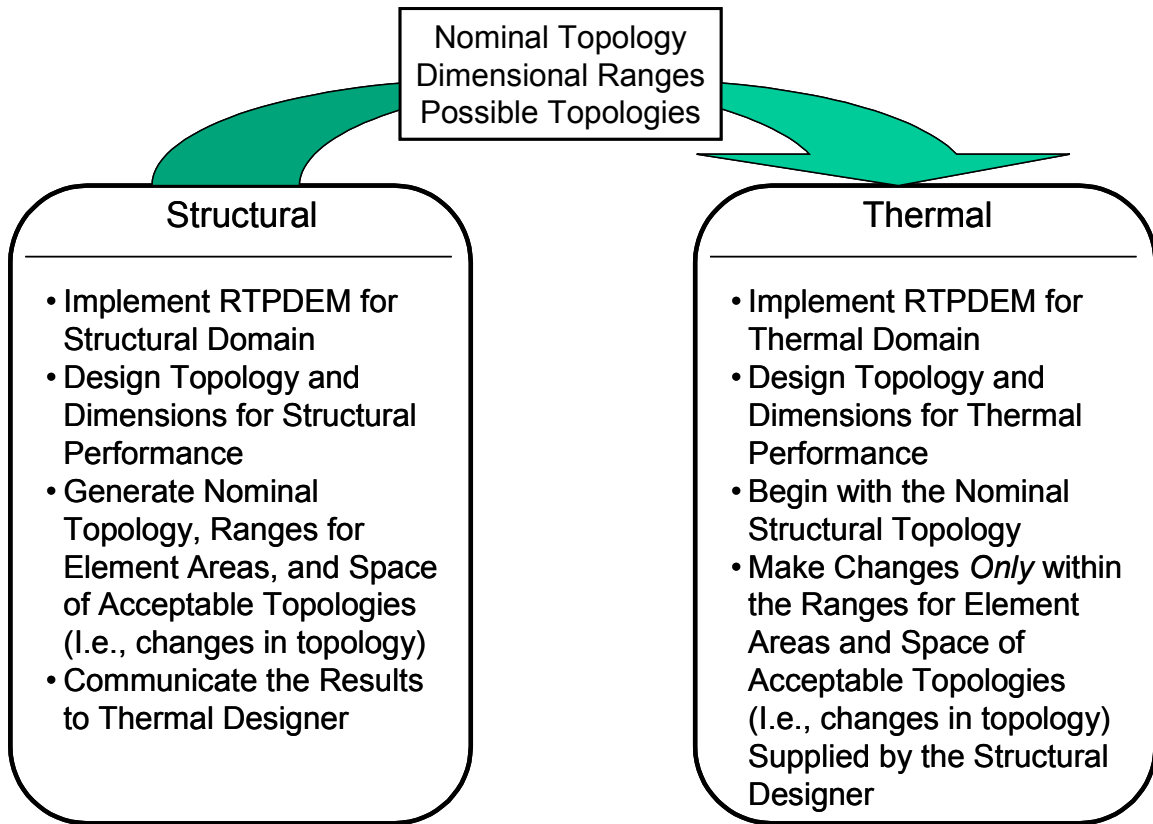


Figure 7.15 – Sequence of Events for Range-Based, Multi-Stage, Multifunctional Topology Design for Stage 1A of Table 7.3

illustrated in Figure 7.16, the structural designer implements the RTPDEM process as for Stage 1A design. In addition to communicating a nominal topology, ranges of dimensions, and sets of possible topologies, the structural designer also creates an approximate physics-based model for the structural domain and communicates it to the thermal designer. The thermal designer uses the approximate structural model to evaluate the impact of design changes (both topological and parametric) on structural performance. With the availability of the approximate structural model, the thermal designer is not limited to the ranges specified by the structural designer; instead, the thermal designer has the capability to make broader topological and parametric design

changes because he/she has the ability to evaluate and balance the impact of those changes on both structural and thermal performance.

The approximate model communicated by the structural designer is essentially the finite element model described in Section 7.3.3. The finite element-based approximate model has several beneficial features. As discussed in Section 7.3.4, the structural model is fast and relatively accurate compared with ANSYS models for evaluating the compliance and stress distribution of the combustor liner. It is important to note that approximate models do not have to be as accurate as their detailed counterparts. Their accuracy should be good enough to permit broad exploration and identification of superior regions of the design space. Computationally expensive, detailed simulations (e.g., FLUENT, ANSYS, etc.) can be used for subsequent detailed design and confirmation of properties and performance once the region of interest has been identified. Also, the finite element models are easily reconfigured to accommodate topological and parametric changes during the design process, in contrast with ANSYS models which require regeneration/recreation of a 3D solid model prior to analysis in order to accommodate topological or parametric changes. Another important feature of the thermal and structural analyses for this example is their compatibility. The control factors (i.e., element identifications and element dimensions) can be imported directly from structural to thermal analyses and vice versa.

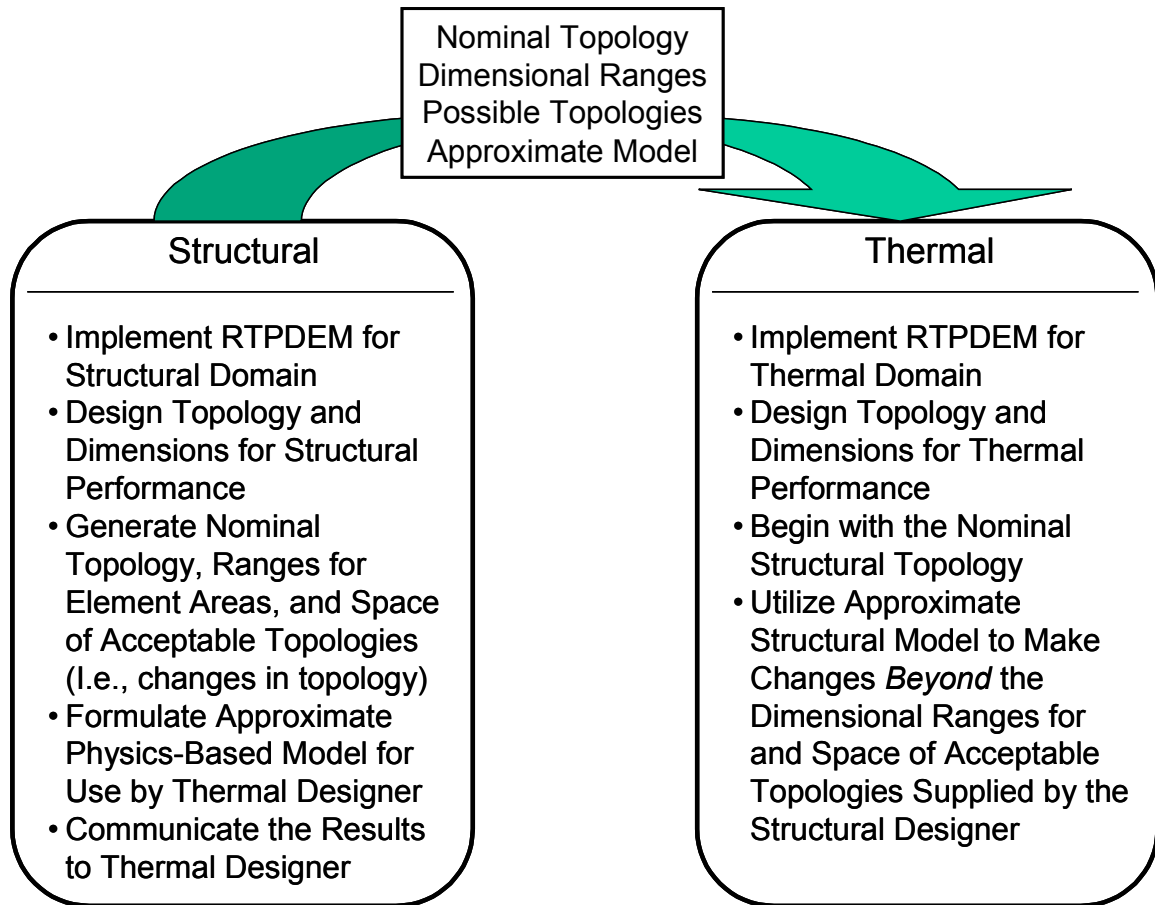


Figure 7.16 – Sequence of Events for Model-Based, Multi-stage, Multifunctional Topology Design for Stage 1B in Table 7.3

7.4 PRESENTATION AND DISCUSSION OF COMBUSTOR LINER DESIGNS

As described in Section 7.3, the RTPDEM has been instantiated for the structural and thermal domains and for distributed, multi-stage, multifunctional design for the combustor liner example. In this section, the multifunctional RTPDEM is applied for designing prismatic cellular materials that fulfill the structural and thermal requirements outlined in the previous sections.

As documented in Table 7.3, the combustor liner example is executed in three stages. In the first stage, multifunctional prismatic cellular materials are designed for the

combustor liner using the multifunctional RTPDEM. The first-stage design results are reported in Sections 7.4.1 through 7.4.3. In the second stage, the results obtained with the RTPDEM are compared with a heuristic design, generated without the benefit of systematic design methods. The details of the heuristically generated design are reported in Section 7.4.4. Finally in the third stage, the capabilities of the customized cellular combustor liner are compared with the general properties and performance of conventional combustor liners comprised of non-cellular alloys and superalloys, as described in the critical discussion in Section 7.5.

The first experimental stage of Table 7.3 includes substages 1A and 1B that correspond to the range-based and model-based approaches for implementing the multi-stage, multifunctional RTPDEM summarized in Figures 7.15 and 7.16, respectively. In each case, the structural designer is the lead designer, solves a robust topology design problem for the structural domain, and communicates ranged sets of design specifications to the subsequent thermal designer. These results serve as the starting point for thermal design for both range-based and model-based multifunctional design approaches. From the structural designer's perspective, the approaches differ because an approximate model of the structural domain must be created and communicated to the thermal designer for the model-based approach. Since the structural designer's implementation of RTPDEM is identical for the two approaches, a common set of structural design results is generated and reported in Section 7.4.1. For range-based design in Stage 1A of Table 7.3, the thermal designer accepts the ranged sets of topology designs from the structural designer and modifies the design for improved thermal performance, strictly within the ranges and sets of acceptable topologies specified by the structural designer. The results of this

design process are reported in Section 7.4.2. For model-based design in Stage 1B of Table 7.3, the thermal designer accepts *both* ranged sets of topology designs *and an approximate* physics-based *model* for the structural domain. The thermal designer makes broader changes to the structural design for improved thermal performance. To support these broader changes, the thermal designer uses the approximate structural model—along with thermal models—to evaluate and balance the impact of potentially extensive design changes on both the thermal and the structural domains. The results of this process are reported in Section 7.4.3.

7.4.1 Structural Design Results for Range-Based and Model-Based, Multi-stage, Multifunctional Topology Design for Stages 1A and 1B of the Experimental Plan of Table 7.3

The structural designer implements the RTPDEM for the structural domain as described in Section 7.3. The goal is to design prismatic cellular materials with structural properties that are robust to small changes in element dimensions or to small changes in topology (i.e., addition or removal of elements). If this can be achieved, then the subsequent thermal designer inherits designs with built-in flexibility for dimensional or topological adjustment, and the thermal designer can use this flexibility to modify the design for improved thermal performance. Robust and non-robust prismatic cellular material designs are presented in Tables 7.10 and 7.11, respectively. Recall that the mesostructures are symmetric; therefore, data is provided for only elements in a symmetric half of each slice of the cellular mesostructure.

The topology of the designs is the first item to investigate. Since the outer boundary of the combustor liner is supported with springs, it is reasonable for elements such as elements 3, 6, and 7 in Table 7.10 and elements 2 and 4 in Table 7.11 to appear in the

Table 7.10 – Robust Structural Design Results

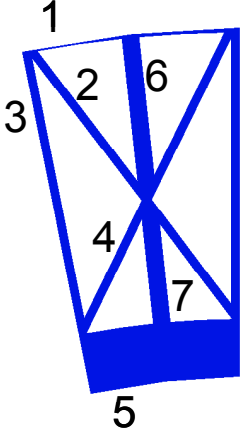
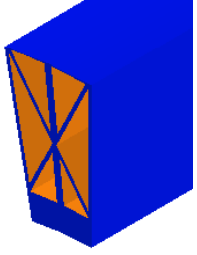
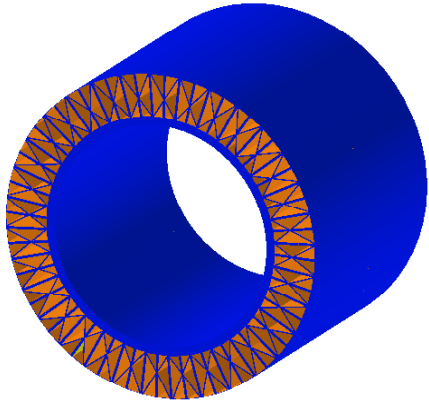
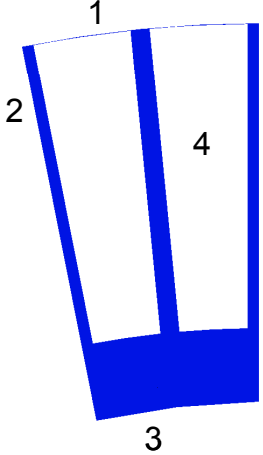
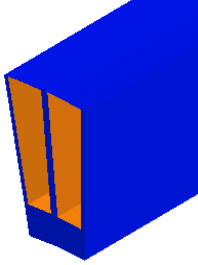
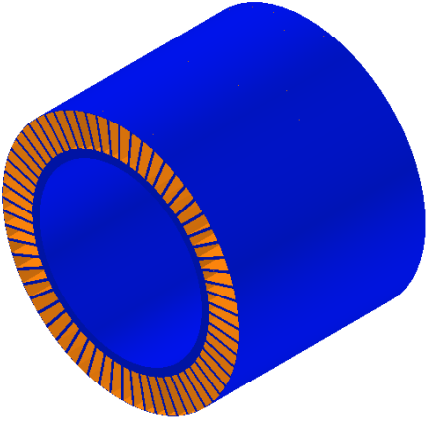
Cross-Section of a 1/32 Slice		Isometric View of 1/32 Slice		Complete Combustor Liner			
							
Element	Dimension and Range (mm)	Stress (MPa)	Nominal Topology	Acceptable Topology 1	Acceptable Topology 2	Sample Unacceptable Topology	Sample Unacceptable Topology
1	0.1 +/- 0.01	430	√	√	√	√	√
2	0.5 +/- 0.07	349	√		√	√	√
3	0.5 +/- 0.07	360	√	√	√	√	
4	0.5 +/- 0.07	403	√	√		√	√
5	3.9 +/- 0.39	437	√	√	√	√	√
6	1.0 +/- 0.1	564	√	√	√		√
7	0.9 +/- 0.09	423	√	√	√	√	√
Final Structure	C, Compliance	402.9		481.2	481.2	541.87	368.5
	Max Stress, S	564		728	728	9545	1410
Converged Ground Structure	C	123.63					
	ΔC	55.38					
	μ_c	142.8					
	$\Delta_\mu C$	62.0					
	σ_c	60.3					

Table 7.11 – Non-Robust Structural Design Results

Cross-Section of a 1/32 Slice		Isometric View of 1/32 Slice		Complete Combustor Liner	
					
Element	Dimension and Range (mm)	Stress (MPa)	Nominal Topology	Sample Unacceptable Topology	Sample Unacceptable Topology
1	0.1 +/- 0.01	430	√	√	√
2	0.6 +/- 0.08	536	√		√
3	4.0 +/- 0.4	430	√	√	√
4	1.3 +/- 0.13	433	√	√	
Final Structure	C, Compliance		337.3	458.70	458.70
	Max Stress, S		536	9830	9830
Converged Ground Structure	C		108.94		
	ΔC		45.6		
	μ_c		143.65		
	$\Delta_\mu C$		58.12		
	σ_c		90.0		

final topology to support the inner, combustion-side surface of the combustor liner which is exposed to pressures of 100 MPa. The support provided by those radial elements reduces the hoop stresses in the elements along the inner surface (i.e., element 5 in Table 7.10 and element 3 in Table 7.11). Additional elements (i.e., elements 2 and 4) are included in the robust design in Table 7.10 to accommodate topological noise, in the form of potential element removal in subsequent design stages and/or cracks or other imperfections in cell walls and joints. Essentially, the extra elements provide additional pathways for transmitting mechanical loads from the inner, combustion-side surface of the combustor liner to the spring-supported outer surface.⁷

The dimensions for the structures are reported in each table below the diagrams. The element numbers refer to the labels in the upper left diagram. The dimensions are reported in terms of nominal values and ranges. The ranges correspond to the ranges calculated with Equation 6.3. Ranges are reported for the non-robust design for completeness (and because they will be used in the thermal design process for comparison purposes), but they are not typically calculated or considered in a non-robust topology design process. Stresses are also indicated for each of the elements in the final topology. Responses are reported in the bottom portion of each table. The notation on each of the responses corresponds to the notation in Equations 7.15 through 7.17, and the values are reported for the nominal topologies illustrated in the tables. Two different sets of responses are reported—one for the final structure (as pictured) and one for the

⁷ As a side note, it is important to note the significance of the spring supports. Of course, the spring supports simulate a semi-rigid structure encasing the combustor liner. In addition, the semi-rigid nature of the springs makes it possible for portions of the load on the inner, combustion-side surface to be transmitted through the inner structure of the combustor liner to outer surface supports. If the outer surface were not supported at all, the hoop stresses in the inner ring would exceed the yield stress of the material. If the outer surface were rigidly supported (i.e., fixed), the structure would not be permitted to expand as it is heated, and stresses throughout the structure would exceed the yield stress of the material by as much as an order of magnitude.

converged ground structure. The final and converged ground structures refer to two different points in the solution process. The solution process begins with the ground structure pictured in Figure 7.2 which converges to a final topology of thick elements and extremely thin elements. This is the converged ground structure. From this converged ground structure, elements with extremely small dimensions (near the lower bound) are removed from the structure. The structure is modified again with an optimization algorithm until the final structure is obtained. The final structure is pictured in the diagrams in the table. Whereas the responses of the final structure are of interest in an engineering sense, the responses of the converged ground structure are important for comparison purposes. Since compliance and all associated responses (e.g., ΔC) are strongly dependent on the number of elements in the structure, it is important to compare robust and non-robust structures with the same number of elements. Then, the magnitudes of each of the responses can be compared and contrasted.

It is evident from the responses that the non-robust topology in Table 7.11 has lower (better) compliance and lower variation in compliance due to dimensional variation (although this objective was not considered during the solution process for the non-robust design). In contrast, the robust topology has a much lower standard deviation of compliance due to topological variation. The robust structural design embodies a tradeoff between nominal compliance (which is higher than the non-robust design) and standard deviation of compliance (which is lower than the non-robust design). It is reasonable for the robust design to exhibit lower standard deviation of compliance because the extra elements in its topology compensate for any missing elements or nodes, thereby improving the compliance of a structure with imperfections.

To illustrate the enhanced capability for topological modification embodied by the robust design, several sample topologies are evaluated for both the robust and the non-robust topology designs. Several possible topologies—in addition to the nominal topology—are listed in Tables 7.10 and 7.11.⁸ As demonstrated by the compliance and maximum stress values, some of the topologies should perform well, even with missing elements, while others perform poorly and are labeled as sample unacceptable topologies. Acceptable topologies 1 and 2 in Table 7.10, along with the nominal topology, represent the space of acceptable topologies to be communicated to the subsequent thermal designer. The thermal designer is then free to choose any of these topologies in order to achieve maximum improvement in thermal performance. In contrast, two sample unacceptable topologies are reported for both robust and non-robust designs. As evidenced by the stress values for the unacceptable topologies, the structures are likely to yield if the indicated elements are removed. Note that *no* elements can be removed from the non-robust structural design. It is sensitive to imperfections (such as cracks or missing joints), and it is also inflexible for potential topological changes during the thermal design process.

Verification of Structural Results

The results reported in Tables 7.10 and 7.11 are verified in several ways. First, as discussed previously, the topologies are inspected and judged to be reasonable from a load-bearing perspective. For example, the additional elements in the robust topology are clearly aimed at lowering the standard deviation of compliance in the event of subsequent element removal or imperfections. Secondly, the iterative search algorithms are monitored for convergence. As illustrated in Figure 7.17, the algorithms converged

⁸ The elements included in a specific topology are denoted with check marks in the table.

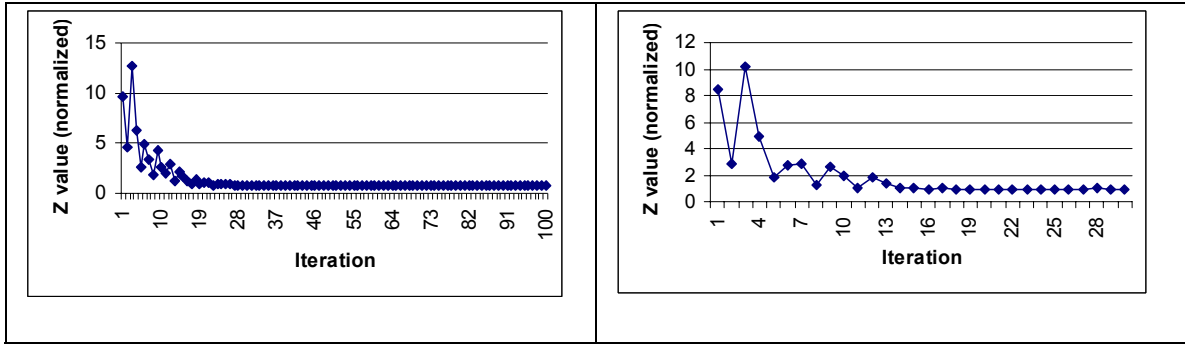


Figure 7.17 – Convergence Plots for Non-Robust (Left) and Robust (Right) Structural Topology Design

smoothly in both cases. In addition, multiple starting points are utilized. Once a topology is obtained, it is re-optimized to improve the results. Thirdly, other local minima are obtained and compared with the reported results. For example, a second dimensionally robust design can be obtained by considering only nominal compliance and variation in compliance due to dimensional variation (without considering standard deviation in compliance due to topological noise). The design is identical to the non-robust design reported in Table 7.11, as expected, because the only impetus for adding additional elements is to reduce the variation in compliance due to topological noise. Fourth, the sensitivity of the designs to the rigidity of the spring supports is investigated. Firmer springs more closely simulate rigid supports and make it difficult to satisfy stress constraints throughout the structure. Finally, alternative starting ground structures are investigated. Increasing the number of nodes in the radial direction does not yield any meaningful structures that differ from those in the tables. Increasing the number of nodes in the circumferential direction yielded a reasonable structure that differs from those in the tables, as illustrated in Figure 7.18. Unfortunately, it is not possible to simultaneously satisfy stress constraints and volume fraction constraints for the structure.

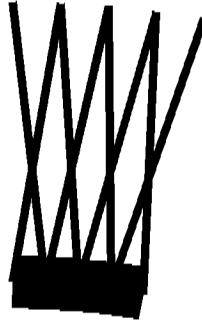


Figure 7.18 – Structural Topology Design Based on a 5x4 Node Mesh

In addition, for validation and verification purposes, the results of this section are compared with the performance of a heuristically derived design in Section 7.4.4 and with the performance of conventional alloy or superalloy-based combustor liners in Section 7.5.

Structural Design for Stage 1B

For Stage 1B, the structural designer also creates an approximate physics-based model for the structural domain and communicates it to the thermal designer. In this case, the approximate model is simply a MATLAB-based implementation of the approximate finite element analysis described in Section 7.3. As noted in Section 7.3, the approximate structural model is particularly well-suited for this role because it is relatively fast and accurate compared with more computationally expensive ANSYS simulations and because it can be reconfigured instantaneously to analyze different topologies and dimensional variations.

7.4.2 Thermal Design Results for Range-Based, Multi-stage, Multifunctional Topology Design for Stage 1A of the Experimental Plan in Table 7.3

In the second multifunctional topology design stage, the thermal designer adjusts the design generated by the structural designer. Two approaches are proposed in Section 3.4 for integrating the two functional domains and associated designers. The first range-based approach involves communicating ranges of design specifications and sets of acceptable topologies from the first (structural) designer to the subsequent (thermal) designer. Implementation of this approach for the combustor liner example is described in this section.

The thermal designer begins his/her design process with the following information:

- The nominal robust structural design reported in Table 7.10,
- The robust ranges for element dimensions reported in Table 7.10,
- And the sets of acceptable topologies, including the nominal topology and the two acceptable modified topologies, as reported in Table 7.10.

According to the range-based multifunctional topology design approach summarized in Figure 7.15, the thermal designer has the flexibility to adjust the design within the ranges and sets of topologies offered by the structural designer. In other words, the thermal designer may choose the nominal topology or any of the acceptable topologies in Table 7.10, and the dimensions of those structures may be adjusted within the ranges specified in Table 7.10 without significantly deteriorating the structural performance of the design.

To identify precise design specifications, the thermal designer solves the compromise DSP presented in Figure 7.5 with the constants and assumptions listed in Tables 7.1, 7.2, and 7.5. The only modified assumption is an adjustment of $T_{\text{hot-inner}}$ from 2000 K to 1700

K to account for the temperature drop across a proposed thin ceramic coating on the interior of the combustor liner. The function of the ceramic coating is to shield the combustor liner from the most extreme combustion temperatures and to prevent melting or yielding at high temperatures. The criteria by which the thermal design is measured include the total rate of steady state heat transfer from the structure to the cooling fluid (air) flowing through its cells. The rate should be maximized to lower the temperature within the cell walls. It is important to reduce the temperature in the walls because yield strength is a function of the temperature of the base material, ranging from 400 MPa at 1650 K to 1500 MPa at 300 K. In other words, a cell wall with an average temperature of 1650 K yields if exposed to stresses greater than 400 MPa. Therefore, it is important to evaluate both the average temperature in each element or wall and the state of stress in the element. The melting temperature of the material is greater than 2200 K, and should not be exceeded.

In Table 7.12, the design specifications and thermal and structural behavior of two designs are compared. On the left-hand side of Table 7.12, design specifications and responses are recorded for the nominal design proposed by the structural designer and recorded in Table 7.10. The dimensional ranges and set of acceptable topologies determined by the structural designer are recorded in Table 7.10, and the ranges are repeated in Table 7.12 along with the nominal design specifications. On the right-hand side of Table 7.12, design specifications and thermal and structural responses are reported for a design that has been modified within the bounds of the dimensional ranges and set of acceptable topologies supplied by the structural designer. It has been modified to maximize the total rate of steady state heat transfer.

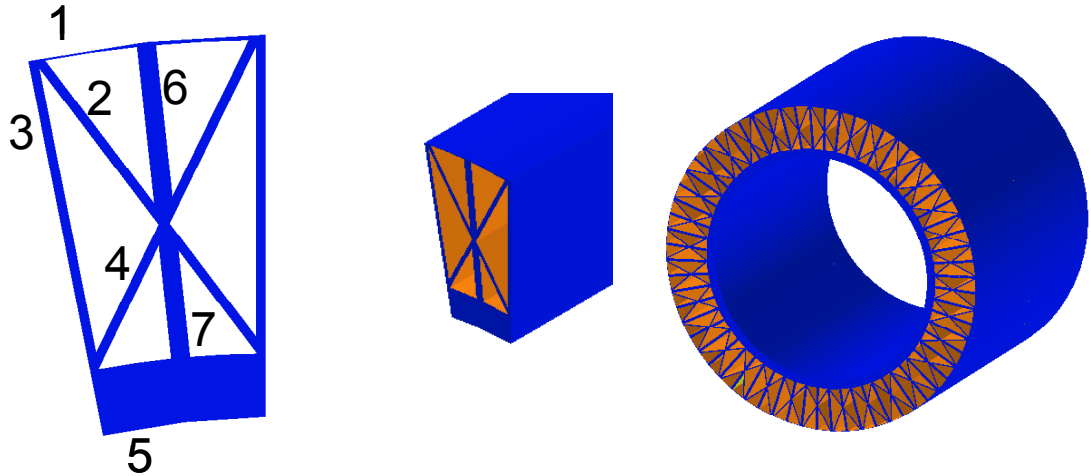
The design specifications for the modified design differ dimensionally but not topologically from the nominal design specifications. There is no topological difference because the nominal topology offers the highest rates of steady state heat transfer among the set of acceptable topologies; therefore, a modified design based on the nominal topology is reported in Table 7.12. In order to increase the rate of steady state heat transfer, most of the dimensions have been increased or decreased to the bounds specified by the structural designer. This pattern suggests that further increases in heat transfer rates are possible if the bounds are broadened—a topic for investigation in Stage 1B design in the next section.

From the data, it is clear that both designs have acceptable stress levels in all of their elements, relative to the average temperatures in those elements. The modified design has slightly higher average temperatures, a phenomenon linked to the dimensional changes (relative to the nominal design) that enhance conductivity throughout the structure and enhance the total rate of steady state heat transfer. The stresses are slightly different in the modified design due to dimensional changes, but the differences are not significant. The increase in the total rate of steady state heat transfer, relative to the nominal unmodified design, is significant at nearly 10%.

For comparison, the thermal properties of the non-robust design from Table 7.11 are reported in Table 7.13 along with the final specifications and properties of a design based on +/- 10% changes in the dimensions of the nominal topology. Since the design is non-robust, no topological changes are permitted. Technically, dimensional changes would not be permitted without iterative reanalysis of structural properties, but modification is performed in this case exclusively for comparison with results based on the robust design.

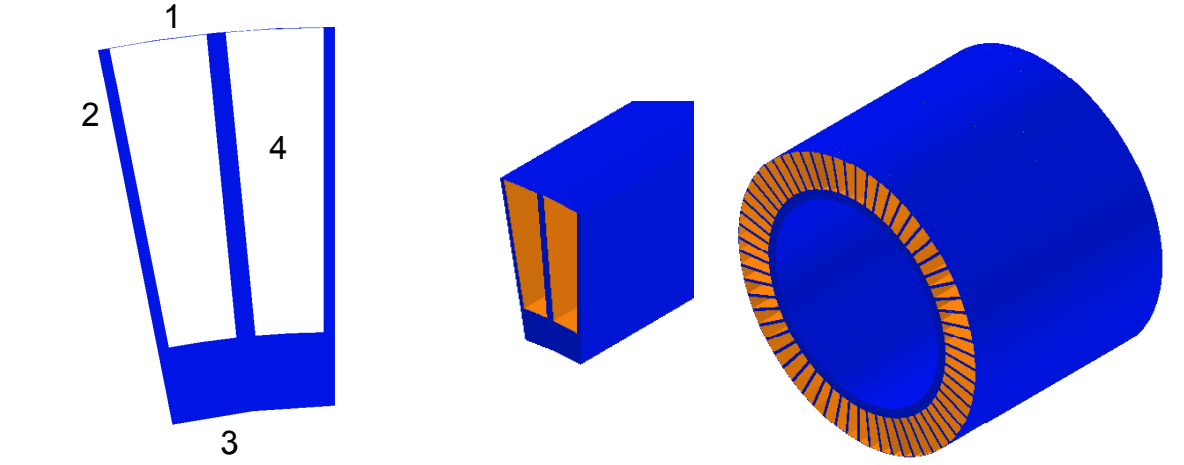
As shown in Table 7.13, dimensional modification improves the thermal performance of the non-robust design by only 3%, compared with a 10% improvement realized with the robust design. More importantly, the total rates of steady state heat transfer achieved by the non-robust design—with or without dimensional modification—are lower than those achieved by the robust design by more than 30%. It is not a coincidence that the robust design performs better in the second domain than the non-robust design. A robust design offers freedom for modification from its nominal dimensions *and topological specifications* in order to enhance multifunctional performance. Therefore, a subsequent designer can add or remove elements from a nominal topology, provided that the resulting topology is equivalent to one of the acceptable topologies specified by the lead (structural) designer. It is possible to remove elements from the robust design to realize the non-robust design; i.e., the non-robust design is a topological subset of the robust design. Such scenarios are likely in robust topological design because topologically robust designs tend to resemble non-robust or dimensionally robust designs with extra elements added to compensate for potential element removal or imperfections, as observed in this example and the example of Chapter 6. When this is the case, the robust design *cannot* exhibit inferior performance to the non-robust design. In fact, the topological and dimensional flexibility are likely to enable superior performance—relative to the non-robust design—by expanding the design space of possible solutions. In this case, performance in the subsequent (thermal) domain was significantly improved by the generation and communication of robust, ranged sets of designs.

Table 7.12 – Results of Range-Based Stage 1A Thermal Design, Based on the Robust Structural Design of Table 7.10, Modified for Thermal Performance within the Ranges Specified by the Structural Designer



Nominal Design				Design Modified within Ranges			
Element	Dimension and Range (mm)	Avg. Temp. @ Outlet(K)	Stress (MPa)	Element	Final Dimension (mm)	Avg. Temp. @ Outlet(K)	Stress (MPa)
1	0.1 +/- 0.01	603	430	1	0.11	625	442
2	0.5 +/- 0.05	691	349	2	0.55	712	295
3	0.5 +/- 0.05	952	360	3	0.55	961	345
4	0.5 +/- 0.05	1129	403	4	0.55	1146	440
5	3.9 +/- 0.39	1621	437	5	3.5	1625	446
6	1.0 +/- 0.1	712	564	6	1.1	736	583
7	0.9 +/- 0.09	1178	423	7	1.0	1194	449
\dot{Q} , Total Rate of Steady State Heat Transfer (W)			3707	\dot{Q} , Total Rate of Steady State Heat Transfer (W)			3910
C, Compliance			402.9	C, Compliance			396.78

Table 7.13 – Results of Range-Based Stage 1A Thermal Design, Based on the Non-Robust Structural Design of Table 7.11, Modified for Thermal Performance within Ranges Consistent with Those for Robust Designs in Table 7.12



Nominal Design				Design Modified within Ranges			
Element	Dimension and Range (mm)	Avg. Temp. @ Outlet(K)	Stress (MPa)	Element	Final Dimension (mm)	Avg. Temp. @ Outlet(K)	Stress (MPa)
1	0.1 +/- 0.01	781	430	1	0.11	801	431
2	0.6 +/- 0.06	1080	536	2	0.66	1088	495
3	4.0 +/- 0.4	1642	430	3	4.4	1634	415
4	1.3 +/- 0.13	1103	433	4	1.43	1112	465
\dot{Q} , Total Rate of Steady State Heat Transfer (W)			2499	\dot{Q} , Total Rate of Steady State Heat Transfer (W)			2571
C, Compliance			342.2	C, Compliance			380

7.4.3 Thermal Design Results for Model-Based, Multi-stage, Multifunctional Topology Design for Stage 1B of the Experimental Plan in Table 7.3

Two approaches are proposed in Section 3.4 for collaboration between multiple domain-specific designers in a multifunctional topology design problem. In the previous section, the first, range-based approach was investigated in which the thermal designer modifies a design within the bounds specified by the lead structural designer. In this section, the second, model-based approach is investigated in which the lead structural designer communicates *not only* ranges of design specifications *but also* an approximate physics-based model of the structural domain. The thermal designer uses the

approximate structural model to evaluate the impact of design changes on structural performance in addition to thermal performance. This capability enables a subsequent thermal designer to make broader changes to the nominal structural design to improve thermal performance while simultaneously minimizing the adverse impact of those changes on the structural performance of the design.

The thermal designer begins the thermal design stage with the following information:

- The nominal robust design reported in Table 7.10,
- The robust ranges of dimensions and sets of acceptable topologies reported in Table 7.10, and
- The approximate physics-based model of the structural domain supplied by the structural designer.

According to the model-based multifunctional topology design approach summarized in Figure 7.16, the thermal designer has the flexibility to adjust the design *beyond* the ranges and sets of topologies offered by the structural designer. However, if he/she chooses to modify the design outside of the ranges and topology sets, he/she must use the approximate structural model along with his own thermal models to evaluate structural performance and to balance achievement of both structural and thermal performance objectives. The approximate structural model is needed because the design specifications are not guaranteed to exhibit robust structural performance outside the robust ranges and sets of topology specified by the structural designer. Outside the bounds, structural performance may deteriorate significantly relative to its nominal values.

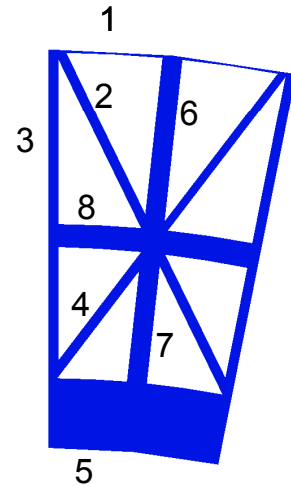
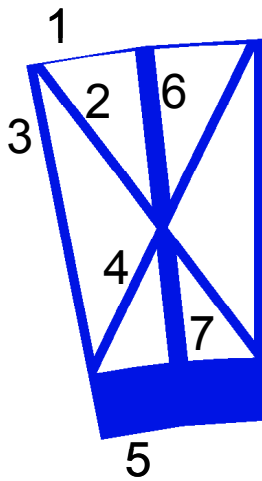
The thermal designer solves the compromise DSP presented in Figure 7.6 with the constants and assumptions listed in Tables 7.1, 7.2, and 7.5. Again, the combustion-side

temperature is adjusted from 2000 K to 1700 K to account for the proposed protective ceramic layer on the inside of the combustor liner. The criteria by which the thermal design is measured include the total rate of steady state heat transfer and the average temperature in each element. As described in Section 7.4.2, the yield stress in the cell walls is an increasing function of temperature. Total rates of steady state heat transfer must be relatively high to lower the temperature within the cellular structure, thereby increasing its threshold for mechanical stress.

In Tables 7.14 and 7.15, the design specifications and thermal and structural behavior of the nominal design generated by the structural designer are compared with specifications and behavior of a design that has been modified extensively according to the model-based, multifunctional topology design approach. The design is modified beyond the bounds specified by the structural designer but within the broader bounds recorded in Table 7.14. The broader modifications include the possibility of removing two elements (#2 and/or #4) and adding another element (#8). The design variable ranges reported in Table 7.14 are also much broader than the ranges reported in Table 7.12 as specified by the lead structural designer. It is important to recall the use of density variables—as described in Section 3.5—to simulate the addition or removal of elements from a thermal topology.

In Table 7.14, the structural and thermal performance of the nominal structural design (without modification) is compared with the performance of the nominal design after it has been modified broadly for maximum heat transfer rate. Compliance and stress are not considered as objectives or constraints for this design. An improvement in the total rate of steady state heat transfer of 500 W is realized relative to the nominal design. As

Table 7.14 – Results of Stage 1B Thermal Design, Based on the Robust Structural Design of Table 7.10, Modified Exclusively for Thermal Performance within Broad Ranges



Nominal Design				Broad Design Ranges			Design Modified within Broad Ranges			
Element	Dimension and Range (mm)	Avg. Temp. @ Outlet (K)	Stress (MPa)	X_L	X_U	Add/Remove Possible	Element	Final Dimension (mm)	Avg. Temp. @ Outlet (K)	Stress (MPa)
1	0.1	603	430	0.09	0.15		1	0.09	851	409
2	0.5	691	349	0.375	0.75	√	2	0.75	970	233
3	0.5	952	360	0.375	0.75		3	0.75	1230	254
4	0.5	1129	403	0.375	0.75	√	4	0.75	1300	339
5	3.9	1621	437	2.9	4.0		5	4.0	1671	350
6	1.0	712	564	0.75	1.5		6	1.49	870	447
7	0.9	1178	423	0.675	1.4		7	1.4	1311	450
8	x	x	x	0.375	0.75	√	8	0.75	1065	410
\dot{Q} , Total Rate of Steady State Heat Transfer (W)			3707				\dot{Q} , Total Rate of Steady State Heat Transfer (W)			4217
C, Compliance			402.9				C, Compliance			523

Table 7.15 – Results of Model-Based Stage 1B Thermal Design, Based on the Robust Structural Design of Table 7.11, Modified for Thermal and Structural Performance within Broad Ranges. A Family of Designs is Illustrated with a Range of Tradeoffs Between Structural and Thermal Performance.

Nominal Structural Design: All Weight on Structural				Balanced Design: Weights Split Between Structural and Thermal				Thermal Design: All Weight on Thermal			
Elem	Dimension and Range (mm)	Avg. Temp. @ Outlet (K)	Stress (MPa)	Elem	Final Dimen (mm)	Avg Temp @ Outlet (K)	Stress (MPa)	Elem	Final Dimension (mm)	Avg. Temp @ Outlet (K)	Stress (MPa)
1	0.1	603	430	1	0.09	690	448	1	0.09	851	409
2	0.5	691	349	2	0.375	824	496	2	0.75	970	233
3	0.5	952	360	3	0.375	1091	430	3	0.75	1230	254
4	0.5	1129	403	4	0.75	1267	346	4	0.75	1300	339
5	3.9	1621	437	5	3.0	1677	457	5	4.0	1671	350
6	1.0	712	564	6	1.25	767	524	6	1.49	870	447
7	0.9	1178	423	7	1.41	1276	337	7	1.4	1311	450
8	x	x	x	8	0.375	937	441	8	0.75	1065	410
\dot{Q} , Total Rate of Steady State Heat Transfer (W)			3707	\dot{Q} , Total Rate of Steady State Heat Transfer (W)			4019	\dot{Q} , Total Rate of Steady State Heat Transfer (W)			4217
C, Compliance			402.9	C, Compliance			384	C, Compliance			523

predicted in the discussion of the previous section, an improvement in thermal performance is also observed relative to the multifunctional design in Table 7.12, obtained with the tighter ranges and topological options of the range-based approach. However, there is a cost in terms of structural performance, measured by a 25% increase in compliance relative to the nominal design and the range-limited design.

In many cases, the deterioration of first-stage (structural) objectives may be so great that it offsets any gains in second-stage (thermal) performance achieved by broadening the range of permissible topological and parametric changes. The approximate model created and shared by the first-stage (structural) designer is intended to alleviate this effect. The approximate model is utilized—along with thermal models possessed by the thermal designer—to generate the compromise design reported in the center columns of Table 7.15. It is clear from the data that utilizing the structural model is an effective technique for minimizing the impact on first-stage objectives. Whereas only structural objectives or thermal objectives are considered for generating the designs in the left-hand and right-hand columns of Table 7.15, respectively, both structural *and* thermal objectives are considered for the design in the center columns. Its topology is identical to that of the thermal design, but its structural and thermal performance is quite different. As recorded in Table 7.15, the design exhibits a total rate of steady state heat transfer that is mid-way between the structural and thermal designs, but its structural compliance is actually *lower* than either of the designs. By utilizing both thermal *and structural* models and broadening the range of permissible parametric and topological changes, it is possible to improve the total rate of steady state heat transfer, relative to the structural design, without worsening its structural performance.

The evidence suggests that utilization of an approximate model improves a subsequent designer's ability to improve his/her own objectives via potentially broad design changes while balancing the objectives of the previous designer. However, there is a computational cost of utilizing the structural model. In this case, the combined thermal and structural analysis requires approximately 90 seconds per iteration on a computer with a Pentium M processor and 768 MB of RAM. Approximately one second of this time is spent on structural analysis; thus, the decrease in computational efficiency caused by including structural analysis is minimal. This is a reflection of the approximate, computationally efficient, but relatively accurate nature of the approximate structural model. These features are important for the reasons discussed in Section 3.5. Another factor contributing to the computational expense of this model-based approach is the larger design space that is likely to require greater numbers of design iterations for effective search.

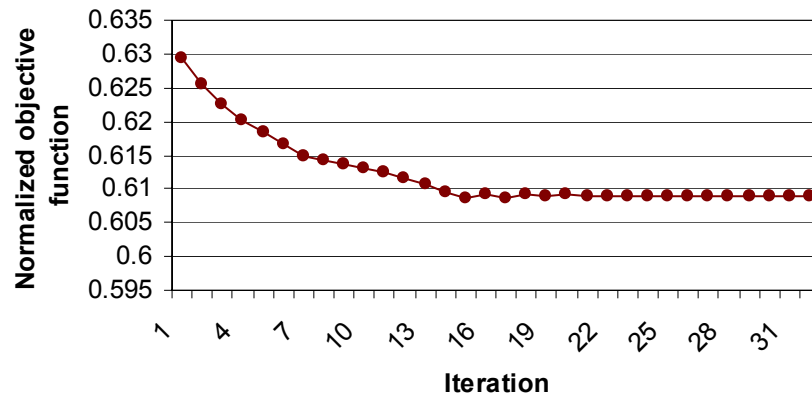


Figure 7.19 – Convergence Plot for Thermal Redesign of the Robust Structural Design

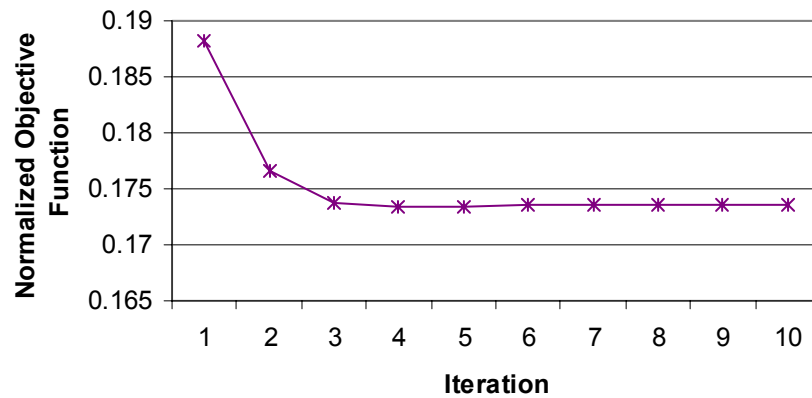
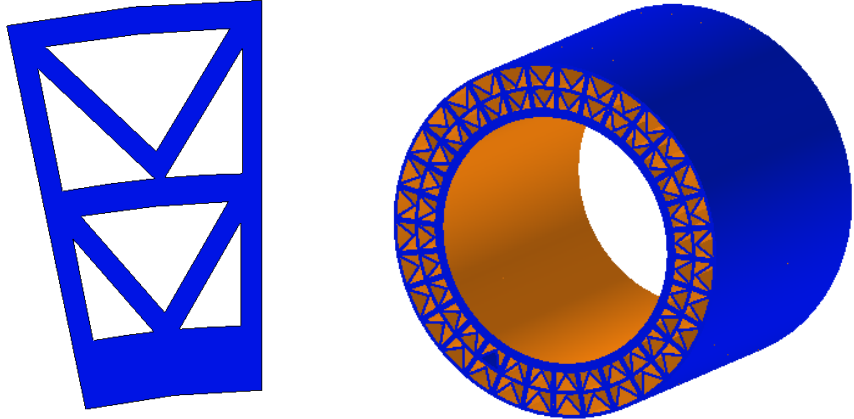


Figure 7.20 – Convergence Plot for Thermal/Structural Design with Broad Ranges. The Resulting Design is on the Right-Hand Side of Tables 7.14 and 7.15.

Verification of Thermal Results

The results presented in Sections 7.4.2 and 7.4.3 have been verified in several ways. First, the results have been interpreted as described in the text to insure that they are reasonable. The designs are compared with other local minima such as nominal designs versus modified designs in Tables 7.12 and 7.13 and families of designs in Table 7.15. This information is valuable to confirm trends in the values of goals, design variables, and constraint functions. For example, the total rates of steady state heat transfer should be higher for the modified designs than for the nominal designs in Tables 7.12 and 7.13 and the rates should be higher for the robust design than for the non-robust design. Similarly, tradeoffs should be apparent between structural and thermal objectives in the family of designs reported in Table 7.16. All of these trends are observed in the actual data. Secondly, the search/optimization algorithms have been monitored for smooth convergence. Sample convergence plots are included in Figures 7.19 and 7.20. Thirdly, the designs are compared with the performance of a heuristic structure that has been

Table 7.16 – Data for a Heuristically Designed Structure			
			
Heuristic Design			
Element	Dimension (mm)	Avg. Temp. @ Outlet(K)	Stress (MPa)
1	1.33	708	263
2	1	767	99
3	0.67	1084	587
4	1.33	911	264
5	1	1269	52
6	3.33	1662	336
\dot{Q} , Total Rate of Steady State Heat Transfer (W)			4020
C, Compliance			697.4

designed by intuition, without the benefit of the RTPDEM or any other systematic design method. The comparison is discussed in the following section.

7.4.4 Results for Stage 2: Comparing the Performance of the Designed Structures with the Performance of a Heuristically Designed Structure

The experimental plan outlined in Table 7.3 includes Stage 2 in which the characteristics of the designs obtained with the RTPDEM are compared with those of a heuristically design structure illustrated in Table 7.16. The heuristic structure was designed ‘by hand’ without the assistance of a systematic design method or search/optimization routine. It was generated in a trial-and-error process using engineering intuition. The basic structure was obtained by simultaneously considering

manufacturing constraints on volume fractions of solid material and maximum and minimum cell wall dimensions. The triangular passageways were added for increased rates of steady state heat transfer and to lower temperatures throughout the structure. Due to the trial-and-error design process, the heuristic structure actually took much *longer* to design than the other alternatives illustrated in Tables 7.10 through 7.15.

With respect to thermal and structural performance, the heuristic structure performs relatively well, but it cannot compete with the designs generated using the model-based, multi-stage, multifunctional RTPDEM with communication of ranged sets of specifications and approximate physics-based models. A comparison of the heuristic design in Table 7.16 with the thermal design in Tables 7.15 and 7.14 reveals that the heuristic design offers higher (worse) levels of compliance and lower levels of the total rate of steady state heat transfer. Also, it is clear that some elements are not fully utilized from a mechanical perspective because the state of stress in the elements is very low (e.g., elements 2 and 5). Designed structures such as those in Table 7.15 are topologically and dimensionally tailored so that all of the elements carry loads *and* contribute to the total rate of steady state heat transfer. In this way, the structures simultaneously achieve superior levels of structural and thermal objectives. As a final note, the design in Table 7.16 is similar to the design used for validation of the thermal and structural analysis codes in Section 7.3.4 (the volume fraction has been reduced to make the structure manufacturable) and the reader is referred to that section for verification of the analysis results.

7.5 CRITICAL DISCUSSION OF THE EXAMPLE RESULTS

The results of this example support many insights into the effectiveness, advantages, and limitations of the RTPDEM and its usefulness for multifunctional materials design applications. First, the combustor liner example provides evidence that the RTPDEM is an effective method for *multifunctional*, robust topology design as proposed in Hypothesis 2. The RTPDEM is implemented in a two-stage sequence for the combustor liner example, with a lead structural designer followed by a subsequent thermal designer. Two alternative RTPDEM-based, multi-stage, multifunctional topology design approaches are implemented: (1) a range-based approach in which ranges of design specifications and sets of acceptable topologies are generated by a lead designer and shared with subsequent designers and (2) a model-based approach in which both ranged sets of design specifications and approximate domain-specific models are shared with subsequent designers. The results are compared with three classes of benchmark designs:

- The *first* class of non-robust designs is generated using the two alternative multi-stage, multifunctional robust topology design approaches *without* the use of robust design techniques. Results are reported in Tables 7.11 and 7.14.
- The *second* class of designs is generated by designing exclusively for structural objectives, without modifying the design for thermal objectives. Results are reported in the left-hand columns of Tables 7.12 through 7.15.
- The *third* class of design is generated heuristically via trial-and-error methods without the benefit of systematic design methods or automated search techniques. Results are reported in Table 7.16.

By comparing the RTPDEM results with the first class of designs, it is observed that the robust designs provide more flexibility and topological options for subsequent designers. In this example, the flexibility is shown to facilitate improvement of performance in a subsequent or secondary functional domain significantly. The space of possible topologies that accompanies a robust design is particularly useful for a subsequent designer who may choose the topology that most significantly improves performance in his/her functional domain. Often, non-robust topologies are subsets of robust topologies, as observed in this example. When this is the case, the robust design *cannot* exhibit inferior performance to the non-robust design; furthermore, the topological flexibility of the robust design can lead to improved subsequent or second-stage functional performance relative to that of the non-robust design, as observed in this example. Further improvements in second-stage functional performance can be obtained by modifying the design within the parametric ranges shared by the lead (structural) designer. Non-robust designs do not offer this topological or parametric flexibility, and their multifunctional performance is significantly worse than that of the robust designs in this example.

By comparing the RTPDEM results with the second class of designs, it is observed that the range-based and model-based methods for sharing information between designers significantly improve second-stage (thermal) design performance with varying effects on the first-stage (structural) performance of the design. The performance of RTPDEM-based designs is compared with the performance of nominal designs in Tables 7.12, 7.14 and 7.15 that have not been modified for improved thermal performance. It is observed that significant improvement in second-stage (thermal) performance is obtained with little

impact on first-stage performance objectives by modifying the nominal design within the ranges and topological sets shared by the lead (structural) designer. By modifying the nominal design *beyond* the ranges and topological sets specified by the lead designer, the subsequent (thermal) designer multiplies the improvement in second-stage (thermal) objectives, at a significant cost in terms of first-stage (structural) objectives. It is observed that deterioration of first-stage (structural) objectives can be alleviated by utilizing the model-based approach. With the model-based approach, the subsequent (thermal) designer can utilize approximate structural models supplied by the structural designer in conjunction with his own thermal models to balance the multifunctional objectives. Results reported in Table 7.15 support the conclusion that this is an effective technique. There are both advantages and computational costs of this approach, as discussed subsequently in this section.

By comparing the RTPDEM results with the third class of designs in Table 7.16, it is observed that the RTPDEM offers improved multifunctional (structural and thermal) performance relative to a structure that is designed without systematic design methods or automated search techniques. Whereas mesostructures generated with the RTPDEM are tailored topologically and dimensionally so that all of the walls carry loads and contribute to heat transfer, material is not used as effectively in the heuristic structure, as demonstrated by the fact that some walls are not supporting significant mechanical loads.

In addition to the observed quantitative, performance-related benefits of utilizing the multifunctional RTPDEM, there are also qualitative benefits of utilizing such an approach. These benefits include reduced iteration compared with ‘over-the-wall’ approaches and enhanced capabilities for leveraging the domain-specific expertise of

multiple designers relative to fully integrated design approaches. Further discussion is provided in Section 3.4.

On the other hand, there are costs of utilizing the RTPDEM. Certainly, there are increased computational costs of utilizing a robust approach compared with a deterministic approach. The computational costs and benefits of robust topology design are discussed in detail in Section 6.5, and the discussion applies straightforwardly to the combustor liner example as well. In a multifunctional, multi-stage design context, there are computational tradeoffs to be made. For example, the range-based approach requires much less computational effort from the subsequent (thermal designer) than the model-based approach, but it significantly limits flexibility for modifying the design to improve thermal performance. Additional computational costs and benefits of the approach are discussed in Section 3.4 and are not repeated here. Another important consideration mentioned in Section 6.5 is the difficulty of identifying suitable initial conditions and starting points for topology design. Convergence behavior can be very sensitive to the problem formulation and choice of initial conditions. Finally, there is no guarantee that the solutions obtained with the RTPDEM are globally superior solutions. A built-in feature of the approach is that the flexibility of a subsequent designer is limited by the decisions of the first-stage designer, especially if the range-based approach is utilized.

There are additional underlying assumptions that limit the scope of the example and the conclusions that can be drawn from it. For example:

- In this example, the lead designer is always the structural designer and the subsequent designer is always the thermal designer. The reasons for this are specified in Section 3.5 and involve the capability of structural topology design methods—relative to

thermal topology design methods introduced in this dissertation—for exploring a broader design space with extremely complicated initial topology. However, the design sequence is very likely to affect the outcome. Clearly, the fact that the structural designer is the leader in this example restricts the design space of the thermal designer. An interesting investigation would be to reverse the order. However, the thermal topology design algorithms are not sophisticated enough at this stage to explore a very complex initial structure. Therefore, if the thermal designer took the lead, it would effectively limit a second-stage structural designer to dimensional adjustment of the design generated by the thermal designer, and prohibit the use of well-developed structural topology design methods.

- One of the advantages of working with these two domains is the ease of creating common topological representations that facilitate the exchange of design specifications. Direct exchange or translation of design specifications between domains is a prerequisite for both the range-based and the model-based multifunctional topology design approaches. In this dissertation, a thermal topology and parametric design approach is established for the thermal domain that utilizes ground structure representations that are similar to the structural representations.
- Only structural and thermal domains are considered in this example. As mentioned in Chapters 2 and 3, it is difficult to develop topology design methods for non-structural domains. A thermal approach has been introduced in this dissertation that works well for the example problem. However, considerable effort is involved in developing such an approach, and it may support only small changes in topology reliably. If other domains are represented in a multifunctional design approach, topology design

methods will have to be developed for the domain *or* changes in the domain will be restricted to parametric adjustments of a topologically static design and/or exhaustive search of a finite set of alternative configurations.

- Only two designers are considered in this example. Introduction of additional designers and functional domains would complicate the dynamics of interactions between designers. The sequence of designers would have to be determined as well as the extent to which each designer is permitted to narrow or restrict the design space.
- Finally, the physical domain considered in this example is relatively small and symmetric. Larger problems would be more challenging computationally.

In addition to providing evidence for validation of Hypothesis 2, the example provides support for Hypothesis 1, as well. Of course, the robust topology design methods proposed in Hypothesis 1 are prerequisites for the multifunctional RTPDEM proposed in Hypothesis 2. As mentioned previously in this section, it is observed that the robust topology design methods within the RTPDEM are extremely useful in a multi-stage, multifunctional topology design problem. Via the results of this example, it is demonstrated that robust topology designs offer built-in flexibility for a subsequent designer in another functional domain to adjust the design both parametrically *and topologically*. These adjustments have been shown to improve domain-specific performance in the second functional domain without significantly deteriorating performance in the initial domain.

The example also provides evidence for Hypothesis 3 that the compromise DSP is a flexible, effective, multiobjective decision support model for *multifunctional*, robust

topology design applications. As documented in Table 7.15, it is possible to achieve a range of multifunctional tradeoffs by adjusting weights, bounds, constraint limits, and targets in the compromise DSP. This is important for generating a corresponding family of multifunctional designs that embody different tradeoffs between multifunctional goals. Families of designs offer multiple potential starting points for subsequent design, and they are useful for comparison purposes to verify the quality of solutions.

Finally, the results of the example have significant implications for the field of materials design. Alternative materials for combustor liners—including metallic superalloys and ceramic matrix composites—are discussed in Section 7.1 and possess advantages and disadvantages. Whereas metal alloys are relatively inexpensive and well-characterized, they have relatively low melting points, and their structural properties begin to degrade at relatively low temperatures. Combustion-side air cooling of metallic combustor liners is a common practice to lower the surface temperature and prevent melting and/or yielding. However, this combustion-side air cooling significantly increases NO_x emissions and reduces the efficiency of the engine. On the other hand, ceramic matrix composites have excellent high temperature properties, but they are particularly vulnerable to corrosive, high-temperature environments—despite decades of research and millions of dollars in development expenditures. Via the results of this example, it has been shown that actively-cooled cellular materials (with internal rather than combustion-side cooling) are promising alternatives to these materials approaches. Based on the data reported in this chapter, the preliminary conclusion is that prismatic cellular materials with a base material of Mo-Si-B intermetallic can be designed to withstand the temperatures and pressures of a high performance combustion chamber

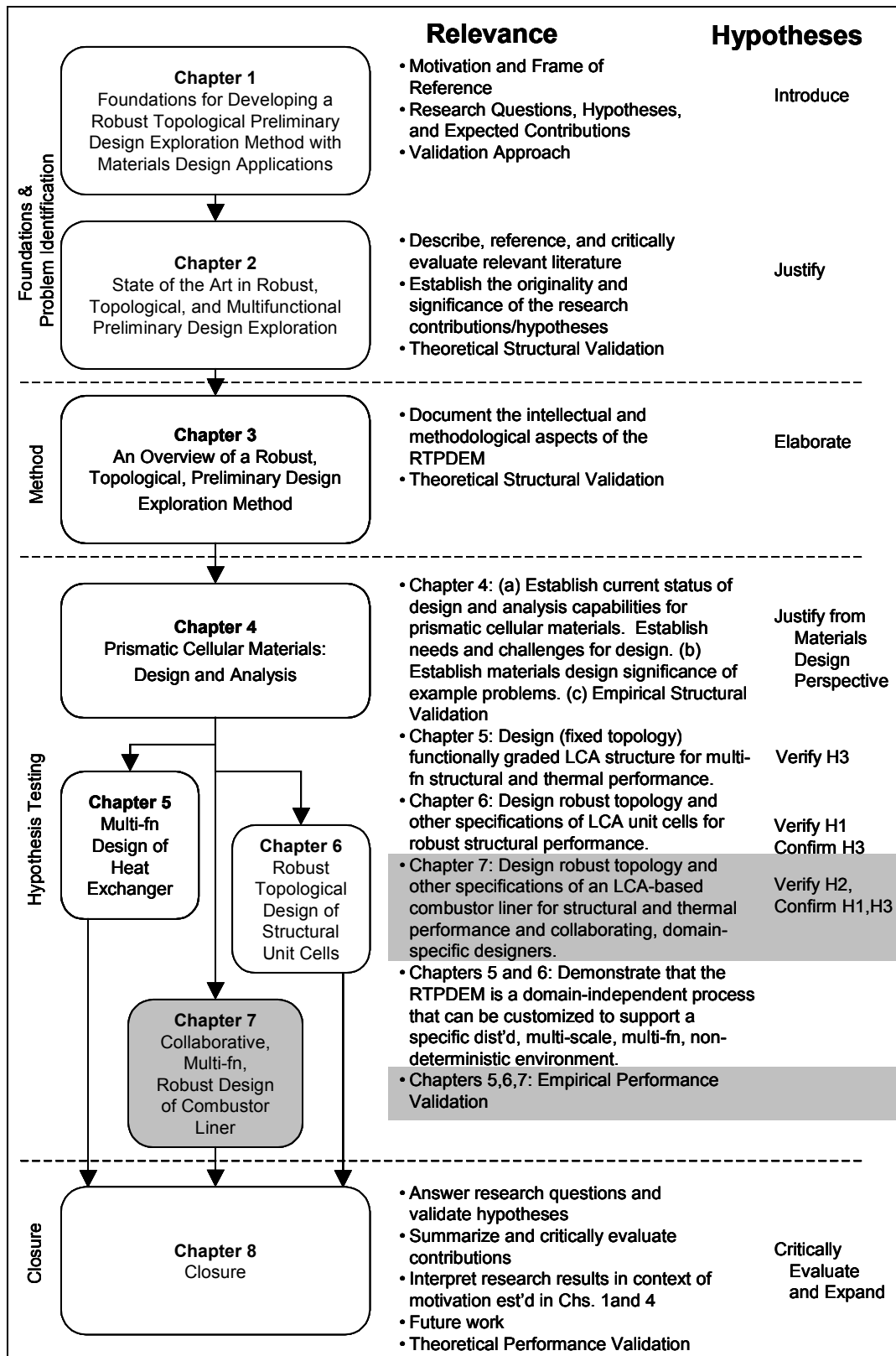


Figure 7.21 – Dissertation Roadmap

without combustion-side air cooling and *without* the design of a new base material. This promises a relatively inexpensive alternative to ceramic matrix composites that does not require combustion-side air cooling, thereby reducing emissions and increasing engine efficiency. In this context, the example provides strong evidence for the utility and effectiveness of strategic materials design methods. In this case, by utilizing a systems-based design approach such as the RTPDEM, it is possible to meet the requirements of advanced, materials-limited applications that have challenged materials scientists for decades ... without even designing a new base material. Imagine what could be accomplished if these design methods were extended for smaller length scales, as well!

7.6 CHAPTER SYNOPSIS

In this example, multifunctional combustor liners comprised of prismatic cellular materials are designed topologically and parametrically for structural and thermal performance in a two-stage, multifunctional, robust topology design process using the RTPDEM. By treating potential topological and parametric design changes by subsequent designers as noise in a robust topology design process, the lead structural designer generates robust designs with built-in topological and parametric flexibility. This flexibility can be used by a subsequent designer—with or without approximate physics-based models for the initial functional domain—to enhance performance in another functional domain without significantly degrading performance in the initial domain. The approach prevents computational intractability associated with fully integrated design approaches, leverages the domain-specific expertise and resources of individual designers, minimizes iterative redesign and information exchange, and avoids the difficulties cited in Section 3.5 of designing for other types of functionality—

particularly scale-dependent phenomena such as internal convection—during a structural topology design process. Although the designs generated with this approach may not be globally ‘optimal’, it is shown in this example that their multifunctional performance is significantly better than heuristically generated or non-robust designs. Therefore, the example results are used in this chapter to verify Hypothesis 2 regarding the effectiveness of the multi-stage RTPDEM for multifunctional applications. Also, from a materials design perspective, the designs meet the challenging requirements of the combustor liner without combustion-side air-cooling, thereby reducing emissions and increasing engine efficiency relative to conventional metallic combustor liners and addressing a materials design challenge for which significant research effort has been devoted for decades.

CHAPTER 8

CLOSURE

The principal goal in this dissertation is to establish a Robust Topological Preliminary Design Exploration Method (RTPDEM) that is suitable for exploring and identifying robust, multifunctional topology and other preliminary design specifications for prismatic cellular materials with the potential for broader application for other materials design applications.

The motivation for establishing the RTPDEM, the details of the method itself, and the results obtained by applying it to cellular materials design problems are summarized in Section 8.1. In Section 8.2, the research questions and hypotheses posed in Chapter 1 are revisited and critically evaluated with a special emphasis on the validity of the research hypotheses beyond the example problems described in this dissertation. Based on the summary and critical review, the achievements and research contributions reported in this dissertation are presented in Section 8.3, followed in Section 8.4 by opportunities for future work.

8.1 A SUMMARY OF THIS DISSERTATION

A paradigm shift is underway in which the classical materials *selection* approach in engineering design is being replaced by the *design* of material structure and processing paths on a hierarchy of length scales for specific multifunctional performance requirements. In this dissertation, the focus is on designing materials on *mesoscopic* length scales that are larger than microscopic features but smaller than the macroscopic characteristics of an overall part or system. The mesoscopic *topology*—or geometric

arrangement of solid phases and voids within a material or product—is increasingly customizable with rapid prototyping and other manufacturing and materials processing techniques that facilitate tailoring topology with high levels of detail. Fully leveraging these capabilities requires not only computational simulation models but also a *systematic, efficient design method* for exploring, refining, and evaluating product and material topology and other design parameters in order to achieve *multifunctional* performance goals and requirements. The performance requirements for materials are typically derived from larger engineering systems in which they are embedded and often require tradeoffs among multiple criteria associated with disparate physical domains such as heat transfer and structural mechanics. The structures and processing paths of these *multifunctional* materials must be designed to simultaneously balance these multi-physics requirements as much as possible. However, the link between preliminary design specifications and realized multifunctional performance is not deterministic. Deviation from nominal or intended performance can be caused by many sources of variability including manufacturing processes, potential operating environments, simulation models, and adjustments in design specifications themselves during a multi-stage product development process. Topology and other preliminary specifications for materials and products should be designed to deliver performance that is *robust* or relatively insensitive to this variability.

In this dissertation, the Robust Topological Preliminary Design Exploration Method (RTPDEM) is presented for designing complex multi-scale products and materials concurrently by topologically and parametrically tailoring them for multifunctional performance that is superior to that of standard designs and less sensitive to variations.

This systems-based design approach is formulated by establishing and integrating principles and techniques for robust design, multiobjective decision support, topology design, collaborative design, and design space exploration along with approximate and detailed simulation models. A comprehensive robust design method is established for topology design applications. Robust topology design problems are formulated as compromise Decision Support Problems, and guidelines are established for modeling sources of variation in topology design, including variations in dimensions and variations or imperfections in topology. Computational techniques are established for evaluating and minimizing the impact of these sources of variation on the performance of a preliminary topological design. Local Taylor-series based approximations of design sensitivities are introduced for evaluating the impact of small changes in control factors such as dimensions or material properties. Strategic experimentation techniques are established for evaluating the impact of variations in topology that require reanalysis of a design.

Robust topology design methods are used in this dissertation not only to design material topologies that are relatively insensitive to manufacturing-related imperfections but also to systematically and intentionally create topological designs with built-in flexibility for subsequent modification. This flexibility is the foundation for the multi-stage, multifunctional robust topology design method introduced in this dissertation. Because it is very difficult to extend complex topology design techniques to non-structural domains—especially if the phenomena are shape- or scale-dependent, in which case it is also difficult to analyze such phenomena during a structural topology design process—multiple functional domains are treated as multiple stages in a multifunctional

topology design process. In the first stage, robust topology design methods are used to explore and generate structural topology that is robust to small changes in the topology itself and the dimensions of its elements. This flexibility is used by a subsequent designer to make small adjustments to the topology and other specifications of a preliminary topological design to enhance performance in an additional functional domain, such as heat transfer, without significant adverse impacts on first-stage structural performance. A modification of the multifunctional design approach involves constructing and sharing approximate, physics-based models of first-stage (structural) performance. To facilitate more extensive changes in topology and other design specifications and potentially more significant enhancement of second-stage performance objectives, the models are utilized by the second-stage designer to evaluate and minimize any associated degradation in first-stage (structural) performance. The multifunctional topology design approach facilitates decomposition and distribution of topology design activities in a manner that is (1) appropriate for highly coupled designs, (2) effective and computationally efficient compared with over-the-wall (iterative) and fully integrated design approaches, (3) appropriate for leveraging the domain-specific expertise of multiple designers, and (4) conducive to multiple functional analyses and topology design techniques that require different design spaces such as the complex initial ground structures of structural topology design versus simpler initial topologies for thermal design. As part of the approach, topology design techniques are established for thermal applications. The techniques are based on a finite element/finite difference heat transfer analysis approach introduced in this dissertation.

Key aspects of the approach are demonstrated by designing linear cellular alloys—ordered metallic cellular materials with extended prismatic cells—for multifunctional applications. For a microprocessor application, structural heat exchangers are designed that increase rates of heat dissipation by approximately 50% and structural load bearing capabilities substantially relative to conventional heat sinks that occupy equivalent volumetric regions. Also, cellular materials are designed with structural properties that are robust to dimensional changes and topological imperfections such as missing cell walls. Although structural imperfections—or deviations from intended structural characteristics—are observed regularly in cellular materials and in other classes of materials, they have not been considered previously during the design process. Finally, cellular combustor liners are designed to increase operating temperatures and efficiencies and reduce harmful emissions in next-generation gas turbine engines via active cooling and load bearing within topologically and parametrically customized cellular materials. Results from these examples are utilized extensively for validating the RTPDEM and the research hypotheses associated with it, as described in the following section.

8.2 ANSWERING THE RESEARCH QUESTIONS AND VALIDATING THE RESEARCH HYPOTHESES

The Robust Topological Preliminary Design Exploration Method (RTPDEM) is established to answer the three research questions posed in Chapter 1, and it is based on the three hypotheses proposed in Chapter 1 for answering each of the research questions. In this section, each of the hypotheses is revisited in turn. In Sections 8.2.1 through 8.2.3, summaries are provided of arguments made throughout the dissertation regarding the theoretical and empirical validity of each hypothesis. In Section 8.2.4, particular

attention is devoted to theoretical performance validity which involves building confidence that the RTPDEM is useful and effective in a general sense beyond the specific example problems.

8.2.1 Hypothesis 1: Robust Topology Design

In Hypothesis 1, a comprehensive method is proposed for formulating and solving robust topology design problems. As proposed in Hypothesis 3, a compromise DSP is used to formulate a robust topology design problem. Guidelines are established in Chapter 3 for identifying and modeling common sources of variation in a topology design problem, including dimensional and topological variation. Two classes of computational techniques are proposed for evaluating the impact of these variations on the performance of a topological design. For evaluating the impact of small changes in control factors such as dimensions or material properties, local Taylor series-based approximations of design sensitivities are proposed. The impact of other sources of variation, such as variations in topology, is evaluated with strategic experiments because reanalysis of a modified structure is required for evaluating the impact of these sources on responses of interest. The accompanying measures of performance variation due to dimensional, topological, and other sources of noise are included in the compromise DSP as objectives, and robust designs are generated by balancing minimization of performance variation with achievement of satisfactory nominal performance levels.

Theoretical Structural Validation

As discussed in Chapters 1 and 2, the need for a comprehensive robust topology design method is supported by a critical review of the literature on robust design and topology design. In documented applications of robust design methodology and

principles—even for the early stages of design—the physical topology or layout of a system is determined *a priori*. Conversely, topology design methods have been established almost exclusively for deterministic contexts in which potential variations in material properties, applied loads, structural dimensions, and other factors are not considered. As discussed in Section 2.3.1, the most closely related work involves designing for worst-case loading and worst-case stress and displacement constraints (i.e., feasibility robustness). Variation in the structure of a design itself (e.g., dimensional or topological variation) have not been considered at all in previously published topology design work.

As discussed in Chapters 2 and 3, it is not a straightforward task to establish robust design methods for topology design applications. Several challenges are overcome in formulating a comprehensive robust topology design method. First, the problem has to be *framed*, as described in Chapter 3, by identifying the critical issues and establishing a methodological and computational framework for formulating and solving robust topology design problems. For example, specific techniques and guidelines are proposed in Chapter 3 for modeling dimensional and topological noise, and the compromise DSP is proposed as an innovative approach for formulating robust topology design problems. Second, several features of topology design problems make it difficult to model variation and propagate it from its sources to relevant responses. These features include the large numbers of variables, non-negligible computational requirements for each analysis of a topological structure, and the ‘on/off’ nature of variables in the topology design process. The ‘on/off’ nature is associated with reduction of the size of the variable set as elements are removed from an initial topology as a result of a topology design process. Together,

these features make both Monte Carlo approaches and statistically designed experiments extremely computationally expensive and place restrictions on models for sources of variation, as described in Chapter 3. Thirdly, the issues of topological noise and robustness have not been addressed previously. The objective here is *not* to select a layout, configuration, or topology as a prerequisite for a robust design process and then design its dimensions and other properties for robustness, as in previous work. Instead, the topology *itself* is designed to be a more robust platform for performance that is less sensitive to variations from many sources including dimensional tolerances and changes in the topology itself. The premise is that the choice of a robust topology has a greater impact on the robustness of a design than relatively modest dimensional and parametric modifications to a design of fixed topology.

The **advantages, limitations, and domain of applicability** of the robust topology design methods included in the RTPDEM are outlined in Table 3.1 and described in Section 3.6. Briefly, the advantages of the robust topology design methods proposed in Hypothesis 1 include the capability of extending robust design methods for the concept design stage in which the layout of a product or system is determined.¹ In this case, the layout or distribution of *material* is determined in the concept or preliminary design stage. The robust topology design methods established in this dissertation facilitate generation of topologies that are robust to parametric or topological noise or variation encountered in the manufacturing process, the operating environment, and/or the remainder of the product development process (e.g., changes made by a subsequent designer). The robust design methods proposed in this dissertation include a flexible compromise DSP formulation for robust topology design problems, guidelines for

¹ The concept design stage occurs before Taguchi's parameter or detailed design stages.

modeling parametric and topological noise and variation, and computational techniques for efficiently solving the compromise DSP via gradient-based mathematical search techniques coupled with Taylor series- and experiment-based assessment of performance variation due to parametric and topological noise, respectively.

On the other hand, the robust topology design methods proposed in this dissertation are limited to applications for which discrete and/or continuum topology design methods are available or can be established. The methods have not been established or applied for configuration-based or modular design, for example. Increased computational time and resources are associated with solving a robust topology design problem, compared with a deterministic topology design problem, but the expense is likely to be balanced by fewer overall design iterations and enhanced quality of a final product. The increased computational requirements for the examples are discussed in Sections 6.5 and 7.4.3. In addition, the robust design methods in the RTPDEM are expected to be applicable for continuum topology design approaches with some minor modifications although they have not been applied in that context in this dissertation. Finally, several potential sources of topological variation are not considered in the examples in this dissertation, including variation in boundary conditions, size and shape of the domain occupied by a ground structure, and nodal positions in an initial ground structure as well as imprecision in analysis models. The robust topology design methods proposed in this dissertation are expected to be directly modifiable for these sources of variation, but the exercise is left for future work.

Empirical Structural and Performance Validation

The effectiveness of the robust topology design method proposed in Hypothesis 1 is demonstrated and validated empirically with the examples presented in Chapters 6 and 7.

In Chapter 6, prismatic cellular materials are designed to possess structural elastic properties that are robust to variations in their dimensions, material properties, and topology. Topological and dimensional variation are modeled as sets of potential permutations of a ground structure and as tolerance ranges with special characteristics as described in Section 3.3.1. The impact of dimensional and topological variation is assessed via Taylor series-based techniques and strategic experiments in potential topological permutations, respectively, as described in Section 3.3.3. Robust topology design problems are formulated as compromise DSPs and solved with gradient-based search algorithms. Three sets of topology designs are generated: (1) designs with structural elastic properties that are robust to dimensional and topological variation, (2) designs with structural elastic properties that are robust to dimensional variation only, and (3) benchmark non-robust topology designs for which variation is not considered. When the robust designs are compared with benchmark, non-robust topology designs, the effectiveness of the robust topology design methods is evident in both the performance and the structure of the resulting designs. Dimensionally robust topology designs tend to have nearly identical levels of nominal performance, much lower levels of performance variation, and much simpler topologies than their non-robust counterparts. The simpler topologies reduce the build-up of tolerance effects on performance variation, and they also tend to be easier to manufacture. On the other hand, the more complex, non-robust topologies tend to be less sensitive to topological variation because element removal has

a smaller impact on a complex topology with large numbers of redundant elements. When both dimensional and topological variation are considered, the robust topology design method yields topologies that offer a compromise between the simpler topologies with superior robustness to dimensional variation and the more complex, non-robust topologies with low levels of robustness to dimensional variation and higher levels of robustness to topological noise.

The example results support the conclusion that the robust topology design method proposed in Hypothesis 1 is effective for generating designs with performance that is more robust than that of designs generated with standard, deterministic topology design techniques and that the methods can be used to achieve a range of tradeoffs between nominal performance, dimensional robustness, and topological robustness. The evidence also supports the conclusion that robust topology design methods facilitate the search for robust local minima for problems for which there may be many local minima with similar nominal performance.

In Chapter 7, combustor liners are designed in a multi-stage, multifunctional topology design process. Robust structural topology design is conducted in the first stage, followed by thermal topology design in the second stage. Robust topology design methods are utilized in the first stage—as in the robust structural topology design example of Chapter 6—to explore and generate topological preliminary design specifications with structural performance that is robust to variations in the topological structure itself, including tolerances and topological imperfections (e.g., missing cell walls). The structural designer shares a set of acceptable topologies and ranges of element dimensions (for which structural properties are designed to be robust) with the

subsequent thermal designer who treats them as design freedom for modifying the structural design to improve thermal performance. By comparing robust and non-robust topology designs, it is shown that the robust designs provide greater flexibility for changes by subsequent designers, and the flexibility is shown to improve second-stage performance significantly. The flexibility takes the form of (1) a robust set of topologies from which to choose and (2) robust ranges of possible dimension values. The space or set of possible topologies that accompanies a robust design is particularly useful for a subsequent designer who may choose the topology that most significantly improves performance in his/her functional domain. It is observed that significant improvement in second-stage (thermal) performance with little impact on first-stage (structural) performance objectives is obtained by modifying the nominal design within the ranges and topological sets shared by the lead (structural) designer. When the non-robust design is modified within similar ranges, a much smaller improvement in second-stage performance is realized at the expense of a much larger deterioration in first-stage performance, as expected from a non-robust design. Via the results of this example, it is demonstrated that robust topology designs generated with the methods proposed in Hypothesis 1 offer built-in flexibility for a subsequent designer in a similar or distinct functional domain to adjust the design both parametrically *and topologically*.

Based on experience with both examples, it is noted that minimal additional computational time is required for dimensional robustness, but computational expense is increased substantially when topological robustness is considered. The robust topology design method is observed to converge to simpler, more robust topologies and typically requires fewer iterations than standard topology design techniques, with robustness

measures acting as penalty functions to encourage convergence to crisp topologies with clearly defined groups of thick and thin elements to be retained and removed, respectively. Due to the customized formulation of tolerance functions described in Chapter 3, the robust topology design problem is smooth and continuous over the entire design space. However, as with standard topology design techniques, convergence behavior can be very sensitive to choice of initial conditions, including design variable bounds, weights, initial ground structure, etc.

8.2.2 Hypothesis 2: Multifunctional, Robust Topology Design

In Hypothesis 2, robust topology design techniques are proposed for *multifunctional* applications. Multiple functions are treated as multiple stages in a topology design process. The first stage is a robust structural topology design process, followed by a more limited topology design process for other functions in the second stage.² There are two alternative approaches for facilitating collaboration between the lead structural designer and a subsequent domain-specific designer. In the first alternative, the structural designer communicates a robust topology design along with associated ranges of element area values and a space of acceptable topologies for which the structural design's performance is robust. The subsequent designer (also known as the thermal designer in Chapter 7) adjusts the structural design *only* within the ranges and sets specified by the structural designer to improve the thermal performance of the design. In the second alternative, the lead structural designer also creates and shares an approximate, physics-

² The first stage is a structural topology design stage because structural topology design techniques are well-established and can operate on very complex initial topologies (i.e., broad topological design spaces). As discussed in Chapters 2 and 3 (particularly Section 2.3.2), it is difficult to establish topology design methods for other physical domains, especially if the phenomena are strongly shape or scale dependent, as in internal heat transfer applications, for example. It is also difficult to analyze these phenomena during a structural topology design process. Topology design methods and topological modifications associated with these functional domains tend to be more limited in scope and better suited for a second stage design process for which a rough topology has already been determined.

based, behavioral model for the structural domain. The thermal designer uses the approximate structural model to evaluate the impact of design changes (both topological and parametric) on structural performance. With the availability of the approximate structural model, the thermal designer is not limited to the ranges specified by the structural designer; instead, the thermal designer has the capability to make broader topological and parametric design changes because he/she has the ability to evaluate and balance the impact of those changes on both structural and thermal performance. Henceforth, the first and second alternative approaches are referred to as the *range-based approach* and the *model-based approach*, respectively.

Theoretical Structural Validation

As discussed in Chapters 1 and 2, the need for a multifunctional topology design approach is motivated by the need to systematically design topology for truly multifunctional applications in which objectives are pursued in multiple physical domains such as heat transfer and structural mechanics. As discussed in Section 2.3.2, multifunctional topology design capabilities are currently limited primarily to coupled field problems in structural mechanics in which the effects of thermal, electrical, or magnetic fields on the state of mechanical stress and deformation in a body are considered with a few applications in thermal conduction, as well.

For several reasons, it is very challenging to establish multifunctional topology design methods. First, as discussed in Chapters 1 and 2 (particularly Section 2.3.2), structural topology design techniques do not apply straightforwardly to other physical domains, and it is difficult to analyze many physical phenomena during a structural topology design process. Therefore, it is necessary to divide a multifunctional topology design process

into multiple stages according to the multiple physical domains and associated domain-specific experts. However, multidisciplinary design methods and techniques such as game theory do not apply straightforwardly to multifunctional topology design applications because they have been developed for nearly decomposable systems with only a few shared or coupled variables. In contrast, topology design spaces are highly coupled and integral rather than decomposable, as discussed in Section 2.4.4. As a result, a theoretical and computational framework is required for facilitating distributed, multifunctional design of integral topology. In addition, systematic techniques are required for topology design in each physical domain under consideration. In response to these needs, the multifunctional robust topology design approach is proposed in Hypothesis 2 and described in Section 3.4, and a thermal topology design technique is introduced in Section 3.5.

The **advantages, limitations, and domain of application** of the multifunctional topology design approach are summarized in Table 3.1 and discussed in Section 3.6. Among its advantages, the multi-stage, multifunctional, robust topology design approach facilitates distribution of topological preliminary design activities across multiple design stages—associated with different functional perspectives and possibly different designers—while simultaneously limiting iteration and facilitating compromise among multiple functional objectives via communication of ranges of parametric design specifications and spaces or sets of possible topologies, with or without approximate physics-based models. Iteration is limited because subsequent designers have the capability of adjusting design specifications—within the specified ranges and sets of potential topologies—to meet their own functional objectives without violating

satisfactory performance levels of previous designers. Generation and communication of approximate behavioral, physics-based models broadens the scope for non-iterative collaboration. Subsequent designers can adjust design specifications, including topology, more extensively by utilizing the approximate behavioral models—along with their own functional models—to evaluate and balance the impact of broader design modifications on both sets of functional objectives. The approach facilitates distributed, multi-stage design for highly coupled, integral, multifunctional products or materials because it does not require near decomposability of a system but accommodates highly coupled systems with large proportions of shared variables. The approach also allows designers with expertise in an area to make decisions in that area and distributes synthesis and computational activities to avoid computational intractability. Finally, it is appropriate for different functional domains with different topological design spaces (e.g., different initial ground structures).

The multi-stage, multifunctional topology design approach does have theoretical limitations. First, the approach facilitates balancing multifunctional objectives, but it does not guarantee Pareto solutions. If all functions, designers, and stages could be considered simultaneously in a fully integrated design process, it is likely that improved solutions would be identified, but a fully integrated design process is not a reasonable option for the reasons cited in Section 3.4. Also, by default, the design freedom of subsequent designers is limited. In the range-based approach, it is limited to the specified parametric ranges and space of potential topological changes. In the model-based approach, the scope for changes is broadened at the cost of creating and repeatedly

executing the approximate behavioral model, but the subsequent designer is bound to begin his/her search with the nominal design supplied by the lead designer.

Empirical Structural and Performance Validation

The effectiveness of the multifunctional robust topology design method proposed in Hypothesis 2 is demonstrated and validated empirically with the combustor liner example described in Chapter 7.

In Chapter 7, combustor liners comprised of prismatic cellular materials are designed with the multifunctional, robust topology design approach proposed in Hypothesis 2. Robust structural topology design is implemented in the first stage followed by thermal topology design in the second stage. Both the range-based and the model-based alternative implementations of the approach are applied to the problem, and the results are compared with one another and with results obtained for (1) a non-robust design, (2) a structurally tailored design that is not modified for thermal performance, and (3) a heuristic design obtained without the benefit of systematic design methods or iterative search techniques. By comparing the RTPDEM results with the first class of non-robust designs, it is observed that the robust designs provide more flexibility for topological and parametric design changes that significantly enhance second-stage (thermal) performance without deteriorating first-stage (structural) performance. Because non-robust designs do not offer this flexibility, their multifunctional performance is significantly worse than that of the robust designs. By comparing RTPDEM results with the second class of structural designs, it is observed that both the range-based and the model-based approaches for multifunctional topology design significantly improve second stage (thermal) performance with varying effects on first-stage (structural) performance relative to

nominal designs that have not been modified for improved thermal performance. It is observed that significant improvement in second-stage (thermal) performance with little impact on first-stage structural performance objectives is obtained by modifying the robust design within the ranges and topological sets shared by the lead (structural) designer. By modifying the robust design beyond the ranges and topological sets, improvement in second-stage (thermal) objectives is multiplied, at a significant cost in terms of structural performance. The deterioration of structural performance is lessened and controlled by utilizing the model-based approach. Results of using the model-based approach indicate that solutions are obtained that are preferred to the results of the range-based approach and offer a range of compromises between improvement in second-stage thermal objectives and sacrifices in first-stage structural objectives. Finally, by comparing the RTPDEM results with the third class of heuristic designs, it is demonstrated that RTPDEM designs offer improved multifunctional performance and more efficient utilization of material than a heuristic structure designed without the benefit of systematic design methods or iterative search techniques.

There are some costs and **limitations** to the approach. Most of them are reported in the theoretical structural validation portion of this section and are not repeated here. An additional item to note is that the approach relies partially on the ease of creating common topological representations for all of the domains that facilitate the exchange of design specifications. Direct exchange or translation of design specifications between domains is a prerequisite for both the range-based and the model-based multifunctional topology design approaches. In the presentation and empirical demonstration of the approach, two designers have been assumed, and the lead designer is assumed to be the

structural designer for the reasons cited previously in this section and in Chapter 2. In principle, the approach should be extensible to more than two designers in varied sequences, but further work is required to formulate and investigate these extensions.

8.2.3 Hypothesis 3: Compromise DSP for Multifunctional, Robust Topology Design

The purpose of Hypothesis 3 is to establish a decision support framework for robust topology design and multifunctional topology design. In Hypothesis 3, the compromise Decision Support Problem is proposed as mathematical model for structuring and supporting decisions in robust, multifunctional topology design. Whereas standard topology design problems are formulated as conventional, single-objective, nonlinear programming problems for pursuing a single objective in a deterministic context, robust multifunctional topology design problem formulations must support exploration of families of compromise solutions that embody ranges of tradeoffs between multiple performance objectives and measures of robustness. Also, when multifunctional topology design problems are distributed among multiple, domain-specific design stages and associated expert decision-makers, a flexible problem formulation is required for formulating and linking multiple sub-problems. In Hypothesis 3, it is proposed that the compromise DSP fulfills these roles for robust, multifunctional topology design.

Theoretical Structural Validation

In Section 2.2, the compromise DSP is described as a hybrid formulation—based on mathematical programming and goal programming—for modeling and achieving multiple goals in engineering design applications. It is used to determine the values of design variables that satisfy a set of constraints and bounds and achieve a set of conflicting, multifunctional goals as closely as possible. In Chapter 2, it is argued that

there is a need for flexible, domain-independent, multiobjective decision support for robust topology design and multifunctional topology design. Whereas several multiobjective formulations—including weighted sum, compromise programming, and min-max formulations—have been applied for considering multiple loads or multiple structural objectives in structural topology design, it is argued that none of these approaches have all of the advantageous characteristics of the compromise DSP for robust, multifunctional topology design. These characteristics include *flexibility* for (1) considering both multiple goals and hard constraints, (2) incorporating and archiving engineering judgment within the problem formulation in the form of assumptions, bounds, goal targets, weights, and constraint limits, (3) utilizing alternative objective function formulations such as preemptive, Archimedean, and utility theory formulations, and (4) adjusting both weights and target values along with bounds and other parameters to facilitate exploration and generation of a family of robust, multifunctional, topology design solutions with a range of tradeoffs between multiple performance objectives and measures of robustness and flexibility. These capabilities are required for the applications addressed in this dissertation but they are *not* characteristic of single-objective optimization formulations.

With respect to **limitations** of the compromise DSP, the user is cautioned that solutions could be inferior to Pareto solutions, especially if unambitious target values are established for one or more goals, but this can be remedied by setting sufficiently high target values for the goals. As discussed in Section 2.2, the compromise DSP's capability for identifying all Pareto solutions depends on the behavior of the solution space as well as the objective function formulation. On the other hand, as discussed in Section 2.2, a

designer may not always wish to obtain Pareto solutions, but may seek robust, satisficing solutions instead. For the advantageous capabilities discussed in the previous paragraph, the compromise DSP is used as a foundational construct for the robust topology design methods and multifunctional robust topology design methods proposed in Hypotheses 1 and 2.

Empirical Structural and Performance Validation

The effectiveness of the compromise DSP as a mathematical decision model for robust, multifunctional topology design problems is demonstrated and validated empirically with the three example problems described in Chapters 5 through 7.

In the structural heat exchanger example, a compromise DSP is formulated for a multifunctional materials design problem with multiple objectives, multiple domains of functionality, and design specifications that include aspect ratios and dimensions (but not the topology) of prismatic cellular materials. The compromise DSP is used as a flexible decision support template for generating a family of compromise solutions by adjusting the weights and target values for each goal in order to achieve a range of tradeoffs between multiple objectives, including the total rate of steady state heat transfer and the overall structural elastic stiffness of the prismatic cellular materials. When compared with single-objective designs, the families of compromise solutions clearly exhibit a range of tradeoff values between thermal and structural objectives. These tradeoffs are clearly manifested in not only the thermal and structural performance measures for the family of designs but also in the actual structures of the materials. Material structures with high overall heat transfer rates tend to have thin walls and very low structural stiffness. Conversely, material structures with thicker walls sacrifice a portion of the

total heat transfer rate in order to achieve higher structural stiffness. The families of designs are generated by adjusting weights and goal target values in a single formulation of the compromise DSP, *without* reformulating the problem. In this example, adjustment of target values is shown to be particularly effective for adjusting and controlling the precise balance between conflicting objectives.

In Chapters 6 and 7, the compromise DSP is used as a mathematical model for formulating robust topology design decisions. In Chapter 6, prismatic cellular materials are designed with elastic properties that are robust with respect to dimensional and topological variation. The designs are compared with deterministic designs that are generated without considering variation or robustness. By formulating the robust topology design problem as a compromise DSP, families of designs are generated with varying levels of robustness and with ranges of tradeoffs between nominal performance and robustness with respect to dimensional and/or topological variation. Once a compromise DSP is formulated for the robust topology design problem, various robust designs are obtained by varying the target values and weights for each goal, and deterministic designs are obtained by assigning negligible or zero-valued weights for robustness goals. The flexibility of the compromise DSP makes that possible *without* reformulating the compromise DSP.

In Chapter 7, the topology and other preliminary design specifications of combustor liners are designed for satisfactory thermal and structural performance in a *multifunctional, multi-stage* robust topology design process. In the first stage, a compromise DSP is formulated for robust structural topology design to generate designs with structural properties that are robust or relatively insensitive to small changes in the

dimensions and topology of the structure. In the second stage, a compromise DSP is formulated and solved for thermal topology design to modify the structural design in order to balance thermal performance objectives with structural performance. By comparison with heuristic designs and benchmark single-objective and non-robust designs, it is demonstrated that the compromise DSP is effective for generating families of topological designs with a range of multifunctional tradeoffs between structural and thermal objectives. It is also demonstrated that the compromise DSP is an effective mathematical model for supporting multiple stages of a multifunctional topology design process by generating, communicating, and accepting ranged sets of design specifications.

8.2.4 Theoretical Performance Validation of Hypotheses 1, 2, and 3

As discussed in Section 1.4, theoretical performance validity involves establishing that the proposed methods are useful beyond the example problems. This involves determining the characteristics of the example problems that make them representative of general classes of problems. Based on the utility of the method for these example problems, its usefulness for general classes of problems is inferred.

For empirical structural validation, it is argued in Sections 5.2, 6.2, and 7.2, that the example problems are collectively representative of a general class of problems, defined by the following characteristics:

- Multiple, conflicting objectives from different functional domains must be balanced in order to achieve families of compromise solutions.
- Manufacturing freedom is available and can be leveraged for adjusting and customizing the structure of the material, including topology, shape, and dimensions.

Any manufacturing limitations are included as constraints or bounds in the problem formulation.

- Motivation exists for tailoring the topology, shape, and dimensions of a design because these factors strongly influence performance characteristics of interest.
- The term topology refers to the distribution of material including solids, voids, and phases. It does not refer to the configuration or arrangement of parts in a larger product or system (e.g., the modular arrangement of parts in an automotive drivetrain).
- Variations in the structure and/or boundary conditions of a design cause significant performance variation—the nature and/or magnitude of which is influenced by the topology, shape, and/or dimensions of the structure. This provides rationale for modeling variability and minimizing its impact on performance characteristics during the topology design process.
- Analytical models are available that relate structure (i.e., topology, shape, dimensions, other properties) to properties and performance, and these models are relatively precise, accurate, and fast enough to permit iterative design exploration.

For the multifunctional topology design example and approach, the following additional characteristics are assumed:

- There is a need to separate multifunctional topology design activities along disciplinary lines associated with multiple domains of functionality. This may be driven by the difficulty of analyzing or topologically designing for other functional domains during a structural topology design process, as discussed previously in this section.

- Designers are clearly sequenced according to their functional domains. In the example in Chapter 7, the structural designer is the lead designer, followed by the thermal designer.
- When viewed from multiple functional perspectives, the design is integral with large proportions of shared or coupled variables, as described in Section 2.4.4. In topology design applications, the entire topology typically influences all or most aspects of functionality.
- Approximate behavioral or physics-based models can be created for the functional domain of a lead designer.
- Common topological representations can be used by all functional domains to facilitate the exchange of design specifications.
- Topology and parametric design techniques are available or can be established for each domain.

This is intended to be a list of the signature properties of the examples for which the effectiveness of the RTPDEM has been demonstrated. It is not a list of the properties the examples do NOT have. Some of these properties and associated opportunities for future work are discussed in Section 8.4.

In Chapters 5, 6, and 7, it has been demonstrated that the RTPDEM is effective for the example problems with these characteristics. Therefore, there is reason to believe that the RTPDEM is effective for *general* classes of problems with these characteristics. In addition, the RTPDEM may be applicable to even broader classes of problems, as discussed in Section 8.4. The capabilities, advantages, and limitations of the RTPDEM

for the general classes of problems represented by the example problems are summarized in Sections 8.2.1 through 8.2.3 and are not repeated here.

The next step is to highlight the achievements and contributions to the fields of design methodology and materials design that have been established by answering the research questions and demonstrating and validating the research hypotheses.

8.3 ACHIEVEMENTS AND CONTRIBUTIONS

The achievements and contributions presented in this dissertation are divided into three categories. First, there are contributions to the field of design methodology. These contributions are directly related to the primary and secondary research hypotheses proposed in Chapter 1 and the establishment of the Robust Topological Preliminary Design Exploration Method (RTPDEM). Second, in the course of applying these design methodologies, thermal topology design and analysis techniques are established. Finally, by applying the design methodology—namely the RTPDEM—to three materials design examples in this dissertation, several achievements are realized in the field of materials design. In this section, the three categories of achievements and contributions are highlighted.

8.3.1 Contributions to the Field of Design Methodology

The primary research contribution corresponds to the principal goal, primary research question, and primary research hypothesis:

- A **M**ethod for **R**obust **T**opological **P**reliminary **D**esign **E**xploration (RTPDEM) is established that is suitable for exploring and identifying robust topology and other preliminary design specifications for multifunctional prismatic cellular materials with the potential for broader application to other materials design applications.

The primary contribution is explained in greater detail by expanding it into several secondary research contributions in the field of design methodology:

- A comprehensive robust topology design method is created by establishing robust design methods and principles for topology design applications. Robust topology design problems are formulated as compromise Decision Support Problems, and guidelines are established for modeling sources of variation in topology design, including variations in dimensions and variations or imperfections in topology. Computational techniques are established for evaluating and minimizing the impact of these sources of variation on the performance of a preliminary topological design. Local Taylor-series based approximations of design sensitivities are established for evaluating the impact of small changes in control factors such as dimensions or material properties. Strategic experimentation techniques are established for evaluating the impact of variations in topology that require reanalysis of a design. The robust topology design method—embodied in the RTPDEM—is shown to be effective for exploring and identifying topology and other preliminary design specifications with performance that is robust with respect to variation in (1) parameters such as dimensions or material constants and (2) topology itself in the form of cracked or missing elements or joints or other topological imperfections. This offers the capability of accommodating processing variations from specimen to specimen without requiring difficult or expensive controls on processing conditions. The capability to generate dimensionally and topologically robust designs also

- provides opportunities for designing flexibility into the design for subsequent changes in dimensions or in the *topology itself*.
- A multifunctional topology design approach that facilitates distributed, multi-stage, robust topology design for multifunctional applications. Two alternative approaches are established for facilitating collaboration between a lead structural designer and a subsequent domain-specific designer—a range-based approach and a model-based approach. In the range-based alternative, the structural designer shares a robust topology design—along with associated robust ranges of element area values and a robust space of possible topologies—with the subsequent designer. The subsequent designer (also known as the thermal designer in Chapter 7) adjusts the structural design *only* within the ranges and sets specified by the structural designer to improve the thermal performance of the design. In the model-based approach, the lead structural designer also creates and shares an approximate, physics-based behavioral model for the structural domain. The subsequent designer uses the approximate structural model to evaluate the impact of design changes (both topological and parametric) on structural performance. With the availability of the approximate structural model, the subsequent designer is not limited to the ranges specified by the structural designer. Instead, the subsequent designer has the capability to make broader topological and parametric design changes because the impact of those changes can be evaluated and balanced for both structural and thermal performance. The multifunctional topology design approach facilitates decomposition and distribution of topology design activities in a manner that is (1) appropriate for highly coupled designs, (2) effective and computationally efficient compared with over-the-

- wall (iterative) and fully integrated design approaches, (3) appropriate for leveraging the domain-specific expertise of multiple designers, and (4) conducive to multiple functional analyses and topology design techniques that require different design spaces such as the very complex initial ground structures of structural topology design versus the simpler initial topologies required for thermal design.
- A flexible, multiobjective, decision support model, based on the compromise Decision Support Problem, is established that facilitates exploration and generation of a *family* of topological and/or parametric designs that embody a *range* of effective compromises among multiple conflicting goals such as (a) nominal performance and performance variation associated with robust design and/or (b) requirements from disparate functional domains such as structural mechanics and heat transfer. The decision support model is a foundational construct for robust topology design and multifunctional topology design. In collaborative topology design contexts, the compromise DSP is the decision support model that enables generation and acceptance of flexible, robust ranges of design specifications and sets of possible topologies that can be used by other designers to modify the design for multifunctional performance. In addition, it is possible to generate families of preliminary designs by adjusting weights, target values, bounds, and constraint limits in the compromise DSP template, *without* reformulating it. The families of solutions offer a balance of multifunctional performance, in contrast with the predominantly single objective performance of designs obtained with single objective, mathematical programming techniques. This is valuable for identifying designs that satisfy multifunctional niches that are not serviceable by standard or conventional designs.

The families of designs can also be used to preserve design freedom and offer a greater variety of choices for subsequent designers who need to fulfill additional functional objectives. Finally, via constraints and bounds, the compromise DSP can be used to consider and impose processing-related limitations on a design space.

8.3.2 Achievements in Thermal Topology Design and Analysis

To support the implementation of the design methodologies, new thermal topology design and analysis techniques are introduced in this dissertation:

- A combined finite element/finite difference heat transfer analysis is introduced in Section 3.5. It is appropriate for analyzing internal and external forced convection heat transfer in the laminar or turbulent flow regimes. As noted in Sections 3.5 and 7.3.4, it is relatively fast, accurate, and reconfigurable compared with other heat transfer analysis approaches, such as FLUENT or finite difference approaches. Because it can be quickly reconfigured, it is particularly useful for investigating the effects of topological changes on thermal system performance. Gradients are also calculated for the total rate of heat transfer with respect to thicknesses and depths of elements; thereby, informing a designer or a gradient-based search/optimization algorithm of design changes that are likely to improve the performance of the system.
- An approximate topology design method for thermal applications with combined conduction and internal or external forced convection is introduced in Section 3.5. The thermal topology design method builds upon the fast, accurate, reconfigurable finite element/finite difference heat transfer analysis technique. An additional technique is introduced for evaluating gradients of thermal performance that approximate the relative contribution of each element in the thermal topology to the

overall thermal performance of the system. These gradients are used to inform a gradient-based search algorithm that modifies the topology and dimensions of the system to improve thermal performance.

8.3.3 Achievements and Contributions in the Field of Materials Design

By applying the design methodologies and analysis techniques to three materials design examples, several achievements in the field of materials design are demonstrated:

- Heat exchangers, comprised of prismatic cellular materials, are designed for representative electronic cooling applications in which they are required to dissipate heat from a high heat flux region (e.g., a microprocessor) and support structural loads. Benchmark comparisons indicate that the cellular heat exchangers presented in Chapter 5 approximately double the heat transfer rate of conventional, state-of-the-art, microprocessor heat sinks with equivalent volumes, while offering the capability of supporting structural loads experienced by portable electronic equipment such as notebook computers. This significant advance in technical performance is achieved by utilizing the compromise DSP along with approximate physics-based models to systematically explore the multifunctional design space and identify families of designs that offer a range of multifunctional performance and satisfy processing constraints. This approach is very different from ad-hoc, trial-and-error materials design approaches and predominantly single objective design approaches that generate designs that inevitably fail to meet one or more functional goals.
- Periodic unit cells are designed to meet overall structural elastic requirements that are not achievable with standard cell topologies. One non-standard cell topology is introduced in this dissertation, but the robust topology design methods could identify

- many more for specific requirements. In addition, the unit cells are designed to be robust to dimensional and topological variation from specimen to specimen in the fabrication process. The example demonstrates the effectiveness of the RTPDEM for tailoring topological preliminary design specifications for multiple performance requirements and robustness for materials design applications.
- Combustor liners, comprised of prismatic cellular materials, are designed for a gas turbine engine application. The designed combustor liners effectively raise the maximum temperature threshold of conventional metal alloy-based combustor liners by several hundred degrees Kelvin while simultaneously promising to increase the efficiency of the engine and reduce harmful NO_x emissions. This is achieved by designing multifunctional cellular materials that simultaneously bear structural loads induced by thermal stresses and combustion pressure while actively cooling themselves via forced air convection through the internal cellular structure. Internal forced convection through the cellular structure reduces the internal temperature of the cellular material to prevent melting and preserve the high-temperature structural properties of the material without requiring combustion-side film cooling of the combustor liner, thereby enabling higher combustion chamber temperatures, increased efficiency, and reduced emissions. The materials offer an alternative to ceramic matrix composites that have excellent high temperature properties but are particularly vulnerable to corrosive, high temperature environments, despite decades of research and millions of dollars in development expenditures. The advanced properties of the cellular combustor liner are achieved by applying the multifunctional, robust topology design approach introduced in this dissertation. In

this case, by utilizing a systems-based approach such as the RTPDEM, it is possible to meet the requirements of an advanced materials-limited application that has challenged material scientists for decades, without even designing a new base material. If such advances can be achieved by strategically arranging known base materials with systematic design methods, one can only imagine the advances that may be achieved by applying such approaches to materials design on smaller length scales.

8.4 LIMITATIONS AND OPPORTUNITIES FOR FUTURE WORK

As summarized in the previous section, several design methodology and materials design achievements are presented in this dissertation. However, there are many limitations to the breadth and extent of the present body of work, and these limitations naturally offer a host of opportunities for future work. In this section, opportunities for future work are outlined in the materials design field and in the areas of design methodology and product realization in general.

8.4.1 Materials Design Opportunities

Whereas the materials design examples in this dissertation are focused on continuum and larger mesoscopic and macroscopic length scales, materials design also needs to be investigated on smaller length and time scales. Also, in the examples in this dissertation, the focus is on structure-property relations and their utilization within a systematic design process for tailoring material structure for targeted properties and performance. Process-structure relations have been simplified as manufacturing-related constraints on the space of realizable material structures. However, in a more comprehensive materials design

effort, the impact of processing path on material structure must be considered more extensively along with the impact of multi-scale structure on properties and performance.

Although broad ranges of length scales and complex process-structure relations are not considered explicitly in this dissertation, it is argued that many of the concepts and methods presented in this dissertation provide a foundation that can be expanded for addressing more complex materials design problems.

As noted in Chapter 1 and illustrated in Figures 1.2 and 1.4, materials properties must be based on process-structure-property relations across length and time scales from angstroms and picoseconds to meters and years. Most material scientists seem to agree that it is unlikely that all of the length and time scales will be bridged in the near future for practical applications. Instead, a hierarchy of models are being developed and applied to specific length and time scales. For example, first principles models, based on theoretical and solid-state physics, are used on atomistic and molecular levels to predict structure and properties of ideal designs, but they are too computationally expensive to model real materials with highly heterogeneous structures that strongly influence their macroscopic properties. On the other hand, continuum-based models, based on classical continuum theory, are useful for describing properties at a macroscopic scale relevant to many engineering applications, but they are inappropriate for smaller scale phenomena that require atomistic resolution. Each model is used to inform the formulation of other models on higher length scales, but it is very difficult to formulate a single model for macroscopic material properties that unifies all of the length scales (McDowell, 1998). Instead of explicitly integrating all of the models across length and time scales, they must

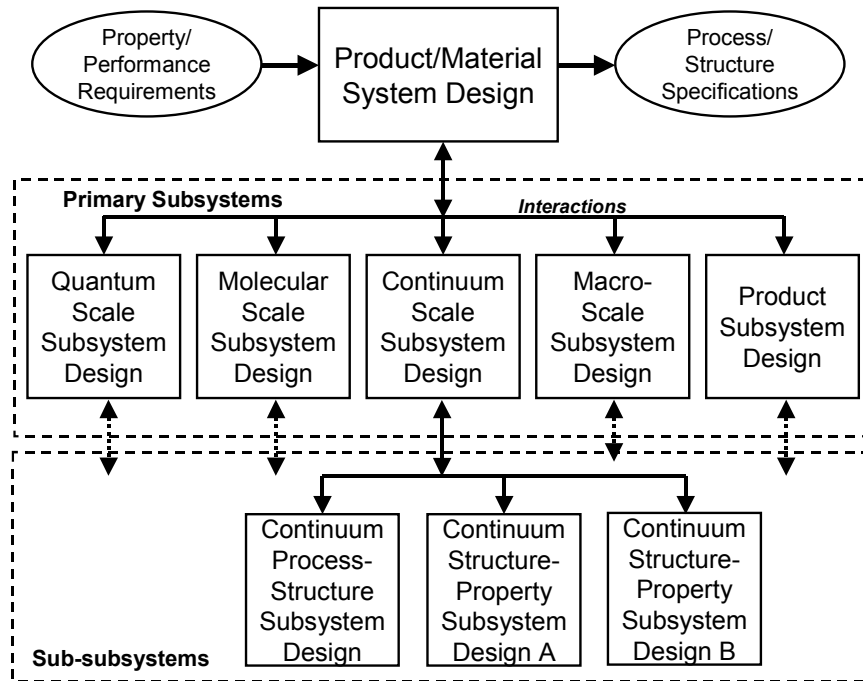


Figure 8.1 – The Hierarchical Nature of Materials Design

be linked as subsystems in an overall systems level design space that is explored by a collaborative team of experts.

As shown in Figure 8.1, a product and its constituent material can be decomposed along the boundaries of modeling domains into levels of contributing subsystems. These subsystems must be analyzed and designed concurrently and collaboratively to realize a product-material system with targeted multifunctional properties. The systems-level design problem has many of the characteristics of the multifunctional topology design problems investigated in this dissertation. For example, the subsystems are likely to be highly coupled in terms of sharing critical parameters. The analyses and associated subsystem level design problems cannot be fully integrated; instead, they must be solved by distributed teams of designers and computing resources and linked via strategic exchanges of information. It is proposed that a design method similar in principle to the

multifunctional robust topology design method introduced in this dissertation could be used to implement the hierarchical design process. Via exchange of approximate physics-based models or surrogate models, along with ranged sets of design specifications, coupled parameters can be shared between designers without unnecessarily closing design freedom.

Several factors complicate the extension of methods like the RTPDEM to multi-scale, hierarchical materials design processes. Further research is required to address them. One of these factors is the prevalence of highly nonlinear relationships and non-local solutions in materials design. Such a poorly conditioned design space may require sophisticated search techniques that can accommodate combinatorial, discrete, and parametric factors. Another factor is the temporal nature of materials design with evolution of material states and meta-stable equilibria over time. This will add another dimension to the design space and may require synthesis methods that account for dynamic behavior and properties.

In addition, materials are complex, hierarchical, heterogeneous systems, and the design of these systems is subject to many sources of variability and imprecision. For example, variation is associated with the structures and morphologies of realized materials due to variations in processing history and other factors. Uncertainty or imprecision is also associated with model-based predictions for several reasons. Models inevitably incorporate assumptions and approximations that impact the precision and accuracy of predictions, and this uncertainty may be magnified when models are utilized near the limits of their domains of application or when models are replaced by approximate surrogate models. Furthermore, experimental data for validating models

may be sparse and affected by measurement errors. It may be impossible or expensive to remove these sources of variation, but their impact on the magnitude and precision of model predictions and final system performance can be profound. Therefore, it is unreasonable to adopt a deterministic approach for materials design. Systems-level design methods need to account for the many sources of variation and facilitate the synthesis of *robust solutions* that are relatively insensitive to them. Robust design methods are introduced and utilized extensively in this dissertation, but multi-scale materials design efforts require significant expansions of currently available methods for modeling uncertainty and achieving robust designs. For example, methods are needed for estimating uncertainty and imprecision in model-based predictions and for propagating this uncertainty and imprecision through a series of coupled subsystem models. In addition, techniques are needed for (1) designing systems that are less sensitive to imprecision and (2) efficiently validating or correcting models using strategic computer or physical experiments. These topics are of major concern to product designers who need to use the designed materials in critical product applications.

Another important aspect of materials design is representation of the design space. As in the topology design problems discussed in this dissertation, representation is often a key step in creating a well-behaved design space that can be explored effectively. In general, process-structure relations in this dissertation are treated as constraints on a design space that is formulated in terms of design variables associated with the material/product structure. Methods for multi-scale materials design are required to treat these process-structure relations much more comprehensively. In fact, it may be advantageous to switch from a structure-centric design space to a process-centric design

space. As in product design, it is fruitless in materials design to explore material structures that cannot be processed or fabricated, regardless of the properties associated with those structures. Because the process-structure relationships for most materials are complex and multi-scale, it is not possible to reduce them to simple parametric constraints on the structure. Instead, process-structure models and relations must be utilized consistently throughout the design process. In addition, material structure cannot be controlled directly; it can be controlled only through processing paths. Therefore, it may be advantageous to center the design space around the factors that can be directly controlled—i.e., the process parameters. The design process would still be driven by properties and performance, but process-structure-property relationships and models would be used to link the process-centric design space to properties and performance via realizable structures.

There are many other factors that need to be considered in a materials design process such as information archiving, storage, and retrieval and distributed computing networks for integrating heterogeneous computing resources. However, those topics are left for further discussion.

8.4.2 Additional Opportunities

In addition to the plethora of opportunities in multi-scale materials design, many opportunities in product design-related areas are motivated by the concepts, methods, and examples presented in this dissertation.

Concurrent Product-Process-Material Design

Although concurrent product and process design has been an active area of research and practice for several years, designers typically *select* materials during the design

process instead of designing them along with the product. Systematic design methods and tools are needed for concurrent design of complex products, processes, and materials. One of the compelling questions involves the interface between materials design and product design. What types of materials parameters should product designers control? What types of information should be available to them, and how should it be represented? How can computer-aided design and computer-aided engineering software be expanded or upgraded to allow product designers to start varying material characteristics along with product features?

Topology and Material Microstructure Design

In this dissertation, the RTPDEM is applied to design the mesostructural topology of materials. A natural progression would be to begin incorporating details of continuum and microstructural scale models into the topology and product design process. One could begin by considering heterogeneous or spatially varying bulk material properties and then progress towards more sophisticated microstructural and smaller scale phenomena.

MEMS Design and Design for Additive Fabrication Applications

The multifunctional, robust topology design methods introduced in this dissertation are not limited in applicability to materials design. They are also applicable for MEMS and other devices for which the characteristic size of the part is on the order of material mesostructure or even microstructure. At these scales, variation in structure, boundary conditions, and other factors can have a very significant impact on the performance of the device, product, or material.

Also, the multifunctional, robust topology design methods are applicable for designing devices or products for additive fabrication. Additive fabrication techniques such as selective laser sintering (SLS) and stereolithography (SLA) are particularly appropriate domains of application for the methods introduced in this dissertation because they provide manufacturing freedom for varying the three-dimensional topology of a product and, increasingly, for varying the spatial distribution of porosity as well as heterogeneous or functionally graded materials. Using the design methods proposed in this dissertation, it is possible to design the topology of products along with some of their material properties and simultaneously to consider processing-induced variations in material properties, dimensions, and other features of the final parts.

Extending the Capabilities of the RTPDEM

There are many opportunities for extending the capabilities of the RTPDEM in its present state of development. For example, only dimensional and topological variation are considered in the examples in this dissertation although the RTPDEM can accommodate many other types of variation, including boundary conditions and bulk material properties. Also, it would be interesting to consider variations in the size and shape of the topological domain and spatially varying material properties. In addition, it would be computationally challenging to consider more complex topological domains with more elements and larger geometric areas. Also, topological design methods are needed for many functional domains in addition to the structural and thermal domains considered in this dissertation. Finally, robust topology design methods have been applied in this dissertation for discrete ground structure topology design approaches, but it would be valuable to extend them for continuum-based approaches, as well.

Comprehensive Methods for Distributed, Multifunctional/Multidisciplinary Design of Highly Coupled or Integral Systems

The multifunctional design methods proposed in this dissertation are applied only for two-stage topology design problems in this dissertation. However, they should be applicable to n-stage topology design problems and to highly coupled systems that do not involve topology design. It would be valuable to explore the use of approximate physics-based models and ranged sets of design specifications for identifying satisfactory compromise design regions that can be sequentially narrowed in subsequent design stages. This is a fundamentally different approach from the decomposition approaches currently utilized in the multidisciplinary optimization (MDO) field.

Several issues need to be addressed to facilitate broader application of the multifunctional, distributed design methods proposed in this dissertation. First, the sequential ordering of designers is likely to affect the outcome of the design process because the design spaces of sequenced designers are increasingly restricted. Principles or guidelines are needed for sequencing designers and for determining the extent to which design freedom and design spaces are reduced by each designer. Also, the approach has been demonstrated for designing topological and dimensional flexibility into designs, but it could also be extended to incorporate flexibility for variable boundary conditions, operating conditions, or other factors that could facilitate concurrent or collaborative design.

APPENDIX A

ADDITIONAL VALIDATION OF THE APPROXIMATE FINITE ELEMENT/FINITE DIFFERENCE SIMULATION MODELS FOR COMBUSTOR LINER DESIGN

In Section 7.3.4, the FE/FD model predictions of total rates of steady state heat transfer were verified. In this appendix, the performance of the FE/FD model is verified for parametric design applications in which element thicknesses are varied for a cellular material of *fixed* topology and for topology design applications in which elements are added or removed to improve the overall rate of steady state heat transfer of the structure.

A.1 PARAMETRIC DESIGN VALIDATION

To support parametric design, predictions of responses (i.e., total rate of steady state heat transfer, volume fraction) are required along with gradients of the responses with respect to element thicknesses. The gradients are used by gradient-based search/optimization algorithms to adjust design variable values in search of improved responses. Accordingly, verification is conducted in two stages:

- First, the predictions of analytical gradients are verified by comparing them with local numerical approximations of the gradients.
- Second, the FE/FD model (including analytical gradients) is used in a sample parametric design process to verify its utility for parametric design.

The basic FE/FD structure for parametric design verification is illustrated in Figure A.1. It is similar to the structure used to validate the FLUENT model (Figure 7.9), but some of the dimensions are slightly different. Specifically, the radii and angles in Figure A.1 are aligned with the nodes, and the elements are centered on the nodes. In the FLUENT structure of Figure 7.9, on the other hand, the radii and angles *bound* the

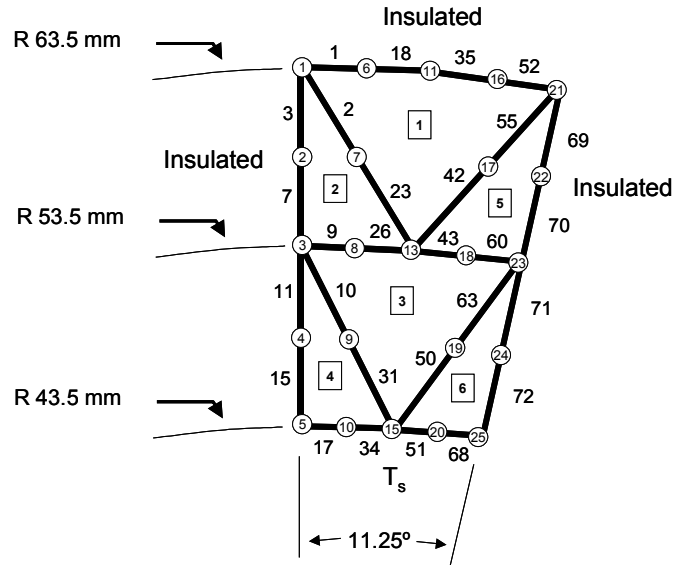


Figure A.1 – Basic Structure for Parametric Design Validation

structure, and solid material does not extend past the radii. The difference is due to the node-based manner of constructing and rendering the finite element model for the FE/FD model. Numerical labels for nodes, elements, and fluid passageways in Figure A.1 are identical to those in Figure 7.12. The boundary and operating conditions for the parametric design trials are recorded in Table A.1.

In the first stage of verification, the analytical gradients computed by MATLAB are compared with local numerical approximations of the gradients. The local numerical approximations are obtained by manually varying the relevant element thicknesses in a forward difference procedure. The results are recorded in Table A.2. All elements are assigned uniform thicknesses of 1 mm, except the elements in the interior wall (17, 34, 51, and 68) which are assigned thicknesses of 1.5 mm. Element numbers are listed in the first column; the numbers correspond to the identifications in Figure A.1. Radial symmetry is imposed on the structure with changes to elements in the left symmetric side

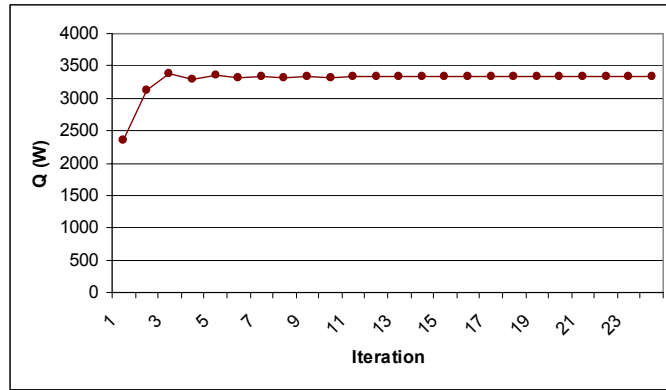
Table A.1 – Boundary and Operating Conditions for Parametric Design Trials	
T_s	1800 K
T_{in}	300 K
\dot{M}	0.02 kg/s
k	100 W/mK
L	0.05 m

of the structure mirrored to the corresponding elements in the right symmetric side of the structure. The approximate analytical gradients calculated within the FE/FD model are listed in the second column, and the numerical approximations are listed in the third column. It is clear from the percentage differences in the fourth column that the analytical gradients calculated within the FE/FD model are not precise. They differ from the numerical estimates, and the differences seem to depend on the location in the structure. Errors are larger for elements nearest the heat source (elements 15 and 31) where temperature gradients are largest. The errors are attributed to simplifications made in the calculation of the gradients, as described in Section x.x. Future work should be devoted to improving the accuracy of these gradient calculations; however, they do not need to be extremely accurate for the purposes of directing a gradient-based search/optimization algorithm. The role of the gradients is to indicate a positive or negative relationship between design variables and responses as well as the relative impact of each design variable on the response. For this purpose, the gradients are sufficiently accurate as will be seen in the next stage of verification.

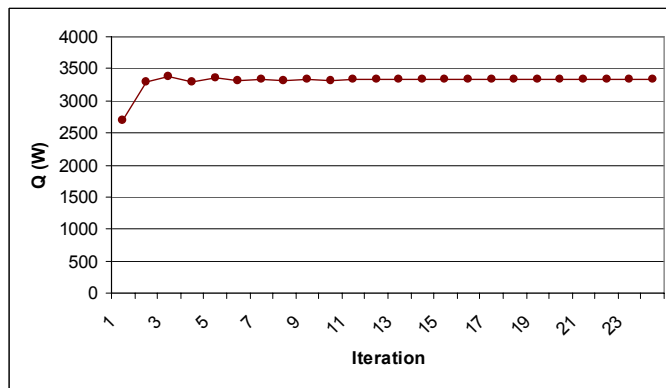
Element ID (see Figure A.1)	$\frac{\partial \dot{Q}}{\partial x}$ --Approximate Analytical (FE/FD)	$\frac{\partial \dot{Q}}{\partial x}$ --Numerical	% difference
1	53920	35000	-35.1
2	210030	132000	-37.2
3	94920	72000	-24.1
7	96380	92000	-4.5
9	75340	81000	7.5
10	240980	156000	-35.3
11	144390	166000	15.0
15	139760	295000	111.1
18	53940	34000	-37.0
23	206790	140000	-32.3
26	74440	68000	-8.7
31	225940	423000	87.2

	Trial 1		Trial 2		Trial 3	
	Initial	Final	Initial	Final	Initial	Final
X ₁ (mm)	0.8	1.39	1.0	1.39	1.3	1.39
X ₂	0.8	1.50	1.0	1.50	1.3	1.50
X ₃	0.8	1.48	1.0	1.48	1.3	1.47
X ₇	0.8	1.39	1.0	1.39	1.3	1.39
X ₉	0.8	1.50	1.0	1.50	1.3	1.50
X ₁₀	0.8	1.50	1.0	1.50	1.3	1.50
X ₁₁	0.8	1.50	1.0	1.50	1.3	1.50
X ₁₅	0.8	1.50	1.0	1.50	1.3	1.50
X ₁₈	0.8	1.50	1.0	1.50	1.3	1.49
X ₂₃	0.8	1.50	1.0	1.50	1.3	1.50
X ₂₆	0.8	1.34	1.0	1.34	1.3	1.35
X ₃₁	0.8	1.50	1.0	1.50	1.3	1.50
X ₁₇	1.5 mm	Fixed	1.5 mm	Fixed	1.5 mm	Fixed
X ₃₄	1.5 mm	Fixed	1.5 mm	Fixed	1.5 mm	Fixed
Q (W)	2350	3330	2694	3330	3192	3331
vf	0.47	0.82	0.58	0.82	0.73	0.82

Trial 1



Trial 2



Trial 3

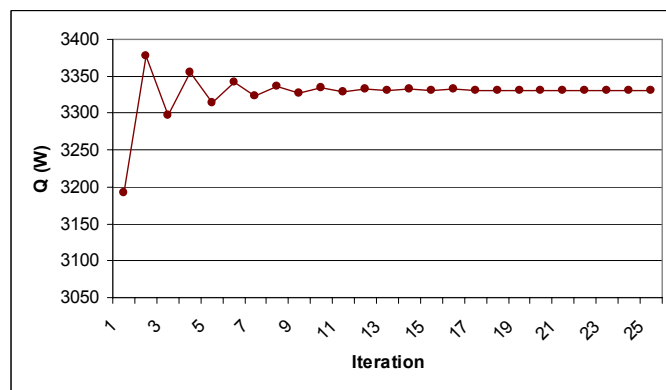


Figure A.2 – Convergence Plots for Parametric Design Trials of Thermal Topology Design Algorithm

In the second phase of parametric design verification, the FE/FD algorithm (including gradients for each response with respect to element thicknesses) is exercised in a trial parametric design study. The boundary and operating conditions are listed in Table A.1. The goal is to maximize the total rate of heat transfer while satisfying a constraint on the volume fraction of solid material of 0.82.¹ Parametric design is conducted from three different starting points: uniform cell wall dimensions of 0.8, 1.0, and 1.3 mm, respectively. The initial and final values for design variables and responses are listed in Table A.3 for each starting point. Values are listed for variables in the left half of the structure in Figure A.1 because symmetry is imposed for the structure. The elements in the interior wall are assigned fixed thicknesses of 1.5 mm (because all of their nodes are assigned fixed source temperatures and they cannot conduct heat through their transverse/out-of-plane thicknesses). It is clear from the table that the algorithm converges to nearly identical final solutions from different starting points. Notice that the total rate of steady state heat transfer is improved by as much as 979 W or 42%. Convergence plots are provided in Figure A.2 for each of the starting points. Notice that the algorithm smoothly converges for each starting point. The algorithm significantly improves the rate of steady state heat transfer, satisfies constraints on the volume fraction, and smoothly reaches nearly identical solutions from three different starting points. Therefore, this trial provides evidence that the parametric design capabilities of the thermal topology design code are working properly.

¹ The numerical value for the volume fraction is misleading. The MATLAB algorithm overestimates the volume fraction by at least 50% because it does not account for overlap among elements, which is substantial in this case.

A.2 VALIDATION OF TOPOLOGY DESIGN

In previous sections the FE/FD algorithm is validated as a tool for prediction and parametric design. In this section, it is validated as a tool for thermal topology design.

Topology design validation is conducted in two stages:

- First, the approximate analytical gradients for each response with respect to the depth of each element are validated by comparing them with forward difference numerical approximations of the gradients.
- Second, a simple topology design trial is conducted to verify the effectiveness of the FE/FD algorithm (with gradients of responses with respect to element depth) for limited thermal topology design in which a few elements are removed from an initial structure.

For both stages, the structure of the cellular heat exchanger is illustrated in Figure A.1. All of the elements are assigned initial thicknesses of 1 mm, except the elements comprising the interior wall (17, 34, 51, and 68) which are assigned thicknesses of 1.5 mm.

In the first stage of topology design validation, the approximate analytical gradients are compared with numerical approximations. The approximate analytical gradients are calculated within the MATLAB code, according to the procedure described in Section x.x. The structure in Figure A.1 is discretized into 100 slices and the last slice (nearest the exit) is used for calculating the approximate analytical gradients. The numerical approximations are calculated by removing the respective element from the structure. (In this dissertation, it is assumed that all structures are symmetric and the FE/FD algorithm is designed to accommodate symmetry by mirroring changes in one symmetric half of a

Element ID (see Figure A.1)	$\frac{\partial \dot{Q}}{\partial d}$ --Approximate Analytical (FE/FD)	$\frac{\partial \dot{Q}}{\partial d}$ --Numerical	% difference
2	1524	2050	34.5
9	4595	2186	-52.4
10	12350	5914	-52.1
23	2325	2326	0.043
26	2996	1448	-51.7
31	23415	12252	-47.7

structure into the other symmetric half.) It is clear from the results in Table A.4 that the approximate analytical gradients in the FE/FD algorithm overestimate the impact of elements near the heat source and underestimate the impact of elements farthest away from the heat source on the total rate of steady state heat transfer. The explanation is associated with the approximations embodied in the analytical gradient calculations. When an element is removed from the structure, the FE/FD algorithm combines its neighboring fluid cells into a single merged cell. Because the merged cell has a larger hydraulic diameter and therefore a lower friction factor, mass flowrate is transferred away from other cells to the merged cell—reducing the mass flowrate in all of the other cells and increasing the flowrate in the merged cell (relative to the sum of flowrates in the two pre-merged cells).² On the other hand, the FE/FD algorithm gradients are based on the assumption that the flowrate in a merged cell is equivalent to the sum of the flowrates in the constituent cells that combine to form it. When elements away from the heat source (e.g., 2) are removed, the mass flowrate is reduced in cells nearest the heat source, resulting in lower overall rates of total heat transfer than predicted by the gradients of the FE/FD algorithm. Conversely, when elements near the heat source are removed, flowrate

² Flowrate is redistributed according to a momentum balance as described in Section x.x.

Table A.5 – Initial and Final Values for Design Variables and Responses for Topology Design Trials of Thermal Topology Design Algorithm			
	Starting Point	Final Design	Comments
Q (W)	2739.8	2505	Reduced by removing elements to satisfy volume fraction constraint
Volume fraction	0.58	0.47	Satisfies volume fraction constraint of 0.47
$X_{17}, X_{34}, X_{51}, X_{68}$	1.5 mm	Fixed	
All other X	1 mm	Fixed	
$d_1, d_3, d_7, d_{11}, d_{15}, d_{17}, d_{18}, d_{34}$	0.05 m (Full length of structure)	Fixed	These are elements along the outer walls that must remain.
d_2	0.05 m	0.001	Removed.
d_9	0.05 m	0.049	
d_{10}	0.05 m	0.049	
d_{23}	0.05 m	0.004	Removed.
d_{26}	0.05 m	0.049	
d_{31}	0.05 m	0.049	

is increased in cells near the heat source, resulting in higher than predicted overall rates of steady state heat transfer. Another source of inaccuracy in the approximate analytical gradients is the fact that they are based on the final slice of the cellular structure. In examples such as this one, temperature gradients in the fluid and in the base material are significant from the inlet to the exit, and gradients based on the final slice do not precisely capture the element's role in conduction and convection throughout the structure. However, as discussed in Section 3.5, the gradients are based on the final slice for purposes of computational efficiency.

In the second phase, the FE/FD algorithm (along with gradients of the responses with respect to element depths) is exercised for a simple thermal topology design example. The starting point is recorded in Table A.5. At the starting point, all elements have full depth equal to the length of the heat exchanger (0.05 m) and *fixed* thicknesses of 1 mm (with the exception of elements 17, 34, 51, and 68 in the combustion-side wall with fixed

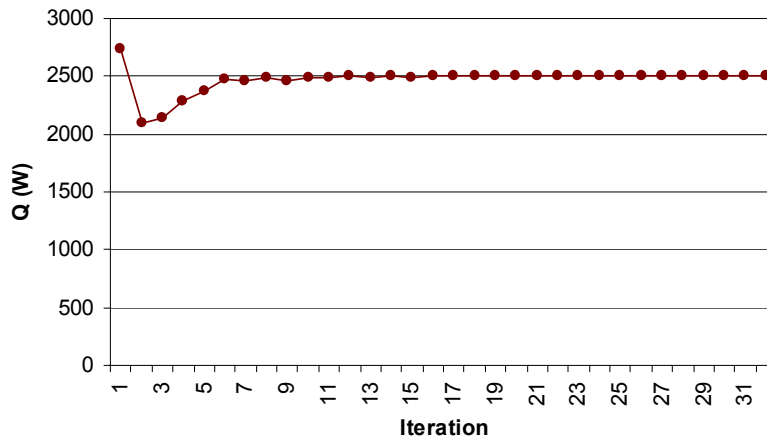


Figure A.3 – A Convergence Plot for the Topology Design Trial of the Thermal Topology Design Algorithm

thicknesses of 1.5 mm). Only the depth of the elements is varied; thicknesses are fixed in this example in order to focus exclusively on modification of element depths and thermal topology design rather than element thicknesses and parametric design. The depth of each element was constrained to vary between 1% and 99% of the full depth of the element. The total rate of steady state heat transfer was maximized. The volume fraction was constrained at 0.47—lower than the starting point volume fraction and low enough to require the removal of two elements from each symmetric side of the initial structure. Since elements must be removed from the initial structure to satisfy the volume fraction constraint, the goal of the example is to determine *which* element(s) are selected for removal by the FE/FD algorithm. As shown in Table A.5, the results of the topology design trial indicate that two elements—elements 2 and 23 in Figure A.1—should be removed from the structure. The final heat transfer rate is 2505 W. As shown in Figure A.3, the algorithm converged smoothly to its final design, as indicated by the smooth

reduction in the total rate of steady state heat transfer in Figure A.3 and the fact that the final design satisfied the volume fraction constraint and design variable bounds.

By exhaustively removing two interior elements from each symmetric half of the structure in Figure A.1, it is possible to determine which element(s) *should* be removed from the initial structure to satisfy the volume fraction constraint while maximizing the total rate of steady state heat transfer. This information can be used to assess the relative quality of the solution obtained by the FE/FD algorithm. By removing elements 9 and 26 and their symmetric counterparts in the right side of the structure in Figure A.1, it is possible to satisfy the volume fraction while achieving a 2% higher heat transfer rate than that achieved by the final design in Table A.5. This is the best possible design solution. Several other potential solutions offer heat transfer rates that differ from the solution in Table A.5 by less than 2%. On the other hand, removing pairs of elements such as 10 and 31 result in total heat transfer rates as much as 21% lower than that reported for the solution in Table A.5. Therefore, the evidence supports the conclusion that the FE/FD algorithm identifies elements for removal that have limited impact on overall objectives, relative to other elements that could potentially be removed. Due to the approximate nature of the gradients, as discussed with respect to Table A.4, it is beyond the precision of the algorithm to distinguish between solutions with objective values that differ by very small amounts (such as 2%). Therefore, it may not always identify the ‘best’ solution, but it should identify a solution that is competitive with other potential solutions.

REFERENCES

- Ananthasuresh, G. K., S. Kota and Y. Gianchandani, 1994, "A Methodological Approach to the Synthesis of Micro Compliant Mechanisms," *Solid-State Sensor and Actuator Workshop*, Hilton Head Island, SC, pp. 189-192.
- Andradottir, S., 1998, "Simulation Optimization," *Handbook of Simulation* (J. Banks, Ed.), John Wiley & Sons, Inc., NY.
- Ashby, M. F., 1999, *Materials Selection in Mechanical Design*, Butterworth-Heinemann, Oxford, UK.
- Bae, K.-R., S. Wang and K. K. Choi, 2002, "Reliability-Based Topology Optimization," *9th AIAA/ISSMO Symposium on Multidisciplinary Analysis and Optimization*, Atlanta, GA. Paper No: AIAA-2002-5542.
- Bailey, J. C., J. Intile, T. F. Fric, A. K. Tolpadi, N. V. Nirmalan and R. S. Bunker, 2002, "Experimental and Numerical Study of Heat Transfer in a Gas Turbine Combustor Liner," *International Gas Turbine Conference and Exposition*, Amsterdam, Netherlands. ASME. Paper Number: GT-2002-30183.
- Bar-Cohen, A. and M. Iyengar, 2003, "Least-Energy Optimization of Air-Cooled Heat Sinks for Sustainable Development," *IEEE Transactions on Components and Packaging Technologies*, Vol. 26, No. 1, pp. 16-25.
- Bejan, A., 1993, *Heat Transfer*, Wiley, New York.
- Bejan, A., 1995, *Entropy Generation Minimization*, CRC Press, Orlando.
- Bejan, A., 2000, *Shape and Structure: From Engineering to Nature*, Cambridge University Press.
- Bejan, A., 2002, "Dendritic Constructal Heat Exchanger with Small-Scale Crossflows and Larger-scale Counterflows," *International Journal of Heat and Mass Transfer*, Vol. 45, pp. 4607-4620.
- Bejan, A. and A. M. Morega, 1994, "The Optimal Spacing of a Stack of Plates Cooled by Turbulent Forced Convection," *International Journal of Heat and Mass Transfer*, Vol. 37, No. 6, pp. 1045-1048.
- Belegundu, A. D. and S. Zhang, 1992, "Robustness of Design through Minimum Sensitivity," *ASME Journal of Mechanical Design*, Vol. 114, pp. 213-217.
- Bendsoe, M. P., 1989, "Optimal Shape Design as a Material Distribution Problem," *Structural Optimization*, Vol. 1, pp. 193-202.

- Bendsoe, M. P., 1995, *Optimization of Structural Topology, Shape, and Material*, Springer, Heidelberg.
- Bendsoe, M. P. and N. Kikuchi, 1988, "Generating Optimal Topologies in Structural Design Using a Homogenization Method," *Computer Methods in Applied Mechanical Engineering*, Vol. 71, pp. 197-224.
- Ben-Haim, Y., 2001, *Information-Gap Decision Theory: Decisions Under Severe Uncertainty*, Academic Press, San Diego.
- Ben-Tal, A. and A. Nemirovski, 1997, "Robust Truss Topology Design via Semidefinite Programming," *SIAM Journal of Optimization*, Vol. 7, No. 4, pp. 991-1016.
- Bisgaard, S. and B. Ankenman, 1995, "Analytic Parameter Design," *Quality Engineering*, Vol. 8, No. 1, pp. 75-91.
- Bocchini, G. F., 1986, "The Influence of Porosity on the Characteristics of Sintered Materials," *The International Journal of Powder Metallurgy*, Vol. 22, No. 3, pp. 185-202.
- Bowman, V. J., 1976, "On the Relationship of the Tchebycheff Norm and the Efficient Frontier of Multiple-Criteria Objectives," *Lecture Notes in Economics and Mathematical Systems*, Vol. 135, pp. 76-85.
- Box, G., 1988, "Signal-to-Noise Ratios, Performance Criteria, and Transformations," *Technometrics*, Vol. 30, No. 1, pp. 1-18.
- Bras, B. A. and F. Mistree, 1993, "Robust Design Using Compromise Decision Support Problems," *Engineering Optimization*, Vol. 2, No. 3, pp. 213-239.
- Buckley, J. D., 1998, "Carbon-Carbon Composites," *Handbook of Composites* (S. T. Peters, Ed.), Kluwer Academic Publishers, pp. 333-351.
- Burns, S. A., Ed., 2002, *Recent Advances in Optimal Structural Design*, American Society of Civil Engineers, Reston, VA.
- Cagan, J. and B. C. Williams, 1993, "First-Order Necessary Conditions for Robust Optimality," *ASME Advances in Design Automation*, Albuquerque, NM. DE-Vol. 65-1, pp. 539-549.
- Callister, W. D., 1994, *Materials Science and Engineering, An Introduction*, Third Ed., Wiley, New York.

- Chang, T. S. and A. C. Ward, 1995, "Conceptual Robustness in Simultaneous Engineering: A Formulation in Continuous Spaces," *Research in Engineering Design*, Vol. 7, pp. 67-85.
- Chang, T. S., A. C. Ward, J. Lee and E. H. Jacox, 1994, "Conceptual Robustness in Simultaneous Engineering: An Extension of Taguchi's Parameter Design," *Research in Engineering Design*, Vol. 6, pp. 211-222.
- Charnes, A. and W. W. Cooper, 1961, *Management Models and Industrial Applications of Linear Programming*, John Wiley & Sons, New York, NY.
- Chen, T.-Y. and S.-C. Wu, 1998, "Multiobjective Optimal Topology Design of Structures," *Computational Mechanics*, Vol. 21, No. 6, pp. 483-492.
- Chen, V. C. P., K.-L. Tsui, R. R. Barton and J. K. Allen, 2003, "A Review of Design and Modeling in Computer Experiments," *Statistics in Industry* (R. Khattree and C. R. Rao, Eds.), Elsevier, Boston, Vol. 22.
- Chen, W., 1995, "A Robust Concept Exploration Method for Configuring Complex Systems," *PhD Dissertation*, G. W. Woodruff School of Mechanical Engineering, Georgia Institute of Technology, Atlanta, GA.
- Chen, W., J. K. Allen, D. Mavris and F. Mistree, 1996a, "A Concept Exploration Method for Determining Robust Top-Level Specifications," *Engineering Optimization*, Vol. 26, No. 2, pp. 137-158.
- Chen, W., J. K. Allen, K.-L. Tsui and F. Mistree, 1996b, "A Procedure for Robust Design: Minimizing Variations Caused by Noise Factors and Control Factors," *ASME Journal of Mechanical Design*, Vol. 118, No. 4, pp. 478-485.
- Chen, W. and K. Lewis, 1999, "A Robust Design Approach for Achieving Flexibility in Multidisciplinary Design," *AIAA Journal*, Vol. 37, No. 8, pp. 982-989.
- Chen, W., A. Sahai, A. Messac and G. Sundararaj, 2000, "Exploration of the Effectiveness of Physical Programming in Robust Design," *ASME Journal of Mechanical Design*, Vol. 122, No. 2, pp. 155-163.
- Chen, W., T. W. Simpson, J. K. Allen and F. Mistree, 1999a, "Satisfying Ranged Sets of Design Requirements Using Design Capability Indices as Metrics," *Engineering Optimization*, Vol. 31, pp. 615-639.
- Chen, W., M. M. Wiecek and J. Zhang, 1999b, "Quality Utility: A Compromise Programming Approach to Robust Design," *ASME Journal of Mechanical Design*, Vol. 121, No. 2, pp. 179-187.

- Chen, W. and C. Yuan, 1999, "A Probabilistic-Based Design Model for Achieving Flexibility in Design," *ASME Journal of Mechanical Design*, Vol. 121, No. 1, pp. 77-83.
- Cheng, G. and X. Guo, 1997, "Epsilon-Relaxed Approach in Structural Topology Optimization," *Structural Optimization*, Vol. 13, pp. 258-266.
- Cherkaev, A. and E. Cherkaeva, 1999, "Optimal Design for Uncertain Loading Conditions," *Homogenization* (V. Berdichevsky, V. Jikov and G. Papanicolaou, Eds.), World Scientific, pp. 193-213.
- Christiansen, S., M. Patriksson and L. Wynter, 2001, "Stochastic Bilevel Programming in Structural Optimization," *Structural and Multidisciplinary Optimization*, Vol. 21, pp. 361-371.
- Christie, D. E., 1976, *Basic Topology*, Macmillan, New York.
- Church, B. C., B. M. Dempsey, J. L. Clark, T. H. Sanders and J. K. Cochran, 2001, "Copper Alloys from Oxide Reduction for High Conductivity Applications," *Proceedings of IMECE 2001, International Mechanical Engineering Congress and Exposition*, New York.
- Cochran, J. K., K. J. Lee, D. L. McDowell and T. H. Sanders, 2000, "Low Density Monolithic Honeycombs by Thermal Chemical Processing," *Proceedings of the 4th Conference on Aerospace Materials, Processes, and Environmental Technology*, Huntsville, AL.
- Cook, R. D., D. S. Malkus and M. E. Plesha, 1989, *Concepts and Applications of Finite Element Analysis*, 3rd Ed., John Wiley and Sons, New York.
- Crawford, R. H. and J. J. Beaman, 1999, "Solid Freeform Fabrication," *IEEE Spectrum*, Vol. 36, No. 2, pp. 34-43.
- Culham, J. R. and Y. S. Muzychka, 2001, "Optimization of Plate Fin Heat Sinks Using Entropy Generation Minimization," *IEEE Transactions on Components and Packaging Technologies*, Vol. 24, No. 2, pp. 159-165.
- Davis, D. M., 2001, "Topology," *Encyclopedia of Mathematics Education* (L. S. Grinstein and S. J. Lipsey, Eds.), Routledge-Falmer, New York.
- Dempsey, B. M., 2002, "Thermal Properties of Linear Cellular Alloys," *M.S. Thesis*, G.W. Woodruff School of Mechanical Engineering, Georgia Institute of Technology, Atlanta, GA.

- Diaz, A. and M. P. Bendsoe, 1992, "Shape Optimization of Structures for Multiple Loading Situations Using a Homogenization Method," *Structural Optimization*, Vol. 4, pp. 17-22.
- Diaz, A., R. Lipton and C. A. Soto, 1995, "A New Formulation of the Problem of Optimum Reinforcement of Reissner-Mindlin Plates," *Computer Methods in Applied Mechanics and Engineering*, Vol. 123, pp. 121-139.
- Dimiduk, D. M. and J. H. Perepezko, 2003, "Mo-Si-B Alloys: Developing a Revolutionary Turbine-Engine Material," *MRS Bulletin*, Vol. September, pp. 639-645.
- Dorn, W. S., R. E. Gomory and H. J. Greenberg, 1964, "Automatic Design of Optimal Structures," *Journal de Mecanique*, Vol. 3, pp. 25-52.
- Du, X. and W. Chen, 2000, "Towards a Better Understanding of Modeling Feasibility Robustness in Engineering Design," *ASME Journal of Mechanical Design*, Vol. 122, No. 4, pp. 385-394.
- Du, X. and W. Chen, 2002, "Efficient Uncertainty Analysis Methods for Multidisciplinary Robust Design," *AIAA Journal*, Vol. 40, No. 3, pp. 545-552.
- Elishakoff, I., R. T. Haftka and J. Fang, 1994, "Structural Design Under Bounded Uncertainty--Optimization with Anti-optimization," *Computers and Structures*, Vol. 53, No. 6, pp. 1401-1405.
- Eschenauer, H. A. and N. Olhoff, 2001, "Topology Optimization of Continuum Structures: A Review," *Applied Mechanics Reviews*, Vol. 54, No. 4, pp. 331-389.
- Evans, A. G., J. W. Hutchinson and M. F. Ashby, 1999, "Multifunctionality of Cellular Metal Systems," *Progress in Materials Science*, Vol. 43, pp. 171-221.
- Evans, A. G., J. W. Hutchinson, N. A. Fleck, M. F. Ashby and H. N. G. Wadley, 2001, "The Topological Design of Multifunctional Cellular Materials," *Progress in Materials Science*, Vol. 46, No. 3-4, pp. 309-327.
- Fernandez, M. G., 2002, "On Decision Support for Distributed Collaborative Design and Manufacture," *M.S. Thesis*, G.W. Woodruff School of Mechanical Engineering, Georgia Institute of Technology, Atlanta, GA.
- Fernandez, M. G., 2003, *A Comparative Study of Optimization Algorithms for the Topological Design of Structures*, ME 6103 Final Project Report, Georgia Institute of Technology, Atlanta, GA.

- Finger, S. and J. R. Dixon, 1989, "A Review of Research in Mechanical Engineering Design. Part I: Descriptive, Prescriptive, and Computer-Based Models of Design Processes," *Research in Engineering Design*, Vol. 1, No. 1, pp. 51-67.
- Fraas, A. P., 1989, *Heat Exchanger Design*, 2nd Ed., Wiley, New York.
- Frecker, M., N. Kikuchi and S. Kota, 1999, "Topology Optimization of Compliant Mechanisms with Multiple Outputs," *Structural Optimization*, Vol. 17, No. 4, pp. 269-278.
- Frecker, M., S. Kota and N. Kikuchi, 1997a, "Use of Penalty Function in Topological Synthesis and Optimization of Strain Energy Density of Compliant Mechanisms," *ASME Advances in Design Automation Conference*, Sacramento, CA. Paper Number: DETC97/DAC-3760.
- Frecker, M. I., G. K. Ananthasuresh, S. Nishiwaki, N. Kikuchi and S. Kota, 1997b, "Topological Synthesis of Compliant Mechanisms Using Multi-Criteria Optimization," *ASME Journal of Mechanical Design*, Vol. 119, No. 2, pp. 238-245.
- Gibson, L. J. and M. F. Ashby, 1997, *Cellular Solids: Structure and Properties*, Cambridge University Press, Cambridge, UK.
- Giunta, A. A., V. Balabanov, D. Haim, B. Grossman, W. H. Mason, L. T. Watson and R. T. Haftka, 1997, "Aircraft Multidisciplinary Design Optimization Using Design of Experiments Theory and Response Surface Modelling," *Aeronautical Journal*, Vol. 101, No. 1008, pp. 347-356.
- Gu, S., T. J. Lu and A. G. Evans, 2001, "On the Design of Two-Dimensional Cellular Metals for Combined Heat Dissipation and Structural Load Capacity," *International Journal of Heat and Mass Transfer*, Vol. 44, No. 11, pp. 2163-2175.
- Gu, X. and J. E. Renaud, 2001, "Implicit Uncertainty Propagation for Robust Collaborative Optimization," *ASME Advances in Design Automation Conference*, Pittsburgh, PA. Paper No: DETC2001/DAC-21118.
- Gu, X., J. E. Renaud, S. M. Batill, R. M. Brach and A. S. Budhiraja, 2000, "Worst Case Propagated Uncertainty of Multidisciplinary Systems in Robust Design Optimization," *Structural and Multidisciplinary Optimization*, Vol. 20, pp. 190-213.
- Guralnik, D. B., Ed., 1973, *Webster's New World Dictionary of the American Language with Student Handbook*, The Southwestern Company, Nashville, TN.
- Haftka, R. T., 1985, "Simultaneous Analysis and Design," *AIAA Journal*, Vol. 23, No. 7, pp. 1099-1103.

- Hajela, P. and E. Lee, 1995, "Genetic Algorithms in Truss Topological Optimization," *International Journal of Solids and Structures*, Vol. 32, No. 22, pp. 3341-3357.
- Hayes, A. M., A. Wang, B. M. Dempsey and D. L. McDowell, 2004, "Mechanics of Linear Cellular Alloys," *Mechanics of Materials*, *in press*.
- Hernandez, G., J. K. Allen and F. Mistree, 2001, "The Compromise Decision Support Problem: Modeling the Deviation Function as in Physical Programming," *Engineering Optimization*, Vol. 33, No. 4, pp. 445-471.
- Hodge, B. K., 1999, *Analysis and Design of Energy Systems*, Simon & Schuster, Upper Saddle River, NJ.
- Hyun, S. and S. Torquato, 2001, "Designing Composite Microstructures with Targeted Properties," *Journal of Materials Research*, Vol. 16, No. 1, pp. 280-285.
- Hyun, S. and S. Torquato, 2002, "Optimal and Manufacturable Two-Dimensional, Kagome-Like Cellular Solids," *Journal of Materials Research*, Vol. 17, No. 1, pp. 137-144.
- Incropera, F. P. and D. P. DeWitt, 1996, *Fundamentals of Heat and Mass Transfer*, 3rd Ed., John Wiley & Sons, New York.
- iSIGHT, 2003, Engineous Software, Inc., Cary, NC, Version 7.0.
- Judex, S., S. Boyd, Y.-X. Qin, S. Turner, K. Ye, R. Muller and C. Rubin, 2003, "Adaptations of Trabecular Bone to Low Magnitude Vibrations Result in More Uniform Stress and Strain under Load," *Annals of Biomedical Engineering*, Vol. 31, No. 1, pp. 12-20.
- Kakac, S., R. K. Shah and W. Aung, Eds., 1987, *Handbook of Single-Phase Convective Heat Transfer*, Wiley-Interscience, New York.
- Kalsi, M., K. Hacker and K. Lewis, 2001, "A Comprehensive Robust Design Approach for Decision Trade-Offs in Complex Systems Design," *ASME Journal of Mechanical Design*, Vol. 123, No. 1, pp. 1-10.
- Keaveny, T. M., 2001, "Trabecular Bone Strength," *Bone Mechanics Handbook* (S. C. Cowin, Ed.), CRC Press, Boca Raton, FL, pp. 16.1-16.42.
- Keeney, R. L. and H. Raiffa, 1976, *Decisions with Multiple Objectives: Preferences and Value Tradeoffs*, John Wiley and Sons, New York.
- Kirsch, U., 1989a, "Optimal Topologies of Structures," *Applied Mechanics Reviews*, Vol. 42, No. 8, pp. 223-239.

- Kirsch, U., 1989b, "Optimal Topologies of Truss Structures," *Computer Methods in Applied Mechanics and Engineering*, Vol. 72, No. 1, pp. 15-28.
- Kirsch, U. and P. Y. Papalambros, 2001, "Structural Reanalysis for Topological Modifications--A Unified Approach," *Structural and Multidisciplinary Optimization*, Vol. 21, No. 5, pp. 333-344.
- Knight, R. W., J. S. Goodling and D. J. Hall, 1991, "Optimal Thermal Design of Forced Convection Heat Sinks--Analytical," *Journal of Electronic Packaging*, Vol. 113, pp. 313-321.
- Koch, P. N., 1997, "Hierarchical Modeling and Robust Synthesis for the Preliminary Design of Large-Scale Complex Systems," *PhD Dissertation*, G.W. Woodruff School of Mechanical Engineering,, Georgia Institute of Technology, Atlanta, GA.
- Koch, P. N., T. W. Simpson, J. K. Allen and F. Mistree, 1999, "Statistical Approximations for Multidisciplinary Design Optimization: The Problem of Size," *Journal of Aircraft*, Vol. 36, No. 1, pp. 275-286.
- Kocvara, M., J. Zowe and A. Nemirovski, 2000, "Cascading--An Approach to Robust Material Optimization," *Computers and Structures*, Vol. 76, pp. 431-442.
- Koehler, J. R. and A. B. Owen, 1996, "Computer Experiments," *Handbook of Statistics* (S. Ghosh and C. R. Rao, Eds.), Elsevier Science, NY, Vol. 13, pp. 261-308.
- Koski, J., 1985, "Defectiveness of Weighting Method in Multicriterion Optimization of Structures," *Communications in Applied Numerical Methods*, Vol. 1, pp. 333-337.
- Kraus, A. D. and A. Bar-Cohen, 1995, *Design and Analysis of Heat Sinks*, Wiley, New York.
- Krog, L. A. and N. Olhoff, 1999, "Optimum Topology and Reinforcement Design of Disk and Plate Structures with Multiple Stiffness and Eigenfrequency Objectives," *Computers and Structures*, Vol. 72, pp. 535-563.
- Kroo, I., S. Altus, R. Braun, P. Gage and I. Sobieski, 1994, "Multidisciplinary Optimization Methods for Aircraft Preliminary Design," *5th AIAA/USAF/NASA/ISSMO Symposium on Multidisciplinary Analysis and Optimization*, Panama City, FL. Paper No. AIAA-94-4325.
- Kroo, I. M., 1997, "Multidisciplinary Optimization Applications in Preliminary Design--Status and Directions," *38th AIAA/ASME/ASCE/AHS/ASC, Structures, Structural Dynamics, and Materials Conference*, Kissimmee, FL. Paper Number: AIAA97-1408.

- Kumar, P., J. K. Santosa, E. Beck and S. Das, 2004, "Direct-Write Deposition of Fine Powders through Miniature Hopper-Nozzles for Multi-Material Solid Freeform Fabrication," *Rapid Prototyping Journal*, Vol. 10, No. 1, pp. 14-23.
- Kumar, R. S. and D. L. McDowell, 2002, "Design of Multifunctional Materials," *9th AIAA/ISSMO Symposium on Multidisciplinary Analysis and Optimization*, Atlanta, GA. Paper Number: AIAA-2002-5569.
- Lee, S., 1995, "Optimum Design and Selection of Heat Sinks," *IEEE Transactions on Components and Packaging Technologies*, Vol. 18, No. 4, pp. 812-817.
- Lewis, K. and F. Mistree, 1998, "The Other Side of Multidisciplinary Design Optimization: Accommodating a Multiobjective, Uncertain, and Non-Deterministic World," *Engineering Optimization*, Vol. 31, No. 2, pp. 161-189.
- Li, Q., G. P. Steven and O. M. Querin, 2000, "Structural Topology Design with Multiple Thermal Criteria," *Engineering Computations*, Vol. 17, No. 6, pp. 715-734.
- Li, Q., G. P. Steven, O. M. Querin and Y. M. Xie, 1999, "Shape and Topology Design for Heat Conduction by Evolutionary Structural Optimization," *International Journal of Heat and Mass Transfer*, Vol. 42, pp. 3361-3371.
- Liu, J. S., 2001, *Monte Carlo Strategies in Scientific Computing*, Springer, NY.
- Lu, T. J., 1999, "Heat Transfer Efficiency of Metal Honeycombs," *International Journal of Heat and Mass Transfer*, Vol. 42, No. 11, pp. 2031-2040.
- Ma, Z.-D., N. Kikuchi and H.-C. Cheng, 1995, "Topological Design for Vibrating Structures," *Computer Methods in Applied Mechanics and Engineering*, Vol. 121, pp. 259-280.
- Malvern, L. E., 1969, *Introduction to the Mechanics of a Continuous Medium*, Prentice-Hall, Upper Saddle River, NJ.
- Marston, M., J. K. Allen and F. Mistree, 2000, "The Decision Support Problem Technique: Integrating Descriptive and Normative Approaches in Decision Based Design," *Journal of Engineering Valuation and Cost Analysis*, Vol. 3, No. 2, pp. 107-129.
- MATLAB, 2001, The Math Works, Inc., Natick, MA, Version 6.5, Release 13.
- Maute, K. and D. M. Frangopol, 2003, "Reliability-Based Design of MEMS Mechanisms by Topology Optimization," *Computers and Structures*, Vol. 81, pp. 813-824.

- Mavris, D. N., O. Bandte and D. A. DeLaurentis, 1999, "Robust Design Simulation: A Probabilistic Approach to Multidisciplinary Design," *Journal of Aircraft*, Vol. 36, No. 1, pp. 298-307.
- McDowell, D. L., 1998, *New Directions in Materials Design Science and Engineering (MDS&E)*, Report of a Workshop Sponsored by the U.S. National Science Foundation, Georgia Institute of Technology and Morehouse College, Atlanta, GA.
- McKay, M. D., R. J. Beckman and W. J. Conover, 1979, "A Comparison of Three Methods for Selecting Values of Input Variables in the Analysis of Output from a Computer Code," *Quality Engineering*, Vol. 11, No. 3, pp. 417-425.
- Messac, A., 1996, "Physical Programming: Effective Optimization for Computational Design," *AIAA Journal*, Vol. 34, No. 1, pp. 149-158.
- Messac, A., S. M. Gupta and B. Akbulut, 1996, "Linear Physical Programming; A New Approach to Multiple Objective Optimization," *Transactions in Operations Research*, Vol. 8, pp. 39-59.
- Michelena, N. F. and A. M. Agogino, 1994, "Formal Solution of N-Type Robust Parameter Design Problems with Stochastic Noise Factors," *ASME Journal of Mechanical Design*, Vol. 116, No. 2, pp. 501-507.
- Michell, A. G. M., 1904, "The Limits of Economy of Materials in Frame Structures," *Philosophical Magazine*, Vol. 8, No. 47, pp. 589-597.
- Min, S., S. Nishiwaki and N. Kikuchi, 2000, "Unified Topology Design of Static and Vibrating Structures Using Multiobjective Optimization," *Computers and Structures*, Vol. 75, No. 1, pp. 93-116.
- Mistree, F., O. F. Hughes and B. A. Bras, 1993a, "The Compromise Decision Support Problem and the Adaptive Linear Programming Algorithm," *Structural Optimization: Status and Promise* (M. P. Kamat, Ed.), AIAA, Washington, D.C., pp. 247-286.
- Mistree, F., W. F. Smith and B. A. Bras, 1993b, "A Decision-Based Approach to Concurrent Engineering," *Handbook of Concurrent Engineering* (H. R. Paresai and W. Sullivan, Eds.), Chapman & Hall, New York, pp. 127-158.
- Mistree, F., W. F. Smith, B. A. Bras, J. K. Allen and D. Muster, 1990, "Decision-Based Design: A Contemporary Paradigm for Ship Design," *Transactions, Society of Naval Architects and Marine Engineers*, Vol. 98, pp. 565-597.
- Mortenson, M. E., 1999, *Mathematics for Computer Graphics Applications*, 2nd Ed., Industrial Press, New York.

- Myers, R. H. and D. C. Montgomery, 1995, *Response Surface Methodology: Process and Product Optimization Using Designed Experiments*, John Wiley and Sons, New York.
- Nair, V. N., 1992, "Taguchi's Parameter Design: A Panel Discussion," *Technometrics*, Vol. 34, pp. 127-161.
- Nemat-Nasser, S. and M. Hori, 1999, *Micromechanics: Overall Properties of Heterogeneous Materials*, 2nd Ed., Elsevier, Amsterdam.
- Neves, M. M., H. Rodrigues and J. M. Guedes, 2000, "Optimal Design of Periodic Linear Elastic Microstructures," *Computers and Structures*, Vol. 76, No. 1-3, pp. 421-429.
- Neves, M. N., O. Sigmund and M. P. Bendsoe, 2002, "Topology Optimization of Periodic Microstructures with a Penalization of Highly Localized Buckling Modes," *International Journal for Numerical Methods in Engineering*, Vol. 54, pp. 809-834.
- Ohsaki, M. and C. C. Swan, 2002, "Topology and Geometry Optimization of Trusses and Frames," *Recent Advances in Optimal Structural Design* (S. A. Burns, Ed.), American Society of Civil Engineers, Reston, VA.
- Olson, G. B., 1997, "Computational Design of Hierarchically Structured Materials," *Science*, Vol. 277, No. 5330, pp. 1237-1242.
- Olson, G. B., 2000, "Designing a New Material World," *Science*, Vol. 288, No. 5468, pp. 993-998.
- Otto, K. N. and E. K. Antonsson, 1993a, "Extensions to the Taguchi Method of Product Design," *ASME Journal of Mechanical Design*, Vol. 115, No. 1, pp. 5-13.
- Otto, K. N. and E. K. Antonsson, 1993b, "Tuning Parameters in Engineering Design," *ASME Journal of Mechanical Design*, Vol. 115, No. 1, pp. 14-19.
- Pahl, G. and W. Beitz, 1996, *Engineering Design: A Systematic Approach*, 2nd Edition Ed., Springer-Verlag, New York.
- Pareto, V., 1909, *Manuel D'Economie Politique*.
- Parkinson, A., C. Sorensen and N. Pourhassan, 1993, "A General Approach for Robust Optimal Design," *ASME Journal of Mechanical Design*, Vol. 115, No. 1, pp. 74-80.
- Pedersen, K., J. Emblemvag, J. K. Allen and F. Mistree, 2000, "Validating Design Methods and Research--The Validation Square," *ASME Design Theory and Methodology Conference*, Baltimore, MD. Paper Number: DETC00/DTM-14579.

- Phadke, M. S., 1989, *Quality Engineering Using Robust Design*, Prentice Hall, Englewood Cliffs, NJ.
- Rajagopalan, S., R. Goldman, K.-H. Shin, V. Kumar, M. Cutkosky and D. Dutta, 2001, "Representation of Heterogeneous Objects During Design, Processing, and Freeform-Fabrication," *Materials and Design*, Vol. 22, No. 3, pp. 185-197.
- Ramakrishnan, B. and S. S. Rao, 1996, "A General Loss Function Based Optimization Procedure for Robust Design," *Engineering Optimization*, Vol. 25, No. 4, pp. 255-276.
- Reddy, G. and J. Cagan, 1995, "Optimally Directed Truss Topology Generation Using Shape Annealing," *ASME Journal of Mechanical Design*, Vol. 117, No. 1, pp. 206-209.
- Reddy, J. N., 1993, *An Introduction to the Finite Element Method*, 2nd Ed., McGraw-Hill, Boston.
- Rozvany, G. I. N., 1972, "Grillages of Maximum Strength and Maximum Stiffness," *International Journal of Mechanical Sciences*, Vol. 14, pp. 651-666.
- Rozvany, G. I. N., 1996, "Difficulties in Truss Topology Optimization with Stress, Local Buckling and System Stability Constraints," *Structural Optimization*, Vol. 11, No. 3-4, pp. 213-217.
- Rozvany, G. I. N., 2001, "Aims, Scope, Methods, History, and Unified Terminology of Computer-Aided Topology Optimization in Structural Mechanics," *Structural and Multidisciplinary Optimization*, Vol. 21, pp. 90-108.
- Rozvany, G. I. N. and W. Prager, 1976, "Optimal Design of Partially Discretized Grillages," *Journal of the Mechanics and Physics of Solids*, Vol. 24, pp. 125-136.
- Rozvany, G. I. N., M. Zhou and T. Birker, 1992, "Generalized Shape Optimization without Homogenization," *Structural Optimization*, Vol. 4, pp. 250-252.
- Sandgren, E. and T. M. Cameron, 2002, "Robust Design Optimization of Structures through Consideration of Variation," *Computers and Structures*, Vol. 80, pp. 1605-1613.
- Saxena, A. and G. K. Ananthasuresh, 2000, "On an Optimal Property of Compliant Topologies," *Structural and Multidisciplinary Optimization*, Vol. 19, No. 1, pp. 36-49.
- Schneibel, J. H., M. J. Kramer, O. Unal and R. N. Wright, 2001, "Processing and Mechanical Properties of a Molybdenum Silicide with the Composition Mo-12Si-8.5B (at. %)," *Intermetallics*, Vol. 9, pp. 25-31.

- Seepersad, C. C., 2001, "A Utility-Based Compromise Decision Support Problem with Applications in Product Platform Design," *M.S. Thesis*, G.W. Woodruff School of Mechanical Engineering, Georgia Institute of Technology, Atlanta, GA.
- Seepersad, C. C., B. M. Dempsey, J. K. Allen, F. Mistree and D. L. McDowell, 2004, "Design of Multifunctional Honeycomb Materials," *AIAA Journal*, Vol. 42, No. 5, pp. 1025-1033.
- Shoemaker, A. C., K.-L. Tsui and C. F. J. Wu, 1991, "Economical Experimentation Methods for Robust Design," *Technometrics*, Vol. 33, pp. 415-427.
- Sigmund, O., 1994, "Materials with Prescribed Constitutive Parameters: An Inverse Homogenization Problem," *International Journal of Solids and Structures*, Vol. 31, pp. 2313-2329.
- Sigmund, O., 1995, "Tailoring Materials with Prescribed Elastic Properties," *Mechanics of Materials*, Vol. 20, pp. 351-368.
- Sigmund, O., 1998, "Topology Optimization in Multiphysics Problems," *7th AIAA/USAF/NASA/ISSMO Symposium on Multidisciplinary Analysis and Optimization*. AIAA, Vol. 1, pp. 1492-1500.
- Sigmund, O., 2000, "A New Class of Extremal Composites," *Journal of the Mechanics and Physics of Solids*, Vol. 48, No. 2, pp. 397-428.
- Sigmund, O., 2001, "A 99 Line Topology Optimization Code Written in Matlab," *Structural and Multidisciplinary Optimization*, Vol. 21, pp. 120-127.
- Sigmund, O. and S. Torquato, 1997, "Design of Materials with Extreme Thermal Expansion Using a Three-Phase Topology Optimization Method," *Journal of the Mechanics and Physics of Solids*, Vol. 45, No. 6, pp. 1037-1067.
- Sigmund, O. and S. Torquato, 1999, "Design of Smart Composite Materials Using Topology Optimization," *Smart Materials and Structures*, Vol. 8, No. 3, pp. 365-379.
- Silva, M. J. and L. J. Gibson, 1997, "Modeling the Mechanical Behavior of Vertebral Trabecular Bone: Effects of Age-Related Changes in Microstructure," *Bone*, Vol. 21, No. 2, pp. 191-199.
- Silva, M. J., W. C. Hayes and L. J. Gibson, 1995, "The Effects of Non-Periodic Microstructure on the Elastic Properties of Two-Dimensional Cellular Solids," *International Journal of Mechanical Sciences*, Vol. 37, No. 11, pp. 1161-1177.
- Simon, H. A., 1983, *Reason in Human Affairs*, Stanford University Press, Stanford, CA.

- Simon, H. A., 1996, *The Sciences of the Artificial*, MIT Press, Cambridge, Mass.
- Simpson, T. W., J. K. Allen and F. Mistree, 1998, "Spatial Correlation Metamodels for Global Approximation in Structural Optimization," *ASME Advances in Design Automation Conference*, Atlanta, GA. Paper Number: DETC98/DAC-5615.
- Simpson, T. W., W. Chen, J. K. Allen and F. Mistree, 1996, "Conceptual Design of a Family of Products Through the Use of the Robust Concept Exploration Method," *6th AIAA/USAF/NASA/ISSMO Symposium on Multidisciplinary Analysis and Optimization*, Bellevue, WA. AIAA Paper Number 96-4161.
- Simpson, T. W., J. R. A. Maier and F. Mistree, 2001, "Product Platform Design: Method and Application," *Research in Engineering Design*, Vol. 13, No. 1, pp. 2-22.
- Sobieszczanski-Sobieski, J., 1988, "Optimization by Decomposition: A Step from Hierarchic to Non-Hierarchic Systems," *NASA Technical Memorandum*, NASA Langley Research Center.
- Sobieszczanski-Sobieski, J. and R. T. Haftka, 1997, "Multidisciplinary Aerospace Design Optimization: Survey of Recent Developments," *Structural and Multidisciplinary Optimization*, Vol. 14, pp. 1-23.
- Su, J. and J. E. Renaud, 1997, "Automatic Differentiation in Robust Optimization," *AIAA Journal*, Vol. 35, No. 6, pp. 1072-1079.
- Summers, E., A. J. Thom, B. Cook and M. Akinc, 2000, "Extrusion and Selected Engineering Properties of Mo-Si-B Intermetallics," *Intermetallics*, Vol. 8, pp. 1169-1174.
- Sundaresan, S., K. Ishii and D. R. Houser, 1995, "A Robust Optimization Procedure with Variations on Design Variables and Constraints," *Engineering Optimization*, Vol. 24, pp. 101-117.
- Svanberg, K., 1987, "The Method of Moving Asymptotes--A New Method for Structural Optimization," *International Journal for Numerical Methods in Engineering*, Vol. 24, pp. 359-373.
- Taguchi, G., 1986, *Introduction to Quality Engineering*, The Asian Productivity Organization, Tokyo.
- Taguchi, G. and D. Clausing, 1990, "Robust Quality," *Harvard Business Review*, Vol. Jan/Feb, pp. 65-75.
- Thampan, C. K. P. V. and C. S. Krishnamoorthy, 2001, "System Reliability-Based Configuration Optimization of Trusses," *Journal of Structural Engineering*, Vol. 127, No. 8, pp. 947-956.

- Tiegs, T. N. and J. M. Wang, 1995, "Strength and Toughness of Ceramic Composites at Elevated Temperatures," *High Temperature Mechanical Behavior of Ceramic Composites* (S. V. Nair and K. Jakus, Eds.), Elsevier, pp. 87-118.
- Topping, B. H. V., 1984, "Shape Optimization of Skeletal Structures: A Review," *Journal of Structural Engineering*, Vol. 109, No. 8, pp. 1933-1951.
- Topping, B. H. V., A. I. Khan and J. P. Leite, 1996, "Topological Design of Truss Structures Using Simulated Annealing," *Structural Engineering Review*, Vol. 8, pp. 301-314.
- Torquato, S., L. V. Gibiansky, M. J. Silva and L. J. Gibson, 1998, "Effective Mechanical and Transport Properties of Cellular Solids," *International Journal of Mechanical Sciences*, Vol. 40, No. 1, pp. 71-82.
- Tsui, K.-L., 1992, "An Overview of Taguchi Method and Newly Developed Statistical Methods for Robust Design," *IIE Transactions*, Vol. 24, No. 5, pp. 44-57.
- Tsui, K.-L., 1996, "A Critical Look at Taguchi's Modeling Approach for Robust Design," *Journal of Applied Statistics*, Vol. 23, No. 1, pp. 81-95.
- Ulrich, K., 1995, "The Role of Product Architecture in the Manufacturing Firm," *Research Policy*, Vol. 24, No. 3, pp. 419-440.
- Vadde, S., R. S. Krishnamachari, J. K. Allen and F. Mistree, 1994, "The Bayesian Compromise Decision Support Problem for Hierarchical Design Involving Uncertainty," *ASME Journal of Mechanical Design*, Vol. 116, pp. 388-395.
- van der Sluis, O., P. J. G. Schreurs, W. A. M. Brekelmans and H. E. H. Meijer, 2000, "Overall Behavior of Heterogeneous Elastoviscoplastic Materials: Effect of Microstructural Modeling," *Mechanics of Materials*, Vol. 32, pp. 449-462.
- Varadarajan, S., W. Chen and C. J. Pelka, 2000, "Robust Concept Exploration of Propulsion Systems with Enhanced Model Approximation Capabilities," *Engineering Optimization*, Vol. 32, No. 3, pp. 309-334.
- Vining, G. G. and R. H. Myers, 1990, "Combining Taguchi and Response Surface Philosophies: A Dual Response Approach," *Journal of Quality Technology*, Vol. 22, pp. 38-45.
- von Neumann, J. and O. Morgenstern, 1947, *The Theory of Games and Economic Behavior*, Princeton University Press, Princeton, NJ.

- Wang, A. and D. L. McDowell, 2004, "Effects of Defects on In-Plane Properties of Periodic Metal Honeycombs," *International Journal of Mechanical Sciences*, Vol. 45, No. 11, pp. 1799-1813.
- Ward, A., J. K. Liker, J. J. Cristiano and D. K. Sobek, 1995, "The Second Toyota Paradox: How Delaying Decisions Can Make Better Cars Faster," *Sloan Management Review*, pp. 43-61.
- Welch, W. J., T. K. Yu, S. M. Kand and J. Sacks, 1990, "Computer Experiments for Quality Control by Parameter Design," *Journal of Quality Technology*, Vol. 22, pp. 15-22.
- Wujek, B. A., J. E. Renaud, S. M. Batill and J. B. Brockman, 1996, "Concurrent Subspace Optimization Using Design Variable Sharing in a Distributed Computing Environment," *Concurrent Engineering: Research and Applications*, Vol. 4, No. 4, pp. 361-377.
- Xiao, A., 2003, "Collaborative Multidisciplinary Decision Making in a Distributed Environment," *Ph.D. Dissertation*, G.W. Woodruff School of Mechanical Engineering, Georgia Institute of Technology, Atlanta, GA.
- Yu, J. and K. Ishii, 1994, "Robust Design by Matching the Design with Manufacturing Variation Patterns," *ASME Design Automation Conference*, Minneapolis, MN. DE-Vol. 69-2, pp. 7-14.
- Yu, J. and K. Ishii, 1998, "Design for Robustness Based on Manufacturing Variation Patterns," *ASME Journal of Mechanical Design*, Vol. 120, No. 2, pp. 196-202.
- Yu, P. L. and G. Leitmann, 1974, "Compromise Solutions, Domination Structures, and Salukvadze's Solution," *Journal of Optimization Theory and Applications*, Vol. 13, No. 3, pp. 362-378.
- Zeleny, M., 1973, "Compromise Programming," *Multiple Criteria Decision-Making* (J. L. Cochrane and M. Zeleny, Eds.), University of South Carolina Press, Columbia, SC, pp. 262-301.
- Zhou, Q.-J., J. K. Allen and F. Mistree, 1992, "Decisions Under Uncertainty: The Fuzzy Compromise Decision Support Problem," *Engineering Optimization*, Vol. 20, pp. 21-43.

VITA

Carolyn Conner Seepersad was born Carolyn Gretchen Conner at Wright Patterson Air Force Base in Ohio on May 12, 1974. She grew up in Clay County, West Virginia and attended Clay County High School. She earned a Bachelor of Science degree, *summa cum laude*, in Mechanical Engineering from West Virginia University in 1996. During her senior year at West Virginia University, she was designated a Rhodes Scholar and earned a Bachelor of Arts in the Honour School of Philosophy, Politics, and Economics at Oxford University in 1998. She earned a Master of Science degree in Mechanical Engineering from the Georgia Institute of Technology in 2001. Her graduate work was funded by a President's Fellowship from the Georgia Institute of Technology, a fellowship from the Achievement Rewards for College Scientists program, a Graduate Research Fellowship from the National Science Foundation, and a Hertz Fellowship from the Fannie and John Hertz Foundation. Carolyn is currently an Assistant Professor of Mechanical Engineering at the University of Texas at Austin.